Dissertation zur Erlangung des Doktorgrades
der Fakultät für Chemie und Pharmazie
der Ludwig-Maximilians-Universität München

Investigations of environmentally benign pyrotechnic formulations based on nitrogen-rich and energetic boron-based compounds

Magdalena Rusan

aus

München

2014

Erklärung

Diese Dissertation wurde im Sinne von § 7 der Promotionsordnung vom 28. November 2011 von Herrn Prof. Dr. Thomas M. Klapötke betreut.

Eidesstattliche Versicherung

Diese Dissertation wurde eigenständig und ohne unerlaubte Hilfe erarbeitet.

München, 03.06.2014

Magdalena Rusan

Dissertation eingereicht am: 03.06.2014
1. Gutachter: Prof. Dr. Thomas M. Klapötke
2. Gutachter: Prof. Dr. Konstantin Karaghiosoff
Mündliche Prüfung am: 07.07.2014

Danksagung

Ich möchte mich ganz besonders bei Herr Prof. Dr. Thomas M. Klapötke für die freundliche Aufnahme in seinen Arbeitskreis, für das sehr interessante und herausfordernde Thema dieser Dissertation, sein Vertrauen und Unterstützung sowie für jede andere Hilfe bedanken. Für die Möglichkeit an zahlreichen Konferenzen teilnehmen zu können, möchte ich mich ebenfalls ganz herzlich bedanken.

Herrn Prof. Dr. Konstantin Karaghiosoff möchte ich zunächst für die Übernahme der Zweitkorrektur danken. Aber ganz besonders möchte ich für seine Hilfe, Diskussionen und Unterstützung danken.

Mein ganz besonderer Dank gilt dem Cusanuswerk für die Förderung im Rahmen eines Promotionsstipendiums. Ich möchte mich nicht nur für die finanzielle Unterstützung, die die Promotion erst ermöglicht hat, bedanken, sondern vor allem und ganz besonders für die „geistige“ Förderung, die Möglichkeit an Graduiertentagungen, Jahrestreffen und vielen anderen Veranstaltungen teilnehmen zu können und so viele neue Erfahrungen sammeln zu können.

Herrn Dr. Burkhard Krumm möchte ich für die vielen guten Vorschläge, Diskussionen und Hilfe danken.

Mein Dank gilt auch Dr. Jörg Stierstorfer für die Hilfe bei den Publikationen, insbesondere beim Kristallstrukturenteil, für alle wertvollen Tipps und die gute Laune.

Stefan Huber möchte ich für die vielen Sensitivitätsmessungen und Chemikalienbestellungen danken, aber vor allem für die netten und lustigen Gespräche.

Besonders bedanken möchte ich mich bei Dr. Jesse J. Sabatini für die wertvollen Ratschläge und die großartige Unterstützung.

Frau Irene S. Scheckenbach gilt mein ganz herzlicher Dank, natürlich für die unermüdliche Hilfe bei allen Anliegen, aber vor allem für ihre grenzenlose Tierliebe die damit verbunden ist jedem einzelnen notleidenden Tier sofort zu helfen. Danke!

Meinen Praktikanten Andreas Drechsel, Thomas G. Müller, Benedikt Stiasny, Katharina A. Hengge, Yvonne Morgenstern, Ines E. Drukenmüller, Matthias R. Becker, Kathleen Nimmrich, Marc F. Bölter, Anne T. M. Friedrichs und Johann Glück möchte ich besonders danken, die einen großen Beitrag zu dieser Arbeit geleistet haben.

Ganz herzlich danke ich auch Véronique Sproll, die während ihrer Masterarbeit wertvolle Beiträge zu dieser Arbeit geleistet hat, aber ganz besonders für die vielen Gespräche und die schöne gemeinsame Zeit.

Ich möchte mich bei meinen Laborkollegen Benedikt Stiasny, Martin Haertel, Marcos Kettner und Vera Hartdegen für die tolle Atmosphäre und die netten Unterhaltungen bedanken.

Dem gesamten Arbeitskreis danke ich ebenfalls für die gute Atmosphäre und Hilfsbereitschaft.

Camilla Evangelisti und Christina Hettstedt (und allen anderen „Köchen“) danke ich für die lustigen, netten und leckeren Kochrunden.

Meinen Lieblingen Felix und Hansi: *„Dass mir mein Hund das Liebste sei, sagst du, oh Mensch, sei Sünde, mein Hund ist mir im Sturme treu, der Mensch nicht mal im Winde.“*
(hl. Franz von Assisi)
Ihr macht jeden Tag besser, schöner, erträglicher und lebenswerter. Danke ihr Süssen!
An dieser Stelle möchte ich aber auch dem „Herrchen“ für seine Tierliebe danken; dafür, dass seine Hilfsbereitschaft, egal wie schwierig es ist, grenzenlos ist.

Meiner Familie und meinen Freunden möchte ich für ihre Unterstützung, Geduld und Verständnis danken.

Table of Contents

1 INTRODUCTION 1

1.1 Energetic Materials 1

1.2 Pyrotechnics 2

1.3 Pyrotechnic Compositions 3

1.3.1 Colorants 3

1.3.2 Oxidizers 4

1.3.4 Fuels 5

1.3.5 Binders 5

1.4 Color Measurements 6

1.4.1 Luminous Intensity 8

1.4.2 Dominant Wavelength 8

1.4.3 Spectral purity 8

1.5 Methods 8

1.6 Objectives 9

1.7 References 10

2 CONCLUSION 11

2.1 Nitrogen-rich Metal Salts 11

2.2 Nitrogen-rich Boron-containing Compounds 13

2.3 Reference Formulations 16

2.4 Green-burning Formulations Based on Boron Compounds 19

2.4.1 Formulations Based on Boron Carbide 19

2.4.2 Formulations Based on Amorphous Boron 19

2.4.3 Formulations Based on Energetic Dihydrobis(azolyl)borates 21

2.4.4 Formulations Based on Tris(2,2,2-trinitroethyl)borate 24
2.5 Formulations Based on Nitrogen-rich Metal Salts 25
2.6 Blue-burning Formulations Based on Copper Iodate 26
2.7 References 27

3 APPENDIX

List of Publications

Curriculum Vitae

1 Introduction

1.1 Energetic materials

According to the American Society for Testing and Materials[1] an energetic material is defined as “a compound or mixture of substances which contains both the fuel and the oxidizer and reacts readily with the release of energy and gas”.[2] Energetic materials can be divided into primary and secondary explosives, fuels and pyrotechnics (Figure 1).

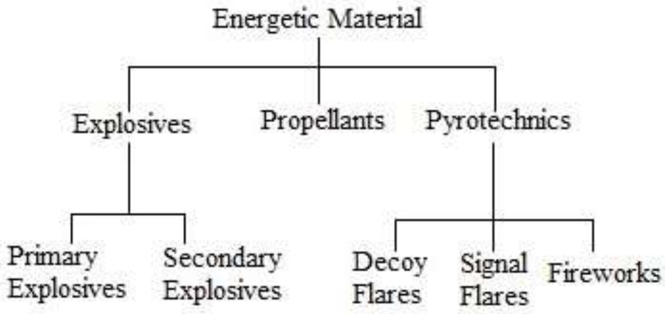

Figure 1. Classification of energetic materials.

Primary explosives are very sensitive and low-performing compounds.[2] They are used to initiate secondary explosives, which are less sensitive but more powerful. The common primary explosives are lead azide ($Pb(N_3)_2$), lead styphnate (2,4,6-trinitroresorcinate), DDNP (diazodinitrophenol) or mercury fulminate ($C_2HgN_2O_2$) (Figure 2). They are very sensitive towards shock, friction and heat and are initiated by burning. Furthermore, primary explosives reveal a very fast transition from burning (deflagration) to detonation, but the energy content is lower compared to secondary explosives.[2]

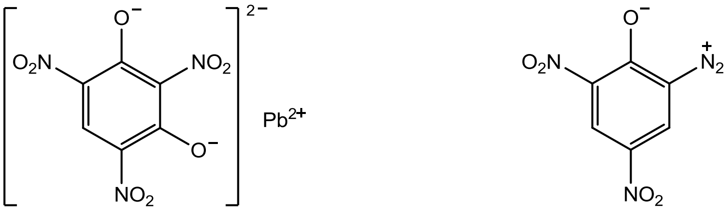

1 **2**

Figure 2. Lead styphnate (**1**) and diazidodinitrophenol (**2**).

Secondary explosives, also called “high explosives” are less or moderate sensitive towards shock, friction or electrostatic discharge and are initiated by the shock wave of a primary explosive. The released energy as well as the power of the shock wave is much higher compared to primary explosives. Examples of mostly used secondary explosives are RDX (1,3,5-trinitro-1,3,5-triazacyclohexane), HMX (1,3,5,7-tetranitro-1,3,5,7-tetraazacyclooctane) and HNS (1,2-bis(2,4,6-trinitrophenyl)ethylene) (Figure 3).[2]

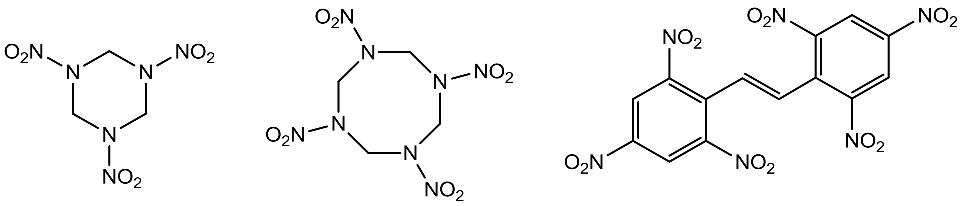

3 **4** **5**

Figure 3. RDX (**3**), HMX (**4**) and HNS (**5**).

In order to obtain more efficient secondary explosives the research interests focus on the development of compounds revealing a high performance, less sensitivity, less toxicity of the compound and the corresponding detonation products.[2] High performance criteria are such as heat of formation (kJ kg^{-1}), detonation velocity (m s^{-1}), detonation pressure (kbar) and released gaseous volume (L kg^{-1}).[2]

Propellants, which can be divided into gun and rocket propellants do not explode but burn. Gun propellants can be single-base such as those based on nitrocellulose using in weapons ranging from pistols to artillery weapons or double-base used in pistols and mortars. The oldest gun propellant is gun powder consisting of 75% potassium nitrate, 10% sulfur and 15% charcoal. Rocket propellants can be separated into solid and liquid propellants. The solid propellants are either double-base or composite propellants. While double-base propellants are homogenous formulations of nitroglycerine and nitrocellulose, composite propellants are mixtures of a crystalline oxidizer such as ammonium perchlorate and a polymeric binder. All kinds of propellants have in common that the specific impulse is the essential parameter describing the efficiency of rockets and engines.[2]

Pyrotechnics are used in military and civilian applications and according to the desired effects they can be divided in heat, noise or gas producing pyrotechnics, delay pyrotechnics as well as colored or colorless light and smoke pyrotechnics.[2]

1.2 Pyrotechnics

The term “pyrotechnic” is derived from the Greek words “pyro” and “techne” and can be translated as the art of fire. Although pyrotechnics are mostly associated with fireworks (Figure 4), in a wide range of applications pyrotechnics is used such as in airbags, fire extinguishers, signal flares, acoustic and optic decay devices and igniters for example.[3]

Figure 4. Color-producing firework (39th IPS, Valencia 2013).

Generally, a pyrotechnic mixture consists of an oxidizer and fuel and a series of different additives such as colorants, binders as well as smoke or noise generating additives depending on their intended use. Noise-producing pyrotechnics, for example, are generated by gas-producing formulations using black powder, which is ignited by a fuse, employing in bangers and aerial bomb shells. Colored smoke-producing pyrotechnics require components, which produce large amounts of gas to increase the colored surface. Colored smokes contain organic dyes, which sublimes and condense in air producing small particles.[2, 3]

1.3 Pyrotechnic compositions

Since this thesis focus on colored light-producing pyrotechnics, the components of such compositions are described below.

1.3.1 Colorants

The production of color requires a color-emitting species and heat, which is obtained from the reaction of the oxidizer and fuel. Light-emitter can be either solid state emitters, which are responsible for the black body radiation or gas phase emitters such as atoms and molecules. Table 1 shows several elements and their compounds (Table 1), which emit the visible light.

Table 1. Visible light-emitting elements and their compounds[4].

Element	**Emitting species**	**Wavelength [nm]**	**Color**	**Compounds**
lithium	atomic Li	670.8 497 460 427, 413	red blue-green blue violet	$LiNO_3$, $LiClO_3$
strontium	SrCl SrCl SrCl SrOH SrOH atomic Sr	675.6, 674.5, 662.0, 661.4 648.5, 636.2, 623.9 400.9, 396.1, 393.7 682.0, 667.5, 659.0 646.0, 605.0 460.7	red orange violet red orange blue	$Sr(NO_3)_2$, $SrCO_3$
sodium	atomic Na	589.6, 589.0	yellow	$Na_2C_2O_4$, NaCl, $NaCO_3$
barium	BaCl BaCl BaOH BaOH BaO atomic Ba atomic Ba	649 532.1, 524.1, 516.2, 513.8, 507 512 487 629, 622, 617, 610, 604 660 553.5	red green green blue-green orange red green	$Ba(NO_3)_2$, $Ba(ClO_3)_2$, $BaSO_4$, BaO
copper	CuCl CuOH CuO	428–452, 476–488 525–555	violet, blue green red	Cu, CuO, $CuSO_4$, CuS, $(NH_4)_2Cu(SO_4)_2$, $Cu(C_2H_3O_2)_2$.

Monochromatic light is light, which is emitted in a particular wavelength range. Visible light, which can be perceived by the human eye emits in the region between 780 nm and 400 nm of the electromagnetic spectrum (Table 2). However, light produced by a pyrotechnic formulation is not monochromatic and contains besides the desired spectral range additional spectral components due to the excitation of atoms or molecules by high temperatures producing several emission lines. Only a few elements such as sodium for examples generate emission lines, which are within the narrow visible range. [4]

Table 2. Wavelength regions of spectral colors[4].

Color	λ [nm]
infrared	> 780
red	780 – 610
yellow	610 – 570
green	570 – 500
blue	500 – 450
violet	450 – 400
ultraviolet	< 400

Red, green, yellow and blue flame colors are obtained using salts of the elements strontium, barium, sodium and copper. Boron is also used to produce green flame colors. The primary light-emitting species are atom sodium for the yellow color, SrOH and SrCl for red color, BaOH, BaO and BaCl for green color and CuCl for blue color.[4] When using boron as green colorant the green-light-emitting species BO_2.[5] Since the chlorides, possessing increased volatility are mainly responsible for red, green and blue flame colors, chlorine-donors must be used in formulations to produces the chlorides. Chlorine-sources such as polyvinyl chloride (PVC), organic chlorine-rich compounds or mostly potassium perchlorate using as the oxidizer at the same time are employed. But the use of these compounds reveals problems regarding the toxicity and environmental aspects. The problems concerning the perchlorates are discussed below (Oxidizers). The combustion of organic compounds in the presence of a chlorine-containing compound results the formation of polychlorinated dibenzo-*p*-dioxins (PCDD) and dibenzofurans (PCDF), which are discussed to be health hazardous.[6]

1.3.2 Oxidizers

Oxidizers, which are usually oxygen-rich ionic solids, decompose at moderate to high temperatures and release oxygen gas.[3] Oxidizers must fit a series of requirements such as wide-range thermal stability, low hygroscopicity, proper particle size and oxygen balance. Compounds, which contain high-energy Cl-O or N-O bonds like in alkali or earth alkaline salts of nitrates, perchlorates, chlorates or chromates as well as ammonium nitrate and ammonium perchlorate are suitable candidates.

Potassium chlorate showing a low hygroscopicity and 39.2% oxygen by weight is used nowadays in colored smoke compositions, firecrackers and some color-producing fireworks.[3] However, it shows a high sensitivity when combining it with acidic components, sulfur or phosphorus.[3] Furthermore, formulations containing potassium chlorate are instable due to the low melting point and low decomposition temperature of the oxidizer.[3] Potassium chlorate decomposes resulting in the formation of potassium chloride and oxygen gas, which is a vigorous reaction becoming violent at temperatures higher than 500°C.[3, 7] Potassium perchlorate, which gradually replaced potassium chlorate, reveals much lower sensitivity towards heat, friction and impact than potassium chlorate due to its higher melting point and less exothermic decomposition.[3, 8] Furthermore, it is used to produce flame colors, can be obtained at reasonable costs and high purity, possess a good stability and shows a good reactivity with a wide range of fuels.[3] However, investigations revealed that the perchlorate anion is teratogenic and has a negative effect on the thyroid gland function since it inhibits the uptake of iodine and can cause hypothyroidism.[4, 9] Also perchlorates are responsible for groundwater contamination.[10] Potassium nitrate, which is the oldest solid oxidizer, is advantageous due to its low hygroscopicity and high-purity. Additionally, it is easy to ignite due its low melting point and decomposes at high temperature. However, when combined with low-energy fuels it burns with difficulty and the reaction stops after potassium nitrite has been formed. A further oxidizer is ammonium perchlorate, which is a powerful oxidizer. When combined with a fuel it can produce high flame temperatures and contributes to the production of color due to hydrogen chloride, which is liberated during the reaction. But since it contains the perchlorate anion, it displays health and environmental concerns. Strontium nitrate, which is often used in red-light-emitting pyrotechnics, is often combined with other oxidizers such as potassium perchlorate. It decomposes near its melting point and strontium nitrite is formed as intermediate at low decomposition temperatures[7], whereas higher reaction temperatures yield strontium oxide and gaseous nitrogen and oxygen resulting an active oxygen content of 37.7%. Strontium nitrate is the main component of highway flares and is mixed with slow-burning fuels such as sulfur to achieve long burning times.[3] In green-color-producing formulations barium nitrate is mostly used as the oxidizer. But it is often combined with potassium perchlorate too. At high decomposition temperatures barium oxide is formed along with nitrogen and oxygen gas giving an active oxygen content of 30.6%, while low reaction temperatures lead to the formation of nitrogen oxides instead of nitrogen gas.[7, 3] But also other oxidizers such as metal oxides Fe_2O_3 or Bi_2O_3 can be used.[3]

1.3.3 Fuels

In a pyrotechnic mixture the fuel is the electron donor, which reacts with the liberated oxygen from the oxidizer to result an oxidized product and heat.[3] This generated heat is necessary to produce color, light, smoke, noise or motion.[3] A series of metals are used as fuels. According to the desired effects the fuel is chosen. For illuminating of colored flame compositions fuels, which lead to the production of high reaction temperatures, should be used. In the case of colored smoke formulations low temperatures are required and therefore low-energy fuels such as sulfur and sugars are employed. For bright-burning formulations and fireworks metal powders such as magnesium, aluminum, titanium, iron, copper, zinc and zirconium are used. Magnesium is widely used because it is a very reactive metal and not expensive but it reveals undesirable and dangerous properties, since it reacts with water resulting in the formation of magnesium hydroxide and hydrogen gas. In green-light-producing pyrotechnics boron is beneficial as it serves not only as fuel but also as colorant.[3, 4]

1.3.4 Binders

Binders are important additives in pyrotechnic formulations since they ensure mechanical stability and seal the surface to protect the mixtures from air moisture.[4] Moreover, binders prevent the separation of the mixture components and are therefore essential for a proper storage of pyrotechnic products. Binders can be divided into energetic and non-energetic binders. Non-energetic binders are for example dextrin or vinyl alcohol, which are water-soluble, or vinyl alcohol acetate resin (VAAR) and polymethyl methacrylate, which are organic-solvents-based.[4] Usually non-energetic binders decrease the reaction rate and behaves as retardants.[4, 11] In contrast energetic binders such as glycidyl azide polymer (GAP) or nitrocellulose contribute to the reaction energy, however they often react with other mixture components as they contain reactive energetic nitro, hydroxyl or azide groups.[4]

1.4 Color measurement

As the sensitivity of the human eye is not equal for all wavelengths of the visible light the measured power at each wavelength is weighted with a factor that represents how sensitive the eye is at that wavelength.[12] Therefore, photometry deals with the measurement of optical radiation as it is perceived by the human eye.[13]

According to literature [14] light sensation is produced by visible radiation, electromagnetic radiation falling within the wavelength limits of 380 nm and 780 nm. Radiation from the short wavelength region of this radiation produces usually the sensation of blue light, radiation with wavelengths between 520 nm and 550 nm are seen as green light, and above about 650 nm we perceive the light usually to be of red color. These limits are not well defined, and the actual perception depends strongly on the adaptation state of the eye and on light stimuli surrounding the test object.[14]

To describe the color perception the CIE 1931 XYZ color space has been introduced by the International Commission on Illumination in 1931. The CIE 1931 Standard Observer has been established a standard based on the average human eye response under normal illumination with a 2° field of view.[13] Three types of cone cells exist in the eye, with each being more sensitive to either short (blue), medium (green), or long (red) wavelength light. The set of signals possible at all three cone cells describes the range of colors that can be seen with the eyes. The diagram below illustrates (Figure 5) the relative sensitivity of each type of cell for the entire visible spectrum. These curves are often also referred to as the tristimulus functions or color matching functions.[15] The CIE color matching functions are mathematical description (Figure 6) of the chromatic response of the observer. Three parameters, corresponding to levels of stimulus of the three types of cone cells, can in principle describe any color sensation. Weighting a total light power spectrum by the individual spectral sensitivities of the three types of cone cells gives three effective stimulus values; these three values make up a tristimulus specification of the objective color of the light spectrum.

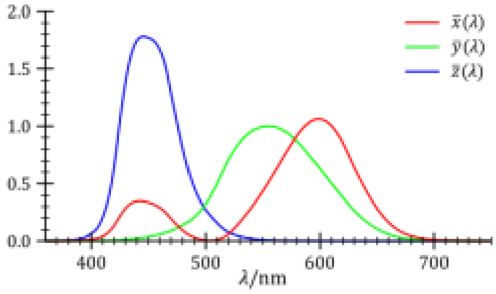

Figure 5. Tristimulus functions.[16]

$$X = \int_{0}^{\infty} I(\lambda)T(\lambda)\overline{x}(\lambda)d\lambda$$

$$Y = \int_{0}^{\infty} I(\lambda)T(\lambda)\overline{y}(\lambda)d\lambda$$

$$Z = \int_{0}^{\infty} I(\lambda)T(\lambda)\overline{z}(\lambda)d\lambda$$

Figure 6. Color matching functions: mathematical description.[17]

The chromaticity diagram displays the entire gamut of human-perceived colors by their xy-coordinates (Figure 7), which are derived from the tristimulus values X, Y and Z.

$$x = \frac{X}{X+Y+Z}; \quad y = \frac{Y}{X+Y+Z}$$

Figure 6. Calculation of xy coordinates.[17]

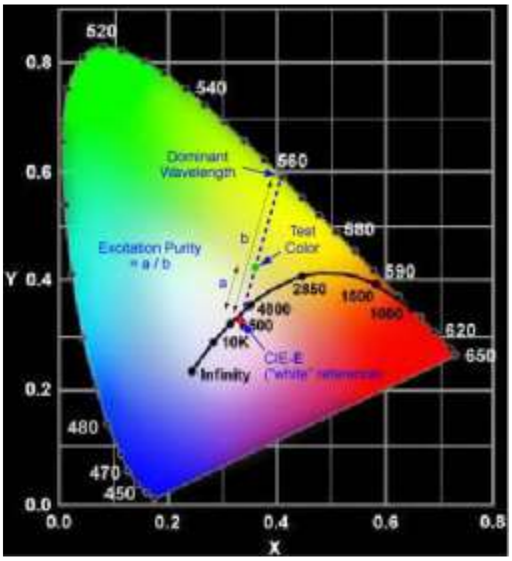

Figure 7. CIE 1931 chromaticity diagram.[17]

The locus of points that define the horseshoe-shaped region are the chromaticity coordinates for spectrally pure colors.

1.4.1 Luminous intensity

Literature [18] describes the luminous intensity to be “the quantity of visible light that is emitted in unit time per unit solid angle. The unit for the quantity of light flowing from a source in any one second (the luminous power, or luminous flux) is called the lumen. The lumen is evaluated with reference to visual sensation. The sensitivity of the human eye is greatest for light having a wavelength of 555 nanometres. At this wavelength there are 685 lumens per watt of radiant power, or radiant flux (the luminous efficiency), whereas at other wavelengths the luminous efficiency is less. The unit of luminous intensity is one lumen per steradian, which is the unit of solid angle—there are 4π steradians about a point enclosed by a spherical surface. This unit of luminous intensity is also called the standard candle, or candela, one lumen per steradian”.[18] The SI unit of luminous intensity is the candela (cd).

1.4.2 Dominant wavelength

As in literature [17] described the dominant wavelength can be determined by drawing a line between the chromaticity coordinates of the reference white point, which is illuminant C in this thesis simulating the daylight, on the diagram and the chromaticity coordinates of a measured color and then extrapolates the line from the end that terminates at the sample point. The wavelength associated with the point on the horseshoe-shaped curve at which the extrapolated line intersects is the dominant wavelength (Figure 7). When the line used to locate the dominant wavelength does not intersect the horseshoe-shaped curve at all, then the complementary wavelength instead of the dominant wavelength is used to describe the color most accurately, and in this case it is called the “complimentary dominant wavelength.”[17]

1.4.3 Spectral purtiy

According to literature [17] the excitation purity is defined to be the ratio of the length of the line segment that connects the chromaticity coordinates of the reference white point and the color of interest to the length of the line segment that connects the reference white point to the dominant wavelength. These line segments are illustrated in Figure 7. As pointed out above, the excitation purity is a welldefined, quantitative measure of the saturation of a particular color. The larger the excitation purity, the more saturated the color appears, or the more similar the color is to its spectrally pure color at the dominant wavelength. The smaller the excitation purity, the less saturated the color appears, or the more white it is.[17]

1.5 Methods

The in this thesis investigated pyrotechnic formulations have been prepared by grinding the oxidizer, fuel, colorant and other additives except the binder in a mortar. Two binder systems – vinyl alcohol acetate resin (VAAR) and Epon 828/Epikure 3140 have been employed. In the case of the VAAR binder, the corresponding amount of binder was diluted in a small amount of ethyl acetate and then added to the mixture and dried at vacuum for several hours. Afterwards the mixtures were grinded again and pellets were pressed using a consolidation dead load of 2000 kg. Formulations using Epon

828/Epikure 3140 binder were prepared by introducing the mixture into the binder system, mixing it by hand with a plastic spatula for 15-30 minutes. After grinding the mixtures again, pellets were pressed using a consolidation dead load of 2000 kg as well and dried over night at 60°C. Pellets of 0.6 g were used. 5-7 pellets were used per formulations and average values were used. The burn down was filmed with a video camera and evaluated with respect to color, smoke production and amount of residues. The burn time (s), dominant wavelength (Dw/nm), spectral purity (Sp/%), luminous intensity (LI/cd) and luminous efficiency (LE/cdsg^{-1}) are measured and compared to the control formulations (see Conclusion). The set-up of the color measurements is shown in Figure 8.

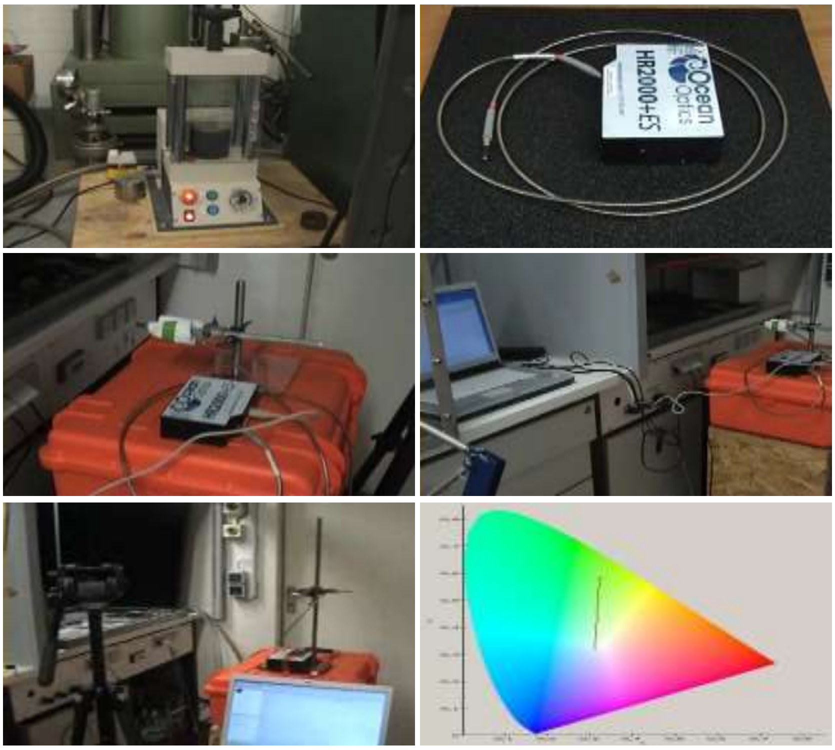

Figure 8. Color measurement set-up.

1.6 Objectives

Novel developments in pyrotechnics focus on the application of environmentally more benign and less toxic compounds. Main objectives are the substitution of toxic perchlorates and heavy metals as well as to reduce the smoke production of the pyrotechnic composition to obtain more brilliant flame colors showing higher spectral purities and luminous intensities. Especially the replacement of highly water-soluble barium compounds such as barium nitrate in green-light emitting pyrotechnics by less toxic boron-containing compounds or water-insoluble barium compounds, which possess a higher performance, is desired. Furthermore, formulations exhibiting long-term stability, high decomposition temperatures and low sensitivities towards ignition stimuli are desired. Therefore, novel nitrogen-rich compounds are synthesized and investigated for their suitability as red and green colorants in pyrotechnical formulations. In this thesis new nitrogen-rich boron-containing compounds have been prepared and investigated as well. Formulations using nitrogen-rich strontium and barium salts as well as energetic boron-compounds as colorants or oxidizers have been investigated. Moreover, chlorine-free blue-burning formulations have been examined as well.

1.7 References

[1] http://www.astm.org/
[2] T. M. Klapötke, *Chemistry of High-energy Materials*, Walter de Gruyter, 2nd Edition, Berlin, **2012**.
[3] J. A. Conkling, C. J. Mocella, *Chemistry of Pyrotechnics: Basic Principles and Theory*, Taylor and Francis Group, 2nd Edition, New York, **2011**.
[4] G. Steinhauser, T. M. Klapötke, *Angew. Chem. Int. Ed.* **2008**, *47*, 3330.
[5] B. T. Sturman, *J. Pyrotech.* **1999**, *9*, 57.
[6] a) O. Fleischer, H. Wichmann, W. Lorenz, *Chemosphere* **1999**, *39*, 925; b) D. Dyke, P. Coleman, *Organohalogen Compounds* **1995**, *24*, 213.
[7] T. Shimizu, Fireworks – The art, science, and technique, Tokyo: T. Shimizu, 1981.
[8] U.S. Army Material Command, *Engineering design handbook: Properties of materials used in pyrotechnic compositions*, Military Pyrotechnic Series, Part Three, Washington, DC, 1963 (AMC Pamphlet 706-187).
[9] a) Natl. Res. Counc. of the Natl. Academies, Health Implications of Perchlorate Ingestion, Washington DC, 2005, pp. 1; b) J. Sass, Int. J. Occup. Environ. Health 2004, 10, 330 ; c) O. P. Soldin, L. E. Braverman, S. H. Lamm, Ther. Drug Monit. 2001, 23, 316; d) J. B. Stanbury, J. B. Wyngaarden, Metab. Clin. Exp. 1952, 1, 533; e) J.Wolff, Pharmacol. Rev. 1998, 50, 89 ; f) J. J. J. Clark in Perchlorate in the Environment (Ed.: E. T. Urbansky), Kluwer Academic/Plenum, New York, 2000.
[10] a) W. E. Motzer, Environ. Forensics 2001, 2, 301; b) C. Hogue, Chem. Eng. News 2003, 81, 37.
[11] B. Berger, Chimia 2004, 58, 363.
[12] http://en.wikipedia.org/wiki/Photometry_(optics)
[13] A. Ryer, *The Light Measurement Handbook*, Technical Publications Dept., International Light Technologies, 10 Technology Drive, Peabody, MA 01960.
[14] J. Schanda, *Colorimetry: Understanding the CIE System*, John Wiley & Sons Inc., New Jersey, 2007.
[15] http://www.cambridgeincolour.com/tutorials/color-perception.htm
[16] http://en.wikipedia.org/wiki/CIE_1931_color_space
[17] T. Erdogan, *How to Calculate Luminosity, Dominant Wavelength, and Excitation Purity*, Shemrock White Paper Series (http://www.semrock.com/how-to-calculate-luminosity-dominant-wavelength-and-excitation-purity.aspx).
[18] http://www.britannica.com/EBchecked/topic/351262/luminous-intensity

2 Conclusion

In the course of the investigation and development of novel non-toxic and environmentally friendly pyrotechnic formulations, a series of nitrogen-rich metal salts and energetic boron-based compounds have been investigated. Major requirements for such novel compounds are no or less smoke production during the combustion obtaining brilliant flame colors and less toxic decomposition products. Also the replacement of highly water-soluble barium nitrate and potassium perchlorate is desired. But also low sensitivities towards ignition stimuli and high temperature stabilities are of high importance as well as a performance equal or higher than that of commonly used compounds.

In literature nitrogen-rich and metal free polynitrated pyrazolates and imidazolates are reported revealing acceptable physical properties such as high densities and thermal stabilities.[1, 2, 3] Thus, metal salts of 4,5-dinitroimidazole, 3,5-dinitropyrazole, 2,4,5-trinitroimidazole and 3,4,5-trinitropyrazole have been synthesized, characterized (Section 2.1) and investigated as potential colorants in pyrotechnic formulations (Section 2.5). Furthermore, formulations containing strontium and barium salts of 5,5’-bistetrazole and 5,5’-bis(tetrazole-1-oxide) have been prepared and investigated as green- and red-burning coloring agents (Section 2.1).

Among energetic materials boron-containing compounds display an interesting class of compounds due to the gain of energy contributing to the formation of B_2O_3 as combustion product. In the course of this investigation energetic borazines, energetic boron esters and energetic poly(azolyl)borate compounds have been synthesized and characterized with respect to their stability and energetic properties (Section 2.2). In order to replace barium compounds in green-burning pyrotechnic formulations, the investigation was focused on energetic boron-containing compounds, employing them as green colorants. A series of energetic dihydrobis(azolyl)borates was synthesized and characterized. Selected compounds were tested as green-burning colorants in pyrotechnic formulations (Section 2.4.3). Furthermore, the energetic boron ester tris(2,2,2-trinitroethyl)borate was investigated as green colorant and the oxidizer at the same time (Section 2.4.4).

Moreover, blue-light-emitting pyrotechnic formulations based on copper iodate and without the use of chlorine-containing compounds are examined (Section 2.6).

2.1 Nitrogen-rich metal salts

Nitrogen-rich compounds are considered to be suitable coloring agents for pyrotechnical applications since they do not obtain their energy from the oxidation of the carbon backbone but rather from the high heats of formation and the main decomposition product is gaseous nitrogen, which means less toxic decomposition products and less or no smoke generation during the combustion yielding brilliant color and thus good color performances. Furthermore, nitrogen-rich five-membered aromatic azole-based compounds show increased stabilities towards thermal conditions and ignition stimuli, which is an important requirement for the use in pyrotechnics. Therefore, a series of nitrogen-rich metal salts have been investigated

The synthesis and characterization of metal dinitro- (**1a**) and trinitropyrazolates (**2b**) as well as dinitro- (**2a**) and trinitroimidazolates (**2b**) are reported (Scheme 1). The starting materials 3,5-dinitropyrazole, 3,4,5-trinitropyrazole, 4,5-dinitroimidazole and 2,4,5-trinitroimidazole were synthesized according to literature procedures.[1, 2, 3] The alkaline and earth alkaline salts of **1a**, **1b**, **2a** and **2b** as well as the copper salt of **2b** were obtained by the reaction of the starting materials with the corresponding metal hydroxides and metal carbonates, respectively.

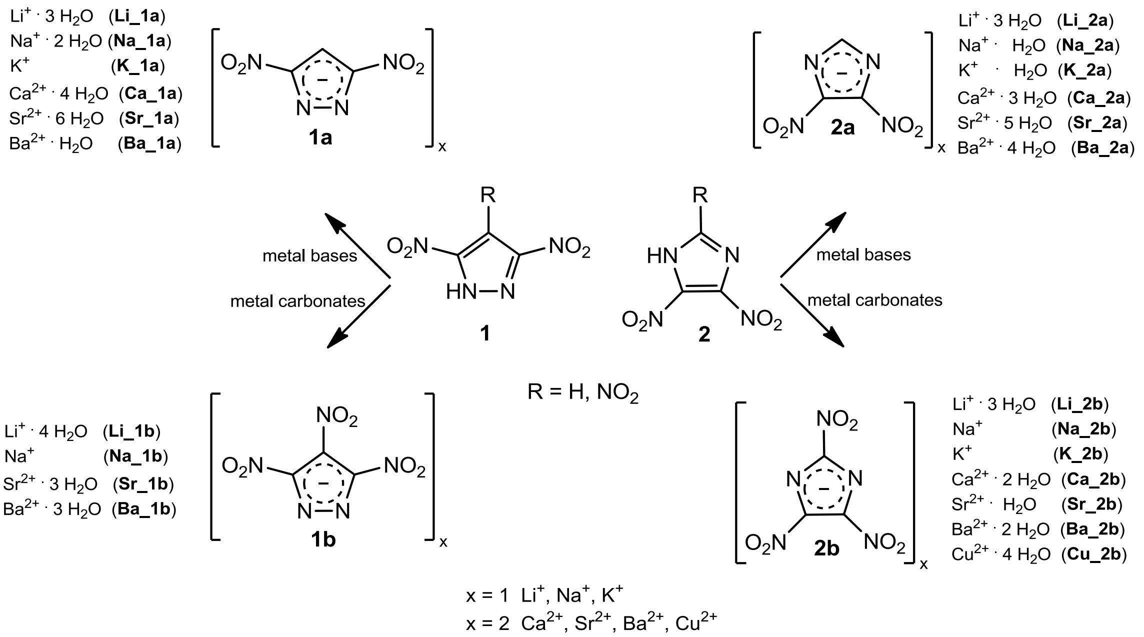

Scheme 1. Syntheses of nitrogen-rich metal salts of polynitrated compounds.

The obtained metal salts show convenient properties such as relative high decomposition temperatures and low sensitivities towards impact, friction and electrostatic discharge. The strontium and barium salts of **1** and **2** were tested in pyrotechnical formulations serving as red and green colorants (Section 2.5). The results of these investigations are described in publications "*Metal Salts of 4,5-Dinitro-1,3-imidazole as Colorants in Pyrotechnic Compositions*", "*Metal Salts of Dinitro-, Trinitropyrazole and Trinitroimidazole*", and "*The Synthesis and Investigation of Nitrogen-rich and Boron-based Compounds as Coloring Agents in Pyrotechnics*".

A further class of energetic nitrogen-rich compounds with promising properties are metal salts of 5,5'-bistetrazole and 5,5'-bis(tetrazole-1-oxide) (Scheme 2), which were synthesized and analyzed. Their barium and strontium salts have been tested as green- and red-burning colorants as well. The examined formulations show intensive green and red flame colors and high spectral purities. Publications "*Alkaline Earth Metal Salts of 5,5'-Bistetrazole – from Academical Interest to Practical Application*" and "*A Selection of Alkali and Alkaline Earth Metal Salts of 5,5'-Bis(1-hydroxytetrazole) in Pyrotechnic Compositions*" describe these results.

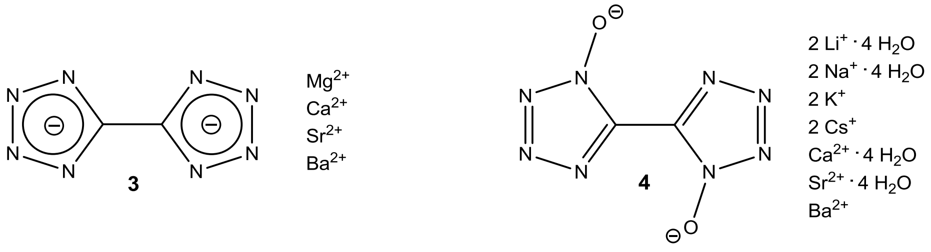

Scheme 2. Metal salts of 5,5’-bistetrazole and 5,5’-bis(tetrazole-1-oxide).

2.2 Nitrogen-rich boron-containing compounds

In order to create highly efficient formulations with a high performance, energetic boron-based colorants are considered to be suitable candidates. The combination of boron with nitrogen-rich energetic moieties in one molecule does not only enhance the energetic character but also could reduce the amount of different additives in pyrotechnical formulations.

Boron esters, which burn with a green flame color are of interest as green colorants for pyrotechnics, whereas borazine and its energetic derivatives are considered to be interesting for the use as propellants. Therefore, several energetic nitrooxy- and nitrosooxyborazine derivatives as well as boron ester compounds based on tetrazole, 5-aminotetrazole and nitrotriazole have been synthesized and characterized. An overview of these molecules is given in Scheme 3. Their thermal and energetic properties have been determined showing acceptable sensitivities and thermal stabilities. The investigations of the borazine compounds are reported in publication “*The synthesis and characterization of nitrooxy- and nitrosooxyborazine compounds*”.

Furthermore, the boron ester compound 6a was tested as green-burning colorant in pyrotechnic formulations revealing smokeless and intensive green flame colors as well as high spectral purities, which is described in publication “*Synthesis and Investigation of Energetic Boron Compounds for Pyrotechnics*”.

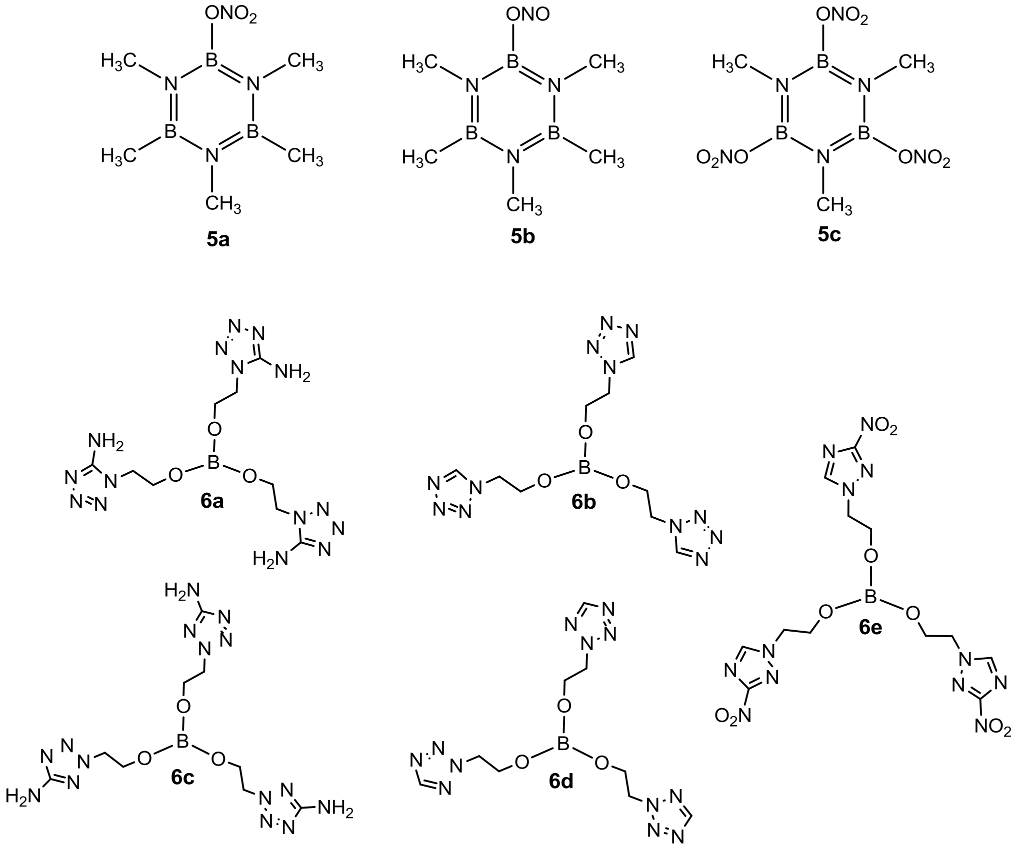

Scheme 3. Nitrooxy- and nitrosooxyborazines and tetrazole- and nitrotriazole based boron esters.

Another group of boron-containing compounds, which are considered as potential green colorants are poly(azolyl)borates.[4] Various poly(azolyl)borates have been reported in literature: there are four classes of poly(azolyl)borates, referring to their grade of substitution – trihydro(azolyl)borates, dihydrobis(azolyl)borates, hydrotris(azolyl)borates and tetrakis(azolyl)borates.[5] Among the different classes of B-N bound azoles, the group of pyrazoles and 1,2,4-triazoles show the greatest variety. Poly(azolyl)borate compounds bearing insensitive groups as alkyl- or aryl-substituents and especially tetrakis(azolyl)borates have been extensively studied by Trofimenko.[6]

Scheme 4 shows four borate compounds, which have been synthesized and analyzed and display possible precursor molecules for the synthesis of metal-free azolyl borates.

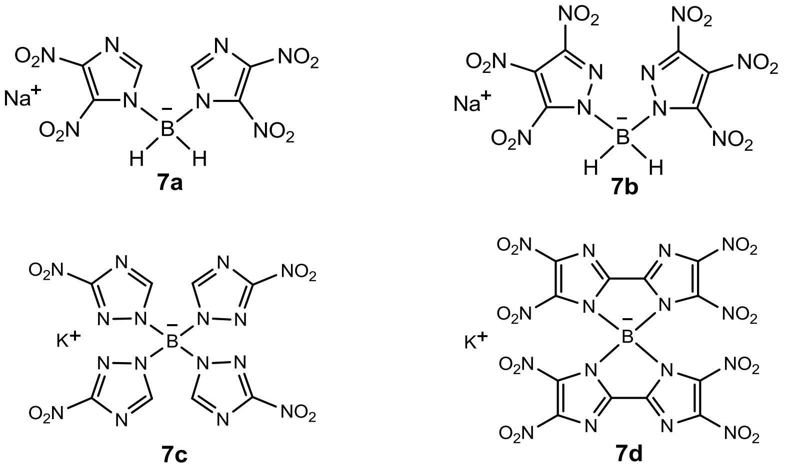

Scheme 4. Dihydrobis(azolyl)borate compounds and tetrakis(azolyl)borate compounds.

As described in the following, a series of metal-free and nitrogen-rich dihydrobis(azolyl)borate salts have been synthesized and analyzed and an overview of these compounds is given in Scheme 6. The starting materials potassium dihydrobis(azolyl)borates were synthesized by the reaction of potassium borohydride and two equivalents of the corresponding azole in a high-boiling solvent (Scheme 5). In the next step the barium salts were obtained by the reaction of the potassium salts with barium hydroxide or barium perchlorate, respectively as it is reported in the publications “*Green Colorants Based on Energetic Azole Borates*” and “*Pyrotechnical Formulations based on metal-free and nitrogen-rich dihydrobis(5-aminotetrazolyl)borates and dihydrobis(1,2,4-triazolyl)borates*”.

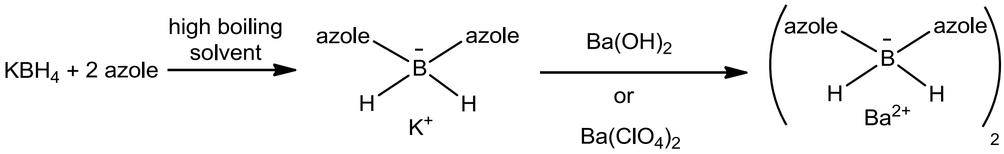

Scheme 5. Synthesis of the starting materials potassium dihydrobis(azolyl)borates and barium dihydrobis(azolyl)borates.

Metal-free dihydrobis(3-nitro-1,2,4-triazolyl)borates (Scheme 6 top), dihydrobis(5-aminotetrazolyl)borates (Scheme 6 middle left), dihydrobis(3,5-dinitropyrazolyl)borates (Scheme 6 middle right), dihydrobis(1,2,4-triazolyl)borates (Scheme 6 bottom left) and dihydrobis(2,4-dinitroimidazolyl)borates (Scheme 6 bottom right) are obtained from the reaction of barium dihydrobis(azolyl)borate with the corresponding sulfates. The products show low sensitivities towards shock, friction and electrostatic discharge as well as relative high decomposition temperatures. Therefore, these compounds display promising candidates for the use as colorants in pyrotechnic formulations.

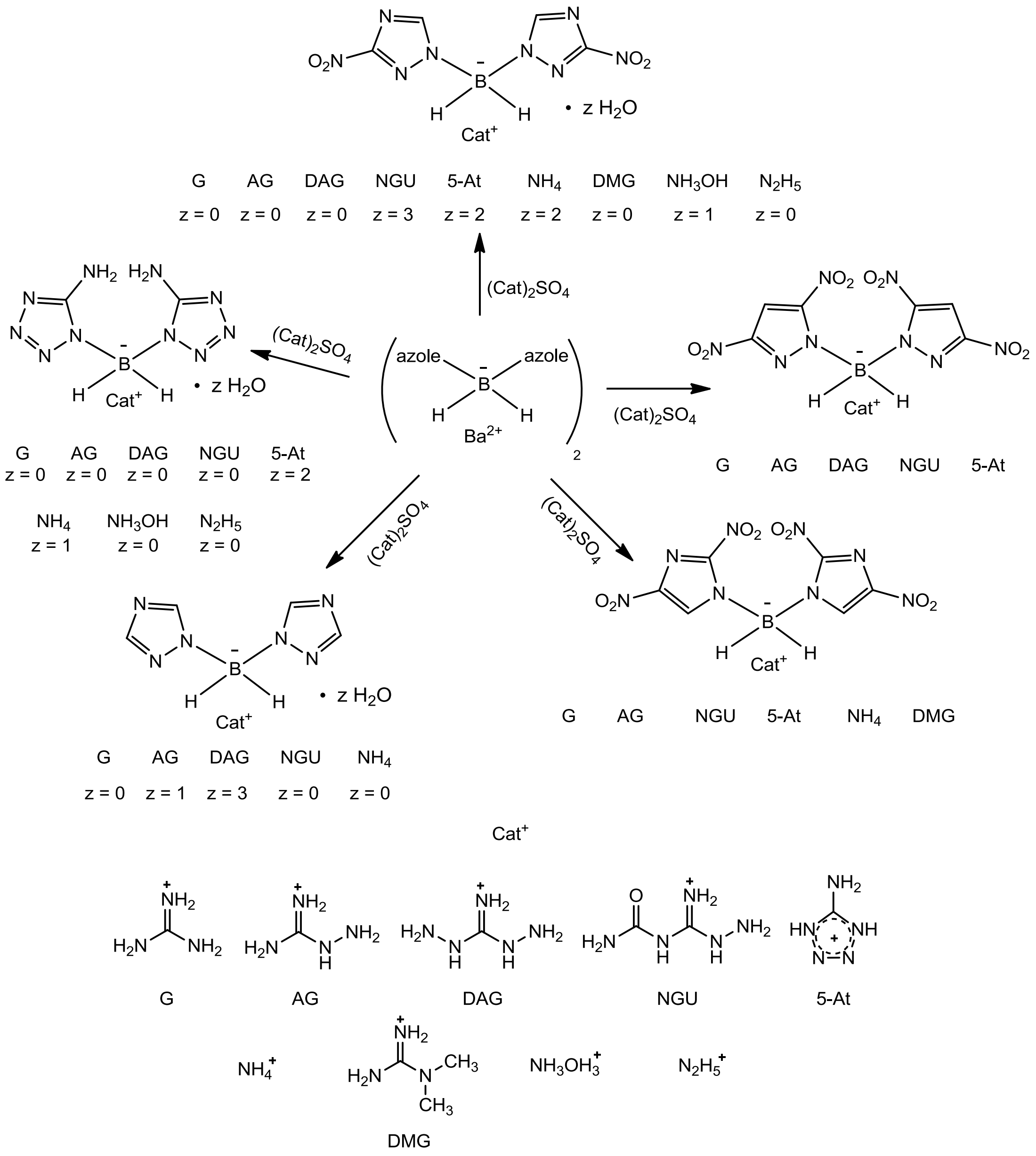

Scheme 6. Synthesis of metal-free dihydrobis(azolyl)borate salts.

2.3 Reference formulations

All new green-burning formulations are compared to the green-burning US Army´s in-service M125A1 formulation consisting of 46% barium nitrate, 33% magnesium, 16% PVC and 5% VAAR binder (Table 1). The small-scale composition (0.6 g pellet) burned smokeless with an intensive green flame color (Figure 1) and no solid residues could be observed after the burn down. Measurements revealed a burn time of 3 seconds, a dominant wavelength of 558 nm, a spectral purity of 75%, a luminous intensity of 390 cd and a luminous efficiency of 1950 cdsg^{-1} (Table 2). The color values are plotted in the CIE 1931 chromaticity diagram in Figure 1.

Table 1. Content of the barium control formulation M125A1.

	$Ba(NO_3)_2$ [wt%]	Mg [wt%]	PVC [wt%]	VAAR [wt%]
Ba-control	46	33	16	5

Table 2. Color properties of the barium control formulation.

	burn time [s]	Dw [nm]	Sp [%]	LI [cd]	LE [$cdsg^{-1}$]
Ba-control	3	558	75	390	1950

Table 3. Energetic and thermal properties of the barium control formulation.

	Impact [J]	Friction [N]	Grain size [µm]	T_{dec} [°C]
Ba-control	15	360	<100	258

The thermal and energetic properties were determined to show an impact sensitivity of 15 J, a friction sensitivity of 360 N and a decomposition temperature of 258 °C.

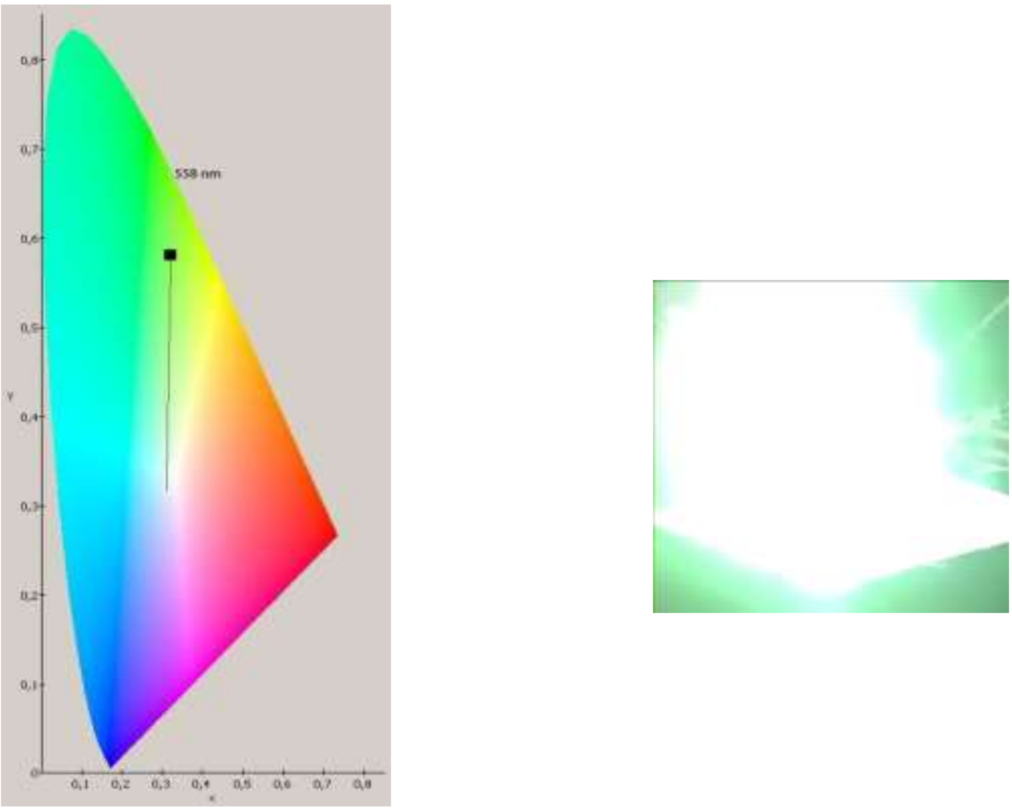

Figure 1. CIE Chromaticity diagram (left) and burn down (right) of the barium control formulation.

Red-burning formulations are compared to the US Army´s in-service M126A1 formulation. The content is given in Table 4 consisting of 39.9% strontium nitrate, 9.8% potassium perchlorate, 29.4% magnesium, 14.7% PVC and 6.8% VAAR binder. A small-scale formulation of 0.6 g was prepared and the performance data is summarized in Table 5 revealing a burn time of 4 seconds, a dominant wavelength of 617 nm, a spectral purity of 91%, a luminous intensity of 992 cd and a luminous efficiency of 6613 cdsg^{-1} (Table 5). The impact and friction sensitivities are measured to be 10 J and 360 N and the decomposition temperature is 266 °C. Figure 2 shows the CIE 1931 chromaticity diagram and the burn down of the strontium control formulation.

Table 4. Content of the strontium control formulation M126A1.

	$Sr(NO_3)_2$ [wt%]	$KClO_4$ [wt%]	Mg [wt%]	PVC [wt%]	VAAR [wt%]
Sr-control	39.9	9.8	29.4	14.7	6.8

Table 5. Color properties of the strontium control formulation.

	burn time [s]	Dw [nm]	Sp [%]	LI [cd]	LE [cdsg^{-1}]
Sr-control	4	617	91	992	6613

Table 6. Energetic and thermal properties of the strontium control formulation.

	Impact [J]	Friction [N]	grain size [µm]	T_{dec} [°C]
Sr-control	10	360	<100	266

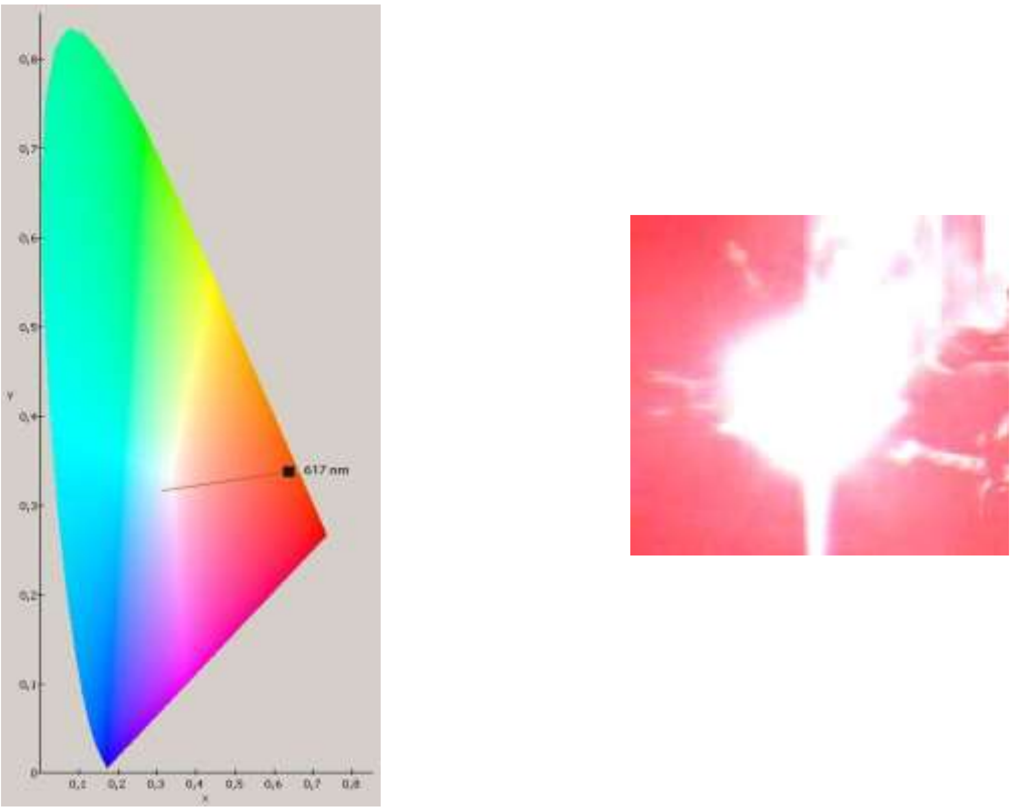

Figure 2. CIE Chromaticity diagram (left) and burn down (right) of the strontium control formulation.

2.4 Green-burning formulations based on boron compounds

2.4.1 Formulations based on boron carbide

The use of boron carbide as green colorant in a pyrotechnic formulation was described by Jesse J. Sabatini.[7] In this formulation 10% boron carbide, 83% potassium nitrate and 7% binder is used (B_4C_1). A small-scale (0.6 g-pellet) formulation was reproduced and measured with the in the introduction mentioned equipment. Formulation B_4C_1 burned with an intensive green flame color and is determined to be impact and friction insensitive with a decomposition temperature higher than 400 °C. The performance data is given in Table 9 revealing a moderate spectral purity of 69% due to the use of potassium nitrate. Therefore, formulations using boron carbide and metal-free oxidizers ammonium nitrate and ammonium dinitramide (ADN) have been investigated. However, NH_4NO_3-containing formulations could not be ignited and ADN-containing formulations did not burn with a green flame color (Figure 3). In all compositions the VAAR binder was employed.

Table 7. Content of formulation B_4C_1.

	B_4C [wt%]	**KNO_3 [wt%]**	**VAAR [wt%]**
B_4C_1	10	83	7

Table 8. Content of formulations B_4C_2 and B_4C_3.

	B_4C [wt%]	**NH_4NO_3 [wt%]**	**ADN [wt%]**	**VAAR [wt%]**
B_4C_2	10	83	-	7
B_4C_3	7	-	90	3

Table 9. Color properties of formulation B_4C_1.

	burn time [s]	**Dw [nm]**	**Sp [%]**	**LI [cd]**	**LE [$cdsg^{-1}$]**
B_4C_1	6	560	69	25	250

Figure 3. Burn down of formulations B_4C_1 (left), B_4C_2 (middle) and B_4C_3 (right).

2.4.2 Formulations based on amorphous boron

Since the use of boron carbide with NH_4NO_3 or ADN did not achieve green flame colors with increased spectral purities, formulations were examined using amorphous boron instead of boron carbide, which is known to be a highly reactive fuel. Formulations combining ammonium nitrate and ammonium dinitramide (ADN) have been prepared and investigated. The content of formulations using NH_4NO_3 as oxidizer are shown in Table 10. The boron content ranges from 7% to 23% and the content of ammonium nitrate is between 70% and 85%. All compositions contain 7% of VAAR binder. All four formulations burn smokeless with a green flame color except composition B_2, which shows some smoke during the combustion. Solid residues remained after the burn down of all four formulations. Also in Table 10 the content of compositions using ADN as oxidizer is given. While formulations B_4 and B_5 contain 75% and 80% of ADN and 18% and 13% of boron, composition B_7 contains 58% ADN, 18% boron and additionally 17% of magnesium. All three formulations burned with an intensive green flame color. While B_5 burned smokeless, B_4 and B_7 showed some smoke during the combustion. No solid residues were observable for B_7, while after the burn down of B_4 and B_5 some residues remained (Figure 4).

Table 10. Content of formulations containing boron.

	B [wt%]	ADN [wt%]	NH_4NO_3 [wt%]	Mg [wt%]	VAAR [wt%]
B_1	13	-	80	-	7
B_2	23	-	70	-	7
B_3	8	-	85	-	7
B_4	18	75	-	-	7
B_5	13	80	-	-	7
B_6	7	-	80	6	7
B_7	18	58	-	17	7

The performance data of all formulations is provided in Table 11. The best performing formulation is B_7 revealing the highest spectral purity of 80% exceeding that of the barium control formulation and a luminous intensity of 320 cd which is comparable with that of the barium control (Table 2).

Table 11. Color properties of formulations containing boron.

	burn time [s]	Dw [nm]	Sp [%]	LI [cd]	LE [$cdsg^{-1}$]
B_1	6	562	40	32	320
B_2	7	562	59	23	268
B_3	14	555	60	24	560
B_4	4	563	63	19	127
B_5	4	567	68	21	140
B_6	7	569	78	196	2287
B_7	2	559	80	320	1067

In Table 12 the energetic and thermal properties of all formulations are summarized. Formulations containing NH_4NO_3 are impact and friction insensitive and show decomposition temperatures higher than 200 °C, whereas formulations using ADN are sensitive and exhibit lower decomposition temperatures.

Table 12. Energetic and thermal properties of formulations containing boron.

	Impact [J]	Friction [N]	grain size [µm]	T_{dec} [°C]
B_1	>40	>360	<100	295
B_2	>40	>360	<100	278
B_3	>40	>360	<100	296
B_4	10	60	<100	169
B_5	10	60	<100	184
B_6	30	>360	<100	220
B_7	10	324	<100	170

Figure 4. Burn down of formulations B_1, B_2, B_3, B_4, B_5, B_6 and B_7.

2.4.3 Formulations based on energetic dihydrobis(azolyl)borates

Although using boron, ADN and magnesium in pyrotechnic formulations brilliant green flame colors with spectral purities exceeding that of the barium control have been achieved, the sensitivities towards ignition stimuli were determined to be rather high. Formulations employing energetic nitrogen-rich azole borates instead of amorphous boron are considered to improve the combustion properties and the performance. Therefore, a series of formulations consisting of ADN or NH_4NO_3, magnesium and an azole borate instead of boron have been investigated. But also formulations employing additionally boron were examined and compared to those without boron. These results are presented in publications "*Green Colorants Based on Energetic Azole Borates*" and "*Pyrotechnical Formulations based on metal-free and nitrogen-rich dihydrobis(5-aminotetrazolyl)borates and dihydrobis(1,2,4-triazolyl)borates*". The best performing formulations are selected and depicted in Tables 13 and 16.

In Table 13 the content of formulations using guandinium dihydrobis(3,5-dinitropyrazolyl)borate ($GH_2B(DNP)_2$) is shown. As the oxidizers ammonium dinitramide and ammonium nitrate were used. All three formulations showed intensive green flame colors (Figure 5) and no smoke could be observed.

Table 13. Content of formulations using compound $GH_2B(DNP)_2$.

	$GH_2B(DNP)_2$ [wt%]	ADN [wt%]	NH_4NO_3 [wt%]	B [wt%]	Mg [wt%]	VAAR [wt%]
GBDNP_1	25	50	-	9	9	7
GBDNP_2	25	50	-	-	18	7
GBDNP_3	25	-	50	-	18	7

The performance values are summarized in Table 14. Formulation GBDNP_3 exhibits the highest spectral purity of 79% exceeding that of the barium control. However, the lowest luminous intensity was observed.

Table 14. Color properties of formulations containing compound $GH_2B(DNP)_2$.

	burn time [s]	Dw [nm]	Sp [%]	LI [cd]	LE [$cdsg^{-1}$]
GBDNP_1	1	554	75	180	300
GBDNP_2	4	571	72	210	1400
GBDNP_3	9	567	79	65	975

Except formulation GBDNP_1, which is impact sensitive, the other formulations are insensitive and show high decomposition temperatures (Table 15).

Table 15. Energetic and thermal properties of formulations containing compound $GH_2B(DNP)_2$.

	Impact [J]	Friction [N]	grain size [µm]	T_{dec} [°C]
GBDNP_1	5	324	<100	189
GBDNP_2	>40	>360	<100	180
GBDNP_3	>40	>360	<100	278

Figure 5. Burn down of formulations GBDNP_1, GBDNP_2 and GBDNP_3.

In order to figure out to what extent the azole borate compounds behaves differently in a pyrotechnic formulation and thus modify the combustion behavior, compositions containing different azole borate were investigated. Table 16 shows the content of formulations using guanidinium dihydrobis(5-aminotetrazolyl)borate ($GH_2B(5\text{-}At)_2$). The first two formulations contain amorphous boron, while formulations GB5At_3 and GB5At_4 contain boron carbide. All four formulations burned smokeless with a green flame color. The burn down is shown in Figure 6.

Table 16. Content of formulations using compound $GH_2B(5\text{-}At)_2$.

	$GH_2B(5\text{-}At)_2$ [wt%]	ADN [wt%]	NH_4NO_3 [wt%]	B [wt%]	B_4C [wt%]	Mg [wt%]	VAAR [wt%]
GB5At_1	10	60	-	15	-	10	5
GB5At_2	20	55	-	9	-	9	7
GB5At_3	15	60	-	-	12	8	5
GB5At_4	15	-	60	-	12	8	5

The performance properties are summarized in Table 17. Formulations GB5At_2 and GB5At_3 reveal higher spectral purities compared to the barium control formulation (Table 2). The lowest spectral purity was obtained when using NH_4NO_3 as the oxidizer.

Table 17. Color properties of formulations containing compound $GH_2B(5\text{-}At)_2$.

	burn time [s]	Dw [nm]	Sp [%]	LI [cd]	LE [cdsg^{-1}]
GB5At_1	4	565	70	51	340
GB5At_2	3	572	80	32	160
GB5At_3	3	562	85	76	380
GB5At_4	9	578	45	21	315

In Table 18 the energetic and thermal properties are gathered. It was observed that the combination of ADN and amorphous boron results high impact sensitivities, while the use of ADN and B_4C reveals lower impact sensitivity. The use of NH_4NO_3 results insensitivity.

Table 18. Energetic and thermal properties of formulations containing compound $GH_2B(5\text{-}At)_2$.

	Impact [J]	Friction [N]	grain size [µm]	T_{dec} [°C]
GB5At_1	1	>360	<100	156
GB5At_2	2	324	<100	164
GB5At_3	10	192	<100	179
GB5At_4	>40	>360	<100	201

Figure 6. Burn down of formulations GB5At_1, GB5At_2 and GB5At_3.

It has been shown, that there are significant differences in color performance, impact and friction sensitivity as well as decomposition temperatures when varying the borate compound and that metal-free and nitrogen-rich azolyl borate compounds are suitable substituents for barium compounds in green-burning pyrotechnics.

2.4.4 Formulations based on tris(2,2,2-trinitroethyl)borate (TNEB)

In literature [8] the synthesis and properties of tris(2,2,2-trinitroethyl)borate (TNEB) are reported. Since TNEB (Scheme 7) burns green and exhibits a good oxygen balance, its possible use as boron-based oxidizer in pyrotechnic formulations was investigated revealing good performance properties.

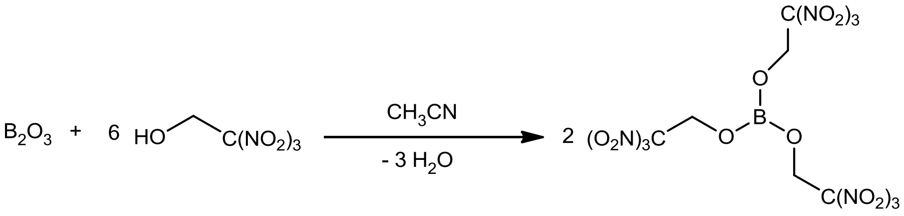

Scheme 7. Synthesis of tris(2,2,2-trinitroethyl)borate (TNEB).

In Table 19 the content of formulations employing TNEB as the oxidizer and coloring agent at the same time, boron carbide and magnesium is depicted. To avoid the hydrolysis of TNEB, and hence to ensure the stability of TNEB-containing formulations, paraffin was added to the formulations in lieu of a binder. Both formulations showed intensive green flame colors (Figure 7) and no smoke was produced during the combustion. The color properties as well as the energetic and thermal properties are summarized in Table 20.

Table 19. Content of TNEB-containing formulations.

	TNEB [wt%]	**B_4C [wt%]**	**Mg [wt%]**	**Paraffin [wt%]**
TNEB_1	75	10	8	7
TNEB_2	79	10	4	7

Table 20. Color, energetic and thermal properties of TNEB-containing formulations.

	burn time [s]	**Dw [nm]**	**Sp [%]**	**LI [cd]**	**LE [$cdsg^{-1}$]**	**Impact [J]**	**Friction [N]**	**grain size [µm]**	**T_{dec} [°C]**
TNEB_1	4	562	85	89	593	>40	>360	<100	168
TNEB_2	7	561	86	50	583	>40	>360	<100	170

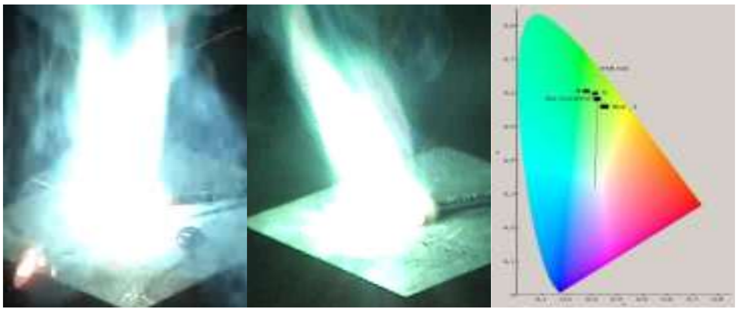

Figure 7. Burn down of formulations TNEB_1 (4) and TNEB_2 (5) and the corresponding CIE chromaticity diagram (TNEB_1 = 4 and TNEB_2 = 5).

Both formulations show high spectral purities of 85% and 86%, which exceed that of the barium control formulations as well as that of the B_4C_1 formulation (Table 9). They are insensitive and exhibit acceptable decomposition temperatures. Thus, green light of high performance and spectral purity can be obtained through the replacement of potassium nitrate with TNEB in the presence of boron carbide, magnesium and paraffin. The detailed investigations are presented in publication "*Improved green-burning formulations for pyrotechnics based on tris(2,2,2-trinitroethyl)borate*".

2.5 Formulations based on nitrogen-rich metal salts

The investigation of perchlorate-free formulations is performed as it is described in publication *"Metal Salts of Dinitro-, Trinitropyrazole and Trinitroimidazole"*. High-nitrogen compounds were used, resulting an ashless combustion, brilliant flame colors and higher spectral purities. In the case of the red-burning formulations one formulation without PVC was examined revealing the same performance like the formulation using PVC. The best-performing green- and red-burning formulations have been chosen and are described herein. These formulations contain Ba_1b or Sr_1b as colorants, ammonium nitrate as the oxidizer and magnesium as fuel. As binder VAAR was employed. Additionally, PVC was added as the chlorine donor. The formulations have been prepared and compared to the US Army´s in-service green (M125A1) and red (M126A1) formulations. Tables 21 and 22 summarize the content of the compositions.

Table 21. Content of formulations using compound Sr_1b.

	Sr_1b [wt%]	**Mg [wt%]**	**PVC [wt%]**	**VAAR [wt%]**
SrTNP_1	68	20	5	7
SrTNP_2	68	25	-	7

Both formulations SrTNP_1 and SrTNP_2 burned smokeless with a red flame color (Figure 8). The performance values are given in Table 23. Although formulation SrTNP_1 contains PVC, formulation SrTNP_2, which does not contain PVC shows a higher spectral purity. Both formulations exhibit the same luminous intensity. Formulation SrTNP_1, which is perchlorate-free and does not contain any other oxidizer as well as no PVC, reveals a higher spectral purity, a longer burn time and a higher impact sensitivity (Table 24) than the strontium control formulation (Table 5).

Table 22. Content of formulations using compound Ba_1b.

	Ba_1b [wt%]	**NH_4NO_3 [wt%]**	**Mg [wt%]**	**PVC [wt%]**	**VAAR [wt%]**
BaTNP_1	35	40	13	5	7
BaTNP_2	53	-	30	10	7
BaTNP_3	58	-	20	15	7

All three compositions BaTNP_1, BaTNP_2 and BaTNP_3 burn with a green flame color and no smoke was observed (Figure 8). Among the formulations containing compound Ba_1b, compositions BaTNP_2 and BaTNP_3, which do not contain NH_4NO_3 in addition, reveal higher spectral purities than that using ammonium nitrate (Table 23). Furthermore, formulations BaTNP_2 and BaTNP_3 show higher spectral purities, longer burn times and higher impact sensitivities than the barium control formulation. The luminous intensities and decomposition temperatures (Table 24) are comparable to that of the barium control (Table 2).

Table 23. Color properties of formulations containing compounds Sr_1b and Ba_1b.

	burn time [s]	Dw [nm]	Sp [wt%]	LI [cd]	LE [cdsg^{-1}]
SrTNP_1	8	608	89	390	5200
SrTNP_2	5	603	94	390	3250
BaTNP_1	3	552	66	169	845
BaTNP_2	6	558	80	359	3590
BaTNP_3	5	559	79	278	2317

Table 24. Energetic and thermal properties of formulations containing compounds Sr_1b and Ba_1b.

	Impact [J]	Friction [N]	grain size [µm]	T_{dec} [°C]
SrTNP_1	40	120	<100	201
SrTNP_2	40	180	<100	196
BaTNP_1	40	192	<100	165
BaTNP_2	40	>360	<100	210
BaTNP_3	35	360	<100	234

Figure 8. Burn down of formulations SrTNP_2 (left) and BaTNP_2 (right).

2.6 Blue-burning formulations based on copper iodate

The generation of blue-light-emitting pyrotechnic formulations based on copper iodate and without the use of chlorine-containing compounds is reported in publication "*Chlorine-Free Pyrotechnics: Copper(I) Iodide as a "Green" Blue-Light-Emitter*". Suitable blue-light-emission has been achieved through the generation of molecular emitting copper(I) iodide. The most optimal copper(I) iodide-based blue-light-emitting formulation was found to have performances exceeding those of chlorine-containing compositions, and was found to be insensitive to various ignition stimuli.

The best-performing formulations as well as Shimizu´s blue formulation[9], which was used as the control formulation are given in Tables 25 and 26.

Table 24. Shimizu´s chlorine-containing blue-light-emitting formulation.

	$KClO_4$ [wt%]	Cu [wt%]	PVC [wt%]	Starch [wt%]
Control	68	15	17	5

Table 25. Blue-burning formulations based on copper iodate.

	$Cu(IO_3)_2$ [wt%]	Guanidine nitrate [wt%]	Mg [wt%]	Urea [wt%]	Cu [wt%]	Epon 828/Epikure 3140 [wt%]
$Cu(IO_3)_2$_1	20	50	10	-	15	5
$Cu(IO_3)_2$_2	30	35	9	21	-	5

Both formulations contain copper iodate, guanidine nitrate and magnesium. While formulation $Cu(IO_3)_2$_1 contains copper, formulation $Cu(IO_3)_2$_2 comprises urea. The binder system Epon 828/Epikure 3140 is employed. Both formulations burned smokeless with a blue flame color (Figure 9). Table 26 shows the performance data of both copper iodate formulations as well as of the control formulation.

Table 26. Performance data of blue-burning formulations.

	burn time [s]	Dw [nm]	Sp [%]	LI [cd]	LE [cdsg^{-1}]	IS [J]	FS [N]	grain size [µm]	T_{dec} [°C]
Control	4	475 (552)	61	54	360	8	324	307	307
$Cu(IO_3)_2$_1	6	477 (555)	64	80	1067	> 40	> 360	< 100	198
$Cu(IO_3)_2$_2	6	476 (525)	63	78	780	> 40	> 360	< 100	180

Formulations $Cu(IO_3)_2$_1 and $Cu(IO_3)_2$_2 both have burn times, spectral purities, and luminosities in excess of the control (Table 26). Formulation $Cu(IO_3)_2$_1 is particularly noteworthy, as this formulation has a luminous intensity 33% brighter and a luminous efficiency value three times better then the control formulation. Moreover, formulations $Cu(IO_3)_2$_1 and $Cu(IO_3)_2$_2 were found to have very low impact and friction sensitivities, with reasonably high decomposition temperatures.

Figure 9. Burn down of formulations $Cu(IO_3)_2$_1 (left) and $Cu(IO_3)_2$_2 (right).

2.7 References

[1] Y. Zhang, Y. Guo, Y-H. Joo, D. A. Parrish, J. M. Shreeve, *Chem. Eur. J.* **2010**, *16*, 10778.

[2] H. Gao, C. Ye, O. D. Gupta, J.-C. Xiao, M. A. Hiskey, B. Twamley, J. M. Shreeve, *Chem. Eur. J.* **2007**, *13*, 3853.

[3] a) A. R. Katritzky, S. Singh, K. Kirichenko, M. Smiglak, J. D. Holbrey, W. M. Reichert, S. K. Spear, R. D. Rogers, *Chem. Eur. J.* **2006**, *12*, 4630; b) M. Smiglak, C. C. Hines, T. B. Wilson, S. Singh, A. S. Vincek, K. Kirichenko, A. R. Katritzky, R. D. Rogers, *Chem. Eur. J.* **2010**, *16*, 1572.

[4] T. M. Klapötke, M. Rusan, J. Stierstorfer, *Proceedings of the 38th International Pyrotechnic Seminars*, Denver, CO, **2012**, 527.

[5] a) C. Pettinari, *Scorpionates II: Chelating Borate Ligands, Dedicated to Swiatoslaw Trofimenko* Imperial College Press: London, **2008**; b) S. Trofimenko, Scorpionates: *The Coordination Chemistry of Poly(pyrazolyl)borate Ligands* Imperial College Press, London, **1999**; c) T. J. Groshens, *J. Coord. Chem.* **2010**, *63*, 1882; d) C. J. Snyder, P. D. Martin, M. J. Heeg, C. H. Winter, *Chem. Eur. J.* **2013**, *19*, 3306; e) M. Pellei, F. Benetollo, G. G. Lobbia, S. Alidori, C. Santini, *Inorg. Chem.* **2005**, *44*, 846; f) Z. Zeng, B. Twamley, J. M. Shreeve, *Organometallics* **2007**, *26*, 1782–1787.

[6] S. Trofimenko, *J. Am. Chem. Soc.* **1966**, *88*, 1842.

[7] J. J. Sabatini, J. C. Poret, R. N. Broad, *Angew. Chem. Int. Ed.* **2011**, *50*, 4624.

[8] T. M. Klapötke, B. Krumm, R. Moll, *Chem. Eur. J.* **2013**, *19*, 12113.

[9] T. Shimizu, *Pyrotechnica* **1980**, *6*, 5.

3 Appendix

The following appendix contains the list of publications, which are already published, in press or submitted during this dissertation. The publications are thematically listed. In the first part publications dealing with energetic boron-containing compounds and its investigations in pyrotechnic formulations are listed. The second part contains publications dealing with nitrogen-rich metal salts and its investigations in pyrotechnic compositions. In the last part formulations are listed investigating chlorine-free blue-burning formulations based on copper iodate.

1. Thomas M. Klapötke, Magdalena Rusan, Véronique Sproll, Preparation of Energetic Poly(azolyl)borates as New Environmentally Benign Green-Light-Emitting Species for Pyrotechnics, *Z. Anorg. Allg. Chem.* **2013**, *639*, (*14*), 2433-2443.

2. Thomas M. Klapötke, Magdalena Rusan, Véronique Sproll, Synthesis and Investigation of Energetic Boron Compounds for Pyrotechnics, *Z. Anorg. Allg. Chem.* **2014**, *640*, (*10*), 1892-1899.

3. Johann Glück, Thomas M. Klapötke, Magdalena Rusan, Jörg Stierstofer, Green Colorants Based on Energetic Azole Borates, *Chem Eur. J.* **2014**, *20*, 15947-15960.

4. Thomas M. Klapötke, Magdalena Rusan, Véronique Sproll, Jörg Stierstorfer, Energetic Materials Based on Azole Borates, *39th International Pyrotechnics Seminar*, Proceedings, Valencia, Spain, May 27-31. **2013**, 1-7.

5. Thomas M. Klapötke, Magdalena Rusan, Jörg Stierstofer, Pyrotechnic formulations based on metal-free and nitrogen-rich dihydrobis(5-aminotetrazoyl)borates and dihydrobis(1,2,4-triazolyl)borates, *J. Pyrotech.* **2014**, in press.

6. Thomas M. Klapötke, Burkhard Krumm, Magdalena Rusan, Jesse J. Sabatini, Improved green-burning formulations for pyrotechnics based on tris(2,2,2-trinitroethyl)borate, *Chem. Commun.* **2014**, *50*, 9581-9583.

7. Thomas M. Klapötke, Magdalena Rusan, The synthesis and characterization of nitrooxy- and nitrosooxyborazine compounds, *Z. Naturforsch.* **2014**, *69b*, 1241-1247.

8. Thomas M. Klapötke, Magdalena Rusan, Jörg Stierstorfer, The Synthesis and Investigation of Nitrogen-rich and Boron-based Compounds as Coloring Agents in Pyrotechnics, *38th International Pyrotechnics Seminar*, Proceedings, Denver, Colorado, USA, June 10-15, **2012**, 527-550.

9. Thomas M. Klapötke, Thomas G. Müller, Magdalena Rusan, Jörg Stierstofer, Metal Salts of 4,5-Dinitro-1,3-imidazole as Colorants in Pyrotechnic Compositions, *Z. Anorg. Allg. Chem.* **2014**, *640*, (*7*), 1347-1354.

10. Thomas M. Klapötke, Thomas G. Müller, Magdalena Rusan, The Synthesis and Characterization of 4,5-Dinitroimidazolate Salts, *New Trends in Research of Energetic Materials*, 14th, Pardubice, Czech Republic, Apr. 13– 15, **2011**, 729-741.

11. Ines E. Drukenmüller, Thomas M. Klapötke, Yvonne Morgenstern, Magdalena Rusan, Jörg Stierstorfer, Metal Salts of Dinitro-, Trinitropyrazole and Trinitroimidazole, *Z. Anorg. Allg. Chem.* **2014**, *640*, (*11*), 2139-2148.

12. Niko Fischer, Thomas M. Klapötke, Kristina Peters, Magdalena Rusan, Jörg Stierstorfer, Alkaline Earth Metal Salts of 5,5´-Bistetrazole – from Academical Interest to Practical Application, *Z. Anorg. Allg. Chem.* **2011**, *637*, 1693-1701.

13. Niko Fischer, Thomas M. Klapötke, Stefan Marcher, Magdalena Rusan, Susanne Scheutzow, Jörg Stierstorfer, A Selection of Alkali and Alkaline Earth Metal Salts of 5,5’-Bis(1-hydroxytetrazole) in Pyrotechnic Compositions, *Propellants Explos. Pyrotech.* **2013**, *35*, 1-12.

14. Thomas M. Klapötke, Magdalena Rusan, Jesse J. Sabatini, Chlorine-Free Pyrotechnics: Copper(I) Iodide as a “Green” Blue-Light-Emitter, *Angew. Chem. Int. Ed.* **2014**, *53*, 9665-9668.

15. Thomas M. Klapötke, Burkhard Krumm, Magdalena Rusan, Jesse J. Sabatini, The investigation of copper iodate and tris(2,2,2-trinitroethyl)borate in pyrotechnical formulations, *40th International Pyrotechnics Seminar,* Proceedings, Colorado Springs, Colorado, USA, **2014**, 15-27.

DOI: 10.1002/zaac.201300259

Preparation of Energetic Poly(azolyl)borates as New Environmentally Benign Green-Light-Emitting Species for Pyrotechnics

Thomas M. Klapötke,*[a] Magdalena Rusan,[a] and Véronique Sproll[a]

Dedicated to Professor Bernt Krebs on the Occasion of His 75th Birthday

Keywords: Poly(azolyl)borates; Pyrotechnics; Borates; Nitrogen-rich compounds; Energetic materials

Abstract. Three different energetic poly(azolyl)borates, potassium dihydridobis(4-nitroimidazolyl)borate, sodium dihydridobis(4,5-dinitroimidazolyl)borate, and sodium dihydridobis(3,4,5-trinitropyrazolyl)borate, were synthesized as starting materials for metal-free environmentally benign green-light-emitting substitutes for barium salts in pyrotechnical mixtures. The compounds were analyzed by NMR and Raman spectroscopy and high mass resolution spectrometry. Moreover, the energetic properties regarding physical and thermal stability were determined. The ^{11}B NMR chemical shifts were calculated and compared to the experimental values and intense investigations on the formation of poly(4-nitroimidazolyl)borates were performed. Furthermore, the solvolytic stability towards alcohol and water was tested.

Introduction

Fireworks, though spectacular and entertaining, come with a gammy leg. Due to their vast sphere of action, aerial fireworks and pyrotechnics are also great environmental polluters, which disperse several hazardous substances over a large area.[1,2] These toxic compounds are released upon explosion, deflagration, or burning of the pyrotechnics, including both reaction products and unburned constituents of a pyrotechnic mixture.[3] In recent years, the number of scientific articles focusing on environmental analysis and development of new energetic compounds increases (see, for example Refs.[1,2,4–6]) thereby emphasizing the importance of this topic.

One of the major toxic components of pyrotechnics form the coloring heavy metals, leading to the emission of heavy metal aerosols.[7] A comprehensive investigation of those aerosols for Beijing in the night of the annual "festival of rows of light" (Diwali festival, a five days remaining celebration traditionally accompanied by fireworks and firecrackers[8]) showed not only a dramatic increase in concentration for sulfur dioxide, nitrogen dioxide and PM_{10}[9] (increase of 57 %, 25 % and 183 %, respectively) but also for toxic metals as barium, lead, copper, aluminum, manganese, and strontium (increase of 8200 %, 800 %, 600 %, 600 %, and 400 %, respectively).[10] Beside lead aerosols, especially the emission of soluble barium salts and aerosols is a cause of concern due to their toxicity.[1,2,7d,11] Regarding an exposure caused by the usage of fireworks, *Kulshrestra* et al.[11] found the barium concentrations in air increased by more than a factor of 1000 in the course of one excessive night of fireworks compared to the usual background. Thus, in terms of green chemistry, the barium nitrate content makes the green-luminescent pyrotechnics the "dirtiest bombs of all".[1]

An alternative is offered by the usage of boron based formulations as barium substitutes for pyrotechnic compositions.[12–14] Most of the boron compounds currently tested have in common that they do not possess any energetic character. Especially with regard to the formulation of highly efficient colorful pyrotechnics, it is of interest to combine the energetic properties with the coloring agent in the same molecule. Therefore, it is essential to create new energetic boron compounds, which could reduce the amount of different additives of pyrotechnics as well as the weight due to a better performance than the currently tested compositions. Among the possible energetic boron compounds nitrogen-rich heterocycles combine both thermal and physical stability and are therefore worthwhile targets for the development of new coloring agents. Through the last decades a variety of poly(azolyl)borates have been reported and become increasingly important, especially as so called scorpionate ligands.[15] Particularly, pyrazolylborates display a versatile class of monoanionic, nitrogen-based and multidentate ligands in coordination, organometallic and bioinorganic chemistry.[15,16,17] Another area of application opens when the relatively unenergetic heterocycle pyrazole gets substituted by triazoles or tetrazoles. For the latter, the Naval Air Warfare Center studied, for example, the transition metal complexes of dihydridobis(5-aminotetrazolyl)borate as potential propellant ingredients containing both metal and boron centers might act as burn rate modifiers.[18] Another interesting example for tetrazole containing poly(azolyl)borates was synthesized recently by *Winter* et al.[19]

---

* Prof. Dr. T. M. Klapötke
Fax: +49-89-2180-77492
E-Mail: tmk@cup.uni-muenchen.de
[a] Department of Chemistry
Energetic Materials Research
Ludwig-Maximilian University
Butenandtstr. 5–13 (D)
81377 München, Germany

Commonly, *Trofimenko*[20] is referred to as the father of poly(azolyl)borate chemistry, especially regarding tetrakis(azolyl)borates. Though *Sazanova* et al.[21] reported the synthesis of potassium tetrakis(pyrrolyl)borate already in 1955, it has been *Trofimenko*[20,22] who provided a synthetic route to afford tetrakis(azolyl)borates in good yields. His thermolytic approach has been applied to most of the known poly(azolyl)borates bearing insensitive groups as alkyl- or aryl-substituents, which are typically synthesized at high temperature using a mixture of the corresponding azole and alkali metal borohydride (e.g. literature[15,17b,17c,17d,17s,20,22]).

In order to increase the energetic character of the borate, nitrated azoles are used in this work. To date only a small number of nitrated poly(azolyl)borates is known. Some examples are given in Figure 1.

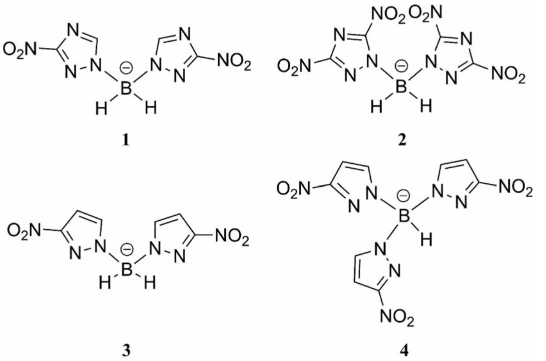

Figure 1. Dihydridobis(3-nitro-1,2,4-triazolyl)borate (**1**),[23] dihydridobis(3,5-dinitro-1,2,4-triazolyl)borate (**2**),[24] dihydridobis (3-nitropyrazolyl)borate (**3**),[25] and hydridotris(3-nitropyrazolyl) borate (**3**)[26] anions.

In this work poly(azolyl)borates of potassium and sodium are synthesized. For further application in pyrotechnic compositions and to further improve the properties, the herein developed compounds will be transformed into nitrogen-rich salts by salt metathesis reactions as shown in Scheme 1. The metal-free salts are generally known to show a more brilliant green color performance and will then be tested for pyrotechnic mixtures.

Results and Discussion

Tetrakis(imidazolyl)borates[27] as well as tris(imidazolyl)borates[28] have been of interest in the construction of new metal-organic framework structures. Nevertheless, to the best of our knowledge there have been no substituted imidazole derivatives reported, especially with regards to the more energetic nitrated compounds. Therefore, it has been of interest to study the properties of the nitrated derivatives as energetic materials.

I. Poly(4-nitroimidazolyl)borates

4-Nitroimidazole (**5**) is commercially available and provided therefore an easily accessible starting material in order to study different reaction conditions for nitrated imidazoles and potassium borohydride (Scheme 2). On the other hand, the extremely low solubility of this compound in common organic solvents limited the possible synthetic routes. Nevertheless, different solvents, stoichiometry, concentrations and temperatures were tested.

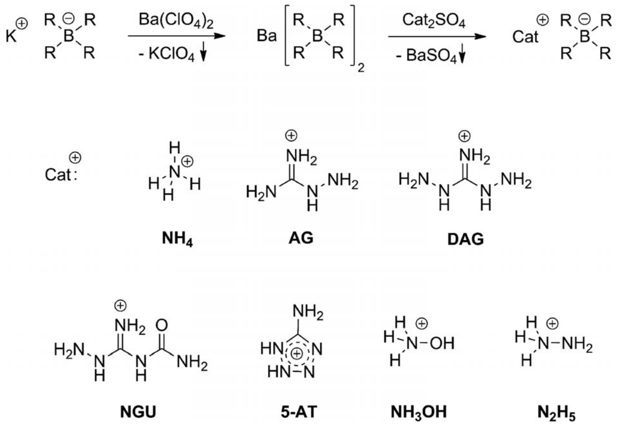

Scheme 1. Schematic metathesis reaction to yield nitrogen-rich, metal-free salts.

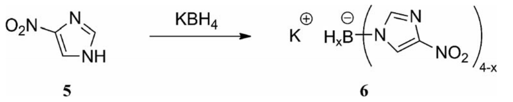

Scheme 2. General reaction scheme for potassium poly(4-nitroimidazolyl)borates (**6**).

The first choice was to go for mild conditions. The reaction of the azole ring and potassium borohydride can be understood as some kind of acid-base reaction with the evolving hydrogen as driving force. Having an electron-withdrawing group attached to the imidazole moiety, it was expected to have a more acidic and therefore mildly activated system where, at least for bissubstitution, relatively low temperatures should be sufficient.

Synthesis of Potassium Dihydridobis(4-nitroimidazolyl)borate (8)

Acetonitrile was chosen as solvent owing to its b.p. of 82 °C and thus also easy removability afterwards as well as its polar character. In order to obtain potassium dihydridobis(4-nitroimidazolyl)borate (**8**), **5** was reacted with potassium borohydride in freshly distilled acetonitrile at reflux conditions (Scheme 3). Immediate gas evolution was observed after adding **5** to the suspension of potassium borohydride in acetonitrile even at room temperature. During the reaction, the suspension discolored and turned from colorless over beige-brown to completely black.

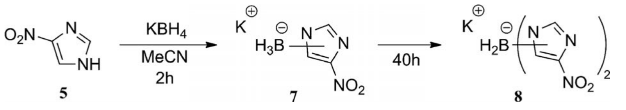

Scheme 3. Synthesis of **8**.

The reaction procedure was monitored by ^{11}B NMR (Figure 2). After 3.5 h the obtained data showed already a complete consumption of potassium borohydride (–38 to –43 ppm) and the formation of two new compounds with signals at –20.1 ppm and –9.8 ppm. Earlier observations on this topic as well as consulted literature[18,29–32] allowed an assignment of these signals to the monosubstituted (–20.1 ppm) and bissubstituted (–9.8 ppm) borate. This first assignment was affirmed by the proton coupled ^{11}B NMR spectra, which showed the expected multiplets, a quartet ($^1J_{B–H}$ = 89 Hz) at –20.1 ppm and a triplet ($^1J_{B–H}$ = 100 Hz) at –9.8 ppm (Figure 2) as well as by calculations (see Table 2).

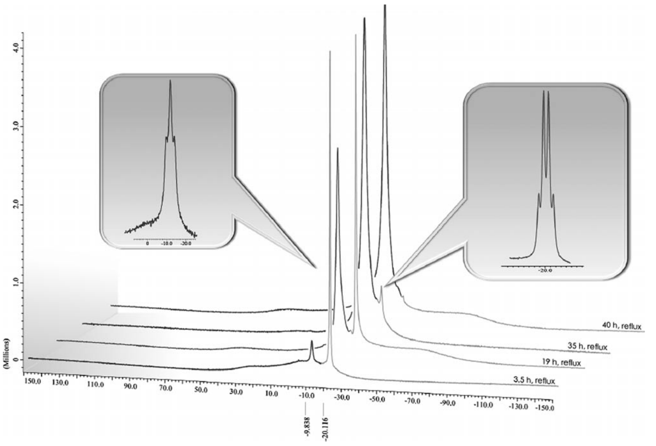

Figure 2. Monitored reaction procedure by $^{11}B\{H\}$ NMR measurements. Due to a better clarity the left part of the spectra with the growing signal at –9.8 ppm (product signal, **8**) was darker colored than the right handed one with the decreasing signal at –20.1 ppm (**7**). The corresponding reaction times are listed at the right edge of the respective spectrum. (solvent: non-deuterated MeCN).

During the reaction procedure further ^{11}B NMR spectra were measured, which show the continuous decline of the signal of trihydridomono(4-nitroimidazolyl)borate (**7**) in favor of the signal of (the higher substituted) compound **8** until after 40 h under reflux conditions the reaction was completed and only the signal of **8** was visible in the NMR spectrum.

To isolate **8** the reaction mixture was simply diluted with further freshly distilled acetonitrile and the insoluble mixture of remaining starting material and impurities was filtered off. Compound **8** was obtained after removal of the solvent as beige solid with a yield of 80 %. The applied procedure captivates with its simplicity and easy work up. This pathway can be easily upscaled and opens access to a possible industrial application of this compound.

Characterization

The product was fully characterized by ^1H, ^{13}C, and ^{11}B NMR as well as elemental analysis, Raman spectroscopy, and high resolution mass spectrometry ($[C_6H_6O_4N_6B]^-$ calcd.: 237.0545; found: 237.0530).

The Raman spectrum exhibits bands attributable to the boron-hydrogen stretching vibration at 2409 cm^{-1}, which is similar to values in complexes containing bis(pyrazolyl)borate ligands[33] or hydridopoly(azolyl)borates in general.[22,24,25,29,34,35] In the region between 3141 cm^{-1} and 3084 cm^{-1} the C–H stretching vibration of the nitroimidazole moiety is clearly visible, as well as the NO_2 asymmetric and symmetric valence vibrations found in the range between 1490–1545 cm^{-1} and 1315–1375 cm^{-1}, respectively.[25,26,34,35] As expected from the obtained NMR spectroscopic data no traces of boric acid can be found.

Due to the asymmetric character of **5** with its two feasible bonding positions for boron (N1 and N3), the formation of three isomeric compounds was regarded possible (Figure 3).

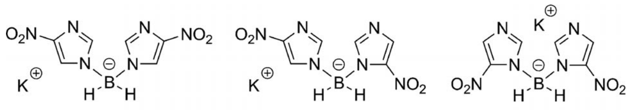

8 a **8 b** **8 c**

Figure 3. Illustration of the isomeric compounds of **8** due to B–N bonding via position 1 (**8a**), position 3 (**8c**), or 1 and 3 (**8b**).

This assumption was corroborated by NMR spectroscopic data. Though there is only one boron signal in the ^{11}B NMR at –10.7 ppm (in [D$_6$]DMSO), there are, despite of the mentioned three possible structures, only two sets of ligand-signals to be found in the ^1H NMR and ^{13}C NMR spectra. These sets can probably be explained by N1 and N3 bound imidazole rings.

The main compound is most reasonably **8a** due to the crystal structure of **5** with the proton bound to N1 and a possible steric repulsion by the nitro group.[36,37] It shows proton shifts in [D$_6$]DMSO at δ = 8.01 ppm (5-C*H*) and 7.50 ppm (2-C*H*)[37] and a broad signal of the BH_2 group centered at δ = 3.30 ppm. It was possible to extract the boron hydrogen coupling and thereby assign this signal unambiguously to the BH_2 group (Figure 4). This was achieved by a measurement at elevated temperature (85 °C) as under these conditions the quadrupole relaxation of the boron core is minored.

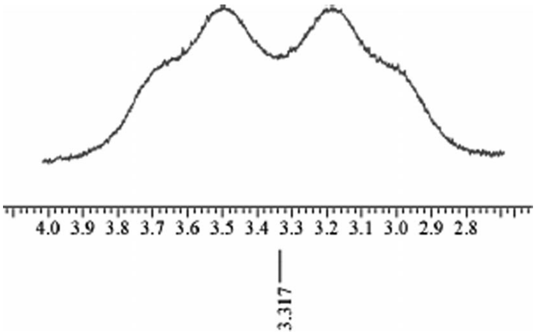

Figure 4. Extract of the ^1H NMR spectrum in [D$_6$]DMSO to visualize the quartet splitting of the BH_2 group ($^1J_{B–H}$ = 123 Hz, *T* = 85 °C).

The ^{13}C NMR signals are located at δ = 148.1 ppm (4-*C*–NO_2), 141.1 ppm and 124.9 ppm and thereby show, as expected when bound to boron, a clear downfield shift compared to the signals of **5** (δ =147.6 ppm, 135.9 ppm and 119.0 ppm).

The second compound is slightly downfield shifted compared to the first one with signals at δ = 8.05 ppm (5-C*H*), 7.52 ppm (2-C*H*)[38] and a very broad one for the corresponding BH_2 group centered around 6.30 ppm (T = 85 °C). The relatively large difference in the chemical shifts of the two BH_2 groups can be rationalized by a possible intramolecular hydrogen bonding between the BH_2 protons and the adjacent nitro group (Figure 5). The assumption of an intramolecular interaction is also supported by a possible formation of the favored structural motif of a six-membered ring as shown in Figure 5. The ^{13}C NMR chemical shifts of 4-*C*–NO_2, 2- and 3-*C*H carbon atoms appear at δ = 147.9 ppm, 140.5 ppm, and 124.8 ppm, respectively.

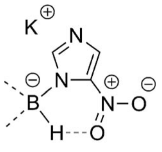

8 b/c

Figure 5. Schematic view of possible intramolecular hydrogen bonding for compound **8b/c**.

Whether all three isomers are present or only two isomers were formed cannot be clearly determined by the obtained analytical data. As the proton shifts of the BH_2 fragment display the greatest sensitivity towards isomeric structure, three different signals for this group would be expected. Whereas the NMR spectrum at 25 °C only shows one signal for a BH_2 group (δ = 3.3 ppm), the signal of the second BH_2 group at 6.3 ppm slowly appears with rising temperature until the spectrum at 65 °C clearly shows the second BH_2 group. The question, whether all three isomers were formed and the NMR shifts of the protons of imidazole rings are independent from the bonding situation of the second imidazole moiety at the boron atom, along with a still missing third BH_2 group that could appear at even higher temperatures, or only two isomers were formed could currently not be solved.

Regarding an ensuing investigation and possible application in pyrotechnical mixtures the insensitive character of compound **8** was confirmed according to BAM standards:[39] impact sensitivity ≥ 40 J, friction sensitivity ≥ 360 N and ESD ≥ 0.85 J. The decomposition point was found to be at 189 °C.

Investigation of Reaction Conditions in Search for a Higher Substitution

As previously mentioned, different reaction conditions were investigated especially with a regard to possible higher substitution of the poly(4-nitroimidazolyl)borate (**6**). Some of these conditions are compiled in Table 1. For the bissubstituted compound **8** a higher dilution deteriorates the reaction conditions and leads to a prolonged reaction time that could not be counteracted by the usage of 4.5 equivalents instead of 2 equivalents 4-nitroimidazole (Table 1, entry 1 and 2).

Concerning a higher substitution, high-boiling solvents as diglyme (b.p. 162 °C) and benzonitrile (b.p. 191 °C) were investigated. These solvents showed at elevated temperatures a rising solubility towards **5**, which was expected to facilitate the reaction. However, reactions in these solvents showed right from the beginning the formation of several different boron compounds.

The reaction of 3 equiv. **5** at 103 °C (Table 1, entry 3) did only yield the bissubstituted compound **8** contaminated with minor signals at 0.9 ppm and 5.3 ppm (^{11}B NMR spectra recorded of the reaction mixture). Even a prolonged reaction time and an increase of temperature (22.5 h, 121 °C and 4 h, 200 °C) did not change the signal ratio and proved therefore these conditions not to be sufficient for a higher substitution.

Due to these results, the reaction was tried with a great excess of **5** in diglyme (Table 1, entry 4) and the temperature was raised to 156 °C right from the beginning. This led to a significantly shortened formation time of compound **8** (–10.4 ppm), which was after 1 h already completed but again also accompanied by the formation of side-products (δ = 0.3 ppm, 4.7 ppm). After 26.75 h the signal of **8** was strongly diminished in favor of the signal at 1.2 ppm whereas the intensity of the third signal (δ = 5.3 ppm) remained the same. With

Table 1. Different reaction conditions for the 4-nitroimidazole (**5**) / potassium borohydride system.

Entry	Stoichiometry **5**:KBH_4	Solvent	Temperature /°C	Concentration mmol(**5**):mL(solvent)	Reaction time /h	δ $^{11}B^{a)}$ /ppm
1	2:1	MeCN	reflux (ca. 90)	0.918	40	–9.84
2	4.5:1	MeCN	reflux (ca. 90)	0.575	164	–10.0
3	3:1	diglyme	103	0.463	20	–10.0 (5.3; 0.9)
4	8:1	diglyme	156	1.405	1	–10.4 (0.3; 4.7)
					26.75	1.2 (–9.2; 5.3)
					45	1.1 (–4.4; 5.2; 7.6)
5	5:1	benzonitrile	163	0.451	5	–10.1
					19.5	–10.1
			187	0.451	9	–9.7 (–4.6)
			reflux (ca. 195)	0.451	15	–4.2
					38	dec.

a) Shifts given in parentheses are minor impurities.

regards to the ^{11}B NMR shifts of other tetrakis(azolyl)borates[40,41] the signal at 1.2 ppm can reasonably be assigned to the tetrakisubstituted compound, in this case tetrakis(4-nitroimidazolyl)borate (**9**) (see also Table 2 for calculations of the NMR chemical shifts). During this reaction the trissubstituted intermediate was not observed.

A further reaction attempt was conducted in benzonitrile, using an excess of **5** (Table 1, entry 5). The reaction mixture was heated to 163 °C, during which time it discolored. Starting from a colorless suspension it turned over a yellow-brown solution with white solid to completely black. After 5 h compound **8** was exclusively formed and remained the only signal in the recorded ^{11}B NMR spectra until the temperature was raised to 187 °C. After 9 h at this temperature a second signal at –4.1 ppm emerged (together with a minor impurity at 0.7 ppm). This signal (most probably assignable to hydridotris(4-nitroimidazolyl)borate **10**, for calculations see also Table 2) was afforded as single boron compound by a further raise of temperature (15 h, 195 °C), yet maintenance of this temperature did not lead to the formation of a higher substituted compound but to complete decomposition.

Investigation of Solvolytic Stability

Sodium tetrakis(imidazolyl)borate is set to be completely stable towards hydrolyses as it was even investigated as gravimetric reagent for proton.[42] Nevertheless, it is commonly known that the general stability of these complexes decrease with the increase of hydrogen atoms attached to the central boron atom.[22]

In order to investigate the stability of **8** towards solvolysis by alcohols, experiments with deuterated methanol were carried out in the scale of NMR-tubes. The results show the rather high stability of **8** against solvolysis in methanol solution. Even after keeping **8** in the system methanol/acetonitrile (0.6:1.0) for 2 d only a slight decomposition could be observed [decomposition product: 11.6 (0.13) ppm; product signal: –9.7 (1.00) ppm].

Carrying out the same experiment in the mixture of methanol/diglyme/DMSO (0.4:0.6:0.2) a faster hydrolysis of **8** [signal at –9.8 (1.00) ppm, decomposition product: 16.6 (1.11) ppm, after 1 d] was observed.

The investigation of the stability of the main compound of entry 4 in Table 1 (shift at 1.2 ppm) under the same conditions showed a much higher sensitivity against solvolysis of this compound. After keeping the compound in the methanol solution for 1 d, the chemical shift at 1.2 ppm nearly disappeared completely and a new signal at δ = 15.2 ppm, probably trimethyl borate, rose as main compound.

II. Poly(4,5-dinitroimidazolyl)borates

*Synthesis of Sodium Dihydridobis(4,5-dinitroimidazolyl)borate (**12**)*

In order to further increase the energetic character the nitration level of the borate was enhanced. Therefore, **5** was further nitrated according to a procedure devised by *Katritzky* et al.[43] to afford 4,5-dinitroimidazole (**11**). Regarding the higher activation due to the presence of two nitro moieties as well as the related possible lower decomposition temperatures, a non-thermolytic approach was chosen to afford the bissubstituted borate. It was expected, that when in solution, the dinitrated imidazole would react with sodium borohydride even at room temperature (Scheme 4). In the first approach a slight excess of **11** was used, but proved difficult to be removed afterwards. Therefore, the reaction was conducted stoichiometric, which led to a prolonged reaction time at ambient temperature. This can be overcome by mildly heating to 45–50 °C.

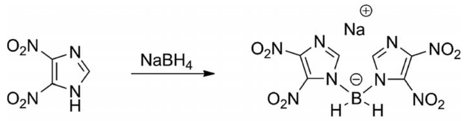

11 **12**

Scheme 4. Synthesis of **12**.

The reaction procedure was monitored by ^{11}B NMR measurements of the crude reaction mixture and showed a smooth transition from the initially formed monosubstituted compound (with a signal at –21.3 ppm, q, $^1J_{B-H}$ = 102 Hz) to the bissubstituted **12** (–11.3 ppm, t, $^1J_{B-H}$ = 102 Hz) (Figure 6).

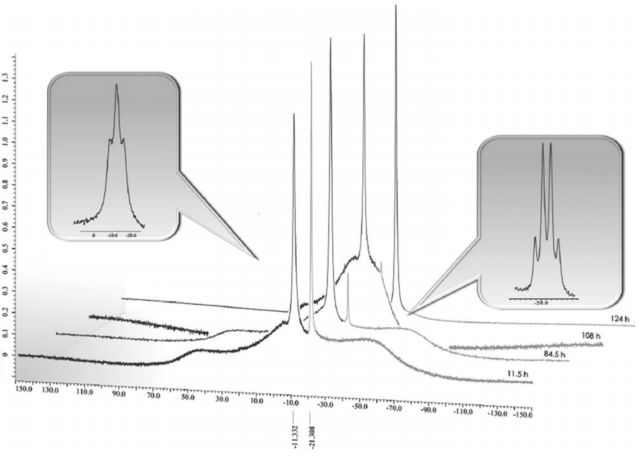

Figure 6. Monitored reaction procedure by ^{11}B{H} ^{nmr} measurements. Due to a better clarity the left part of the spectra with the growing signal at –11.3 ppm (product signal, **12**) was darker colored than the right handed one with the decreasing signal at –21.3 ppm (intermediate product). The corresponding reaction times are listed at the right edge of the respective spectrum. (solvent: undeuterated MeCN).

After removal of the solvent, compound **12** was obtained as pale yellow solid in almost quantitative yield. Despite drying under high vacuum at elevated temperature, a small amount of acetonitrile remained in the solid product. It was assumed that the acetonitrile is part of the solid structure.

Characterization

The product was fully characterized by ^{1}H, ^{13}C, ^{14}N, and ^{11}B NMR as well as elemental analysis, vibrational spec-

Dedicated Cluster

troscopy, and high resolution mass spectrometry ($[C_6H_4O_8N_8B]^-$ calcd.: 327.0246; found: 327.0254).

The Raman spectrum shows the clear evidence of the BH_2 fragment by exhibiting a band at 2449 cm^{-1} which is characteristic for boron–hydrogen stretching vibrations in comparable complexes.[22,24,25,29,33–35] At 3140 cm^{-1} the band corresponding to the C–H stretching vibration of the imidazole moiety is visible as well as the NO_2 asymmetric and symmetric valence vibrations found in the range between 1490–1564 cm^{-1} and 1301–1375 cm^{-1}, respectively.[25,26,34,35] As already mentioned, small residues of acetonitrile remained in the solid product and the corresponding bands are displayed in the Raman spectrum [pure acetonitrile: 2943 (100), 2253 (73), 921 (26), 382 (20) cm^{-1};[44] acetonitrile residues: 2944 (10), 2266 (4), 955 (3), 388 (2) cm^{-1}]. As expected from the obtained NMR spectroscopic data no traces of boric acid can be found.

The ^1H NMR chemical shift of the 2-C*H* protons (in CD_3CN solution) is observed at δ = 7.40 ppm and the BH_2 protons appear as a broad signal at δ = 3.29 ppm, while the ^{13}C chemical shifts of 2-*C*H and 4/5-*C*–NO_2 carbon atoms are at δ = 139.6 ppm and 138.7 ppm. ^{14}N NMR shows the signal of the imidazolyl moiety at a shift of –185.3 ppm and the signals of the two nitro groups at a shift of –17.3 ppm and –20.6 ppm. In the ^{11}B NMR spectrum the signal appears at a shift of –12.2 ppm with a coupling constant *J*(B–H) between the boron and the hydrogen atoms of 98 Hz.

NMR spectroscopic data of compound **12** was also measured in deuterated acetone with the only major difference that the protons of the BH_2 fragment spread over the range of 1.39 ppm (3.89–2.50 ppm).

Regarding an ensuing investigation and possible application in pyrotechnical mixtures the sensitivities of compound **12** were determined according to BAM standards:[39] impact sensitivity ≥ 10 J and friction sensitivity ≥ 240 N. These results show that compound **12** is, in contrast to the complete insensitive compound **8**, sensitive towards impact and friction. This behavior of **12** is in accordance with the expected tendency that more nitro groups at the imidazole ring will lead to a higher energetic character along with a higher sensitivity. This trend is also supported by the drop of the decomposition point from 189 °C (**8**) to 127 °C of compound **12**.

Investigation of Solvolytic Stability of Compound 12

Experiments regarding the stability of **12** towards solvolysis were conducted in aqueous and methanol solutions. In the system water/acetone (0.6:1.0) compound **12** showed only a minor decomposition to boric acid [boric acid signal: 18.5 (0.085) ppm; product signal: –12.5 (1.00) ppm] after 2 h. The intensities of the boric acid were corrected by the intensity of the signal of boric acid resulting from hydrolysis by the water impurities of deuterated acetone (measured after several days of storage in deuterated acetone).

In the system methanol/acetonitrile (0.6:1.0) compound **12** has a comparable sensitivity towards solvolysis. After 3.5 h the decomposition signal (δ = 17.9 ppm) showed an intensity of 0.19 compared to the signal of **12** at –11.9 ppm (1.00). These results point out that compound **12** is mostly stable towards hydrolysis. Nevertheless, longer times of storage in aqueous solution will lead to a degradation of the compound.

In conclusion, the novel borate **12** is a pale yellow solid, soluble in water, methanol, DMSO, acetonitrile, and THF. It can be kept in aqueous and methanol solutions without significant hydrolysis to boronic acids and trimethyl borate, respectively. Moreover, the synthesis was optimized and could be upscaled without further problems.

III. Poly(3,4,5-trinitropyrazolyl)borates

Among the numerous known poly(azolyl)borates the group of pyrazole based borates display the greatest variety. Though, electron withdrawing substituents on the pyrazolyl moiety are relatively less common compared to the scorpionate ligands with electron donating substituents like methyl or *iso*propyl on the pyrazolyl rings.[16] The groups of *Santini* and *Dias* reported a view of these rare compounds, e.g. trihydrido(5-CF_3-pyrazolyl) borate as well as the mono-, bis-, and tris-substituted 3-nitropyrazolyl-borates.[17b,25,45]

Synthesis of Sodium Dihydridobis(3,4,5-trinitropyrazolyl)-borate (14)

2,4,5-Trinitropyrazole (**13**) was synthesized via a multi-step reaction sequence of nitrations and ensuing rearrangements starting from commercially available 1*H*-pyrazol. After the experiences with **12** similar mild reaction conditions were chosen for the synthesis of sodium dihydridobis(3,4,5-trinitropyrazolyl)borate (**14**) (Scheme 5). As the trinitrated pyrazole is well soluble in organic solvents the reaction was performed in freshly distilled diethyl ether at ambient temperature.

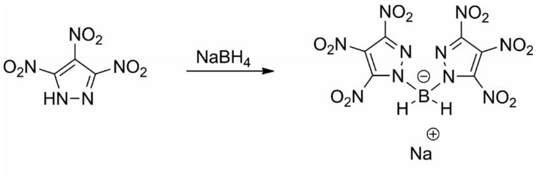

13 **14**

Scheme 5. Synthesis of **14**.

An excess of **13** was reacted with sodium borohydride for 16 h, during which time a pale yellow precipitate was formed. The reaction solid was filtered off and washed with diethyl ether to obtain **14** in a good yield of 83 %.

Characterization

The product was fully characterized by ^1H, ^{13}C, ^{14}N, and ^{11}B NMR as well as elemental analysis, vibrational spectroscopy, and high resolution mass spectrometry ($[C_6H_2O_{12}N_{10}B]^-$ calcd.: 416.9948; found: 416.9916).

The Raman spectrum shows the clear evidence of the BH_2 fragment by exhibiting a band at 2476 cm^{-1} which is characteristic for boron-hydrogen stretching vibrations in comparable complexes.[22,24,25,29,33–35] The asymmetric and symmetric valence vibrations of the NO_2 group appear at 1567 cm^{-1} and 1408 cm^{-1}, respectively, in accordance with the values generally found for polynitropyrazolyl moieties.[46,47]

Furthermore, small diethyl ether residues remained in the solid product and the typical "triplet" centered at 2945 cm^{-1} can be found in the Raman spectrum. These small residues can be reduced by prolonged storage under high vacuum at elevated temperature of 75–80 °C. However, these diethyl ether residues are assumed to stabilize the structure of compound **14** as after removal some kind of decomposition is detected in NMR spectroscopic data. This decomposition led not only to the formation of some boric acid or presumably triethyl borate when resolved in deuterated acetone or acetonitrile (signal at δ = 18.5 ppm and 18.6 ppm, respectively) but also to the formation of a second set of signals for the ethoxy moiety in the ^1H NMR (4.70, 1.54 ppm, diethyl ether, 3.45, 1.14 ppm, CD_3CN).

The ^1H chemical shift of the BH_2 group was observed at δ = 3.80 ppm as broad signal (in CD_3CN solution). In addition, the ^{13}C spectrum of **14** showed two signals for the C–NO_2 carbon atoms at δ = 146.6 ppm and 144.6 ppm, while ^{14}N NMR displayed the signals of the three nitro groups at a shift of –23.7 ppm, –25.5 ppm, and –27.3 ppm. In the ^{11}B NMR spectrum the signal appears at a shift of –7.4 ppm.

The analysis of the energetic properties of **14** was performed according to BAM standards:[39] impact sensitivity ≥ 10 J and friction sensitivity ≥ 120 N. These results show only a small increase of sensitivity for compound **14** compared to the dinitrated imidazolyl derivative **12**, which is in accordance with the already observed tendency that more nitro groups at the azole moiety will lead to a higher energetic character along with a higher sensitivity. In contrast to this finding, the decomposition temperature raises from 127 °C (**12**) to 170 °C of compound **14**. Of course, compound **12** is based on an imidazole scaffold, whereas **14** has two pyrazole moieties, nevertheless, this raise of decomposition temperature is noteworthy.

Investigation of Solvolytic Stability of Compound 14

As well as for the other synthesized borates, the solvolytic stability of compound **14** was also investigated. But in this case the obtained data does not only show the relative stability towards solvolysis but also allows an assumption of the degradation process. In the system methanol/acetonitrile (0.6:1.0) compound **14** showed after 3.5 h the formation of two new compounds with signals at δ = 27.9 ppm and 18.3 ppm. The latter can be clearly assigned to the expected solvolysis to trimethyl borate,[30] whereas the former signal refers to the intermediate formation of dimethyl boronate [$HB(OMe)_2$]. This signal displays in the proton coupled ^{11}B NMR a doublet with a coupling constant of 162 Hz, in accordance with the values generally found for B–H coupling in the $HB(OR)_2$ scaffold [$HB(OR)_2$: 26–28 ppm, $^1J_{B-H}$ = 160–168 Hz].[30] Therefore, the solvolysis of **14** could reasonably follow the pathway suggested in Scheme 6 where the trinitropyrazolyl moiety gets substituted before the final hydrogen atom, indicating that this moiety is bound to boron less strong than the hydrogen atom.

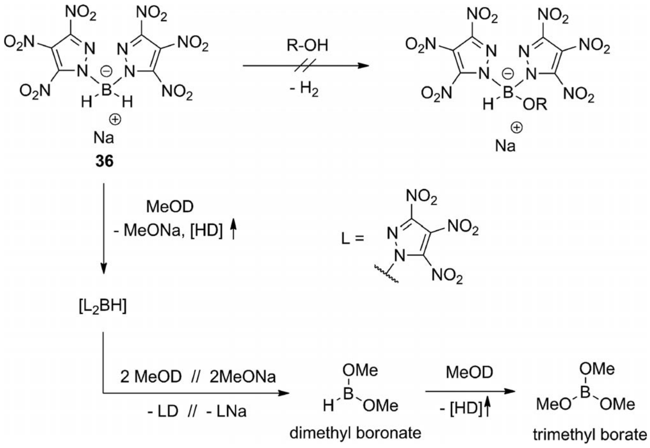

Scheme 6. Proposed degradation pathway of compound **14**.

This is corroborated by the fact that the signal at δ = 27.9 ppm cannot correspond to the scaffold L_2BH with L standing for the trinitropyrazolyl moiety. For such a species the B–H coupling ranges between 126–131 Hz [$HB(NR_2)_2$: 26–29 ppm, $^1J_{B-H}$ = 126–131 Hz][30] instead of the found 162 Hz. Furthermore, it has to be the original hydrogen, as only deuterated solvents were used and no coupling of a BD fragment could be observed, as for this fragment a triplet with a coupling constant of 24 Hz would be expected.[30]

After 4 d the signal at δ = 27.9 ppm was completely converted to trimethyl borate, which remained the only signal.

Experiments regarding the stability of **14** towards solvolysis were not only conducted in methanol solution but in aqueous solution as well. In the system water/acetonitrile (0.6:1.0) compound **14** showed noticeable decomposition to boric acid [boric acid signal: 18.6 (0.66) ppm; product signal: –12.5 (1.00) ppm] after 3.5 h, as well as the intermediate formation of a third compound with a shift at δ = 26.3 ppm.

IV Calculation of ^{11}B Chemical Shifts

As additional verification of the analytical data, the ^{11}B NMR chemical shifts were calculated and compared to the experimental data.

In order to compute the ^{11}B NMR chemical shifts for various high-nitrogen boron compounds, the isotropic magnetic shielding was computed using the GIAO (Gauge-Independent Atomic Orbital) method implemented in G03.[48,49] The structures were fully optimized and the frequencies calculated (NIMAG = 0) at MPW1PW91/aug-cc-pVDZ level of theory. Subsequently, the NMR shielding tensors were calculated at the same level of theory using the GIAO method.[49] Table 2 summarizes the computed isotropic magnetic shielding and relative ^{11}B NMR chemical shifts (ppm) referenced to $BF_3{\cdot}Et_2O$.

The comparison of the calculated values with the experimentally determined shifts shows a good accordance thereof. In case of the mono- and bissubstituted nitroimidazolyl, dinitroimidazolyl and trinitropyrazolyl borates, all compounds

Table 2. Computed isotropic magnetic shieldings (GIAO method[48,49] MPW1PW91/aug-cc-pVDZ) and relative ^{11}B chemical shifts /ppm referenced to $BF_3{\cdot}Et_2O$.

Compound	–*E*/ a.u.	*NIMAG*	***p.g.***	δ ^{11}B /ppm, calcd. isotr. shielding	δ ^{11}B /ppm, calcd. (ref. to $BF_3{\cdot}Et_2O$)	δ ^{11}B /ppm, exptl., (ref. to $BF_3{\cdot}Et_2O$)
$BF_3{\cdot}Et_2O$	558.164166	0	C_1	+110.0	0.0	0.0
BH_4^-	27.246888	0	T_d	+159.0	–49.0	–41.6 [50]
$B(OH)_3$	252.468079	0	C_{3h}	92.4	+17.6	18.4–19.6 [30]
$B(OH)_4^-$	328.333947	0	S_4	107.9	+2.1	+1.1 [30]
$BH_3(DNT)^-$ c)	677.334541	0	C_1	+130.2	–20.2	–17.2 [24]
$BH_2(DNT)_2^-$ c)	1327.389843	0	C_1	+117.5	–7.5	–6.2 [24]
$BH_3(NIM)^-$ (**7**)	456.829447	0	C_s	133.0	–23.0	–20.1 a)
$BH_2(NIM)_2^-$ (**8**)	886.389580	0	C_1	121.8	–11.8	–9.8 a)
$BH(NIM)_3^-$ (**9**)	1315.931096	0	C_1	115.8	–5.8	–4.1 b)
$B(NIM)_4^-$ (**10**)	1745.446360	0	C_1	112.8	–2.8	+1.1 b)
$BH_2(DNIM)_2^-$ (**12**)	1295.333327	0	C_1	122.5	–12.5	–12.2 a)

a) Compounds verified by high resolution mass spectrometry. b) Compounds not isolated and fully verified up to now. c) DNT stands for 3,5-dinitro-1,2,4-triazole.

were unambiguously proven by high-resolution mass spectrometry and can therefore be used as control for the calculated values. The calculated chemical shifts of the trissubstituted and tetrakissubstituted imidazolyl borates reveal a good accordance to in the course of the investigations obtained NMR shifts (Table 1, entry 4 and 5). Therefore, two systems were found that most likely open access to higher substituted 4-nitroimidazolyl borates and consequently will be further investigated.

Conclusions

4-Nitroimidazole was used for the investigation of various reaction conditions leading to mono-, bis-, tris- or tetrakissubstituted borates. These experiments showed that the formation of the bissubstituted compound potassium dihydridobis(4-nitroimidazolyl)borate (**8**) proceeds smoothly in acetonitrile and can easily be upscaled. In order to increase the oxygen content, the higher nitrated derivative 3,4-dinitroimidazole (**11**) was used. The increased reactivity of **11** due to the second nitro group facilitates milder reaction conditions for the formation of sodium dihydridobis(4,5-dinitroimidazolyl)borate (**12**). Furthermore, sodium dihydridobis(3,4,5-trinitropyrazolyl)borate (**14**) was synthesized as fully nitrated compound in high yields and could easily be upscaled. The energetic properties were determined, whereas two compounds, potassium dihydridobis(4-nitroimidazolyl)borate (**8**) and sodium dihydridobis(3,4,5-trinitropyrazolyl)borate (**14**), showed very promising properties regarding an application in pyrotechnics (decomposition points of 189 °C and 170 °C, respectively). Furthermore, the compounds exhibit a moderate stability towards solvolysis. Especially when subjected to metathesis reactions these compounds are very promising candidates as coloring agents in pyrotechnic formulations. Moreover, the high oxygen content of compound **14** can influence the oxygen balance of the whole pyrotechnic mixture positively.

Experimental Section

All manipulations were carried out in an atmosphere of dry argon using standard vacuum line techniques. Experimental reaction procedures to yield boron compounds were monitored by ^{11}B NMR measurements and every reaction setting thereof was equipped with a bubble counter to track gas evolution. Solvents were dried by standard procedures. Deuterated NMR solvents were purchased from Eurisotop. 4,5-Dinitroimidazole (**11**)[43] and 3,4,5-trinitropyrazole (**13**)[51–53] were prepared as stated in the corresponding references. All other chemicals were commercially available and used as received. The NMR spectra were recorded with a JEOL Eclipse 400, JEOL Eclipse 270 or JEOL EX400 instrument at an ambient temperature of 25 °C if not stated otherwise. All ^{13}C NMR spectra were recorded {^{1}H}-decoupled. Chemical shifts (δ) were calibrated using the residual undeuterated solvent as an internal reference and are according to the common convention reported in parts per million (ppm) downfield relative to tetramethylsilane (TMS, ^{13}C, 100.6 MHz resp. 67.9 MHz; ^{1}H, 399.8 MHz resp. 270.2 MHz), nitromethane (^{14}N) or boron trifluoro etherate (^{11}B) as external standards. The chemical shifts of the reference solvents were defined concurrent with the data from Nudelman.[54] For the designation of multiplicities the following abbreviations were used: s (singlet), d (doublet), t (triplet), q (quartet), br (broad) and m (multiplet) or combinations thereof; coupling constants (*J*) are given in Hertz (Hz). Raman spectra were recorded with a Bruker FT-Raman-MultiRAM Spectrometer instrument equipped with a Klaastech DENICAFC LC-3/40 laser device. The intensities are reported in percentages relative to the most intense peak and are given in parentheses. High resolution (HRMS) and low resolution (LRMS) mass spectra were recorded by the mass spectrometry facility of the Department of Chemistry and Pharmacy of the Ludwig Maximilian University Munich on a JEOL MS station JMS 700 instrument. Ionization of the samples was achieved using fast atom bombardment (FAB) as indicated in the experimental section. Elemental analyses were performed with an Elementar Vario EL or an Elementar Vario EL micro cube. DSC-measurements were performed with a Perkin-Elmer Pyris 6 DSC- instrument at a heating rate of 5 °C min^{-1} in closed aluminum containers with a hole (1 µm) on the top for gas release and a nitrogen flow of 5 mL·min^{-1}. The reference sample was an empty closed aluminum container. The impact and friction sensitivity was determined using a BAM drophammer and a BAM friction tester.[39] The sensitivities of the compounds are indicated according to the UN Recommendations on the Transport of Dangerous Goods (+):[39] impact: insensitive $>$ 40 J, less sensitive $>$ 35 J, sensitive $>$ 4 J, very sensitive $<$ 4 J; friction: insensitive $>$ 360 N, less sensitive = 360 N, sensitive $<$ 360 N and $>$ 80 N, very sensitive $<$ 80 N, extreme sensitive $<$ 10 N.

CAUTION! The compounds described in this work are potential explosives, which are sensitive to environmental stimuli such as impact, friction, heat or electrostatic discharge. While we encountered no issues in the handling of these materials, appropriate precautions, and proper protective measures (safety glasses, face shields, leather coat, Kevlar gloves, and ear protectors) should be taken when preparing and manipulating these materials.

Potassium Dihydridobis(4-nitroimidazolyl)borate (8): 4-Nitroimidazole (**5**) 4.15 g, 36.7 mmol) was added in portions to a suspension of potassium borohydride (990 mg, 18.4 mmol) in acetonitrile (40 mL). The obtained colorless suspension was stirred under reflux conditions for 40 h, during this period the suspension discolored and turned from colorless over beige-brown to completely black. After cooling to ambient temperature the reaction mixture was strongly diluted with further acetonitrile and the insoluble impurities were filtered off. After removal of the solvent in vacuo compound **8** was obtained as off-white solid in high yields (4.06 g, 80 %). Isomer 1 and isomer 2 were obtained in the ratio of 2 to 1. **DSC**: T_{dec} = 189 °C. $C_6H_6BKN_6O_4{\cdot}1/2MeCN$: calcd. C 28.35, H 2.55, N 30.70 %, found C 28.80, H 2.59, N 29.39 %. **^{11}B NMR** ([D$_6$]DMSO): δ = –10.7 ppm. Isomer 1: **^{1}H NMR** ([D$_6$]DMSO, 25 °C): δ = 8.01 (d, $^4J_{C,H,\ C-H}$ = 1.4 Hz, 2 H, C–H), 7.50 (d, $^4J_{C,H,\ C-H}$ = 1.4 Hz, 2 H, C–H), 3.30 (br. s, 2 H, BH$_2$) ppm. ([D$_6$]DMSO, 85 °C): δ = 7.86 (d, $^4J_{C,H,\ C-H}$ = 1.1 Hz, 2 H, C–H), 7.42 (d, $^4J_{C,H,\ C-H}$ = 1.1 Hz, 2 H, C–H), 3.34 (br. q, $^1J_{B-H}$ = 123 Hz, 2 H, BH$_2$) ppm. **^{13}C NMR** ([D$_6$]DMSO, 25 °C): δ = 148.1 (C–NO$_2$), 141.1 (C–H), 124.9 (C–H) ppm. Isomer 2: **^{1}H NMR** ([D$_6$]DMSO, 25 °C): δ = 8.05 (d, $^4J_{C,H,\ C-H}$ = 1.1 Hz, 2 H, C–H), 7.52 (d, $^4J_{C,H,\ C-H}$ = 1.1 Hz, 2 H, C–H) ppm. ([D$_6$]DMSO, 85 °C): δ = 7.97 (br. s, 2 H, C–H), 7.46 (br. s, 2 H, C–H), 6.30 (br. s, 2 H, BH$_2$) ppm. **^{13}C NMR** ([D$_6$]DMSO, 25 °C): δ = 147.9 (C–NO$_2$), 140.5 (C–H), 124.8 (C–H) ppm. **Raman** (300 mW): $\tilde{\nu}$ = 3141 (10), 3124 (3), 3117 (5), 3106 (3), 3084 (2), 2409 (8), 1544 (6), 1519 (36), 1510 (3), 1474 (23), 1467 (5), 1434 (3), 1404 (96), 1379 (21), 1340 (18), 1288 (21), 1279 (100), 1261 (23), 1219 (72), 1152 (43), 1112 (10), 1033 (13), 991 (62), 915 (3), 877 (4), 829 (7), 811 (19), 705 (8), 640 (6), 551 (8), 342 (3), 314 (11) cm^{-1}. **HRMS** (FAB$^-$): *m/z* for $C_6H_6O_4N_6B^-$: calcd. 237.0545, found 237.0530. **IS** (grain $<$ 100 µm): $>$ 40 J. **FS** (grain $<$ 100 µm): $>$ 360 N. **ESD** (grain $<$ 100 µm): $>$ 0.85 J.

Sodium Dihydridobis(4,5-dinitroimidazol-1-yl)borate (12): Sodium borohydride (265 mg, 7.00 mmol) was suspended in acetonitrile (60 mL) before 4,5-dinitroimidazole (**11**) (2.21 g, 14.0 mmol) was added in small portions. Immediate strong gas evolution was visible and the reaction mixture was stirred at ambient temperature for 12 h, followed by additional 15 h at 45 °C. After removal of the solvent, compound **12** was obtained as pale yellow solid in almost quantitative yield (2.51 g, 97 %). Despite drying under high vacuum at elevated temperature, a small amount of acetonitrile remained in the solid product. It was assumed that the acetonitrile is part of the solid structure. **DSC**: T_{dec} = 127 °C. $C_6H_4BN_8NaO_8{\cdot}1/2MeCN$: calcd. C 22.69, H 1.50, N 32.14 %, found C 22.72, H 1.95, N 30.50 %. **^{1}H NMR** (CD$_3$CN): δ = 7.40 (s, 2 H, C–H), 3.29 (br. s, 2 H, BH$_2$) ppm. **^{13}C NMR** (CD$_3$CN): δ = 139.6, 138.7 ppm. **^{14}N NMR** (CD$_3$CN): δ = –17.3 (NO$_2$), –20.6 (NO$_2$), –185.3 (ring) ppm. **^{11}B NMR** (CD$_3$CN): δ = –12.2 ppm. **Raman** (300 mW): $\tilde{\nu}$ = 3172 (2), 3137 (6), 2985 (2), 2848 (3), 2449 (6), 1563 (40), 1528 (11), 1473 (11), 1398 (19), 1363 (26), 1336 (5), 1308 (100), 1280 (13), 1251 (7), 1216 (13), 1182 (16), 1127 (2), 1016 (7), 900 (2), 855 (22), 817 (4), 763 (8), 725 (2), 654 (3), 512 (3), 423 (3), 267 (4) cm^{-1}. **HRMS** (FAB$^-$): *m/z* for $C_6H_4O_8N_8B^-$: calcd. 327.0246, found 327.0254. **IS** (grain $<$ 100 µm): $>$ 10 J. **FS**(grain $<$ 100 µm): $>$ 240 N.

Sodium Dihydridobis(3,4,5-trinitropyrazol-1-yl)borate (14): Sodium borohydride (167 mg, 4.40 mmol) was suspended in diethyl ether (25 mL) before 3,4,5-trinitropyrazole (**13**) (2.69 g, 13.2 mmol) was added in small portions. Immediate gas evolution was visible and the yellow reaction solution was stirred for 16 h at ambient temperature, during which time a pale yellow precipitate was formed. The reaction solid was filtered off and washed with diethyl ether to obtain **14** in high yields (1.61 g, 83 %). **DSC**: T_{dec} = 170 °C. $C_6H_2BN_{10}NaO_{12}{\cdot}4/11Et_2O$: calcd. C 19.18,H 1.22, N 30.00 %, found C 19.07, H 1.17, N 29.55 %. **^{1}H NMR** (CD$_3$CN): δ = 3.80 (br. s, 2 H, BH$_2$) ppm. **^{13}C NMR**(CD$_3$CN): δ = 146.6, 144.6 ppm. **^{14}N NMR** (CD$_3$CN): δ = –23.7 (NO$_2$), –25.5 (NO$_2$), –27.3 (NO$_2$) ppm. **^{11}B NMR** (CD$_3$CN): δ = –7.4 ppm. **Raman** (500 mW): $\tilde{\nu}$ = 2476 (8), 1567 (17), 1478 (12), 1457 (3), 1409 (100), 1331 (18), 1302 (4), 1223 (7), 1181 (22), 1135 (2), 1066 (3), 850 (46), 808 (5), 769 (3), 750 (10), 561 (4), 503 (2), 430 (2), 390 (3), 328 (6), 293 (2) cm^{-1}. **HRMS** (FAB$^-$): *m/z* for $C_6H_2O_{12}N_{10}B^-$: calcd. 416.9948, found 416.9916. **IS** (grain $<$ 100 µm): $>$ 10 J. **FS** (grain $<$ 100 µm): $>$ 120 N.

Acknowledgments

Financial support of this work by the Ludwig-Maximilian University of Munich (LMU), the U.S. Army Research Laboratory (ARL) under grant no. W911NF-09–2-0018, the Armament Research, Development, and Engineering Center (ARDEC) under grant no. W911NF-12–1-0467, and the Office of Naval Research (ONR) under grant nos. ONR.N00014–10–1-0535 and ONR.N00014–12–1-0538 is gratefully acknowledged. The authors acknowledge collaborations with *Dr. Mila Krupka* (OZM Research, Czech Republic) in the development of new testing and evaluation methods for energetic materials and with *Dr. Muhamed Suceska* (Brodarski Institute, Croatia) in the development of new computational codes to predict the detonation and propulsion parameters of novel explosives. We are indebted to and thank *Drs. Betsy M. Rice* and *Brad Forch* (ARL, Aberdeen, Proving Ground, MD) for many inspired discussions. The authors want to thank *St. Huber* for measuring the sensitivities. The Cusanuswerk is gratefully acknowledged for the award of a PhD scholarship (M. Rusan).

References

[1] T. M. Klapötke, G. Steinhauser, *Angew. Chem. Int. Ed.* **2008**, *47*, 3330.

[2] T. M. Klapötke, G. Steinhauser, *J. Chem. Educ.* **2010**, *87*, 150.

[3] K. R. Tarantik, Dissertation, Ludwig Maximilian University Munich, **2010**.

[4] R. P. Singh, R. D. Verma, D. T. Meshri, J. M. Shreeve, *Angew. Chem. Int. Ed.* **2006**, *45*, 3584.

[5] a) O. P. Murty, *J. Forensic Med. Toxicol.* **2000**, *17*, 23; b) T. M. Klapötke, G. Holl, *Green Chem.* **2001**, *3*, G75.

[6] a) G. Steinhauser, K. Tarantik, T. M. Klapötke, *J. Pyrotech.* **2008**, *27*, 3; b) T. M. Klapötke, K. R. Tarantik, *11th Conference New Trends in Research of Energetic Materials*, Pardubice, Czech Republic, Apr. 9–11, **2008**, *Part 2*, pp. 586; c) T. M. Klapötke, J. Stierstorfer, K. R. Tarantik, *12th Conference New Trends in Research of Energetic Materials*, Pardubice, Czech Republic, Apr. 1–3, **2009**, *Part 2*, pp. 647; d) T. M. Klapötke, J. Stierstorfer, K. R. Tarantik, *J. Pyrotech.* **2009**, *28*, 61.

[7] a) R. Mandal, B. K. Sen, S. Sen, *Chem. Environ. Res.* **1996**, *5*, 307; b) A. Dutschke, C. Lohrer, S. Seeger, L. Kurth, *Chem. Ing. Tech.* **2009**, *81*, 167; c) G. Croteau, R. Dills, M. Beaudreau, *Atmos. Environ.* **2010**, *40*, 4316; d) G. Steinhauser, J. H. Sterba, M. Foster, F. Grass, M. Bichler, *Atmos. Environ.* **2008**, *42*, 8616.

[8] http://www.diwalifestival.org/diwali-festival-in-india.html 07.03.2013, 17:55.

[9] http://www.umweltbundesamt.at/umweltsituation/luft/luftschadstoffe/staub/pm10/ 07.03.2013, 18:18.

[10] Y. Wang, G. Zhuang, C. Xu, Z. An, *Atmos. Environ.* **2007**, *41*, 417.

[11] U. C. Kulshrestha, T. Nageswara Rao, S. Azhaguvel, M. J. Kulshrestha, *Atmos. Environ.* **2004**, *38*, 4421.

[12] S. Yuasa, H. Isoda, *Combust. Flame* **1991**, *86*, 216.

[13] K. J. Smit, R. J. Hancox, D. J. Hatt, S. P. Murphy, L. V. de Yong, *Appl. Spectrosc.* **1997**, *51*, 1400.

[14] J. J. Sabatini, J. C. Poret, R. N. Broad, *Angew. Chem. Int. Ed.* **2011**, *50*, 4624.

[15] S. Trofimenko, *Scorpionates: The Coordination Chemistry of Poly(pyrazolyl)borate Ligands*, Imperial College Press, London, **1999**.

[16] C. Pettinari, C. Santini, *Comput. Coord. Chem. II* **2004**, *1*, 159.

[17] a) H. V. R. Dias, C. J. Lovely, *Chem. Rev.* **2008**, *108*, 3223; b) C. Pettinari, *Scorpionates II: Chelating Borate Ligands*, (dedicated to Swiatoslaw Trofimenko), Imperial College Press, London, **2008**; c) H. V. R. Dias, M. Fianchini, *Comments Inorg. Chem.* **2007**, *28*, 73; d) M. M. Diaz-Requejo, P. J. Perez, *J. Organomet. Chem.* **2005**, *690*, 5441; e) M. Pellei, G. Papini, G. G. Lobbia, S. Ricci, M. Yousufuddin, H. V. R. Dias, C. Santini, *Dalton Trans.* **2010**, *39*, 8937; f) H. V. R. Dias, M. Fianchini, *Angew. Chem. Int. Ed.* **2007**, *46*, 2188; g) H. V. R. Dias, J. Wu, *Angew. Chem. Int. Ed.* **2007**, *46*, 7814; h) C. G. Young, A. G. Wedd, *Chem. Commun.* **1997**, 1251; i) H. Vahrenkamp, *Acc. Chem. Res.* **1999**, *32*, 589; j) G. Parkin, *Chem. Rev.* **2004**, *104*, 699; k) W. B. Tolman, *J. Biol. Inorg. Chem.* **2006**, *11*, 261; l) C. Santini, M. Pellei, *Applications of Scorpionate Ligands in Enzyme Modeling and Biological Studies*, Bentham Science, **2009**; m) K. Rangan, M. Fianchini, S. Singh, H. V. R. Dias, *Inorg. Chim. Acta* **2009**, *362*, 4347; n) H. V. R. Dias, R. M. G. Rajapakse, D. M. M. Krishantha, M. Fianchini, X. Y. Wang, R. L. Elsenbaumer, *J. Mater. Chem.* **2007**, *17*, 1762; o) H. V. R. Dias, X. Wang, R. M. G. Rajapakse, R. L. Elsenbaumer, *Chem. Commun.* **2006**, 976; p) M. M. Diaz-Requejo, P. J. Perez, *J. Organomet. Chem.* **2001**, *617*, 110; q) J. M. Munoz-Molina, A. Caballero, M. M. Diaz-Requejo, S. Trofimenko, T. R. Belderrain, P. J. Perez, *Inorg. Chem.* **2007**, *46*, 7725; r) G. P. A. Yap, F. Jove, J. Urbano, E. Alvarez, S. Trofimenko, M. M. Diaz-Requejo, P. J. Perez, *Inorg. Chem.* **2007**, *46*, 780; s) T. Tietz, C. Limberg, R. Stößer, B. Ziemer, *Chem. Eur. J.* **2011**, *17*, 10010.

[18] T. J. Groshens, *J. Coord. Chem.* **2010**, *63*, 1882.

[19] C. J. Snyder, P. D. Martin, M. J. Heeg, C. H. Winter, *Chem. Eur. J.* **2013**, *19*, 3306.

[20] S. Trofimenko, *J. Am. Chem. Soc.* **1966**, *88*, 1842.

[21] V. A. Sazonova, L. P. Sorokina, *Dokl. Akad. Nauk SSSR* **1955**, *105*, 993.

[22] S. Trofimenko, *J. Am. Chem. Soc.* **1967**, *89*, 3170.

[23] M. Pellei, F. Benetollo, G. G. Lobbia, S. Alidori, C. Santini, *Inorg. Chem.* **2005**, *44*, 846.

[24] a) K. O. Christe, R. Haiges, R. I. Wagner, C. J. Jones, *Synthesis of New High-oxygen Carriers and Ditetrazinetetroxide (DTTO)*, Final Report for the Office of Naval Reasearch, **2008–2009**, under Contr. N00014–08–1-0590; b) K. O. Christe, R. Haiges, G. Belanger-Chabot, M. Rahm, R. Wagner, W. Wilson, *ONR 6.1 Advanced Energetic Materials Program Review*, February 12–13, **2013**, CALTECH, Pasadena, CA and USC, Los Angeles, CA.

[25] M. Pellei, S. Aldori, G. Papini, G. G. Lobbia, J. D. Gorden, H. V. R. Dias, C. Santini, *Dalton Trans.* **2007**, 4845.

[26] M. Pellei, G. Papini, G. G. Lobbia, S. Ricci, M. Yousufuddin, H. V. R. Dias, C. Santini, *Dalton Trans.* **2010**, *39*, 8937.

[27] B. H. Hamilton, K. A. Kelly, W. Malasi, C. J. Ziegler, *Inorg. Chem.* **2003**, *42*, 3067.

[28] a) C. Janiak, T. G. Scharmann, P. Albrecht, F. Marlow, R. Macdonald, *J. Am. Chem. Soc.* **1996**, *118*, 6307; b) C. Janiak, S. Temizdemir, S. Dechert, *Inorg. Chem. Commun.* **2000**, *3*, 271.

[29] D. Lu, C. H. Winter, *Inorg. Chem.* **2010**, *49*, 5795.

[30] H. Nöth, B. Wrackmeyer, *NMR – Basic Prinicples and Progress (14), Nuclear Magnetic Resonance Spectroscopy of Boron Compounds*, Springer Verlag, Berlin, **1978**.

[31] a) C. Lopez, R. M. Claramunt, D. Sanz, C. Foces, F. H. Cano, R. Faure, E. Cayon, J. Elguero, *Inorg. Chim. Acta* **1990**, *176*, 195; b) T. O. Northcutt, R. J. Lachicotte, W. D. Jones, *Organometallics* **1998**, *17*, 5148; c) U. E. Bucher, A. Currao, R. Nesper, H. Ruegger, L. M. Venanzi, E. Younger, *Inorg. Chem.* **1995**, *34*, 66.

[32] R. T. Pardasani, P. Pardasani, *Chemical Shifts and Coupling Constants for Boron-11*, Springer, Berlin, **2009**.

[33] C. E. Webster, M. B. Hall, *Inorg. Chim. Acta* **2002**, *330*, 268.

[34] a) M. O. Albers, S. F. A. Crosby, D. C. Liles, D. J. Robinson, A. Shaver, E. Singleton, *Organometallics* **1987**, *6*, 2014; b) J. C. Bommer, K. W. Morse, *J. Am. Chem. Soc.* **1974**, *96*, 6222; c) J. C. Bommer, K. W. Morse, *Inorg. Chem.* **1979**, *18*, 531; d) J. C. Bommer, K. W. Morse, *Inorg. Chem.* **1980**, *19*, 587.

[35] a) G. Socrates, *Infrared and Raman Characteristic Group Frequencies – Tables and Charts*, 3rd ed., John Wiley & Sons: Chichester, **2004**; b) M. Hesse, H. Meier, B. Zeeh, *Spektroskopische Methoden in der Organischen Chemie*, 6. Auflage, Thieme, Stuttgart, **2002**.

[36] H. L. De Bondt, E. Ragia, N. M. Blaton, O. M. Peeters, C. J. De Ranter, *Acta Crystallogr., Sect. C Cryst. Struct. Commun.* **1993**, *49*, 693.

[37] A. Grimmson, J. H. Ridd, B. V. Smith, *J. Chem. Soc.* **1960**, 1352.

[38] The assignment was taken in accordance with the shift sequence of the free ligand and not calculated.

[39] a) M. Suceska, *Test Methods for Explosives*, Springer, New York, **1995**, p. 21 (impact), p. 27 (friction); b) http://www.bam.de/; c) *UN Recommendations on the Transport of Dangerous Goods*, *Model Regulations*, 15th ed., United Nations, New York a. Geneva, **2007**.

[40] a) Z. Zeng, B. Twamley, J. M. Shreeve, *Organometallics* **2007**, *26*, 1782; b) L. G. Gioia, B. Flavio, C. Patrizio, *Synth. React. Inorg. Met.-Org. Chem.* **1991**, *21*, 1141.

[41] B. H. Hamilton, K. A. Kelly, W. Malasi, C. J. Ziegler, *Inorg. Chem.* **2003**, *42*, 3067.

[42] S. Chao, C. E. Moore, *Anal. Chim. Acta* **1978**, *100*, 457.

[43] A. R. Katritzky, S. Singh, K. Kirichenko, M. Smiglak, J. D. Holbrey, W. M. Reichert, S. K. Spear, R. D. Rogers, *Chem. Eur. J.* **2006**, *12*, 4630.

[44] Characteristic frequencies taken from: http://sdbs.riodb.aist.go.jp/sdbs/cgi-bin/direct_frame_top.cgi 16.02.213, 20:48.

[45] H. V. R. Dias, S. Alidori, G. Gioia Lobbia, G. Papini, M. Pellei, C. Santini, *Inorg. Chem.* **2007**, *46*, 9708.

[46] A. Penger, Dissertation Ludwig-Maximilian University Munich, **2011**.

[47] M. Feller, Master Thesis, Ludwig-Maximilian-University Munich, **2011**.

[48] Gaussian 03, Revision A.1, Frisch, M. J.; Trucks, G. W.; Schlegel, H. B.; Scuseria, G. E.; Robb, M. A.; Cheeseman, J. R.; Montgomery Jr., J. A.; Vreven, T.; Kudin, K. N.; Burant, J. C.; Millam, J. M.; Iyengar, S. S.; Tomasi, J.; Barone, V.; Mennucci, B.; Cossi, M.; Scalmani, G.; Rega, N.; Petersson, G. A.; Nakatsuji, H.; Hada, M.; Ehara, M.; Toyota, K.; Fukuda, R.; Hasegawa, J.; Ishida, M.; Nakajima, T.; Honda, Y.; Kitao, O.; Nakai, H.; Klene, M.; Li, X.; Knox, J. E.; Hratchian, H. P.; Cross, J. B.; Adamo, C.; Jaramillo, J.; Gomperts, R.; Stratmann, R. E.; Yazyev, O.; Austin, A. J.; Cammi, R.; Pomelli, C.; Ochterski, J. W.; Ayala, P. Y.; Morokuma, K.; Voth, G. A.; Salvador, P.; Dannenberg, J. J.; Zakrzewski, V. G.; Dapprich, S.; Daniels, A. D.; Strain, M. C.; Farkas, O.; Malick, D. K.; Rabuck, A. D.; Raghavachari, K.; Foresman, J. B.; Ortiz, J. V.; Cui, Q.; Baboul, A. G.; Clifford, S.; Cioslowski, J.; Stefanov, B. B.; Liu, G.; Liashenko, A.; Piskorz,

P.; Komaromi, I.; Martin, R. L.; Fox, D. J.; Keith, T.; Al-Laham, M. A.; Peng, C. Y.; Nanayakkara, A.; Challacombe, Gill, P. M. W.; Johnson, B.; Chen, W.; Wong, M. W.; Gonzalez, C.; Pople, J. A.; Gaussian, Inc., Pittsburgh PA, **2003**.

[49] a) K. Wolinski, J. F. Hilton, P. Pulay, *J. Am. Chem. Soc.* **1990**, *112*, 8251; b) J. L. Dodds, R. McWeeny, A. Sadlej, *Mol. Phys.* **1980**, *41*, 1419; c) R. Ditchfield, *Mol. Phys.* **1974**, *27*, 789; d) R. McWeeny, *Phys. Rev.* **1962**, *126*, 1028.

[50] H. C. Brown, T. P. Stocky, *J. Am. Chem. Soc.* **1977**, *99*, 8218.

[51] J. W. A. M. Janssen, H. J. Koeners, C. G. Kruse, C. L. Habrakern, *J. Org. Chem.* **1973**, *38*, 1777.

[52] R. Hüttel, F. Büchele, *Chem. Ber.* **1955**, *88*, 1586.

[53] G. Hervé, C. Roussel, H. Graindorge, *Angew. Chem.* **2010**, *122*, 3245.

[54] H. E. Gottlieb, V. Kotlyar, A. Nudelman, *J. Org. Chem.* **1997**, *62*, 7512.

Received: May 21, 2013

DOI: 10.1002/zaac.201400218

Synthesis and Investigation of Energetic Boron Compounds for Pyrotechnics

Thomas M. Klapötke,*[a] Magdalena Rusan,[a] and Véronique Sproll[a]

Keywords: Energetic boron esters; Green pyrotechnics; Tetrakis(azolyl)borate; Nitrogen-rich compounds; Energetic materials

Abstract. The energetic boron esters tris(1-ethyl-5-aminotetrazolyl) borate, tris(2-ethyl-5-aminotetrazolyl) borate, tris(1-ethyltetrazolyl) borate, tris(2-ethyltetrazolyl) borate, and tris(2-(3-nitro-1,2,4-triazolyl)ethyl) borate were synthesized and analyzed by NMR and IR spectroscopy, elemental analysis, and mass spectrometry. Two tetracoordinate borates potassium tetrakis(3-nitro-1,2,4-triazolyl)borate and potassium bis(4,4′,5,5′-tetranitro-2,2′-bisimidazolyl)borate were synthesized and fully characterized as well. Moreover, the energetic and thermal properties of the energetic boron esters and tetracoordinate borates were determined. The ^{11}B NMR chemical shifts of potassium tetrakis(3-nitro-1,2,4-triazolyl)borate and potassium bis(4,4′,5,5′-tetranitro-2,2′-bisimidazolyl)borate were calculated and compared to the experimental values. Tris(1-ethyl-5-aminotetrazolyl) borate was tested as colorant in pyrotechnic formulations with respect to the combustion behavior and color properties as well as the energetic and thermal properties.

Introduction

In pyrotechnical applications green light is traditionally produced by using barium nitrate in combination with magnesium, a chlorine source to generate metastable BaCl, which is the green-light-emitting species and often a perchlorate oxidizer to enhance the burn rate and improve the color properties.[1] But due to environmental issues and health concerns caused by barium compounds like barium oxide, barium hydroxide, and barium chloride formed as by-products during the combustion, the goal is the replacement by green-burning boron compounds. Several boron compounds like boric acid, amorphous boron, or boron carbide were tested in pyrotechnic formulations.[2] But these boron compounds have in common that they do not possess any energetic character. The development of a compound, which combines color-producing and energetic properties, would be advantageous with regard to the creation of highly efficient pyrotechnics, which could reduce the amount of different additives of pyrotechnics as well as the weight due to a better performance. As energetic boron esters consisting of a boron center and energetic ligands fit these requirements, they have attracted the research interests.

Energetic boron esters were first mentioned by *Klapötke* et al., reporting the synthesis of tris(2,2,2-trinitroethyl)borate, which was investigated as oxidizer.[3] The synthesis was performed by the reaction of boron oxide and trinitroethanol at slightly elevated temperature. Other boron esters like tris(aminoalkoxy)boranes were prepared by *Niedenzu* and coworkers by transesterification reaction of triethyl borate and several alkanolamines.[4] Another synthesis method, which was also examined by *Klapötke* and co-workers, is the reaction of tris(2-chloroethyl)borate with 1-nitropron-2-ol and methylaminoethanol resulting in the formation of the corresponding boron esters.[5]

Another group of boron-containing compounds, which are considered as potential green colorants are poly(azolyl)borates.[6] Various poly(azolyl)borates have been reported in literature: there are four classes of poly(azolyl)borates, referring to their grade of substitution – trihydro(azolyl)borates, dihydrobis(azolyl)borates, hydrotris(azolyl)borates, and tetrakis(azolyl)borates.[7] Among the different classes of B–N bound azoles, the group of pyrazoles and 1,2,4-triazoles show the greatest variety. Poly(azolyl)borate compounds bearing insensitive groups as alkyl- or aryl substituents and especially tetrakis(azolyl)borates have been extensively studied by *Trofimenko*.[8] The synthesis approach implies high temperatures using a mixture of the corresponding azole and alkali metal borohydride obtaining tetrakis(azolyl)borates in good yields.[7b,8,9] Borates bearing four energetic ligands are only scarcely reported. Several attempts were done to synthesize tetracoordinate tetrazole-based borates, but only tris-substituted borates based on tetrazole could be obtained.

In this contribution several energetic boron esters based on tetrazole, 5-aminotetrazole, and nitrotriazole as well as three tetracoordinated azole borate compounds were synthesized. These compounds were characterized by IR and NMR spectroscopy, mass spectrometry, and elemental analysis, and investigated with regard to their thermal and energetic character.

Results and Discussion

Boron esters, which burn with a green flame color are of interest as green colorants in pyrotechnics. Although *Chavez* et al. tested pyrotechnic formulations based on boric acid,[10]

---

* Prof. Dr. T. M. Klapötke
Fax: +49-89-2180-77492
E-Mail: tmk@cup.uni-muenchen.de
[a] Department of Chemistry
Energetic Materials Research
Ludwig-Maximilian University
Butenandtstr. 5–13 (D)
81377 München, Germany

no energetic boron esters have been investigated as green colorant so far. The synthesis of three energetic boron esters like tris(2-methylamino)ethyl) borate, tris(2-nitroethyl) borate, and tris(1-nitropropan-2-yl) borate have been performed.[5] Herein, the preparation of boron esters tris(1-ethyl-5-aminotetrazolyl) borate (**3**), tris(2-ethyl-5-aminotetrazolyl) borate (**4**), tris(1-ethyltetrazolyl) borate (**7**), tris(2-ethyltetrazolyl) borate (**8**), and tris(2-(3-nitro-1,2,4-triazolyl)ethyl) borate (**10**) is reported.

Since decades trihydro(azolyl)borates, dihydrobis(azolyl) borates, hydrotris(azolyl)borates, and tetrakis(azolyl)borates have been widely investigated.[7] But only a few of such borate containing energetic character have been prepared. Among the trihydro(azolyl)borates the synthesis of metal complexes containing nitrogen-rich hydrotris(tetrazolyl)orates is reported.[7d] The energetic tetracoordinate compound tetrakis(dinitrotriazolyl)borate has been reported by *K. O. Christe* et al.[11] Two tetracoordinate borate compounds, potassium tetrakis(3-nitro-1,2,4-triazolyl)borate (**12**) and potassium bis(4,4′,5,5′-tetranitro-2,2′-bisimidazolyl)borate (**14**) were synthesized.

I. Boron Esters

Boron esters can be derived from boric acid and by transesterification reaction the alcohol moieties can be replaced so that many different moieties can be introduced and a variety of compounds can be obtained (Scheme 1).

$$3\,\mathrm{HO{-}R^1} + \mathrm{B}\left(\!-\mathrm{OR^2}\right)_3 \xrightarrow[-\,3\,\mathrm{R^2OH}]{} \mathrm{B}\left(\!-\mathrm{OR^1}\right)_3$$

Scheme 1. General reaction scheme for nitrogen-rich boron esters.

Most suitable ligands are high-boiling alcohols. By combining them with trimethyl- or triethylborate low-boiling alcohols methanol and ethanol, respectively, are formed and can be easily removed from the reaction mixture.

Several nitrogen-rich boron esters are synthesized and characterized. Trimethylborate is commercially available and hydroxyethyltetrazole,[12] hydroxyethyl-5-aminotetrazole,[13] and 2-(3-nitro-1,2,4-triazolyl)ethanol[14] can be easily synthesized.

Synthesis of Tris(ethyl-5-aminotetrazolyl) Borates (3 and 4)

The starting materials were synthesized according to a literature procedure.[13] 5-Aminotetrazole was deprotonated by sodium hydroxide and stirred with chloroethanol at reflux conditions for 18 h resulting in the formation of a mixture of isomers, which were separated through different solubility in acetone and ethanol.

Compound **3** was synthesized by reacting trimethyl borate and compound **1** in stoichiometric amounts in *N*,*N*-dimethylformamide (DMF) at elevated temperatures. After 24 h the reaction was completed, which was determined by ^{11}B NMR spectroscopy. A slightly yellow solution was obtained and after removing the solvent a colorless solid was gained as product (Scheme 2).

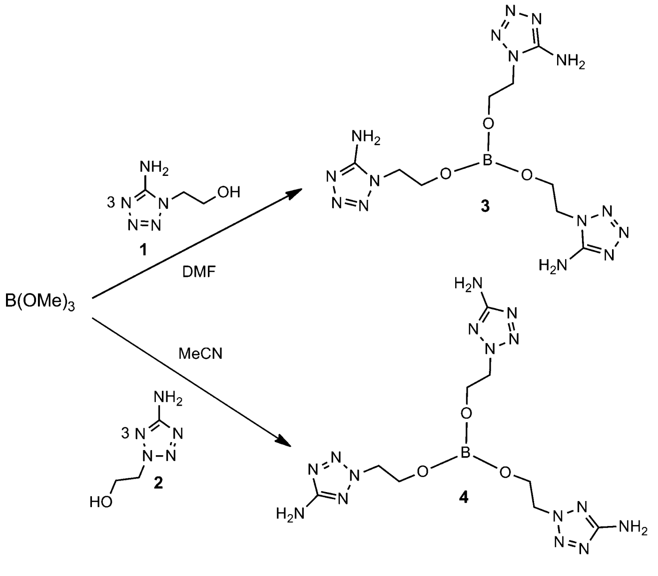

Scheme 2. Synthesis of compounds **3** and **4**.

Product **4** was synthesized by the reaction of compound **2** and trimethyl borate in acetonitrile at elevated temperature as well. Monitoring by ^{11}B NMR spectroscopy revealed that trimethyl borate was completely consumed after 24 h and product **4** was formed. Product **4** was obtained as a colorless solid.

Both products were obtained in high yields and after drying in high vacuum also in high purity.

Characterization

The products were fully characterized by ^{1}H-, ^{13}C- and ^{11}B NMR spectroscopy (in [D$_6$]DMSO) as well as elemental analysis, mass spectrometry, and infrared spectroscopy. The ^{11}B NMR spectra show for both compounds a shift at about 18 ppm. In the ^{13}C NMR spectra two shifts at around 59 ppm and around 52 ppm could be observed, which can be assigned to the ethyl carbon atoms. Furthermore, compounds **3** and **4** show peaks at δ = 159 ppm and 167 ppm corresponding to the 5-aminotetrazolyl ring carbon atoms. The ^{1}H NMR spectra reveal triplet signals at around 4.3 ppm and 3.8 ppm, which can be attributed to the protons of the ethyl group. The protons of the amino groups of both products were found to be at around 6.5 ppm. In the IR spectra of both products bands at 1325 cm^{-1} were observed, which can be assigned to the boron-oxygen stretching vibrations.

Both compounds did not hydrolyze by storing them at air atmosphere, as the ^{11}B NMR spectrum revealed, which was recorded after four weeks exposure to air.

Synthesis of Tris(ethyltetrazolyl) Borates (7 and 8)

The starting materials 1- and 2-(2-hydroxyethyl)tetrazole (**5** and **6**) were synthesized according to literature synthesis protocols.[12] From the reaction of tetrazole with sodium hydroxide and chloroethanol at high temperatures a mixture of compounds **5** and **6** was obtained, which were separated by column chromatography.

Two derivatives tris(1-ethyltetrazolyl) borate (**7**) and tris(2-ethyltetrazolyl) borate (**8**) were synthesized. Acetonitrile was chosen as solvent owing to its rather low boiling point of 82 °C and therefore easy removability and due to the good solubility of both isomers of hydroxyethyltetrazole. The starting materials were employed in stoichiometric amounts and the slightly yellow solution was stirred at room temperature for 24 h. The removal of the solvent gave compound **7** as a slightly yellow viscous liquid and compound **8** as a colorless solid (Scheme 3).

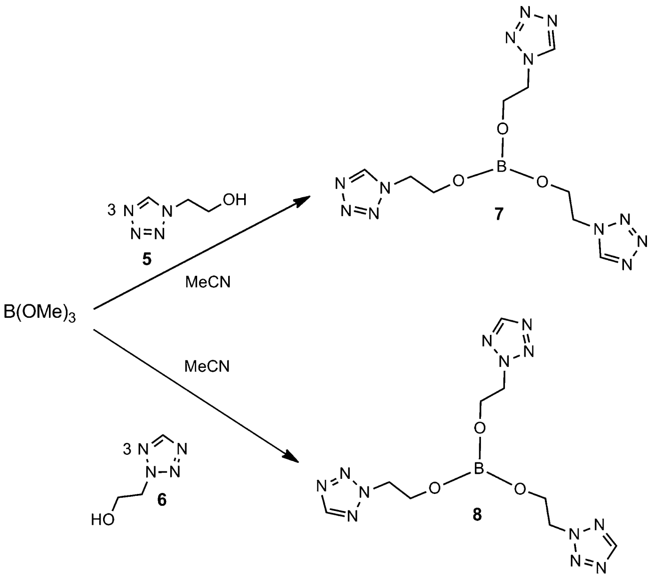

Scheme 3. Synthesis of compounds **7** and **8**.

Both products were obtained in high yields and after drying in high vacuum for 2 d compounds **7** and **8** were also gained in high purity.

Characterization

The products were fully characterized by ^{1}H-, ^{13}C-, and ^{11}B NMR spectroscopy (in $CDCl_3$) as well as elemental analysis, mass spectrometry, and infrared spectroscopy. The ^{11}B NMR spectra show for both compounds a shift at about 16 ppm. Signals at around 61 ppm and 52 ppm in the ^{13}C NMR spectrum of both products can be assigned to the carbon atoms of the ethyl groups. Compound **7** shows a peak at δ = 143 ppm and compound **8** exhibits a peak at δ = 152 ppm, which both can be attributed to the tetrazolyl ring carbon atoms. The ^{1}H NMR spectra of both products show triplet peaks at 4.7 ppm and 4.1 ppm corresponding to the ethyl group protons. The protons of the ring system are observable at around 8.6 ppm for both products. The IR spectra exhibit bands at 1325 cm^{-1} and 1328 cm^{-1} for compound **7** and **8**, respectively, which can be attributed to the boron-oxygen stretching vibrations.

The exposure to air moisture did not hydrolyze both compounds as the ^{11}B NMR indicated, which was recorded after four weeks.

*Synthesis of Tris(2-(3-nitro-1,2,4-triazolyl)ethyl) Borate (**10**)*

2-(3-Nitro-1*H*-1,2,4-triazol-1-yl)ethanol (**9**) is a literature known compound. For the preparation of compound **9**, *Kofman* et al.[14] recommend two synthetic pathways, either via the usage of 2-chloroethanol and sodium bromide in H_2O/DMF, affording only 25 % of **9**, or via a reaction of epoxyethanol in a sealed vessel to obtain after 40 h 55 % of the hydroxyethyl derivative **9**. However, following the first route did not afford any **9** at all and the second route was not further investigated due to the excessive costs of epoxyethanol. Nevertheless, a slight modification of the first variant led to the formation of 2-(3-nitro-1,2,4-triazol-1-yl)ethanol (**9**) in much higher yields compared to the original procedure.

An excess of **9** was reacted with boron trichloride in dry chloroform under reflux conditions resulting in the formation of product **10** (Scheme 4). During the reaction a yellow colored second liquid phase emerged from the colorless reaction solution and after 21.5 h the colorless supernatant with the excess **9** was removed. The remaining yellow liquid was repeatedly washed with dry chloroform and dichloromethane, stored under high vacuum. Compound **10** was finally obtained as colorless glassy solid.

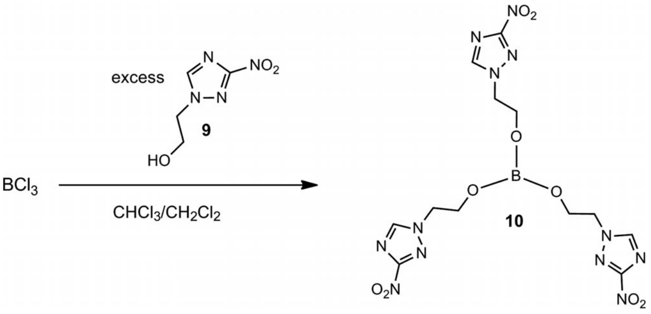

Scheme 4. Synthesis of compound **10**.

Tris(2-(3-nitro-1,2,4-triazol-1-yl)ethyl) borate (**10**) was characterized by ^{1}H-, ^{13}C- and ^{11}B NMR spectroscopy (in CD_3OD) as well as elemental analysis and vibrational spectroscopy. The ^{11}B chemical shift of compound **10** is found at δ = 17.6 ppm. The corresponding ^{13}C chemical shifts are at 163.8 (C–NO_2), 147.9 (CH), 60.5 (CH_2–O) and 54.8 (CH_2–N) ppm, whereas the ^{14}N NMR spectrum shows the signal of the nitro group at –22.6 ppm. The ^{1}H NMR spectrum shows the signal of the CH proton at a shift of 8.60 ppm while the two different CH_2 protons have a signal at δ = 4.41 ppm and 3.94 ppm, respectively. These signals show, as expected, a triplet splitting due to their coupling with each other. The IR vibrational spectrum shows a very strong absorbance at 1310 cm^{-1}, which resembles the B–O stretching vibration.

Energetic and Thermal Properties

The friction (FS), impact (IS), and electrostatic discharge (ESD) sensitivities as well as the melting (T_m) and decomposition (T_{dec}) temperatures were measured and are summarized in Table 1. All compounds are impact insensitive. The friction sensitivities are in the range from 80 N to 192 N, revealing that

Table 1. Energetic and thermal properties of boron ester compounds.

	3	**4**	**7**	**8**	**10**
FS /N	192	160	120	160	80
IS /J	>40	>40	>40	>40	>40
ESD /J	0.3	0.7	0.5	0.3	0.3
Grain size /µm	100–500	<100	–	100–500	<100
T_m /°C	232	234	–	226	145
T_{dec} /°C	262	253	204	258	178

the nitro compound **10** shows the highest friction sensitivity followed by compound **7**. Compound **3** shows the lowest friction sensitivity. The measurement of the sensitivity towards electric discharge (ESD) exhibits values between 0.3 J and 0.7 J. The decomposition temperatures are in the range from 178 °C to 262 °C.

II. Tetracoordinate Azolylborates

In order to obtain tetracoordinate azolylborates the reactions were performed at high temperatures in the high-boiling solvent diglyme and the starting materials were employed in stoichiometric amounts.

*Synthesis of Potassium Tetrakis(3-nitro-1,2,4-triazolyl)borate (**12**)*

3-Nitro-1,2,4-triazole was synthesized via a two-step reaction sequence according to literature.[15] As the successful reaction of potassium borohydride and 3-nitro-1,2,4-triazole requires a high temperature, high-boiling diglyme was used as the solvent. 3-Nitro-1,2,4-triazole and potassium borohydride were employed in stoichiometric amounts giving a yellow solution, from which a slightly yellow solid precipitated after heating for several hours. The reaction procedure was monitored by ^{11}B NMR spectroscopy. After 48 h, the obtained data already showed a complete consumption of potassium borohydride and the formation of the target compound **12**, which precipitated as a yellow solid (Scheme 5).

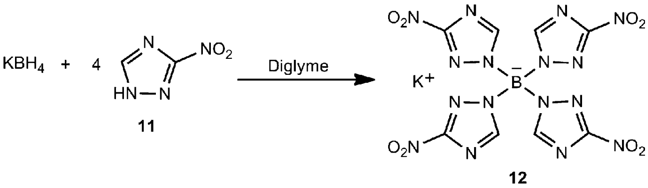

Scheme 5. Synthesis of **12**.

Filtration and washing with ethyl ether and drying at 60 °C for 2 d yielded a pure product in high quantity.

Characterization

The product was fully characterized by ^{1}H-, ^{13}C-, ^{14}N- and ^{11}B NMR spectroscopy ([D$_6$]DMSO) as well as elemental analysis, vibrational spectroscopy, and mass spectrometry.

The ^{11}B NMR spectrum shows a signal at –3.6 ppm. The corresponding ^{13}C chemical shifts are at δ = 164.1 ppm (C–NO$_2$) and 148.8 ppm (CH). In the ^{1}H NMR spectrum only the CH shift at δ = 8.30 ppm is visible. No signal between 3.0 ppm and 4.5 ppm, which is characteristic for the appearance of the BH$_2$ group peak, was observable. The ^{14}N NMR spectrum displayed the signals of the nitro groups at a shift of –22 ppm. The IR spectrum did not show any bands in the region of 2640–2350 cm^{-1}, where usually the BH- and BH$_2$-fragment vibrations appear, so that the formation of the tetracoordinate compound can be assumed. Additionally the B–N stretching vibrations were detected between 1433 cm^{-1} and 1337 cm^{-1}.[16]

The ^{11}B NMR spectrum of compound **12** was measured after four weeks exposure to air moisture and no decomposition of **12** could be observed.

*Synthesis of Potassium Bis(4,4′,5,5′-tetranitro-2,2′-bisimidazolyl)borate (**14**)*

The investigation of 4,4′,5,5′-tetranitro-2,2′-bisimidazole (TNBI) as energetic compound has been reported by *Klapötke* et al.[17] The synthesis compound **13** was accomplished according to the procedure described in literature.[17]

Product **14** was obtained by the reaction of two equivalents of TNBI and one equivalent of KBH$_4$, which were stirred in diglyme at reflux conditions (Scheme 6).

The reaction was monitored by ^{11}B NMR spectroscopy and after 72 h all potassium borohydride was completely consumed and only the product peak was observable. From a yellow solu-

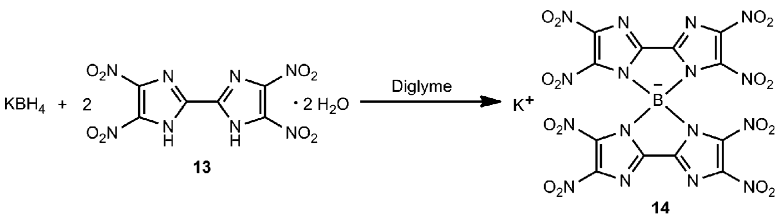

Scheme 6. Synthesis of **14**.

tion a brown solid precipitated and was isolated. After washing with ethyl ether and drying in high vacuum a brownish solid in high yield and purity was obtained. Although compound **13** was employed as hydrate, no traces of boric acid were visible in the ^{11}B NMR spectrum, so that it can be assumed, that the formed product is not highly sensitive towards hydrolysis. The exposure to air moisture did not lead to decomposition.

Characterization

Herein, characterization by ^{1}H-, ^{13}C-, ^{14}N-, and ^{11}B NMR spectroscopy ([D$_6$]DMSO) as well as elemental analysis and IR spectroscopy was performed. In the ^{11}B NMR spectrum one signal at 7.2 ppm is observable. The ^{13}C NMR spectrum shows two shifts at δ = 140.9 ppm and 139.1 ppm, which can assigned to the C–NO$_2$ groups and CH groups, respectively. Since in the ^{1}H NMR spectrum no signal is visible, the formation of compound **14**, which is coordinated by four nitrogen atoms of two 4,4′,5,5′-tetranitro-2,2′-bisimidazole moieties can be assumed. The ^{14}N NMR spectrum exhibits a signal at –28 ppm corresponding to the nitro groups. A further evidence for the formation of the tetracoordinate compound is the absence of IR vibrations in the region of 2640–2350 cm^{-1}, which are typical for B–H vibrations of BH and BH$_2$ groups. The B–N stretching vibrations are visible in the region from 1460 cm^{-1} to 1330 cm^{-1}.[16]

Energetic and Thermal Properties

The energetic and thermal properties such as the friction (FS), impact (IS), and electrostatic discharge (ESD) sensitivities as well as the melting (T_m) and decomposition temperatures (T_{dec}) of compounds **12** and **14** are summarized in Table 2. Both compounds are neither friction nor impact sensitive. Also both compounds are insensitive towards electrostatic discharge and show high decomposition temperatures of 303 °C and 230 °C.

Table 2. Energetic and thermal properties of tetracoordinate borate compounds.

	12	**14**
FS /N	>360	>360
IS /J	>40	>40
ESD /J	1.5	1.0
Grain size /µm	100–500	<100
T_m /°C	–	–
T_{dec} /°C	303	230

Calculation of ^{11}B NMR Chemical Shifts

As additional verification of the analytical data, the ^{11}B NMR chemical shifts of compounds **12** and **14** were calculated and compared to the experimental data.

In order to compute the ^{11}B NMR chemical shifts for various high-nitrogen boron compounds, the isotropic magnetic shielding were computed using the GIAO (Gauge-Independent Atomic Orbital) method implemented in G03.[18,19] The structures were fully optimized and the frequencies calculated (NIMAG = 0) at MPW1PW91/aug-cc-pVDZ level of theory. Subsequently, the NMR shielding tensors were calculated at the same level of theory using the GIAO method[19]. Table 3 summarizes the computed isotropic magnetic shielding and relative ^{11}B NMR chemical shifts (ppm) referenced to $BF_3\cdot Et_2O$.

The comparison of the calculated values with the experimentally determined shifts shows a very good accordance for potassium tetrakis(3-nitro-1,2,4-triazolyl)borate (**12**). In the case of bis(4,4′,5,5′-tetranitro-2,2′-bisimidazolyl)borate (**14**) the calculated and experimental values do not concur. The difference between the calculated and the experimentally measured values could probably be due to coordination effects of 4,4′,5,5′-tetranitro-2,2′-bisimidazole on the boron atom (Table 3).

Pyrotechnical Formulations

The replacement of toxic and environmentally hazardous barium nitrate by a green-burning boron-containing compound was investigated. The boron ester **3** was chosen due to its thermal stability and the lowest friction and impact sensitivity among the boron esters. Three pyrotechnic formulations containing compound **3** as green colorant were investigated and compared to the US Army's in-service green burning composition M125A1 (Ba-control) (Table 4). The pyrotechnical compositions were prepared by mixing all substances, except the binder, in a mortar. Afterwards the binder, a solution of 25 % vinyl alcohol acetate resin (VAAR), was added. After drying in high vacuum for 3 h the mixtures were grinded again. Pellets of 0.6 g each were pressed using a consolidation dead load

Table 3. Computed isotropic magnetic shieldings (GIAO method[18,19] MPW1PW91/aug-cc-pVDZ), and relative ^{11}B chemical shifts /ppm referenced to $BF_3\cdot Et_2O$.

Compound	–*E* /a.u.	NIMAG	Point Group	δ = ^{11}B /ppm calcd. isotr. shielding	δ = ^{11}B /ppm calcd. (ref. to $BF_3\cdot Et_2O$)	δ = ^{11}B /ppm, exp. (ref. to $BF_3\cdot Et_2O$)
$BF_3\cdot Et_2O$	558.164166	0	C_1	+110.0	0.0	0.0
BH_4^-	27.246888	0	T_d	+159.0	–49.0	–41.6[20]
$B(OH)_3$	252.468079	0	C_{3h}	92.4	+17.6	18.4–19.6[21]
$B(OH)_4^-$	328.333947	0	S_4	107.9	+2.1	+1.1[21]
12	1809.431116	0	S_4	113.6	–3.6	–3.6
14	2560.937467	0	C_1	113.1	–3.1	+7.2

of 2000 kg. The pellets were dried overnight at ambient temperature. The controlled burn down was filmed with a digital video camera recorder (SONY, DCR-HC37E). The performance of each composition was evaluated with respect to color emission, smoke generation, and the amount of solid residues. Spectrometric measurements were performed using a HR2000+ES spectrometer with an ILX511B linear silicon CCD-array detector and included software from Ocean Optics with a detector-sample distance of 1 m. The dominant wavelength and spectral purity was measured based on the 1931 CIE method using illuminant C as the white reference point. Five samples were measured for each formulation and all given values are averaged based on the full burn of the mixture. Ammonium dinitramide (ADN) and ammonium nitrate were used as the oxidizers and magnesium and amorphous boron as fuels, respectively.

Table 4. US Army's composition M125A1.

	$Ba(NO_3)_2$ /wt-%	Mg /wt-%	PVC /wt-%	VAAR /wt-%
Ba-control	46	33	16	5

The barium control M125A1 was mixed in a small-scale (0.6 g) and the color properties as well as thermal and energetic properties were measured and are summarized in Table 4, Table 5, and Table 6.

Table 5. US Army's composition M125A1.

	Burn time /s	Dw /nm	Sp /%	LI /cd	LE /(cds)g^{-1}
Ba-control	3	558	75	390	1950

Table 6. US Army's composition M125A1.

	Impact /J	Friction /N	Grain size /μm	T_{dec} /°C
Ba-control	15	360	<100	258

Table 7 summarizes the content of formulations 1–3 using compound **3** as colorant. Formulation 1 contains ammonium nitrate as the oxidizer and formulations 2 and 3 contain ammonium dinitramide (ADN). Formulations 1 and 3 comprise boron and magnesium as fuels, whereas formulation 2 contains only magnesium as fuel. All three formulations burned with a green flame color and no smoke and residues could be observed.

Table 7. Formulations 1–3 /wt-% containing compound **3**.

	3	NH_4NO_3	ADN	Mg	B	VAAR
1	24	60	–	8	3	5
2	37	–	50	8	–	5
3	34	–	50	8	3	5

In Table 8 the color performance values are shown. As can be seen formulation 3 achieved the highest luminous intensity of 80 % exceeding that of the barium control (Table 5). Formulation 1 shows the lowest spectral purity of 70 % and the lowest luminous intensity of 60 cd using NH_4NO_3 as the oxidizer. The highest luminous intensity of 130 cd revealed formulation 3.

Table 8. Color performance of formulations 1–3.

	Burn time /s	Dw /nm	Sp /%	LI /cd	LE /(cds)g^{-1}
1	4	565	70	60	400
2	4	562	72	73	487
3	3	559	80	130	650

The impact and friction sensitivities as well as the decomposition temperatures were determined and are summarized in Table 9. Formulation 1 is neither impact nor friction sensitive, whereas formulations 2 and 3 are both impact and friction sensitive. Formulation 3 containing boron and magnesium shows higher impact sensitivity than formulation 2 containing no boron. As expected the highest decomposition temperature exhibits formulation 1. Formulations 2 and 3 reveal similar decomposition temperatures (Table 9).

Table 9. Energetic and thermal properties of formulations 1–3.

	Impact /J	Friction /N	Grain size /μm	T_{dec} /°C
1	>40	>360	<100	230
2	35	324	<100	174
3	10	324	<100	170

Conclusions

Several energetic boron esters tris(1-ethyl-5-aminotetrazolyl) borate (**3**), tris(2-ethyl-5-aminotetrazolyl) borate (**4**), tris(1-ethyltetrazolyl) borate (**7**), tris(2-ethyltetrazolyl) borate (**8**), and tris(2-(3-nitro-1,2,4-triazolyl)ethyl) borate (**10**) as well as the tetracoordinate azolyl borates potassium tetrakis(3-nitro-1,2,4-triazolyl)borate (**12**) and potassium bis(4,4′,5,5′-tetranitro-2,2′-bisimidazolyl)borate (**14**) were synthesized and characterized. The ^{11}B NMR shifts of the azolyl borates were calculated and compared to the experimental values. All compounds are stable at air atmosphere and do not hydrolyze. The boron esters are impact insensitive but friction sensitive, whereas the azolyl borate compounds are neither impact nor friction sensitive. Additionally all compounds show high decomposition temperatures. Compound **3** was tested as green colorant in pyrotechnic mixtures. Formulation 3 containing compound **3**, ADN, boron, and magnesium showed the best color properties among the investigated formulations. The spectral purity of formulation 3 was found to be higher than that of the barium control formulation.

Experimental Section

CAUTION! The compounds described in this work are potential explosives, which are sensitive to environmental stimuli such as impact, friction, heat, or electrostatic discharge. No issues in the handling of these materials were encountered, but appropriate precautions and proper protective measures (safety glasses, face shields, leather coat, Kevlar gloves, and ear protectors) should be taken when preparing and manipulating these materials.

All syntheses were performed in a dry argon atmosphere using standard vacuum line techniques and dry solvents. All reagents and solvents were purchased from Sigma-Aldrich, Fluka, and Acros Organics. Melting and decomposition points were measured with a Linseis PT10 DSC using heating rates of 5 °C min^{-1}, which were checked with a Büchi Melting Point B-450 apparatus. ^{1}H, ^{13}C, and ^{14}N NMR spectra were measured with a JEOL Eclipse 400, JEOL Eclipse 270, or JEOL EX400 instrument at an ambient temperature of 25 °C if not stated otherwise. All chemical shifts are quoted in ppm relative to TMS (^{1}H, ^{13}C), nitromethane (^{14}N), or boron trifluoro etherate (^{11}B) as external standards. Infrared spectra were measured with a Perkin-Elmer Spectrum BX-FTIR spectrometer with a Smiths DuraSampl IR-ATR unit. Elemental analyses were performed with an Elementar Vario EL or an Elementar Vario EL micro cube. Mass spectra were measured with a JEOL MS station JMS 700 instrument. The impact and friction sensitivity was determined using a BAM drophammer and a BAM friction tester.[22] The sensitivities of the compounds are indicated according to the UN Recommendations on the Transport of Dangerous Goods (+):[22] impact: insensitive $>$ 40 J, less sensitive $>$ 35 J, sensitive $>$ 4 J, very sensitive $<$ 4 J; friction: insensitive $>$ 360 N, less sensitive = 360 N, sensitive $<$ 360 N $>$ 80 N, very sensitive $<$ 80 N, extreme sensitive $<$ 10 N.

Tris(1-ethyl-5-aminotetrazolyl) Borate (3): 1-(2-Hydroxyethyl)-5-aminotetrazole (0.50 g, 3.87 mmol) was dissolved in DMF (40 mL), and trimethyl borate (0.15 mL, 1.29 mmol) was added. The solution was stirred at reflux conditions for 24 h. After removing the solvent in vacuo and washing with ethyl ether (100 mL) a colorless solid (0.41 g, 80 %) was obtained. **IR** (ATR): $\tilde{\nu}$ = 3317 (s), 3146 (s), 2964 (w), 2941 (m), 2886 (w), 2740 (w), 1663 (s), 1596 (s), 1486 (w), 1438 (w), 1396 (w), 1388 (w), 1332 (w), 1290 (w), 1276 (w), 1243 (w), 1122 (w), 1100 (w), 1069 (m), 1035 (m), 983 (w), 949 (w), 860 (w), 779 (w), 745 (w), 698 (w) cm^{-1}. **^{11}B NMR** ([D$_6$]DMSO): δ = 18.5 (1B) ppm. **^{13}C NMR** ([D$_6$]DMSO): δ = 155.8 (3C, C–NH$_2$), 58.8 (3C, C–H$_2$), 47.1 (3C, C–H$_2$) ppm. **^{1}H NMR** ([D$_6$]DMSO): δ = 6.51 (t, 6 H, NH$_2$), 4.16 (t, 6 H, CH$_2$), 3.78 (t, 6 H, CH$_2$) ppm. **EA**: $C_9H_{18}N_{15}O_3B$ (395.15): calcd. N 53.17, C 27.36, H 4.59 %; found N 51.92, C 27.55, H 4.83 %. **MS**: *m/z* (DCI$^+$): 267.2 [M-OCH$_2$CH$_2$(N$_4$CNH$_2$)]$^+$. **IS**: >40 J (grain size 100–500 µm). **FS**: 192 N (grain size 100–500 µm). **ESD**: 0.3 J (grain size 100–500 µm). **DSC**: 262 °C (dec.).

Tris(2-ethyl-5-aminotetrazolyl) Borate (4): 2-(2-Hydroxyethyl)-5-aminotetrazole (0.50 g, 3.87 mmol) was dissolved in acetonitrile (40 mL), and trimethyl borate (0.15 mL, 1.29 mmol) was added. The yellow solution was stirred at reflux conditions for 24 h. After removing the solvent in vacuo and recrystallization from acetonitrile a colorless solid (0.37 g, 73 %) was obtained. **IR** (ATR): $\tilde{\nu}$ = 3418 (s), 3333 (s), 3232 (s), 2961 (w), 2254 (w), 1624 (s), 1543 (s), 1477 (m), 1416 (s), 1360 (s), 1324 (s), 1266 (m), 1196 (s), 1070 (m), 1015 (m), 962 (w), 870 (w), 791 (m), 756 (m) cm^{-1}. **^{11}B NMR** ([D$_6$]DMSO): δ = 18.9 (1B) ppm. **^{13}C NMR** ([D$_6$]DMSO): δ = 167.1 (3C, C–NH$_2$), 59.0 (3C, C–H$_2$), 54.9 (3C, C–H$_2$) ppm. **^{1}H NMR** ([D$_6$]DMSO): δ = 6.54 (t, 6 H, NH$_2$), 4.42 (t, 6 H, CH$_2$), 3.82 (t, 6 H, CH$_2$) ppm. **EA**: $C_9H_{18}N_{15}O_3B$ (395.15): calcd. N 53.17, C 27.36, H 4.59 %; found N 50.04, C 26.91, H 4.91 %. **MS**: *m/z* (DEI$^+$): 267.2 [M-OCH$_2$CH$_2$(N$_4$CNH$_2$)]$^+$. **IS**: >40 J (grain size <100 µm). **FS**: 160 N (grain size <100 µm). **ESD**: 0.7 J (grain size <100 µm). **DSC**: 253 °C (dec.).

Tris(1-ethyltetrazolyl) Borate (7): 1-(2-Hydroxyethyl)tetrazole (0.30 g, 2.63 mmol) was dissolved in acetonitrile (30 mL), and trimethyl borate (0.10 mL, 0.88 mmol) was added. The slightly yellow solution was stirred at reflux conditions for 24 h. After removing the solvent in vacuo a yellow viscous liquid (0.20 g, 65 %) was gained as product. **IR** (ATR): $\tilde{\nu}$ = 3351 (m), 3135 (m), 2963 (w), 2902 (w), 2364 (w), 2336 (w), 1484 (m), 1414 (s), 1328 (s), 1268 (m), 1248 (m), 1170 (s), 1104 (s), 1075 (m), 1052 (m), 1025 (m), 966 (w), 869 (m), 720 (w), 680 (m) cm^{-1}. **^{11}B NMR** ([D$_6$]DMSO): δ = 16.9 (1B) ppm. **^{13}C NMR** ([D$_6$]DMSO): δ = 143.4 (3C, C–H), 60.2 (3C, C–H$_2$), 49.5 (3C, C–H$_2$) ppm. **^{1}H NMR** ([D$_6$]DMSO): δ = 8.71 (t, 3 H, C–H), 4.65 (t, 6 H, CH$_2$), 4.15 (t, 6 H, CH$_2$) ppm. **EA**: $C_9H_{15}N_{12}O_3B$ (350.11): calcd. N 48.00, C 30.88, H 4.32 %; found N 45.51, C 30.21, H 4.45 %. **MS**: *m/z* (DCI$^+$): 351.2 [M + H]$^+$. **IS**: >40 J (liquid). **FS**: 120 N (liquid). **ESD**: 0.5 J (liquid). **DSC**: 204 °C (dec.).

Tris(2-ethyltetrazolyl) Borate (8): 2-(2-Hydroxyethyl)tetrazole (0.30 g, 2.63 mmol) was dissolved in acetonitrile (30 mL), and trimethyl borate (0.10 mL, 0.88 mmol) was added. The slightly yellow solution was stirred at reflux conditions for 24 h and after removing the solvent in vacuo as product a colorless solid (0.26 g, 85 %) was obtained. **IR** (ATR): $\tilde{\nu}$ = 3141 (w), 2963 (w), 1476 (m), 1417 (s), 1362 (s), 1328 (s), 1282 (s), 1194 (m), 1133 (m), 1027 (s), 1009 (m), 874 (m), 698 (m) cm^{-1}. **^{11}B NMR** ([D$_6$]DMSO): δ = 16.3 (1B) ppm. **^{13}C NMR** ([D$_6$]DMSO): δ = 152.9 (3C, C–H), 61.3 (3C, C–H$_2$), 53.8 (3C, C–H$_2$) ppm. **^{1}H NMR** ([D$_6$]DMSO): δ = 8.51 (t, 3 H, C–H), 4.75 (t, 6 H, CH$_2$), 4.11 (t, 6 H, CH$_2$) ppm. **EA**: $C_9H_{15}N_{12}O_3B$ (350.11): calcd. N 48.00, C 30.88, H 4.32 %; found N 46.21, C 39.99, H 4.46 %. **IS**: >40 J (grain size 100–500 µm). **MS**: *m/z* (DEI$^+$): 237.2 [M-OCH$_2$CH$_2$N$_4$CH]$^+$. **FS**: 160 N (grain size 100–500 µm). **ESD**: 0.3 J (grain size 100–500 µm). **DSC**: 258 °C (dec.).

Tris(2-(3-nitro-1,2,4-triazolyl)ethyl) Borate (10): 2-(3-Nitro-1,2,4-triazol-1-yl)ethanol (711 mg, 4.50 mmol) was dissolved in dry chloroform (57 mL) and boron trichloride (1 M in dichloromethane, 1.00 mL, 1.00 mmol) was added. A fine milky precipitate emerged and the reaction mixture was heated to reflux conditions for 22.5 h. During this period emerging hydrogen chloride could be detected as ammonium chloride fog via aqueous ammonia and a second liquid phase (yellow) emerged from the colorless reaction solution. The colorless supernatant with the excess **9** was removed via a syringe and the remaining yellow liquid was repeatedly washed with dry chloroform, stored under high vacuum, washed again and stored under high vacuum afterwards. This procedure was repeated until first solidification was observable. The residue was dissolved in dry dichloro methane and the solvent was removed in vacuo to afford **10** as colorless solid (193 mg, 40 %). **IR** (ATR): $\tilde{\nu}$ = 3400 (w), 3128 (w), 2960 (w), 2714 (w), 1547 (s), 1501 (s), 1476 (w), 1410 (s), 1380 (m), 1362 (m), 1328 (s), 1310 (s), 1264 (m), 1199 (m), 1054 (m), 1038 (s), 1016 (w), 968 (w), 872 (w), 833 (s), 772 (w), 734 (w), 688 (w), 657 (w) cm^{-1}. **^{11}B NMR** (CD$_3$OD): δ = 17.6 (1B) ppm. **^{13}C NMR** (CD$_3$OD): δ = 163.8 (C–NO$_2$), 147.9 (C–H), 60.5 (C–O), 54.8 (C–N) ppm. **^{1}H NMR** (CD$_3$OD): δ = 8.60 (s, 1H, C–H), 4.41 (t, 2H, CH$_2$), 3.94 (t, 2H, CH$_2$) ppm. **^{14}N NMR** (CD$_3$OD): δ = –23 ppm. **EA**: $C_{12}N_{12}H_{15}O_9B$ (482.14): calcd. N 34.86, C 29.89 H 3.14 %; found N 33.48, C 29.52, H 3.17 %. **IS**: >40 J (grain size <100 µm). **FS**: 80 N (grain size <100 µm). **ESD**: 0.3 J (grain size <100 µm). **DSC**: 178 °C (dec.).

Potassium Tetrakis(3-nitro-1,2,4-triazol-1-yl)borate (12): Potassium borohydride (0.58 g, 10 mmol) was dissolved in dry diglyme (20 mL) and 3-nitro-1,2,4-triazole (4.6 g, 40 mmol) was added. The mixture was heated up to 160 °C and stirred at this temperature for 48 h, whereas a yellow precipitate was formed. After filtration and washing with ethyl ether the product **12** (80 %) was obtained. **IR** (ATR): $\tilde{\nu}$ = 3444 (w), 334 (w), 3130 (w), 3113 (w), 2964 (w), 2916 (w), 1732 (w), 1647 (w), 1552 (m), 1504 (s), 1432 (m), 1424 (m), 1413 (m), 1386 (m), 1359 (m), 1337 (m), 1303 (s), 1253 (w), 1221 (m), 1174 (s), 1109 (m), 1033 (m), 1105 (m), 1033 (m), 1018 (s), 925 (m), 905 (m), 887 (w), 842 (m), 835 (m), 782 (w), 750 (m), 734 (m), 725 (m), 695 (m), 657 (m) cm^{-1}. **^{11}B NMR** ([D$_6$]DMSO): δ = –3.6 (1B) ppm. **^{13}C NMR**

([D$_6$]DMSO): δ = 151.1 (4C, C–H), 164.9 (4C, C–NO_2) ppm. **^{1}H NMR** ([D$_6$]DMSO): δ = 8.62 (s, 4 H, C–H) ppm. **^{14}N NMR** ([D$_6$]DMSO): δ = –22 ppm. **EA**: $C_8H_4N_{16}O_8BK$ (502.13): calcd. N 44.63, C 19.14, H 0.80 %; found N 45.00, C 19.71, H 1.12 %. **IS**: >40 J (grain size 100–500 µm). **FS**: >360 N (grain size 100–500 µm). **ESD**: 1.5 J (grain size 100–500 µm). **DSC**: 303 °C (dec.).

Potassium Bis(4,4′,5,5′-tetranitro-2,2′-bisimidazolyl)borate (14): Potassium borohydride (0.03 g, 0.6 mmol) was dissolved in dry diglyme (10 mL) and 4,4′,5,5′-tetranitro-2,2′-bisimidazole (0.38 g, 1.2 mmol) was added. The yellow solution was heated to 160 °C and stirred at this temperature for 72 h, whereas a brown precipitate was formed. After filtration and washing with ethyl ether the product (73 %) was obtained as a brownish solid. **IR** (ATR): ṽ = 3262 (w), 1746 (m), 1682 (m), 1532 (m), 1514 (m), 1452 (m), 1431 (m), 1350 (m), 1300 (m), 1199 (m), 1106 (s), 979 (w), 927 (w), 858 (w), 808 (m), 757 (m) cm^{-1}. **^{11}B NMR** ([D$_6$]DMSO): δ = 7.2 (1B) ppm. **^{13}C NMR** ([D$_6$]DMSO): δ = 139.1 (4C, C–C), 140.9 (8C, C–NO_2) ppm. **^{14}N NMR** ([D$_6$]DMSO): δ = –28 ppm. **EA**: $C_{12}N_{16}O_{16}BK$ (674.14): calcd. N 33.24, C 21.38 %; found N 31.23, C 21.00 %. **IS**: >40 J (grain size <100 µm). **FS**: >360 N (grain size <100 µm). **ESD**: 1.0 J (grain size <100 µm). **DSC**: 230 °C (dec.).

Acknowledgements

Financial support of this work by the Ludwig-Maximilian University of Munich (LMU), the U.S. Army Research Laboratory (ARL) under grant no. W911NF-09–2-0018, the Armament Research, Development and Engineering Center (ARDEC) under grant no. W911NF-12–1-0467, and the Office of Naval Research (ONR) under grant nos. ONR.N00014–10–1-0535 and ONR.N00014–12–1-0538 is gratefully acknowledged. The authors acknowledge collaborations with *Dr. Mila Krupka* (OZM Research, Czech Republic) in the development of new testing and evaluation methods for energetic materials and with *Dr. Muhamed Suceska* (Brodarski Institute, Croatia) in the development of new computational codes to predict the detonation and propulsion parameters of novel explosives. The authors are indebted to and thank *Drs. Betsy M. Rice* and *Brad Forch* (ARL, Aberdeen, Proving Ground, MD) for many inspired discussions. The Cusanuswerk is gratefully acknowledged for the award of a PhD scholarship (*M. Rusan*).

References

[1] a) J. C. Poret, J. J. Sabatini, *J. Energ. Mater.* **2013**, *31*, 27; b) J. A. Conkling, C. J. Mocella, *Chemistry of Pyrotechnics: Basic Principles and Theory*, 2nd ed, **2011**, Boca Raton, FL: Taylor and Francis Group; c) T. M. Klapötke, G. Steinhauser, *Angew. Chem. Int. Ed.* **2008**, *47*, 3330.

[2] a) J. J. Sabatini, J. C. Poret, R. N. Broad, *Angew. Chem. Int. Ed.* **2011**, *50*, 4624; b) R. M. Blunt, P. J. Keitel, US Pat. US 3453157, **1969**.

[3] T. M. Klapötke, B. Krumm, R. Moll, *Chem. Eur. J.* **2013**, *19*, 12113.

[4] a) K. D. Edwards, G. H. Pearson, M. K. Woodrum, K. Niedenzu, *Inorg. Chim. Acta* **1992**, *194*, 81; b) R. Duggal, R. C. Mehrotra, *Inorg. Chim. Acta* **1980**, *43*, 179.

[5] V. Ernst, Master Thesis, Ludwig Maximilian University Munich, Germany **2008**.

[6] T. M. Klapötke, M. Rusan, J. Stierstorfer, *Proceedings of the 38th International Pyrotechnic Seminar*, Denver, CO, USA, **2012**, pp. 527.

[7] a) C. Pettinari, *Scorpionates II: Chelating Borate Ligands*, Dedicated to Swiatoslaw Trofimenko Imperial College Press, London, **2008**; b) S. Trofimenko, *Scorpionates: The Coordination Chemistry of Poly(pyrazolyl)borate Ligands* Imperial College Press, London, **1999**; c) T. J. Groshens, *J. Coord. Chem.* **2010**, *63*, 1882; d) C. J. Snyder, P. D. Martin, M. J. Heeg, C. H. Winter, *Chem. Eur. J.* **2013**, *19*, 3306; e) M. Pellei, F. Benetollo, G. G. Lobbia, S. Alidori, C. Santini, *Inorg. Chem.* **2005**, *44*, 846; f) Z. Zeng, B. Twamley, J. M. Shreeve, *Organometallics* **2007**, *26*, 1782–1787.

[8] S. Trofimenko, *J. Am. Chem. Soc.* **1966**, *88*, 1842.

[9] S. Trofimenko, *J. Am. Chem. Soc.* **1967**, *89*, 3170.

[10] D. E. Chavez, M. A. Hiskey, D. L. Naud, *J. Pyrotech.* **1999**, *10*, 17.

[11] a) K. O. Christe, R. Haiges, R. I. Wagner, C. J. Jones, *Synthesis of New High-Oxygen Carriers and Ditetrazinetetroxide (DTTO)*, Final Report for the Office of Naval Reasearch, **2008–2009**, Under Contr. N00014–08–1-0590; b) K. O. Christe, R. Haiges, G. Belanger-Chabot, M. Rahm, R. Wagner, W. Wilson, *ONR 6.1 Advanced Energetic Materials Program Review*, February 12–13, **2013**, CALTECH, Pasadena, CA and USC, Los Angeles, CA.

[12] W. G. Finnegan, R. A. Henry, *J. Org. Chem.* **1959**, *24*, 1565.

[13] R. A. Henry, W. G. Finnegan, *J. Am. Chem. Soc.* **1954**, *76*, 923.

[14] T. P. Kofman, G. Y. Kartseva, *Russ. J. Org. Chem.* **2001**, *37*, 707.

[15] A. Preimesser, Dipoma Thesis, Ludwig Maximilian University Munich, **2010**.

[16] G. Socrates, *Infrared and Raman Characteristic Group Frequencies – Tables and Charts*, 3rd ed., John Wiley & Sons, Chichester, UK **2004**.

[17] T. M. Klapötke, A. Preimesser, J. Stierstorfer, *Z. Anorg. Allg. Chem.* **2012**, *638*, 1278.

[18] *Gaussian 03, Revision A.1*, Frisch, M. J.; Trucks, G. W.; Schlegel, H. B.; Scuseria, G. E.; Robb, M. A.; Cheeseman, J. R.; Montgomery Jr., J. A.; Vreven, T.; Kudin, K. N.; Burant, J. C.; Millam, J. M.; Iyengar, S. S.; Tomasi, J.; Barone, V.; Mennucci, B.; Cossi, M.; Scalmani, G.; Rega, N.; Petersson, G. A.; Nakatsuji, H.; Hada, M.; Ehara, M.; Toyota, K.; Fukuda, R.; Hasegawa, J.; Ishida, M.; Nakajima, T.; Honda, Y.; Kitao, O.; Nakai, H.; Klene, M.; Li, X.; Knox, J. E.; Hratchian, H. P.; Cross, J. B.; Adamo, C.; Jaramillo, J.; Gomperts, R.; Stratmann, R. E.; Yazyev, O.; Austin, A. J.; Cammi, R.; Pomelli, C.; Ochterski, J. W.; Ayala, P. Y.; Morokuma, K.; Voth, G. A.; Salvador, P.; Dannenberg, J. J.; Zakrzewski, V. G.; Dapprich, S.; Daniels, A. D.; Strain, M. C.; Farkas, O.; Malick, D. K.; Rabuck, A. D.; Raghavachari, K.; Foresman, J. B.; Ortiz, J. V.; Cui, Q.; Baboul, A. G.; Clifford, S.; Cioslowski, J.; Stefanov, B. B.; Liu, G.; Liashenko, A.; Piskorz, P.; Komaromi, I.; Martin, R. L.; Fox, D. J.; Keith, T.; Al-Laham, M. A.; Peng, C. Y.; Nanayakkara, A.; Challacombe, Gill, P. M. W.; Johnson, B.; Chen, W.; Wong, M. W.; Gonzalez, C.; Pople, J. A.; Gaussian, Inc., Pittsburgh PA, **2003**.

[19] a) K. Wolinski, J. F. Hilton, P. Pulay, *J. Am. Chem. Soc.* **1990**, *112*, 8251; b) J. L. Dodds, R. McWeeny, A. Sadlej, *Mol. Phys.* **1980**, *41*, 1419; c) R. Ditchfield, *Mol. Phys.* **1974**, *27*, 789; d) R. McWeeny, *Phys. Rev.* **1962**, *126*, 1028.

[20] H. C. Brown, T. P. Stocky, *J. Am. Chem. Soc.* **1977**, *99*, 8218.

[21] H. Nöth, B. Wrackmeyer, *NMR – Basic Principles and Progress (14), Nuclear Magnetic Resonance Spectroscopy of Boron Compounds*, Springer Verlag, Berlin, **1978**.

[22] a) *UN Recommendations on the Transport of Dangerous Goods, Model Regulations*, 15th ed., United Nations, New York a. Geneva, **2007**; b) http://www.bam.de.

Received: May 7, 2014

ChemPubSoc Europe
DOI: 10.1002/chem.201403451
CHEMISTRY
A European Journal
Full Paper

Pyrotechnics

Green Colorants Based on Energetic Azole Borates

Johann Glück, Thomas M. Klapötke,* Magdalena Rusan, and Jörg Stierstorfer[a]

Abstract: The investigation of green-burning boron-based compounds as colorants in pyrotechnic formulations as alternative for barium nitrate, which is a hazard to health and to the environment, is reported. Metal-free and nitrogen-rich dihydrobis(5-aminotetrazolyl)borate salts and dihydrobis(1,3,4-triazolyl)borate salts have been synthesized and characterized by NMR spectroscopy, elemental analysis, mass spectrometry, and vibrational spectroscopy. Their thermal and energetic properties have been determined as well. Several pyrotechnic compositions using selected azolyl borate salts as green colorants were investigated. Formulations with ammonium dinitramide and ammonium nitrate as oxidizers and boron and magnesium as fuels were tested. The burn time, dominant wavelength, spectral purity, luminous intensity, and luminous efficiency as well as the thermal and energetic properties of these compositions were measured.

Introduction

In recent years, the interest to develop environmentally friendly pyrotechnics has increased.[1] Particularly the research of non-polluting green-burning pyrotechnic colorants has been the focus. The most common green-light-emitting compound (which is however known to be a health hazard) is the highly water-soluble barium(II) nitrate. During combustion, the metastable green-light emitter BaCl in the presence of a chlorinated organic compound is formed.[2] Therefore, its replacement by less-toxic compounds is one major goal. Furthermore, widely used potassium perchlorate is banned as it is known to cause thyroid defects. As alternative green colorants, boron and boron compounds, which produce the metastable and green-light-emitting species BO_2 in the gas phase, are current objects of investigation. The boric ester trimethyl borate is reported to emit in the green region and was investigated in green-flame military signal flares.[3] Formulations containing amorphous boron and potassium nitrate were also investigated, but they are reported to be not convenient for practical use owing to too fast burning.[4] Other green-burning formulations based on boron carbide and potassium nitrate have been investigated by Sabatini et al. and are shown to be an alternative for amorphous boron and barium compounds.[4]

To create highly efficient formulations with a high performance, energetic boron-based colorants are considered to be suitable candidates. The combination of boron with nitrogen-rich energetic moieties in one molecule not only enhances the energetic character but could also reduce the amount of different additives. A further advantage of such nitrogen-rich boron-based colorants is the decrease of smoke during the combustion owing to the generation of nitrogen as the main decomposition product and thus could improve the brilliance.

Various azolyl borate compounds have been described. Trofimenko et al. reported the synthesis of many different poly(azolyl)borates, which are important ligands in coordination, organometallic, and bioinorganic chemistry.[5] Azolyl borates can be grouped into four classes, referring to their grade of substitution, such as the trihydro(azolyl)borates, the dihydrobis(azolyl)borates, the hydrotris(azolyl)borates, and the tetrakis(azolyl)borates. Several tetrakis(azolyl)borates have been reported by Trofimenko as well.[5] Also azolyl borates with a high nitrogen content are known and have been described.[6] The synthesis of triazolyl and nitrotriazolyl borates has been reported. Shreeve et al. synthesized imidazolium, triazolium, and tetrazolium dihydrobis(triazolyl)borate and hydrotris(triazolyl)borate salts, respectively, investigating them as ionic liquids.[6] The synthesis and characterization of potassium dihydro(3-nitro-1,2,4-triazolyl)borate and their zinc and cadmium complexes was reported by Pellei et al.,[7] as well as the copper phosphane complexes of dihydrobis(3-nitro-1,2,4-triazolyl)borate, which were examined for their cytotoxic properties.[8] Pellei et al. also reported the synthesis of nitrated poly(-pyrazolyl)borates.[9,10] Metal complexes of dihydrobis(tetrazolyl)borates have been described by Janiak and co-workers[11] and Winter and co-workers.[12] The synthesis of hydrotris(tetrazolyl)borates and its metal complexes was also performed by Winter et al. using metal borohydrides with tetrazoles at high temperatures in ether solvents.[13] The analogous dihydrobis(5-aminotetrazolyl)borates were reported by Groshens, investigating them as coordination ligands.[14]

Herein, the synthesis of several metal-free and nitrogen-rich dihydrobis(3-nitro-1,2,4-triazolyl)borate, diyhdrobis(3,5-dinitropyrazolyl)borate and dihydrobis(2,4-dinitroimiazolylborate salts as well as their characterization by NMR and vibrational spectroscopy, elemental analysis, and mass spectrometry is report-

---

[a] J. Glück, Prof. Dr. T. M. Klapötke, M. Rusan, Dr. J. Stierstorfer
Department of Chemistry
Ludwig-Maximilian University of Munich
Butenandtstrasse 5–13 (D), 81377 Munich (Germany)
Fax: +(49) 89-2180 77492
E-mail: tmk@cup.uni-muenchen.de

ed. All of the compounds were also examined for their thermal and energetic properties. The main goal of the synthesis and examination of these compounds is the investigation of their potential suitability as green burning colorants serving as barium substitutes. Therefore, selected borate salts have been tested in several pyrotechnic formulations and compared with the in-service US Army's M125A1 barium-containing formulation as well as with formulations using amorphous boron as green colorant. Their color performances also have been investigated by the measurement of the dominant wavelength, spectral purity, luminous intensity, and luminous efficiency. Additionally, the energetic and thermal properties of these formulations were determined as well.

Results and Discussion

All of the reactions start with the synthesis of the potassium azole borate salt by reacting KBH_4 with two equivalents of the azole in a high-boiling solvent. The synthesis of potassium dihydrobis(3-nitro-1,2,4-triazol-1-yl)borate (**2**) was first described by Pellei et al.[7] In this work, the synthesis of **2** was performed by reacting potassium borohydride with two equivalents of 3-nitro-1,2,4-triazole in dimethylacetamide. Potassium dihydrobis(3,5-dinitropyrazolyl)borate (**4**) and potassium dihydrobis(2,4-dinitroimidazlyl)borate (**6**) were synthesized according to the same procedure using potassium borohydride and two equivalents of 3,5-dinitropyrazole and 2,4-dinitroimidazole in DMAc and acetonitrile, respectively (Scheme 1). The starting materials 3-nitro-1,2,4-triazole (**1**), 3,5-dinitropyrazole (**3**), and 2,4-dinitroimidazole (**5**) were synthesized according to previously reported procedures (see the Experimental Section).

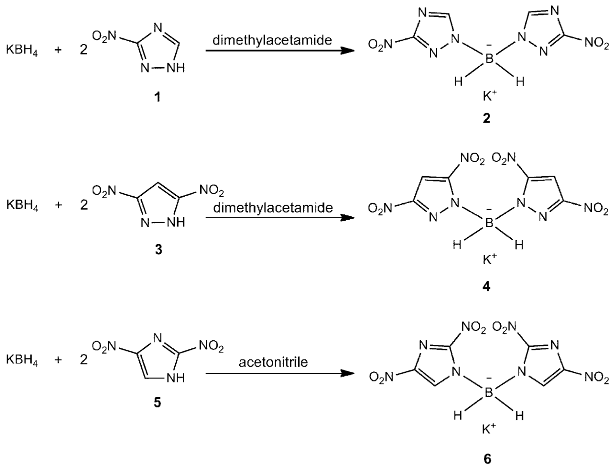

Scheme 1. Synthesis of potassium dihydrobis(azolyl)borate salts.

The potassium azolyl borate salts (**2**, **4**, **6**) served as starting materials and were transformed in a second step into the corresponding barium azolyl borate salts (**7**, **8**, **9**). The potassium salts were combined with barium perchlorate in stochiometric amounts in water and/or methanol, whereas low solubility potassium perchlorate was formed and filtered off (Scheme 2).

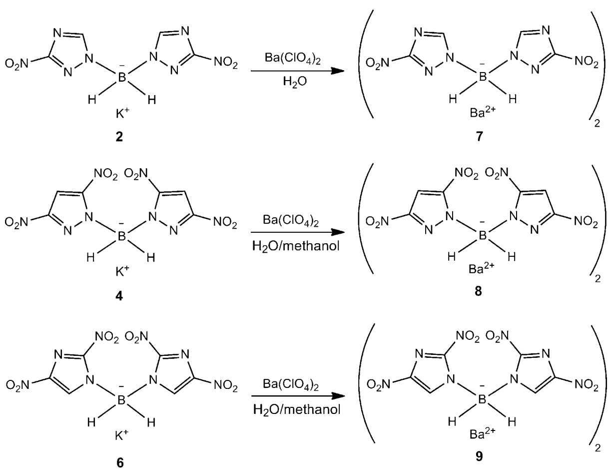

Scheme 2. Synthesis of barium dihydrobis(azolyl)borate salts.

The metal-free dihydrobis(3-nitro-1,2,4-triazol-1-yl)borate salts were synthesized by the reaction of the barium salt **7** and the corresponding nitrogen-rich sulfates in water. The driving force of these reactions is the formation of insoluble barium sulfate, which was filtered off, and as colorless products the guanidinium (**10**), aminoguanidinium (**11**), diaminoguanidinium (**12**), N-guanylurea (**13**), 5-aminotetrazolium (**14**), ammonium (**15**), *N*,*N*-dimethylguanidinium (**16**), hydroxylammonium (**17**), and hydrazinium (**18**) salts of dihydrobis(3-nitro-1,2,4-triazol-1-yl)borate were obtained in high yields (Scheme 3).

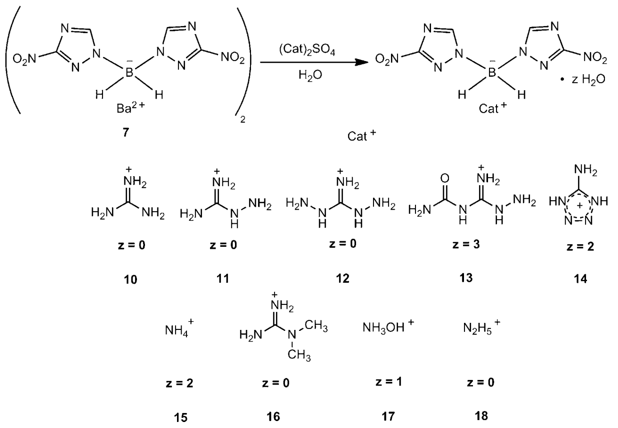

Scheme 3. Synthesis of metal-free dihydrobis(3-nitro-1,2,4-triazolyl)borate salts.

The metal-free dihydrobis(3,5-dinitropyrazolyl)borate and dihydrobis(2,4-dinitroimidazolyl)borate salts were synthesized according the same procedure, like the dihydrobis(3-nitro-1,2,4-triazolyl)borate salts. The barium compounds **4** and **6** were stirred with the sulfates in a water/methanol solution (70:30 ratio) at room temperature and then filtered off. After removing the solvent and recrystallization from methanol, slightly yellow (dihydrobis(3,4-dinitropyrazolyl)borate salts **19**-**23**) and yellow (dihydrobis(2,4-dinitroimidazolyl)borate salts **24**-**29**) products were obtained in good yields (Scheme 4 and Scheme 5).

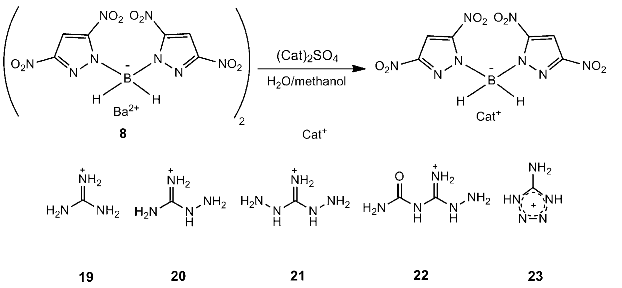

Scheme 4. Synthesis of metal-free dihydrobis(3,5-dinitropyrazolyl)borate salts.

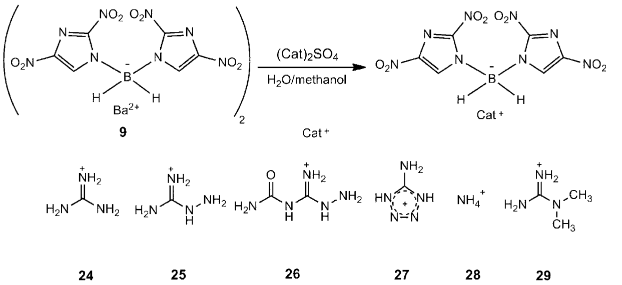

Scheme 5. Synthesis of metal-free dihydrobis(2,4-dinitroimidazolyl)borate salts.

Characterization

The ^{1}H, ^{13}C, ^{14}N and ^{11}B NMR spectra of all of the borate compounds (**2**, **4**, **6**–**29**) were measured in [D$_6$]DMSO.

In the ^{1}H NMR spectra of all of the borate compounds, a broad resonance at about 3.3 ppm is visible and can be assigned to the protons of the BH$_2$ group. A second resonance in the ^{1}H NMR spectra of all of the dihydrobis(3-nitro-1,2,4-triazolyl)borate compounds (**2**, **7**, **10**–**16**) appears at around 8.4 ppm, corresponding the proton on the 3-nitro-1,2,4-triazole ring. The ^{1}H NMR spectra of the dihydrobis(3,5-dinitropyrazolyl)borate anion of compounds **4**, **8**, and **19**–**23** show, apart from the BH$_2$ group resonance, a further signal at around 7.3 ppm, which can be assigned to the proton at the 3,5-dinitropyrazole ring. In the case of the dihydrobis(2,4-dinitroimidazolyl)borate compounds (**6**, **9**, **24**–**29**), the 2,4-dinitroimidazole ring proton appears in the ^{1}H NMR spectra at about 7.7 ppm. The guanidinium cation has resonances in the ^{1}H NMR spectra of all of the borate compounds at about 7.1 ppm, corresponding to the protons of the three NH$_2$ groups. The aminoguanidinium cation reveals a shift at about 4.6 ppm, which can be assigned to the nitrogen-bonded amino group. Two further signals at 7.3 ppm and 6.7 ppm, corresponding to the two carbon-connected amino groups, are visible. A further sharp signal at around 8.6 ppm can be assigned to the NH group. The ^{1}H NMR resonances of the diaminoguanidinium cation appear at around 7.1, 7.5, and 4.6 ppm, which are caused by the NH_2^+, NH, and NH$_2$ groups.[15] The N-guanylurea cation shows three signals at around 10.2, 8.0, and 7.3 ppm corresponding to the NH-, NH$_2$-, and NH_2^+ groups.[16] The ammonium cation shows a peak at 7.3 ppm, the hydroxylammonium cation reveals a broad peak at about 10 ppm, and the hydrazinium cation causes a resonance at 7.2 ppm. The 5-aminotetrazolium cation shows a signal at about 8 ppm for both the amino group and ring protons.[17] *N*,*N*-Dimethylguanidinium shows peaks at about 3 ppm and 7 ppm corresponding to the methyl groups and the amino groups, respectively.

The diyhdrobis(3-nitro-1,2,4-triazolyl)borate salts exhibit two signals in the ^{13}C NMR spectra at about 151 ppm and 165 ppm corresponding to the C–H and C–NO$_2$ groups of the 3-nitro-1,2,4-triazole ring system of the borate anion. The ^{13}C NMR spectra of the dihydrobis(3,5-dinitropyrazolyl)borates show two resonances at around 98 ppm and 147 ppm, which can be assigned to the dinitropyrazole ring carbon atoms of the borate anion. In the ^{13}C NMR spectra of the dihydrobis(2,4-dinitroimidazolyl)borate salts, three signals at about 131, 147, and 155 ppm corresponding to the dinitroimidazole ring carbon atoms of the borate anion are observable. The guanidinium cation exhibits in the ^{13}C NMR spectra a shift at about 158 ppm, the aminoguanidinium cation at about 159 ppm, and the diaminoguanidinium cation at around 160 ppm. The N-guanylurea cation exhibits two carbon signals at around 154 ppm and 155 ppm. 5-Aminotetrazolium cation shows a signal at about 152 ppm and *N*,*N*-dimethylguanidinium cation at about 38 ppm and 157 ppm.

The ^{11}B NMR spectra of dihydrobis(3-nitro-1,2,4-triazolyl)borate salts, of dihydrobis(3,5-dinitropyrazolyl)borate salts, and of dihydrobis(2,4-dinitroimidazolyl)borate salts show resonances at about −9, −6, and −10 ppm.

The NO$_2$ groups of dihydrobis(3-nitro-1,2,4-triazolyl)borate, dihydrobis(3,5-dinitropyrazolyl)borate, and dihydrobis(2,4-dinitroimidazolyl)borate anions show in the ^{14}N NMR spectra resonances in the region between −10 and −20 ppm.

The infrared spectra of all borate salts were taken. The assignments were carried according to previous reports.[18] The boron–hydrogen stretching vibration is visible between 2410 and 2450 cm^{-1} and the B–H in-plane deformation vibration for the borate anion of all of the compounds. Additionally, the borate anions show NO$_2$-group symmetric and asymmetric stretching vibrations at about 1300 cm^{-1} and 1500 cm^{-1}, respectively.

Energetic and Thermal Properties

The thermal behavior, impact and friction sensitivities, and also the sensitivity towards electric discharge of all salts were determined and are summarized in Tables 1-4. As can be seen from Table 1 and Table 2, the dihydrobis(3-nitro-1,2,4-triazolyl)borate salts are not friction-sensitive, and except the metal salts **2** and **7** and the 5-aminotetrazolium (**14**) and hydroxylammonium (**17**) salts all of the other salts are also not impact-sensitive. Except the 5-aminotetrazolium (**14**), hydroxylammonium (**17**), and hydrazinium (**18**) salts, all of the other salts show a decomposition temperatures that are higher than 200 °C (Tables 1 and 2). Table 3 shows the data of dihydrobis(3,5-dinitropyrazolyl)borates salts. All metal-free salts are friction-insensitive, whereas the potassium and barium salts show a friction sensi-

Table 1. Energetic and thermal properties of dihydrobis(3-nitro-1,2,4-triazolyl)borate compounds **2**, **7**, and **10**–**13**.

	2	**7**	**10**	**11**	**12**	**13**
formula	$C_4H_4N_8O_4BK$	$C_8H_8N_{16}O_8B_2Ba$	$C_5H_{10}N_{11}O_4B$	$C_5H_{11}N_{12}O_4B$	$C_5H_{12}N_{13}O_4B$	$C_6H_{18}N_{13}O_8B$
MW [g mol^{-1}]	278.04	615.20	299.02	314.03	329.05	411.10
Ω[a] [%]	−54.67	−41.61	−66.88	−66.23	−65.64	−56.43
N [%]	40.30	36.43	51.52	53.52	55.34	44.29
impact[b] [J]	4	5	>40	>40	>40	>40
friction[b] [N]	360	360	>360	>360	>360	>360
ESD [J]	1.2	1.2	1.5	1.5	1.5	1.0
grain size [µm]	<100	<100	100–500	100–500	100–500	100–500
T_{dehydr} (onset)[c] [°C]	–	–	–	–	–	98
T_{melt} (onset)[c] [°C]	–	–	–	161	–	–
T_{decomp} (onset)[c] [°C]	242	224	189	221	175	225

[a] Oxygen balance. [b] According to BAM drophammer/friction tester. [c] DSC/TGA (5 °C min^{-1}).

Table 2. Energetic and thermal properties of dihydrobis(3-nitro-1,2,4-triazolyl)borate compounds **14**–**18**.

	14	**15**	**16**	**17**	**18**
formula	$C_5H_{12}N_{13}O_6B$	$C_4H_{12}N_9O_6B$	$C_7H_{14}N_{11}O_4B$	$C_4H_{10}N_9O_6B$	$C_4H_9N_{10}O_4B$
MW [g mol^{-1}]	361.04	293.01	327.07	290.99	271.99
Ω[a] [%]	−50.96	−51.87	−90.50	−46.74	−58.82
N [%]	50.43	43.02	47.12	43.32	51.50
impact[b] [J]	10	40	>40	10	>40
friction[b] [N]	288	360	360	>360	360
ESD [J]	1.5	1.0	1.5	1.0	1.0
grain size [µm]	100–500	100–500	<100	100–500	100–500
T_{dehydr} (onset)[c] [°C]	92	89	-	87	-
T_{melt} (onset)[c] [°C]	–	–	114	–	64
T_{decomp} (onset)[c] [°C]	136	209	236	152	144

[a] Oxygen balance. [b] According to BAM drophammer/friction tester. [c] DSC/TGA (5 °C min^{-1}).

Table 3. Energetic and thermal properties of dihydrobis(3,5-dinitropyrazolyl)borate compounds **4**, **8**, and **19**–**23**.

	4	**8**	**19**	**20**	**21**	**22**	**23**
formula	$C_6H_4N_8O_8BK$	$C_{12}H_8N_{16}O_{16}B_2Ba$	$C_7H_{10}N_{11}O_8B$	$C_7H_{11}N_{12}O_8B$	$C_7H_{12}N_{13}O_8B$	$C_8H_{11}N_{12}O_9B$	$C_7H_8N_{13}O_8B$
MW [g mol^{-1}]	366.05	791.24	387.04	402.05	417.06	430.06	413.03
Ω[a] [%]	−41.52	−32.35	−51.67	−51.73	−51.79	−52.08	−44.55
N [%]	30.61	28.32	39.81	41.81	43.66	39.08	44.09
impact[b] [J]	3	5	>40	8	20	>40	>40
friction[b] [N]	216	180	>360	>360	>360	>360	>360
ESD [J]	1.0	0.4	1.5	1.5	1.5	1.5	1.0
grain size [µm]	100–500	100–500	<100	<100	100–500	<100	100–500
T_{melt} (onset)[c] [°C]	316	298	210	174	178	–	167
T_{decomp} (onset)[c] [°C]	344	342	318	346	231	353	344

[a] Oxygen balance. [b] According to BAM drophammer/friction tester. [c] DSC/TGA (5 °C min^{-1}).

tivity of 216 N and 180 N. The impact sensitivities vary from very sensitive (**4**), sensitive (**8**, **20**, **21**), to insensitive (**19**, **22**, **23**). The decomposition temperatures of all of the dihydrobis(3,5-dinitropyrazolyl)borate compounds, except the diaminoguanidinium compound, are higher than 300 °C (Table 3). All of the dihydrobis(2,4-dinitroimidazolyl)borate salts are impact- and friction-insensitive (Table 4). The decomposition temperatures are in the range between 165 °C and 349 °C as it is summarized in Table 4. The ESD values are between 1.0 and 1.5 J, except compound **8** (0.4 J), which can be classified as not sensitive.

Crystal Structures

Suitable single crystals of compounds (**11, 12**, and **16**) were measured by low-temperature X-ray diffraction. For all of the compounds, an Oxford Xcalibur3 diffractometer with a CCD area detector was employed for data collection using Mo$_{K\alpha}$ ra-

Table 4. Energetic and thermal properties of dihydrobis(2,4-dinitroimidazolyl)borate compounds **6**, **9**, and **24**–**29**.

	6	**9**	**24**	**25**	**26**	**27**	**28**	**29**
formula	$C_6H_4N_8O_8BK$	$C_{12}H_8N_{16}O_{16}B_2Ba$	$C_7H_{10}N_{11}O_8B$	$C_7H_{11}N_{12}O_8B$	$C_8H_{11}N_{12}O_9B$	$C_7H_8N_{13}O_8B$	$C_6H_8N_9O_8B$	$C_9H_{14}N_{11}O_8B$
MW [g mol^{-1}]	366.05	791.24	387.04	402.05	430.06	413.03	344.99	415.09
Ω[a] [%]	−41.52	−32.35	−51.67	−51.73	−52.08	−44.55	−44.06	−71.31
N [%]	30.61	28.32	39.81	41.81	39.08	44.09	36.54	37.12
impact[b] [J]	>40	>40	>40	>40	>40	>40	>40	>40
friction[b] [N]	>360	>360	>360	>360	360	>360	>360	>360
ESD [J]	1.5	1.5	1.5	1.5	1.5	1.5	1.0	1.5
grain size [μm]	100–500	100–500	<100	<100	<100	100-500	<100	100–500
T_{melt} (onset)[c] [°C]	–	–	–	–	120	–	200	162
T_{decomp} (onset)[c] [°C]	165	349	249	228	242	192	243	261

[a] Oxygen balance. [b] According to BAM drophammer/friction tester. [c] DSC/TGA (5 °C min^{-1}).

diation ($\lambda = 0.71073$ Å). The data collection and reduction were performed by using the CrysAlisPro software.[19] The structures were solved by direct methods (SIR92,[20] or Shelxs-97[21]) and refined by full-matrix least-squares on F^2 (Shelxl[22]) and finally checked using the platon software[23] integrated in the WinGX software suite.[24] The non-hydrogen atoms were refined anisotropically and the hydrogen atoms were located and freely refined. The absorptions were corrected by a Scale3 Abspack multiscan method.[25] In the case of the chiral space groups in the structures of **11** and **16**, "Friedel pairs" were merged using the SHELX command "MERG 3". Diamond2 plots are shown with ellipsoids set at the 50 % probability level.

Unfortunately we failed to obtain single crystals of borates linked to dinitroimidazole (**6**, **9**, **24**–**29**) and dinitropyrazole (**4**, **8**, **19**–**23**). However we were able to obtain single crystals of 3-nitro-1,2,4-triazolylborates **11**, **12**, and **16**, which are described herein. Details of the X-ray data collection and structure refinements are gathered in Table 5.

Crystal structures containing the dihydrobis(3-nitro-1,2,4-triazolyl)borate moiety have been reported before. Examples are potassium dihydrobis(3-nitro-1,2,4-triazolyl)borate[7] and a complex phosphine silver salt.[9] The molecular moieties of **11**, **12**, and **16** are depicted in Figure 1, Figure 2, and Figure 3. Compounds **11**, **12**, and **16** show comparable crystal structures and densities (**11** 1.56 g cm^{-3}, **12** 1.60 g cm^{-3}, **16** 1.52 g cm^{-3}) at 173 K without any solvent inclusion. Four cation/anion pairings are observed per unit cell crystallizing in different space groups (**11**: $Pca2_1$, **12**: $P2_1/n$, **16**: $Pna2_1$). They all show comparable anion structures, which are similar to those described for the potassium salt.[7] The averaged B–N distances of **11**, **12**, and (**16**) (each 1.56 Å) are identical with the value (1.56 Å) given for a B–N single bond.[26] Selected bond lengths, angles, and torsion angles are listed in the caption of Figure 1. The nitrotriazole moiety is almost planar, which has also been described for 3-nitro-1,2,4-triazole itself.[27] The cation structures are in agreement to values observed for bis(aminoguanidinium) and bis(diaminoguanidnium) sulfate[28] and dimethylguanidinium chloride.[29] Owing to the large numbers of N–H protons in the cations, all of the structures are dominated by several strong hydrogen bonds. The B–H hydrogen atoms do not participate in any non-classical hydrogen bonding.

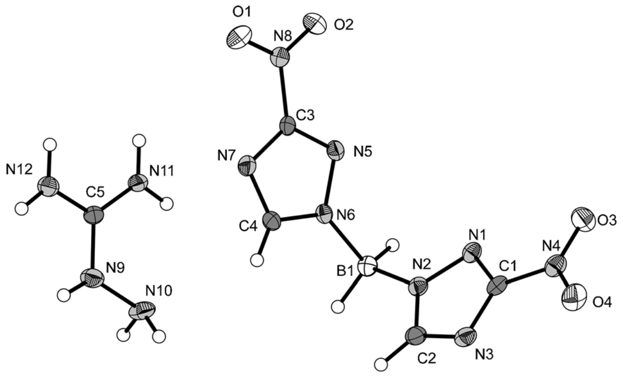

Figure 1. Representation of the molecular unit of **11** with atom labeling. Ellipsoids are set at 50 % probability; hydrogen atoms are shown as small spheres of arbitrary radius. Selected anion bond lengths [Å]: N2–B1 1.571(3), N6–B1 1.556(3), O1–N8 1.219(3), O2–N8 1.226(3), O3–N4 1.221(3), O4–N4 1.230(2), N5–C3 1.322(2), N5–N6 1.366(2), N3–C2 1.329(3), N3–C1 1.339(3), N8—C3 1.454(3), N1—C1 1.324(3), N1—N2 1.364(3), N4—C1 1.445(3), N7—C4 1.328(3), N7—C3 1.337(3), N2—C2 1.337(3), N6—C4 1.338(3); selected anion angles [°]: C2–N2–B1 128.2(2), N1–N2–B1 123.3(2), C2–N3–C1 100.6(2), C1–N1–N2 101.6(2), O3–N4–O4 123.5(2), O3–N4–C1 119.0(2), O4–N4–C1 117.5(2), C2–N2–N1 108.4(2), N3–C2–N2 112.3(2), N2–B1–H1B 106.6(13), H1A–B1–H1B 118.1(17); selected anion torsion angles [°]: O3–N4–C1–N1 −3.4(3), N1–N2–B1–N6 −80.2(2), B1–N2–C2–N3 −176.9(2).

Pyrotechnic Formulations

To replace toxic and environmentally hazardous formulations containing barium nitrate as green-burning coloring agent, investigations on boron-containing colorants were performed. Several pyrotechnic formulations containing different nitrogen-rich and metal-free dihydrobis(azolyl)borate salts as green colorants were investigated and compared to the US Army's in-service green-burning composition M125A1 (**Ba-control**; Table 6). The pyrotechnical compositions were prepared by mixing all substances, except the binder, in a mortar. Then the binder, a solution of 25 % vinyl alcohol acetate resin (VAAR), was added. After drying in high vacuum for 3 h, the mixture was ground again. Pellets of 0.6 g each were pressed using a consolidation dead load of 2000 kg. The pellets were dried overnight at ambient temperature. The controlled burn down was filmed with a digital video camera recorder (SONY, DCR-

Table 5. Crystallographic data of **11**, **12**, and **16**.

Compound	**11**	**12**	**16**
formula	$C_5H_{11}BN_{12}O_4$	$C_5H_{12}BN_{13}O_4$	$C_7H_{14}BN_{11}O_4$
FW [g mol^{-1}]	314.07	329.09	327.10
crystal system	orthorhombic	monoclinic	orthorhombic
space group	$Pca2_1$ (No. 29)	$P2_1/n$ (No. 14)	$Pna2_1$ (No. 33)
color/habit	colorless block	colorless platelet	colorless block
size [mm]	0.11×0.14×0.18	0.10×0.10×0.30	0.09×0.10×0.17
a [Å]	22.2636(16)	4.5115(2)	16.0958(9)
b [Å]	4.2661(4)	16.1546(10)	18.4098(11)
c [Å]	14.0568(13)	18.7627(9)	4.8292(4)
α [°]	90	90	90
β [°]	90	90.447(4)	90
γ [°]	90	90	90
V [Å^3]	1335.1(2)	1367.41(12)	1430.99(17)
Z	4	4	4
ρ_{calcd} [g cm^{-3}]	1.563	1.599	1.518
μ [mm^{-1}]	0.131	0.134	0.123
F(000)	648	680	680
$\lambda_{MoK\alpha}$ [Å]	0.71073	0.71073	0.71073
T [K]	173	173	173
θ min, max [°]	4.7, 27.5	4.1, 26.0	4.4, 27.0
dataset h; k; l	−27:28; −4:5; −18:17	−5:5; −19:19; −23:23	−20:18; −10:23; −3:6
reflections collected	7265	9966	3871
independent reflections	1595	2685	1713
R_{int}	0.031	0.032	0.041
reflection obs.	1398	2243	1392
no. parameters	243	256	264
R_1 (obs)	0.0276	0.0332	0.0420
wR_2 (all data)	0.0589	0.0819	0.0829
S	1.03	1.06	1.07
residual density [e Å^{-3}]	−0.13, 0.12	−0.20, 0.18	−0.22, 0.20
device type	Oxford Xcalibur3 CCD	Oxford Xcalibur3 CCD	Oxford Xcalibur3 CCD
solution	SIR-92	SHELXS-97	SIR-92
refinement	SHELXL-97	SHELXL-97	SHELXL-97
absorption corr.	multi-scan	multi-scan	multi-scan
CCDC	1 001 407	1 001 408	1 001 409

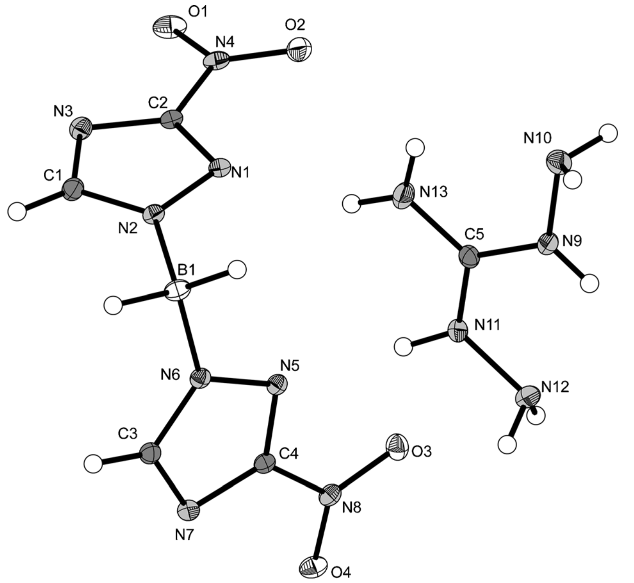

Figure 2. Representation of the molecular unit of **12** with atom labeling. Ellipsoids are set at 50 % probability; hydrogen atoms are shown as small spheres of arbitrary radius.

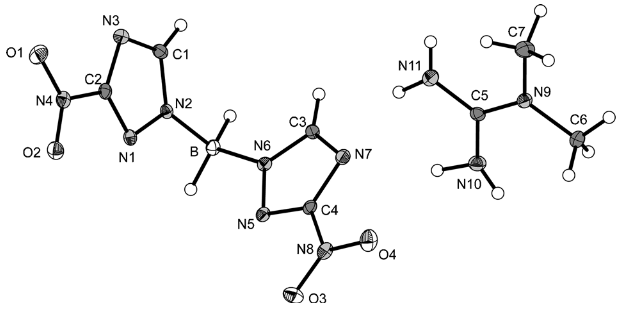

Figure 3. Representation of the molecular unit of **16** with atom labeling. Ellipsoids are set at 50 % probability; hydrogen atoms are shown as small spheres of arbitrary radius.

Table 6. US Army's composition M125A1.

	$Ba(NO_3)_2$ [wt %]	Mg [wt %]	PVC [wt %]	VAAR [wt %]
Ba-control	46	33	16	5

HC37E). The performance of each composition has been evaluated with respect to color emission, smoke generation, and the amount of solid residues. Spectrometric measurements were performed using a HR2000+ES spectrometer with an ILX511B linear silicon CCD-array detector and included software from Ocean Optics with a detector-sample distance of 1 meter. The dominant wavelength (Dw) and spectral purity (Sp) were measured based on the 1931 CIE method using illuminant C as the white reference point. Luminous intensities (LI) and luminous efficiencies (LE) were determined using pellets of 0.6 g each. Five samples were measured for each formulation and all of the given values are averaged based on the full burn of the mixture. Amorphous boron was used as fuel and green coloring agent. Ammonium dinitramide (ADN), ammonium nitrate, and magnesium were used as oxidizers and fuel, respectively. The thermal and energetic properties of the formulations were determined according to the above-mentioned methods.

The barium containing US Army's in-service M125 A1 green-burning formulation was used as the barium control formulation, consisting of 46% barium nitrate, 33% magnesium, 16% polyvinylchloride (PVC), and 5% binder (Table 6). Although the dominant wavelength and the spectral purity of this formulation have been described,[30] a small-scale M125A1 formulation (0.6 g) was prepared and measured, using VAAR binder and the above mentioned equipment. The Ba-control formulation revealed a burn time of 3 seconds, a dominant wavelength (Dw) of 558 nm, a spectral purity (Sp) of 75%, a luminous intensity (LI) of 390 cd, and a luminous efficiency (LE) of 1950 cdsg^{-1} (Table 7). The impact and friction sensitivity as well as the decomposition temperature were measured and are summarized in Table 8.

Table 7. Performances of US Army's composition M125A1.

	Burn time [s]	Dw [nm]	Sp [%]	LI [cd]	LE [cdsg^{-1}]
Ba-control	3	558	75	390	1950

Table 8. Energetic and thermal properties of US Army's composition M125A1.

	Impact [J]	Friction [N]	grain size [µm]	T_{decomp} [°C]
Ba-control	15	360	<100	258

As green burning barium nitrate substituent amorphous boron has been investigated. In Table 9, three formulations (**B_1**, **B_2**, and **B_3**) using ADN as oxidizer are shown. Additionally, formulation **B_3** contains magnesium.

The combustion of all three compositions revealed no smoke and no residues. The dominant wavelengths, spectral purities, luminous intensities, and luminous efficiencies are summarized in Table 10.

While the formulations **B_1** and **B_2** show lower spectral purities than the barium control formulation, the spectral purity of **B_3** with 80% exceeds that of the **Ba-control**. Also the luminous intensities of **B_1** and **B_2**, are far below the barium control (Table 10), which is most likely due to the absence of magnesium. Only the luminous intensity of **B_3** (320 cd) is comparable to the control.

Table 9. Formulations containing amorphous boron.

	B [wt%]	ADN [wt%]	Mg [wt%]	VAAR [wt%]
B_1	18	75	-	7
B_2	13	80	-	7
B_3	18	58	17	7

Table 10. Performances of formulations containing amorphous boron.

	Burn time [s]	Dw [nm]	Sp [%]	LI [cd]	LE [cdsg^{-1}]
Ba-control	3	558	75	390	1950
B_1	4	563	63	19	127
B_2	4	567	68	21	140
B_3	2	559	80	320	1067

The impact and friction sensitivities and the decomposition temperatures were measured (Table 11). All three compositions are impact- (10 J) and friction-sensitive (60 N and 324 N). The decomposition temperatures are below 200 °C.

Among the dihydrobis(3-nitro-1,2,4-triazolyl)borate salts, the diaminoguanidinium (**12**) and the N-guanylurea (**13**) salts have been investigated as colorants. Three formulations containing compound **12** and one formulation containing compound **13** and ADN, amorphous boron, magnesium, and binder are summarized in Table 12 and Table 13.

All four formulations (**DAGBNTr_1**, **DAGBNTr_2**, **DAGBNTr_3**, and **NGUBNTr**) burned smokeless and no residues remained. Except formulation **DAGBNTr_3** with a spectral purity of 75%, all of the other mixtures show spectral purities that are lower than that of the **Ba-control** (Table 14). Only the luminous in-

Table 11. Energetic and thermal properties of formulations containing amorphous boron.

	Impact [J]	Friction [N]	Grain size [µm]	T_{decomp} [°C]
B_1	10	60	<100	169
B_2	10	60	<100	184
B_3	10	324	<100	170

Table 12. Formulations containing compound **12**.

	12 [wt%]	ADN [wt%]	B [wt%]	Mg [wt%]	VAAR [wt%]
DAGBNTr_1	18	58	13	4	7
DAGBNTr_2	10	60	15	10	5
DAGBNTr_3	20	55	9	9	7

Table 13. Formulation containing compound **13**.

	13 [wt %]	ADN [wt %]	B [wt %]	VAAR [wt %]
NGUBNTr	25	50	18	7

Table 14. Performances of formulations containing compounds **12** and **13**.

	Burn time [s]	Dw [nm]	Sp [%]	LI [cd]	LE [(cds)g^{-1}]
Ba-control	3	558	75	390	1950
DAGBNTr_1	3	564	59	93	465
DAGBNTr_2	3	560	64	300	1500
DAGBNTr_3	3	560	75	212	1060
NGUBNTr	4	566	73	59	393

tensities of **DAGBNTr_2** and **DAGBNTr_3** are in the range of the barium control (Table 14). Compositions **DAGBNTr_1** and **NGUBNTr** show low luminous intensities and longer burn times.

As shown in Table 15, all of the formulations, except **DAGBNTr_1**, are sensitive towards impact but less or not sensitive towards friction. The decompositions temperatures are in the range between 169 °C and 183 °C.

Table 15. Energetic and thermal properties of formulations containing compounds 12 and 13.

	Impact [J]	Friction [N]	Grain size [μm]	T_{decomp} [°C]
Ba-control	15	360	<100	258
DAGBNTr_1	>40	>360	<100	183
DAGBNTr_2	1	252	<100	180
DAGBNTr_3	2	>360	<100	162
NGUBNTr	4	>360	<100	169

The following investigated formulations contain the guanidinium-, aminoguanidinium-, diaminoguanidinium-, N-guanylurea- and 5-aminotetrazolium dihydrobis(3,5-dinitropyrazolyl)borate salts as green colorants.

Two compositions containing compound **19**, ADN, boron, magnesium, and binder and one composition containing **19**, ammonium nitrate, magnesium, and binder were examined (Table 16). All three formulations showed a smokeless burndown without residues.

Table 16. Formulations containing compound **19**.

	19 [wt %]	ADN [wt %]	NH_4NO_3 [wt %]	B [wt %]	Mg [wt %]	VAAR [wt %]
GBDNP_1	25	50	–	9	9	7
GBDNP_2	25	50	–	–	18	7
GBDNP_3	25	–	50	–	18	7

As can be seen from Table 20, formulations **GBDNP_1** and **GBDNP_2** show similar spectral purities of 75 % and 72 % and luminous intensities of 180 cd and 210 cd. **GBDNP_2**, with an increased magnesium content, reveals a higher luminous intensity of 258 cd, as expected. The highest spectral purity of 79 % could be achieved by the mixture using ammonium nitrate and magnesium (**GBDNP_3**), and a long burn time of 9 s could be observed. However, the luminous intensity of 65 cd is rather low (Table 20).

In further two formulations, the aminoguanidinium dihydrobis(3,5-dinitropyrazolyl)borate (**20**) compound was employed as the colorant. In these formulations only the content of the salt and magnesium was differed (Table 17). Both mixtures burned smokeless and no residues could be observed. The spectral purities of 72 % and 71 % are lower than the **Ba-control**, showing 75 % (Table 20). Although composition **AGBDNP_1** contains only 5 % more of magnesium than **AGBDNP_2**, the luminous intensity of 258 cd is much higher than that of the second formulation with only 57 cd (Table 20).

Table 17. Formulations containing compound **20**.

	20 [wt %]	ADN [wt %]	B [wt %]	Mg [wt %]	VAAR [wt %]
AGBDNP_1	25	50	9	9	7
AGBDNP_2	30	50	9	4	7

The next two formulations DAGBDNP and 5-AtBDNP contain the borate salts 21 and 23, ADN, amorphous boron and binder of the same weight percent (Tables 18 and 19). A smokeless and residue-free combustion of both compositions could be observed. Although varying only the borate salt, the spectral purities are significantly different. While DAGBDNP shows a low spectral purity of only 51 %, composition 5-AtBDNP reveals a much higher spectral purity of 78 %, which also exceeds that of the barium control (Table 20). In contrast, the luminous intensities are similar with 58 cd and 55 cd and are quite low, which is most likely due to the absence of magnesium.

Comparing the formulations containing dihydrobis(3,5-dinitropyrazolyl)borates, the highest and barium control-exceeding spectral purities were achieved by the two formulations

Table 18. Formulation containing compound **21**.

	21 [wt %]	ADN [wt %]	B [wt %]	VAAR [wt %]
DAGBDNP	30	50	13	7

Table 19. Pyrotechnic composition containing compound **23**.

	23 [wt %]	ADN [wt %]	B [wt %]	VAAR [wt %]
5-AtBDNP	30	50	13	7

Table 20. Performances of formulations containing compounds **19**, **20**, **21**, and **23**.

	burn time [s]	Dw [nm]	Sp [%]	LI [cd]	LE [cdsg^{-1}]
Ba-control	3	558	75	390	1950
GBDNP_1	1	554	75	180	300
GBDNP_2	4	571	72	210	1400
GBDNP_3	9	567	79	65	975
AGBDNP_1	1	560	72	258	430
AGBDNP_2	2	555	71	57	190
DAGBDNP	2	559	51	58	193
5-AtBDNP	3	554	78	234	1170

GBDNP_3 and **5-AtBDNP**. The highest luminous intensity of 258 cd could be observed for composition **AGBDNP_1** (Table 20).

Except compositions **GBDNP 1** and **AGBDNP 2**, which show an impact sensitivity of 5 J and 30 J and can therefore be classed as sensitive, all other formulations containing a dihydrobis(3,5-dinitropyrazolyl)borate salt are less or not impact-sensitive (Table 21). Also all formulations (except **GBDNP_1**, which is friction-sensitive) are friction-insensitive. All of the formulations containing ADN exhibit decomposition temperatures that are lower than 200 °C; only the composition with NH_4NO_3 as oxidizer shows a decomposition temperature of 278 °C (Table 21).

Table 21. Energetic and thermal properties of formulations containing compounds **19**, **20**, **21** and **23**.

	Impact [J]	Friction [N]	Grain size [μm]	T_{decomp} [°C]
Ba-control	15	360	<100	258
GBDNP_1	5	324	<100	189
GBDNP_2	>40	>360	<100	180
GBDNP_3	>40	>360	<100	278
AGBDNP_1	>40	>360	<100	185
AGBDNP_2	30	>360	<100	183
DAGBDNP	>40	>360	<100	161
5-AtBDNP	40	>360	<100	142

It could be shown that formulations using amorphous boron and ADN reveal intensive green flame colors, but only the composition with additional magnesium exhibits higher spectral purity and comparable luminous intensity compared to the barium control formulation. However, these formulations are rather impact- and friction-sensitive. When adding a dihydrobis(azolyl)borate salt to such a formulation, the friction sensitivity is remarkably decreased. Only two formulations **DAGBNTr_2** and **GBDNP_1** are friction-sensitive. In the case of compositions using dihydrobis(3,5-dinitropyrazolyl)borates, the impact sensitivity is also decreased. Comparing dihydrobis(3-nitro-1,2,4-triazolyl)borate-containing formulations with dihydrobis(3,5-dinitropyrazolyl)borate-containing formulations, the latter show better color and sensitivity properties. Especially formulation **GBDNP 3** is noteworthy, which exhibits the highest spectral purity of 79 % among the dihydrobis(azolyl)borate-containing mixtures, an impact and friction insensitivity, and the highest decomposition temperature of 278 °C owing to the absence of ADN. However, a low luminous intensity of 65 cd and the longest burn time of 9 seconds were observed.

Conclusion

A series of dihydrobis(azolyl)borate salts was synthesized and characterized comprehensively by NMR and IR spectroscopy, elemental analysis, and mass spectrometry. Crystal structures were obtained of compounds **11**, **12**, and **16**. Pyrotechnic formulations were investigated employing selected dihydrobis(azolyl)borate salts as green colorants. Ammonium dinitramide and ammonium nitrate were used as oxidizers and boron and magnesium as fuels. The color properties were determined of all formulations and compared to the US Army's M125A1 formulation. Additionally, the thermal and energetic properties of all of the compositions were measured as well. The best-performing formulations regarding their color properties and insensitivity towards stimuli are **GBDNP_3** and **5-AtBDNP**.

Experimental Section

CAUTION! The compounds described in this work are potential explosives, which are sensitive to environmental stimuli such as impact, friction, heat, or electrostatic discharge. While we encountered no issues in the handling of these materials, appropriate precautions and proper protective measures (safety glasses, face shields, leather coat, Kevlar gloves, and ear protectors) should be taken when preparing and manipulating these materials.

All reagents and solvents were used as received (Sigma–Aldrich, Fluka, Acros Organics) if not stated otherwise. N-Guanylurea sulfate monohydrate, ammonium sulfate, hydroxylammonium sulfate, *N*,*N*-dimethylguanidinium sulfate and hydrazinium hydrogensulfate were purchased and used as received (Sigma–Aldrich, Fluka, Acros Organics). Guanidinium sulfate, aminoguanidinium sulfate, diaminoguanidinium sulfate, and 5-aminotetrazolium sulfate were synthesized by mixing the corresponding chloride salts[15] with silver sulfate in stoichiometric amounts in water. The mixtures were stirred at room temperature under exclusion of light for 15 min and then filtered off. After drying at ambient temperatures the products were obtained as colorless solids and were characterized by elemental analysis. 3,5-Dinitropyrazole[31] and 2,4-dinitroimidazole[32] were synthesized according to literature procedure. Melting and decomposition points were measured with a Linseis PT10 DSC using heating rates of 5 °C min^{-1}, which were checked with a Büchi Melting Point B-450 apparatus. ^{1}H, ^{13}C, and ^{14}N NMR spectra were measured with a JEOL Eclipse 400, JEOL Eclipse 270 or JEOL EX400 instrument at an ambient temperature of 25 °C if not stated otherwise. All chemical shifts are quoted in ppm relative to TMS (^{1}H, ^{13}C), nitromethane (^{14}N), or borontrifluoride etherate ok(^{11}B) as external standards. Infrared spectra were measured using a PerkinElmer Spectrum BX-FTIR spectrometer with a Smiths DuraSampl IR-ATR unit. Elemental analyses were performed with an Elementar Vario EL or an Elementar Vario EL micro cube. Mass spectra were measured on a JEOL MS station JMS 700 instrument. The impact and friction sensitivity was determined using a BAM drophammer and a BAM friction tester.[33] The sensitivities of the compounds are indicated according to the UN Recommendations on the Transport of Dangerous Goods (+):[33] impact: insensitive > 40 J, less sensitive > 35 J, sensitive > 4 J, very sensitive 4 J; friction: insensitive > 360 N, less sensitive = 360 N, sensitive < 360 N > 80 N, very sensitive < 80 N, extreme sensitive < 10 N.

Salts of dihydrobis(3-dinitro-1,2,4-triazolyl)borate

Potassium dihydrobis(3-nitro-1,2,4-triazolyl)borate (2): According to a previously reported method,[7] potassium borohydride (0.66 g, 12.2 mmol) was dissolved in *N*,*N*-dimethylacetamide (9 mL) and 3-nitro-1,2,4-triazole (4.17, 36.6 mmol) was slowly added. The reaction mixture was heated up to 160 °C and stirred at this temperature for 5 h. After cooling down to room temperature, chloroform (150 mL) was added to the solution and a slightly brownish precipitate was formed immediately and then filtered off. After recrystallization from acetone/diethyl ether (1:3), a colorless product (2.73 g, 82 %) was obtained. IR (ATR): $\tilde{\nu}=3368$ (w), 3133 (w), 2839 (w), 2470 (w), 2441 (w), 2285 (w), 1763 (w), 1634 (w), 1540 (s), 1495 (s), 1425 (m), 1396 (m), 1366 (w), 1334 (w), 1303 (s), 1207 (w), 1171 (s), 1149 (s), 1076 (w), 1036 (s), 1020 (m), 984 (w), 925 (w), 894 (m), 886 (w), 878 (m), 844 (s), 835 (s), 782 (w), 772 (w), 739 (w), 728 (m), 678 cm^{-1} (w); ^{1}H NMR ([D$_6$]DMSO): $\delta=3.32$ (br s, 2H, BH_2), 8.45 ppm (s, 2H, CH); ^{13}C NMR ([D$_6$]DMSO): $\delta=150.7$ (2C, C-H), 164.9 ppm (2C, C-NO_2); ^{14}N NMR ([D$_6$]DMSO): $\delta=-14$ ppm (2N, C-NO_2); ^{11}B NMR ([D$_6$]DMSO): $\delta=-9.4$ ppm (1B); EA: $C_4H_4N_8O_4BK$ (278.04): calculated N 40.30, C 17.28, H 1.45; found N 40.01, C 17.54, H 1.46. MS (FAB$^+$): *m/z* for K^+: calculated 39.10; found 39.0. MS (FAB$^-$): *m/z* for $C_4H_4N_8O_4B^-$: calculated 238.94; found 239.3. IS: 4 J (grain size < 100 μm). FS: 360 N (grain size < 100 μm). ESD: 1.2 J (grain size < 100 μm). DSC: 242 °C (decomp).

Barium dihydrobis(3-nitro-1,2,4-triazolyl)borate (7): Compound **2** (2.00 g, 7.19 mmol) was dissolved in water (40 mL), and barium perchlorate (1.21 g, 3.59 mmol) was then added. The solution was stirred at room temperature for 24 h whereas potassium perchlorate was formed and filtered off. The solvent was evaporated and a colorless solid (2.20 g, 52 %) was obtained. IR (ATR): $\tilde{\nu}=3355$ (w), 2436 (w), 2359 (w), 1738 (w), 1548 (s), 1502 (s), 1428 (m), 1397 (m), 1362 (w), 1336 (w), 1305 (s), 1214 (w), 1164 (s), 1142 (s), 1043 (m), 1027 (s), 878 (w), 838 (s), 725 cm^{-1} (m); ^{1}H NMR ([D$_6$]DMSO) $\delta=3.76$ (br s, 2H, BH_2), 8.42 ppm (s, 2H, CH); ^{13}C NMR ([D$_6$]DMSO): $\delta=150.2$ (2C, C-H), 164.2 ppm (2C, C-NO_2); ^{14}N NMR ([D$_6$]DMSO): $\delta=-23$ ppm (2N, C-NO_2); ^{11}B NMR ([D$_6$]DMSO): $\delta=-9.8$ ppm (1B); EA: $C_8H_8N_{16}O_8B_2Ba$ (615.20): calculated N 36.43, C 15.62, H 1.31; found N 33.81, C 15.24, H 1.38. MS (FAB$^+$): *m/z* for $C_4H_4N_8O_4BBa^+$: calculated 376.30; found 376.8. MS (FAB$^-$): *m/z* for $C_4H_4N_8O_4B^-$: calculated 238.94; found 239.0. IS: 5 J (grain size < 100 μm). FS: 360 N (grain size < 100 μm). ESD: 1.2 J (grain size < 100 μm). DSC: 224 °C (decomp).

General procedure for the synthesis of metal-free dihydrobis(3-nitro-1,2,4-triazolyl)borate salts

Compound **7** was dissolved in water and the corresponding sulfates were added in stoichiometric amounts. The formation of a colorless precipitate could immediately be observed. After stirring at room temperature for 10 min to complete the reaction, the mixture was filtered off and washed with water. After the evaporation of the solvent colorless solids were obtained.

Guanidinium dihydrobis(3-nitro-1,2,4-triazolyl)borate (10): A colorless solid (81 %) was formed as the product. IR (ATR): $\tilde{\nu}=3342$ (s), 3265 (s), 3177 (s), 2817 (w), 2478 (w), 2450 (w), 2283 (w), 1656 (s), 1547 (m), 1529 (m), 1482 (m), 1427 (w), 1418 (m), 1395 (m), 1367 (w), 1325 (w), 1304 (m), 1255 (w), 1212 (w), 1162 (m), 1147 (m), 1077 (s), 1040 (s), 1024 (s), 988 (m), 975 (m), 939 (w), 900 (w), 878 (w), 836 cm^{-1} (w); ^{1}H NMR ([D$_6$]DMSO): $\delta=3.35$ (br s, 2H, BH_2), 7.12 (s, 6H, 3·NH_2), 8.34 ppm (s, 2H, CH); ^{13}C NMR ([D$_6$]DMSO): $\delta=150.6$ (2C, C-H), 158.4 (1C, C-NH_2), 163.9 ppm(2C, C-NO_2); ^{14}N NMR ([D$_6$]DMSO): $\delta=-14$ ppm (2N, C-NO_2); ^{11}B NMR ([D$_6$]DMSO): $\delta=-9.4$ ppm (1B); EA: $C_5H_{10}N_{11}O_4B$ (299.02): calculated N 51.53, C 20.08, H 3.37; found N 51.01, C 20.32, H 3.26. MS (FAB$^+$): *m/z* for $CH_6N_3^+$: calculated 60.08; found 60.1. MS (FAB$^-$): *m/z* for $C_4H_4N_8O_4B^-$: calculated 238.94; found 239.3. IS: > 40 J (grain size 100–500 μm). FS: > 360 N (grain size 100–500 μm). ESD: 1.5 J (grain size 100–500 μm). DSC: 189 °C (decomp.).

Aminoguanidinium dihydrobis(3-nitro-1,2,4-triazolyl)borate (11): As product a colorless solid (87 %) was obtained. IR (ATR): $\tilde{\nu}=3476$ (w), 3422 (m), 3345 (w), 3148 (m), 3128 (m), 2474 (w), 2444 (w), 2364 (w), 2282 (w), 2040 (w), 1788 (w), 1668 (s), 1540 (s), 1498 (s), 1417 (m), 1394 (m), 1365 (m), 1343 (m), 1305 (s), 1261 (w), 1220 (w), 1212 (w), 1185 (m), 1168 (s), 1159 (s), 1071 (m), 1036 (s), 1022 (m), 985 (m), 942 (m), 896 (m), 882 (m), 834 (s), 750 (m), 720 (m), 652 cm^{-1} (s); ^{1}H NMR ([D$_6$]DMSO): $\delta=3.54$ (br s, 2H, BH_2), 4.66 (s, 2H, N-NH_2), 6.73 (s, 2H, C-NH_2) 7.25 (s, 2H, C-NH_2), 8.45 (s, 2H, CH), 8.55 ppm (s, 1H, NH); ^{13}C NMR ([D$_6$]DMSO): δ: 150.7 (2C, C-H), 159.3 (1C, C-NH_2), 164.4 ppm (2C, C-NO_2); ^{14}N NMR ([D$_6$]DMSO): $\delta=-14$ ppm (2N, C-NO_2); ^{11}B NMR ([D$_6$]DMSO): $\delta=-9.5$ ppm (1B); EA: $C_5H_{11}N_{12}O_4B$ (314.03): calculated N 53.52, C 19.12, H 3.53; found N 50.49, C 18.89, H 3.48. MS (FAB$^+$): *m/z* for $CH_7N_4^+$: calculated 75.09; found 75.1. MS (FAB$^-$): *m/z* for $C_4H_4N_8O_4B^-$: calculated 238.94; found 239.2. IS: > 40 J (grain size 100–500 μm). FS: 360 N (grain size 100–500 μm). ESD: 1.5 J (grain size 100–500 μm). DSC: 221 °C (decomp)

Diaminoguanidinium dihydrobis(3-nitro-1,2,4-triazolyl)borate (12): Colorless crystals were obtained as product (91 %). IR (ATR): $\tilde{\nu}=3469$ (w), 3376 (m), 3349 (m), 3311 (m), 3273 (m), 3136 (m), 2825 (w), 2464 (w), 2444 (w), 2430 (w), 2349 (w), 2281 (w), 1675 (s), 1627 (m), 1534 (s), 1490 (s), 1415 (s), 1393 (m), 1330 (m), 1301 (s), 1210 (m), 1159 (s), 1145 (s), 1032 (m), 1017 (w), 989 (w), 906 (w), 879 (w), 837 (s), 786 (w), 720 (w), 658 cm^{-1} (s); ^{1}H NMR ([D$_6$]DMSO): $\delta=3.36$ (br s, 2H, BH_2), 4.49 (s, 4H, NH_2), 7.15 (s, 2H, NH_2^+), 7.51 (s, 2H, NH), 8.39 ppm (s, 2H, CH); ^{13}C NMR ([D$_6$]DMSO): $\delta=150.8$ (2C, C-H), 159.9 (1C, C-NH_2), 164.6 ppm(2C, C-NO_2); ^{14}N NMR ([D$_6$]DMSO): $\delta=-14$ ppm (2N, C-NO_2). ^{11}B NMR ([D$_6$]DMSO): $\delta=-9.6$ ppm (1B); EA: $C_5H_{12}N_{13}O_4B$ (329.05): calculated N 55.34, C 18.25, H 3.68; found N 53.49, C 18.31, H 3.62. MS (FAB$^+$): *m/z* for $CH_8N_5^+$: calculated 90.11; found 90.1. MS (FAB$^-$): *m/z* for $C_4H_4N_8O_4B^-$: calculated 238.94; found 239.3. IS: > 40 J (grain size 500–1000 μm). FS: > 360 N (grain size 500–1000 μm). ESD: 1.5 J (grain size 500–1000 μm). DSC: 175 °C (decomp).

***N*-Guanylurea dihydrobis(3-nitro-1,2,4-triazolyl)borate trihydrate (13)**: A colorless solid (80 %) was obtained as product. IR (ATR): $\tilde{\nu}=3578$ (w), 3277 (m), 3149 (m), 2478 (w), 2436 (w), 2280 (w), 1752 (m), 1696 (m), 1661 (w), 1603 (m), 1539 (s), 1500 (vs), 1424 (m), 1397 (m), 1340 (m), 1307 (s), 1214 (m), 1170 (s), 1155 (s), 1075 (m), 1038 (m), 1028 (m), 882 (m), 836 (vs), 770 (m), 723 cm^{-1} (s); ^{1}H NMR ([D$_6$]DMSO): δ: 3.32 (br s, 2H, BH_2), 3.40 (H_2O), 6.99 (s, 2H, NH_2^+), 8.02 (s, 4H, NH_2), 8.41 (s, 2H, CH), 10.16 ppm (s, 1H, NH); ^{13}C NMR ([D$_6$]DMSO): $\delta=150.6$ (2C, C-H), 154.7 (1C), 155.5 (1C), 164.6 ppm (2C, C-NO_2); ^{14}N NMR ([D$_6$]DMSO): $\delta=-16$ ppm (2N, C-NO_2); ^{11}B NMR ([D$_6$]DMSO): $\delta=-9.6$ ppm (1B); EA: $C_6H_{11}O_5N_{12}B\cdots 3H_2O$ (396.09): calculated N 42.44, C 18.19, H 4.33; found N 41.58, C 18.06, H 3.54. MS (FAB$^+$): *m/z* for $C_2H_7N_4O^+$: calculated 103.10; found 103.1. MS (FAB$^-$): *m/z* for $C_4H_4N_8O_4B^-$: calculated 238.94; found 239.1. IS: > 40 J (grain size 100–500 μm). FS: >

360 N (grain size 100–500 μm). ESD: 1.0 J (grain size 100–500 μm). DSC: 225 °C (decomp).

5-Aminotetrazolium dihydrobis(3-nitro-1,2,4-triazolyl)borate dihydrate (14): Recrystallization from water led to the formation of a colorless solid (67 %). IR (ATR): $\tilde{\nu}=2483$ (w), 2296 (w), 3187 (w), 2950 (w), 2438 (w), 1982 (vw), 1666 (m), 1548 (m), 1504 (s), 1426 (m), 1396 (m), 1336 (m), 1309 (m), 1225 (w), 1149 (s), 1028 (s), 995 (m), 914 (m), 893 (m), 875 (m), 836 (vs), 829 (s), 722 cm^{-1} (s); ^{1}H NMR ([D$_6$]DMSO): $\delta=3.20$ (s, H_2O), 3.52 (br s, 2 H, BH_2), 8.42 (s, 2 H, CH), 8.68 ppm (br s, 4 H, NH_2/NH); ^{13}C NMR ([D$_6$]DMSO): $\delta=$ 150.7 (2C, C-H), 154.8 (1C, C-NH_2), 164.6 ppm (2C, C-NO_2); ^{14}N NMR ([D$_6$]DMSO): δ: −18 ppm (2N, C-NO_2); ^{11}B NMR ([D$_6$]DMSO): −9.6 ppm (1B); EA: $C_5H_8N_{13}O_4B\cdots2H_2O$ (361.05) calculated N 50.43, C 16.63, H 3.35; found N 49.26, C 16.93, H 3.63. MS (FAB$^+$): m/z for $CH_4N_5^+$: calculated 86.08; found 86.10. MS (FAB$^-$): m/z for $C_4H_4N_8O_4B^-$: calculated 238.94; found 239.3. IS: 10 J (grain size 100–500 μm). FS: 288 N (grain size 100–500 μm). ESD: 1.5 J (grain size 100–500 μm). DSC: 136 °C (decomp).

Ammonium dihydrobis(3-nitro-1,2,4-triazolyl)borate dihydrate (15): Colorless crystals (86 %) were obtained as product. IR (ATR): $\tilde{\nu}=3314$ (w), 3110 (w), 2855 (w), 2435 (w), 2349 (w), 2272 (w), 1562 (m), 1506 (m), 1454 (m), 1424 (s), 1396 (m), 1338 (w), 1307 (s), 1216 (w), 1164 (s), 1149 (s), 1046 (w), 1024 (m), 937 (w), 897 (w), 884 (w), 835 (s),722 cm^{-1} (m); ^{1}H NMR ([D$_6$]DMSO): $\delta=3.10$ (s, H_2O), 3.32 (br s, 2 H, BH_2), 7.04 (4 H, NH_4^+), 8.42 ppm (s, 2 H, CH); ^{13}C NMR ([D$_6$]DMSO): $\delta=150.7$ (2C, C-H), 164.6 ppm (2C, C-NO_2); ^{14}N NMR ([D$_6$]DMSO): $\delta=-20$ (2N, C-NO_2), −354 ppm (1N, NH_4^+); ^{11}B NMR ([D$_6$]DMSO): −9.7 ppm (1B); EA: $C_4H_8N_9O_4B\cdots2H_2O$ (293.01) calculated N 43.02, C 16.39, H 4.13; found N 40.99, C 15.91, H 3.97. MS (FAB$^+$): m/z for NH_4^+: calculated 18.04; found 18.10. MS (FAB$^-$): m/z for $C_4H_4O_4N_8B^-$: calculated 238.94; found 239.4. IS: 40 J (grain size 100–500 μm). FS: 360 N (grain size 100–500 μm). ESD: 1.0 J (grain size 100–500 μm). DSC: 209 °C (decomp).

***N,N*-Dimethylguanidinium dihydrobis(3-nitro-1,2,4-triazolyl)borate (16)**: A colorless solid (63 %) was obtained after recrystallization from water. IR (ATR): $\tilde{\nu}=3484$ (w), 3401 (w), 3340 (w), 3240 (w), 3103 (w), 2484 (w), 2426 (w), 2167 (w), 1829 (w), 1638 (s), 1552 (s), 1524 (m), 1501 (s), 1423 (m), 1394 (m), 1324 (w), 1300 (s), 1249 (w), 1216 (m), 1159 (s), 1141 (s), 1059 (m), 1042 (m), 1032 (m), 1019 (m), 920 (w), 872 (w), 840 (s), 774 (w), 722 cm^{-1} (m); ^{1}H NMR ([D$_6$]DMSO): $\delta=2.91$ (s, 6 H, N-(CH_3)$_2$), 3.30 (br s, 2 H, BH_2), 7.06 (s, 4 H, 2⋯NH_2), 8.42 ppm (s, 2 H, CH); ^{13}C NMR ([D$_6$]DMSO): $\delta=38.3$ (2C, 2⋯CH_3), 150.6 (2C, C-H), 157.5 (1C, C-NH_2^+), 164.6 ppm (2C, C-NO_2); ^{14}N NMR ([D$_6$]DMSO): $\delta=-16$ ppm (2N, C-NO_2); B NMR ([D$_6$]DMSO):$\delta=-9.5$ ppm (1B) . EA: $C_7H_{14}N_{11}O_4B$ (327.07) calculated N 47.11, C 25.71, H 4.31; found N 45.92, C 25.22, H 4.25. MS (FAB$^+$): m/z for $C_3N_3H_{10}^+$: calculated 88.13; found 88.1. MS (FAB$^-$): m/z for $C_4H_4O_4N_8B^-$: calculated 238.94; found 239.4. IS: > 40 J (grain size < 100 μm). FS: 360 N (grain size < 100 μm). ESD: 1.5 J (grain size < 100 μm). DSC: 236 °C (decomp).

Hydroxylammonium dihydrobis(3-nitro-1,2,4-triazolyl)borate monohydrate (17): After recrystallization from water as colorless (72 %) solid was obtained. IR (ATR): $\tilde{\nu}=3161$ (w), 2850 (w), 2712 (w), 2447 (w), 2283 (w), 1697 (w), 1558 (m), 1504 (s), 1430 (m), 1400 (m), 1338 (w), 1305 (s), 1259 (w), 1216 (m), 1166 (s), 1151 (vs), 1106 (m), 1033 (s), 1004 (m), 981 (w), 884 (m), 829 (vs), 769 (w), 722 cm^{-1} (m); ^{1}H NMR ([D$_6$]DMSO): $\delta=3.41$ (br s, 2 H, BH_2), 8.42 (s, 2 H, CH), 10.04 ppm (NH_3OH^+); ^{13}C NMR ([D$_6$]DMSO): $\delta=150.7$ (2C, C-H), 164.6 ppm (2C, C-NO_2); ^{14}N NMR ([D$_6$]DMSO): $\delta=-17$ ppm (2N, NO_2); ^{11}B NMR ([D$_6$]DMSO): −9.5 ppm (1B); EA: $C_4H_8N_9O_5B\cdots H_2O$ (290.99) calculated N 43.32, C 16.51, H 3.46; found N 39.85, C 16.08, H 3.14. MS (FAB$^+$): m/z for NH_4O^+: calculated 34.04; found 34.1. MS (FAB$^-$): m/z for $C_4H_4N_8O_4B^-$: calculated 238.94; found 239.4. IS: 10 J (grain size 100–500 μm). FS: > 360 N (grain size 100–500 μm). ESD: 1.0 J (grain size 100–500 μm). DSC: 152 °C (decomp).

Hydrazinium dihydrobis(3-nitro-1,2,4-triazolyl)borate (18): As product, a colorless solid (76 %) was obtained. IR (ATR): $\tilde{\nu}=3532$ (w), 3343 (w), 3135 (w), 2864 (w), 2463 (w), 2438 (w), 2281 (w), 2152 (w), 2006 (w), 1918 (w), 1785 (w), 1606 (w), 1550 (m), 1505 (s), 1424 (m), 1396 (w), 1338 (w), 1306 (m), 1270 (w), 1214 (w), 1154 (s), 1069 (w), 1046 (w), 1033 (m), 982 (w), 943 (w), 894 (w), 884 (w), 837 (s), 772 (w), 721 cm^{-1} (m); ^{1}H NMR ([D$_6$]DMSO): $\delta=3.47$ (br s, 2 H, BH_2), 6.40 (s, $N_2H_5^+$), 8.46 ppm (s, 2 H, CH); ^{13}C NMR ([D$_6$]DMSO): $\delta=146.7$ (2C, CH), 164.6 ppm (2C, C-NO_2); ^{14}N NMR ([D$_6$]DMSO): δ: −18 (2N, NO_2) ppm. ^{11}B NMR ([D$_6$]DMSO): $\delta=$ −9.8 ppm (1B); EA: $C_4H_9N_{10}O_4B$ (271.99) calculated N 51.50, C 17.66, H 3.34; found N 48.50, C 17.10, H 3.50. MS (FAB$^+$): m/z for $N_2H_5^+$: calculated 33.05; found 33.1. MS (FAB$^-$): m/z for $C_4H_4N_8O_4B^-$: calculated 238.94; found 239.2. IS: > 40 J (grain size 100–500 μm). FS: 360 N (grain size 100–500 μm). ESD: 1.0 J (grain size 100–500 μm). DSC: 144 °C (decomp).

Salts of dihydrobis(3,5-dinitropyrazolyl)borate

Potassium dihydrobis(3,5-dinitropyrazolyl)borate (4): A suspension of KBH_4 (0.44 g, 8.16 mmol) and 3,5-dinitropyrazole[31] (2.58 g, 16.3 mmol) in benzonitrile (50 mL) was heated up to 120 °C and stirred at this temperature for 4 h, whereas a slightly brown solid was formed. After cooling to room temperature, filtration and drying at 60 °C for 2 days the product was obtained as a slightly brownish solid (2.99 g, 65 %). IR (ATR): $\tilde{\nu}=3320$ (w), 3156 (w), 2923 (w), 2853 (w), 2595 (w), 2296 (w), 1792 (w), 1706 (w), 1666 (w), 1619 (w), 1580 (w), 1536 (m), 1469 (m), 1440 (s), 1377 (m), 1335 (s), 1307 (s), 1269 (m), 1249 (m), 1149 (m), 1063 (w), 1001 (m), 992 (m), 829 (s), 749 (s), 696 (w), 672 cm^{-1} (w); ^{1}H NMR ([D$_6$]DMSO): $\delta=3.32$ (br s, 2 H, BH_2), 7.26 ppm (s, 2 H, CH); ^{13}C NMR ([D$_6$]DMSO): $\delta=98.4$ (2C, C-H), 156.4 ppm (4C, C-NO_2); ^{14}N NMR ([D$_6$]DMSO): $\delta=$ −15 ppm (4N, NO_2); ^{11}B NMR ([D$_6$]DMSO): $\delta=-15.1$ ppm (br, 1B); EA: $C_6H_4N_8O_8BK$ (366.05) calculated N 30.61, C 19.69, H 1.10; found N 28.74, C 19.47, H 1.21. MS (FAB$^+$): m/z for K^+: calculated 39.10; found 39.1. MS (FAB$^-$): m/z for $C_6H_4N_8O_8B^-$: calculated 326.96; found 157.2 ($C_3HN_4O_4^-$). IS: 3 J (grain size 100–500 μm). FS: 216 N (grain size 100–500 μm). ESD: 1.0 J (grain size 100–500 μm). DSC: 344 °C (decomp).

Barium dihydrobis(3,5-dinitropyrazolyl)borate (8): $Ba(ClO_4)_2$ (0.54 g, 1.60 mmol) was added to a solution of **4** (1.17 g, 3.19 mmol) in methanol/water (50:50; 40 mL), and the mixture was stirred for 24 h at room temperature. After filtration the solvent was evaporated and the product as yellow solid obtained (2.52 g, 79 %). IR (ATR): $\tilde{\nu}=3568$ (w), 3140 (m), 2884 (w), 1680 (w), 1627 (w) 1518 (m), 1506 (m), 1479 (m), 1443 (w), 1385 (w), 1357 (m), 1288 (s), 1148 (w), 1003 (m), 864 (w), 836 (m), 821 (s), 757 (m), 680 cm^{-1} (m); ^{1}H NMR ([D$_6$]DMSO): $\delta=3.28$ (br s, 2 H, BH_2), 7.24 (s, 2 H, CH) ppm. ^{13}C NMR ([D$_6$]DMSO): $\delta=98.2$ (2C, C-H), 156.1 ppm (4C, C-NO_2); ^{14}N NMR ([D$_6$]DMSO): $\delta=-17$ ppm (4N, NO_2); ^{11}B NMR ([D$_6$]DMSO): $\delta=-15.6$ ppm (br, 1B); EA: $C_{12}H_8N_{16}O_{16}B_2Ba$ (791.24) calculated N 28.32, C 18.22, H 1.02; found N 26.74, C 18.47, H 0.98. MS (FAB$^-$): m/z for $C_6H_4N_8O_8B^-$: calculated 326.96; found 157.2 ($C_3HN_4O_4^-$). IS: 5 J (grain size 100–500 μm). FS: 180 N (grain size 100–500 μm). ESD: 0.4 J (grain size 100–500 μm). DSC: 342 °C (decomp).

General procedure for the synthesis of metal-free dihydrobis(3,5-dinitropyrazolyl)borate salts

Pertinent sulfate salts were added in stoichiometric amounts to a solution of barium dihydrobis(3,5-dinitropyrazolyl)borate (**8**) in methanol. The mixture was stirred at room temperature for 15 min and then filtered off. After removing the solvent, slightly yellow to slightly brownish solids were obtained.

Guanidinium dihydrobis(3,5-dinitropyrazolyl)borate (19): Slightly yellow needles (83 %) were obtained as product. IR (ATR): $\tilde{\nu}=3751$ (w), 3675 (w), 3629 (w), 3476 (w), 3434 (w), 3370 (w), 3146 (w), 2814 (w), 2338 (w), 2026 (w), 2017 (w), 1878 (w), 1667 (m), 1575 (w), 1534 (m), 1470 (s), 1441 (m), 1370 (s), 1351 (s), 1313 (s), 1277 (m), 1166 (m), 1147 (m), 1068 (m), 1010 (s), 994 (m), 836 (s), 815 (m), 762 (w), 744 (s), 705 (w), 672 cm^{-1} (w); ^{1}H NMR ([D$_6$]DMSO): $\delta=3.35$ (br s, 2H, BH_2), 7.02 (s, 6H, 3·NH_2), 7.29 ppm (s, 2H, CH); ^{13}C NMR ([D$_6$]DMSO): $\delta=98.9$ (2C, C-H), 156.9 (4C, C-NO_2), 158.6 ppm (1C, C-NH_2); ^{14}N NMR ([D$_6$]DMSO): $\delta=-9$ ppm (4N, NO_2); ^{11}B NMR ([D$_6$]DMSO): $\delta=-15.8$ ppm (br, 1B); EA: $C_7H_{10}N_{11}O_8B$ (387.04) calculated N 39.81, C 21.72, H 2.60; found N 34.74, C 21.04, H 2.30. MS (FAB$^+$): m/z for $CH_6N_3^+$: calculated 60.08; found 60.1. MS (FAB$^-$): m/z for $C_6H_4N_8O_8B^-$: calculated 326.96; found 157.2 ($C_3HN_4O_4^-$). IS: > 40 J (grain size < 100 μm). FS: > 360 N (grain size < 100 μm). ESD: 1.5 J (grain size < 100 μm). DSC: 318 °C (decomp).

Aminoguanidinium dihydrobis(3,5-dinitropyrazolyl)borate (20): Slightly yellow-brownish needles (79 %) were obtained as product. IR (ATR): $\tilde{\nu}=3625$ (w), 3544 (w), 3480 (w), 3436 (w), 3371 (w), 3319 (w), 3270 (w), 3186 (w), 3155 (w), 2953 (w), 2857 (w), 2804 (w), 2714 (w), 2597 (w), 2221 (w), 2138 (w), 1987 (w), 1947 (w), 1792 (w), 1682 (w), 1651 (w), 1607 (w), 1537 (m), 1479 (s), 1441 (s), 1343 (s), 1310 (s), 1275 (m), 1185 (m), 1174 (m), 1165 (m), 1150 (m), 1065 (m), 1011 (m), 1001 (s), 994 (m), 922 (m), 843 (m), 829 (s), 763 (m), 750 (s), 672 cm^{-1} (m); ^{1}H NMR ([D$_6$]DMSO): $\delta=3.33$ (br s, 2H, BH_2), 4.58 (s, 2H, N-NH_2), 6.52 (s, 2H, C-NH_2) 7.21 (s, 2H, C-NH_2), 7.27 (s, 2H, CH), 8.50 ppm (s, 1H, NH); ^{13}C NMR ([D$_6$]DMSO): $\delta=98.9$ (2C, C-H), 157.0 (4C, C-NO_2), 159.3 ppm (1C, C-NH_2); ^{14}N NMR ([D$_6$]DMSO): $\delta=-11$ ppm (4N, NO_2); ^{11}B NMR ([D$_6$]DMSO): $\delta=-16.2$ ppm (br, 1B); EA: $C_7H_{11}N_{12}O_8B$ (402.05) calculated N 41.81, C 20.91, H 2.76; found N 39.32, C 19.96, H 2.92. MS (FAB$^+$): m/z for $CH_7N_4^+$: calculated 75.09; found 75.1. MS (FAB$^-$): m/z for $C_6H_4N_8O_8B^-$: calculated 326.96; found 157.2 ($C_3HN_4O_4^-$). IS: 8 J (grain size < 100 μm). FS: > 360 N (grain size < 100 μm). ESD: 1.5 J (grain size < 100 μm). DSC: 346 °C (decomp).

Diaminoguanidinium dihydrobis(3,5-dinitropyrazolyl)borate (21): Slightly yellow-brownish crystals (62 %) were obtained as product. IR (ATR): $\tilde{\nu}=3682$ (w), 3624 (w), 3575 (w), 3544 (w), 3459 (w), 3356 (w), 3336 (w), 3303 (w), 3266 (w), 3197 (w), 3156 (w), 3141 (w), 2859 (w), 2614 (w), 2481 (w), 2271 (w), 2071 (w), 1986 (w), 1802 (w), 1675 (w), 1635 (w), 1607 (w), 1539 (s), 1504 (m), 1482 (s), 1441 (s), 1421 (m), 1370 (m), 1343 (s), 1324 (m), 1315 (s), 1277 (m), 1166 (m), 1069 (m), 1012 (s), 1000 (m), 955 (w), 886 (w), 843 (s), 824 (m), 811 (m), 805 (m), 762 (w), 743 (s), 703 (w), 673 cm^{-1} (m); ^{1}H NMR ([D$_6$]DMSO): $\delta=3.36$ (br s, 2H, BH_2), 4.58 (s, 4H, NH_2), 7.18 (s, 2H, NH_2^+), 7.26 (s, 2H, CH), 7.59 ppm (s, 2H, NH); ^{13}C NMR ([D$_6$]DMSO): $\delta=98.9$ (2C, C-H), 157.0 (4C, C-NO_2), 159.3 ppm (1C, C-NH_2); ^{14}N NMR ([D$_6$]DMSO): $\delta=-11$ ppm (4N, NO_2); ^{11}B NMR ([D$_6$]DMSO): $\delta=-16.1$ ppm (br, 1B); EA: $C_7H_{12}N_{13}O_8B$ (417.07) calculated N 43.66, C 20.16, H 2.90; found N 39.79, C 20.36, H 2.92. MS (FAB$^+$): m/z for $CH_8N_5^+$: calculated 90.11; found 90.1. MS (FAB$^-$): m/z for $C_6H_4N_8O_8B^-$: calculated 326.96; found 157.2 ($C_3HN_4O_4^-$). IS: 20 J (grain size 100–500 μm). FS: > 360 N (grain size 100–500 μm). ESD: 1.5 J (grain size 100–500 μm). DSC: 231 °C (decomp).

***N*-Guanylurea dihydrobis(3,5-dinitropyrazolyl)borate (22)**: As product a slightly yellow-brownish powder (75 %) was obtained. IR (ATR): $\tilde{\nu}=3625$ (w), 3583 (w), 3544 (w), 3478 (w), 3425 (w), 3360 (w), 3315 (w), 3270 (w), 3196 (w), 3156 (w), 2806 (w), 2596 (w), 2455 (w), 2333 (w), 2295 (w), 2146 (w), 1997 (w), 1971 (w), 1900 (w), 1791 (w), 1726 (w), 1680 (w), 1657 (w), 1606 (w), 1595 (w), 1538 (m), 1473 (s), 1441 (s), 1340 (s), 1325 (s), 1309 (s), 1277 (m), 1269 (m), 1165 (m), 1150 (m), 1127 (m), 1065 (m), 1012 (m), 1001 (s), 831 (s), 762 (m), 751 (s), 714 (m), 700 (m), 672 cm^{-1} (m); ^{1}H NMR ([D$_6$]DMSO): $\delta=3.29$ (br s, 2H, BH_2), 6.87 (s, 2H, NH_2^+), 7.29 (s, 2H, CH), 8.02 (s, 4H, NH_2), 10.19 ppm (s, 1H, NH); ^{13}C NMR ([D$_6$]DMSO): $\delta=99.0$ (2C, C-H), 154.5 (1C), 155.6 (1C), 156.9 (4C, C-NO_2) ppm. ^{14}N NMR ([D$_6$]DMSO): $\delta=-11$ ppm (4N, NO_2); ^{11}B NMR ([D$_6$]DMSO): $\delta=-16.0$ ppm (br, 1B); EA: $C_8H_{11}N_{12}O_9B$ (430.06) calculated N 39.08, C 22.34, H 2.58; found N 35.99, C 22.02, H 2.20. MS (FAB$^+$): m/z for $C_2H_7N_4O^+$: calculated 103.10; found 103.1. MS (FAB$^-$): m/z for $C_6H_4N_8O_8B^-$: calculated 326.96; found 157.2 ($C_3HN_4O_4^-$). IS: > 40 J (grain size < 100 μm). FS: > 360 N (grain size < 100 μm). ESD: 1.5 J (grain size < 100 μm). DSC: 353 °C (decomp).

5-Aminotetrazolium dihydrobis(3,5-dinitropyrazolyl)borate (23): Slightly yellow crystals (82 %) were obtained as product. IR (ATR): $\tilde{\nu}=3977$ (w), 3682 (w), 3629 (w), 3443 (w), 3318 (w), 3249 (w), 31 250 (w), 2955 (w), 2772 (w), 2622 (w), 2440 (w), 2294 (w), 2168 (w), 2147 (w), 2084 (w), 2047 (w), 2035 (w), 1971 (w), 1911 (w), 1640 (m), 1593 (m), 1539 (s), 1484 (s), 1446 (s), 1357 (s), 1325 (s), 1285 (m), 1186 (m), 1165 (m), 1134 (w), 1081 (m), 1069 (m), 1043 (m), 1013 (m), 992 (s), 831 (s), 760 (m), 747 (s), 741 (s), 674 (s), 665 cm^{-1} (s); ^{1}H NMR ([D$_6$]DMSO): $\delta=3.30$ (br s, 2H, BH_2), 7.24 (s, 2H, CH), 8.70 ppm (br s, 4H, NH_2/NH); ^{13}C NMR ([D$_6$]DMSO): $\delta=98.8$ (2C, C-H), 157.0 (4C, C-NO_2), 154.5 ppm (1C, C-NH_2); ^{14}N NMR ([D$_6$]DMSO): $\delta=-11$ ppm (4N, NO_2); ^{11}B NMR ([D$_6$]DMSO): $\delta=-16.2$ ppm (br, 1B, BH_2); EA: $C_7H_8N_{13}O_8B$ (413.03) calculated N 44.09, C 20.36, H 1.95; found N 39.99, C 20.02, H 2.05. MS (FAB$^+$): m/z for $CH_4N_5^+$: calculated 86.08; found 86.10. MS (FAB$^-$): m/z for $C_6H_4N_8O_8B^-$: calculated 326.96; found 157.2 ($C_3HN_4O_4^-$). IS: > 40 J (grain size 100–500 μm). FS: > 360 N (grain size 100–500 μm). ESD: 1.0 J (grain size 100–500 μm). DSC: 344 °C (decomp).

Salts of dihydrobis(2,4-dinitroimidazolyl)borate

Potassium dihydrobis(2,4-dinitroimidazolyl)borate (6): A solution of KBH_4 (0.74 g, 13.71 mmol) and 2,4-dinitroimidazole[32] (4.33 g, 27.39 mmol) in dry acetonitrile (50 mL) was stirred under an argon atmosphere at 82 °C for 24 h. Evaporation of the solvent led to the formation of a yellow solid (3.05 g, 61 %). IR: $\tilde{\nu}=3594$ (w), 3437 (w), 3148 (w), 2791 (w), 2486 (w), 2404 (w), 1945 (w), 1730 (w), 1685 (w), 1626 (w), 1550 (m), 1526 (s), 1518 (s), 1500 (s), 1470 (s), 1432 (m), 1370 (m), 1327 (s), 1301 (s), 1264 (s), 1211 (m), 1154 (s), 1094 (m), 1000 (m), 914 (m), 903 (m), 874 (m), 850 (s), 838 (m), 825 (s), 758 (s), 702 cm^{-1} (m); ^{1}H NMR ([D$_6$]DMSO): $\delta=3.47$ (br s, 2H, BH_2), 7.72 ppm (s, 2H, CH); ^{13}C NMR ([D$_6$]DMSO): $\delta=129.7$ ppm (2C, C-H); ^{14}N NMR ([D$_6$]DMSO): $\delta=-17$ ppm (br, NO_2); ^{11}B NMR ([D$_6$]DMSO): -10.0 ppm (br, 1B); EA: $C_6H_4N_8O_8BK$ (366.06) calculated N 30.61, C 19.69, H 1.10; found N 29.11, C 20.51, H 1.19. MS (FAB$^+$): m/z for K^+: calculated 39.10; found 39.1. MS (FAB$^-$): m/z for $C_6H_4O_8N_8B^-$: calculated 326.96; found 326.8. IS: > 40 J (grain size 100–500 μm). FS: 360 N (grain size 100–500 μm). ESD: 1.5 J (grain size 100–500 μm). DSC: 165 °C (decomp).

Barium dihydrobis(2,4-dinitroimidazolyl)borate (9): $Ba(ClO_4)_2$ (0.54 g, 1.60 mmol) was added to a solution of **6** (1.17 g, 3.19 mmol) in methanol/water (50:50; 70 mL) and the mixture was stirred for 24 h at room temperature. After filtration the solvent was evaporated and the product was obtained as a yellow-brown solid (1.53 g, 60%). IR: $\tilde{\nu}=3568$ (w), 3140 (m), 2884 (w), 1680 (w), 1627 (w) 1518 (m), 1506 (m), 1479 (m), 1443 (w), 1385 (w), 1357 (m), 1288 (s), 1148 (w), 1003 (m), 864 (w), 836 (m), 821 (s), 757 (m), 680 cm^{-1} (m); ^{1}H NMR ([D_6]DMSO): $\delta=3.31$ (br s, 2H, BH_2), 7.70 ppm (s, 2H, CH); ^{13}C NMR ([D_6]DMSO): $\delta=129.8$ ppm (2C, C-H); ^{14}N NMR ([D_6]DMSO): $\delta=-17$ ppm (br, NO_2); ^{11}B NMR ([D_6]DMSO): $\delta=-9.9$ ppm (br, 1B); EA: $C_{12}H_8N_{16}O_{16}B_2Ba$ (791.24) calculated N 28.32, C 18.22, H 1.02; found N 25.74, C 18.19, H 1.10. MS (FAB$^-$): m/z for $C_6H_4O_8N_8B^-$: calculated 326.96; found 326.8. IS: > 40 J (grain size 100–500 μm). FS: 360 N (grain size 100–500 μm). ESD: 1.5 J (grain size 100–500 μm). DSC: 349 °C (decomp).

General procedure for the synthesis of metal-free dihydrobis(2,4-dinitroimidazol-1-yl)borate salts

Guanidinium dihydrobis(2,4-dinitroimidazolyl)borate (24): A brownish solid was obtained as product (79%). IR: $\tilde{\nu}=3500$ (w), 3432 (m), 3383 (m), 3341 (m), 3111 (m), 2506 (w), 2440 (w), 2362 (w), 2242 (w), 2190 (w), 2148 (w), 2163 (w), 2103 (w), 2074 (w), 2026 (w), 2018 (w), 1986 (w), 1971 (w), 1960 (w), 1909 (w), 1731 (m), 1659 (s), 1614 (m), 1502 (m), 1463 (m), 1434 (m), 1404 (m), 1384 (m), 1357 (m), 1287 (s), 1221 (m), 1180 (m), 1080 (s), 1003 (s), 940 (m), 874 (m), 839 (m), 824 (m), 771 (m), 756 (m), 716 cm^{-1} (m); ^{1}H NMR ([D_6]DMSO): $\delta=3.36$ (br s, 2H, BH_2), 7.21 (br s, 6H, $3{\cdot}NH_2$), 7.71 ppm (s, 2H, CH); ^{13}C NMR ([D_6]DMSO): $\delta=130.8$ (2C, C-H), 158.9 ppm (1C, C-NH_2); ^{14}N NMR ([D_6]DMSO): $\delta=-10$ ppm (br, NO_2); ^{11}B NMR ([D_6]DMSO): −10.0 ppm (br, 1B); EA: $C_7H_{10}N_{11}O_8B$ (387.04) calculated N 39.81, C 21.72, H 2.60; found N 38.04, C 21.20, H 2.79. MS (FAB$^+$): m/z for $CH_6N_3^+$: calculated 60.08; found 60.10. MS (FAB$^-$): m/z for $C_6H_4O_8N_8B^-$: calculated 326.96; found 326.8. IS: > 40 J (grain size < 100 μm). FS: > 360 N (grain size < 100 μm). ESD: 1.5 J (grain size < 100 μm). DSC: 249 °C (decomp).

Aminoguanidinium dihydrobis(2,4-dinitroimidazolyl)borate (25): Yellow-orange crystals were obtained as product (77%). IR: $\tilde{\nu}=3571$ (w), 3437 (w), 3310 (w), 3146 (m), 2821 (w), 2783 (w), 2263 (w), 2152 (w), 2020 (w), 1729 (w), 1680 (m), 1667 (m), 1548 (m), 1503 (s), 1473 (s), 1429 (s), 1401 (m), 1376 (m), 1338 (s), 1297 (s), 1288 (s), 1254 (m), 1227 (m), 1201 (m), 1143 (m), 1102 (s), 1013 (m), 1000 (s), 933 (m), 866 (m), 835 (s), 818 (s), 756 (s), 654 cm^{-1} (s); ^{1}H NMR ([D_6]DMSO): $\delta=3.59$ (br s, 2H, BH_2), 4.63 (s, 2H, N-NH_2), 6.69 (s, 2H, C-NH_2) 7.35 (s, 2H, C-NH_2), 7.69 (s, 2H, CH), 8.52 ppm (s, 1H, NH). ^{13}C NMR ([D_6]DMSO): $\delta=130.6$ (2C, C-H), 159.3 ppm (1C, C-NH_2); ^{14}N NMR ([D_6]DMSO): $\delta=-12$ ppm(br, NO_2); ^{11}B NMR ([D_6]DMSO): −10.2 ppm (br, 1B); EA: $C_7H_{11}N_{12}O_8B$ (402.05) calculated N 41.81, C 20.91, H 2.76; found N 39.54, C 21.08, H 2.92. MS (FAB$^+$): m/z for $CH_7N_4^+$: calculated 75.09; found 75.1. MS (FAB$^-$): m/z for $C_6H_4O_8N_8B^-$: calculated 326.96; found 326.8. IS: > 40 J (grain size < 100 μm). FS: > 360 N (grain size < 100 μm). ESD: 1.5 J (grain size < 100 μm). DSC: 228 °C (decomp).

***N*-Guanylurea dihydrobis(2,4-dinitroimidazolyl)borate (26)**: As product a yellow-orange solid was obtained (83%). IR: $\tilde{\nu}=3577$ (w), 3424 (w), 3329 (w), 2348 (w), 1743 (m), 1648 (m), 1636 (m), 1583 (m), 1506 (m), 1473 (s), 1428 (m), 1380 (m), 1352 (m), 1274 (s), 1222 (m), 1143 (m), 1108 (m), 1081 (m), 999 (m), 929 (w), 864 (w), 835 (m), 821 (m), 756 cm^{-1} (m); ^{1}H NMR ([D_6]DMSO): $\delta=3.47$ (br s, 2H, BH_2), 6.37 (s, 2H, NH_2^+), 7.69 (s, 2H, CH), 8.26 (s, 4H, NH_2), 10.07 ppm (s, 1H, NH); ^{13}C NMR ([D_6]DMSO): $\delta=130.5$ (2C, C-H), 154.3 (1C), 154.8 ppm (1C); ^{14}N NMR ([D_6]DMSO): $\delta=-11$ ppm (br, NO_2); ^{11}B NMR ([D_6]DMSO): $\delta=-10.18$ ppm (br, 1B); EA: $C_8H_{11}N_{12}O_9B$ (430.06) calculated N 39.08, C 22.34, H 2.58; found N 37.45, C 22.19, H 2.33. MS (FAB$^+$): m/z for $C_2H_7N_4O^+$: calculated 103.10; found 103.1. MS (FAB$^-$): m/z for $C_6H_4O_8N_8B^-$: calculated 326.96; found 326.8. IS: > 40 J (grain size < 100 μm). FS: 360 N (grain size < 100 μm). ESD: 1.5 J (grain size < 100 μm). DSC: 242 °C (decomp).

5-Aminotetrazolium dihydrobis(2,4-dinitroimidazolyl)borate (27): A yellow solid was obtained as product (91%). IR: $\tilde{\nu}=3476$ (w), 3341 (w), 3278 (w), 3193 (w), 3145 (w), 3004 (w), 2944 (w), 2782 (w), 1732 (w), 1641 (m), 1510 (s), 1474 (s), 1435 (s), 1379 (m), 1355 (m), 1338 (m), 1294 (vs), 1220 (s),1152 (m), 1107 (s), 1061 (s), 1000 (s), 930 (m), 866 (m), 836 (s), 820 (s), 756 (s), 737 (m), 688 cm^{-1} (m); ^{1}H NMR ([D_6]DMSO): $\delta=3.43$ (br s, 2H, BH_2), 7.76 (s, 2H, CH), 8.65 ppm (br s, 4H, NH_2/NH); ^{13}C NMR ([D_6]DMSO): $\delta=130.7$ (2C, C-H), 154.2 ppm (1C, C-NH_2); ^{14}N NMR ([D_6]DMSO): $\delta=-10$ ppm (br, NO_2); ^{11}B NMR ([D_6]DMSO): −9.5 ppm (br, 1B); EA: $C_7H_8N_{13}O_8B$ (413.03) calculated N 44.09, C 20.36, H 1.95; found N 30.11, C 20.40, H 1.85. MS (FAB$^+$): m/z for $CH_4N_5^+$: calculated 86.08; found 86.10. MS (FAB$^-$): m/z for $C_6H_4O_8N_8B^-$: calculated 326.96; found 326.8. IS: > 40 J (grain size 100–500 μm). FS: > 360 N (grain size 100–500 μm). ESD: 1.5 J (grain size 100–500 μm). DSC: 192 °C (decomp).

Ammonium dihydrobis(2,4-dinitroimidazolyl)borate (28): An orange solid was obtained as product (80%). IR: $\tilde{\nu}=3315$ (w), 3256 (w), 3142 (w), 3115 (w), 2985 (w), 2943 (w), 2807 (w), 2464 (w), 1730 (w), 1682 (m), 1504 (s), 1474 (s), 1420 (s), 1356 (m), 1280 (s), 1233 (s), 1142 (s), 1082 (s), 1001 (s), 929 (m), 870 (m), 836 (s), 819 (s), 794 (m), 756 cm^{-1} (s); ^{1}H NMR ([D_6]DMSO): $\delta=3.68$ (br s, 2H, BH_2), 7.12 (4H, NH_4^+), 7.77 ppm (s, 2H, CH); ^{13}C NMR ([D_6]DMSO): $\delta=130.7$ ppm (2C, C-H); ^{14}N NMR ([D_6]DMSO): $\delta=-12$ (br, NO_2), −354 ppm (1N, NH_4^+); ^{11}B NMR ([D_6]DMSO): $\delta=-9.8$ ppm (br, 1B); EA: $C_6H_8N_9O_8B$ (344.99) calculated N 36.54, C 20.89, H 2.34; found N 35.11, C 20.80, H 2.45. MS (FAB$^+$): m/z for NH_4^+: calculated 18.04; found 18.10. MS (FAB$^-$): m/z for $C_6H_4O_8N_8B^-$: calculated 326.96; found 326.8. IS: > 40 J (grain size < 100 μm). FS: > 360 N (grain size < 100 μm). ESD: 1.0 J (grain size < 100 μm). DSC: 243 °C (decomp).

***N*,*N*-Dimethylguanidinium dihydrobis(2,4-dinitroimidazolyl)borate (29)**: An yellow-orange solid was obtained as product (93%). IR: $\tilde{\nu}=3566$ (w), 3421 (w), 3143 (w), 2443 (w), 2058 (w), 1733 (w), 1672 (m), 1631 (s), 1516 (m), 1471 (s), 1436 (s), 1418 (m), 1356 (m), 1288 (s), 1224 (s), 1156 (m), 1104 (m), 1058 (m), 1022 (m), 1000 (s), 850 (w), 836 (s), 820 (s), 778 (w), 758 cm^{-1} (s); ^{1}H NMR ([D_6]DMSO): $\delta=2.87$ (s, 6H, N-$(CH_3)_2$), 3.42 (br s, 2H, BH_2), 7.25 (s, 4H, $2{\cdots}NH_2$), 7.77 ppm (s, 2H, CH); ^{13}C NMR ([D_6]DMSO): $\delta=38.7$ (2C, $2{\cdots}CH_3$), 130.1 (2C, C-H), 157.9 ppm (1C, C-NH_2^+); ^{14}N NMR ([D_6]DMSO): $\delta=-10$ ppm (br, NO_2); ^{11}B NMR ([D_6]DMSO): $\delta=-10.5$ ppm (br, 1B); EA: $C_9H_{14}N_{11}O_8B$ (415.09) calculated N 37.12, C 26.04, H 3.40; found N 35.98, C 25.97, H 3.45. MS (FAB$^+$): m/z for $C_3N_3H_{10}^+$: calculated 88.13; found 88.1. MS (FAB$^-$): m/z for $C_6H_4O_8N_8B^-$: calculated 326.96; found 326.8. IS: > 40 J (grain size 100–500 μm). FS: > 360 N (grain size 100–500 μm). ESD: 1.5 J (grain size 100–500 μm). DSC: 261 °C (decomp).

Acknowledgements

Financial support of this work by the Ludwig-Maximilian University of Munich (LMU), the U.S. Army Research Laboratory (ARL) under grant no. W911NF-09-2-0018, the Armament Research, Development and Engineering Center (ARDEC) under grant no. W911NF-12-1-0467, and the Office of Naval Research (ONR) under grant nos. ONR.N00014-10-1-0535 and ONR.N00014-12-1-0538 is gratefully acknowledged. The authors acknowledge collaborations with Dr. Mila Krupka (OZM Research, Czech Republic) in the development of new testing and evaluation methods for energetic materials, and with Dr. Muhamed Suceska (Brodarski Institute, Croatia) in the development of new computational codes to predict the detonation and propulsion parameters of novel explosives. We are indebted to and thank Dr. Betsy M. Rice and Dr. Brad Forch (ARL, Aberdeen, Proving Ground, MD) for many inspired discussions. The Cusanuswerk is gratefully acknowledged for the award of a PhD scholarship (M.R.).

Keywords: azole borates · colorants · energetic materials · pyrotechnics · X-ray diffraction

[1] a) G. Steinhauser, T. M. Klapötke, *Angew. Chem.* **2008**, *120*, 3376; *Angew. Chem. Int. Ed.* **2008**, *47*, 3330; b) J. J. Sabatini, A. V. Nagori, E. A. Latalladi, J. C. Poret, G. Chen, R. Damavarapu, T. M. Klapötke, *Propellants Explos. Pyrotech.* **2011**, *36*, 373; c) J. J. Sabatini, A. V. Nagori, G. Chen, P. Chu, R. Damavarapu, T. M. Klapötke, *Chem. Eur. J.* **2012**, *18*, 628; d) J. J. Sabatini, J. M. Raab, R. K. Hann Jr., C. T. Freeman, *Z. Anorg. Allg. Chem.* **2013**, *639*, 25.

[2] a) G. Steinhauser, T. M. Klapötke, *J. Chem. Educ.* **2010**, *87*, 150; b) R. Mandal, B. K. Sen, S. Sen, *Chem. Environ. Res.* **1996**, *5*, 307; c) A. Dutschke, C. Lohrer, S. Seeger, L. Kurth, *Chem. Ing. Tech.* **2009**, *81*, 167; d) A. L. Reeves, *Handbook on the Toxicology of Metals*, Elsevier/North Holland Biomedical Press, New York **1979**, 321; e) G. Steinhauser, J. H. Sterba, M. Foster, F. Grass, M. Bichler, *Atmos. Environ.* **2008**, *42*, 8616; f) J. A. Conkling, *Chemistry of Pyrotechnics: Basic Principles and Theory*, Taylor & Francis Group, New York, **1985**, 156.

[3] R. M. Blunt, P. J. Keitel, US Pat. US 3453157, **1969**.

[4] J. J. Sabatini, J. C. Poret, R. N. Broad, *Angew. Chem.* **2011**, *123*, 4720; *Angew. Chem. Int. Ed.* **2011**, *50*, 4624.

[5] S. Trofimenko, *Scorpionates: The Coordination Chemistry of Poly(pyrazolyl)borate Ligands*, Imperial College Press, London, **1999**.

[6] a) R. Haiges, C. Bigler Jones, K. O. Christe, *Inorg. Chem.* **2013**, *52*, 5551; b) Z. Zeng, B. Twamley, J. M. Shreeve, *Organometallics* **2007**, *26*, 1782.

[7] M. Pellei, F. Benetollo, G. G. Lobbia, S. Alidori, C. Santini, *Inorg. Chem.* **2005**, *44*, 846.

[8] C. Marzano, M. Pellei, S. Alidori, A. Brossa, G. G. Lobbia, F. Tisato, C. Santini, *J. Inorg. Biochem.* **2006**, *100*, 299.

[9] M. Pellei, S. Aldori, G. Papini, G. G. Lobbia, J. D. Gorden, H. V. R. Dias, C. Santini, *Dalton Trans.* **2007**, 4845.

[10] M. Pellei, G. Papini, G. G. Lobbia, S. Ricci, M. Yousufuddin, H. V. R. Dias, C. Santini, *Dalton Trans.* **2010**, *39*, 8937.

[11] a) C. Janiak, T. G. Scharmann, W. Gunther, F. Girgsdies, H. Hemling, W. Hinrichs, D. Lentz, *Chem. Eur. J.* **1995**, *1*, 637; b) C. Janiak, *J. Chem. Soc. Chem. Commun.* **1994**, 545; c) C. Janiak, L. Esser, *Z. Naturforsch. B* **1993**, *48*, 394; d) C. Janiak, T. G. Scharmann, *Polyhedron* **2003**, *22*, 1123.

[12] D. Lu, C. H. Winter, *Inorg. Chem.* **2010**, *49*, 5795.

[13] C. J. Snyder, P. D. Martin, M. J. Heeg, C. H. Winter, *Chem. Eur. J.* **2013**, *19*, 3306.

[14] T. J. Groshens, *J. Coord. Chem.* **2010**, *63*, 1882.

[15] T. M. Klapötke, P. Mayer, J. Stierstorfer, *Phosphorus Sulfur Silicon Relat. Elem.* **2009**, *184*, 2393.

[16] T. M. Klapötke, C. Miró Sabaté, *Heteroat. Chem.* **2008**, *63*, 301.

[17] M. von Denffer, T. M. Klapötke, C. Miró Sabaté, *Z. Anorg. Allg. Chem.* **2008**, *634*, 2575.

[18] G. Socrates, *Infrared and Raman Characteristic Group Frequencies—Tables and Charts*, 3edrd edWiley, Chichester, **2004**.

[19] CrysAlisPro, Oxford Diffraction Ltd., version 171.33.41, **2009**.

[20] SIR-92, A program for crystal structure solution: A. Altomare, G. Cascarano, C. Giacovazzo, A. Guagliardi, *J. Appl. Crystallogr.* **1993**, *26*, 343.

[21] a) A. Altomare, G. Cascarano, C. Giacovazzo, A. Guagliardi, A. G. G. Moliterni, M. C. Burla, G. Polidori, M. Camalli, R. Spagna, SIR97 **1997**; b) A. Altomare, M. C. Burla, M. Camalli, G. L. Cascarano, C. Giacovazzo, A. Guagliardi, A. G. G. Moliterni, G. Polidori, R. Spagna, *J. Appl. Crystallogr.* **1999**, *32*, 115.

[22] a) G. M. Sheldrick, SHELX-97, University of Göttingen, Göttingen, Germany, **1997**; b) G. M. Sheldrick, *Acta Crystallogr. Sect. A* **2008**, *64*, 112.

[23] A. L. Spek, PLATON, A Multipurpose Crystallographic Tool, Utrecht University, The Netherlands, **1999**.

[24] L. J. Farrugia, *J. Appl. Crystallogr.* **1999**, *32*, 837.

[25] SCALE3 ABSPACK – An Oxford Diffraction program (1.0.4, gui: 1.0.3), Oxford Diffraction Ltd., **2005**.

[26] N. Wiberg in *Lehrbuch der Anorganischen Chemie* (Eds.: A. F. Holleman, E. Wiberg), 101 Auflage, de Gruyter, Berlin, **1995**, Anhang V.

[27] M. Hemamalini, H.-K. Fun, *Acta Crystallogr. E* **2011**, *67*, o15.

[28] T. M. Klapötke, P. Mayer, J. Stierstorfer, *Phosphorus Sulfur Silicon Relat. Elem.* **2009**, *184*, 2393.

[29] M. Weinmann, J. Nuss, M. Jansen, *Acta Crystallogr. E* **2007**, *63*, o2767.

[30] J. C. Poret, J. J. Sabatini, *J. Energ. Mater.* **2013**, *31*, 27.

[31] J. W. A. M. Janssen, H. J. Koeners, C. G. Kruse, C. L. Habraken, *J. Org. Chem.* **1973**, *38*, 1777.

[32] G. Wüllner, F.-W. Herkenrath, WO 021409, Dynamit Nobel AG/Asahi Chemical Corp. 2010.

[33] *UN Recommendations on the Transport of Dangerous Goods, Model Regulations*, 15edth edUnited Nations, New York, **2007**.

Received: May 8, 2014

39th International Pyrotechnics Seminar
Valencia 2013

Energetic Materials Based on Azole Borates

Thomas M. Klapötke[1], Magdalena Rusan[1], Véronique Sproll[1], Jörg Stierstorfer[1].

[1] Ludwig Maximilian University Munich, Butenandtstr. 5-13 Haus D, 81377 Munich, Germany, Phone: +49 89 2180 77491, Fax: +49 89 2180 77492

march@cup.uni-muenchen.de

Keywords: Nitrogen-rich, Azole Borates, Pyrotechnics, Flame Colors

ABSTRACT

The replacement of environmentally critical and toxic compounds is of high importance. Especially the replacement of barium compounds in green-light emitting pyrotechnics by less toxic boron-containing compounds is desirable. Therefore the development of nitrogen-rich azole borates is of interest. The syntheses and characterization of several azole borates are presented. In addition, promising pyrotechnic formulations containing boron compounds as colorants has been investigated.

1. INTRODUCTION

Novel developments in pyrotechnics focus on the application of environmentally more benign compounds. Main objectives are the substitution of toxic perchlorates and heavy metals like barium as well as to reduce the smoke production of the pyrotechnic composition. Therefore, new coloring agents should possess a lower toxicity as well as nontoxic combustion products while at the same time offering at least comparable or even better color performance and combustion behaviour than currently used compounds.

Nitrogen-rich heterocycles are very promising candidates in the development of environmentally friendly high-energy-density materials. In contrast to conventional energetic materials, nitrogen-rich compounds do not gain their energy from oxidation of a carbon backbone or a fuel, but rather from high heats of formation due to their large number of inherently energetic N-N and C-N bonds (Hiskey et al 2000). Furthermore, they combine several advantages, such as high flame temperatures and the formation of mostly gaseous products, which is important for a smokeless combustion (Klapötke et al 2010).

Taking these advantages into account, nitrogen-rich azole borate compounds are promising barium substitutes and therefore worthwhile targets for the development of new coloring agents. Several boron compounds like elemental boron, boric acid, boron esters (Blunt and Keitel 1969) and boron carbide have been investigated as coloring agents in green-light-emitting pyrotechnic compositions (Sabatini et al 2011). But these boron compounds have in common that they do not possess any energetic character. Especially with regard to the formation of highly efficient colourful pyrotechnics, it is of interest to combine the energetic properties with the coloring agent in the same molecule. To date, a number of different energetic boron compounds were investigated such as boron azides and boron esters for example (Wiberg et al 1954, Paetzold 1987 and Guibert and Marshall 1966). The disadvantage of these compounds is the sensitivity towards chemical and physical stimulations. More stable and less sensitive boron-~~containing compounds are azole borate salts. Various azole borates~~ haven been reported in literature: there are four classes of azolylborates, referring to their grade of substitution – trihydro(azolyl)borates, dihydrobis(azolyl)borates, hydrotris(azolyl)borates and tetrakis(azolyl)borates. Among the different classes of B-N bound azoles, the group of pyrazoles and 1,2,4-triazoles show the greatest variety (Trofimenko et al 1999, Shreeve et al 2007, Gioia et al 1991 and Pellei et al 2005). But also azole borates based on tetrazole have been investigated (Groshens 2010, Janiak et al 1993 and Winter and Lu 2010). In this work, nitrogen-rich borates based on 3-nitro-1,2,4-triazole and 3,5-dinitropyrazole are investigated as colorants in pyrotechnic mixtures.

2. SYNTHESIS

In the following the synthesis of a series of nitrogen-rich azole borate salts is reported. Salts of dihydrobis(3,5-dinitropyrazol-1-yl)borate and di-hydrobis-(3-nitro-1,2,4-triazol-1-yl)borate as well as the potassium salt of tetrakis(3-nitro-1,2,4-triazol-1-yl) have been synthesised and characterized.

2.1. Dihydrobis(3,5-dinitropyrazol-1-yl)borate Salts

In order to obtain metal free dihydrobis(3,5-dinitropyrazol-1-yl)borate salts, the starting material is the corresponding potassium salt. In the first step of the synthesis potassium dihydrobis(3,5-dinitropyrazol-1-yl)borate was synthesized by reacting KBH_4 with two equivalents of 3,5-dinitropyrazole in benzonitrile at elevated temperatures. The second synthesis step is the generation of the corresponding barium salt by the reaction of the potassium salt with barium perchlorate in methanol at room temperature. The metal-free salts guanidinium (**G_H$_2$B(DNP)$_2$ 1**)-, aminoguanidinium (**AG_H$_2$B(DNP)$_2$ 2**)-, diaminoguanidinium (**DAG_H$_2$B(DNP)$_2$ 3**)-, N-guanylurea (**NGU_H$_2$B(DNP)$_2$ 4**)- and 5-aminotetrazolium dihydrobis(3,5-dinitropyrazol-1-yl)borate (**5-At_H$_2$B(DNP)$_2$ 5**) were synthesized by mixing the barium salt with the nitrogen-rich sulfates (Figure 1) in methanol at room temperature. All compounds crystallize water-free.

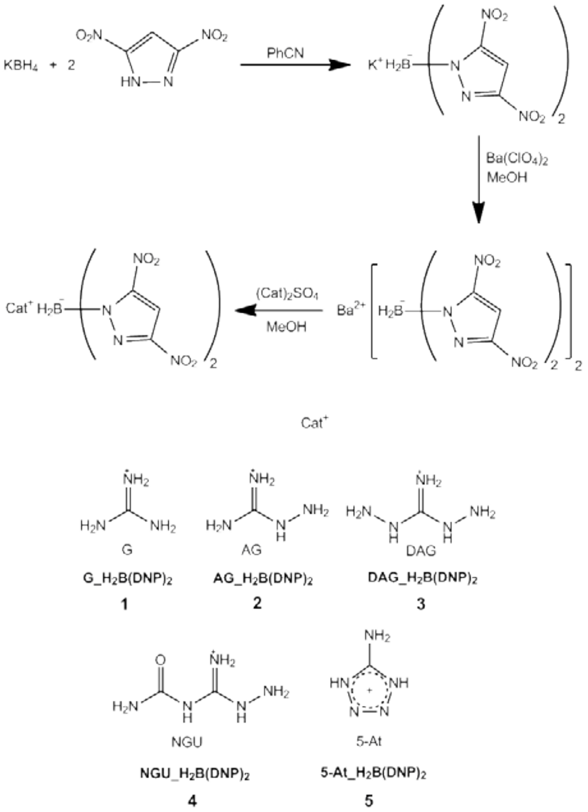

Figure 1: Syntheses of dihydrobis(3,5-dinitropyrazol-1-yl)borate salts.

All compounds have been fully characterized using ^{1}H, ^{13}C and ^{11}B NMR spectroscopy as well as mass spectrometry, elemental analysis and vibrational spectroscopy.

2.2.Dihydrobis(3-nitro-1,2,4-triazol-1-yl)borate Salts

The synthesis of potassium dihydrobis(3-nitro-1,2,4-triazolyl)borate was performed according to literature (Pellei et al 2005) reacting potassium borohydride with 3-nitro-1,2,4-triazole in a molar ratio of 1:2 in dimethylacetamide at high temperatures. Then the corresponding barium salt was synthesized by mixing the potassium salt with barium perchlorate in water at room temperature. In the last step all nitrogen-rich dihydrobis(3-nitro-1,2,4-triazol-1-yl)borate salts were obtained by the reaction of the barium salt with the corresponding sulfates using water and methanol as solvents. The obtained metal-free borate salts are ammonium (**NH$_4$_H$_2$B(3-NTr)$_2$ 6**)-, aminoguanidiunium (**AG_ H$_2$B(3-NTr)$_2$ 7**)-, diaminoguanidinium (**DAG_ H$_2$B(3-NTr)$_2$ 8**)-, N-guanylurea (**NGU_H$_2$B(3-NTr)$_2$ 9**)-, 5-aminotetrazolium (**5-At_H$_2$B(3-NTr)$_2$ 10**)-, dimethylguanidinium (**DMG_H$_2$B(3-NTr)$_2$ 11**)-, hydroxylammonium (**NH$_3$OH_H$_2$B(3-NTr)$_2$ 12**) and hydrazinium dihydrobis(3-nitro-1,2,4-triazol-1-yl)borate (**N$_2$H$_5$_H$_2$B(3-NTr)$_2$ 13**) (Figure 2).The ammonium salt crystallizes as a dihydrate, the N-guanylurea salt as a trihydrate, the 5-aminotetrazolium salt as a dihydrate, the dimethylguanidiunium salt as a monohydrate and the hydroxylammonium salt as a monohydrate.

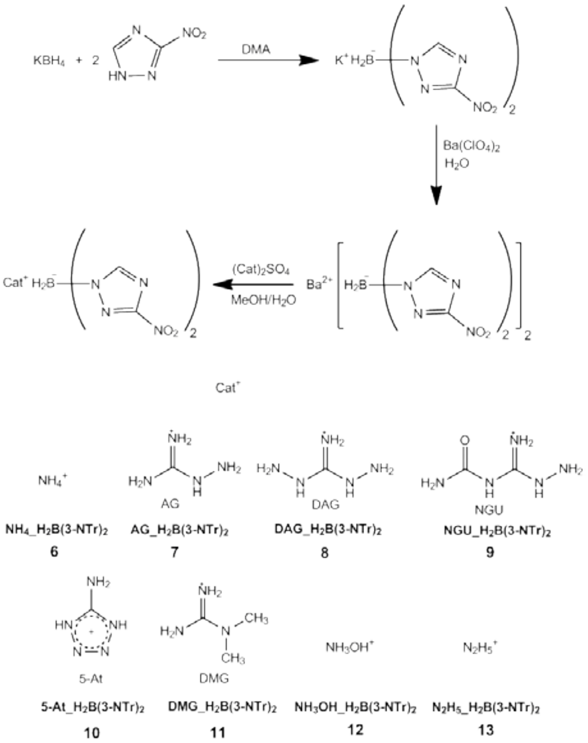

Figure 2: Syntheses of dihydrobis(3-nitro-1,2,4-triazol-1-yl)borate salts.

All compounds have been fully characterized using ^{1}H, ^{13}C and ^{11}B NMR spectroscopy as well as mass spectrometry, elemental analysis and vibrational spectroscopy.

2.3. Four-fold coordinated borate – Potassium tetrakis(3-nitro-1,2,4-triazol-1-yl)borate

Potassium tetrakis(3-nitro-1,2,4-triazol-1-yl)borate (**14**) was synthesized by reacting potassium borohydride and 3-nitro-1,2,4-triazole with a molar ratio of 1:4 in diglyme at high temperature (Figure 3).

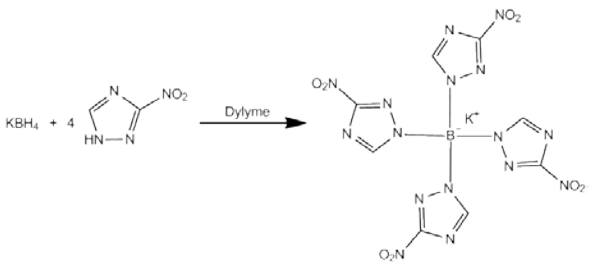

Figure 3: Synthesis of potassium tetrakis(3-nitro-1,2,4-triazol-1-yl)borate.

Compound **14** was characterized using ^{1}H, ^{13}C and ^{11}B NMR spectroscopy and elemental analysis. The measured ^{11}B NMR shift in DMSO-d^6 can be observed at -3.8 ppm. In addition the ^{11}B NMR shift was calculated in order to compare the experimentally measured value with the theoretically calculated value. The isotropic magnetic shielding was computed using the GIAO (Gauge-Independent Atomic Orbital) method implemented in G03 (Frisch et al and Wolinski et al 1990). The structures were fully optimized and the frequencies calculated (NIMAG = 0) at MPW1PW91/aug-cc-pVDZ level of theory, Subsequently, the NMR shielding tensors were calculated at the same level of theory using the GIAO method[2]. Table 1 summarizes the computed isotropic magnetic shieldings and relative ^{11}B NMR chemical shifts (ppm) referenced to $BF_3 \cdot Et_2O$.

Table 1: ^{11}B NMR chemical shift calculation.

	-*E*/ a.u.	*NIMAG*	*p.g.*	δ ^{11}B / ppm, calcd. isotr. shielding	δ ^{11}B / ppm, calcd. (ref. to $BF_3 \cdot Et_2O$)
14	1809.431116	0	S_4	113.6	-3.6

3. THERMAL AND ENERGETIC PROPERTIES

Melting and decomposition points were measured with a Linseis PT10 DSC using heating rates of 5 °C min^{-1}, which were checked with a Büchi Melting Point B-450 apparatus. The sensitivity data were performed using BAM methods. The following tables indicate the results obtained from submitting the compounds to shock and friction stimuli as well as to electrostatic discharge (ESD). Furthermore, the decomposition (T_{dec}) temperatures are listed below (Tables 2-3).

All dihydrobis(3,5-dinitropyrazol-1-yl)borate salts show high decomposition temperatures ranking from 231 to 353 °C. All salts except the aminoguanidinium- and diaminoguanidinium dihydrobis(3,5-dinitropyrazol-1-yl)borates are insensitive towards shock and all salts are friction insensitive (Table 2).

Table 2: Thermal and energetic properties of dihydrobis(3,5-dinitropyrazol-1-yl)borates salts.

	Impact[a] [J]	Friction[a] [N]	grain size [µm]	T_{dec} (onset)[b] [°C]
G_H$_2$B(DNP)$_2$	>40	>360	<100	311
AG_H$_2$B(DNP)$_2$	8	>360	<100	346
DAG_H$_2$B(DNP)$_2$	20	>360	100-500	231
NGU_H$_2$B(DNP)$_2$	>40	>360	<100	353
5-At_H$_2$B(DNP)$_2$	>40	>360	100-500	345

[a]BAM standards, method 1 of 6, [b]DSC heating rate 5 °/min

The decomposition temperatures of dihydrobis(3-nitro-1,2,4-triazol-1-yl)borate salts are summarized in table 3 and are in the range of 136 to 236 °C. All salts are not or less sensitive towards friction. Impact sensitive are only the 5-aminotetrazolium and hydroxylammonium salts, both show a value of 10 J. All other salts can be classified as insensitive (Table 3).

Table 3: Thermal and energetic properties of dihydrobis(3-nitro-1,2,4-triazol-1-yl)borates salts.

	Impact[a] [J]	Friction[a] [N]	grain size [µm]	T_{dec} (onset)[b] [°C]
NH$_4$_H$_2$B(3-NTr)$_2$	40	360	100-500	209
AG_H$_2$B(3-NTr)$_2$	>40	360	100-500	221
NGU_H$_2$B(3-NTr)$_2$	>40	>360	100-500	225
5-At_H$_2$B(3-NTr)$_2$	10	288	100-500	136
DMG_H$_2$B(3-NTr)$_2$	>40	>360	<100	236
NH$_3$OH_H$_2$B(3-NTr)$_2$	10	>360	100-500	152
N$_2$H$_5$_H$_2$B(3-NTr)$_2$	>40	360	100-500	143

[a]BAM standards, method 1 of 6, [b]DSC heating rate 5 °/min

The decomposition temperature and the impact and friction sensitivities of compound **14** were measured as well. With an impact sensitivity of >40 J and a friction sensitivity of >360 N compound **14** can be classified as insensitive. Compound **14** shows a high decomposition temperature of 303 °C.

3. PYROTECHNIC FORMULATIONS

In order to replace toxic and environmentally hazardous formulations containing barium nitrate as green-burning coloring agent, investigations on boron-containing colorants were performed. Several pyrotechnic formulations containing the compounds **1**, **2**, **3**, **4** and **7** as green coloring agent were investigated and compared to the US Army´s in-service green (M125A1 Ba-control) burning compositions (Table 4). The pyrotechnical compositions were prepared by mixing all substances, except the binder, in a mortar.

Then the binder, a solution of 25 % vinyl alcohol acetate resin (VAAR), was added. The mixtures of 0.6 g each were formed by hand and dried under high vacuum for three hours. The controlled burn down was filmed with a digital video camera recorder (SONY, DCR-HC37E). The performance of each composition has been evaluated with respect to color emission, smoke generation and the amount of solid residues. Spectrometric measurements were performed using a *HR2000+ES* spectrometer with an ILX511B linear silicon CCD-array detector and included software from OCEAN OPTICS with a detector-sample distance of 1 meter. The dominant wavelength and spectral purity was measured based on the 1931 CIE method using illuminant C as the white reference point. 5 samples were measured for each formulation and all given values are averaged based on the full burn of the mixture. Amorphous boron was used as fuel and green coloring agent. Ammonium dinitramide (ADN), Ammonium nitrate and magnesium were used as oxidizer and fuel, respectively. In the tables 4-10 the content of the compositions (mass percent) is summarized.

The used barium control formulation containing barium nitrate as oxidizer and green colorant is shown in table 4.

Table 4: US Army composition M125 A1.

	$Ba(NO_3)_2$ [wt%]	Mg [wt%]	PVC [wt%]	VAAR [wt%]
Ba-control	46	33	16	5

In Table 5 the compositions of the formulations containing compound **1** as colorant are shown.

Table 5: Pyrotechnic compositions containing compound 1 as coloring agent.

	1 [wt%]	ADN [wt%]	NH_4NO_3 [wt%]	B [wt%]	Mg [wt%]	VAAR [wt%]
GBDNP_1	25	50	-	9	9	7
GBDNP_2	25	50	-	-	18	7
GBDNP_3	25	-	50	-	18	7

All three formulations GBDNP_1, GBDNP_2 and GBDNP_3 burned smokeless with an intense green flame color (Figure 4). While GBDNP_1 showed no residues, after the burn down of GBDNP_2 and GBDNP_3 no residues remained.

Figure 4: Burn down of formulations GBDNP_1 (left), GBDNP_2 (middle) and GBDNP_3 (right).

Compositions containing compound **2** as green colorant are shown in Table 6.

Table 6: Pyrotechnic compositions containing compound 1 as coloring agent.

	2 [wt%]	ADN [wt%]	B [wt%]	Mg [wt%]	VAAR [wt%]
AGBDNP_1	25	50	9	9	7
AGBDNP_2	30	50	9	4	7

Both formulations burned smokeless with an intense green flame color and no residues were observable (Figure 5).

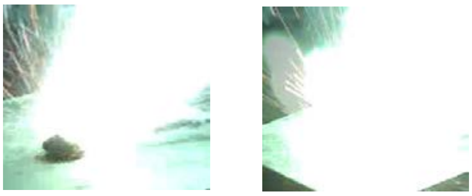

Figure 5: Burn down of formulations AGBDNP_1 (left) and AGBDNP_2 (right).

The Tables 7 and 8 show the compositions of the formulations containing compounds **3** and **4** as green colorants.

Table 7: Pyrotechnic compositions containing compound 3 as coloring agent.

	3 [wt%]	ADN [wt%]	B [wt%]	VAAR [wt%]
DAGBDNP	30	50	13	7

Table 8: Pyrotechnic compositions containing compound 4 as coloring agent.

	4 [wt%]	ADN [wt%]	B [wt%]	Mg [wt%]	VAAR [wt%]
NGUBDNP	25	55	10	3	7

Both formulations burned smokeless with an intense green flame color and no residues remained (Figure 6).

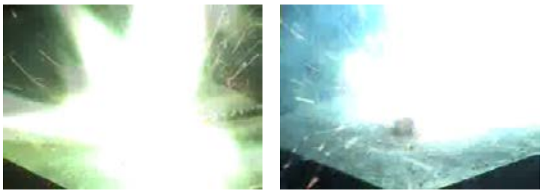

Figure 6: Burn down of formulations DAGBDNP (left) and NGUBDNP (right).

Among the dihydrobis(3-nitro-1,2,4-triazol-1-yl)borates compound **7** was investigated as coloring agent. Three formulations with different compositions were tested as shown in Table 9.

Table 9: Pyrotechnic compositions containing compound 7 as coloring agent.

	7 [wt%]	ADN [wt%]	B [wt%]	Mg [wt%]	VAAR [wt%]
AGBNTr_1	34	60	-	-	6
AGBNTr_2	29	60	5	-	6
AGBNTr_3	25	50	9	9	7

All three formulations burned smokeless with a green flame color and no residues were observable (Figure 7).

Figure 7: Burn down of formulations AGBNTr_1 (left), AGBNTr _2 (middle) and AGBNTr _3 (right).

Additionally, formulations containing amorphous boron as colorant and fuel were also investigated. In Table 10 the content of the compositions is summarized.

Table 10: Pyrotechnic compositions containing amorphous boron as coloring agent.

	B [wt%]	ADN [wt%]	Mg [wt%]	VAAR [wt%]
B_1	18	75	-	7
B_2	13	80	-	7
B_3	18	58	17	7

As can be seen from Figure 8 all three formulations burned with an intense green flame color. Composition B_1 produced some smoke and some residues remained. Composition B_2 burned smokeless, but less residues were observable. Formulation B_3 showed less smoke and no residues remained.

Figure 8: Burn down of formulations B_1 (left), B_2 (middle) and B_3 (right).

From spectrometrical measurements the dominant wavelengths (Dw), spectral purities (Sp) and luminous intensities (LI) as well as burn times – referring to 0.6 g samples – were obtained and are summarized in the following Tables 11-17. Also the impact and friction sensitivities and the decomposition temperature of the formulations are given (Tables 12-17).

The GBDNP formulations of 0.6 g each show burning times from 1 to 9 s, while GBDNP_1 burns very fast formulations GBDNP_3 shows a long burning time compared to those of the barium control with a burning time of 3 s (Table 11). Compositions AGBDNP_1, AGBDNP_2, DAGBDNP and NGUBDNP show burning times 1-2 s and are in the range of the barium control. The spectral purities of the GBDNP and AGBDNP formulations (Table 13) are in the range of 65 % to 71 % and are slightly lower than that of the barium control with 75 % (Table 11). The AGBDNP compositions show higher spectral purities than the GBDNP formulations. Compositions GBDNP_1 and GBDNP_2 using ADN as oxidizer reveal higher luminous intensities than GBDNP_3 with NH_4NO_3 as oxidizer. The luminous intensity of formulation GBDNP_2 exceeds that of the barium control. Both compositions DAGBDNP and NGUBDNP show with 51 % and 55 % lower spectral purities as well as lower luminous intensities compared to the barium control and the other formulations.

Table 11: Performance of the barium control.

	burn time [s]	Dw [nm]	Sp [%]	LI [cd]
Ba-control	3	558	75	$4.35 \cdot 10^{-3}$

Table 12: Thermal and energetic properties of the barium control.

	Impact[a] [J]	Friction[a] [N]	grain size [µm]	T_{dec} [°C]
Ba-control	15	360	< 100	258

T_{dec} = decomposition temperature (DSC onset), [a]BAM standards, method 1 of 6

Table 13: Performance of formulations containing compounds 1, 2, 3 and 4 as colorants.

	burn time [s]	Dw [nm]	Sp [%]	LI [cd]
GBDNP_1	1	554	65	$3.69 \cdot 10^{-3}$
GBDNP_2	4	571	68	$8.76 \cdot 10^{-3}$
GBDNP_3	9	556	70	$5.03 \cdot 10^{-4}$

AGBDNP_1	1	560	72	$9.35{\cdot}10^{-4}$
AGBDNP_2	2	555	71	$5.52{\cdot}10^{-3}$
DAGBDNP	2	559	51	$4.23{\cdot}10^{-4}$
NGUBDNP	2	557	55	$2.13{\cdot}10^{-3}$

Due to the oxidizer ADN in the formulations, the decomposition temperatures going from 180 °C to 189 °C (Table 14) are all lower than that of the barium control of 258 °C (Table 12). Only GBDNP_3 possess a high decomposition temperature of 278 °C, due to NH_4NO_3 used as oxidizer. Except the formulations GBDNP_1 and AGBDNP_2, which are impact sensitive, all other compositions are not impact sensitive. Regarding the friction sensitivity, only GBDNP_1 is less friction sensitive. The other formulations are not friction sensitive (Table 14).

Table 14: Thermal and energetic properties of formulations containing compounds 1, 2, 3 and 4 as colorants.

	Impact[a] [J]	Friction[a] [N]	grain size [µm]	T_{dec} [°C]
GBDNP_1	5	324	< 100	189
GBDNP_2	40	360	< 100	180
GBDNP_3	40	360	< 100	278
AGBDNP_1	40	360	< 100	185
AGBDNP_2	30	360	< 100	183

T_{dec} = decomposition temperature (DSC onset), [a]BAM standards, method 1 of 6

The formulations AGBNTr_1, AGBNTr_2 and AGBNTr_3 with burning times of 3-4 s show slightly lower spectral purities than the barium control as well (Table 15). The luminous intensity of AGBNTr_3 containing magnesium is higher than the luminous intensities of the other two formulations without magnesium, but is lower than that of the barium control (Table 15).

Table 15: Performance of formulations containing compound 7 as colorant.

	burn time [s]	Dw [nm]	Sp [%]	LI [cd]
AGBNTr_1	4	556	68	$8.56{\cdot}10^{-4}$
AGBNTr_2	4	560	69	$4.78{\cdot}10^{-4}$
AGBNTr_3	3	555	71	$3.47{\cdot}10^{-3}$

For comparison three formulations containing only boron as green colorant were investigated. The first two compositions B_1 and B_2 show a burning time of 2-3 s and are in the range of the control, whereas B_1 has a long burning time of 11 s. The spectral purities are also only slightly lower than that of the barium control. The luminous intensities of B_1 and B_2 are lower than that of the control, whereas the luminous intensity of B_3 exceeds that of the barium control (Table 16).

Table 16: Performance of formulations containing amorphous boron as colorant.

	burn time [s]	Dw [nm]	Sp [%]	LI [cd]
B_1	2	563	63	$6.25{\cdot}10^{-4}$
B_2	3	567	68	$6.97{\cdot}10^{-4}$
B_3	11	566	72	$3.15{\cdot}10^{-2}$

As shown in Table 17 all formulations are impact and friction sensitive and show decompositions temperatures lower than 200 °C.

Table 17: Thermal and energetic properties of formulations containing amorphous boron as colorant.

	Impact[a] [J]	Friction[a] [N]	grain size [µm]	T_{dec} [°C]
B_1	10	60	< 100	169
B_2	10	60	< 100	184
B_3	10	324	< 100	170

T_{dec} = decomposition temperature (DSC onset), [a]BAM standards, method 1 of 6

3. CONCLUSIONS

Several nitrogen-rich dihydrobis(3,5-dinitropyrazol-1-yl)borate and dihydrobis(3-nitro-1,2,4-triazol-1-yl)borate salts were synthesized and characterized. Decomposition temperatures, impact and friction sensitivities were measured and showed, that most of the salts possess high thermal stability and are not or less sensitive. Furthermore, the four coordinated potassium tetrakis(3-nitro-1,2,4-triazol-1-yl)borate was synthesized and characterized. In addition the ^{11}B NMR shift was calculated.

Pyrotechnical formulations with selected azole borates as colorants were prepared and investigated and compared to the US Army in-service M125 A1 barium formulation. Formulations containing only amorphous boron as colorant were investigated as well. The combustion behaviour was observed and the dominant wavelengths, spectral purities and luminous intensities as well as the decomposition temperature and the shock and friction sensitivities were measured. The results show that the spectral purities are in the range of 51 % to 72 % and are only slightly lower than that of the barium control. The luminous intensities of formulations using magnesium and ADN are higher and are comparable or even higher (B_3) than that of the barium control. Formulations containing ADN show lower thermal stability. Almost all compositions are less or not impact and friction sensitive, except the formulations containing amorphous boron which are sensitive towards shock and friction. For this reasons, formulations containing azole borates as green colorants are promising candidates in the ongoing investigations to replace toxic barium compounds by environmentally friendly and less toxic boron-containing compounds.

REFERENCES

M. A. Hiskey, D. E. Chavez, D. L. Naud, S. F. Son, H. L. Berghout, C. A. Bolme, *27th Proc. Int. Pyrotech. Sem.*, Co, USA, July 16–21, **2000**, 3.

T. M. Klapötke, J. Stierstorfer, K. R. Tarantik, *Propellants, Explos., Pyrotech.*, **2010**, *35*, 395.

R. M. Blunt, P. J. Keitel, *US Pat.* US 3453157, **1969**.

J. J. Sabatini, J. C. Poret, R. N. Broad, *Angew. Chem., Int. Ed.*, **2011**, *50*, 4624.

a) E. Wiberg, H. Michaud, *Z. Naturforsch.*, **1954**, *9b*, 497; b) P. Paetzold, *Adv. Inorg. Chem.*, **1987**, **31**, 123; c) F. Liu, X. Zeng, J. Zhang, L. Meng, S. Zheng, M. Ge, D. Wang, D. K. W. Mok, F. Chau, *Chem. Physics Letters*, **2006**, *419*, 213.

C. R. Guibert, M. D. Marshall, *J. Am. Chem. Soc.*, **1966**, *88*, 189.

S. Trofimenko, *Scorpionates: The Coordination Chemistry of Poly(pyrazolyl)borate Ligands*, Imperial College Press, London, **1999**.

a) Z. Zeng, B. Twamley, J. M. Shreeve, *Organometallics*, **2007**, *26*, 1782; b) L.G. Gioia, B. Flavio, C. Patrizio, *Synth. React. Inorg. Met.-Org. Chem.*, **1991**, *21*, 1141.

M. Pellei, F. Benetollo, G. G. Lobbia, S. Alidori, C-Santini, *Inorg. Chem.*, **2005**, *44*, 846.

T. J. Groshens, *J. Coord. Chem.*, **2010**, *63*, 1882.

a) C. Janiak, L. Esser, *Z. Naturforsch. B* , **1993**, *48*, 394; b) C. Janiak, T. G. Scharmann, W. Gunther, F. Girgsdies, H. Hemling, W. Hinrichs, D. Lentz, *Chem. Eur. J.*, **1995**, *1*, 637; c) C. Janiak, T. G. Scharmann, *Polyhedron*, **2003**, *22*, 1123.

(a) Wolinski, K.; Hilton, J. F.; Pulay, P. *J. Am. Chem. Soc*. **1990**, *112*, 8251;
(b) Dodds, J. L.; McWeeny, R.; Sadlej, A. J. *Mol. Phys*. **1980**, *41*, 1419;
(c) Ditchfield, R. *Mol. Phys*. **1974**, *27*, 789;
(d) McWeeny, R. *Phys. Rev*. **1962**, *126*, 1028.

Gaussian 03, Revision A.1, Frisch, M. J.; Trucks, G. W.; Schlegel, H. B.; Scuseria, G. E.; Robb, M. A.; Cheeseman, J. R.; Montgomery, Jr., J. A.; Vreven, T.; Kudin, K. N.; Burant, J. C.; Millam, J. M.; Iyengar, S. S.; Tomasi, J.; Barone, V.; Mennucci, B.; Cossi, M.; Scalmani, G.; Rega, N.; Petersson, G. A.; Nakatsuji, H.; Hada, M.; Ehara, M.; Toyota, K.; Fukuda, R.; Hasegawa, J.; Ishida, M.; Nakajima, T.; Honda, Y.; Kitao, O.; Nakai, H.; Klene, M.; Li, X.; Knox, J.E.; Hratchian, H. P.; Cross, J. B.; Adamo, C.; Jaramillo, J.; Gomperts, R.; Stratmann, R. E.; Yazyev, O.; Austin, A. J.; Cammi, R.; Pomelli, C.; Ochterski, J. W.; Ayala, P. Y.; Morokuma, K.; Voth, G. A.; Salvador, P.; Dannenberg, J. J.; Zakrzewski, V. G.; Dapprich, S.; Daniels, A.D.; Strain, M. C.; Farkas, O.; Malick, D. K.; Rabuck, A. D.; Raghavachari, K.; Foresman, J. B.; Ortiz, J. V.; Cui, Q.; Baboul, A. G.; Clifford, S.; Cioslowski, J.; Stefanov, B. B.; Liu, G.; Liashenko, A.; Piskorz, P.; Komaromi, I.; Martin, R. L.; Fox, D. J.; Keith, T.; Al-Laham, M. A.; Peng, C. Y.; Nanayakkara, A.; Challacombe, Gill, P. M. W.; Johnson, B.; Chen, W.; Wong, M. W.; Gonzalez, C.; and Pople, J. A.; Gaussian, Inc., Pittsburgh PA, 2003.

D. Lu, C. H. Winter, *Inorg. Chem.*, **2010**, *49*, 5795.

Acknowledgements

Financial support of this work by the Ludwig-Maximilian University of Munich (LMU), the U.S. Army Research Laboratory (ARL) under grant no. W911NF-09-2-0018, the Armament Research, Development and Engineering Center (ARDEC) under grant no. W911NF-12-1-0467, and the Office of Naval Research (ONR) under grant nos. ONR.N00014-10-1-0535 and ONR.N00014-12-1-0538 is gratefully acknowledged. The authors acknowledge collaborations with Dr. Mila Krupka (OZM Research, Czech Republic) in the development of new testing and evaluation methods for energetic materials and with Dr. Muhamed Suceska (Brodarski Institute, Croatia) in the development of new computational codes to predict the detonation and propulsion parameters of novel explosives. We are indebted to and thank Drs. Betsy M. Rice and Brad Forch (ARL, Aberdeen, Proving Ground, MD) for many inspired discussions. The Cusanuswerk is gratefully acknowledged for the award of a PhD scholarship (M. Rusan).

Green Pyrotechnic Formulations Based on Metal-Free and Nitrogen-Rich Tetrazolylborate Salts

Thomas M. Klapötke,* Magdalena Rusan and Jörg Stierstorfer
Department of Chemistry and Biochemistry, University of Munich (LMU), Butenandtstr. 5-13, D-81377 Munich, Germany
email: tmk@cup.uni-muenchen.de

Abstract: *The investigation of green-burning boron-based compounds as colorants in pyrotechnic formulations as an alternative for environmentally and health hazardous barium nitrate is reported here. Metal-free and nitrogen-rich dihydrobis(5-aminotetrazolyl)borate salts and dihydrobis(1,3,4-triazolyl)borate salts have been synthesized and characterized by NMR spectroscopy, elemental analysis, mass spectrometry and vibrational spectroscopy. The energetic and thermal properties have been determined as well. Crystal structures of compounds* ***5b****, 7 and* ***13*** *were obtained. Pyrotechnic compositions have been prepared using selected dihydrobis(azolyl)borate salts as green colorants. In these compositions ammonium dinitramide and ammonium nitrate haven been used as oxidizers, and boron and magnesium as fuels. The burn time, dominant wavelength, spectral purity, luminous intensity and luminous efficiency as well as the thermal and energetic properties of these compositions were measured.*

Introduction

In the course of the elimination of hazardous materials from the wide field of pyrotechnics, the search for alternatives has become important.[1] In green-light emitting pyrotechnic formulations barium nitrate is mostly used as both the flame colorant and the oxidant.[2] Despite producing intense green colored flames in the presence of a chlorine source, barium nitrate is known to be toxic to humans and the environment and therefore it is desirable to replace it by non-toxic green colorants. As alternatives boron and boron compounds are taken into consideration. In particular boron compounds with nitrogen-rich moieties are considered to be interesting green colorants.

The use of nitrogen-rich compounds in pyrotechnics was reported by Douda and co-workers in the 1960s.[3] Later publications describe further investigations of nitrogen-rich compounds like dihydrazinotetrazine in pyrotechnic formulations.[4] A boron-based pyrotechnic formulation has been investigated by Sabatini using boron carbide as green colorant.[2b] The combination of boron carbide and potassium nitrate resulted in an intense green-burning and insensitive formulation revealing good color properties. The synthesis of nitrogen-rich and therefore energetic boron-containing compounds like sodium and potassium dihydrobis(5-aminotetrazolyl)borates has been described in the literature.[5] The reaction of sodium and potassium borohydrides and two equivalents of 5-aminotetrazole led to the formation of the corresponding metal dihydrobis(5-aminotetrazolyl) borates. In addition, a series of metal complexes containing dihydrobis(tetrazolyl)borate as ligand have been described in the literature.[6] Higher coordinated compounds like hydrotris(tetrazolyl)borate moieties have been synthesized using the solvent diglyme, high temperatures and a crown ether revealing unique properties in metal complexes and representing nitrogen-rich and energetic metal complexes.[7] Shreeve and co-workers investigating ionic liquids for solvent applications reported the synthesis of triazole-based borates, which fit the ionic liquid criteria. The synthesis of potassium and barium dihydrobis(1,2,4-triazolyl)borates as well as metal and metal-free hydrotris(triazolyl)borates has been described.[8] Also, the preparation and investigation of silver(ɪ) poly(1,2,4-triazolyl)borate complexes containing phosphane ligands have been reported.[9]

In this work the synthesis and characterization of nitrogen-rich and metal-free dihydrobis(5-aminotetrazolyl)borate and dihydrobis(1,2,4-triazolyl)borate salts are reported. Their thermal and energetic properties were determined as well. Several selected metal-free dihydrobis(azolyl)borate salts are employed as colorants in pyrotechnic formulations. Mixtures of those salts and ammonium dinitramide (ADN), ammonium nitrate, magnesium, boron and vinyl alcohol acetate resin binder (VAAR) were made and their color performance and thermal and energetic properties investigated.

Results and discussion

Syntheses

The starting materials potassium dihydrobis(5-aminotetrazolyl)borate (**1**), (5-aminotetrazole)dihydro(5-aminotetrazolyl)borane hemihydrate (**2**), potassium dihydrobis(1,2,4-triazolyl)borate (**11**) and barium dihydrobis(1,2,4-triazolyl)borate trihydrate (**13**) were described in the literature and synthesized according to those literature procedures.[5a,8] The reaction of potassium borohydride and

Article Details | *Article No:- 0104*
Manuscript Received:- | *Final Revisions:-*
Publication Date:- | *Archive Reference:-*

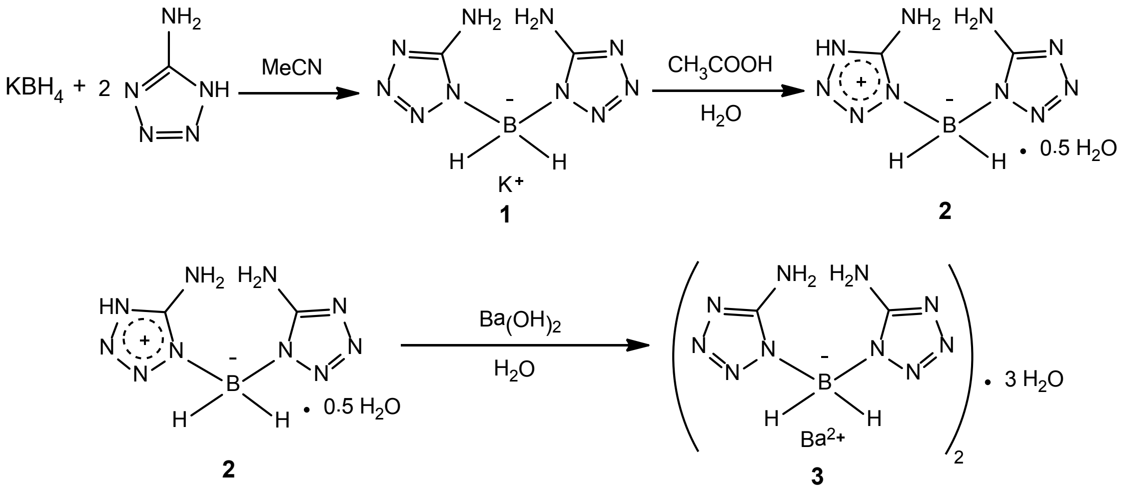

Scheme 1. *Synthesis of potassium and barium dihydrobis(5-aminotetrazolyl)borate salts.*

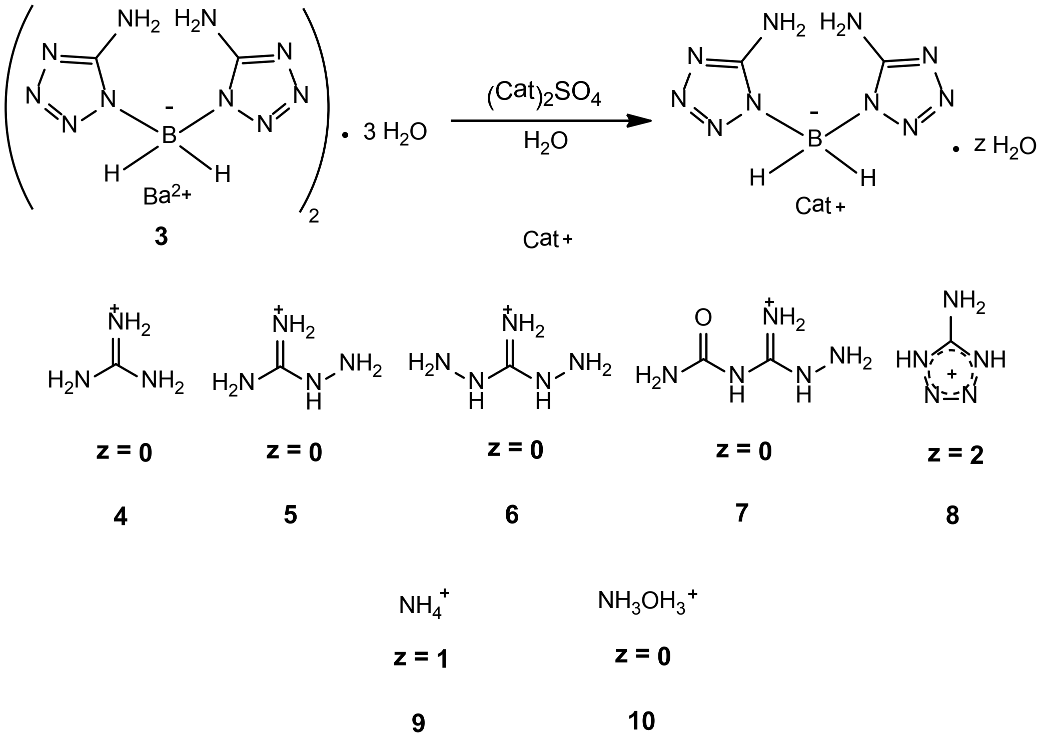

Scheme 2. *Synthesis of metal-free dihydrobis(5-aminotetrazolyl)borate salts.*

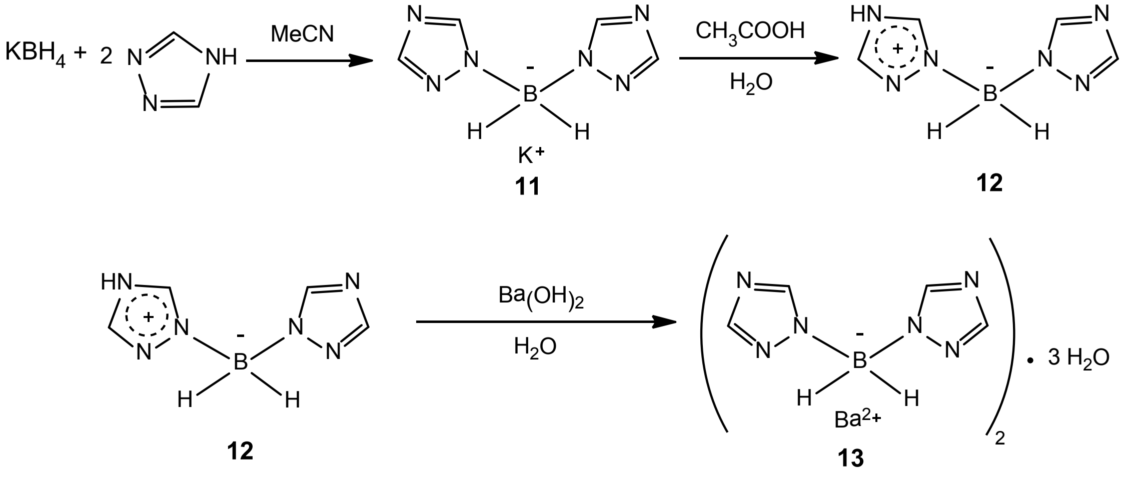

Scheme 3. *Synthesis of potassium and barium dihydrosbis(1,2,4-triazolyl)borate salts.*

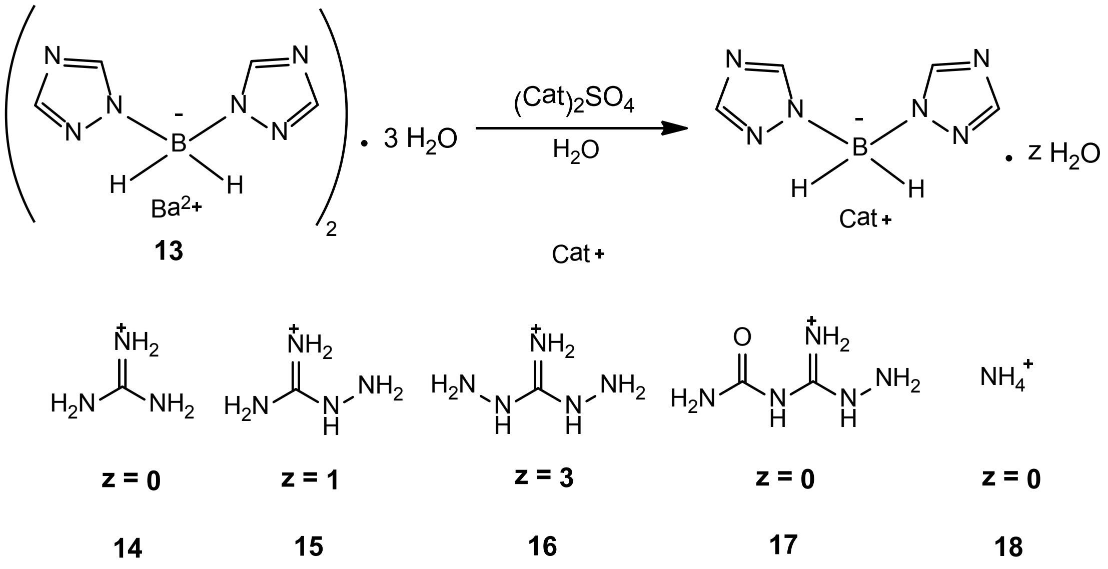

Scheme 4. *Synthesis of metal-free dihydrobis(1,2,4-triazolyl)borate salts.*

two equivalents of 5-aminotetrazole or 1,2,4-triazole, respectively, led to the formation of the corresponding potassium dihydrobis(azolyl)borate salts. By the acidification of the potassium dihydrobis(azolyl)borate salts the corresponding (azole)dihydrobis(azolyl) boranes were obtained. The following reaction with barium hydroxide resulted in the formation of the barium dihydrobis(azolyl)borate trihydrate salts (Schemes 1 and 3). Both barium compounds **3** and **13** served as starting compounds in the synthesis of the metal-free dihydrobis(azolyl)borates (Schemes 2 and 4).

Metal-free dihydrobis(5-aminotetrazolyl)borates were obtained by mixing **3** with nitrogen-rich sulfates in water at room temperature (Scheme 2). The compounds **4–10** could be obtained as colorless solids in high yields and high purity. Recrystallization of the aminoguanidinium salt **5** from water/acetone yielded single crystals of hydrazone **5b**.

According to the literature[8] the dihydrobis(1,2,4-triazolyl)borate compounds have been synthesized in the same manner as the dihydrobis(5-aminotetrazolyl)borate salts (Scheme 3). First the potassium salt **11** and then the barium salt **13** were synthesized and served as starting materials for the preparation of metal-free compounds.

Metal-free dihydrobis(1,2,4-triazolyl)borates were prepared like the dihydrobis(5-aminotetrazolyl)borates by combining compound **13** and nitrogen-rich sulfates in water and at room temperature, obtaining colorless solids in high yields and high purities as well (Scheme 4).

Characterization

All salts have been identified and characterized by ^{1}H, ^{13}C, ^{14}N, and ^{11}B NMR spectroscopy, elemental analysis, mass spectrometry and IR spectroscopy. The ^{1}H and ^{13}C NMR shifts of the 5-aminotetrazolyl and 1,2,4-triazolyl moieties as well as those of the cations are in accordance with the literature values.[5a,8] Dihydrobis(5-aminotetrazolyl) borates show ^{11}B NMR shifts at around −15 ppm. The ^{11}B NMR signals of dihydrobis(1,2,4-triazolyl)borate compounds have been observed at around −10 ppm. The ^{1}H NMR spectra of the borate anions show broadened shifts between 3.2 and 3.7 ppm attributed to the BH_2 group. The IR spectra of all borate anions show B–H stretching vibrations between 2410 and 2450 cm^{-1}. Additionally B–N stretching vibrations between 1548 and 1540 cm^{-1} could be observed.[10]

Molecular structures

Crystal structures of compounds **5b**, **6** and **13** were measured by low temperature X-ray diffraction. Suitable single crystals were picked from the crystallization mixture and mounted in Kel-F oil, transferred to the N_2 stream of an Oxford Xcalibur3 diffractometer with a Spellman generator (voltage 50 kV, current 40 mA) and a KappaCCD detector using a $\lambda_{\mathrm{MoK}\alpha}$ radiation wavelength of 0.71073 Å. All structures were measured at −173 °C. The data collection and data reduction were carried out with the CrysAlisPro software.[11] The structures were solved with Sir-92,[11] refined with Shelxl 97[12] and finally checked using the Platon software[13] integrated in the WINGX software suite.[14] The non-hydrogen atoms were refined anisotropically and the hydrogen atoms were located and freely refined. The absorptions were corrected by a SCALE3 ABSPACK multi-scan method.[15] Detailed data and parameters of the X-ray measurements and refinements are included in Table 1. Further information regarding the crystal-structure determination has been deposited as cif files with the Cambridge Crystallographic Data Centre[16] as supplementary publications with the Nos. 1001410 (**5b**), 1001412 (**6**), 1001410 (**13**).

Both guanidinium bis(azolyl)borates **5b** and **6** crystallize in the monoclinic space group $P2_1/c$. The molecular moieties are depicted in Figures 1 and 2. The density of the hydrazone **5b** (1.357 g cm^{-3}) is significantly lower than that of the diaminoguanidinium salt **6** (1.551 g cm^{-3}). This might be a consequence of missing hydrogen bonds of the missing hydrazine NH_2 group. Nevertheless both structures are dominated by a large variety of hydrogen bonds. The B–H protons in both structures do not participate in any non-

Table 1. *Crystallographic data of **5b**, **6** and **13**.*

Compound	**5b**	**6**	**13**
Formula	$C_6H_{17}BN_{14}$	$C_3H_{14}BN_{15}$	$C_8H_{18}B_2BaN_{12}O_3$
FW [g mol^{-1}]	296.15	271.10	489.30
Crystal system	Monoclinic	Monoclinic	Orthorhombic
Space Group	$P2_1/c$ (No. 14)	$P2_1/c$ (No. 14)	$C222_1$ (No. 20)
Color/Habit	Colorless plate	Colorless block	Colorless rod
Size [mm]	0.09 × 0.21 × 0.40	0.12 × 0.18 × 0.28	0.13 × 0.14 × 0.30
a [Å]	11.8627(6)	9.2353(3)	7.0683(2)
b [Å]	8.5858(5)	13.3916(5)	13.6825(3)
c [Å]	14.8565(9)	9.3994(3)	18.0720(4)
α [°]	90	90	90
β [°]	106.642(6)	92.738(3)	90
γ [°]	90	90	90
V [Å^3]	1449.77(15)	1161.15(7)	1747.78(7)
Z	4	4	4
ρ_{calc} [g cm^{-3}]	1.357	1.551	1.860
μ [mm^{-1}]	0.099	0.118	2.311
$F(000)$	624	568	960
$\lambda_{MoK\alpha}$[Å]	0.71073	0.71073	0.71073
T [K]	173	173	173
θ min-max [°]	4.2, 26.0	4.3, 26.5	4.5, 26.0
Dataset h; k; l	−14:14; −9:10; −18:18	−11:11; −16:16; −11:11	−8:8; −16:16; −22:22
Reflect. coll.	7298	18224	8824
Independ. refl.	2833	2400	1716
R_{int}	0.021	0.037	0.030
Reflections obs	2371	1809	1676
No. parameters	258	228	155
R_1 (obs)	0.0325	0.0296	0.0138
wR_2 (all data)	0.0862	0.0743	0.0303
S	1.02	0.96	1.07
Resd. Dens. [e Å^{-3}]	−0.17, 0.19	−0.17, 0.17	−0.32, 0.71
Device type	Oxford Xcalibur3 CCD	Oxford Xcalibur3 CCD	Oxford Xcalibur3 CCD
Solution	SIR-92	SIR-92	SIR-92
Refinement	SHELXL-97	SHELXL-97	SHELXL-97
Absorpt. corr.	multi-scan	multi-scan	multi-scan
CCDC	1001410	1001412	1001411

classical hydrogen bond. The 5-aminotetrazole moieties are comparable to similar structures of alkali aminotetrazolates[17] in which the N–H protons are bent out of the ring plane. The cations are almost planar. The B–N distances in both structures are observed similarly (**5b**: B–N1 1.5587(18), B–N6 1.5659(18); **6**: B–N1 1.5594(18), B–N6 1.5540(18) Å). In the structure of **5b** (and in contrast to **6**) the amino groups of the tetrazole ligand show a *cis*-like conformation.

The barium bis(dihydrobis(triazolyl)borate salt **13** as its trihydrate crystallizes in the non-centrosymmetric orthorhombic space group $C222_1$ with four complexes in the unit cell. Its density of 1.860 g cm^{-3} is relatively low in comparison to other barium azole salts.[18] The barium cation and oxygen atom O1 lie on the C_2 axis. Taking into account coordination distances up to 3.6 Å, the barium cations are ninefold coordinated. The bistriazolyl anions act as a bidentate ligand coordinating with their nitrogen atoms N4

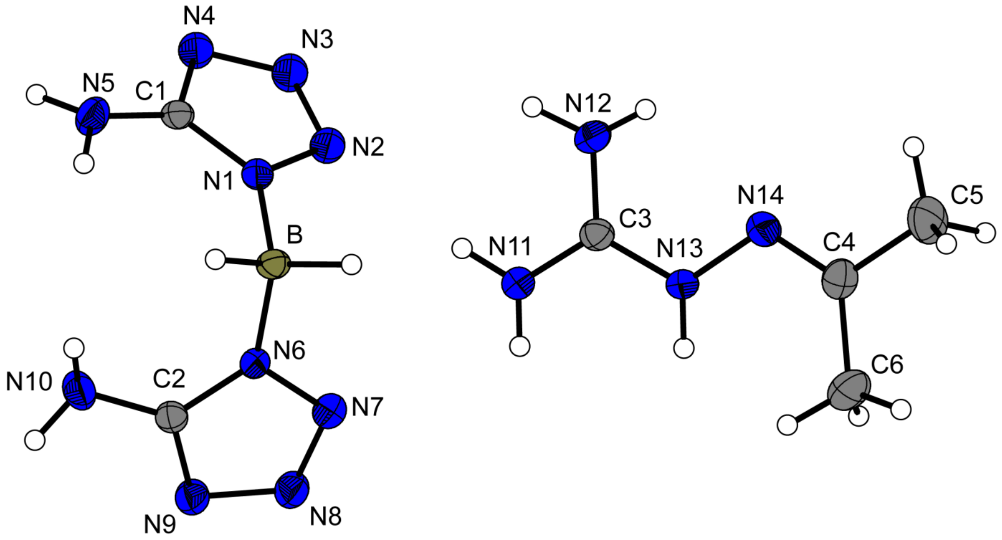

Figure 1. *Representation of the molecular unit of* ***5b****, showing the atom-labeling scheme. Thermal ellipsoids represent the 50% probability level and hydrogen atoms are shown as small spheres of arbitrary radius. Selected anion bond lengths [Å]: N1–B 1.5587(17), N6–B 1.5659(17), N1–C1 1.3477(16), N1–N2 1.3676(14), N2–N3 1.2936(15), N3–N4 1.3621(16), N4–C1 1.3335(16), N5–C1 1.3553(16); selected anion bond angles [°]: N1–B–N6 108.50(10), C1–N1–B 130.80(10), N2–N1–B 122.33(10).*

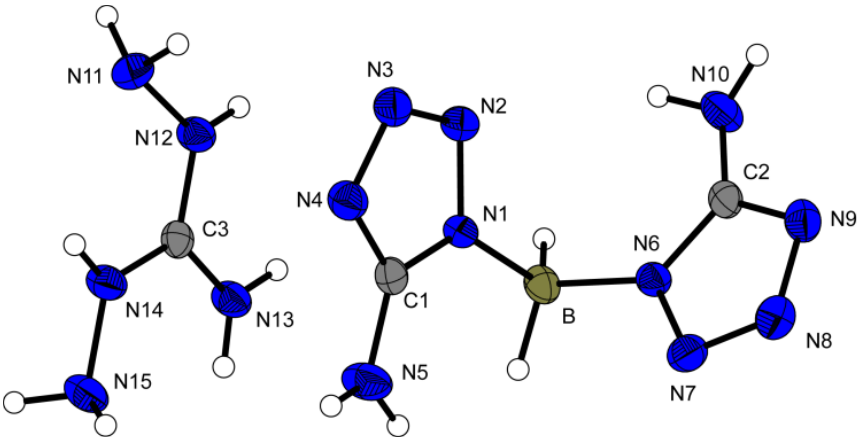

Figure 2. *Molecular unit of* ***6****, showing the atom-labeling scheme. Thermal ellipsoids represent the 50% probability level and hydrogen atoms are shown as small spheres of arbitrary radius. Selected anion bond lengths [Å]: N1–B 1.5593(17), N6–B 1.5541(17), C1–N1 1.3395(14) N1–N2 1.3630(13), N2–N3 1.2937(14), N4–N3 1.3572(14), N4–C1 1.3273(15), C1–N5 1.3499(16), selected anion bond angles [°]: N6–B–N1 106.51(9), C1–N1–B 130.44(10), N2–N1–B 122.29(9).*

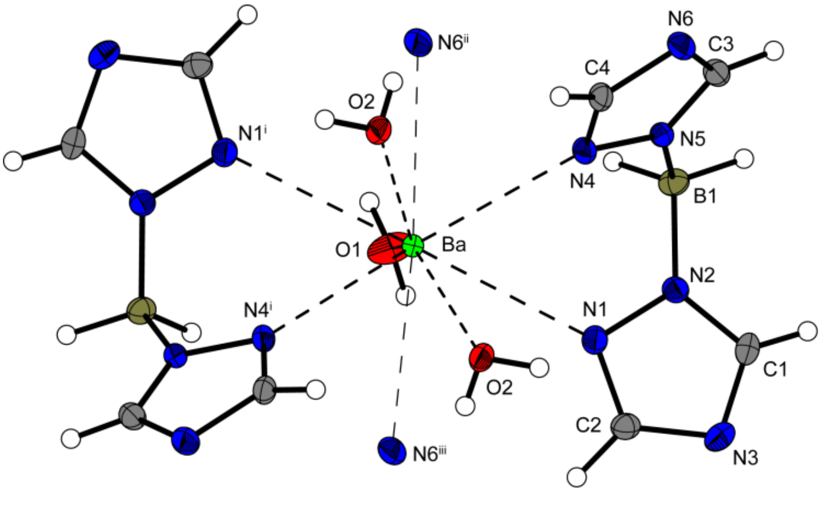

Figure 3. *Advanced molecular unit of barium salt* ***13****, showing the atom-labelling scheme. Thermal ellipsoids represent the 50% probability level and hydrogen atoms are shown as small spheres of arbitrary radius. B–N and barium coordination distances [Å]: B1–N5 1.559(3), B1–N2 1.543(3) Ba–N4 3.0058(19), Ba–N1 3.0001(18), Ba–O1 2.723(2), Ba–O2 2.7863(18), Ba–N6ii 3.070(2); Symmetry codes: (i) x, −y, −z; (ii) 0.5+x, 0.5−y, −z; (iii) 0.5+x, −0.5+y, z.*

and N1. A 3-D structure is formed by the coordination of the triazolyl nitrogen atoms N6 of two other anions.

Energetic properties

The sensitivities towards ignition stimuli and the decomposition temperatures of the products have been determined. Table 2 shows the impact (IS) and friction (FS) sensitivities. Also the sensitivities towards electrostatic discharge (ESD), the dehydration (T_{dehydr}), melting (T_{melt}) and decomposition temperatures (T_{dec}) are summarized in Table 2. All compounds are barely or not at all impact and friction sensitive. The decomposition temperatures vary between 140 °C and 320 °C. Compound **17** shows a decomposition temperature that is higher than 400 °C. Additionally, the DSC curves of compounds **8**, **9**, **15** and **16** show peaks between 81 °C and 101 °C corresponding to the loss of crystal water.

Pyrotechnic formulations

The replacement of toxic and environmentally hazardous barium nitrate as green-burning colorant by boron-containing colorants has been investigated. Several pyrotechnic formulations containing different nitrogen-rich and metal-free dihydrobis(azolyl)borate salts as green colorants were investigated and compared to the US Army's in-service green burning composition M125A1 (Ba-control) (Table 3). The pyrotechnic compositions were prepared by mixing all substances, except the binder, in a mortar. Then the binder, a solution of 25% vinyl alcohol acetate resin (VAAR), was added. After drying under high vacuum for 3 hours the mixtures were ground again. Pellets of 0.6 g each were pressed using a consolidation dead load of 2000 kg. The pellets were dried overnight at ambient temperature. The controlled burn down was filmed with a digital video camera recorder (SONY, DCR-HC37E). The performance of each composition has been evaluated with respect to color emission, smoke generation (perceived by the naked eye) and the amount of solid residues. Spectrometric measurements were performed using an HR2000+ES spectrometer with an ILX511B linear silicon CCD-array detector and included software from Ocean Optics with a detector–sample distance of 1 m. The dominant wavelength and spectral purity were measured based on the 1931 CIE method using illuminant C as the white reference point. Five samples were measured for each formulation and all given values are averaged based on the full burn of the mixture. Amorphous boron was used as fuel and green coloring agent. Ammonium dinitramide (ADN) and ammonium nitrate were used as oxidizer and magnesium and amorphous boron as fuel, respectively.

Two types of metal-free dihydrobis(azolyl)borates – the dihydrobis(5-aminotetrazolyl)borate and the dihydrobis(1,2,4-triazolyl)borate salts – have been investigated as green colorants in several pyrotechnic mixtures. Formulations containing different borate salts but the same content and ratio have been tested, investigating the influence of the borate salts on combustion behavior, color properties and sensitivities. The guanidinium, aminoguanidinium, diaminoguanidinium and *N*-guanylurea salts of both dihydrobis(azolyl)borates were employed.

The barium control M125A1 was mixed on a small scale (0.6 g) and the color properties as well as thermal and energetic properties were measured and are summarized in Tables 3–5.

Table 3. *US Army composition M125A1.*

	$Ba(NO_3)_2$ [wt%]	Mg [wt%]	PVC [wt%]	VAAR [wt%]
Ba-control	46	33	16	5

Table 4. *US Army composition M125A1.*

	Burn time [s]	Dw [nm]	Sp [%]	LI [cd]	LE [cd s g^{-1}]
Ba-control	3	558	75	390	1950

Table 2. *Overview of the physico-chemical properties of **4–18**.*

	Formula	MW [g mol^{-1}]	Ω^a [%]	N^b [%]	IS [J]	FS [N]	grain size [μm]	ESD [J]	T_{dehydr} [°C]	T_{melt} [°C]	T_{dec} [°C]
4	$C_3H_{12}N_{13}B$	241.03	−89.61	75.55	>40	>360	100–500	1.5	—	120	173
5	$C_3H_{13}N_{14}B$	256.04	−87.48	76.59	>40	>360	100–500	1.0	—	143	193
6	$C_3H_{14}N_{15}B$	271.06	−85.59	77.51	>40	324	100–500	0.3	—	153	165
7	$C_4H_{13}N_{14}OB$	284.05	−84.49	69.04	>40	>360	<100	1.5	—	115	164
8	$C_3H_{14}N_{15}O_2B$	303.06	−65.99	69.33	>40	>360	<100	1.0	82	190	320
9	$C_2H_{14}N_{11}O_2B$	235.02	−71.48	65.56	>40	>360	<100	0.5	86	160	201
10	$C_2H_{10}N_{11}OB$	214.98	−70.70	71.67	30	360	<100	1.0	—	—	140
14	$C_5H_{12}N_9B$	209.02	−133.95	60.31	>40	>360	100–500	1.0	—	111	262
15	$C_5H_{15}N_{10}OB$	242.05	−118.98	57.89	>40	>360	100–500	1.0	81	—	164
16	$C_5H_{20}N_{11}O_3B$	293.10	−100.99	52.57	>40	>360	100–500	1.0	101	143	212
17	$C_6H_{13}N_{10}OB$	252.05	−120.61	55.57	>40	>360	<100	1.5	—	139	>400
18	$C_4H_{10}N_7B$	166.98	−138.93	58.72	40	288	100–500	0.7	—	154	285

[a] Oxygen balance assuming the formation of CO_2. [b] Nitrogen content.

Table 5. *US Army composition M125A1.*

	Impact [J]	Friction [N]	Grain size [µm]	T_{dec} [°C]
Ba-control	15	360	<100	258

Table 6 shows the formulations containing guanidinium dihydrobis(5-aminotetrazolyl)borate (**4**) as colorant. In these two formulations the amounts of the colorant, ADN, boron, magnesium and binder were varied. Both compositions burned without smoke and no solid residues were observable. The spectral purity of **GB5At_1** is 70% and lower than that of the barium control, whereas composition **GB5At_2** shows with 80% a higher spectral purity than the Ba-control with 75% (Table 4).

Two further formulations **GB5At_3** and **GB5At_4** containing compound **4** (Tables 7 and 8) have been investigated. Formulations **GB5At_3** and **GB5At_4** contain boron carbide instead of amorphous boron. In order to compare the influence of compound **4** on the combustion behavior, formulations **A** and **B** containing only B_4C and ADN and NH_4NO_3, respectively (Tables 11 and 12) were examined.

Formulation **GB5At_3** burned with an intense green flame color and no smoke and no residues were observable. Composition **GB5At_4** also burned smokeless, but the flame color was rather pale-green. This observation is in accordance with the spectral purities. While **GB5At_3** exhibits a spectral purity of 85%, which also exceeds that of the barium control, **GB5At_4** shows a spectral purity of only 45% (Table 9). Among these four formulations **GB5At_3** shows the highest luminous intensity of 76 cd, which is however much lower than that of the barium control formulation (Table 4).

Table 6. *Formulations **GB5At_1** and **GB5At_2** containing compound **4**.*

	4 [wt%]	ADN [wt%]	B [wt%]	Mg [wt%]	VAAR [wt%]
GB5At_1	10	60	15	10	5
GB5At_2	20	55	9	9	7

Table 7. *Formulation **GB5At_3** containing compound **4**.*

	4 [wt%]	ADN [wt%]	B4C [wt%]	Mg [wt%]	VAAR [wt%]
GB5At_3	15	60	12	8	5

Table 8. *Formulation **GB5At_4** containing compound **4**.*

	4 [wt%]	NH_4NO_3 [wt%]	B4C [wt%]	Mg [wt%]	VAAR [wt%]
GB5At_4	15	60	12	8	5

Table 9. *Color performance of formulations containing compound **4**.*

	Burn time [s]	Dw [nm]	Sp [%]	LI [cd]	LE [cd s g^{-1}]
GB5At_1	4	565	70	51	340
GB5At_2	3	572	80	32	160
GB5At_3	3	562	85	76	380
GB5At_4	9	578	45	21	315

The energetic and thermal properties of these formulations were determined as well. Both formulations **GB5At_1** and **GB5At_2** using ADN, boron and magnesium show very high impact sensitivities of 1 J and 2 J, but are not (>360 N) or only slightly (324 N) friction sensitive (Table 10). Formulation **GB5At_3** employing ADN, B_4C and Mg shows a lower impact sensitivity of 10 J, but is at 192 N friction sensitive. The combination of NH_4NO_3, B_4C and magnesium in formulation **GB5At_4** reveals a composition which is friction and impact insensitive but however shows worse color properties. The decomposition temperatures are in the range between 156 °C and 179 °C in the case of the ADN-containing formulations. The NH_4NO_3-containing formulation shows a higher decomposition temperature of 201 °C (Table 10).

In formulations **A** and **B** (Tables 11 and 12) no dihydrobis(azolyl)borate salt was employed. Composition **A** was compared with **GB5At_3** and composition **B** with **GB5At_4**. While formulation **B** burned with no green flame color, formulation **A** was not ignitable, so that it can be concluded that compound **4** possesses a significant influence on the combustion behavior.

Table 10. *Energetic and thermal properties of formulations containing compound **4**.*

	Impact [J]	Friction [N]	Grain size [µm]	T_{dec} [°C]
GB5At_1	1	>360	<100	156
GB5At_2	2	324	<100	164
GB5At_3	10	192	<100	179
GB5At_4	>40	>360	<100	201

Table 11. *T Formulation **A** containing ADN and boron carbide.*

	ADN [wt%]	B_4C [wt%]	Mg [wt%]	VAAR [wt%]
A	75	10	8	7

Table 12. *Formulation **B** containing ammonium nitrate and boron carbide.*

	NH_4NO_3 [wt%]	B_4C [wt%]	Mg [wt%]	VAAR [wt%]
B	75	10	8	7

In order to figure out to what extent compound **5**, which compared to compound **4** differs only in the cation, behaves differently in a pyrotechnic formulation and therefore modifies the combustion behavior, three compositions containing **5** were investigated. Formulations **AGB5At_1**, **AGB5At_2** and **AGB5At_3** (Table 13) were prepared in the same ratios as the previously discussed compositions **GB5At_1**, **GB5At_2** and **GB5At_3**.

All three formulations revealed green flame colors and a smokeless and residue-free burn down. In Table 14 the performances are summarized. The spectral purities are 61% (**AGB5At_1**), 71% (**AGB5At_2**) and 77% (**AGB5At_3**). Only the spectral purity of **AGB5At_3** exceeds the barium control. All three formulations show a burn time of 3 seconds, but different luminous intensities. The highest luminous intensity of 378 cd, which is in the range of the barium control formulation (Table 4), is shown by composition **AGB5At_2**. The lowest luminous intensity of 37 cd is revealed by formulation **AGB5At_1** (Table 14).

The comparison of formulations **AGB5At_1**, **AGB5At_2** and **AGB5At_3** with **GB5At_1**, **GB5At_2** and **GB5At_3** shows that although they only differ in the borate compound the performances are quite different. **GB5At_1** and **GB5At_2** show higher spectral purities than **AGB5At_1** and **AGB5At_2**, but the latter ones show much higher luminous intensities (Tables 9 and 14). But all three **AGB5At**-formulations possess burn times of 3 seconds. Only formulation **AGB5At_2** shows a luminous intensity of 378 cd, which is comparable with the barium control (Table 4).

Table 13. *Formulations **AGB5At_1**, **AGB5At_2** and **AGB5At_3** containing compound **5**.*

	5 [wt%]	ADN [wt%]	B [wt%]	Mg [wt%]	VAAR [wt%]
AGB5At_1	10	60	—	25	5
AGB5At_2	10	60	15	10	5
AGB5At_3	20	55	9	9	7

Table 14. *Color performance of formulations containing compound **5**.*

	Burn time [s]	Dw [nm]	Sp [%]	LI [cd]	LE [cdsg^{-1}]
AGB5At_1	3	571	61	37	185
AGB5At_2	3	560	71	378	1890
AGB5At_3	3	561	77	135	675

Table 15. *Energetic and thermal properties of formulations containing compound **5**.*

	Impact [J]	Friction [N]	Grain size [µm]	T_{dec} [°C]
AGB5At_1	3	>360	<100	169
AGB5At_2	2	>360	<100	180
AGB5At_3	4	>360	<100	145

In Table 15 the sensitivities towards impact and friction as well as the decomposition temperatures of **AGB5At**-compositions are shown.

All three formulations are impact but not friction sensitive and thus differ from the **GB5At**-formulations, which are friction sensitive (Table 10). The decomposition temperatures range from 145 °C to 180 °C (Table 15).

Since there is a difference in combustion behavior, color, thermal and energetic properties when using different dihydrobis(5-aminotetrazolyl)borate salts, two further dihydrobis(5-aminotetrazolyl)borate salts **6** and **7** were tested in formulations employing the same components and ratios as the previously discussed formulations. Table 16 summarizes formulations using compound **6**.

All three formulations burned smokeless, residue-free and with a green flame color. The measured spectral purities (Table 17) and luminous intensities are lower compared with the spectral purity and luminous intensity of the barium control (Table 4). The comparison of the color performances and sensitivity data (Tables 17 and 18) with those of the **GB5At**-formulations (Tables 9 and 10) or **AGB5At**-formulations (Tables 14 and 15) reveals differences. Only the decomposition temperatures are comparable.

The next compositions contain compound *N*-guanylurea

Table 16. *Formulations **DAGB5At_1**, **DAGB5At_2** and **DAGB5At_3** containing compound **6**.*

	6 [wt%]	ADN [wt%]	B [wt%]	Mg [wt%]	VAAR [wt%]
DAGB5At_1	10	60	—	25	5
DAGB5At_2	10	60	15	10	5
DAGB5At_3	20	55	9	9	7

Table 17. *Color performance of formulations containing compound **6**.*

	Burn time [s]	Dw [nm]	Sp [%]	LI [cd]	LE cd s g^{-1}]
DAGB5At_1	3	580	42	55	275
DAGB5At_2	3	571	74	139	695
DAGB5At_3	3	572	60	63	315

Table 18. *Energetic and thermal properties of formulations containing compound **6**.*

	Impact [J]	Friction [N]	Grain size [µm]	T_{dec} [°C]
DAGB5At_1	2	120	<100	162
DAGB5At_2	1	>360	<100	180
DAGB5At_3	3	144	<100	154

dihydrobis(5-aminotetrazolyl)borate (**7**) as colorant. In Table 19 the content of formulations using ADN as the oxidizer is summarized. Table 20 shows the composition with ammonium nitrate used as the oxidizer.

Formulations **NGUB5At_1**, **NGUB5At_2** and **NGUB5At_3** burned green, smokeless and no residues remained. Composition **NGUB5At_4** also showed a green flame color and no smoke, but after the burn down some solid residue remained. Except for **NGUB5At_3**, revealing a spectral purity of 82% (Table 21), which exceeds that of the barium control formulation, all other formulations show a lower spectral purity than the barium control (Table 4). The luminous intensities of all four formulations are rather low.

Formulations **NGUB5At_1**, **NGUB5At_2** and **NGUB5At_3** are friction and impact sensitive. Formulation **NGUB5At_4** is friction insensitive but impact sensitive. As expected the highest decomposition temperature was achieved in formulation **NGUB5At_4** using ammonium nitrate as the oxidizer. The other formulations show decomposition temperatures between 165 °C and 170 °C (Table 22).

Table 19. *Formulations **NGUB5At_1**, **NGUB5At_2** and **NGUB5At_3** containing ADN and compound **7**.*

	7 [wt%]	ADN [wt%]	B [wt%]	Mg [wt%]	VAAR [wt%]
NGUB5At_1	10	60	—	25	5
NGUB5At_2	10	60	15	10	5
NGUB5At_3	20	55	9	9	7

Table 20. *Formulation NGUB5At_4 containing NH_4NO_3 and compound 7.*

	7 [wt%]	NH_4NO_3 [wt%]	B [wt%]	Mg [wt%]	VAAR [wt%]
NGUB5At_4	10	60	15	10	5

Table 21. *Color performance of formulations containing compound 7.*

	burn time [s]	Dw [nm]	Sp [%]	LI [cd]	LE [cd s g^{-1}]
NGUB5At_1	3	578	55	35	175
NGUB5At_2	4	571	54	54	360
NGUB5At_3	5	573	82	24	200
NGUB5At_4	3	566	70	30	150

Table 22. *Energetic and thermal properties of formulations containing compound 7.*

	Impact [J]	Friction [N]	Grain size [µm]	T_{dec} [°C]
NGUB5At _1	10	216	<100	165
NGUB5At _2	5	144	<100	169
NGUB5At _3	3	216	<100	170
NGUB5At _4	5	>360	<100	210

In the following section formulations containing dihydrobis(1,2,4-triazolyl)borate compounds are investigated as colorants and compared among themselves and with the corresponding formulations containing dihydrobis(5-aminotetrazolyl)borates.

In Table 23 formulations using compound **16** as colorant are summarized. Table 24 shows the composition employing ammonium nitrate as the oxidizer.

All four formulations showed green flame colors and a smokeless burn down. While no residues could be observed for compositions **DAGBTr_1** and **DAGBTr_2**, formulations **DAGBTr_3** and **DAGBTr_4** revealed small amounts of residues. However, the spectral purities are significantly lower than that of the barium control but in the range of the corresponding **DAGB5At**-formulations (Table 17). The highest spectral purity of 70% was obtained in formulation **DAGBTr_4**. In the case of formulation **DAGBTr_2** a high luminous intensity of 334 cd was achieved, which is in the range of the barium control formulation (Table 25).

The first three formulations are impact and friction sensitive. Only composition **DAGBTr_4** containing NH_4NO_3 instead of ADN is friction insensitive. But in contrast to the impact-insensitive formulation **GB5At_4** also containing NH_4NO_3, **DAGBTr_4** is impact sensitive. As in the case of all ammonium nitrate containing formulations the highest decomposition temperature of 279 °C was observed for formulation **DAGBTr_4** (Table 26).

Table 23. *Formulations **DAGBTr_1**, **DAGBTr_2** and **DAGBTr_3** containing ADN and compound **16**.*

	16 [wt%]	ADN [wt%]	B [wt%]	Mg [wt%]	VAAR [wt%]
DAGBTr_1	10	60	—	25	5
DAGBTr_2	10	60	15	10	5
DAGBTr_3	20	55	9	9	7

Table 24. *Formulation **DAGBTr_4** containing NH_4NO_3 and compound **16**.*

	16 [wt%]	NH_4NO_3 [wt%]	B [wt%]	Mg [wt%]	VAAR [wt%]
DAGBTr_4	10	60	15	10	5

Table 25. *Color performance of formulations containing compound **16**.*

	Burn time [s]	Dw [nm]	Sp [%]	LI [cd]	LE [cd s g^{-1}]
DAGBTr_1	3	577	55	118	590
DAGBTr_2	3	560	65	334	1670
DAGBTr_3	4	572	62	46	307
DAGBTr_4	5	564	70	75	625

Table 26. *Energetic and thermal properties of formulations containing compound **16**.*

	Impact [J]	Friction [N]	Grain size [µm]	T_{dec} [°C]
DAGBTr_1	2	216	<100	160
DAGBTr_2	2	96	<100	165
DAGBTr_3	4	144	<100	173
DAGBTr_4	3	>360	<100	279

Among the dihydrobis(1,2,4-triazolyl)borates the *N*-guanylurea dihydrobis(1,2,4-triazolyl)borate salt (**17**) was tested as colorant as well. The content of the formulations is summarized in Table 27.

While formulations **NGUBTr_1** and **NGUBTr_2** burned smokeless and no residues could be observed, composition **NGUBTr_3** showed some solid residues and a smokeless burn down as well. Formulation **NGUBTr_2** achieved a high spectral purity of 80% (Table 28), exceeding that of the barium control of 75% (Table 4). While in the case of formulations **NGUBTr_1** and **NGUBTr_3** spectral purities were measured which show values which are comparable to the **DAGBTr**-formulations (Table 25), **NGUBTr_2** exhibits a deviant value (Table 28).

All three formulations are friction and impact sensitive. The decomposition temperatures are in the range from 165 °C to 180 °C (Table 29).

The comparison of either dihydrobis(5-aminotetrazolyl) borate-containing formulations or dihydrobis(1,2,4-triazolyl)borate-containing formulations among themselves revealed that there are significant differences in color performance, impact and friction sensitivity as well as decomposition temperatures when varying the borate compound. All formulations have in common that they exhibit high impact sensitivity, when combining ADN, boron, magnesium and an azolylborate salt. When using NH_4NO_3 instead of ADN, only formulation **GB5At_4** revealed friction and impact insensitivity.

Table 27. *Formulations **NGUBTr_1**, **NGUBTr_2** and **NGUBTr_3** containing compound **17**.*

	17 [wt%]	ADN [wt%]	B [wt%]	Mg [wt%]	VAAR [wt%]
NGUBTr_1	10	60	—	25	5
NGUBTr_2	10	60	15	10	5
NGUBTr_3	20	55	9	9	7

Table 28. *Color performance of formulations containing compound **17**.*

	burn time [s]	Dw [nm]	Sp [%]	LI [cd]	LE [cdsg^{-1}]
NGUBTr_1	4	573	55	179	1193
NGUBTr_2	4	573	80	90	600
NGUBTr_3	3	574	50	25	125

Table 29. *Energetic and thermal properties of formulations containing compound **17**.*

	Impact [J]	Friction [N]	grain size [µm]	T_{dec} [°C]
NGUBTr _1	3	120	<100	180
NGUBTr _2	2	144	<100	165
NGUBTr _3	2	216	<100	171

Conclusions

Metal-free and nitrogen-rich salts of dihydrobis(5-aminotetrazolyl)borate and dihydrobis(1,2,4-triazolyl) borate have been synthesized and characterized by NMR and IR spectroscopy, elemental analysis and mass spectrometry. Crystal structures of compounds **5b**, **6** and **13** were obtained. The impact and friction sensitivities as well as the sensitivity towards electrostatic discharge have been determined to be low or not sensitive for all compounds. Formulations using selected borate salts as colorants have been investigated with respect to their performance and sensitivity properties. Formulations employing the same content except for the borate salt have been compared among themselves and with the barium control formulation. It was observed that the use of different borate salts influences significantly the combustion behaviour and the performance and sensitivity properties. Additionally, formulations **GB5At_2**, **GB5At_3**, **AGB5At_3**, **NGUB5At_3** and **NGUBTr_2** using different borate salts as colorants reveal higher spectral purities than the barium control formulation.

Experimental part

All reagents and solvents were used as received (Sigma-Aldrich, Fluka, Acros Organics) if not stated otherwise. Melting and decomposition points were measured with a Linseis PT10 DSC using heating rates of 5 °C min^{-1}, which were checked with a Büchi Melting Point B-450 apparatus. ^{1}H, ^{13}C and ^{14}N NMR spectra were measured with a JEOL Eclipse 400, JEOL Eclipse 270 or JEOL EX400 instrument at an ambient temperature of 25 °C if not stated otherwise. All chemical shifts are quoted in ppm relative to TMS (^{1}H, ^{13}C), nitromethane (^{14}N) or boron trifluoroetherate (^{11}B) as external standards. Infrared spectra were measured using a Perkin Elmer Spectrum BX-FTIR spectrometer with a Smiths DuraSampl IR-ATR unit. Elemental analyses were performed with an Elementar Vario EL or an Elementar Vario EL micro cube. Mass spectra were measured on a JEOL MS station JMS 700 instrument. The impact and friction sensitivity was determined using a BAM drophammer and a BAM friction tester.[19] The sensitivities of the compounds are indicated according to the UN Recommendations on the Transport of Dangerous Goods (+):[19] impact: insensitive >40 J, less sensitive >35 J, sensitive >4 J, very sensitive <4 J; friction: insensitive >360 N, less sensitive = 360 N, sensitive <360 N >80 N, very sensitive <80 N, extremely sensitive <10 N.

The syntheses of potassium dihydrobis(azolyl)borate (**1** and **11**) salts were performed under an argon atmosphere, using standard Schlenk techniques according to the literature procedure.[5a,8] Guanidinium, aminoguanidinium, diaminoguanidinium and 5-aminotetrazolium sulfates were synthesized by combining the corresponding chlorides[20,21] and silver nitrate in water and room temperature under exclusion of light.

CAUTION!

The compounds described in this work are potential explosives, which are sensitive to environmental stimuli such as impact, friction, heat or electrostatic discharge. While we encountered no issues in the handling of these materials, appropriate precautions and proper protective measures (safety glasses, face shields, leather coat, Kevlar gloves and ear protectors) should be taken when preparing and manipulating these materials.

Salts of dihydrobis(5-aminotetrazolyl)borate

All compounds **4–10** were obtained by the reaction of compound **3** with the corresponding nitrogen-rich sulfates. To a solution of **3** in water the sulfates were added in stoichiometric amounts. The reaction mixtures were stirred at room temperature for 15 minutes, whereupon barium sulfates precipitated. After filtration and evaporation of the solvent, colorless solids were yielded as products.

Guanidinium dihydrobis(5-aminotetrazolyl)borate (4)

As product a colorless solid (94%) was gained. IR (ATR): $\tilde{\nu}$ [cm^{-1}] = 3416 (m), 3338 (s), 3184 (s), 2775 (w), 2472 (m), 1778 (w), 1635 (s), 1563 (m), 1542 (m), 1514 (m), 1447 (m), 1296 (m), 1221 (w), 1155 (w), 1126 (w), 1060 (m), 1011 (w), 994 (w), 905 (w), 862 (w), 754 (w), 740 (w), 687 (w). ^{1}H NMR (DMSO-d$_6$) δ: 3.37 (br s, 2H, BH$_2$), 5.58 (s, 4H, C–NH2), 7.19 (s, 6H, 3·NH2) ppm. ^{13}C NMR (DMSO-d$_6$): δ: 158.3 (1C, C-NH$_2$), 159.3 (2C, C-NH$_2$) ppm. ^{11}B NMR (DMSO-d$_6$): δ: −15.3 (1B) ppm. EA: $C_3H_{12}N_{13}B$ (241.03): calculated N 75.55, C 14.95, H 5.02; found N 73.00, C 14.84, H 5.17%. MS (FAB+): *m*/*z* for $CH_6N_3^+$: calculated 60.08; found 60.1. MS (FAB−): *m*/*z* for $C_2H_6N_{10}B$−: calculated 180.95; found 181.3. IS: >40 J (grain size 100–500 μm). FS: >360 N (grain size 100–500 μm). ESD: 1.5 J (grain size 100–500 μm). DSC: 173 °C (dec.).

Aminoguanidinium dihydrobis(5-aminotetrazolyl) borate (5)

A colorless solid was obtained as product (60%). IR (ATR): $\tilde{\nu}$ [cm^{-1}] = 3480 (w), 3420 (w), 3150 (m), 3063 (w), 2908 (w), 2817 (w), 2470 (w), 2348 (m), 1685 (m), 1661 (m), 1620 (s), 1561 (s), 1468 (m), 1455 (m), 1304 (w), 1295 (w), 1278 (w), 1236 (w), 1214 (w), 1189 (w), 1141 (m), 1117 (m), 1103 (m), 1071 (m), 1011 (w), 929 (w), 860 (w), 761 (s). ^{1}H NMR (DMSO-d$_6$): δ: 3.52 (br s, 2H, BH$_2$), 4.63 (s, 2H, N–NH$_2$), 5.59 (s, 4H, C–NH$_2$), 6.74 (s, 2H, C–NH$_2$) 7.22 (s, 2H, C–NH$_2$), 8.55 (s, 1H, NH) ppm. ^{13}C NMR (DMSO-d$_6$): δ: 159.2 (2C, C-NH$_2$), 159.3 (1C, C–NH$_2$) ppm. ^{11}B NMR (DMSO-d$_6$): δ: −14.5 (1B) ppm. EA: $C_3H_{13}N_{14}B$ (256.04): calculated N 76.59, C 14.07, H 5.12; found N 74.03, C 14.49, H 4.98%. MS (FAB+): *m*/*z* for $CH_7N_4^+$: calculated 75.09; found 75.1. MS (FAB−): *m*/*z* for $C_2H_6N_{10}B$−: calculated 180.95; found 181.2. IS: >40 J (grain size 100–500 μm). FS: >360 N (grain size 100–500 μm). ESD: 1.0 J (grain size 100–500 μm). DSC: 193 °C (dec.).

Diaminoguanidinium dihydrobis(5-aminotetrazolyl) borate (6)

As product a colorless solid (78%) was gained. IR (ATR): $\tilde{\nu}$ [cm^{-1}] = 3440 (m), 3357 (w), 3311 (m), 3214 (m), 2980 (w), 2480 (w), 2436 (w), 1667 (s), 1621 (s), 1546 (w), 1514 (w), 1500 (w), 1450 (w), 1353 (w), 1325 (w), 1298 (w), 1278 (w), 1199 (w), 1157 (w), 1133 (w), 1117 (w), 1060 (w), 993 (w), 950 (w), 862 (w), 757 (w), 683 (w). ^{1}H NMR (DMSO-d$_6$): δ: 3.54 (br s, 2H, BH$_2$), 4.57 (s, 4H, NH$_2$), 5.58 (s, 4H, C–NH$_2$), 7.21 (s, 2H, NH$_2^+$), 7.68 (s, 2H, NH) ppm. ^{13}C NMR (DMSO-d$_6$): δ: 159.2 (2C, C–NH$_2$), 159.5 (1C, C–NH$_2$) ppm. ^{11}B NMR (DMSO-d$_6$): δ: −14.3 (^{1}B) ppm. EA: $C_3H_{14}N_{15}B$ (271.06): calculated N 77.51, C 13.29, H 5.21; found N 76.46, C 13.19, H 5.20%. MS (FAB+): *m*/*z* for $CH_8N_5^+$: calculated 90.11; found 90.1. MS (FAB−): *m*/*z* for $C_2H_6N_{10}B^-$: calculated 180.95; found 181.3. IS: >40 J (grain size 100–500 μm). FS: 324 N (grain size 100–500 μm). ESD: 0.3 J (grain size 100–500 μm). DSC: 165 °C (dec.).

N-Guanylurea dihydrobis(5-aminotetrazolyl)borate (7)

As product a colorless crystals (83%) were obtained. IR (ATR): $\tilde{\nu}$ [cm^{-1}] = 3458 (w), 3295 (s), 3129 (s), 3009 (m), 2477 (w), 2422 (w), 2356 (w), 2200 (w), 1718 (s), 1702 (s), 1601 (s), 1548 (s), 1462 (s), 1376 (m), 1353 (s), 1300 (m), 1293 (s), 1228 (m), 1191 (m), 1156 (m), 1124 (s), 1099 (s), 1079 (s), 1048 (s), 1025 (m), 976 (m), 933 (m), 868 (m), 781 (s), 749 (s), 730 (s), 702 (s). ^{1}H NMR (DMSO-d$_6$): δ: 3.30 (br s, 2H, BH$_2$), 5.55 (s, 4H, C-NH$_2$), 6.78 (s, 2H, NH$_2^+$), 8.15 (s, 4H, NH$_2$), 10.07 (s, 1H, NH) ppm. ^{13}C NMR (DMSO-d$_6$): δ: 154.8 (1C), 155.6 (1C), 159.2 (2C, C-NH$_2$) ppm. ^{11}B NMR (DMSO-d$_6$): δ: −14.6 (1B) ppm. EA: $C_4H_{13}N_{14}OB$ (284.05): calculated N 69.04, C 16.91, H 4.61; found N 66.51, C 17.18, H 4.46%. MS (FAB+): *m*/*z* for $C_2H_7N_4O^+$: calculated 103.10; found 103.1. MS (FAB−): *m*/*z* for $C_2H_6N_{10}B^-$: calculated 180.95; found 181.1. IS: >40 J (grain size <100 μm). FS: >360 N (grain size <100 μm). ESD: 1.5 J (grain size <100 μm). DSC: 164 °C (dec.).

5-Aminotetrazolium dihydrobis(5-aminotetrazolyl) borate dihydrate (8)

A colorless solid (95%) was gained. IR (ATR): $\tilde{\nu}$ [cm^{-1}] = 3472 (m), 3374 (m), 3190 (m), 2360 (s), 1782 (w), 1638 (s), 1450 (m), 1297 (m), 1156 (m), 1057 (s), 994 (s), 907 (s), 755 (s), 740 (s), 668 (s). ^{1}H NMR (DMSO-d$_6$): δ: 3.17 (s, H$_2$O), 3.27 (br s, 2H, BH$_2$), 6.45 (br s, 4H, C-NH$_2$), 8.10 (br s, 4H, C-NH$_2$/NH) ppm. ^{13}C NMR (DMSO-d$_6$): δ: 156.7 (3C, C-NH$_2$) ppm. ^{11}B NMR (DMSO-d$_6$): δ: −15.4 (1B) ppm. EA: $C_3H_{10}N_{15}B\cdot 2H_2O$ (303.06): calculated N 69.33, C 11.89, H 4.66; found N 64.71, C 11.68, H 4.56%. MS (FAB+): *m*/*z* for $CH_4N_5^+$: calculated 86.08; found 86.10. MS (FAB−): *m*/*z* for $C_2H_6N_{10}B^-$: calculated 180.95; found 181.1. IS: >40 J (grain size <100 μm). FS: >360 N (grain size <100 μm). ESD: 1.0 J (grain size <100 μm). DSC: 320 °C (dec.).

Ammonium dihydrobis(5-aminotetrazolyl)borate hydrate (9)

A colorless solid (85%) was obtained. IR (ATR): $\tilde{\nu}$ [cm^{-1}] = 3138 (w), 3122 (w), 3047 (w), 2439 (w), 2397 (w), 2348 (w), 2287 (w), 1783 (w), 1513 (m), 1428 (m), 1323 (m), 1280 (m), 1216 (m), 1183 (m), 1171 (s), 1157 (s), 1131 (s), 1113 (s), 1015 (m), 990 (s), 895 (m), 886 (m), 870 (s), 718 (m), 677 (s). ^{1}H NMR (DMSO-d$_6$): δ: 3.23 (s, H_2O), 3.36 (br s, 2H, BH_2), 5.57 (br s, 4H, C-NH_2), 7.20 (4H, NH_4^+) ppm. ^{13}C NMR (DMSO-d$_6$): δ: 158.3 (3C, C-NH_2) ppm. ^{11}B NMR (DMSO-d$_6$): δ: −15.2 (1B) ppm. EA: $C_2H_{10}N_{11}B{\cdot}H_2O$ (217.00): calculated N 71.00, C 11.07, H 5.57; found N 70.94, C 11.13, H 5.47%. MS (FAB+): *m/z* for NH_4^+: calculated 18.04; found 18.10. MS (FAB−): *m/z* for $C_2H_6N_{10}B^-$: calculated 180.95; found 181.2. IS: >40 J (grain size <100 μm). FS: >360 N (grain size <100 μm). ESD: 0.5 J (grain size <100 μm). DSC: 201 °C (dec.).

Hydroxylammonium dihydrobis(5-aminotetrazolyl)borate (10)

As product a colorless solid (91%) was gained. IR (ATR): $\tilde{\nu}$ [cm^{-1}] = 3436 (w), 3414 (w), 3323 (w), 3222 (w), 3166 (w), 3111 (w), 2936 (w), 2676 (w), 2489 (w), 2348 (m), 2129 (w), 1655 (m), 1625 (s), 1595 (m), 1563 (m), 1472 (m), 1455 (m), 1299 (m), 1282 (w), 1266 (w), 1218 (w), 1195 (w), 1149 (s), 1131 (s), 1113 (m), 1073 (s), 1024 (m), 992 (m), 877 (w), 867 (m), 762 (s), 750 (m). ^{1}H NMR (DMSO-d$_6$): δ: 3.41 (br s, 2H, BH_2), 5.58 (br s, 4H, C-NH_2), 10.04 (NH_3OH^+) ppm. ^{13}C NMR (DMSO-d$_6$): δ: 158.8 (3C, C-NH_2) ppm. ^{11}B NMR (DMSO-d$_6$): δ: −15.2 (1B) ppm. EA: $C_2H_{10}N_{11}OB$ (214.99): calculated N 71.67, C 11.17, H 4.69; found N 68.81, C 11.13, H 4.78%. MS (FAB+): *m/z* for NH_4O^+: calculated 34.04; found 34.1. MS (FAB−): *m/z* for $C_2H_6N_{10}B^-$: calculated 180.95; found 181.1. IS: 30 J (grain size <100 μm). FS: 360 N (grain size <100 μm). ESD: 1.0 J (grain size <100 μm). DSC: 140 °C (dec.).

Salts of dihydrobis(1,2,4-triazolyl)borate

The compounds **14–18** were gained by the reaction of compound **13** with the corresponding nitrogen-rich sulfates. To a solution of **13** in water the sulfates were added in stoichiometric amounts. The reaction mixtures were stirred at room temperature for 15 minutes, whereupon the barium sulfates precipitated. After filtration and evaporation of the solvent, colorless solids were obtained as products.

*Guanidinium dihydrobis(1,2,4-triazolyl)borate (**14**)*

As product a colorless solid (90%) was obtained. IR (ATR): $\tilde{\nu}$ [cm^{-1}] = 3585 (w), 3432 (m), 3326 (m), 3232 (m), 3151 (m), 3121 (m), 3103 (m), 2424 (w), 2402 (w), 2267 (w), 2183 (w), 2133 (w), 2040 (w), 2010 (w), 1997 (w), 1971 (w), 1957 (w), 1943 (w), 1774 (w), 1736 (w), 1646 (s), 1540 (w), 1503 (s), 1415 (m), 1317 (m), 1267 (m), 1216 (w), 1178 (m), 1160 (s), 1143 (s), 1128 (s), 1031 (w), 1020 (m), 970 (m), 902 (w), 88 (w), 872 (m), 863 (m), 735 (w), 723 (w), 705 (vw), 676 (m), 666 (s). ^{1}H NMR (DMSO-d$_6$) δ: 3.31 (br s, 2H, BH_2), 7.60 (s, 2H, CH), 7.99 (s, 2H, CH), 7.43 (s, 6H, 3·NH_2) ppm. ^{13}C NMR (DMSO-d$_6$): δ: 147.2 (2C, CH), 151.5 (2C, CH), 158.4 (1C, C-NH_2) ppm. ^{11}B NMR (DMSO-d$_6$): δ: −10.1 (1B) ppm. EA: $C_5H_{12}N_9B$ (209.02): calculated N 60.31, C 28.73, H 5.79; found N 58.14, C 27.86, H 5.61%. MS (FAB+): *m/z* for $CH_6N_3^+$: calculated 60.08; found 60.1. MS (FAB−): *m/z* for $C_4H_6N_6B^-$: calculated 148.94; found 149.1. IS: >40 J (grain size 100–500 μm). FS: >360 N (grain size 100–500 μm). ESD: 1.0 J (grain size 100–500 μm). DSC: 262 °C (dec.).

*Aminoguanidinium dihydrobis(1,2,4-triazolyl)borate hydrate (**15**)*

A slightly yellow solid was obtained as product (70%). IR (ATR): $\tilde{\nu}$ [cm^{-1}] = 3133 (w), 3121 (w), 3114 (w), 3045 (w), 2439 (w), 2398 (w), 2287 (w), 1783 (w), 1513 (m), 1428 (m), 1323 (m), 1280 (m), 1216 (w), 1183 (w), 1171 (m), 1157 (s), 1131 (s), 1113 (m), 1015 (m), 996 (s), 884 (m), 870 (s), 756 (m), 718 (m), 677 (m). ^{1}H NMR (DMSO-d$_6$): δ: 3.21 (s, H_2O), 3.46 (br s, 2H, BH_2), 4.68 (s, 2H, N–NH_2), 6.93 (s, 2H, C–NH_2) 7.28 (s, 2H, C–NH_2), 7.66 (s, 2H, CH), 7.97 (s, 2H, CH), 8.28 (s, 1H, NH) ppm. ^{13}C NMR (DMSO-d$_6$): δ: 147.9 (2C, CH), 151.6 (2C, CH), 159.3 (1C, C–NH_2) ppm. ^{11}B NMR (DMSO-d$_6$): δ: −9.9 (1B) ppm. EA: $C_5H_{13}N_{10}B$ (224.04): calculated N 62.52, C 26.81, H 5.85; found N 60.00, C 26.39, H 5.93%. MS (FAB+): *m/z* for $CH_7N_4^+$: calculated 75.09; found 75.1. MS (FAB−): *m/z* for $C_4H_6N_6B^-$: calculated 148.94; found 149.1. IS: >40 J (grain size 100–500 μm). FS: >360 N (grain size 100–500 μm). ESD: 1.0 J (grain size 100–500 μm). DSC: 164 °C (dec.).

*Diaminoguanidinium dihydrobis(1,2,4-triazolyl)borate trihydrate (**16**)*

As product a colorless solid (99%) was gained. IR (ATR): $\tilde{\nu}$ [cm^{-1}] = 3585 (w), 3432 (m), 3326 (m), 3232 (m), 3151 (m), 3121 (m), 3103 (m), 2424 (m), 2402 (m), 2267 (w), 2133 (w), 1774 (w) 1736 (w), 1646 (s),1540 (w), 1503 (s), 1415 (m), 1317 (m), 1267 (m), 1216 (w), 1178 (m), 1160 (s), 1143 (s), 1128 (s), 1031 (m), 1020 (m), 989 (w), 970 (m), 902 (w), 888 (w), 972 (m), 863 (m), 735 (w) 723 (w), 872 (m), 863 (m), 735 (w) 723 (m), 676 (m), 666 (s), 656 (m). ^{1}H NMR (DMSO-d$_6$): δ: 3.10 (s, H2O), 3.54 (br s, 2H, BH_2), 4.53 (s, 4H, NH_2), 7.29 (s, 2H, NH_2^+), 7.65 (s, 2H, CH), 7.98 (s, 2H, CH), 7.79 (s, 2H, NH) ppm. ^{13}C NMR (DMSO-d$_6$): δ: 147.9 (2C, CH), 151.6 (2C, CH), 159.2 (1C, C–NH_2) ppm. ^{11}B NMR (DMSO-d$_6$): δ: −9.8 (1B) ppm. EA: $C_5H_{14}N_{11}B$ (239.05): calculated N 64.45, C 25.12, H 5.90; found N 58.67, C 25.19, H 5.98%. MS (FAB+): *m/z* for $CH_8N_5^+$: calculated 90.11; found 90.1. MS (FAB−): *m/z* for $C_4H_6N_6B^-$: calculated 148.94; found 149.1. IS: >40 J (grain size 100–500 μm). FS: >360 N (grain size 100–500 μm). ESD: 1.0 J (grain size 100–500 μm). DSC: 212 °C (dec.).

*N-Guanylurea dihydrobis(1,2,4-triazolyl)borate (**17**)*

A colorless solid (82%) was obtained as product. IR (ATR): $\tilde{\nu}$ [cm^{-1}] = 3447 (w), 3322 (w), 3130 (w), 3087 (w), 2920 (w), 2761 (w), 2356 (w), 2274 (w), 2042 (w), 1724 (m), 1681 (m), 1586 (m), 1541 (w), 1507 (s), 1453 (m), 1417 (w), 1395 (w), 1321 (m), 1270 (m), 1197 (w), 1185 (w), 1171 (m), 1161 (s), 1132 (m), 1074 (m), 1019 (m), 997 (w), 972 (s), 899 (m), 886 (m), 801 (w), 784 (w), 719 (m). ^{1}H NMR (DMSO-d$_6$): δ: 3.46 (br s, 2H, BH$_2$), 7.67 (s, 2H, CH), 6.81 (s, 2H, NH$_2^+$), 7.87 (s, 2H, CH), 8.34 (s, 4H, NH2), 10.03 (s, 1H, NH) ppm. ^{13}C NMR (DMSO-d$_6$): δ: 147.3 (2C, CH), 152.1 (2C, CH), 154.4 (1C), 155.1 (1C) ppm. ^{11}B NMR (DMSO-d$_6$): δ: −9.5 (1B) ppm. EA: C$_6$H$_{13}$N$_{10}$OB (252.05): calculated N 55.57, C 28.59, H 5.20; found N 51.61, C 28.39, H 5.15%. MS (FAB+): *m/z* for C$_2$H$_7$N$_4$O$^+$: calculated 103.10; found 103.1. MS (FAB−): *m/z* for C$_4$H$_6$N$_6$B$^-$: calculated 148.94; found 149.1. IS: >40 J (grain size <100 µm). FS: >360 N (grain size <100 µm). ESD: 1.5 J (grain size <100 µm). DSC: >400 °C (dec.).

*Ammonium dihydrobis(1,2,4-triazolyl)borate (**18**)*

As product a colorless solid (91%) was obtained. IR (ATR): $\tilde{\nu}$ [cm^{-1}] = 3138 (w), 3122 (w), 3047 (w), 2439 (w), 2397 (w), 2287 (w), 1783 (w), 1513 (m), 1428 (m), 1323 (m), 1280 (m), 1216 (w), 1183 (w), 1171 (m), 1157 (s), 1131 (s), 1113 (m), 1015 (m), 990 (s), 886 (m), 870 (s), 718 (m), 677 (m). ^{1}H NMR (DMSO-d$_6$): δ: 3.51 (br s, 2H, BH$_2$), 7.25 (4H, NH$_4^+$), 7.51 (s, 2H, CH), 7.61 (s, 2H, CH) ppm. ^{13}C NMR (DMSO-d$_6$): δ: 147.9 (2C, CH), 152.6 (2C, CH) ppm. ^{11}B NMR (DMSO-d$_6$): δ: −9.9 (1B) ppm. EA: C$_4$H$_{10}$N$_7$B (116.98): calculated N 58.72, C 28.77, H 6.04; found N 53.81, C 28.59, H 5.97%. MS (FAB+): *m/z* for NH$_4^+$: calculated 18.04; found 18.10. MS (FAB−): *m/z* for C$_4$H$_6$N$_6$B$^-$: calculated 148.94; found 149.1. IS: 40 J (grain size 100–500 µm). FS: 288 N (grain size 100–500 µm). ESD: 0.7 J (grain size 100–500 µm). DSC: 285 °C (dec.).

Acknowledgements

Financial support of this work by the Ludwig-Maximilian University of Munich (LMU), the U.S. Army Research Laboratory (ARL) under grant no. W911NF-09-2-0018, the Armament Research, Development and Engineering Center (ARDEC) under grant no. W911NF-12-1-0467, and the Office of Naval Research (ONR) under grant nos. ONR.N00014-10-1-0535 and ONR.N00014-12-1-0538 is gratefully acknowledged. The authors acknowledge collaborations with Dr. Mila Krupka (OZM Research, Czech Republic) in the development of new testing and evaluation methods for energetic materials and with Dr. Muhamed Suceska (Brodarski Institute, Croatia) in the development of new computational codes to predict the detonation and propulsion parameters of novel explosives. We are indebted to and thank Drs. Betsy M. Rice and Brad Forch (ARL, Aberdeen, Proving Ground, MD) for many inspired discussions. The Cusanuswerk is gratefully acknowledged for the award of a PhD scholarship (M. Rusan).

References

1 (a) G. Steinhauser and T. M. Klapötke, *Angewandte Chemie International Edition*, Vol. 47, 2008, p. 3330; (b) J. J. Sabatini, A. V. Nagori, E. A. Latalladi, J. C. Poret, G. Chen, R. Damavarapu and T. M. Klapötke, *Propellants, Explosives, Pyrotechnics*, Vol. 36, 2011, p. 373; (c) J. J. Sabatini, A. V. Nagori, G. Chen, P. Chu, R. Damavarapu and T. M. Klapötke, *Chemistry – A European Journal*, Vol. 18, 2012, p. 628; (d) J. J. Sabatini, J. M. Raab, R. K. Hann Jr. and C. T. Freeman, *Zeitschrift für Anorganische und Allgemeine Chemie*, Vol. 639, 2013, p. 25.

2 (a) J. A. Conkling, *Chemistry of Pyrotechnics: Basic Principles and Theory*, Taylor & Francis Group, New York, 1985, 156; (b) J. J. Sabatini, J. C. Poret and R. N. Broad, *Angewandte Chemie International Edition*, Vol. 50, 2011, p. 4624.

3 B. E. Douda, *DTIC Report*, Accession Number 447410, 1969.

4 (a) D. E. Chavez, M. A. Hiskey and D. L. Naud, *Journal of Pyrotechnics*, Issue 7, 1998, p. 11; (b) D. E. Chavez and M. A. Hiskey, *Journal of Pyrotechnics*, Issue 10, 1999, p. 17.

5 (a) T. J. Groshens, *Journal of Coordination Chemistry*, Vol. 63, 2010, p. 1882; (b) D. Lu and C. H. Winter, *Inorganic Chemistry*, Vol. 49, 2010, p. 5795; (c) C. Janiak, *Journal of the Chemical Society, Chemical Communications*, 1994, p. 545; (d) C. Janiak and T. G. Scharmann, *Polyhedron*, Vol. 22, 2003, p. 1123.

6 D. Lu and C. H. Winter, *Inorganic Chemistry*, Vol. 49, 2010, p. 5795.

7 C. J. Snyder, P. D. Martin, M. J. Heeg and C. H. Winter, *Chemistry – A European Journal*, Vol. 19, 2013, p. 3306.

8 Z. Zeng, B. Twamley and J. M. Shreeve, *Organometallics*, Vol. 26, 2007, p. 1782.

9 G. G. Lobbia, M. Pellei, C. Pettinari, C. Santini, B. W. Skelton and A. H. White, *Inorganica Chimica Acta*, Vol. 358, 2005, p. 1162.

10 G. Socrates, *Infrared and Raman Characteristic Group Frequencies – Tables and Charts*, 3rd edn, John Wiley & Sons, Chichester, 2004.

11 SIR-92, 1993, A program for crystal structure solution, A. Altomare, G. Cascarano, C. Giacovazzo and A. Guagliardi, *Journal of Applied Crystallography*, Vol. 26, 1993, p. 343.

12 G. M. Sheldrick SHELXS-97, Program for Crystal Structure Solution, Universität Göttingen, 1997.

13 PLATON, A Multipurpose Crystallographic Tool, Utrecht University, Utrecht, The Netherlands, A. L. Spek, 1998.

14 L. J. Farrugia, *Journal of Applied Crystallography*, Vol. 32, 1999, p. 837.

15 Empirical absorption correction using spherical harmonics, implemented in SCALE3 ABSPACK scaling algorithm (CrysAlisPro Oxford Diffraction Ltd., Version 171.33.41, 2009).

16 Crystallographic data for the structure(s) have been deposited with the Cambridge Crystallographic Data Centre. Copies of the data can be obtained free of charge on application to The Director, CCDC, 12 Union Road, Cambridge CB2 1EZ, UK (Fax: int.code

(1223)336-033; e-mail for inquiry: fileserv@ccdc.cam.ac.uk; e-mail for deposition: deposit-@ccdc.cam.ac.uk).

17 V. Ernst, T. M. Klapötke and J. Stierstorfer, *Zeitschrift für Anorganische und Allgemeine Chemie*, Vol. 633, 2007, p. 879.

18 R. Damavarapu, T. M. Klapötke, J. Stierstorfer and K. R. Tarantik, *Propellants, Explosives, Pyrotechnics*, Vol. 35, 2010, p. 395.

19 UN Recommendations on the Transport of Dangerous Goods. Model Regulations 15th edn, United Nations, New York a. Geneva, 2007.

20 T. M. Klapötke, P. Mayer and J. Stierstorfer, *Phosphorus, Sulfur, and Silicon and the Related Elements*, Vol. 184, Issue 9, 2009, p. 2393.

21 T. M. Klapötke and C. Miró Sabaté, *Heteroatom Chemistry*, Vol. 63, 2008, p. 301.

ChemComm

COMMUNICATION

View Article Online
View Journal | View Issue

Cite this: *Chem. Commun.*, 2014, **50**, 9581

Received 18th June 2014,
Accepted 5th July 2014

DOI: 10.1039/c4cc04616a

www.rsc.org/chemcomm

Improved green-light-emitting pyrotechnic formulations based on tris(2,2,2-trinitroethyl)-borate and boron carbide

Thomas M. Klapötke,*[a] Burkhard Krumm,[a] Magdalena Rusan[a] and Jesse J. Sabatini*[b]

Green-light-emitting pyrotechnic compositions based on tris(2,2,2-trinitroethyl)borate (TNEB) and boron carbide have been investigated. The best performing formulations were found to be insensitive to various ignition stimuli, and exhibited very high spectral purities and luminosities compared to previously reported green-light-emitting formulations.

Traditional green-light-emitting pyrotechnic formulations rely on a combination of barium compounds and chlorine donors to achieve a suitable green-light-emitting species.[1] In these mixtures, barium nitrate is combined with a chlorine donor such as poly(vinyl) chloride to form metastable barium(I) chloride as the green-light-emitting species.[1] Spectral purities of barium-based green-light-emitting illuminants are typically in the low-to-high 60% range. This relatively low spectral purity is a result of large amounts of white-light-emitting incandescent particles (*i.e.* MgO, BaO) formed during the combustion of a given formulation. Unfortunately, barium compounds are suspected cardiotoxins and have been linked to hazards associated with occupational health.[2] Furthermore, there is concern that the combustion of chlorine donors such as PVC leads to the production of significant amounts of carcinogenic materials such as polychlorinated biphenyls (PCBs), polychlorinated dibenzodioxins (PCDDs), and polychlorinated dibenzofurans (PCDFs).[3] Thus, the removal of barium- and chlorine-containing materials from green-light-emitting pyrotechnic formulations is of high interest in "greening" this class of green-light-emitting pyrotechnic formulations.

In 2011, Sabatini *et al.* developed a barium- and chlorine-free green-light-emitting pyrotechnic formulation by burning a mixture of potassium nitrate/boron carbide/epoxy binder.[4] Green-light-emission occurred due to the formation and emission of metastable boron dioxide (BO_2) as opposed to the traditional barium(I) chloride species. While this mixture gives decent green-light-emission and is very insensitive to impact friction and electrostatic discharge, it has a relatively low spectral purity. Low spectral purities are a consequence of "washing out" of the flame colour. This phenomenon likely occurred due to the presence of high levels of potassium nitrate, which produces white-light-emitting KOH.[5] Therefore, it was believed that replacement of potassium nitrate with a metal-free oxidizer would improve the colour properties through the minimization of incandescent particle emission. Although it was initially postulated that mixtures of ammonium nitrate/boron carbide or ammonium dinitramide/boron carbide may result in high quality green-light-emission,[5,6] attempts to produce green light by these means were unsuccessful. Since the production of metastable BO_2 favours green-light-emission, attention was then turned to a boron-containing oxidizer to maximize the quality of a green-light-emitting flame based on boron carbide. Tris(2,2,2-trinitroethyl)-borate (TNEB), which was synthesized previously,[7] was considered to be the compound of interest in this study. TNEB contains both a boron centre and trinitroethyl energetic ligands. With an oxygen balance of +13.1, TNEB was determined to be a suitable oxidizing material for this research investigation.

The green-light-emitting formulation containing potassium nitrate and boron carbide reported by Sabatini *et al.*[4] was reinvestigated with the herein used equipment to establish a relevant data point (Table 1). This green-light-emitting formulation had a spectral purity of 69% (Table 2). It should be noted that TNEB (Fig. 1) is a moisture sensitive material, owing to the highly reactive nature and the vacant p-orbital of the boron centre. When synthesized, the material decomposes after several

Table 1 Formulation **1**

Formulation	KNO_3 [wt%]	B_4C [wt%]	Epon 828/Epikure 3140 [wt%]
1	83	10	7

---

[a] Department of Chemistry, Energetic Materials Research, Ludwig-Maximilian University of Munich, Butenandtstr. 5-13, D-81377 Munich, Germany. E-mail: tmk@cup.uni-muenchen.de; Fax: +49 89 2180 77492; Tel: +49 89 2180 77491

[b] Pyrotechnics Technology and Prototyping Division US Army RDECOM-ARDEC, Picatinny Arsenal, NJ 08706-5000, USA. E-mail: jesse.j.sabatini.civ@mail.mil; Fax: +1-973-724-7375

Table 2 Color properties of formulation **1**

Formulation	BT^a [s]	DW^b [nm]	SP^c [%]	LI^d [cd]	LE^e [cd s g^{-1}]
1	6	560	69	25	250

[a] BT = Burn time. [b] DW = Dominant wavelength. [c] SP = Spectral purity. [d] LI = Luminous intensity. [e] LE = Luminous efficiency.

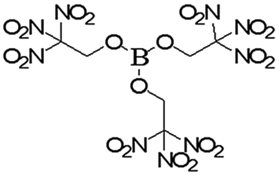

Fig. 1 Structure of tris(2,2,2-trinitroethyl)borate.

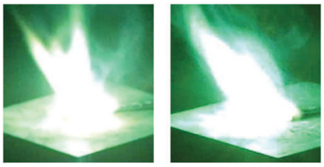

Fig. 2 Formulation **2** (left) and formulation **3** (right) at mid-burn.

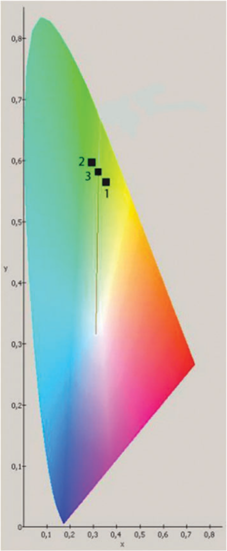

Fig. 3 CIE 1931 chromaticity diagram of formulations **1–3**.

days of storage. When preparing pyrotechnic mixtures containing this oxidizer, it is recommended that non-basic materials be used to prevent any undesired side-reactions from occurring with TNEB. Therefore, the use of epoxy-based binder systems that typically employ polyamine-based curing agents is not recommended.

To help minimize the decomposition of TNEB, and to assist in providing sealant-like properties for the TNEB-containing formulations, paraffin was added to the formulations in lieu of the polyamine-based binder system. Mixing all solid ingredients in liquid paraffin offered a moisture resistant quality to the formulations detailed in Table 3. The presence of magnesium in formulations **2** and **3** was critical in order to maintain a high combustion temperature. Green-light-emission was not observed when magnesium was omitted from these formulations.

The performances of both mixtures and their energetic and thermal properties are summarized in Table 4. Formulations **2** and **3** burned with little smoke, and yielded an intensive green flame (Fig. 2). These formulations reveal respective spectral purities of 86% and 85%, which exceed the spectral purity of formulation **1** due to the absence of large quantities of potassium-based white-light-emission. The luminous intensities of formulations **2** and **3** are appreciably higher than the luminosity observed in formulation **1**, a phenomenon due to the presence of magnesium in the former formulations. Formulation **2** was observed to be the best of the TNEB-based formulations tested on the basis of the performance obtained. Formulation **2** not only had an equivalent burn time to formulation **1**, but it also surpassed the latter formulation in all performance categories by wide margins. Further pictorial evidence of the superior spectral purities of formulations **2** and **3** is provided in the CIE 1931 chromaticity diagram (Fig. 3).

Table 3 Formulations **2** and **3**

	TNEB [wt%]	B_4C [wt%]	Mg [wt%]	Paraffin [wt%]
2	79	10	4	7
3	75	10	8	7

Table 4 Color performances and energetic and thermal properties of formulations **2** and **3**

Formulation	BT^a [s]	DW^b [nm]	SP^c [%]	LI^d [cd]	LE^e [cd s g^{-1}]	IS^f [J]	FS^g [N]	T_{dec}^{h} [°C]
2	7	561	86	50	583	>40	>360	170
3	4	562	85	89	593	>40	>360	168

[a] BT = Burn time. [b] DW = Dominant wavelength. [c] SP = Spectral purity. [d] LI = Luminous intensity. [e] LE = Luminous efficiency. [f] IS = Impact sensitivity. [g] FS = Friction sensitivity. [h] T_{dec} = Temperature of decomposition.

Formulations **2** and **3** were found to respond to various ignition stimuli, each having an impact sensitivity higher than 40 J and a friction sensitivity in excess of 360 N. The respective decomposition temperatures were 170 °C and 168 °C.

In summary, a green-light-emitting pyrotechnic formulation with high performance and spectral purity has been obtained by means of replacing potassium nitrate with TNEB in the presence of boron carbide, magnesium, and paraffin wax. In particular, formulation **2** exceeds the performance of potassium nitrate-based formulation **1** in all categories, while formulation **3** yields the highest overall luminosity. The aforementioned compositions are very insensitive to impact and friction. Although further study is needed to address potential concerns associated with moisture sensitivity, the research is of potential interest to those in the pyrotechnics community concerned with finding environmentally friendly alternatives to barium- and chlorine-based green-light-emitting pyrotechnics of high luminosity and spectral purity.

Caution! Tris(2,2,2-trinitroethyl) borate is an energetic material and formulations **1–3** are energetic formulations with high sensitivity towards heat, impact and friction. Although no incidents occurred during preparation and manipulation, additional proper protective precautions like face shield, leather coat, earthed equipment and shoes, Kevlar gloves, and ear plugs should be used when undertaking work with these compounds.[8]

TNEB was synthesized according to the literature procedure.[7] Boron carbide, amorphous boron, potassium nitrate, and paraffin were purchased from Aldrich and were used as received. The pyrotechnical compositions were prepared by grinding all substances in a mortar. The mixture was then introduced slowly into warm liquid paraffin. After cooling to room temperature, the mixtures were grinded again. Pellets of 0.6 g each were pressed using a consolidation dead load of 2000 kg. The pellets were dried overnight at ambient temperature. The controlled burn was filmed using a digital video camera recorder (SONY, DCR-HC37E). The performance of each composition was evaluated with respect to color emission, smoke generation, and the amount of solid residues. Spectrometric measurements were performed using a HR2000+ES spectrometer equipped with an ILX511B linear silicon CCD-array detector and included software from Ocean Optics with a detector-sample distance of 1 meter. The dominant wavelength and spectral purity were measured based on the 1931 CIE method using illuminant C as the white reference point. Luminous intensities and luminous efficiencies were determined using pellets of 0.6 g each. Five samples were measured for each formulation and all given values are averaged based on the full burn of the mixture. Decomposition points were measured using a Linseis PT10 DSC at heating rates of 5 °C min^{-1}.[9] The impact[10] and friction[11] sensitivity was determined using a BAM drop hammer and a BAM friction tester. The sensitivities of the compounds are indicated according to the UN Recommendations on the Transport of Dangerous Goods (+):[12] impact: insensitive $>$ 40 J, less sensitive $>$ 35 J, sensitive $>$ 4 J, very sensitive $<$ 4 J; friction: insensitive $>$ 360 N, less sensitive = 360 N, sensitive $<$ 360 N $>$ 80 N, very sensitive $<$ 80 N, extremely sensitive $<$ 10 N.

Financial support of this work by the Ludwig-Maximilian University of Munich (LMU), the U.S. Army Research Laboratory (ARL) under grant no. W911NF-09-2-0018, the Armament Research, Development and Engineering Center (ARDEC) under grant no. W911NF-12-1-0467, and the Office of Naval Research (ONR) under grant no. ONR.N00014-10-1-0535 and ONR.N00014-12-1-0538 is gratefully acknowledged. The authors acknowledge collaborations with Dr Mila Krupka (OZM Research, Czech Republic) in the development of new testing and evaluation methods for energetic materials and with Dr Muhamed Suceska (Brodarski Institute, Croatia) in the development of new computational codes to predict the detonation and propulsion parameters of novel explosives. We are indebted to and thank Drs Betsy M. Rice and Brad Forch (ARL, Aberdeen, Proving Ground, MD) for many inspired discussions. The Cusanuswerk is gratefully acknowledged for the award of a PhD scholarship (M. Rusan).

Notes and references

1 (*a*) G. Steinhauser and T. M. Klapötke, *Angew. Chem., Int. Ed.*, 2008, **47**, 3330; (*b*) J. A. Conkling, *Chemistry of Pyrotechnics: Basic Principles and Theory*, Taylor & Francis Group, New York, 1985, 156; (*c*) G. Steinhauser and T. M. Klapötke, *J. Chem. Educ.*, 2010, **87**, 150.

2 (*a*) R. Hicks, L. Q. Caldas, P. R. Dare and P. J. Hewitt, *Arch. Toxicol. Supplement*, **9**, 415–420; (*b*) A. L. Reeves, *Handbook on the Toxicology of Metals*, Elsevier/North Holland Biomedical Press, New York, 1979, pp. 321–328.

3 D. Dyke and P. Coleman, *Organohalogen Compounds*, 1995, **24**, 213.

4 J. J. Sabatini, J. C. Poret and R. N. Broad, *Angew. Chem., Int. Ed.*, 2011, **50**, 4624.

5 (*a*) T. M. Klapötke, M. A. Rusan, J. Stierstorfer, *Proceedings of the 38th International Pyrotechnic Seminars*, Denver, CO, **2012**, 527-550; (*b*) J. J. Sabatini, in *Green Energetic Materials*, ed. T. Brinck, Wiley-VCH, Weinheim, 2014, 78.

6 T. M. Klapötke, M. A. Rusan, and J. Stierstorfer, *Proceedings of the 38th International Pyrotechnic Seminars*, Denver, CO, **2012**, 527-550.

7 T. M. Klapötke, B. Krumm and R. Moll, *Chem. – Eur. J.*, 2013, **19**, 12113.

8 T. M. Klapötke, B. Krumm, F. X. Steemann and G. Steinhauser, *Safety Science*, 2010, **48**, 28–34.

9 http://www.linseis.com.

10 NATO standardization agreement (STANAG) on explosives, *impact sensitivity tests*, no. 4489, 1st edn, Sept. 17, **1999**.

11 NATO standardization agreement (STANAG) on explosive, *friction sensitivity tests*, no. 4487, 1st edn, Aug. 22, **2002**.

12 UN Recommendations on the Transport of Dangerous Goods, Model Regulations, 15th edn, United Nations, New York a. Geneva, **2007**.

The Synthesis and Characterization of Nitrooxy- and Nitrosooxyborazine Compounds

Thomas M. Klapötke and Magdalena Rusan

Department of Chemistry, Ludwig-Maximilian University of Munich, Butenandtstr. 5 – 13 (D),
81377 Munich, Germany

Reprint requests to Prof. Dr. Thomas M. Klapötke. Fax: +49-89-2180-77492.
E-mail: tmk@cup.uni-muenchen.de

Z. Naturforsch. **2014**, *69b*, 1241 – 1247 / DOI: 10.5560/ZNB.2014-4101
Received May 19, 2014

Dedicated to Professor Hubert Schmidbaur on the occasion of his 80th birthday

B-Nitrosooxypentamethylborazine, *B*-nitrooxypentamethylborazine and *B*-trinitrooxy-*N*-trimethylborazine have been synthesized and characterized by ^{1}H, ^{13}C, ^{11}B, and ^{14}N NMR spectroscopy, mass spectrometry, vibrational spectroscopy and elemental analysis. The ^{11}B NMR shifts were calculated and compared to the experimental results. The decomposition temperatures and the impact and friction sensitivities of these compounds have been determined as well.

Key words: Nitrosooxyborazines, Nitrooxyborazines, ^{11}B NMR Spectroscopy, Energetic Materials, Impact and Friction Sensitivities

Introduction

The investigation of borazine, which was first isolated by Stock and Pohland in 1926, and its derivatives has been of interest for decades [1 – 5]. Borazine, the "inorganic benzene", which shows a different reactivity compared to benzene due to the polarity of the BN bonds, is calculated to possess substantial aromatic character assuming that the resonance energy is a criterion for aromaticity [6]. Numerous fields of applications and a plenty of borazine compounds have been reported in literature [2 – 8]. The preparation of various symmetrically and unsymmetrically substituted borazine derivatives is well-known and has been extensively investigated. Derivatives of borazine with alkyl, alkoxy, halogen, pseudohalogen, and amino substituents on the nitrogen and boron atoms are described [9 – 14]. Metal π-complexes containing alkylborazine compounds as ligands are reported as well [15]. Borazine is described to be a convenient precursor compound for the synthesis of polyborazines and hence for boron nitride ceramics. *B*,*B*,*B*-Triaminoborazine was prepared as a molecular precursor for hexagonal boron nitride showing excellent thermal and mechanical properties and structural similarities with graphite [7]. Among the various fields of applications of borazine derivatives, their use in propellants and related areas has also been considered and investigated [16]. Niedenzu and co-workers reported the synthesis of the energetic borazine compound *B*-trichloro-*N*-trihydroxyborazine, which could not be isolated due to its too sensitive character [17]. More stable and isolatable energetic borazine compounds are azidoborazines such as *B*-azidopentamethylborazine and *B*-triazidoborazine, which were obtained by Paine *et al.* [18]. Additionally, Meller and Wechsberg reported the preparation of *B*-triazido-*N*-trimethylborazin from *B*-trichloroborazine and sodium azide [19]. Besides energetic azido borazine molecules, borazine derivatives containing energetic nitro groups are also of high interest.

The investigation of *N*-nitroborazines was performed by Hirata [16]. Several syntheses of borazine using nitryl chloride and gaseous hydrogen chloride are described. The results of these examinations showed that borazine reacts violently with nitryl chloride in the absence of a diluent, and decomposition occurred instead of the formation of the target compound. Synthesis attempts to indroduce ONO_2 or ONO groups into the borazine molecule were performed by Brennan *et al.* using *B*-trichloroborazine and silver nitrate and silver nitrite, respectively, but no stable products could be isolated [20].

Decades later, the synthesis and crystal structure of the first compound containing a nitrooxy group, 2,4-bis(dimethylamino)-1,3,5-trimethyl-6-(nitrooxy)borazine, was reported by Rodriguez and Borek [21]. The reaction of 2,4-bis(dimethylamino)-6-chloro-1,3,5-trimethylborazine with silver nitrate in acetonitrile resulted in the formation of 2,4-bis(dimethylamino)-1,3,5-trimethyl-6-(nitrooxy)borazine.

Although several syntheses of borazine derivatives using borazine as starting material are reported, borazine is not a suitable starting material for further syntheses due to its unfavorable properties like decomposition and polymerization tendencies at room temperature [16]. However, halogen-substituted borazines such as *B*-trichloroborazine, *B*-trichloro-*N*-trimethylborazine or *B*-bromopentamethylborazine do not polymerize or decompose at room temperature and are therefore suitable starting materials for further syntheses [22 – 24].

In this contribution the synthesis of *B*-nitrosooxypentamethylborazine (**2**), *B*-nitrooxypentamethylborazine (**3**) and *B*-trinitrooxy-*N*-trimethylborazine (**5**) is described. Their characterization by NMR spectroscopy, elemental analysis, mass spectrometry and IR spectroscopy, as well as their thermal and energetic properties are reported. Additionally calculations of ^{11}B NMR shifts of compounds **2**, **3** and **5** have been performed.

Results and Discussion

Synthesis

The starting material *B*-bromopentamethylborazine (**1**) was synthesized according to the literature procedure by the reaction of hexamethylborazine and BBr_3 in dichloromethane at room temperature [24]. The products *B*-nitrosooxypentamethylborazine (**2**) and *B*-nitroxypentamethylborazine (**3**) were synthesized using *B*-bromopentamethylborazine (**1**) and silver nitrite and silver nitrate, respectively, in stoichiometric ratios (Scheme 1). Both reactions were performed in dry acetonitrile at ambient temperature and under exclusion of light. The driving force of these reactions is the formation of silver bromide. The reaction was monitored *via* ^{11}B NMR spectroscopy, and after 24 hours the ^{11}B NMR shift indicated that a complete substitution of the bromo group by the nitrosooxy and nitrooxy moieties, respectively, had occurred. Af-

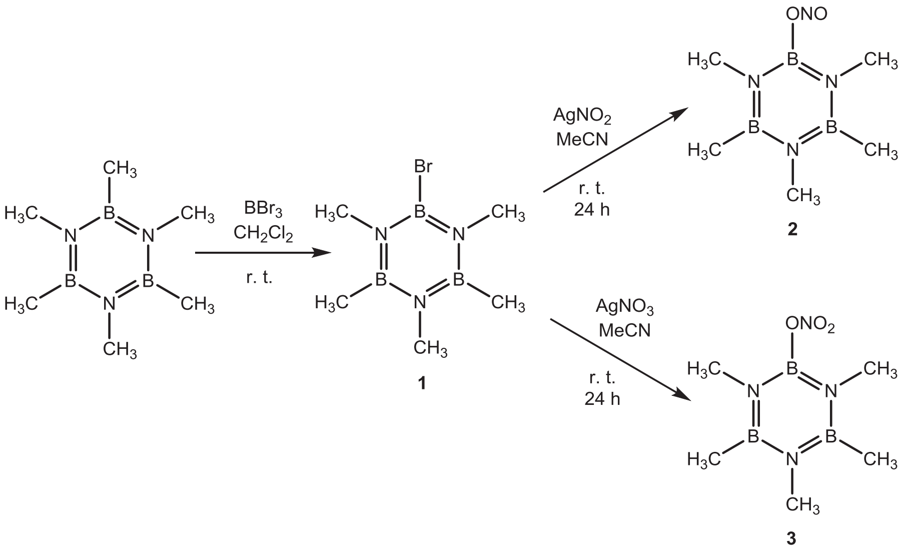

Scheme 1. Synthesis of compounds **1**–**3**.

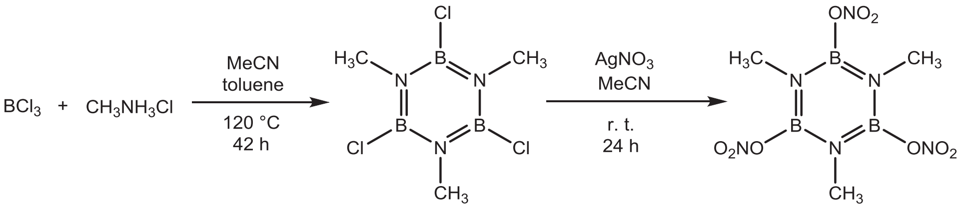

4

5

Scheme 2. Synthesis of compounds **4** and **5**.

ter filtration the products were washed with dry diethyl ether and recrystallized from dry acetonitrile. Colorless solids were obtained in high purity and yield.

The synthesis of *B*-trichloro-*N*-trimethylborazine (**4**) was performed according to the literature procedure for *B*-trichloroborazine [22] by reacting methylammonium chloride with boron trichloride (1-molar solution in toluene) in acetonitrile (Scheme 2). *B*-Trinitrooxy-*N*-trimethylborazine (**5**) was obtained by the reaction of *B*-trichloro-*N*-trimethylborazine and silver nitrate in stoichiometric amounts in dry acetonitrile at room temperature and under exclusion of light. Here again, the driving force of the reaction is the formation of silver chloride. After filtration and recrystallization from dry acetonitrile, compound **5** was obtained as a colorless solid of high yield and purity.

Characterization

Compounds **2**, **3** and **5** were characterized by ^{11}B, ^{1}H, ^{13}C, and ^{14}N NMR spectroscopy, as well as elemental analysis, mass spectrometry and infrared spectroscopy.

The ^{11}B NMR spectra of compounds **2** and **3** reveal chemical shifts near $+36$ ppm, which can be attributed to boron atoms containing methyl substituents. The substitution of the Br atom by the ONO group is indicated by the ^{11}B signal shift from $+31$ ppm to $+22$ ppm, and the ^{11}B chemical shift of compound **3** is found at $+24$ ppm suggesting the formation of the nitrato compound **3**. In the ^{1}H NMR spectra both compounds show signals at around $+2.9$ ppm corresponding to the protons of the two *ortho* *N*-methyl groups. The protons of the *para* *N*-methyl groups exhibit chemical shifts at around $+2.7$ ppm. The protons of the boron-connected methyl groups of **2** and **3** show signals at $+0.5$ ppm. In the ^{13}C NMR spectra of compounds **2** and **3** the *N*-methyl groups in *ortho* position appear at $+34$ ppm, while the carbon atoms in *para* position exhibit a signal at $+31$ ppm. The boron-connected methyl groups of both compounds show a signal at $+1$ ppm. In the ^{14}N NMR spectra of both compounds a signal at -286 ppm corresponds to nitrogen atoms of the borazine ring. The ^{14}N signal of the ONO-group appears at -22 ppm. In the case of compound **3** a signal at -46 ppm corresponding to the ONO_2-group is observed. The assignment of infrared absorptions was performed according to the literature [25]. In the IR spectra of both compounds strong bands of B–N stretching vibrations are visible in the region between 1455 and 1369 cm^{-1}, and of B–N deformation vibrations in the 706 – 702 cm^{-1} region. In the IR spectrum of compound **1** strong bands of B–Br stretching vibrations appear in the range between 1032 and 946 cm^{-1}, which are not visible in the IR spectra of compounds **2** and **3**. However, these two compounds show B–O stretching vibrations in the range 1371 to 1335 cm^{-1}.

In the ^{11}B NMR spectrum of compound **5** one signal at $+25.6$ ppm is observed. Since the starting material **4** shows a ^{11}B chemical shift at $+30.3$ ppm, the formation of **5** can be assumed. In the ^{1}H NMR spectrum compound **5** shows a signal at $+2.83$ ppm corresponding to the three methyl protons, and in the ^{13}C NMR spectrum a signal at $+35.1$ ppm for the carbon atoms of the three *N*-methyl groups. The ^{14}N NMR spectrum of **5** reveals a shift of -46 ppm corresponding to the three ONO_2 substituents and a second signal at -139 ppm, which can be assigned to the ring nitrogen atoms. The assignments of IR vibrations were done according to ref. [25]. The B–O stretching vibrations are found in the 1387 – 1340 cm^{-1} region, the B–N stretching vibrations appear between 1450 and 1359 cm^{-1}, whereas the B–N deformation vibrations appear between 706 and 704 cm^{-1}.

Table 1. Calculated isotropic magnetic shielding (GIAO method [26–30], MPW1PW91/aug-cc-p VDZ) and relative ^{11}B chemical shifts (ppm) referenced to $BF_3{\cdot}Et_2O$.

Compound	$-E$ (a. u.)	NIMAG	P. g.	δ ^{11}B (ppm) calcd. isotr. shielding	δ ^{11}B (ppm) calcd. (ref. to $BF_3{\cdot}Et_2O$)	δ ^{11}B (ppm) exptl. (ref. to $BF_3{\cdot}Et_2O$)
2	643.690087	0	C_s	74.6 (2)	35.4 (2)	36 (2)
				81.9	28.1 (1)	22 (1)
3	718.874416	0	C_s	74.8 (2)	35.4 (2)	36 (2)
				86.3 (1)	23.7 (1)	24 (1)
5	1199.653977	0	C_s	84.4 (2)	25.6 (2)	25.6
				86.8 (1)	23.2 (1)	
$BF_3{\cdot}Et_2O$	558.164166	0	C_1	+110.0	0.0	0.0

Calculation of ^{11}B chemical shifts

As additional verification of the analytical data, the ^{11}B NMR chemical shifts were calculated and compared to the experimental data.

In order to compute the ^{11}B NMR chemical shifts for various high-nitrogen boron compounds, the isotropic magnetic shieldings were calculated using the GIAO (Gauge-Independent Atomic Orbital) method implemented in G03 [26–30]. The structures were fully optimized and the frequencies calculated (NIMAG = 0) at MPW1PW91/aug-cc-pVDZ level of theory (Fig. 1). Subsequently, the NMR shielding tensors were calculated at the same level of theory using the GIAO method [27–30]. Table 1 summarizes the computed isotropic magnetic shieldings and relative ^{11}B NMR chemical shifts (ppm) referenced to $BF_3{\cdot}Et_2O$.

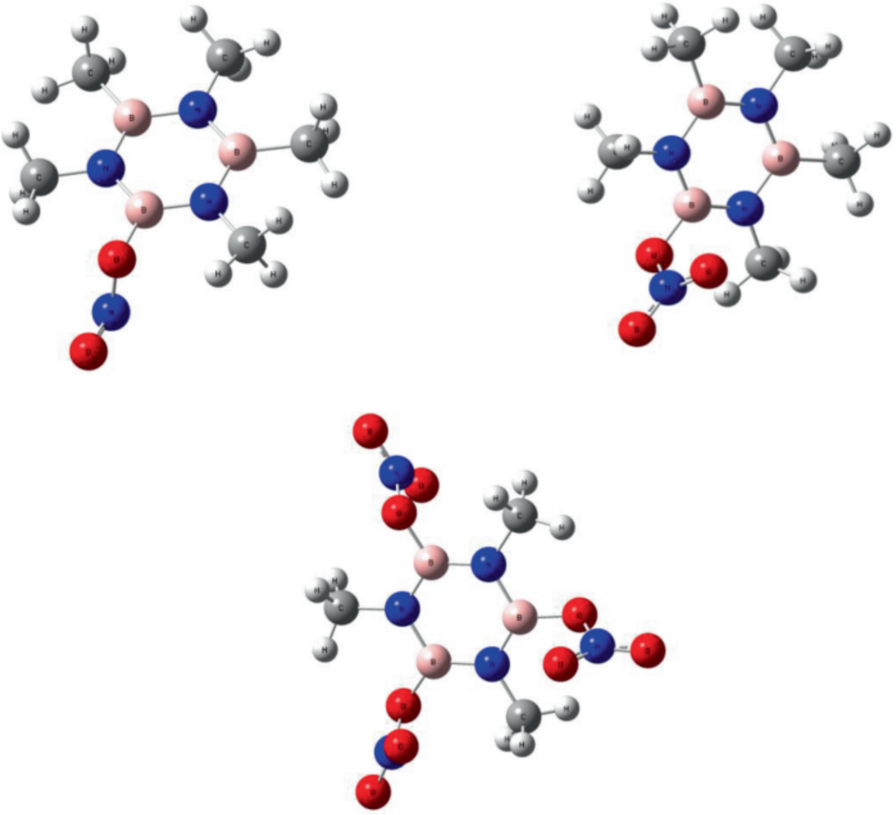

Fig. 1 (color online). MPW1PW91/aug-cc-pVDZ-optimized structures of compounds **2** (top left), **3** (top right) and **5** (bottom center) in idealized C_s symmetry.

Table 2. Energetic and thermal properties of compounds **2**, **3** and **5**.

	2	**3**	**5**
Chemical formula	$C_5H_{15}N_4O_2B_3$	$C_5H_{15}N_4O_3B_3$	$C_3H_9N_6O_9B_3$
Formula weight, g mol^{-1}	195.63	211.63	305.57
N, %[a]	28.64	26.48	27.50
Ω_{CO}, %[b]	−122.68	−105.84	−15.71
Ω_{CO_2}, %[c]	−163.57	−143.64	−31.42
Grain size, μm	< 100	< 100	< 100
IS, J	> 40	> 40	> 40
FS, N	120	80	80
T_m, °C	–	76	83
T_{dec}, °C	127	117	154

[a] Nitrogen content; [b] oxygen balance assuming the formation of CO; [c] oxygen balance assuming the formation of CO_2.

The comparison of the calculated values with the experimentally determined shifts shows a good accordance. In the case of compound **5** experimentally only one ^{11}B NMR chemical shift at 25.6 ppm was detected, whereas the calculation requires two ^{11}B NMR signals at 25.6 ppm and 23.2 ppm for the assumed C_s symmetry (Table 1). In solution, molecular dynamics seem to lead to a coalescence of these signals.

Energetic and thermal properties

The impact (IS) and friction (FS) sensitivities as well as the melting (T_m) and decomposition (T_{dec}) temperatures of compounds **2**, **3** and **5** are summarized in Table 2. Furthermore, the oxygen balance and the nitrogen content are given in Table 2. All three borazine derivatives are impact insensitive but show friction sensitivities of 120 N (**2**), and 80 N (**3** and **5**). The decomposition temperatures have been determined to be 127 °C (**2**), 117 °C (**3**) and 154 °C (**5**).

Conclusion

The borazine compounds *B*-nitrosooxypentamethylborazine (**2**), *B*-nitrooxypentamethylborazine (**3**) and *B*-trinitrooxy-*N*-trimethylborazine (**5**) have been synthesized and characterized *via* NMR and IR spectroscopy as well as elemental analysis and mass spectrometry. Calculations of ^{11}B NMR chemical shifts were performed showing a good accordance of calculated and experimentally determined values. The measurement of the impact and friction sensitivities revealed that all compounds are impact insensitive but friction sensitive. The decomposition temperatures have been determined to be moderate.

Experimental Section

All manipulations were carried out in an atmosphere of dry argon using standard vacuum line techniques. Solvents were dried by standard procedures. All other chemicals were commercially available and used as received. The NMR spectra were recorded using Jeol Eclipse 400, Jeol Eclipse 270 or Jeol EX400 instruments at an ambient temperature of 25 °C if not stated otherwise. Chemical shifts (δ) were calibrated using the residual undeuterated solvent as an internal reference and are reported according to the common convention in parts per million (ppm) downfield relative to tetramethylsilane (TMS, ^{13}C, ^{1}H), nitromethane (^{14}N) or boron trifluoride etherate (^{11}B) as external standards. Infrared (IR) spectra were measured with a Perkin-Elmer Spectrum BX-FTIR spectrometer equipped with a Smiths DuraSampl*IR* II ATR device. All spectra were recorded at ambient temperature, the samples were neat solids. Mass spectrometric data were obtained with a Jeol MStation JMS 700 spectrometer ((+)-DEI, (+)-DCI). The fragments are referred to the isotope with the highest natural abundance. Elemental analyses were performed with an Elementar Vario EL or an Elementar Vario EL micro cube, DSC measurements with a Perkin Elmer Pyris 6 DSC instrument at a heating rate of 5 °C min^{-1} in closed aluminum containers with a hole (1 μm) on the top for gas release and a nitrogen flow of 5 mL min^{-1}. The reference sample was an empty closed aluminum container. The impact and friction sensitivity was determined using a BAM drophammer and a BAM friction tester [31–35]. The sensitivities of the compounds are indicated according to the UN Recommendations on the Transport of Dangerous Goods [36]: impact: insensitive > 40 J, less sensitive > 35 J, sensitive > 4 J, very sensitive < 4 J; friction: insensitive > 360 N, less sensitive = 360 N, sensitive < 360 N > 80 N, very sensitive < 80 N, extreme sensitive < 10 N.

CAUTION! *The compounds described in this work are potential explosives, which are sensitive to environmental stimuli such as impact, friction and heat. While we encoun-*

tered no problems in the handling of these materials, appropriate precautions and proper protective measures (safety glasses, face shields, leather coat, Kevlar gloves and ear protectors) should be taken when preparing and manipulating these materials.

*Synthesis of B-nitrosooxypentamethylborazine (**2**)*

B-Bromopentamethylborazine [24] (**1**) (0.5 g, 2.18 mmol) was dissolved in dry acetonitrile (12 mL) and cooled in an ice bath. To the cooled and stirred solution silver nitrite (0.34 g, 2.18 mmol) was added, and a yellow precipitate was immediately formed. Under exclusion of light the mixture was stirred at room temperature for 24 h and then filtered. After removing the solvent and recrystallization from dry acetonitrile a colorless solid (0.30 g, 71 %) was obtained. – IR (ATR): $\tilde{\nu} = 3358$ (m), 3074 (s), 3017 (s), 2943 (s), 2849 (s), 2779 (m), 2745 (m), 2530 (w), 2469 (w), 2379 (w), 2210 (w), 1580 (m), 1443 (s), 1415 (s), 1371 (s), 1360 (s), 1341 (s), 1330 (m), 1335 (s), 1316 (s), 1279 (s), 1251 (s), 1158 (m), 1109 (s), 915 (s), 896 (m), 882 (m), 846 (w), 807 (w), 785 (w), 754 (w), 713 (m), 675 (m), 528 (w), 481 (w) cm^{-1}. – ^{1}H NMR ($CDCl_3$): $\delta = 2.91$ (s, 6H, 2·N–CH_3), 2.73 (s, 3H, N–CH_3), 0.59 (s, 6H, B–CH_3) ppm. – ^{13}C NMR ($CDCl_3$): $\delta = 34.9$ (2C, N–CH_3), 31.8 (1C, N–CH_3), 1.9 (2C, B–CH_3) ppm. – ^{11}B NMR ($CDCl_3$): $\delta = 36.4$ (2B, B–CH_3), 22.4 (1B, B–ONO) ppm. – ^{14}N NMR ($CDCl_3$): $\delta = -22$ (1N, ONO), −286 (3N, borazine ring) ppm. – MS ((+)-DEI): $m/z = 149.5$ $[\text{M-ONO}]^+$ (calcd. 195.63 for $C_5H_{15}N_4O_2B_3$). – EA: $C_5H_{15}N_4O_2B_3$ (195.63): calcd. N 28.64, C 30.70, H 7.73; found N 26.56, C 30.35, H 7.54 %. – IS: > 40 J (grain size < 100 µm). – FS: 120 N (grain size < 100 µm). – DSC: 127 °C (dec.).

*Synthesis of B-nitrooxypentamethylborazine (**3**)*

To a cooled solution of *B*-bromopentamethylborazine [24] (**1**) (0.14 g, 0.62 mmol) in dry acetonitrile (4 mL) silver nitrate (0.32 g, 1.86 mmol) was added, and a slightly yellow precipitate was immediately formed. The reaction mixture was stirred at room temperature and under exclusion of light for 24 h and then filtered. The solvent was removed *in vacuo*, and the obtained solid was recrystallized from dry acetonitrile. As product a colorless solid was gained (0.10 g, 80 %). – IR (ATR): $\tilde{\nu} = 3360$ (m), 3073 (s), 3022 (s), 2949 (s), 2855 (s), 2779 (m), 2745 (m), 2530 (w), 2469 (w), 2379 (w), 2210 (w), 1580 (m), 1440 (s), 1415 (s), 1371 (s), 1360 (s), 1344 (s), 1330 (m), 1335 (s), 1318 (s), 1277 (s), 1251 (s), 1152 (m), 1109 (s), 910 (s), 896 (m), 895 (m), 841 (w), 800 (w), 790 (w), 754 (w), 721 (m), 672 (m), 528 (w), 488 (w) cm^{-1}. – ^{1}H NMR ($CDCl_3$): $\delta = 2.98$ (s, 6H, 2·N–CH_3), 2.86 (s, 3H, N–CH_3), 0.55 (s, 6H, B–CH_3) ppm. – ^{13}C NMR ($CDCl_3$): $\delta = 34.3$ (2C, N–CH_3), 31.4 (1C, N–CH_3), 1.4 (2C, B–CH_3) ppm. – ^{11}B NMR ($CDCl_3$): $\delta = 36.4$ (2B, B–CH_3), 24.3 (1B, B–ONO_2) ppm. – ^{14}N NMR ($CDCl_3$): $\delta = -46$ (1N, ONO_2), −286 (3N, borazine ring) ppm. – MS ((+)-DEI): $m/z = 196.1$ $[\text{M-O}]^+$ (calcd. 211.63 for $C_5H_{15}N_4O_3B_3$). – EA: $C_5H_{15}N_4O_3B_3$ (211.63): calcd. N 26.47, C 28.38, H 7.14; found N 24.78, C 18.29, H 6.99 %. – IS: > 40 J (grain size < 100 µm). – FS: 80 N (grain size < 100 µm). – DSC: 117 °C (dec.).

*Synthesis of B-trinitrooxy-N-trimethylborazine (**5**)*

B-Trichloro-*N*-trimethylborazine (according to ref. [22]) (**4**) (0.5 g, 2.18 mmol) was dissolved in dry acetonitrile (20 mL) and cooled in an ice bath. To the cooled and stirred solution silver nitrate (1.11 g, 6.54 mmol) was added, and a yellow precipitate was immediately formed. Under exclusion of light the mixture was stirred at room temperature for 24 h and then filtered. Evaporation of the solvent and recrystallization of the residue from dry acetonitrile gave a colorless solid (0.54 g, 81 %). – IR (ATR): $\tilde{\nu} = 3440$ (s), 3335 (s), 3210 (s), 2930 (s), 2851 (m), 2831 (m), 2521(w), 2390 (w), 2259 (w), 2092 (w), 2038 (w), 1683 (m), 1640 (m), 1470 (s), 1415 (s), 1256 (m), 1231 (m), 1387 (s), 1361 (s), 1340 (s), 1197 (m), 882 (w), 795 (m), 709 (m), 656 (w), 520 (w) cm^{-1}. – ^{1}H NMR ($CDCl_3$): $\delta = 2.83$ (s, 9H, 3·N–CH_3) ppm. – ^{13}C NMR ($CDCl_3$): $\delta = 35.1$ (3C, 3·N–CH_3) ppm. – ^{11}B NMR ($CDCl_3$): $\delta = 25.6$ (3B, B–ONO_2) ppm. – ^{14}N NMR ($CDCl_3$): $\delta = -46$ (1N, ONO_2), −139 (3N, borazine ring) ppm. – MS ((+)-DEI): $m/z = for 243.5$ $[\text{M-ONO}_2]^+$ (calcd. 305.57 for $C_3H_9N_6O_9B_3$). – EA: $C_3H_9N_6O_9B_3$ (305.57): calcd. N 27.50, C 11.79, H 2.97; found N 25.88, C 11.59, H 2.48 %. – IS: > 40 J (grain size < 100 µm). – FS: 80 N (grain size < 100 µm). – DSC: 154 °C (dec.).

Acknowledgement

Financial support of this work by the Ludwig-Maximilian University of Munich (LMU), the U. S. Army Research Laboratory (ARL) under grant no. W911NF-09-2-0018, the Armament Research, Development and Engineering Center (ARDEC) under grant no. W911NF-12-1-0467, and the Office of Naval Research (ONR) under grant nos. ONR.N00014-10-1-0535 and ONR.N00014-12-1-0538 is gratefully acknowledged. The authors acknowledge collaborations with Dr. Mila Krupka (OZM Research, Czech Republic) in the development of new testing and evaluation methods for energetic materials and with Dr. Muhamed Suceska (Brodarski Institute, Croatia) in the development of new computational codes to predict the detonation and propulsion parameters of novel explosives. We are indebted to and thank Drs. Betsy M. Rice and Brad Forch (ARL, Aberdeen, Proving Ground, MD) for many inspiring discussions. The Cusanuswerk is gratefully acknowledged for the award of a PhD scholarship (M. Rusan).

[1] A. Stock, E. Pohland, *Ber. Dtsch. Chem. Ges.* **1926**, *59*, 2215.
[2] O. T. Beachley, *J. Amer. Chem. Soc.* **1971**, *93*, 5066.
[3] H. Nöth, H. Sachdev, *Z. Naturforsch.* **1997**, *52b*, 1345.
[4] A. Stock, E. Wiberg, H. Martini, *Chem. Ber.* **1930**, *62B*, 90.
[5] K. Niedenzu, J. W. Dawson, *Boron-Nitrogen Compounds*, Springer Verlag, **1965**.
[6] D. Benker, T. M. Klapötke, G. Kuhn, J. Li, C. Miller, *Heteroatom. Chem.* **2005**, *16*, 311.
[7] Y. Kimura, Y. Kubo, N. Hayashi, *J. Inorg. Organometal. Polym.* **1992**, *2*, 231.
[8] C. K. Narula, D. A. Lindquist, M.-M. Fan, T. T. Borek, E. N. Duesler, A. K. Datye, R. Schaeffer, R. T. Paine, *Chem. Mater.* **1990**, *2*, 377.
[9] B. M. Mikhailov, *Russ. Chem. Rev.* **1960**, *29*, 459.
[10] A. Meller, M. Armbrecht, *Chem. Ber.* **1986**, *119*, 1.
[11] R. H. Toeniskoetter, F. R. Hall, *Inorg. Chem.* **1963**, *2*, 29.
[12] M. Oertel, R. F. Porter, *Inorg. Chem.* **1970**, *9*, 904.
[13] J. M. Miller, G. L. Wilson, *J. Fluorine Chem.* **1974**, *4*, 207.
[14] B. Anand, H. Nöth, H. Schwenk-Kircher, A. Troll, *Eur. J. Inorg. Chem.* **2008**, 3186.
[15] K. Deckelmann, H. Werner, *Helv. Chim. Acta* **1970**, *53*, 139.
[16] T. Hirata, *Study on Synthesis of N-Nitroborazine Compounds. II. Borazine Derivatives*, Technical Memorandum 2011, Picatinny Arsenal, Dover, NJ, **1971**.
[17] K. Niedenzu, D. H. Harrelson, J. W. Dawson, *J. Amer. Chem. Soc.* **1961**, *94*, 671.
[18] R. T. Paine, W. Koestle, T. T. Borek, G. L. Wood, E. A. Pruss, E. N. Duesler, M. A. Hiskey, *Inorg. Chem.* **1999**, *38*, 3738.
[19] A. Meller, M. Wechsberg, *Monatsh. Chem.* **1967**, *98*, 513.
[20] G. L. Brennan, G. H. Dahl, R. Schaeffer, *J. Am. Chem. Soc.* **1960**, *82*, 6248.
[21] M. A. Rodriguez, T. T. Borek, *Acta Crystallogr.* **2013**, *E69*, o634.
[22] H. Nöth, H. Sachdev, *Z. Naturforsch.* **1997**, *52b*, 1345.
[23] A. Meller, K. Niedenzu (ed.), *Gmelin Handbuch der Anorganischen Chemie*, Vol. 51, Supplement Boron Compounds 17, Springer-Verlag, West Berlin, **1978**.
[24] J. Bai, K. Niedenzu, J. Serwatowska, J. Serwatowski, *Inorg. Chem.* **1992**, *31*, 228.
[25] G. Socrates, *Infrared and Raman Characteristic Group Frequencies – Tables and Charts*, 3rd edition, John Wiley & Sons, Chichester, **2004**.
[26] M. J. Frisch, G. W. Trucks, H. B. Schlegel, G. E. Scuseria, M. A. Robb, J. R. Cheeseman, J. A. Montgomery Jr., T. Vreven, K. N. Kudin, J. C. Burant, J. M. Millam, S. S. Iyengar, J. Tomasi, V. Barone, B. Mennucci, M. Cossi, G. Scalmani, N. Rega, G. A. Petersson, H. Nakatsuji, M. Hada, M. Ehara, K. Toyota, R. Fukuda, J. Hasegawa, M. Ishida, T. Nakajima, Y. Honda, O. Kitao, H. Nakai, M. Klene, X. Li, J. E. Knox, H. P. Hratchian, J. B. Cross, C. Adamo, J. Jaramillo, R. Gomperts, R. E. Stratmann, O. Yazyev, A. J. Austin, R. Cammi, C. Pomelli, J. W. Ochterski, P. Y. Ayala, K. Morokuma, G. A. Voth, P. Salvador, J. J. Dannenberg, V. G. Zakrzewski, S. Dapprich, A. D. Daniels, M. C. Strain, O. Farkas, D. K. Malick, A. D. Rabuck, K. Raghavachari, J. B. Foresman, J. V. Ortiz, Q. Cui, A. G. Baboul, S. Clifford, J. Cioslowski, B. B. Stefanov, G. Liu, A. Liashenko, P. Piskorz, I. Komaromi, R. L. Martin, D. J. Fox, T. Keith, M. A. Al-Laham, C. Y. Peng, A. Nanayakkara, Challacombe, P. M. W. Gill, B. Johnson, W. Chen, M. W. Wong, C. Gonzalez, J. A. Pople, GAUSSIAN 03, (revision A.1), Gaussian, Inc., Pittsburgh PA (USA) **2003**.
[27] K. Wolinski, J. F. Hilton, P. Pulay, *J. Am. Chem. Soc.* **1990**, *112*, 8251.
[28] J. L. Dodds, R. McWeeny, A. Sadlej, *Mol. Phys.* **1980**, *41*, 1419.
[29] R. Ditchfield, *Mol. Phys.* **1974**, *27*, 789.
[30] R. McWeeny, *Phys. Rev.* **1962**, *126*, 1028.
[31] BAM Bundesanstalt für Materialforschung und -prüfung, Berlin: http://www.bam.de/.
[32] NATO standardization agreement (STANAG) on explosives, *impact sensitivity tests*, no. 4489, 1st edition, Sept. 17, **1999**.
[33] WIWEB-Standardarbeitsanweisung 4–5.1.02, Ermittlung der Explosionsgefährlichkeit, hier der Schlagempfindlichkeit mit dem Fallhammer, Nov. 8, **2002**.
[34] NATO standardization agreement (STANAG) on explosives, *friction sensitivity tests*, no. 4487, 1st edition, Aug. 22, **2002**.
[35] WIWEB-Standardarbeitsanweisung 4–5.1.03, Ermittlung der Explosionsgefährlichkeit order Reibeempfindlichkeit mit dem Reibeapparat, Nov. 8, **2002**.
[36] *UN Recommendations on the Transport of Dangerous Goods. Model Regulations*, (15th edition), United Nations, New York, Geneva, **2007**.

The Synthesis and Investigation of Nitrogen-rich and Boron-based Compounds as Coloring Agents in Pyrotechnics

Thomas M. Klapötke, Magdalena Rusan, Jörg Stierstorfer, Energetic Materials Research, University of Munich (LMU), Butenandtstr. 5-13, 81377 Munich, Germany, Fax: +49 89 2180 77492, tmk@cup.uni-muenchen.de

ABSTRACT

The development of ecologically friendly energetic materials is nowadays of high relevance. Therefore both nitrogen-rich compounds as well as boron-containing compounds, especially for green-light emitting pyrotechnics, are of significant interest due to their smoke-reduced combustion and less toxic decomposition products. The syntheses and characterization of selected alkali and alkaline earth metal salts of trinitroimidazole and di- and trinitropyrazole are presented. In addition, promising boron derivatives of nitro-heterocycles are reported. Their potential use as colorants in pyrotechnic compositions has been investigated.

Introduction

The creation of environmentally friendly pyrotechnics for military and civilian application is intended by many research groups.[1] The major requirements for such pyrotechnics are less or no smoke generation during the combustion and less toxic decomposition products. Suitable candidates are therefore nitrogen-rich compounds because of the formation of molecular nitrogen as main decomposition product.[2-5] Besides the ecological aspect a high performance of the compounds as well as thermal stability and low impact and friction sensitivity are desired.

3,5-Dinitropyrazole as well as salts of 3,4,5-trinitropyrazole and 2,4,5-trinitroimidazole with nitrogen-rich cations are reported to be insensitive and reveal good oxygen balance, high thermal stability and high positive molar enthalpies of formation.[6-7] Although metal 3,4,5-trinitropyrazolate salts are mentioned in patents[8], their characterization and properties are not described. For these reasons alkali and earth alkali salts of 3,5-dinitropyrazolate (3,5-DNP), 3,4,5-trinitropyrazole (TNP) and 2,4,5-trinitroimidazole (TNI) are interesting compounds for the use in pyrotechnic compositions as coloring agents since high thermal stability and safe handling of pyrotechnic components is required. Therefore alkali and earth alkali salts of 3,5-DNP, TNP and TNI were synthesized and characterized and additionally investigated in pyrotechnic compositions with regard to color performance and smoke generation.

Mostly barium compounds are used in green-light-emitting pyrotechnics. But many of these barium compounds are toxic and environmentally harmful. Thus, the development of barium-free green burning compounds is of importance. Boron containing compounds are therefore promising compounds because of their green-burning character and less toxic decomposition product B_2O_3. The synthesis and investigation of nitrogen-rich azolylborate salts is therefore focused. 5-aminotetrazolylborates, 1,2,4-triazolyl- and 3-nitro-1,2,4-triazolylborates as well as 3,5-dinitropyrazolylborates and 2,4-dinitroimidazolylborates are synthesized and investigated. Especially the metal-free azolylborates are of high interest with regard to their suitability as green coloring agents in pyrotechnics.

Experimental

All reagents and solvents were used as received (Sigma-Aldrich, Fluka, Acros Organics) if not stated otherwise. ^{1}H, ^{13}C, ^{11}B and ^{14}N NMR spectra were measured with a JEOL instrument. All chemical shifts are quoted in ppm relative to TMS (^{1}H, ^{13}C), $BF_3{\cdot}Et_2O$ (^{11}B) or nitromethane (^{14}N). Infrared spectra were measured with a PERKIN ELMER Spectrum BX-59343 FT-IR instrument. For detection a Smiths Detection DuraSampl*IR* II Diamond ATR sensor was used. Elemental analyses (EA) were performed with a Netsch STA 429 simultaneous thermal analyzer. Mass spectra were recorded on JEOL JMS-700, Finnigan MAT 95Q and Finnigan Mat 90 instruments.

Metal-3,5-dinitropyrazolates

The synthesis of 3,5-dinitropyrazole was performed according to literature (9)(10). All salts were synthesized by the same procedure. To a solution of 3,5-dinitropyrazole in ethanol (LiDNP, NaDNP, KDNP) or water ($Ca(DNP)_2$, $Sr(DNP)_2$, $Ba(DNP)_2$) the corresponding metal carbonate or metal hydroxide in stoichiometric amount was added. The reaction mixture was stirred at room temperature for 24 hours and then filtered off. After removing the solvent and recrystallization from water yellow solids as products were obtained.

Lithium-3,5-dinitropyrazolate trihydrate (Li_1)

Yield: 97%
IR: [cm^{-1}] = 3156 (w), 1738 (m), 1641 (m), 1531 (m), 1470 (m), 1443 (s), 1353 (s), 1318 (m), 1273 (m), 1171 (m), 1016 (m), 997 (m), 821 (m), 749 (m), 681 (w). **^{1}H-NMR** (acetone-*d$_6$*) δ: 4.07 (s, H_2O), 7.26 (s, 1H, CH) ppm. **^{13}C-NMR** (acetone-*d$_6$*) δ: 97.60 (CH), 156.41 (CNO_2) ppm. **^{14}N-NMR** (acetone-*d$_6$*) δ: −17.95 (CNO_2) ppm. **EA**: $LiC_3HN_4O_4{\cdot}(H_2O)_3$ (218.05): calculated: C, 16.53; H, 3.24; 25.69; found: C, 16.97; H, 3.01; N, 25.84. **M/z (FAB$^-$)**: 156.9 (anion), **(FAB$^+$)**: 7.0 (cation).

Sodium-3,5-dinitropyrazolate dihydrate (Na_1)

Yield: 99%
IR: [cm^{-1}] = 3570 (m), 3156 (m), 2362 (m), 2337 (m), 1683 (m), 1645 (m), 1560 (w), 1532 (m), 1507 (m), 1472 (s), 1443 (s), 1355 (s), 1316 (s), 1272 (m), 1166 (m), 1072 (w), 1012 (m), 994 (m), 837 (s), 820 (s), 750 (s), 686 (w). **^{1}H-NMR** (acetone-*d$_6$*) δ: 3.42 (s, H_2O), 7.30 (s, 1H, CH) ppm. **^{13}C-NMR** (acetone-*d$_6$*) δ: 97.84 (CH), 156.36 (CNO_2) ppm. **^{14}N-NMR** (acetone-*d$_6$*) δ: −18.17 (CNO_2) ppm. **EA**: $NaC_3HN_4O_4{\cdot}(H_2O)_2$ (216.09): calculated: C, 16.67; H, 2.33; N, 25.92; found: C, 16.51; H, 2.77; N, 25.23. **M/z (FAB$^-$)**: 157.0 (anion), **(FAB$^+$)**: 23.0 (cation).

Potassium-3,5-dinitropyrazolate dihydrate (K_1)

Yield: 99%
IR: [cm^{-1}] = 3156 (w), 2596 (w), 2294 (w), 1738 (w), 1539 (m), 1476 (s), 1443 (s), 1378 (m), 1353 (s), 1338 (s), 1310 (s), 1270 (m), 1151 (m), 1064 (w), 1003 (s), 993 (m), 830 (s), 754 (s). **^{1}H-NMR** (acetone-*d$_6$*) δ: 7.21 (s, 1H, CH) ppm. **^{13}C-NMR** (acetone-*d$_6$*) δ: 97.80 (CH), 156.89 (br, CNO_2) ppm. **^{14}N-NMR** (acetone-*d$_6$*) δ: −49.54, −16.04 (CNO_2) ppm. **EA**: $KC_3HN_4O_4$ (196.16): calculated: C, 18.37; H, 0.51; N, 28.56; found: C, 18.52; H, 0.62; N, 27.76. **M/z (FAB$^-$)**: 156.9 (anion), **(FAB$^+$)**: 39.0 (cation).

Calcium-*bis*(3,5-dinitropyrazolate) tetrahydrate (Ca_1)

Yield: 77%

IR: [cm^{-1}] = 3638 (m), 3549 (m), 3166 (m), 1636 (m), 1540 (m), 1511 (m), 1483 (s), 1450 (m), 1344 (s), 1318 (s), 1280 (m), 1204 (w), 1175 (m), 1017 (s), 998 (m), 842 (s), 818 (w), 748 (s). **^{1}H-NMR** (acetone-*d$_6$*) δ: 3.91 (s, H_2O), 7.29 (s, 1H, CH) ppm. **^{13}C-NMR** (acetone-*d$_6$*) δ: 97.63 (CH), 156.29 (CNO_2) ppm. **^{14}N-NMR** (acetone-*d$_6$*) δ: −17.95 (CNO_2) ppm. **EA**: $CaC_6H_2N_8O_8{\cdot}(H_2O)_4$ (426.27): calculated: C, 16.91; H, 2.36; N, 26.29; found: C, 17.05; H, 2.34; N, 25.72. **M/z (FAB$^-$)**: 157.0 (anion), **(FAB$^+$)**: 197.0 ($CaC_3HN_4O_4^+$).

Strontium- *bis*(3,5-dinitropyrazolate) hexahydrate (Sr_1)

Yield: 98%

IR: [cm^{-1}] = 2971 (w), 2170 (w), 1739 (s), 1618 (m), 1540 (m), 1475 (m), 1443 (m), 1354 (s), 1322 (m), 1279 (w), 1229 (m), 1217 (m), 1073 (w), 1017 (m), 999 (w), 835 (m), 826 (m), 749 (m). **^{1}H-NMR** (acetone-*d$_6$*) δ: 3.68 (s, H_2O), 7.27 (s, 1H, CH) ppm. **^{13}C-NMR** (acetone-*d$_6$*) δ: 98.33 (CH), 156.98 (CNO_2) ppm. **^{14}N-NMR** (acetone-*d$_6$*) δ: −18.17 (CNO_2) ppm. **EA**: $SrC_6H_2N_8O_8{\cdot}(H_2O)_6$ (509.84): calculated: C, 14.14; H, 2.77; N, 21.98; found: C, 14.43; H, 2.68; N, 21.71. **MS/z (FAB$^-$)**: 157.0 (anion), **(FAB$^+$)**: 245.0 ($SrC_3HN_4O_4^+$).

Barium- *bis*(3,5-dinitropyrazolate) hydrate (Ba_1)

Yield: 29%

IR: [cm^{-1}] = 3610 (w), 3156 (w), 2361 (w), 1739 (m), 1611 (m), 1548 (s), 1494 (s), 1444 (m), 1369 (m), 1342 (s), 1321 (s), 1230 (w), 1172 (m), 1070 (w), 1010 (m), 1000 (w), 840 (s), 821 (w), 744 (s), 669 (w). **^{1}H-NMR** (acetone-*d$_6$*) δ: 2.88 (s, H_2O), 7.28 (s, 1H, CH) ppm. **^{13}C-NMR** (acetone-*d$_6$*) δ: 98.63 (CH) ppm. **^{14}N-NMR** (acetone-*d$_6$*) δ: −18.63 (CNO_2) ppm. **EA**: $BaC_6H_2N_8O_8{\cdot}(H_2O)$ (487.49): calculated: C, 15.32; H, 0.86; N, 23.84; found: C, 15.08; H, 1.01; N, 22.66. **M/z (FAB$^-$)**: 157.0 (anion), **(FAB$^+$)**: 448.0 ($BaC_6H_2N_8O_8^+$).

Metal-3,4,5-trinitropyrazolates

According to literature (11) 3,4,5-Trinitropyrazole was synthesized. All metal salts were synthesized by the same procedure. An ethanolic solution of 3,4,5-Trinitropyrazole and the corresponding metal carbonates was stirred at room temperature for 24 hours. After the removal of the solvent and recrystallization in ethanol yellow solids as products were obtained.

Lithium-3,4,5-trinitropyrazolate tetrahydrate (Li_2)

Yield: 86%

IR: [cm^{-1}] = 3620 (m), 3582 (w), 3512 (m), 3343 (w), 3209 (w), 2628 (w), 1668 (m), 1630 (w), 1540 (m), 1522 (s) 1456 (s), 1351 (s), 1325 (s), 1299 (s), 1172 (w), 1133 (m), 1024 (m), 850 (s), 806 (m), 763 (m), 731 (m), 680 (m). **^{1}H-NMR** (acetone-*d$_6$*) δ: 3.30 (H_2O) ppm. **^{13}C-NMR** (acetone-*d$_6$*): no signals could be observed. **^{14}N-NMR** (acetone-*d$_6$*) δ: -22.45 (CNO_2) ppm. **EA**: $LiC_3N_5O_6{\cdot}(H_2O)_4$ (281.06): calculated: C 12.82, N 24.92, H 2.87; found: C 13.24, N 24.41, H 2.72. **M/z (FAB$^-$):** 201.9 (anion), **(FAB$^+$):** 7.0 (cation).

Sodium-3,4,5-trinitropyrazolate (Na_2)

Yield: 96%

IR: [cm^{-1}] = 3638 (w), 1605 (w), 1560 (w), 1546 (m), 1512 (s), 1456 (m), 1357 (m), 1319 (s), 1296 (w), 1170 (w), 1132 (w), 1024 (w), 850 (s), 808 (m), 762 (w), 682 (w). ^{13}**C-NMR** (acetone-*d$_6$*): no signals could be observed. ^{14}**N-NMR** (acetone-*d$_6$*) δ: -21.92 (CNO_2) ppm. **EA**: $NaC_3N_5O_6$ (225.05): calculated: C 16.01, N 31.12; found: C 16.15, N 30.22. **M/z (FAB$^-$):** 202.0 (anion), **(FAB$^+$):** 32.0 (cation).

Strontium-bis(3,4,5)-trinitropyrazolate (Sr_2)

Yield: 74%
IR: [cm^{-1}] = 3616 (w), 3139 (m), 2924 (m), 1596 (w), 1518 (s), 1493 (m), 1454 (m), 1358 (m) 1328 (s), 1131 (m), 1025 (s), 841 (m), 787 (w), 760 (m), 672 (w). ^{13}**C-NMR** (acetone-*d$_6$*) δ: 146.93 (CNO_2) ppm. ^{14}**N-NMR** (acetone-*d$_6$*) δ: -22.37 (CNO_2) ppm. **EA**: $SrC_6N_{10}O_{12}$ (491.75): calculated: C 14.65, N 28.48; found: C 14.13, N 27.96. **M/z (FAB$^-$):** 202.0 (anion).

Barium-bis(3,4,5)-trinitropyrazolate trihydrate (Ba_2)

Yield: 96%
IR: [cm^{-1}] = 3582 (m), 1619 (m), 1540 (s), 1514 (s), 1457 (m), 1354 (m), 1322 (s), 1303 (m), 1132 (m), 1028 (w), 850 (s), 806 (m), 766 (w). ^{1}**H-NMR** (acetone-*d$_6$*) δ: 2.99 (s, H_2O) ppm. ^{13}**C-NMR** (acetone-*d$_6$*): no signals could be observed. ^{14}**N-NMR** (acetone-*d$_6$*) δ: -23.02 (CNO_2) ppm. **EA**: $BaC_6N_{10}O_{12}\cdot(H_2O)_3$ (595.50): calculated: C 12.10, H 1.02, N 23.52; found: C 12.13, H 1.04, N 22.58. **M/z (FAB$^-$):** 202.1 (anion).

Metal-2,4,5-trinitroimidazolates

2,4,5-Trinitroimidazole and potassium 2,4,5-trinitroimidazolate were synthesized according to (12). All other 2,4,5-trinitroimidazolate salts were obtained by adding saturated aqueous solutions of metal carbonates/metal hydroxides to a solution of 2,4,5-trinitroimidazole until the pH=7 was achieved. After stirring at room temperature for 24 hours the reaction mixture was filtered and the products were extracted with ethylacetate. After removing the solvent orange solids as products were gained.

Lithium-2,4,5-trinitroimidazolate trihydrate (Li_3)

Yield: 76%
IR: [cm^{-1}] = 3563 (m), 3321 (w), 1648 (m), 1538 (s), 1467 (s), 1426 (m), 1328 (s), 1301 (s), 1111 (m), 868 (s), 832 (m), 812 (s), 755 (w). 650 (m). ^{1}**H-NMR** (DMSO-*d$_6$*) δ: 3.37 (s, H_2O) ppm. ^{13}**C-NMR** (DMSO-*d$_6$*) δ: no signals detectable. ^{14}**N-NMR** (DMSO-d$_6$) δ: -21.27 (NO_2) ppm. **EA**: $LiC_3N_5O_6\cdot(H_2O)_3$ (263.05): calculated: C 13.70, H 2.30, N 26.62; found: C 14.49, H 2.18, N 26.67. **M/z (FAB$^-$):** 201.9 (anion), **(FAB$^+$):** 7.0 (cation).

Sodium-2,4,5-trinitroimidazolate (Na_3)

Yield: 86%
EA: $NaC_3N_5O_6$ (225.05): calculated: C 16.01, N 31.11 found: C 17.27, N 30.34. **M/z (FAB$^-$):** berechnet 202 (anion), **(FAB$^+$):** 23 (cation).

Calcium-*bis*(2,4,5-trinitroimidazolate)·$(C_4H_8O_2)_2$ dihydrate (Ca_3)

Yield: 78%
IR: [cm^{-1}] = 3582 (m), 3347 (w), 1643 (w), 1619 (m), 1535 (s), 1468 (s), 1422 (w), 1327 (s), 1304 (s), 1109 (m) 865 (s), 830 (w), 808 (s), 752 (m), 672 (m) **^{13}C-NMR** (DMSO-*d*$_6$) δ: no signals detectable. **^{14}N-NMR** (DMSO-d$_6$) δ: -19.24 (CNO_2) ppm. **EA:** $CaC_6N_{10}O_{12}·(C_4H_8O_2)_2·(H_2O)_2$ (656.44): calculated: C 25.62, H 3.07, N 21.34; found: C 25.48, H 3.21, N 21.23. **M/z (FAB$^-$):** 202.0 (anion).

Strontium-*bis*(2,4,5-trinitroimidazolate)·$(C_4H_8O_2)_{1.5}$ hydrate (Sr_3)

Yield: 78%
IR: [cm^{-1}] = 3616 (w), 2988 (w), 1693 (s), 1545 (s), 1470 (s), 1425 (m), 1378 (m), 1321 (s), 1297 (s), 1189 (w), 1111 (s), 1041 (s), 867 (s), 833 (m), 810 (s), 753 (m), 650 (m) **^{13}C-NMR** (DMSO-*d*$_6$) δ: 14.06 (CH_2CH_3) 20.73 (CH_3), 59.73 (OCH_2), 170.31 (CO) ppm. **^{14}N-NMR** (DMSO-d$_6$) δ: -20.13 (NO_2) ppm. **EA:** $SrC_6N_{10}O_{12}·(C_4H_8O_2)_{1.5}·H_2O$ (641.92): calculated: C 22.45, H 2.20, N 21.82; found: C 20.98, H 2.43, N 21.66. **M/z (FAB$^-$):** 202.0 (anion).

Copper-*bis*(2,4,5-trinitroimidazolate) tetrahydrate (Cu_3)

Yield: 85%
^{1}H-NMR (DMSO- *d*$_6$) δ: 3.35 (H_2O) ppm. **^{13}C-NMR** (DMSO- *d*$_6$) δ: no signals detectable. **^{14}N-NMR** (DMSO- *d*$_6$) δ: -20.24 (CNO_2), -359.27 ppm. **EA**: $CuC_6N_{10}O_{12}·(H_2O)_4$ (539.73) calculated: C 13.35, H 1.49, N 25.95 found: C 13.49, H 1.49, N 25.95. **M/z (FAB$^-$):** 201.9 (anion).

Salts of dihydrobis(5-aminotetrazol-1-yl)borate

The synthesis of potassium dihydro*bis*(5-aminotetrazol-1-yl)borate and (5-amino-1-H-tetrazole)dihydro(5-aminotetrazol-1-yl)borane was performed according to literature (13). Barium dihydro*bis*(5-aminotetrazol-1-yl)borate was synthesized by stirring **H_4** with bariumhydroxide in stoichiometric amount in water for 4 hours. After filtration and removal of the solvent a colorless solid was obtained. The metal-free borate salts were synthesized by mixing **Ba_4** with the corresponding sulfates in stoichiometric amount in water, stirring 5 minutes, followed by filtration and removal of the solvent. The obtained colorless solids were air-dried.

Ammonium dihydrobis(5-aminotetrazol-1-yl)borate hydrate (NH_4_4)

Yield: 64%
^{1}H-NMR (DMSO-*d*$_6$) δ: 3.39 (s, 2H, BH_2), 5.62 (s, 4H, NH_4), 7.13 (s, 4H, C-NH_2) ppm. **^{13}C-NMR** (DMSO-*d*$_6$) δ: 159.69 (s, 2C, C_{ring}) ppm. **^{11}B-NMR** (DMSO-*d*$_6$) δ: - 14.40 (s, BH_2) ppm. **EA:** $C_2H_{10}BN_{11}·H_2O$ (217.00): calculated: C, 11.07; H, 5.57; N, 71.00 found: C, 11.46; H, 5.27; N, 69.21. **M/z (FAB$^-$):** 181.2 (anion), **(FAB$^+$):** 18.1 (cation).

Aminoguanidinium dihydrobis(5-aminotetrazol-1-yl)borate (AG_4)

Yield: 60%
^{1}H-NMR (DMSO-*d*$_6$) δ: 3.51 (s, 2H, BH_2), 4.68 (s, 2H, N-NH_2), 5.59 (s, 4H, C_{ring}-NH_2), 7.23 (s, 4H, C*AG*-NH_2), 8.60 (s, 1H, NH-N) ppm. **^{13}C-NMR** (DMSO-*d*$_6$) δ: 159.31 (2C, C_{ring}), 159.69 (1C, C*AG*) ppm. **^{11}B-NMR** (DMSO-*d*$_6$) δ: -14.31 (1B, BH_2) ppm. **EA:** $C_3N_{14}H_{13}B$ (256.15): calculated: C, 14.07; H, 5.12; N, 76.59. found: C, 14.69; H, 4.80; N, 74.03. **M/z (FAB$^-$):** 181.2 ($C_2H_6N_{10}B^-$), **(FAB$^+$):** 75.1 ($CH_7N_4^+$).

Diaminoguanidinium dihydrobis(5-aminotetrazol-1-yl)borate (DAG_4)

Yield: 92 %
^{1}H-NMR (DMSO-d_6) δ: 3.34 (s, 2H, BH_2), 4.65 (s, 4H, N-NH_2), 5.58 (s, 4H, C_{ring}-NH_2), 7.17 (s, 2H, *CDAG*-NH_2), 8.60 (s, 2H, NH-N) ppm. **^{13}C-NMR** (DMSO-d_6) δ: 159.16 (2C, C_{ring}), 159.71 (1C, C*DAG*) ppm. **^{11}B-NMR** (DMSO-d_6): δ: -15.56 (s, 1B, BH_2). **EA:** $C_3N_{15}H_{14}B$ (271.06): calculated: C, 13.29; H, 5.21; N, 77.51. found: C, 13.74; H, 4.92; N, 75.10. **M/z (FAB$^-$):** 181.1 ($C_2H_6N_{10}B^-$), **(FAB$^+$):** 90.1 ($CH_8N_5^+$).

N-Guanylurea dihydrobis(5-aminotetrazol-1-yl)borate (NGU_4)

Yield: 88%
IR: [cm^{-1}] = 3458.8 (w), 3295.5 (s), 3129.0 (s), 3009.9 (m), 2477.8 (w), 2422.0 (w), 2356.8 (w), 2200.2 (w), 1718.1 (vs), 1702.1 (vs), 1601.0 (vs), 1548.5 (s), 1462.3 (s), 1376.3 (m), 1353.1 (vs), 1300.9 (m), 1293.6 (s), 1228.3 (m), 1191.6 (m), 1156.2 (m), 1124.4 (vs), 1099.1 (vs), 1079.3 (vs), 1048.4 (s), 1025.8 (m), 976.4 (m), 933.0 (m), 868.9 (m), 781.5 (s), 749.2 (vs), 730.8 (vs), 702.5 (vs). **^{1}H-NMR** (DMSO-d_6): δ: 5.55 (s, 4H, NH_2), 3.30 (s, 2H, BH_2). **^{13}C-NMR** (DMSO-d_6): δ: 159.12 (2C, C-NH_2), 155.58 (1C, C=N), 154.85 (1C, C=O). **^{11}B-NMR** (DMSO-d_6): δ: -14.64 (s, 1B, BH_2). **EA:** $C_4H_{13}BN_{14}O$ (284.05); calculated: N: 69.03; C: 16.91; H: 4.61; found: N: 66.51; C: 17.27; H: 4.46. **M/z (FAB$^-$):** 181 ($C_2H_6BN_{10}^-$), **(FAB$^+$):** 103.0 ($C_2H_7N_4O^+$): 103.1.

5-Aminotetrazolium dihydrobis(5-aminotetrazol-1-yl)borate dihydrate (5At_4)

Yield: 90%
IR: (cm^{-1}) = 3472.1 (m), 3374.0 (m), 3190.7 (m), 2360.6 (s), 1782.1 (w), 1638.6 (vs), 1450.5 (m), 1297.1 (m), 1156.4 (m), 1057.3 (vs), 994.7 (s), 907.7 (s), 755.7 (s), 740.1 (s), 668.0 (s). **^{1}H-NMR** (DMSO-d_6): δ: 6.45 (br, 6H, NH_2). **^{13}C-NMR** (DMSO-d_6): δ: 156.69 (3C, C-NH_2). **^{11}B-NMR** (DMSO-d_6): δ: -7.29 (s, 1B, BH_2). **EA:** $C_3H_{14}BN_{15}O_2$ (303.05); calculated: N: 69.32; C: 11.89; H: 4.65; found: N: 63.34; C: 11.50; H: 4.47. **M/z (ESI):** 181.09 ($C_2H_6BN_{10}^-$).

Salts of dihydrobis(1,2,4-triazolyl)borate

Potassium dihydro*bis*(1,2,4-triazolyl)borate and barium dihydro*bis*(1,2,4-triazolyl)borate were synthesized according to literature (14). All metal-free borate salts were obtained by stirring the barium salt with the corresponding sulfates in stoichiometric amount in water for 1 minute. After filtration and removing the water colorless solids as products were obtained.

Ammonium dihydrobis(1,2,4-triazolyl)borate (NH_4_5)

Yield: 80%
^{1}H-NMR (DMSO-d_6) δ: 3.49 (2H, BH_2), 4.61 (4H, NH_4), 8.26 (2H, C-H), 8.80 (2H, C-H) ppm. **^{13}C-NMR** (DMSO-d_6) δ: 146.11 (1C, CH), 148.09 (1C, CH) ppm. **^{11}B-NMR** (DMSO-d_6) δ: -9.12 (1B, BH_2) ppm. **EA:** $C_4H_{10}BN_7$ (166.98): calculated: C, 28.77; H, 6.04; N, 58.72; found: C, 28.98; H, 4.37; N, 51.13. **M/z (FAB$^-$):** 149.1 ($C_4H_6BN_6^-$).

Aminoguanidinium dihydrobis(1,2,4-triazolyl)borate hydrate (AG_5)

Yield: 64%
^{1}H-NMR (DMSO-*d$_6$)* δ: 3.35 (s, 2H, BH_2), 4.68 (s, 2H, N-NH_2), 7.28 (s, 4H, C-NH_2), 7.66 (s, 2H, CH), 7.97 (s, 2H, CH), 8.28 (s, 1H, C-NH) ppm. **^{13}C-NMR** (DMSO-*d$_6$)* δ: 147.99 (2C, CH), 151.61 (2C, CH), 159.34 (1C, AG^+) ppm. **^{11}B-NMR** (DMSO-*d$_6$)* δ: -9.85 (1B) ppm. **EA:** $C_5H_{13}BN_{10}\cdot H_2O$ (242.05): calculated: C, 24.81; H, 6.25; N, 57.87; found: C, 25.32; H, 5.58; N, 55.97. **M/z (FAB$^-$):** 149.1 ($C_4H_6BN_6^-$), **(FAB$^+$):** 75.1 ($CH_7N_4^+$).

Diaminoguanidinium dihydrobis(1,2,4-triazolyl)borate trihydrate (DAG_5)

Yield: 88%
^{1}H-NMR (DMSO-*d$_6$)* δ: 3.48 (s, 2H, BH_2), 4.59 (s, 4H, N-NH_2), 7.15 (s, 2H, C-NH_2), 7.70 (s, 2H, CH), 8.03 (s, 2H, CH), 8.57 (s, 2H, NH-N) ppm. **^{13}C-NMR** (DMSO-*d$_6$)* δ: 147.80 (2C, CH), 151.29 (2C, CH), 160.21 (1C, DAG^+) ppm. **^{11}B-NMR** (DMSO-*d$_6$)* δ: - 9.91 (1B) ppm. **EA:** $C_5H_{14}BN_{11}\cdot 3H_2O$ (293.10): calculated: C, 20.49; H, 6.88; N, 52.57; found: C, 16.63; H, 5.36; N, 54.51. **M/z (FAB$^-$):** 149.1 ($C_4H_6N_6B^-$), **(FAB$^+$):** 90.1 ($CH_8N_5^+$).

Salts of dihydrobis(3-nitro-1,2,4-triazolyl)borate

The starting material potassium dihydrobis(3-nitro-1,2,4-triazolyl)borate was synthesized according to literature (15). To a solution of potassium dihydrobis(3-nitro-1,2,4-triazolyl)borate in water barium perchlorate was added in stoichiometric amount. The mixture was stirred at room temperature for 24 hours, then filtrated. After evaporation of the solvent barium dihydrobis(3-nitro-1,2,4-triazolyl)borate as slight yellow solid was obtained. The metal-free compounds were synthesized by stirring **Ba_6** with the corresponding sulfates (1:1) in water for a few minutes. The products as slight yellow solids were gained after filtration and evaporation of the solvent.

Barium dihydrobis(3-nitro-1,2,4-triazolyl)borate (Ba_6)

Yield: 65%
IR: [cm^{-1}] = 3354.7 (w), 2435.8 (w), 2358.7 (w), 1738.3 (w), 1548.4 (s), 1502.2 (vs), 1427.8 (m), 1397.3 (m), 1361.8 (w), 1335.8 (w), 1305.2 (s), 1213.5 (w), 1163.9 (s), 1142.1 (vs), 1042.5 (m), 1026.5 (s), 878.2 (w), 838.0 (vs), 725.0 (m). **^{1}H-NMR** (DMSO-*d$_6$*,): δ: 8.42 (s, 4H, CH), 3.76 (br, 4H, BH_2). **^{13}C-NMR** (DMSO-*d$_6$*,): δ = 164.18 (4C, C-NO_2); 150.22 (4C, CH). **^{11}B-NMR** (DMSO-*d$_6$*,): δ: -9.85 (s, 2B, BH_2). **^{14}N-NMR** (DMSO-*d$_6$*,): δ: -21.99 (s, 4N, NO_2), -131.82 (s, 8N, C=N). **EA:** $C_8H_8B_2BaN_{16}O_8$ (615.20); calculated: N: 36.43; C: 15.62; H: 1.31; found: N: 28.82; C: 15.45; H: 2.10. **M/z (FAB$^-$):** 239.0($C_4H_4BN_8O_4^-$) 239.0, **(FAB$^+$):** 376.8 ($C_4H_4BBaN_8O_4^+$): 376.3.

Ammonium dihydrobis(3-nitro-1,2,4-triazolyl)borate (NH_4_6)

Yield: 65%
IR: [cm^{-1}] = 3592.0 (w), 3112.0 (w), 2901.3 (w), 2431.7 (w), 1548.8 (s), 1507.1 (s), 1457.6 (m), 1423.7 (s), 1393.8 (m), 1304.8 (s), 1221.0 (w), 1161.2 (s), 1149.4 (vs), 1046.2 (m), 1026.0 (m), 896.0 (w), 879.8 (w), 719.8 (s), 657.3 (vs). **^{1}H-NMR** (DMSO-*d_6*): δ: 8.45 (s, 2H, CH), 7.09 (br, 4H, N*H_2*), 3.46 (br, 2H, BH_2). **^{13}C-NMR** (DMSO-*d_6*): δ: 150.14 (2C, CH). **^{11}B-NMR** (DMSO-*d_6*): δ: -9.51 (s, 1B, BH_2). **^{14}N-NMR** (DMSO-*d_6*): δ: -21.69 (s, 2N, NO_2). **EA:** $C_4H_8BN_9O_4$ (256.98); calculated: N: 49.06; C: 18.70; H: 3.14; found: N: 38.73; C: 15.09; H: 3.47. **M/z (ESI):** 239.0 ($C_4H_4BN_8O_4^-$).

N-Guanylurea dihydrobis(3-nitro-1,2,4-triazolyl)borate (NGU_6)

Yield: 70%
IR: [cm^{-1}] = 3575.0 (w), 3149.4 (w), 2477.7 (w), 2436.5 (w), 2360.2 (w), 1751.1 (m), 1694.7 (m), 1659.8 (w), 1602.6 (m) 1538.0 (m), 1499.1 (s), 1423.8 (m), 1395.1 (m), 1339.8 (m), 1306.3 (s), 1214.3 (m), 1154.1 (s), 1074.7 (m), 1038.2 (m), 1028.0 (m), 882.0 (w), 835.7 (vs), 722.6 (m), 657.8 (vs). **^{1}H-NMR** (DMSO-*d_6*): δ = 8.42 (s, 2H, CH), 8.01 (s, 2H, N*H_2*), 3.30 (br, 2H, BH_2). **^{13}C-NMR** (DMSO-*d_6*): δ: 155.44 (1C, C=N), 154.56 (1C, C=O), 150.14 (2C, CH). **^{11}B-NMR** (DMSO-*d_6*): δ: -9.94 (s, 1B, BH_2). **^{14}N-NMR** (DMSO-*d_6*): δ: -23.52 (s, 2N, NO_2). **EA:** $C_6H_{11}BN_{12}O_5$ (342.04); calculated: N: 49.14; C: 21.07; H: 3.24; found: N: 40.71; C: 17.77; H: 3.68. **M/z (ESI):** 239.0 ($C_4H_4BN_8O_4^-$).

5-Aminotetrazolium dihydrobis(3-nitro-1,2,4-triazolyl)borate (5At_6)

Yield: 62%
IR: [cm^{-1}] = 3394.6 (w), 3162.0 (w), 2471.8 (w), 2438.5 (w), 2282.9 (w), 1697.8 (w), 1548.5 (m), 1503.5 (s), 1424.0 (m), 1399.3 (w), 1380.1 (w), 1306.5 (s), 1269.7 (w), 1216.8 (w), 1164.0 (m), 1149.2 (s), 1106.8 (w), 1028.0 (m), 981.7 (w), 877.1 (m), 836.0 (vs), 722.6 (m). **^{1}H-NMR** (DMSO-*d_6*): δ: 8.45 (s, 2H, CH), 6.63 (s, 2H, N*H_2*), 3.47 (br, 2H, BH_2). **^{13}C-NMR** (DMSO-*d_6*): δ: 164.18 (2C, C-NO_2), 150.18 (2C, CH), 146.19 (1C, C-NH_2). **^{11}B-NMR** (DMSO-*d_6*): δ: -9.14 (s, 1B, BH_2). **^{14}N-NMR** (DMSO-*d_6*): δ: -28.16 (s, 2N, NO_2). **EA:** $C_5H_8BN_{13}O_4$ (325.02); calculated: N: 56.02; C: 18.48; H: 2.48; found: N: 47.44; C: 16.05; H: 2.40. **M/z (ESI):** 239.0 ($C_4H_4BN_8O_4^-$).

Salts of dihydrobis(3,5-dinitropyrazolyl)borate

Potassium dihydrobis(3,5-dinitropyrazolyl)borate (K_7)

A suspension of KBH_4 (8.16 mmol) and 3,5- dinitropyrazole[9-10] (16.3 mmol) in benzonitrile was heated up to 120 °C and stirred at this temperature for 5 hours. After cooling to room temperature, filtration and drying at 60 °C for 2 days the product as colorless solid was obtained.

Yield: 65%
IR: [cm^{-1}] = 3320 (w), 3156 (w), 2923 (w), 2853 (w), 2595 (w), 2296 (w), 1792 (w), 1706 (w), 1666 (w), 1619 (w), 1580 (w), 1536 (m), 1469 (m), 1440 (s), 1377 (m), 1335 (s), 1307 (s), 1269 (m), 1249 (m), 1149 (m), 1063 (w), 1001 (m), 992 (m), 829 (s), 749 (s), 696 (w), 672 (w). **^{1}H-NMR** (DMSO-*d_6*) δ: 3.32 (s, 2H, BH_2), 7.26 (d, 1H, *5J*=0.8 Hz, CH) ppm. **^{13}C-NMR** (DMSO-*d_6*) δ: 98.36 (CH), 156.45 (CNO_2) ppm. **^{14}N-NMR** (DMSO-*d_6*) δ: −15.43 (CNO_2) ppm. **^{11}B-NMR** (acetone-*d_6*) δ: −0.96. **EA**: $KBC_6H_4N_8O_8$

(366.06): calculated: C, 19.69; H, 1.10; N**,** 30.61; found: C, 18.69; H, 0.63; N, 28.33. **M/z (FAB$^-$)**: 352.9 ($KC_6H_2N_8O_8^-$), **(FAB$^+$)**: 39.0 (cation).

Barium dihydrobis(3,5-dinitropyrazolyl)borate (Ba_7)

To a solution of **K_7** (3.19 mmol) in methanol $Ba(ClO_4)_2$ (1.60 mmol) was added and the mixture was stirred for 24 hours at room temperature. After filtration the solvent was evaporated and the product as yellow solid was obtained.

Yield: 79%
IR: [cm^{-1}] = 3568 (w), 3140 (m), 2884 (w), 1680 (w), 1627 (w) 1518 (m), 1506 (m), 1479 (m), 1443 (w), 1385 (w), 1357 (m), 1288 (s), 1148 (w), 1003 (m), 864 (w), 836 (m), 821 (s), 757 (m), 680 (m). **^{1}H-NMR** (DMSO-*d$_6$*) δ: 7.70 (CH), 3.31 (H_2B) ppm. **^{13}C-NMR** (DMSO-*d$_6$*) δ: 129.89 (CH) ppm. **^{14}N-NMR** (DMSO-*d$_6$*) δ: -17.25 (NO_2), -137.01 (CNC) ppm. **^{11}B-NMR** (DMSO-*d$_6$*) δ: not observable. **EA**: $BaH_4B_2(C_3HN_4O_4)_4$: calculated: C 16.03, H 2.24, N 24.92; found: C 16.14, H 2.21, N 23.04. **M/z (FAB$^-$)**: 157.0 ($C_3HN_4O_4^-$).

Salts of dihydrobis(2,4-dinitroimidazolyl)borate

Potassium dihydrobis(2,4-dinitroimidazolyl)borate (K_8)

A solution of KBH_4 (8.16 mmol) and 3,5- dinitroimidazole[16] (16.3 mmol) in acetonitrile was stirred at 82 °C for 24 hours. Evaporation of the solvent led to the formation of a yellow solid.

Yield: 80%
IR: [cm^{-1}] = 3378 (w), 2454 (w), 1498 (m), 1473 (m), 1432 (m), 1283 (s), 1223 (w), 1098 (m), 1000 (m), 923 (w), 872 (w), 837 (m), 818 (s), 782 (w), 757 (s), 695 (m), 662 (m). **^{1}H-NMR** (DMSO-*d$_6$*) δ: 7.72 (CH), 3.47 (br, H_2B) ppm. **^{13}C-NMR** (DMSO-*d$_6$*) δ: 39.50 (m, CH), 129.70 (CNO_2) ppm. **^{14}N-NMR** (DMSO-*d$_6$*) δ: -16.80 (CNO_2), -359.28 (NH) ppm. **^{11}B-NMR** (DMSO-*d$_6$*) δ: -10.03 (br, H_2B), 18.74 ppm. **EA**: $KBC_6H_4N_8O_8$ (366.06) calculated: C 19.69, H 1.10, N 30.61; found: C 22.51, H 2.12, N 29.11 **M/z (FAB$^-$)**: 156.09 (C3HN4O4$^-$), 326.8 ($BC_6H_4N_8O_8^-$**)**, **(FAB$^+$):** 38.9.

Barium dihydrobis(2,4-dinitroimidazolyl)borate (Ba_8)

To a solution of **K_8** (3.19 mmol) in methanol $Ba(ClO_4)_2$ (1.60 mmol) was added and the mixture was stirred for 24 hours at room temperature. After filtration the solvent was evaporated and the product as yellow solid was obtained.

Yield: 60%
IR: [cm^{-1}] = 3568 (w), 3140 (m), 2884 (w), 1680 (w), 1627 (w) 1518 (m), 1506 (m), 1479 (m), 1443 (w), 1385 (w), 1357 (m), 1288 (s), 1148 (w), 1003 (m), 864 (w), 836 (m), 821 (s), 757 (m), 680 (m). **^{1}H-NMR** (DMSO-*d$_6$*) δ: 7.70 (CH), 3.31 (H_2B) ppm. **^{13}C-NMR** (DMSO-*d$_6$*) δ: 129.89 (CH) ppm. **^{14}N-NMR** (DMSO-*d$_6$*) δ: -17.25 (NO_2), -137.01 (CNC) ppm. **^{11}B-NMR** (DMSO-*d$_6$*) δ: signal not observable. **EA**: BaH_4B_2(C3HN4O4)4*(H2O)6 (791.24): calculated: C 18.21, H 1.02, N 28.32; found: C 16.14, H 2.21, N 23.04. **M/z (FAB$^-$)**: 157.0 ($C_3HN_4O_4^-$)**, (FAB$^+$)**: 137.1 (cation).

Results and Discussion

1 Synthesis

1.1 Metal Salts of di-, trinitropyrazole and trinitroimidazole

The synthesis of 3,5-Dinitropyrazole was performed according to literature by successive nitration of commercially available Pyrazole followed by isomerisation in benzonitrile.[9-10] The alkali and earth alkali salts of 3,5-Dinitropyrazole were synthesized by deprotonation with corresponding metal carbonates in ethanol and metal hydroxides in water, respectively (Scheme 1). The products were obtained in high yields.

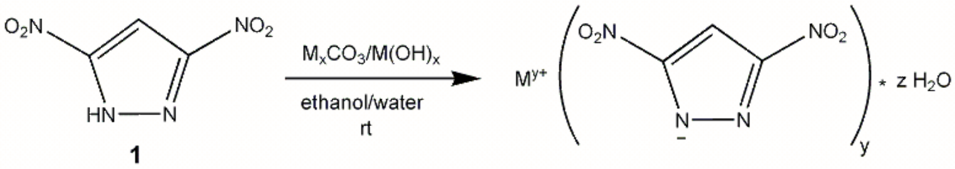

M = **Li**	x = 2	y = 1	z = 3	**LiDNP·3H$_2$O**	**Li_1**
M = **Na**	x = 2	y = 1	z = 2	**NaDNP·2H$_2$O**	**Na_1**
M = **K**	x = 2	y = 1	z = 0	**KDNP**	**K_1**
M = **Ca**	x = 2	y = 2	z = 4	**Ca(DNP)$_2$·4H$_2$O**	**Ca_1**
M = **Sr**	x = 2	y = 2	z = 6	**Sr(DNP)$_2$·6H$_2$O**	**Sr_1**
M = **Ba**	x = 2	y = 2	z = 1	**Ba(DNP)$_2$·H$_2$O**	**Ba_1**

Scheme 1: Synthesis of 3,5-dinitropyrazolate salts.

All salts crystallize as hydrates and were characterized by NMR spectroscopy, mass spectrometry, elemental analysis and IR spectroscopy (see **Experimental**).

According to literature 3,4,5-trinitropyrazole was synthesized by nitration of 3,5-dinitropyrazole with concentrated sulfuric and nitric acid.[11] The deprotonation of 3,4,5-trinitropyrazole with metal carbonates in ethanol at room temperature led to the formation of the corresponding metal salts in high yields (Scheme 2).

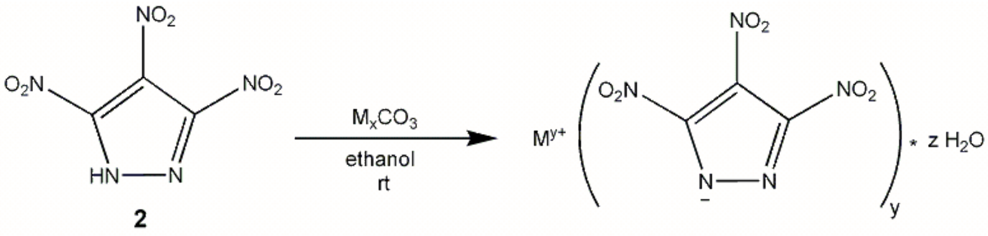

M = **Li**	x = 2	y = 1	z = 3	**LiTNP·4H_2O**	**Li_2**
M = **Na**	x = 2	y = 1	z = 3	**NaTNP**	**Na_2**
M = **Sr**	x = 1	y = 2	z = 3	**Sr(TNP)$_2$**	**Sr_2**
M = **Ba**	x = 1	y = 2	z = 3	**Ba(TNP)$_2$·3H_2O**	**Ba_2**

Scheme 2: Synthesis of 3,4,5-trinitropyrazolate salts.

All salts were analyzed by NMR spectroscopy, mass spectrometry, elemental analysis and IR spectroscopy (see **Experimental**).

The nitration of 2,4-dinitroimidazole with glacial acetic acid, nitric acid and acetic anhydride led to the formation of 2,4,5-trinitroimidazole.[16] The alkali metal salts and the copper salt were synthesized by deprotonating 2,4,5-trinitroimidazole with the corresponding metal carbonates, whereas the earth alkali salts were obtained by the deprotonation with the corresponding metal hydroxides (Scheme 3). Recrystallization from ethylacetate gave the products in high yields.

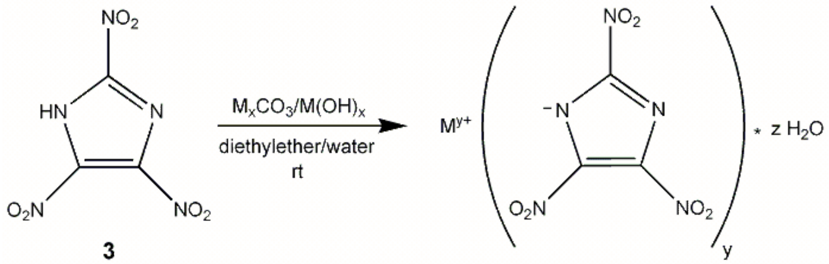

M = **Li**	x = 2	y = 1	z = 3	**LiTNI·3H_2O**	**Li_3**
M = **Na**	x = 2	y = 1	z = 0	**NaTNI**	**Na_3**
M = **K**	x = 2	y = 1	z = 0	**KTNI**	**K_3**
M = **Ca**	x = 2	y = 2	z = 4	**Ca(TNI)$_2$·2H_2O/2$C_4H_8O_2$**	**Ca_3**
M = **Sr**	x = 2	y = 2	z = 2.5	**Sr(TNI)$_2$·H_2O/1.5$C_4H_8O_2$**	**Sr_3**
M = **Cu**	x = 2	y = 2	z = 4	**Cu(TNI)$_2$·4H_2O**	**Cu_3**

Scheme 3: Synthesis of 3,4,5-trinitropyrazolate salts.

All salts were analyzed by NMR spectroscopy, mass spectrometry, elemental analysis and IR spectroscopy (see **Experimental**). The elemental analysis of the strontium and calcium salt led to the assumption that these salts contain coordinated ethylacetate, which could not be removed by drying the salts at 60 °C.

1.2 Nitrogen-rich azolylborate salts

All potassium azolylborate salts were synthesized by the reaction of potassium borohydride with the corresponding azole at different reaction conditions. **K_4**, **K_6**, **K_7** and **K_8** were obtained by stirring the reaction mixture at elevated temperatures in acetonitrile and dimethylacetamide, respectively, whereas **K_5** was synthesized in a solid-solid reaction of the starting components, also at high temperature of 120 °C (Scheme 4 left). The acidification of **K_4** and **K_5** with glacial acetic acid (Scheme 4 right) led to the formation of the protonated forms, which served as starting materials for the synthesis of the corresponding barium salts **Ba_4** and **Ba_5** (Scheme 5).

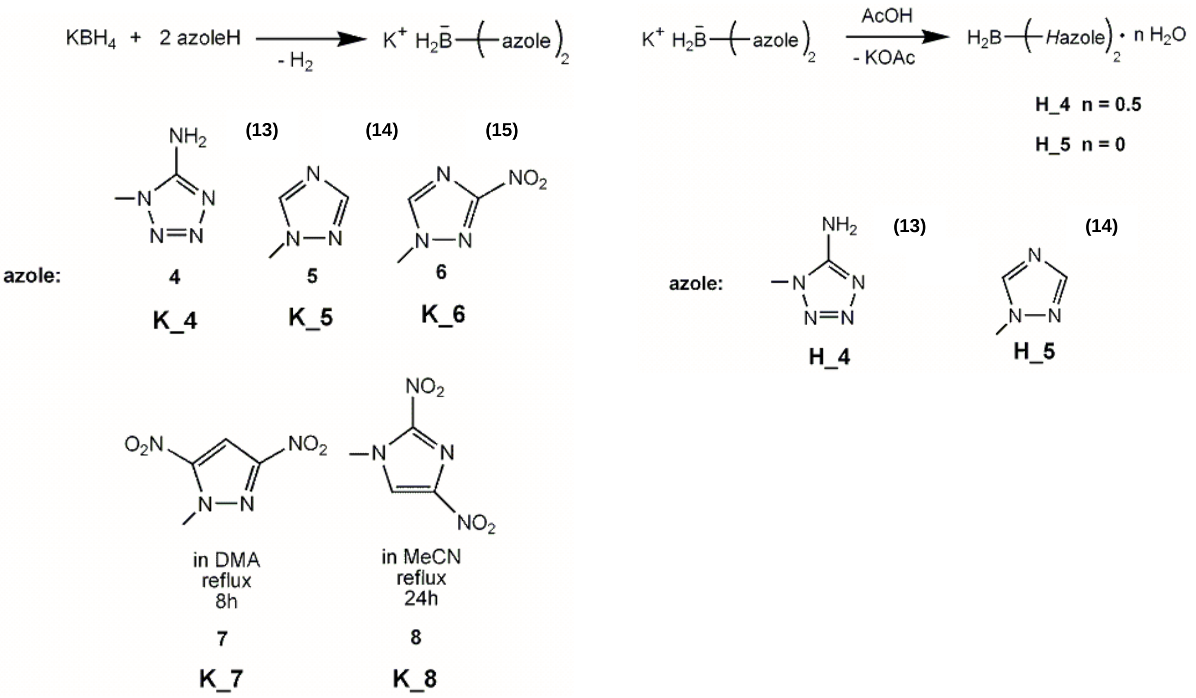

Scheme 4: Synthesis of potassium azolylborate salts (left) and the protonated forms (right).

The barium salts **Ba_4** and **Ba_5** were obtained by deprotonation of **H_4** and **H_5** with barium hydroxide in water at room temperature. The salts **Ba_6**, **Ba_7** and **Ba_8** were synthesized by the reaction of the corresponding potassium salts with barium perchlorate whereat hardly soluble potassium perchlorate precipitated (Scheme 5).

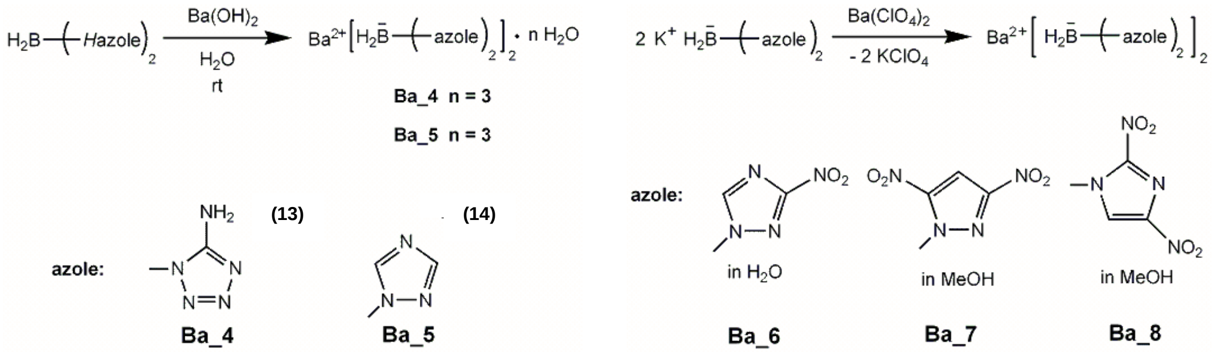

Scheme 5: Synthesis of barium azolylborate salts.

All salts were characterized by NMR spectroscopy, mass spectrometry, elemental analysis and IR spectroscopy (see **Experimental**).

The synthesis of the metal-free azolylborate salts was performed by the reaction of the barium salts with selected nitrogen-rich sulfates in water or methanol at room temperature, whereat barium sulfate precipitated and was removed. The isolated products were obtained as solids and in high yields. As nitrogen-rich cations ammonium, aminoguanidinium, diaminoguanidinium, N-guanylurea and 5-aminotetrazolium were selected (Scheme 6).

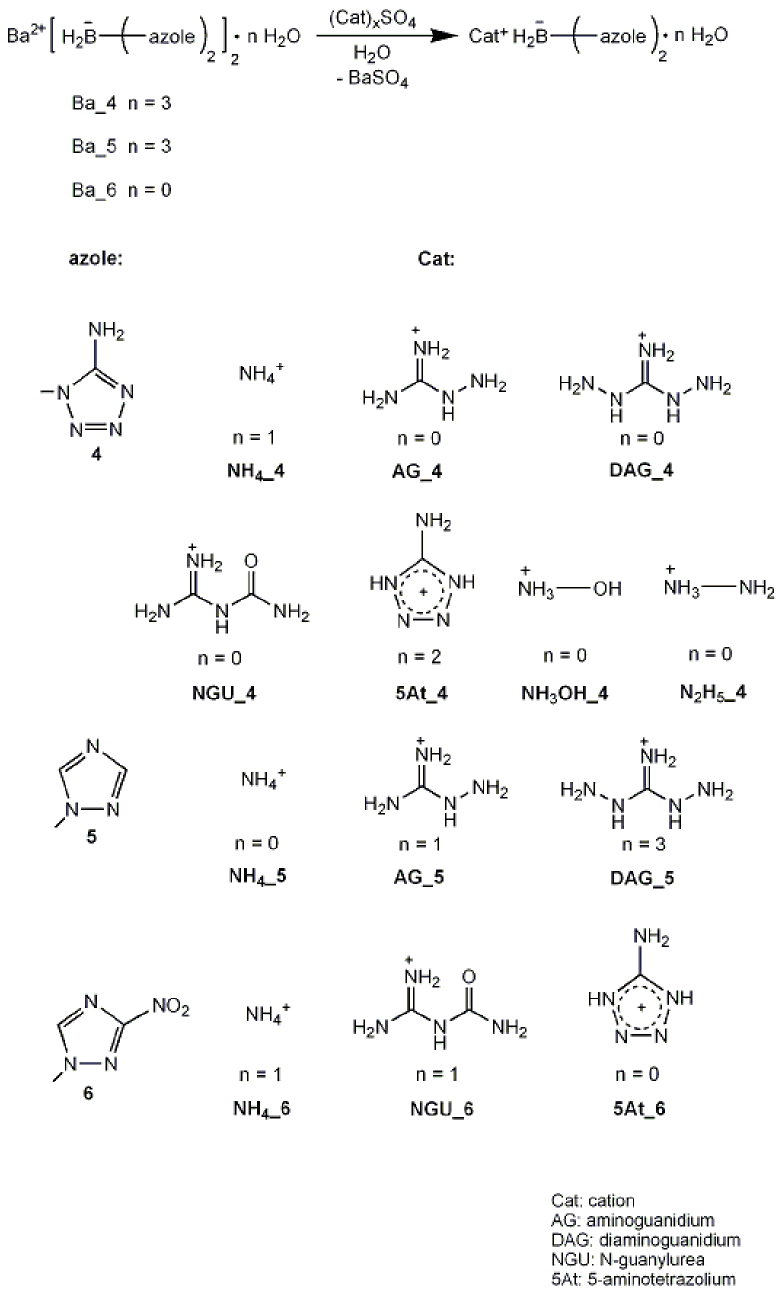

Scheme 6: Synthesis of metal-free azolylborate salts.

All salts were characterized by NMR spectroscopy, mass spectrometry, and elemental analysis (see **Experimental**).

2 Crystal Structures

Suitable single crystals of the described compounds (**DAG_4**, **K_1**, **Ba_1** and **Ba_5**) were picked from the crystallization mixture and mounted in Kel-F oil, transferred to the N_2 stream of an Oxford Xcalibur3 diffractometer with a Spellman generator (voltage 50 kV, current 40 mA) and a KappaCCD detector using a $\lambda_{MoK\alpha}$ radiation wavelength of 0.71073 Å. All structures were measured at -100 °C. The data collection and data reduction was carried out with the CrysAlisPro software.[17] The structures were solved with Sir-92[18] refined with Shelxl-97[19] and finally checked using the Platon software[20] integrated in the WINGX software suite.[21] The non-hydrogen atoms were refined anisotropically and the hydrogen atoms were located and freely refined. The absorptions were corrected by a SCALE3 ABSPACK multi-scan method.[22] Further data and parameters of the X-ray measurements and refinements are included in Table 1. Further information regarding the crystal-structure determination have been deposited as cif files with the Cambridge Crystallographic Data Centre [23] as supplementary publications.

Table 1: XRD data and parameters.

	DAG_4	**K_1**	**Ba_1·MeOH·Et$_2$O**	**Ba_5·3H$_2$O**
Formula	$C_3H_{14}BN_{15}$	$C_3HKN_4O_4$	$C_{11}H_{16}BaN_8O_{10}$	$C_8H_{18}B_2BaN_{12}O_3$
FW [g mol^{-1}]	271.10	196.18	557.65	489.30
Crystal system	Monoclinic	Triclinic	Monoclinic	Orthorhombic
Space Group	$P2_1/c$	P-1	$P2_1/c$	$C222_1$
Color / Habit	colorless rods	yellow blocks	yellow plates	colorless blocks
Size [mm]	0.12 x 0.18 x 0.28	0.10 x 0.20 x 0.25	0.09 x 0.18 x 0.34	0.35 x 0.30 x 0.25
a [Å]	9.2353(3)	4.7304(5)	10.1288(3)	7.0683(2)
b [Å]	13.3916(5)	8.0724(9)	9.4139(2)	13.6825(3)
c [Å]	9.3994(3)	9.1070(12)	21.4156(8)	18.0720(4)
α [°]	90	105.521(11)	90	90
β [°]	92.738(3)	102.423(10)	103.197(3)	90
γ [°]	90	97.273(9)	90	90
V [Å^3]	1161.15(7)	320.90(7)	1988.08(11)	1747.78(7)
Z	4	2	4	4
$\rho_{calc.}$ [g cm^{-3}]	1.551	2.030	1.863	1.860
μ [mm^{-1}]	0.118	0.806	2.066	2.311
F(000)	568	196	1096	960
$\lambda_{MoK\alpha}$ [Å]	0.71073	0.71073	0.71073	0.71073
T [K]	173	173	173	173
θ Min–Max [°]	4.3, 26.5	4.5, 26.0	4.2, 26.0	4.5, 26.0
Dataset	-11:11; -16:16; -11:11	-5:5; -9:8; -10:11	-12:12; -11:11; -26:26	-8:8; -16:16; -22:22
Reflections collected	18224	1660	19502	8824
Independent refl.	2400	1245	3892	1716
R_{int}	0.037	0.014	0.048	0.030
Observed reflections	1809	1129	3283	1676
Parameters	228	114	283	155
R_1 (obs)	0.0296	0.0283	0.0254	0.0138
wR_2 (all data)	0.0743	0.0710	0.0580	0.0303
S^c	0.96	1.05	1.03	1.07
Resd. Dens. [e Å^{-3}]	-0.17, 0.17	-0.28, 0.27	-0.41, 0.61	-0.32, 0.71
Device type	Oxford Xcalibur3 CCD	Oxford Xcalibur3 CCD	Oxford Xcalibur3 CCD	Oxford Xcalibur3 CCD
Solution	SIR-92	SIR-92	SIR-92	SIR-92
Refinement	SHELXL-97	SHELXL-97	SHELXL-97	SHELXL-97
Absorption correction	multi-scan	multi-scan	multi-scan	multi-scan

Diaminoguanidinium dihydrobis(5-aminotetrazolyl)borate (**DAG_4**) crystallizes in the monoclinic space group $P2_1/c$ with four formula units in the unit cell and a density of 1.551 g cm^{-3}. One anion/cation pair is shown in Figure 1.

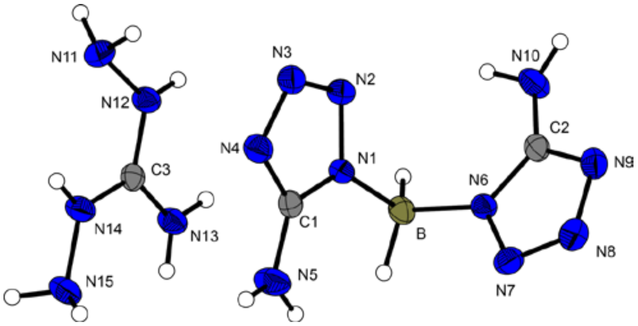

Figure 1: Molecular unit of diaminoguanidinium dihydrobis(5-aminotetrazolyl)borate (**DAG_4**). Thermal ellipsoids represent the 50 % probability level. Selected bond distances [Å]: N1–B 1.5593(17), C1–N1 1.3395(14), C1–N5 1.3499(16), N4–C1 1.3273(15), N4–N3 1.3572(14), N12–C3 1.3304(15), N8–N7 1.2905(14), N8–N9 1.3651(15), N10–C2 1.3602(17), N7–N6 1.3663(14), N1–N2 1.3630(13), N9–C2 1.3298(16), N2–N3 1.2937(14), N6–C2 1.3414(15), N6–B 1.5541(17), N12–C3 1.3304(15), N14–C3 1.3175(15), N15–N14 1.4077(14), N13–C3 1.3237(16), N12–N11 1.4095(15); selected bond angle [°]: N6–B–N1 106.51(9).

Potassium 3,5-dinitropyrazolate, shown in Figure 2, with a density of 2.030 g cm^{-3} crystallizes within the triclinic space group *P*-1. Up to now, no 3,5-dinitropyrazole structure can be found in the CCDC database. The aromatic pyrazole ring is planar. The nitro groups are slightly twisted out of the ring plane (torsion angles O3–N4–C3–C2 5.9(3)° and O2–N3–C1–C2 4.6(3)°.

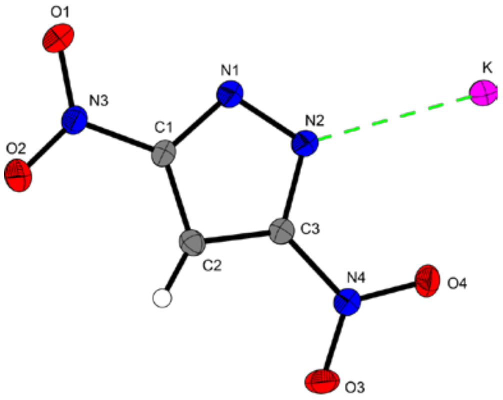

Figure 2: Asymmetric unit of potassium 3,5-dinitropyrazolate (**K_1**). Thermal ellipsoids represent the 50 % probability level. Selected bond and coordination distances [Å]: O1–N3 1.235(2), O2–N3 1.2314(19), N2–

K2.942(12), O2–K 3.0152(14), O3–N4 1.2297(19), O4–N4 1.2396(19), N1–N2 1.343(2), N1–C1 1.357(2), N2–C3 1.356(2), N3–C1 1.439(2), N4–C3 1.429(2), C1–C2 1.381(3), C2–C3 1.383(2).

Barium 3,5-dinitropyrazolate (**Ba_1**) could only obtained crystalline with the inclusion of one methanol and one diethyl ether molecule. The diethyl ether is fixed by the strong hydrogen bond O9–H9 ··O10 (d(D–A): 2.772(5) Å) to the barium coordinated methanol molecule. Complex **Ba_1** crystallizes in the monoclinic space group $P2_1/c$ with four formula units in the unit cell and a density of 1.863 g cm^{-3}. In agreement to the corresponding potassium structure **K_1** the 3,5-dinitropyrazolate anions are nearly planar.

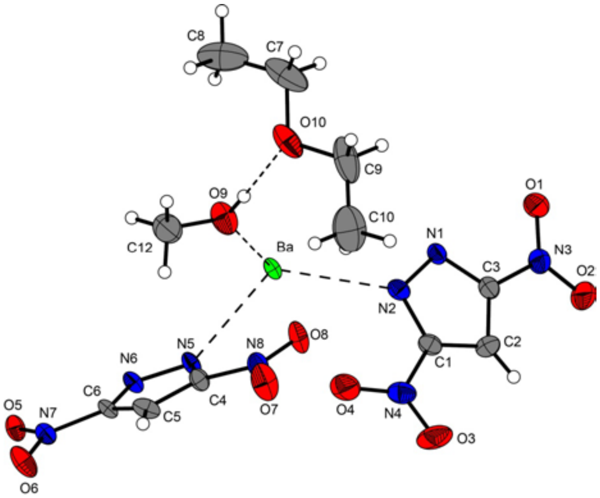

Figure 3: Asymmetric unit of barium 3,5-dinitropyrazolate (**Ba_1**). Thermal ellipsoids represent the 50 % probability level. Selected bond and coordination distances [Å]: O1–N3 1.238(3), O2–N3 1.227(3), O3–N4 1.224(4), O4–N4 1.242(4), O4–Ba 2.956(3), N1–C3 1.347(4), N1–N2 1.355(3), N2–C1 1.352(4), N2–Ba 2.961(3), N3–C3 1.439(4), N4–C1 1.431(4), C1–C2 1.373(5), C2–C3 1.372(4), O5–N7 1.243(3), O6–N7 1.236(3), O7–N8 1.225(3), O8–N8 1.237(3), O8–Ba 2.943(2), N5–N6 1.340(3), N5–C4 1.355(4), N5–Ba 2.909(2), N6–C6 1.350(4), N7–C6 1.425(4), N8–C4 1.437(4), C4–C5 1.393(4), C5–C6 1.366(4), O10–C7 1.424(5), O10–C9 1.431(5), C8–C7 1.508(7), C9–C10 1.470(7), O9–C12 1.411(4), O9–Ba 2.784(3).

The molecular unit of barium dihydrobis(1,2,4-triazolyl)borate trihydrate (**Ba_5**), which crystallizes in the monoclinic space group C2/c is depicted in Figure 4.

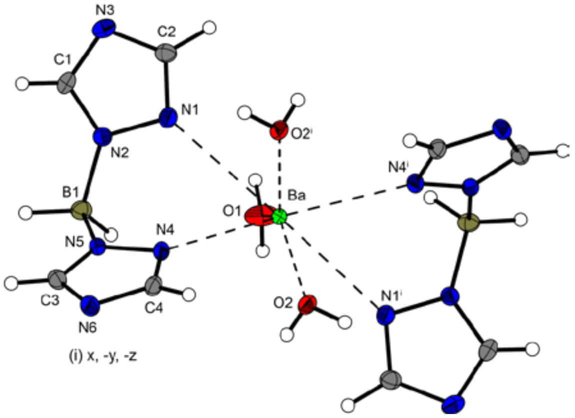

Figure 4: Molecular unit of barium dihydrobis(1,2,4-triazolyl)borate trihydrate (**Ba_5**). Thermal ellipsoids represent the 50 % probability level. Selected bond and coordination distances [Å]: N2–C1 1.330(3), N2–N1 1.375(2), N2–B1 1.543(3), N4–C4 1.323(3), N4–N5 1.380(3), N5–C3 1.335(3), N5–B1 1.559(3), N3–C1 1.335(3), N3–C2 1.354(3), N6–C3 1.332(3), N6–C4 1.361(3), N1–C2 1.321(3), N1–Ba 3.0001(18), Ba–N4 3.0058(19), Ba–N6 3.070(2), O1–Ba 2.723(2), O2–Ba 2.7863(18), Ba–N1 3.0001(18), Ba–N4 3.0058(19).

3 Thermal and Energetic Properties

Melting and decomposition points were measured with a Linseis PT10 DSC using heating rates of 5 °C min^{-1}, which were checked with a Büchi Melting Point B-450 apparatus. The sensitivity data were performed using BAM methods.[24] The following tables indicate the results obtained from submitting the compounds to shock and friction stimuli as well as to electrostatic discharge (ESD). Furthermore, the melting (T_m) and decomposition (T_{dec}) temperatures are listed below (Tables 2-8).

Table 2: Thermal and energetic properties of 3,5-dinitropyrazolate salts.

	Li_1	**Na_1**	**K_1**	**Ca_1**	**Sr_1**	**Ba_1**
T_m (°C) (onset[a])	145	295	-	-	-	150
T_{dec} (°C) (onset[a])	325	324	306	>400	400	361
Friction[b] (N)	360	360	216	360	360	72
Impact[b] (J)	>40	>40	20	8	>40	30
grain size (µm)	<100	<100	100-500	100-500	100-500	500-1000

[a] Differential Scanning Calorimetry (DSC)
[b] according to BAM standards (www.bam.de)

All salts are with temperatures higher than 200 °C thermally very stable. Except the **Ba_1** all salts are less friction sensitive. **Li_1** and **Na_1** are impact insensitive, all other salts are sensitive[24] (Table 2). Therefore **Li_1** and **Sr_1** are suitable candidates for the use as coloring agents in pyrotechnics.

Table 3: Thermal and energetic properties of 3,4,5-trinitropyrazolate salts.

	Li_2	**Na_2**	**Sr_2**	**Ba_2**
T_m (°C) (onset[a])	-	-	-	158
T_{dec} (°C) (onset[a])	274	254	193	302
Friction[b] (N)	96	80	80	144
Impact[b] (J)	40	25	40	5
grain size (µm)	100-500	100-500	100-500	100-500

[a] Differential Scanning Calorimetry (DSC)

[b] according to BAM standards (www.bam.de)

The 3,4,5-trinitropyrazolate salts are also thermally stable but with an additional nitro group friction sensitive.[24] Toward impact the lithium and strontium salts are less sensitive and the sodium and barium salt sensitive (Table 3).[24]

Table 4: Thermal and energetic properties of 2,4,5-trinitroimidazolate salts.

	Li_3	**K_3**	**Ca_3**	**Cu_3**
T_m (°C) (onset[a])	152	-	-	-
T_{dec} (°C) (onset[a])	252	231	188	170
Friction[b] (N)	360	120	360	80
Impact[b] (J)	40	25	40	3
grain size (µm)	100-500	100-500	100-500	100-500

[a] Differential Scanning Calorimetry (DSC)

[b] according to BAM standards (www.bam.de)

In contrast to lithium trinitropyrazolate lithium trinitroimidazolate is less sensitive towards impact and friction. [24] In addition the decomposition temperature is higher than 200 °C. These properties make **Li_3** an interesting compound for red burning pyrotechnics (Table 4).

All metal-free nitrogen-rich salts of 5-aminotetrazolylborate and 1,2,4-triazolylborate as well as barium dihydrobis(1,2,4-triazolyl)borate are not or less sensitive towards impact, friction and electrostatic discharge[24] and thermally stable (Table 5-6).

Table 5: Thermal and energetic properties of dihydrobis(5-aminotetrazolyl)borate salts.

	NH_4_4	**AG_4**	**DAG_4**	**NGU_4**	**5At_4**
T_m (°C) (onset[a])	157	143	153	n.d.	n.d.
T_{dec} (°C) (onset[a])	201	193	165	n.d.	n.d.
Friction[b] (N)	>360	>360	324	>360	>360
Impact[b] (J)	>40	>40	>40	>40	>40
ESD[b] (J)	0.5	1	0.3	n.d.	n.d.
grain size (µm)	<100	100-500	100-500	<100	<100

[a] Differential Scanning Calorimetry (DSC)
[b] according to BAM standards (www.bam.de)
n.d. (not determined)

Table 6: Thermal and energetic properties of dihydrobis(1,2,4-triazolyl)borate salts.

	NH_4_5	**AG_5**	**DAG_5**	**Ba_5**
T_m (°C) (onset[a])	154	-	143	-
T_{dec} (°C) (onset[a])	285	164	212	348
Friction[b] (N)	288	>360	>360	>360
Impact[b] (J)	40	>40	>40	>40
ESD[b] (J)	0.7	1	1	0.8
grain size (µm)	100-500	100-500	100-500	100-500

[a] Differential Scanning Calorimetry (DSC)
[b] according to BAM standards (www.bam.de)

Compounds **NH_4_6** and **NGU_6** reveal insensitivity toward impact and friction and are therefore promising compounds for metal-free green-burning pyrotechnics (Table 7).

Table 7: Thermal and energetic properties of dihydrobis(3-nitro-1,2,4-triazolyl)borate salts.

	NH_4_6	**NGU_6**	**5At_6**	**Ba_6**
T_m (°C) (onset[a])	163	154	n.d.	-
T_{dec} (°C) (onset[a])	207	220	n.d.	224
Friction[b] (N)	>360	>360	288	360
Impact[b] (J)	>40	>40	10	5
grain size (µm)	100-500	100-500	100-500	100-500

[a] Differential Scanning Calorimetry (DSC)
[b] according to BAM standards (www.bam.de)
n.d. (not determined)

The potassium and barium dihydrobis(3,5-dinitropyrazolyl)borate is impact and friction sensitive in contrast to potassium and barium dihydrobis(2,4-dinitroimidazolyl)borate, which are both insensitive. All salts reveal high thermal stability (Table 8).

Table 8: Thermal and energetic properties of dihydrobis(3,5-dinitropyrazolyl)borate (**7**) and dihydrobis(2,4-dinitroimidazolyl)borate (**8**) salts.

	K_7	**Ba_7**	**K_8**	**Ba_8**
T_m (°C) (onset[a])	-	298	-	-
T_{dec} (°C) (onset[a])	316	342	165	349
Friction[b] (N)	216	180	360	360
Impact[b] (J)	3	5	40	40
grain size (µm)	100-500	100-500	100-500	100-500

[a] Differential Scanning Calorimetry (DSC)

[b] according to BAM standards (www.bam.de)

4 Investigation of Pyrotechnic Compositions

Compounds **Ba_1**, **Sr_1**, **AG_4**, **DAG_4** and **AG_5** were investigated in pyrotechnic mixtures. The pyrotechnic mixtures were prepared by mixing all substances (given in weight percent), except the binder, in a mortar. Then the binder, a solution of 25 % vinyl alcohol acetate resin (VAAR), was added. The mixture was formed by hand and dried under high vacuum for three hours. The controlled burn down was filmed with a digital video camera recorder (SONY, DCR-HC37E). The performance of each composition has been evaluated with respect to color emission, smoke generation and the amount of solid residues.

Table 9: Pyrotechnic compositions.

	compound	*oxidizer*	*fuel*	*binder*
composition 1	**Ba_1** 25%	NH_4NO_3 60%	B 8%	VAAR[a] 7%
composition 2	**Ba_1** 35%	NH_4NO_3 50%	B/Mg 3%/5%	VAAR[a] 7%
composition 3	**Ba_1** 35%	NH_4NO_3 50%	B/Mg 4%/4%	VAAR[a] 7%
composition 4	**Sr_1** 25%	NH_4NO_3 60%	Mg 8%	VAAR[a] 7%
composition 5	**Sr_1** 40%	NH_4NO_3 45%	Mg 8%	VAAR[a] 7%
composition 6	**Sr_1** 40%	$KMnO_4$ 45%	Mg 8%	VAAR[a] 7%
composition 7	**DAG_4** 35%	NH_4NO_3 40%	B 18%	VAAR[a] 7%

composition 8	**AG_4** 35%	NH_4NO_3 40%	B 18%	VAAR[a] 7%
composition 9	**AG_5** 25%	NH_4NO_3 60%	B 8%	VAAR[a] 7%

[a] vinyl alcohol acetate resin

Composition 1 and **3** burned fast with a deep green flame color. No smoke was observable and almost no residues remained. In contrast **composition 2** burned fast with a slight green flame color without smoke but some residues could be observed (Figure 5).

Composition 4 and **5** burned with an intense red flame color, whereas **composition 6** showed a less intensive red flame color (Figure 6). The combustion velocity of **composition 4** and **5** was moderate and of **composition 6** very fast. All three compositions burned without smoke generation. No residues were observable for **composition 6**, some residues remained in the case of **composition 4** and **5**.

The burn down of the borate salts in **compositions 7-9** showed green flame colors without smoke generation and almost no residues (Figure 7). The combustion velocities of all three compositions were fast.

Figure 5: Burn down of **compositions 1** (left), **2** (middle) and **3** (right).

Figure 6: Burn down of **compositions 4** (left), **5** (middle) and **6** (right).

Figure 7: Burn down of **compositions 7** (left), **8** (middle) and **9** (right).

Summary and Conclusions

The synthesis, characterization and the investigation of thermal and energetic properties of new alkali and earth alkali salts of 3,5-dinitropyrazole as well as of selected alkali and earth alkali salts of 3,4,5-trinitropyrazole and 2,4,5-trinitroimidazole were performed. All salts are thermally stable. Except barium 3,5-dinitropyrazolate (**Ba_1**), potassium 2,4,5-trinitroimidazolate (**K_3**) and the 3,4,5-trinitropyrazolates, all salts are friction insensitive, which is an important requirement for their use in pyrotechnic compositions.

Dihydrobisazolylborate salts with nitrogen-rich cations were synthesized and characterized. The borate salts are no or less sensitive (Impact, Friction, ESD) and show high thermal stability.

Crystal structures of the compounds **Ba_1**, **K_1**, **DAG_4** and **Ba_5** were determined by single crystal diffraction.

Pyrotechnic compositions of selected compounds **Ba_1**, **Sr_1**, **AG_4**, **DAG_4** and **AG_5** were investigated. Good color performance and smokeless combustion could be observed.

Acknowledgements

Financial support of this work by the Ludwig-Maximilian University of Munich (LMU), the U.S. Army Research Laboratory (ARL), the Armament Research, Development and Engineering Center (ARDEC), the Strategic Environmental Research and Development Program (SERDP) and the Office of Naval Research (ONR Global, title: “Synthesis and Characterization of New High Energy Dense Oxidizers (HEDO) - NICOP Effort ”) under contract nos. W911NF-09-2-0018 (ARL), W911NF-09-1-0120 (ARDEC), W011NF-09-1-0056 (ARDEC) and 10 WPSEED01-002 / WP-1765 (SERDP) is gratefully acknowledged. The authors acknowledge collaborations with Dr. Mila Krupka (OZM Research, Czech Republic) in the development of new testing and evaluation methods for energetic materials and with Dr. Muhamed Sucesca (Brodarski Institute, Croatia) in the development of new computational codes to predict the detonation and propulsion parameters of novel explosives. We are indebted to and thank Drs. Betsy M. Rice and Brad Forch (ARL, Aberdeen, Proving Ground, MD) and Mr. Gary Chen (ARDEC, Picatinny Arsenal, NJ) for many helpful and inspired discussions and support of our work. The Cusanuswerk is gratefully acknowledged for the award of a PhD scholarship (MR).

References

(1) Steinhauser, G.; Klapötke, T. M.; *Angew. Chem. Int. Ed.* **2008**, *47*, 3330.

(2) Sabatini, J. J.; Poret, J. C.; Nagori, A. V.; Chen, G.; Damavarapu, R.; Klapötke, T. M.; *Prop. Expl. Pyrotech.* **2011**, *36*, 373.

(3) Sabatini, J. J.; Nagori, A. V.; Poret, J. C.; Damavarapu, R.; Klapötke, T. M.; *Chemistry – Europ. J.* **2011**, DOI: 10.1002/chem.201102485.

(4) Sabatini, J. J.; Poret, J. C.; Broad, R. N.; *Angew. Chem., Int. Ed.* **2011**, *50*, 4624.

(5) Sabatini, J. J.; Poret, J. C.; Broad, R. N.; *Journal of Energetic Materials* **2011**, *29*, 360.

(6) Zhang, Y.; Guo, Y.; Joo, Y. H.; Parrish, D. A.; Shreeve, J. M.; *Chem. Eur. J.* **2010**, *16*, 10778.

(7) Gao, H.; Ye, Ch.; Gupta, O. D.; Xiao, J. Ch.; Hiskey, M. A.; Twamley, B.; Shreeve, J.M.; *Chem. Eur. J.* **2007**, *13*, 3853.

(8) a) Hervé, G.; FR Patent 2917409, **2008**; b) Hervé, G.; WO Patent 2008152524, **2008**; c) Hervé, G.; US Patent 20090186931, **2009**.

(9) Hüttel, R.; Büchele, F; *Chem. Ber.* **1955**, *88*, 1586.

(10) Janssen, J. W. A. M.; Koeners, H. J.; Kruse, C. G.; Habraken, C. L.; *J. Org. Chem.* **1973**, *38*, 1777.

(11) Hervé, G.; Roussel, C.; Graindorge, H; *Angew. Chem. Int. Ed.* **2010**, *49*, 3177.

(12) Katriszky, A. R.; Cundy, D. J.; Chen, J.; *J. Ener. Mat.* **1993**, *11*, 345.

(13) Groshens, T. J.; *Journal of Coordination Chemistry* **2010**, *63*, 1882.

(14) Zeng, Z.; Twamley, B.; Shreeve, J. M.; *Organometallics* **2007**, *26*, 1782.

(15) Pellei, M.; Benetollo, F.; Lobbia, G. G.; Alidori, S.; Santini, C.; *Inorg. Chem.* **2005**, *44*, 846.

(16) Wüllner, G.; Herkenrath, F. W., WO 021409, Dynamit Nobel AG/Asahi Chemical Corp. **2010**.

(17) CrysAlisPro Oxford Diffraction Ltd., Version 171.33.41, **2009**.

(18) SIR-92, 1993, A program for crystal structure solution, Altomare, A.; Cascarano, G.; Giacovazzo, C.; Guagliardi, A.; *J. Appl. Cryst.* **1993**, *26*, 343.

(19) G. M. Sheldrick SHELXS-97, Program for Crystal Structure Solution, Universität Göttingen, **1997**.

(20) PLATON, A Multipurpose Crystallographic Tool, Utrecht University, Utrecht, The Netherlands, A. L. Spek, **1998**.

(21) Farrugia, L. J.; *J. Appl. Cryst.* **1999**, *32*, 837.

(22) Empirical absorbtion correction using spherical harmonics, implemented in SCALE3 ABSPACK scaling algorithm (CrysAlisPro Oxford Diffraction Ltd., Version 171.33.41, **2009**)

(23) Crystallographic data for the structure(s) have been deposited with the Cambridge Crystallographic Data Centre. Copies of the data can be obtained free of charge on application to the Director, CCDC, 12 Union Road, Cambridge CB2 1EZ, UK (Fax: int.code (1223)336-033: email for inquiry: fileserv@ccdc.cam.ac.uk; e.mail for deposition: deposit-@ccdc.cam.ac.uk).

(24) www.bam.de

DOI: 10.1002/zaac.201400082

Metal Salts of 4,5-Dinitro-1,3-imidazole as Colorants in Pyrotechnic Compositions

Thomas M. Klapötke,*[a] Thomas G. Müller,[a] Magdalena Rusan,[a] and Jörg Stierstorfer[a]

In Memory of Professor Alan Katritzky

Keywords: 4,5-Dinitroimidazole; Alkali metals; Alkaline earth metals; Crystal structure; Green and red colorants; Nitrogen-rich compounds; Pyrotechnics

Abstract. 4,5-Dinitroimidazole (**1**) (4,5-DNI) was synthesized by nitration of commercially available 4-nitro-imidazole. Several alkaline and alkaline earth metal salts of 4,5-dinitro-1,3-imidazole were synthesized by reaction of DNI with stoichiometric amounts of the corresponding metal hydroxides and carbonates. The synthesized salts, LiDNI·3H_2O (**2**), NaDNI·H_2O (**3**), KDNI·H_2O (**4**), Ca$(DNI)_2$·5H_2O (**5**), Sr$(DNI)_2$·3H_2O (**6**), and Ba$(DNI)_2$·4H_2O (**7**) were characterized comprehensively by means of single-crystal X-ray diffraction, NMR and vibrational (IR/Raman) spectroscopy, mass spectrometry, elemental analysis, and differential scanning calorimetry (DSC). A detailed description of their potential use as flame colorants in pyrotechnical compositions is also given. Their color properties regarding the dominant wavelength, spectral purity, luminous intensity and luminous efficiency were measured. Last but not least the investigated salts were found to be insensitive in terms of friction and impact tested with BAM methods.

Introduction

The development of environmentally friendly pyrotechnics for military and civilian application is intended by many research groups.[1] Major requirements for such pyrotechnics are less or no smoke generation during the combustion and less toxic decomposition products. But also low sensitivities towards ignition stimuli and high temperature stabilities are of high importance as well as a performance equal or higher than that of commonly used compounds. Suitable compounds are therefore nitrogen-rich salts, as their energy is not obtained from the oxidation of the carbon backbone but rather from the high heats of formation.[2] Furthermore, their main decomposition product is gaseous nitrogen, which leads to brilliant color and thus good color performances.

In literature five-membered nitrogen-containing heterocycles like tetrazolates and triazolates are described as energetic materials, and especially their strontium and barium salts have been investigated as coloring agents in pyrotechnics.[3] By the introduction of nitro groups into energetic compounds the oxygen balance and density, and thus the detonation properties are improved.[4] Dinitroimidazole, which can exist as several different isomers with respect to the positions of the substituted nitro groups, is reported to be an energetic compound with an excellent thermal stability and highly insensitive behavior towards shock and friction.[4,5] Nitration on the ring carbon atoms is preferable than on the nitrogen atom because nitro groups are usually more stable than nitramino groups.[5] The synthesis and investigation of various metal-free 4,5-dinitroimidazolate salts have been reported by *Katritzky* and *Rogers* and co-workers investigating them as ionic liquids.[6,7] The synthesis of the metal salt potassium 4,5-dinitroimidazolate was performed by the reaction of 4,5-dinitroimidazole and potassium carbonate in acetone.[6] According to this procedure the synthesis of the herein reported metal 4,5-dinitro-1,3-imidazolate salts was accomplished.

The synthesis and the full characterization by NMR spectroscopy, mass spectrometry, elemental analysis, and vibrational spectroscopy of alkali metal and alkaline earth metal salts of 4,5-dinitro-1,3-imidazole is reported herein as well as their energetic and thermal sensitivities. Also all compounds were characterized by X-ray analysis. The strontium and barium compounds were investigated for their suitability as colorants in pyrotechnic formulations. Several formulations with different oxidizers and fuels were prepared and examined regarding their burn down properties and performances like dominant wavelength, spectral purity, luminous intensity, and luminous efficiency. Their sensitivity towards impact and friction as well as their decomposition temperatures were determined.

---

* Prof. T. M. Klapötke
Fax: +49-89-2180-77492
E-Mail: tmk@cup.uni-muenchen.de
[a] Department of Chemistry
Energetic Materials Research
Ludwig-Maximilian University of Munich (LMU)
Butenandtstraße 5–13 (D)
81377 Munich, Germany

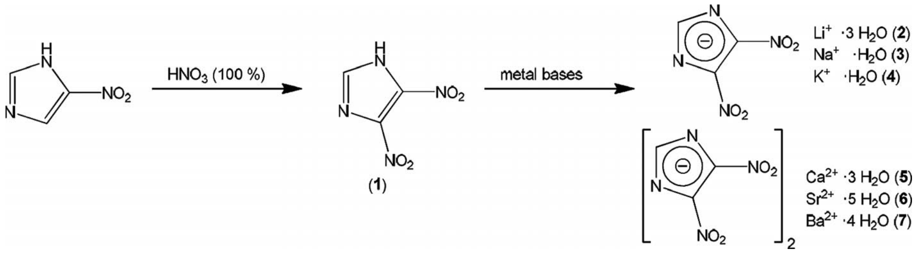

Scheme 1. Synthesis of compounds **1**–**7**.

Results and Discussion

Synthesis

The starting material 4,5-dinitroimidazole (**1**) was synthesized according to literature by nitration of commercially available 4-nitroimidazole.[6] Due to the good solubility of **1** in acetone, all syntheses of the metal salts were performed by reaction of 4,5-dinitroimidazole with metal bases in acetone at room temperature like described for the potassium salt in literature.[6] After stirring for 24 h the reaction mixtures were filtered off and the solvent was evaporated. Recrystallization from ethyl acetate led to the formation of crystals suitable for X-ray analysis. The lithium (**2**) and calcium (**5**) salts crystallize as trihydrates, the sodium (**3**) and potassium (**4**) salts as monohydrates, the strontium salt (**6**) as a pentahydrate, and the barium salt (**7**) as a tetrahydrate (Scheme 1). This was confirmed by single-crystal X-ray diffraction and elemental analysis.

Crystal Structures

Suitable single crystals of the described compounds **2**–**7** were picked from the crystallization mixture and mounted in Kel-F oil, transferred to the N_2 stream of an Oxford Xcalibur3 diffractometer with a Spellman generator (voltage 50 kV, current 40 mA) and a KappaCCD detector using a λ(Mo-K_α) radiation wavelength of 0.71073 Å. All structures were measured at –100 °C. The data collection and data reduction was carried out with the CRYSALISPRO software.[8] The structures were solved with SIR-92,[9] refined with SHELXL-97,[10] and finally checked using the PLATON software[11] integrated in the WINGX software suite.[12] The non-hydrogen atoms were refined anisotropically and the hydrogen atoms were located and freely refined. The absorptions were corrected by a SCALE3 ABSPACK multi-scan method.[13] Further data and parameters of the X-ray measurements and refinements are included in Table 1.

With respect to energetic interest, up to now, only the crystal structures of neutral 4,5-dinitroimidazole ($P2_1/c$, 1.781 g·cm^{-3}),[5] 1-methyl-4,5-dinitroimidazole ($Pna2_1$, 1.637 g·cm^{-3}),[15] and potassium 4,5-dinitroimidazolate (waterfree, $P6_1$, 1.987 g·cm^{-3})[16] have been published and described in the literature.

The structures shortly described in the following all contain the 4,5-dinitroimidazolate anion, whose structure is comparable to its neutral form.[5] The overall anion is not planar but its imidazole moiety is planar. The ring bond lengths are all observed slightly longer than in its neutral form and are exemplarily listed in the caption of Figure 1. In the vicinal configuration of the nitro groups, there is not sufficient space for both nitro groups substituted on adjacent carbon atoms to lie in the plane of the imidazole ring, and so, to compensate for this lack of space, the nitro groups would have to twist out of the plane or the twist axes (C–N), would have to bend out of the plane, or laterally away from each other. In our observed structure the nitro groups are twisted between 2° (**6**) and 39° (**5**) out of the plane. The "step aside" of the nitro groups can be best described by the facing O–C3–C4–O torsion angles (**2**: 11°, **3**: 29°, **4**: 28°, **5**: 21°/23°, **6**: 27°/17°, and **7**: 25°).

All of the crystalline compounds have crystal water included. In contrast to the alkaline earth metal salts the alkaline salts do not show the trend of increasing densities. The monohydrated potassium salt **4** has a lower density (1.852 g·cm^{-3}) in comparison to the monohydrated sodium salt **3** (1.918 g·cm^{-3}).

The structure **2**, in which the lithium cations are pentacoordinate is shown in Figure 1. The isolated complexes are connected by various hydrogen bonds involving the crystal water molecules.

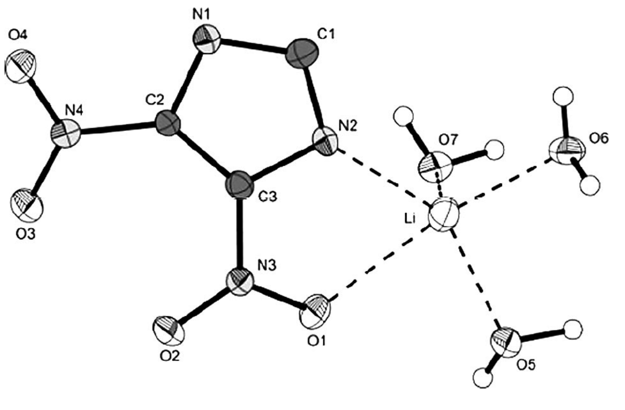

Figure 1. Molecular unit of lithium 4,5-dinitroimidazolate trihydrate (**2**). Thermal ellipsoids represent the 50 % probability level. Selected bond lengths /Å: O1–N3 1.235(2), O2–N3 1.226(2), O3–N4 1.224(2), O4–N4 1.230(2), N1–C1 1.350(3), N1–C2 1.350(3), N2–C3 1.353(3), N2–C1 1.359(3), N3–C3 1.433(3), N4–C2 1.431(3), C2–C3 1.391(3), N2–Li 2.166(4), O1–Li 2.270(4), O5–Li 2.005(4), Li–O6 2.051(4), Li–O7 2.011(4).

Compounds **3** and **4** crystallize similarly. In both structures the metal cations are arranged to strands connected by bridging

Table 1. XRD data and parameters.

	2 Li	**3** Na	**4** K	**5** Ca	**6** Sr	**7** Ba
Formula	$C_3H_6LiN_4O_7$	$C_3H_3N_4NaO_5$	$C_3H_3KN_4O_5$	$C_6H_8CaN_8O_{11}$	$C_6H_{12}N_8O_{13}Sr$	$C_6H_{10}BaN_8O_{12}$
FW /g·mol^{-1}	217.06	198.08	214.19	408.28	491.86	523.44
Crystal system	triclinic	orthorhombic	orthorhombic	monoclinic	monoclinic	monoclinic
Space group	$P\bar{1}$ (No. 2)	$Pca2_1$ (No. 29)	$Pca2_1$ (No. 29)	$P2_1/n$ (No. 14)	$P2_1/c$ (No. 14)	$C2/c$ (No. 15)
Color / habit	yellow needle	yellow platelet	yellow block	yellow block	yellow platelet	yellow needle
Size /mm	0.03 × 0.08 × 0.35	0.03 × 0.15 × 0.20	0.14 × 0.15 × 0.22	0.10 × 0.20 × 0.20	0.04 × 0.20 × 0.23	0.11 × 0.13 × 0.56
a /Å	7.0037(9)	12.8420(6)	13.2738(14)	6.4701(3)	17.720(4)	18.9556(15)
b /Å	7.2642(9)	3.6205(2)	3.8034(4)	14.2942(5)	6.534(5)	6.5074(3)
c /Å	10.3337(11)	14.7551(6)	15.2172(15)	15.8828(6)	15.031(6)	14.4955(12)
α /°	69.633(11)	90	90	90	90	90
β /°	84.14(1)	90	90	99.779(4)	106.672(5)	118.804(10)
γ /°	63.730(13)	90	90	90	90	90
V /Å^3	441.12(11)	686.03(6)	768.25(14)	1447.58(10)	1667.2(15)	1566.8(2)
Z	2	4	4	4	4	4
$\rho_{\text{calcd.}}$ /g·cm^{-3}	1.634	1.918	1.852	1.873	1.960	2.220
μ /mm^{-1}	0.157	0.229	0.691	0.519	3.324	2.622
F(000)	222	400	432	832	984	1016
λ(Mo-K_α) /Å	0.71073	0.71073	0.71073	0.71073	0.71073	0.71073
T /K	173	173	173	173	173	173
θ Min-max /°	4.2, 26.0	4.2, 26.0	5.1, 26.2	4.2, 26.5	4.2, 26.0	4.4, 26.0
Dataset	–8:7; –8:8; –12:12	–15:15; –4:4; –18:18	–13:16; –3:4; –10:18	–8:8; –17:17; –19:19	–21:21; –8:7; –11:18	–12:23; –7:8; –17:17
Reflections collected	3023	7300	1734	11879	6354	3022
Independent refl.	1723	705	803	2984	3247	1527
R_{int}	0.028	0.033	0.034	0.046	0.036	0.029
Observed reflections	1112	654	573	2292	2198	1334
Parameters	160	130	103	267	301	98
R_1 (obs)	0.0413	0.0214	0.0340	0.0326	0.0284	0.0258
wR_2 (all data)	0.1028	0.0546	0.0601	0.0826	0.0388	0.0482
S	0.94	1.06	0.89	0.95	0.79	0.96
Resd. dens. /e·Å^{-3}	–0.23, 0.69	–0.12, 0.16	–0.24, 0.25	–0.22, 0.69	–0.32, 0.42	–0.70, 0.64
Device type	Oxford Xcalibur3 CCD	Oxford Xcalibur3 CCD	Oxford Xcalibur3 CCD	Oxford Xcalibur3 CCD	Oxford Xcalibur3 CCD	Oxford Xcalibur3 CCD
Solution	SIR-92	SIR-92	SIR-92	SIR-92	SIR-92	SIR-92
Refinement	SHELXL-97	SHELXL-97	SHELXL-97	SHELXL-97	SHELXL-97	SHELXL-97
Absorption correction	multi-scan	multi-scan	multi-scan	multi-scan	multi-scan	multi-scan
CCDC [14]	864602	864599	864600	864604	864601	864603

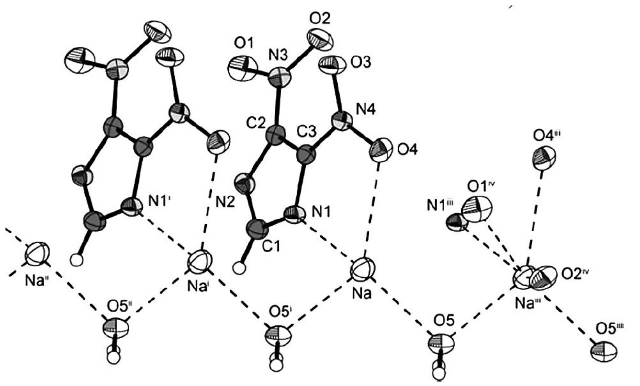

Figure 2. View on an extract of the structure of sodium 4,5-dinitroimidazolate monohydrate (**3**). Thermal ellipsoids represent the 50 % probability level. Symmetry codes: (i) *x*, –1+*y*, *z*; (ii) *x*, –3+*y*, *z*; (iii) *x*, 1+*y*, *z*; (iv) 1.5–*x*, 1+*y*, 0.5+*z*.

water molecules (Figure 2 and Figure 3). In contrast to the potassium cations, which are coordinated distorted octahedrally the potassium cations are trigonal coordinated (taking account into K–O and K–N distances smaller than 2.9 Å).

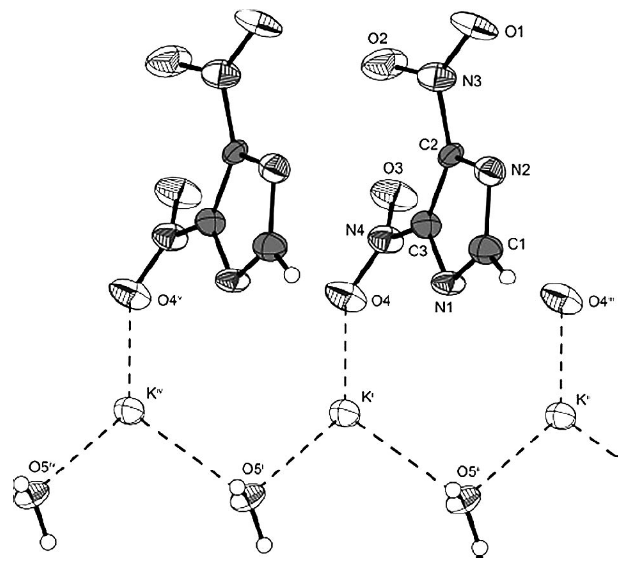

Figure 3. View on an extract of the structure of potassium 4,5-dinitroimidazolate monohydrate (**4**). Thermal ellipsoids represent the 50 % probability level. Symmetry codes: (i) 0.5–*x*, 1+*y*, –0.5+*z*; (ii) 0.5–*x*, *y*, –0.5+*z*; (iii) *x*, –1+*y*, *z*; (iv) 0.5–*x*, 2+*y*, –0.5+*z*; (v) *x*, 1+*y*, *z*.

The coordination sphere of the calcium atoms in **5** are depicted in Figure 4. The cations are surrounded by two chelating 4,5-DNI ligands, three oxygen atoms of included crystal water, and one oxygen atom of a close nitro group. Latter interaction leads to a complex three-dimensional structure.

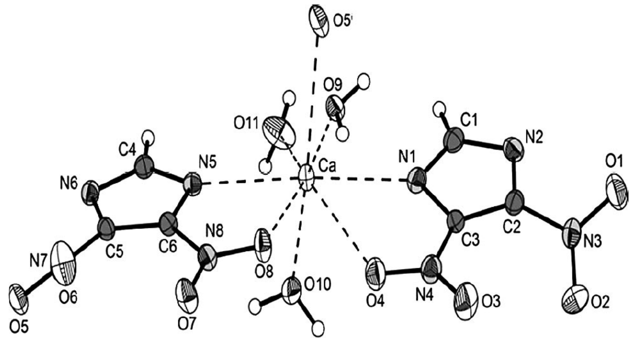

Figure 4. Molecular unit of calcium bis(4,5-dinitroimidazolate) trihydrate (**5**). Thermal ellipsoids represent the 50 % probability level. Selected coordination distances /Å: Ca–O4 2.6048(16), Ca–O5^{i} 2.7549(15), Ca–O8 2.5547(14), Ca–O9 2.4217(15), Ca–O10 2.3158(15), Ca–O11 2.3564(17), Ca–N1 2.5041(17), Ca–N5 2.5213(16). Symmetry code: (i) 0.5+*x*, 0.5–*y*, 0.5+*z*. 0.5+*z*; (iii) *x*, –1+*y*, *z*; (iv) 0.5–*x*, 2+*y*, –0.5+*z*; (v) *x*, 1+*y*, *z*.

The monoclinic ($P2_1/c$) strontium salt **6** forms isolated complexes, in which the strontium cations are eightfold coordinated (Figure 5). All five crystal water molecules are connected to the central strontium cations within distances of 2.54 and 2.61 Å.

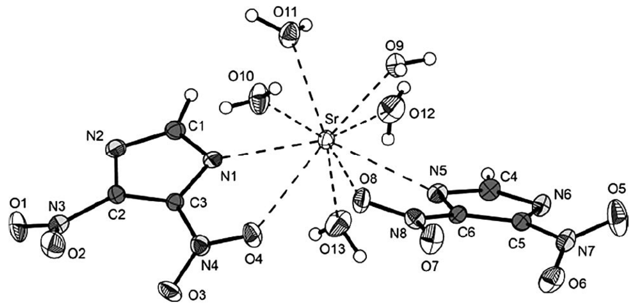

Figure 5. Molecular unit of strontium bis(4,5-dinitroimidazolate) pentahydrate (**6**). Thermal ellipsoids represent the 50 % probability level. Selected coordination distances /Å: Sr–N1 2.716(2), Sr–N5 2.707(2), Sr–O4 2.7695(18), Sr–O8 2.794(2), Sr–O9 2.606(2), Sr–O10 2.581(2), Sr–O11 2.579(2), Sr–O12 2.633(3), Sr–O13 2.541(3).

The asymmetric unit of **7** as well as the coordination sphere of the barium atoms is shown in Figure 6. This salt crystallizes in the monoclinic space group *C*2/*c* with four formula units in the unit cell. The density of 2.220 g·cm^{-3} is the highest observed in this work.

Thermal and Energetic Properties

The melting (T_m) and decomposition (T_dec) temperatures, as well as the temperatures of dehydration (T_dehydr) of **2**–**7** were measured by differential scanning calorimetry (DSC) and are listed in Table 2. About 1 mg of each substance was placed in covered aluminum container with a hole in the lid for gas release and a nitrogen flow of 20 mL per minute with a Linseis PT 10 DSC[17] calibrated by standard pure indium and zinc at a heating rate of 5 °C•min^{-1}.

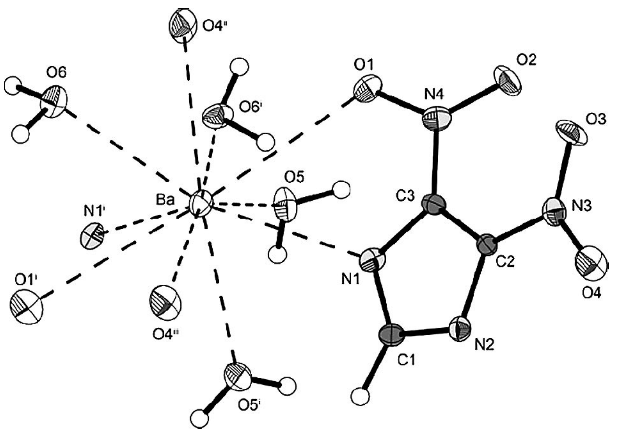

Figure 6. Depiction of the coordination sphere (< 3.2 Å) of the barium cations in the solid-state structure of barium bis(4,5-dinitroimidazolate) tetrahydrate **7**. Thermal ellipsoids represent the 50 % probability level. Selected coordination distances /Å: Ba–N1/Ba–N1^{i} 2.895(14), Ba–O1/ Ba–O1^{i} 3.095(8), Ba–O4^{ii}/Ba–O4^{iii} 3.015(13), Ba–O5/ Ba–O5^{i} 2.723(4), Ba–O6/Ba–O6^{i} 2.780(5). Symmetry codes: (i) –*x*, *y*, 0.5–*z*; (ii) –0.5+*x*, 0.5–*y*, –0.5+*z*; (iii) 0.5–*x*, 0.5–*y*, 1–*z*.

Table 2. Thermal properties of compounds **2**–**7**.

	2	3	4	5	6	7
T_dehydr /°C	128	110	80	132	91	85
T_m /°C	132	–	–	–	–	–
T_dec /°C	231	235	253	268	261	239

The DSC curves of all salts reveal endothermic peaks between 80 °C and 125 °C, which can be assigned to the loss of crystal water of the salts. Only the lithium salt shows a melting point of 132 °C. All compounds show high decomposition points, which are in the range from 231 °C to 268 °C.

The impact sensitivity (IS) tests were performed according to STANAG 4489[18] modified instruction[19] using a BAM (Bundesanstalt für Materialforschung) drophammer.[20] The friction sensitivity (FS) tests were carried out according to STANAG 4487[21] modified instruction[22] using the BAM friction tester. The classification of the tested compounds results from the "UN Recommendations on the Transport of Dangerous Goods".[23] All compounds were tested upon the sensitivity towards electrical discharge (ESD) using the Electric Spark Tester ESD 2010 EN.[24]

As shown in Table 3, all metal salts, except the sodium and calcium salt, are insensitive towards impact, whereas the sodium salt (25 J) and the calcium salt (3 J) can be considered as moderate sensitive and sensitive, respectively. The sensitivities towards electric discharge are in the range from 0.10 to 0.60 J implying low ESD sensitivities (Table 3).

Pyrotechnical Formulations

The investigation of energetic nitrogen-rich red and green colorants in pyrotechnical formulations is reported herein. The

Table 3. Energetic properties of compounds **2**–**7**.

	2	**3**	**4**	**5**	**6**	**7**
IS [a] /J	> 40	25	> 40	3	> 40	40
FS [b] /N	> 360	> 360	288	360	> 360	324
ESD [c] /J	0.25	0.60	0.60	0.10	0.20	0.17
Grain size /µm	100–500	500–1000	100–500	100–500	500–1000	500–1000

a) Impact sensitivity (BAM drophammer, method 1 of 6). b) Friction sensitivity (BAM friction tester, method 1 of 6). c) Electrostatic discharge sensitivity (OZM ESD tester).

use of nitrogen-rich compounds in pyrotechnics is beneficial due to gaseous nitrogen as the main decomposition product. This yields to a reduction of smoke during the combustion and therefore higher color brilliance is obtained. Several formulations containing the strontium (**6**) and barium (**7**) salts are investigated herein and compared to the US Army′s in-service red (M126A1) strontium and green (M125A1) barium control formulations.

All pyrotechnic formulations were prepared by grinding all substances (given in weight percent), except the binder, in a mortar. When using the VAAR binder – a solution of 25 % vinyl alcohol acetate resin – the binder was diluted in a few milliliter of ethyl acetate and then added to the other mixed components. Mixtures of 0.6 g each were formed by hand and dried under high vacuum for 3 h. In the case of Epon 828/Epicure 1340 binder system all grinded components were introduced to the binder and then hand-blended until a homogeneous bulk was obtained. After grinding the mixtures again in a mortar, pellets of 0.6 g each were pressed using a consolidation dead load of 2000 kg. The pellets were dried overnight at ambient temperature. The controlled burn down was filmed with a digital video camera recorder (SONY, DCR-HC37E). The performance of each composition has been evaluated with respect to color emission, smoke generation and the amount of solid residues. The color properties like dominant wavelength (DW), spectral purity (Sp) and luminous intensity (LI) were performed using a HR2000+ES spectrometer with an ILX11B linear silicon CCD-array detector and included software from Ocean Optics. The dominant wavelength and spectral purity were measured based on the 1931 CIE method using illuminant C as the white reference point. Luminous efficiencies (LE) were determined using pellets of 0.6 g each. Five samples were measured for each formulation and all given values are averaged based on the complete burning of the mixture. Potassium nitrate, ammonium nitrate, and ammonium dinitramide (ADN) are used as oxidizers, magnesium and 5-aminotetrazole (5-At) as fuels. The thermal and energetic properties of the formulations were determined according to the procedure described in the previous chapter.

Strontium-containing Formulations

Table 4 shows the content of the intensive red-burning strontium control formulation (US Army in-service M126A1).

Table 4. Content of strontium control formulation (US Army M126A1).

	$Sr(NO_3)_2$ /wt %	$KClO_4$ /wt %	Mg /wt %	PVC /wt %	VAAR /wt %
Sr-control	39.3	9.8	29.4	14.7	6.8

In Table 5 the content of formulation SrDNI_1 is given, using 11 % of strontium dinitroimidazolate pentahydrate (**6**) as coloring agent, 70 % KNO_3 as oxidizer, and 10 % Mg as fuel. Poly(vinyl chloride) (PVC, 5 %) was used as the chlorine source. As the binder 4 % of Epon 828/Epikure 3140 with a 80/20 ratio was used. The composition burned with a purple flame color and some smoke and residues were observed.

Table 5. Content of formulation SrDNI_1.

	6 /wt %	KNO_3 /wt %	Mg /wt %	PVC /wt %	VAAR /wt %
SrDNI_1	11	70	10	5	4

To avoid a purple flame color caused by KNO_3, ammonium nitrate, and ammonium dinitramide were used as oxidizers in the following investigated formulations. Table 6 shows a formulation with 60 % of ammonium nitrate as oxidizer, 6 % of the strontium salt **6**, 6 % of magnesium, 2 % of PVC, and 7 % of VAAR binder. The formulation burned with a red flame color and some smoke and residues could be observed.

Table 6. Content of formulation SrDNI_2.

	6 /wt %	NH_4NO_3 /wt %	Mg /wt %	PVC /wt %	VAAR /wt %
SrDNI_2	25	60	6	2	7

The next two compositions contain 25 % of the colorant **6**, 60 % of ADN, 8 % of magnesium and 5-aminotetrazole, respectively and 7 % of VAAR binder (Table 7 and Table 8).

Table 7. Content of formulation SrDNI_3.

	6 /wt %	ADN /wt %	Mg /wt %	VAAR /wt %
SrDNI_3	25	60	8	7

Table 8. Content of formulation SrDNI_4.

	6 /wt %	ADN /wt %	5-At /wt %	VAAR /wt %
SrDNI_4	25	60	8	7

Both formulations burned without generation of smoke with an intensive red flame color and no residues remained.

Measurements were performed to investigate the color properties of these three formulations containing compound **6** and compared to the strontium control. The spectral purities of formulations SrDNI_2 and SrDNI_4 with 80 % and 83 % are below that of the control composition. Only formulation SrDNI_3 shows like the control a spectral purity of 91 %. All three formulations exhibit longer burn times and low luminous intensities compared to the strontium control (Table 9). Among the three formulations SrDNI_3 containing ADN and magnesium reveals the highest luminous intensity of 135cd.

Table 9. Color properties of formulations containing compound **6**.

	Burn time /s	Dw /nm	Sp /%	LI /cd	LE /cd•s•g^{-1}
Sr-control	4	617	91	992	6613
SrDNI_2	7	607	80	23	268
SrDNI_3	6	606	91	135	1350
SrDNI_4	9	600	83	18	270

All compositions are neither sensitive towards impact nor friction. The ADN containing formulations show decompositions temperatures, which are lower than 200 °C. Only SrDNI_2, which contains NH_4NO_3, exhibits a decomposition temperature of 210 °C (Table 10).

Table 10. Energetic and thermal properties of formulations containing compound **6**.

	Impact /J	Friction /N	Grain size /µm	T_{dec} /°C
Sr-control	10	360	< 100	266
SrDNI_2	> 40	> 360	< 100	210
SrDNI_3	> 40	> 360	< 100	151
SrDNI_4	> 40	> 360	< 100	159

Barium-containing Formulations

Two formulations using the barium salt **7** as colorant were investigated and compared with the barium nitrate containing control formulation US Army′s M125A1 (Table 11). Formulation BaDNI_1 comprises of 15 % of 7, 60 % of ADN, 8 % of magnesium, 10 % of PVC, and 7 % of VAAR binder (Table 12). Formulation BaDNI_2 consists of 13 % of 7, 55 % of ADN, 15 % of magnesium, 10 % of PVC, and 7 % of VAAR binder (Table 12). Both compositions burned smokeless with a green flame color and no solid residues could be observed.

Table 11. Content of barium control formulation (US Army M125A1).

	$Ba(NO_3)_2$ /wt%	Mg /wt %	PVC /wt %	VAAR /wt %
Ba-control	46	33	16	5

Table 12. Content of formulations BaDNI_1 and BaDNI_2.

	7 /wt %	ADN /wt %	Mg /wt %	PVC /wt %	VAAR /wt %
BaDNI_1	15	60	8	10	7
BaDNI_2	13	55	15	10	7

With respect to the spectral purities both BaDNI_1 (80 %) and BaDNI_2 (78 %) exceed that of the barium control mixture (75 %). Compared to the barium control formulation both compositions show long burn times of seven and six seconds, respectively. Both compositions exhibit very low luminous intensities of 20cd for BaDNI_1 and 67cd for BaDNI_2, which contains higher magnesium content (Table 13). Both compositions are neither sensitive towards impact nor friction insensitive, but show rather low decomposition temperatures of 155 °C and 130 °C, respectively (Table 14).

Table 13. Color properties of formulations containing compound **7**.

	Burn time /s	Dw /nm	Sp /%	LI /cd	LE /cd•s•g^{-1}
Ba-control	3	558	75	390	1950
BaDNI_1	7	564	80	20	233
BaDNI_2	6	558	78	67	670

Table 14. Energetic and thermal properties of formulations containing compound **7**.

	Impact /J	Friction /N	Grain size /µm	T_{dec} /°C
Ba-control	10	360	< 100	266
BaDNI_1	> 40	> 360	< 100	155
BaDNI_2	> 40	> 360	< 100	130

Higher spectral purities could be obtained by using the barium compound **7** in formulations, however the luminous intensities are rather low and long burn times could be observed. In the case of the formulations containing the strontium compound **6** only the composition using ADN and magnesium shows the same high spectral purity like the strontium control. The other two formulations exhibit lower spectral purities. Among these three Sr-containing formulations the formulation comprising ADN and magnesium reveals the highest luminous intensity, which is however low compared to that of the strontium control composition. Both BaDNI formulations show a higher spectral purity, longer burn times, and rather low luminous intensities compared to the control composition. All SrDNI- and BaDNI formulations are impact and friction insensitive. All compositions containing ADN as oxidizer decompose below 200 °C. Only formulation SrDNI_2 using ammonium nitrate reveals a decomposition temperature of 210 °C.

Conclusions

Alkali and earth alkaline salts of 4,5-dinitroimidazole were synthesized and fully characterized. Crystal structures of all metal salts were determined. Energetic and thermal analysis of these compounds were performed and showed that only the sodium (**3**) and calcium dinitroimidazolate (**5**) salts are sensitive towards impact. Potassium (**4**) and barium dinitroimidazolate (**7**) salts are sensitive towards friction. All salts decompose upon 200 °C. Pyrotechnic formulations using the strontium (**6**) and barium (**7**) compounds as red and green colorants were investigated. Among the SrDNI-formulations only SrDNI_3 containing ADN and magnesium reveals a spectral purity as high as the control formulation, whereas compositions using NH_4NO_3 as oxidizer or 5-aminotetrazole as fuel showed lower spectral purities. The luminous intensities of all three formulations are rather low compared to the control as well as longer burn times. Concerning the BaDNI-formulations higher spectral purities than that of the Ba-control could be achieved. Like the SrDNI-formulations also the BaDNI-formulations show low luminous intensities and longer burn times. All compositions containing ADN decompose at temperatures lower than 200 °C, except SrDNI_2 using ammonium nitrate shows a decomposition temperature higher than 200 °C. All formulations are impact and friction insensitive.

Experimental Section

All reagents and solvents were used as received (Sigma-Aldrich, Fluka, Acros Organics) if not stated otherwise. Melting and decomposition points were measured with a Linseis PT10 DSC using heating rates of 5 °C·min^{-1}, which were checked with a Büchi Melting Point B-450 apparatus. ^{1}H, ^{13}C and ^{14}N NMR spectra were measured with a JEOL Eclipse 400, JEOL Eclipse 270, or JEOL EX400 instrument at an ambient temperature of 25 °C if not stated otherwise. All chemical shifts are quoted in ppm relative to TMS (^{1}H, ^{13}C) or nitromethane (^{14}N). Raman spectra were recorded with a Bruker FT-Raman-MultiRAM Spectrometer instrument equipped with a Klaastech DENICAFC LC-3/40 laser device. Infrared spectra were measured with a Perkin-Elmer Spectrum BX-FTIR spectrometer with a Smiths DuraSampl IR-ATR unit. Elemental analyses were performed with an Elementar Vario EL or an Elementar Vario EL micro cube. Mass spectra were measured on a JEOL MS station JMS 700 instrument. The impact and friction sensitivity was determined using a BAM drophammer and a BAM friction tester.[23] The sensitivities of the compounds are indicated according to the UN Recommendations on the Transport of Dangerous Goods (+):[23] impact: insensitive $>$ 40 J, less sensitive $>$ 35 J, sensitive $>$ 4 J, very sensitive $<$ 4 J; friction: insensitive $>$ 360 N, less sensitive = 360 N, sensitive $<$ 360 N and $>$ 80 N, very sensitive $<$ 80 N, extreme sensitive $<$ 10 N.

CAUTION! The compounds described in this work are potential explosives, which are sensitive to environmental stimuli such as impact, friction, heat, or electrostatic discharge. While we encountered no issues in the handling of these materials, appropriate precautions and proper protective measures (safety glasses, face shields, leather coat, Kevlar gloves, and ear protectors) should be taken when preparing and manipulating these materials.

The synthesis of 4,5-dinitroimidazole was performed according to literature.[6] All salts were synthesized by the same procedure. To a solution of 4,5-dinitroimidazole in acetone the corresponding metal carbonate (1.5 mol excess) was added. The reaction mixture was stirred at room temperature for 24 h and filtered off. After removing the solvent and recrystallization from ethyl acetate yellow solids as products were obtained.

Lithium 4,5-Dinitroimidazolate Trihydrate (2): As product a slightly yellow solid (75 %) was obtained. **^{1}H NMR** ([D$_6$]DMSO): δ = 3.41 (s, H_2O), 6.90 (s, 1 H, CH) ppm. **^{13}C NMR** ([D$_6$]DMSO): δ = 139.8 (2C, C–NO_2), 140.5 (1C, CH) ppm. **^{14}N NMR** ([D$_6$]DMSO): δ: –17 (2N, C–NO_2) ppm. $C_3HN_4O_4Li·3\ H_2O$ (218.07): calcd. C 16.52, H 3.24, N 25.69 %; found C 15.97, H 3.47, N 24.99 %. **MS** (FAB^{-}): *m/z* for $C_3HN_4O_4$: calculated 157.07, found 156.9. **MS** (FAB^{+}): *m/z* for Li^{+}: calculated 6.94, found 7.0. **IR** (ATR): $\tilde{\nu}$ = 3502 (s), 3454.5 (s), 3151 (m), 3142 (m), 2925 (m), 2644 (w), 2571 (w), 2423 (w), 1791 (w), 1765 (w), 1649 (m), 1538 (m), 1524 (m), 1498 (m), 1451 (m), 1412 (m), 1336 (s), 1303 (s), 1272 (m), 1250 (m), 1186 (m), 1169 (m), 1102 (m), 1050 (m), 990 (m), 956 (m), 902 (m), 884 (m), 864 (m), 820 (m), 789 (m), 752 (m), 736 (m), 654 (m), 637 (m) cm^{-1}. **RAMAN** (300 mW): $\tilde{\nu}$ = 3130 (w), 1540 (m), 1474 (s), 1459 (m), 1428 (w), 1385 (s), 1354 (m), 1334 (w), 1305 (s), 1248 (m), 1188 (m), 1171 (s), 1143 (w), 1068 (w), 984 (w), 955 (w), 860 (m), 830 (w), 757 (w), 622 (w), 520 (w) cm^{-1}. **IS** (grain size 100–500 µm): $>$ 40 J. **FS** (grain size 100–500 µm): $>$ 360 N. **ESD** (grain size 100–500 µm): 0.25 J. **DSC**: 231 °C (dec.).

Sodium 4,5-Dinitroimidazolate Monohydrate (3): Yellow crystals (60 %) were obtained as products. **^{1}H NMR** ([D$_6$]DMSO): δ = 3.36 (s, 2 H, H_2O), 6.93 (s, 1 H, CH) ppm. **^{13}C NMR** ([D$_6$]DMSO): δ = 139.4 (2C, C–NO_2), 140.3 (1C, CH) ppm. **^{14}N NMR** ([D$_6$]DMSO): δ: –16 (2N, C–NO_2) ppm. $C_3HN_4O_4Na·H_2O$ (198.07): calcd. C 18.19, H 1.53, N 28.29 %; found C 18.40, H 1.49, N 27.91 %. **MS** (FAB^{-}): *m/z* for $C_3HN_4O_4$: calculated 157.07, found 156.9. **MS** (FAB^{+}): *m/z* for Na^{+}: calculated 22.98, found 23.1. **IR** (ATR): $\tilde{\nu}$ = 3624 (m), 3589 (m), 3565 (m), 3420 (m), 3145 (m), 3009 (m), 2960 (m), 2923 (s), 2854 (m), 2637 (m), 2570 (m), 2419 (w), 2340 (w), 2192 (w), 1647 (m), 1624 (m), 1535 (m), 1494 (m), 1454 (s), 1376 (m), 1356 (s), 1329 (s), 1306 (s), 1257 (s), 1173 (m), 1154 (m), 1087 (s), 1015 (s), 990 (m), 953 (w), 935 (w), 862 (m), 805 (s), 754 (m), 652 (m), 615 (m) cm^{-1}. **RAMAN** (300 mW): $\tilde{\nu}$ = 3144 (w), 1528 (m), 1470 (s), 1377 (m), 1339 (w), 1306 (s), 1269 (m), 1184 (s), 1104 (w), 1068 (w), 954 (w), 865 (w), 756 (w), 668 (w), 641 (w), 619 (w), 521 (w) cm^{-1}. **IS** (grain size 500–1000 µm): 25 J. **FS** (grain size 500–1000 µm): $>$ 360 N. **ESD** (grain size 500–1000 µm): 0.60 J. **DSC**: 235 °C (dec.).

Potassium 4,5-Dinitroimidazolate Monohydrate (4): As product a yellow solid (78 %) was obtained. **^{1}H NMR** ([D$_6$]DMSO): δ = 3.40 (s, 2 H, H_2O), 6.88 (s, 1 H, CH) ppm. **^{13}C NMR** ([D$_6$]DMSO): δ = 139.4 (2C, C–NO_2), 140.0 (1C, CH) ppm. **^{14}N NMR** ([D$_6$]DMSO): δ: –17 (2N, C–NO_2) ppm. $C_3HN_4O_4K·H_2O$ (214.18): calcd. C 16.82, H 1.41, N 26.16 %; found C 17.16, H 1.43, N 25.78 %. **MS** (FAB^{-}): *m/z* for $C_3HN_4O_4^{-}$: calculated 157.07, found 156.9. **MS** (FAB^{+}): *m/z* for K^{+}: calculated 39.09, found 38.9. **IR** (ATR): $\tilde{\nu}$ = 3752 (w), 3618 (w), 3564 (m), 3379 (m), 3198 (m), 3124 (m), 2923 (m), 2853 (m), 2642 (w), 2426 (w), 2192 (w), 2027 (w), 1752 (w), 1654 (m), 1559 (w), 1493 (m), 1470 (m), 1447 (s), 1349 (m), 1300 (m), 1240 (m), 1174 (m), 1097 (m), 949 (w), 897 (w), 877 (w), 856 (m), 810 (m), 754 (m), 670 (m), 617 (w) cm^{-1}. **RAMAN** (300 mW): $\tilde{\nu}$ = 3111 (w), 1534 (w), 1513 (w), 1468 (s), 1427 (w), 1365 (m), 1348 (m), 1317 (w), 1298 (m), 1281 (w), 1258 (w), 1239 (s), 1183 (s), 948 (w), 857 (w), 758 (w), 624 (w), 518 (w), 421 (w), 244 (w) cm^{-1}. **IS** (grain size 100–500 µm): $>$ 40 J. **FS** (grain size 100–500 µm): 288 N. **ESD** (grain size 100–500 µm): 0.60 J. **DSC**: 253 °C (dec.).

Calcium Bis(4,5-dinitroimidazolate) Trihydrate (5): A yellow solid (50 %) was obtained as product. **^{1}H NMR** ([D$_6$]DMSO): δ = 3.31 (s, 2 H, H_2O), 6.83 (s, 1 H, CH) ppm. **^{13}C NMR** ([D$_6$]DMSO): δ = 139.9 (2C, C–NO_2), 140.6 (1C, CH) ppm. **^{14}N NMR** ([D$_6$]DMSO): δ: –17 (2N, C–NO_2) ppm. $C_6H_2N_8O_8Ca·3\ H_2O$ (408.25): calcd. C 17.65, H 1.98, N 27.45 %; found C 18.24, H 1.87, N 26.76 %. **MS** (FAB^{-}): *m/z* for $C_3HN_4O_4^{-}$: calculated 157.07, found 156.9. **IR** (ATR): $\tilde{\nu}$ = 3460 (s), 2467 (w), 2164 (w), 1772 (w), 1638 (m), 1563 (m), 1544 (m), 1414 (s), 1320 (s), 1262 (m), 1249 (s), 1184 (m), 1104 (m), 1045 (m), 964 (w), 867 (w), 816 (m), 742 (m), 662 (m), 648 (m) cm^{-1}. **RAMAN** (300 mW): $\tilde{\nu}$ = 3111 (w), 1530 (w), 1489 (s), 1457 (w), 1367 (m), 1353 (w), 1303 (m), 1249 (s), 1189 (m), 1178 (s), 1102 (w), 965 (w), 863 (w), 818 (w), 760 (w), 649 (w), 619 (w), 545 (w), 434 (w), 386 (w), 233 (w) cm^{-1}. **IS** (grain size 100–500 µm): 3 J. **FS** (grain size 100–500 µm): 360 N. **ESD** (grain size 100–500 µm): 0.10 J. **DSC**: 268 °C (dec.).

Strontium Bis(4,5-dinitroimidazolate) Pentahydrate (6): As product a slightly yellow crystals (68 %) were gained. **^{1}H**

NMR ([D$_6$]DMSO): δ = 3.40 (s, 2 H, H$_2$O), 6.95 (s, 1 H, CH) ppm. **^{13}C NMR** ([D$_6$]DMSO): δ = 139.9 (2C, C–NO$_2$), 140.6 (1C, CH) ppm. **^{14}N NMR** ([D$_6$]DMSO): δ: –16 (2N, C–NO$_2$) ppm. $C_6H_2N_8O_8Sr{\cdot}5H_2O$ (491.83): calcd. C 14.65, H 2.46, N 22.78 %; found C 14.40, H 2.39, N 22.19 %. **MS** (FAB$^-$): m/z for $C_3HN_4O_4$: calculated 157.07, found 156.9. **IR** (ATR): $\tilde{\nu}$ = 3585 (s), 3539 (s), 3398 (s), 3148 (m), 3061 (m), 2914 (m), 2651 (m), 2426 (m), 2191 (w), 1771 (w), 1623 (m), 1525 (m), 1498 (m), 1452 (s), 1354 (m), 1303 (m), 1248 (m), 1175 (m), 1100 (m), 954 (w), 886 (w), 858 (m), 812 (m), 752 (m), 671 (m), 657 (m) cm^{-1}. **RAMAN** (300 mW): $\tilde{\nu}$ = 3131 (w), 3112 (w), 1533 (w), 1524 (w), 1480 (m), 1471 (m), 1453 (w), 1380 (w), 1354 (w), 1307 (m), 1250 (m), 1175 (s), 956 (w), 860 (w), 756 (w), 657 (w), 620 (w), 526 (w), 432 (w), 240 (w) cm^{-1}. **IS** (grain size 500–1000 µm): > 40 J. **FS** (grain size 500–1000 µm): > 360 N. **ESD** (grain size 500–1000 µm): 0.20 J. **DSC**: 261 °C (dec.).

Barium Bis(4,5-dinitroimidazolate) Tetrahydrate (7): Yellow crystals (70 %) were obtained as product. **^{1}H NMR** ([D$_6$]DMSO): δ = 3.38 (s, 2 H, H$_2$O), 6.92 (s, 1 H, CH) ppm. **^{13}C NMR** ([D$_6$]DMSO): δ = 139.5 (2C, C–NO$_2$), 140.3 (1C, CH) ppm. **^{14}N NMR** ([D$_6$]DMSO): δ: –16 (2N, C–NO$_2$) ppm. $C_6H_2N_8O_8Ba{\cdot}4H_2O$ (523.52): calcd. C 13.77, H 1.92, N 21.40 %; found C 14.01, H 1.88, N 21.03 %. **MS** (FAB$^-$): m/z for $C_3HN_4O_4^-$: calculated 157.07, found 156.9. **IR** (ATR): $\tilde{\nu}$ = 3644 (m), 3572 (m), 3381 (m), 3146 (m), 3125 (m), 2923 (m), 2853 (m), 2650 (w), 2427 (w), 2358 (w), 1782 (w), 1654 (w), 1614 (w), 1556 (m), 1542 (m), 1528 (m), 1505 (m), 1469 (m), 1451 (s), 1382 (w), 1346 (s), 1302 (s), 1242 (s), 1178 (s), 1099 (m), 954 (w), 893 (w), 858 (w), 812 (m), 753 (w), 668 (m), 629 (w) cm^{-1}. **RAMAN** (300 mW): $\tilde{\nu}$ = 3127 (w), 1535 (w), 1510 (w), 1465 (s), 1375 (m), 1306 (s), 1271 (m), 1187 (s), 1102 (w), 955 (w), 860 (m), 755 (w), 531 (w), 422 (w) cm^{-1}. **IS** (grain size 500–1000 µm): 40 J. **FS** (grain size 500–1000 µm): 324 N. **ESD** (grain size 500–1000 µm): 0.17 J. **DSC**: 239 °C (dec.).

Further information regarding the crystal-structure determination have been deposited as cif files with the Cambridge Crystallographic Data Centre [14] as supplementary publications.

Acknowledgements

Financial support of this work by the Ludwig-Maximilian University of Munich (LMU), the U.S. Army Research Laboratory (ARL) under grant no. W911NF-09–2-0018, the Armament Research, Development and Engineering Center (ARDEC) under grant no. W911NF-12–1-0467, and the Office of Naval Research (ONR) under grant nos. ONR.N00014–10–1-0535 and ONR.N00014–12–1-0538 is gratefully acknowledged. The authors acknowledge collaborations with *Dr. Mila Krupka* (OZM Research, Czech Republic) in the development of new testing and evaluation methods for energetic materials and with *Dr. Muhamed Suceska* (Brodarski Institute, Croatia) in the development of new computational codes to predict the detonation and propulsion parameters of novel explosives. We are indebted to and thank *Drs. Betsy M. Rice* and *Brad Forch* (ARL, Aberdeen, Proving Ground, MD) for many inspired discussions. The authors want to thank *St. Huber* for measuring the sensitivities. The Cusanuswerk is greatfully acknowledged for the award of a PhD scholarship (*M. Rusan*).

References

[1] a) G. Steinhauser, T. M. Klapötke, *Angew. Chem. Int. Ed.* **2008**, *47*, 3330; b) J. J. Sabatini, A. V. Nagori, E. A. Latalladi, J. C. Poret, G. Chen, R. Damavarapu, T. M. Klapötke, *Propellants Explos. Pyrotech.* **2011**, *36*, 373; c) J. J. Sabatini, A. V. Nagori, G. Chen, P. Chu, R. Damavarapu, T. M. Klapötke, *Chem. Eur. J.* **2012**, *18*, 628; d) J. J. Sabatini, J. M. Raab, R. K. Hann Jr., C. T. Freeman, *Z. Anorg. Allg. Chem.* **2013**, *639*, 25.

[2] a) M. A. Hiskey, D. E. Chavez, D. L. Naud, S. F. Son, H. L. Berghout, C. A. Bolme, *27th Proc. Int. Pyrotech. Sem.*, Co, USA, July 16–21, **2000**, 3; b) R. P. Singh, R. D. Verma, D. T. Meshri, J. M. Shreeve, *Angew. Chem.* **2006**, *118*, 3682.

[3] a) G. Steinhauser, K. Tarantik, T. M. Klapötke, *J. Pyrotech.* **2008**, *27*, 3; b) T. M. Klapötke, J. Stierstorfer, K. R. Tarantik, *J. Pyrotech.* **2009**, *28*, 61.

[4] a) H. Gao, C. Ye, O. D. Gupta, J.-C. Xiao, M. A. Hiskey, B. Twamley, J. M. Shreeve, *Chem. Eur. J.* **2007**, *13*, 3853; b) G.-F. Zhang, M.-Y. Cai, P. Jing, C. He, P. Li, F.-Q. Zhao, J.-Z. Li, X.-Z. Fan, S. W. Ng, *J. Chem. Crystallogr.* **2010**, *40*, 278.

[5] A. J. Bracuti, *J. Chem. Crystallogr.* **1998**, *28*, 367.

[6] A. R. Katritzky, S. Singh, K. Kirichenko, M. Smiglak, J. D. Holbrey, W. M. Reichert, S. K. Spear, R. D. Rogers, *Chem. Eur. J.* **2006**, *12*, 4630.

[7] M. Smiglak, C. C. Hines, T. B. Wilson, S. Singh, A. S. Vincek, K. Kirichenko, A. R. Katritzky, R. D. Rogers, *Chem. Eur. J.* **2010**, *16*, 1572.

[8] *CRYSALISPRO*, Oxford Diffraction Ltd., Version 171.33.41, **2009**.

[9] *SIR-92*, 1993, A Program for Crystal Structure Solution, A. Altomare, G. Cascarano, C. Giacovazzo, A. Guagliardi, *J. Appl. Crystallogr.* **1993**, *26*, 343.

[10] G. M. Sheldrick *SHELXS-97*, Program for Crystal Structure Solution, Universität Göttingen, **1997**.

[11] *PLATON*, A Multipurpose Crystallographic Tool, Utrecht University, Utrecht, The Netherlands, A. L. Spek, **1998**.

[12] L. J. Farrugia, *J. Appl. Crystallogr.* **1999**, *32*, 837–838.

[13] Empirical absorption correction using spherical harmonics, implemented in SCALE3 ABSPACK scaling algorithm (*CRYSALISPRO*, Oxford Diffraction Ltd., Version 171.33.41, **2009**).

[14] Crystallographic data (excluding structure factors) for the structures in this paper have been deposited with the Cambridge Crystallographic Data Centre, CCDC, 12 Union Road, Cambridge CB21EZ, UK. Copies of the data can be obtained free of charge on quoting the depository numbers CCDC-864602, CCDC-864599, CCDC-864600, CCDC-864604, CCDC-864601, and CCDC-864603. (Fax: +44-1223-336-033; E-Mail: deposit@ccdc.cam.ac.uk, http://www.ccdc.cam.ac.uk).

[15] Y.-X. Li, X.-J. Wang, J.-L. Wang, *Acta Crystallogr. Sect. E* **2009**, *65*, o3073.

[16] A. Kowalski, *Z. Kristallogr.* **1993**, *208*, 244.

[17] http://www.linseis.com.

[18] NATO Standardization Agreement (STANAG) on Explosives, *Impact Sensitivity Tests*, no. 4489, 1st ed., Sept. 17, **1999**.

[19] WIWEB-Standardarbeitsanweisung 4–5.1.02, Ermittlung der Explosionsgefährlichkeit, hier der Schlagempfindlichkeit mit dem Fallhammer, Nov. 8, **2002**.

[20] http://www.bam.de.

[21] NATO Standardization Agreement (STANAG) on Explosives, *Friction Sensitivity Tests*, no. 4487, 1st ed., Aug. 22, **2002**.

[22] WIWEB-Standardarbeitsanweisung 4–5.1.03, Ermittlung der Explosionsgefährlichkeit oder der Reibeempfindlichkeit mit dem Reibeapparat, Nov. 8, **2002**.

[23] Impact: Insensitive > 40 J, less sensitive > 35 J, sensitive > 4 J, very sensitive < 4 J; friction: Insensitive > 360 N, less sensitive = 360 N, sensitive 360 N to 80 N, very sensitive < 80 N, extreme sensitive < 10 N; According to the UN Recommendations on the Transport of Dangerous Goods (+) indicates: not safe for transport.

[24] http://www.ozm.cz.

Received: February 21, 2014
Published Online: March 14, 2014

The synthesis and characterization of 4,5-dinitroimidazolate salts

Thomas M. Klapötke*, Thomas G. Müller* and Magdalena Rusan*

* Department of Chemistry, Energetic Material Research, Ludwig-Maximilian-University of Munich,
Butenandtstr. 5-13 (D), D-81377 Munich, Germany

tmk@cup.uni-muenchen.de

Abstract:

The syntheses of the alkali and earth alkali salts of 4,5-dinitroimidazole is reported as well as their characterization by NMR-spectroscopy, mass spectrometry and elemental analysis. The structures were determined by single crystal diffraction and the impact and friction sensitivities were measured. With the regard to their potential use as coloring agents in pyrotechnic compositions several mixtures have been investigated.

Keywords: Pyrotechnics; Nitration; Imidazoles, Crystal structure.

---

1 Introduction

Dinitroimidazole, which can exist as several different isomers with respect to the positions of the substituted nitro groups, is reported to be an energetic compound with an excellent thermal stability and highly insensitive behavior towards shock and friction [1, 2]. Nitration on the ring carbon atoms is preferable to substitution on the nitrogen atom because nitro groups are usually more stable than nitramino groups [1]. For these reasons alkali and earth alkali salts of 4,5-dinitroimidazolate are interesting compounds for the use in pyrotechnic compositions as coloring agents since high thermal stability and safe handling of pyrotechnic components is required.

2 Results and discussion

2.1 Synthesis

The starting material 4,5-dinitroimidazol was prepared according to literature [3] by nitration of commercially available 4-nitroimidazole. According to the literature reported synthesis of potassium 4,5-dinitroimidazolate [3] the alkali- and earth alkali salts of 4,5-dinitroimidazole were synthesized by deprotonation with the corresponding metal carbonates in acetone (Scheme 1). All compounds were recrystallized from ethylacetate and obtained in moderate yields and high purity.

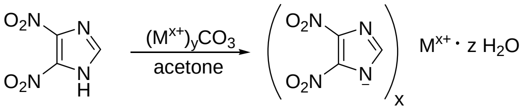

M = Li, x=1, y=1, z=3	4,5-LiDNI*3H_2O	**1**
M = Na, x=1, y=1, z=1	4,5-NaDNI*H2O	**2**
M = K, x=1, y=1, z=1	4,5-KDNI*H_2O	**3**
M = Ca, x=2, y=2, z=3	4,5-Ca$(DNI)_2$*3H_2O	**4**
M = Sr, x=2, y=2, z=5	4,5-Sr$(DNI)_2$*5H_2O	**5**
M = Ba, x=2, y=2, z=4	4,5-Ba$(DNI)_2$*4H_2O	**6**

Scheme 1. Syntheses of 4,5-dinitroimidazolate salts.

2.2 NMR-spectroscopy

The ^{1}H NMR resonance for the CH-group of all salts in DMSO-d^6 occurs at around 6.9 ppm. Since all salts crystallize as hydrates an addition signal at ~ 3.4 ppm corresponding to the water molecules is observable. In the ^{13}C-NMR spectra one signal at around 139.5 ppm corresponding to the nitro group containing carbon atoms and a further resonance at ~ 140.4 ppm corresponding to the CH-group occur.

2.3 Crystal structures

X-ray suitable crystals were obtained by slow crystallization from ethylacetate. Data sets for compounds **1** to **6** were collected on an Oxford Diffraction Xcalibur 3 diffractometer equipped with a CCD detector. All structures were solved by direct methods (SHELXS-97 and SIR97) [4] and refined by means of full-matrix least-squares procedures using SHELXL-97 [5]. Thermal ellipsoids in the figures represent the 50 % probability level. Crystallographic data are summarized in Table 1.

Table 1: Crystallographic data for compounds **1** to **6**.

	1	**2**	**3**	**4**	**5**	**6**
Formula	$C_3H_7N_4O_7Li$	$C_3H_3N_4O_5Na$	$C_3H_3N_4O_5K$	$C_6H_8N_8O_{11}Ca$	$C_6H_{12}N_8O_{13}Sr$	$C_6H_{10}N_8O_{12}Ba$
M/(g/mol)	218.07	198.07	214.18	408.25	491.83	523.52
T/K	173(2)	173(2)	173(2)	173(2)	173(2)	173(2)
λ/Å	0.71073	0.71073	0.71073	0.71073	0.71073	0.71073
Crystal system	triclinic	orthorhombic	orthorhombic	monoclinic	monoclinic	monoclinic
Space group	P-1 (2)	$Pca2_1$ (29)	$Pca2_1$ (29)	$P2_1/n$ (14)	$P2_1/c$ (14)	$C2/c$ (15)
a/Å	7.0037(9)	12.8420(6)	13.2738(14)	6.4701(3)	17.720(5)	18.9556(15)
b/Å	7.2642(9)	3.6205(2)	3.8034(4)	14.2942(5)	6.534(5)	6.5074(3)
c/Å	10.3337(11)	14.7551(6)	15.2172(15)	15.8828(6)	15.031(5)	14.4955(12)
α/°	69.63(1)	90	90	90	90	90
β/°	84.14(1)	90	90	99.779(4)	106.67(0)	118.80(1)
γ/°	63.73(1)	90	90	90	90.0)	90
V/Å³	441.12(358)	686.03(6)	768.25(14)	1447.58(10)	1667.17(290)	1566.81(19)
Z	2	4	4	4	4	4
ρ_{calc}/ (g cm^{-3})	1.64168	1.9177	1.99007	1.87315	1.81592	2.23583
μ/mm^{-1}	0.157	0.229	0.708	0.491	3.308	2.623
θ range/°	4.22-26.00	4.21-25.99	5.06-26.00	4.16-26.50	4.20-26.00	4.38-25.99
R_{int}	0.0276	0.0319	0.0291	0.0464	0.0357	0.0293
Parameters	164	130	130	267	301	131
Indep. Refl.	1723	1353	1087	2984	3256	1527
Observ. Refl.	1112	1224	772	2292	2206	1334
R_{all} (R_{obs})	0.0637 (0.0346)	0.0275 (0.0233)	0.0580 (0.0339)	0.0450 (0.0326)	0.0505 (0.0286)	0.0328 (0.0258)
wR_{all} (wR_{obs})	0.0719 (0.0671)	0.05554 (0.0544)	0.0642 (0.0599)	0.0825 (0.0796)	0.0442 (0.0425)	0.0486 (0.0478)
F(000)	224	400	464	712	904	1032
S	0.88	1.03	0.89	0.96	0.80	0.96

Lithium 4,5-dinitroimidazolate (**1**) crystallizes triclinic in the space group P-1 with two molecular moieties in the unit cell and a density of 1.641 g/cm^3. The asymmetric unit comprises of one lithium cation and one 4,5-dinitroimidazole anion as well as three water molecules. The molecular moiety is shown in Figure 1. The view of the unit cell along the a axis indicates an antiparallel layer alignment of the anions (see Figure 2).

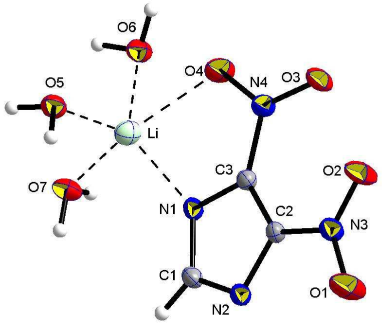

Figure 1: Molecular structure of 1 with the numbering scheme.

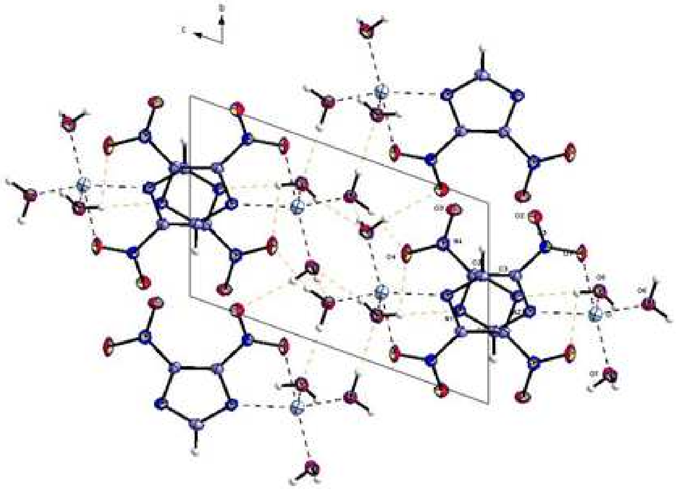

Figure 2: View of the unit cell of 1 along a-axis.

Diamond representations of the asymmetric unit for sodium 4,5-dinitroimidazolate (**2**) and potassium 4,5-dinitroimidazolate (**3**) are shown in Figure 3 and Figure 5. Compound **2** and **3** crystallize orthorhombic in the space group *Pca*2_1 with four molecular moieties in the unit cell and a density of 1.917 g/cm^3 and 1.990 g/cm^3, respectively. In both cases, the sodium and potassium cation, respectively, is coordinated by one 4,5-dinitroimidazolate anion and one water molecule. As it can be seen from the view of the unit cell along the b axis (Figure 4 and 6) the structure consists of chains of alternating 4,5-dinitroimidazolate units, which form hydrogen-bonds to the water molecules.

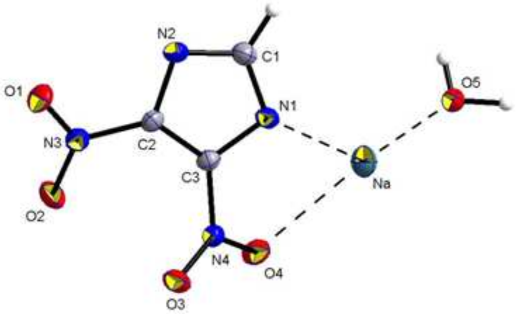

Figure 3: Molecular structure of 2 with the numbering scheme.

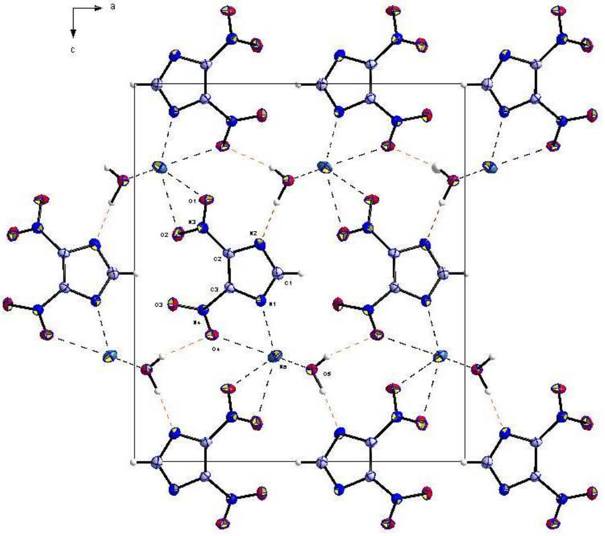

Figure 4: View of the unit cell of 2 along b-axis.

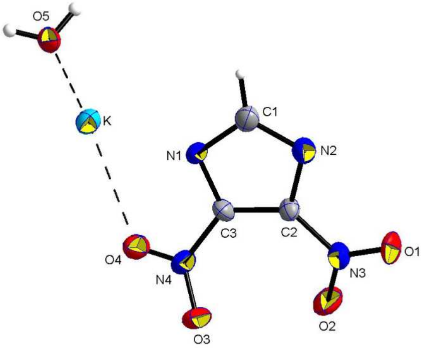

Figure 5: Molecular structure of 3 with the numbering scheme.

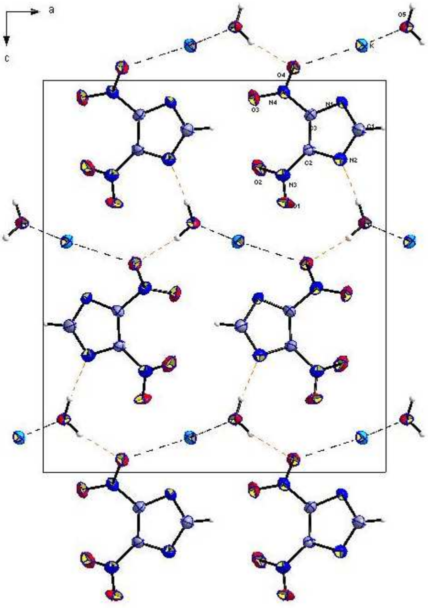

Figure 6: View of the unit cell of 3 along b-axis.

Calcium 4,5-dinitroimidazolate (**4**) crystallizes in the monoclinic crystal system $P2_1/n$ and a density of 1.873 g/cm^3 was calculated. Figure 7 shows the asymmetric unit of compound **4**. The calcium cation is coordinated by two 4,5-dinitroimidazolate anions and three water molecules. The unit cell contains four molecular moieties. The view of the unit cell along the a axis shows antiparallel chains of anions with calcium cations in between. (Figure 8).

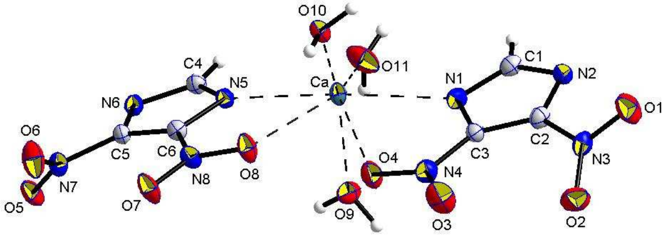

Figure 7: Molecular structure of 4 with the numbering scheme.

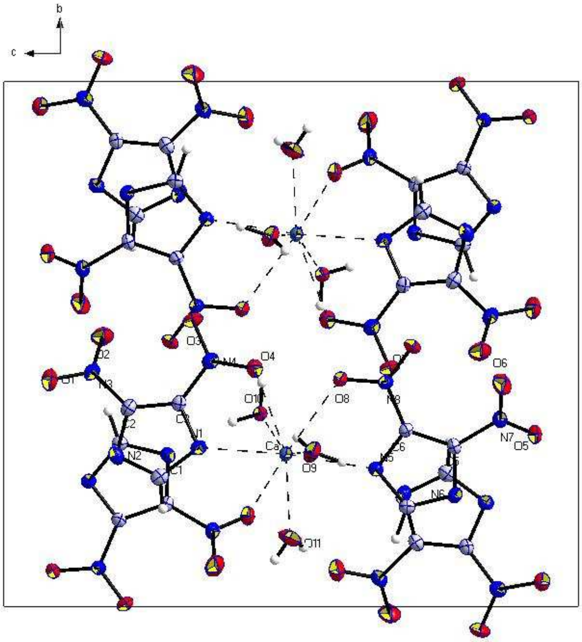

Figure 8: View of the unit cell of 4 along a-axis.

Crystals of strontium 4,5-dinitroimidazolate (**5**) are monoclinic with the space group $P2_1/c$. The unit cell contains four molecular moieties and the density is 1.816 g/cm^3. In Figure 9 the molecular structure is shown whereas strontium is coordinated by two 4,5-dinitroimidazolate anions and five water molecules. The unit cell with a view along the b axis indicates an anti-parallel chain-like arrangement of the anions with water molecules coordinated strontium cations between them (Figure 10).

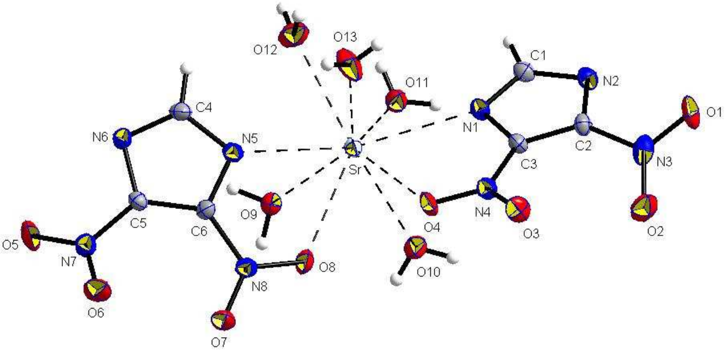

Figure 9: Molecular structure of 5 with the numbering scheme.

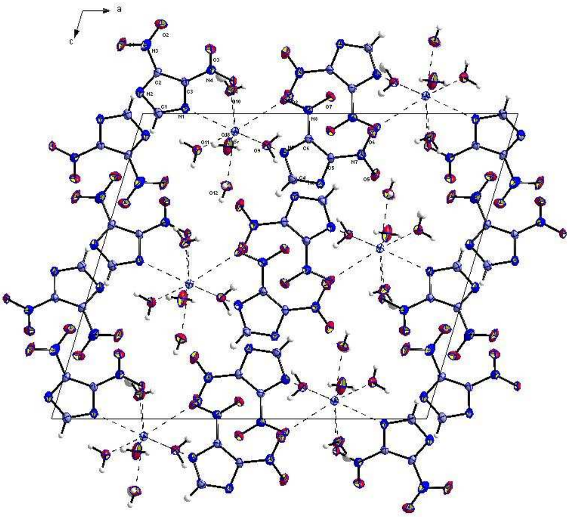

Figure 10: View of the unit cell of 5 along b-axis.

Barium 4,5-dinitroimidazolate (**6**) crystallizes monoclinic in the space group *C*2/*c* with a density of 2.236 g/cm^3 and contains four molecular moieties in the unit cell. Figure 11 shows the asymmetric unit of compound **6** with the labelling scheme, while in Figure 12 left (unit cell with view along a axis) the wavelike layer structure of the 4,5-dinitroimidazolate anions is represented. In Figure 12 right the antiparallel layers of the anions with four water molecules surrounded barium cations similar to the structure of compound **5** are illustrated.

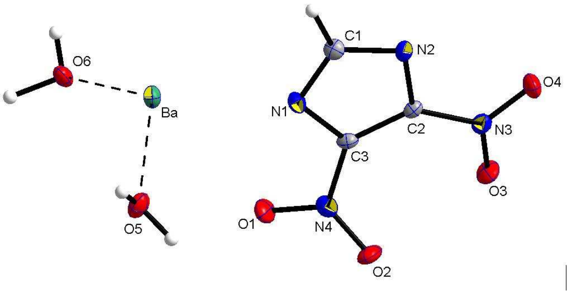

Figure 11: Molecular structure of 6 with the numbering scheme.

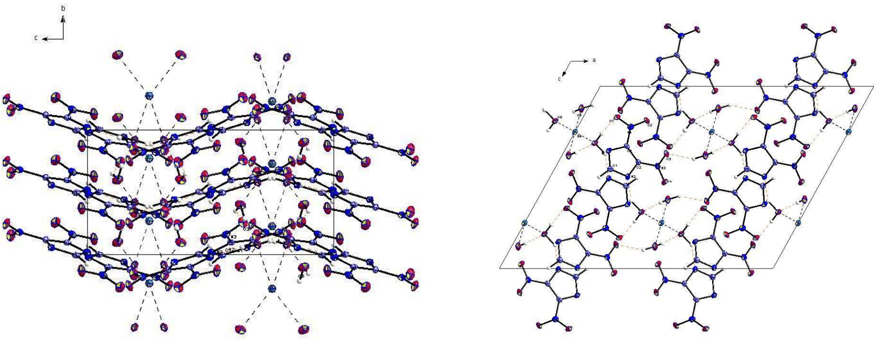

Figure 12: View of the unit cell of 6 along a-axis (left) and along b-axis (right).

Generally, all structures show a planar 4,5-dinitroimidazolate moiety and the cations are coordinated by one imidazole ring nitrogen and one oxygen atom of the nitro groups and water molecules. The ring C-N bonds are shorter than a C-N single bond length. The bonding lengths and angles of the 4,5-dinitroimidazolate anions are in accordance to those described in literature [1].

2.4 Thermal and energetic properties

The melting and decomposition points (onsets) were determined by DSC-measurements (Linseis PT10) with a heating rate of 5 °/min in a nitrogen flow. The sensitivity data were performed using BAM methods [6].
The following table indicates the results obtained from submitting the compounds to shock and friction stimuli as well as to electrostatic discharge (ESD). Furthermore, the melting (T_m) and decomposition (T_{dec}) temperatures are listed below (Table 2).

Table 2: Sensitivity and Thermal Data.

	1	**2**	**3**	**4**	**5**	**6**
Impact (J)	> 40	25	> 40	3	> 40	40
Friction (N)	> 360	360	288	360	288	324
ESD (J)	0.25	0.60	0.60	0.10	0.20	0.17
grain size (µm)	100-500	500-1000	100-500	100-500	500-1000	500-1000
T_m (°C)	128	111	80	63	91	165
T_{dec} (°C)	231	235	252	275	261	239

All salts, except the calcium salt, are insensitive and less sensitive, respectively. The decomposition temperatures are above 200 °C for all salts which makes them useful for pyrotechnic mixtures.

2.5 Pyrotechnic compositions

Compounds **1**, **5** and **6** were investigated in pyrotechnic mixtures. The pyrotechnic mixtures were prepared by mixing all substances, except the binder, in a mortar. Then the binder, a solution of 25 % vinyl alcohol acetate resin (VAAR), was added. The mixture was formed by hand and dried under high vacuum for three hours. The controlled burn down was filmed with a digital video camera recorder (SONY, DCR-HC37E). The performance of each composition has been evaluated with respect to color emission, smoke generation and the amount of solid residues.

2.5.1 Red color

LiDNI · 3 H_2O:

Two mixtures with LiDNI · 3 H_2O as coloring agent are reported here.
The composition **Li1** (28 % LiDNI · 3 H_2O; 41 % KNO_3; 14% Mg; 17 % VAAR) containing KNO_3 as oxidizer and Mg as fuel shows a deep red flame color and during the burn down less smoke was produced without residues (Figure 13 left).
The composition **Li2** (28 % LiDNI · 3 H_2O; 41 % NH_4NO_3; 14% Mg; 17 % VAAR) with NH_4NO_3 as oxidizer shows faster burning with a bright red flame color (Figure 13 right). Almost no smoke was produced and less residues remained.

Figure 13: Burn down of compostion **Li1** (left) and **Li2** (right).

Sr(DNI)$_2$ · 5 H_2O:

This compound was used as coloring agent in the mixtures **Sr1** and **Sr2**.
Composition **Sr1** (28 % Sr(DNI)$_2$ · 5 H_2O; 41 % KNO_3; 14% Mg; 17 % VAAR) shows a purple-red flame color and a moderate burn down, but no smoke and almost no residues (Figure 14 left). The fast and smokeless burn down of composition **Sr2** (28 % Sr(DNI)$_2$ · 5 H_2O; 41 % NH_4NO_3; 14% Mg; 17 % VAAR) shows a deep red flame color (Figure 14 right) but some residues remained.

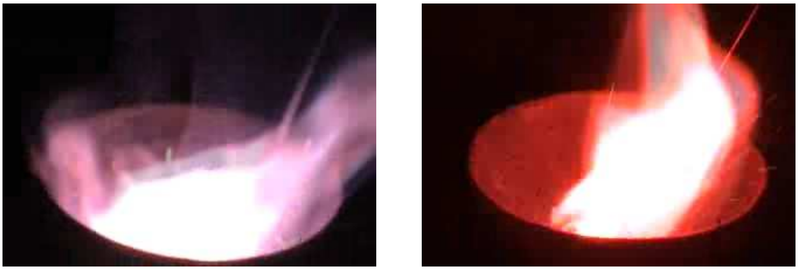

Figure 14: Burn down of composition **Sr1** (left) and **Sr2** (right).

2.5.2 Green Color

Ba(DNI)$_2$ · 4 H$_2$O:

In two compositions **Ba1** and **Ba2** barium 4,5-dinitroimidazolate tetrahydrate was combined with KNO_3 and NH_4NO_3 as oxidizers and boron (powder, amorphous-325 mesh) as fuel. Composition **Ba1** (28 % $Ba(DNI)_2 \cdot 4\ H_2O$; 41 % NH_4NO_3; 14% B; 17 % VAAR) burns fast and smokeless with a green flame color, whereas composition **Ba2** (28 % $Ba(DNI)_2 \cdot 4\ H_2O$; 41 % KNO_3; 14% B; 17 % VAAR) shows an extremly fast and also smokeless burn down with a white flame color. Some residues were observed for both compositions.

Figure 15: Burn down of composition **Ba1** (left) and **Ba2** (right).

3 Conclusions

Several new 4,5-dinitroimidazolate salts were synthesized and characterized. The sensitivities (friction, impact, ESD) were measured and reveal a less sensitivity of the salts. Due to their high decomposition temperatures the salts are useful compounds for pyrotechnic use. Compounds **1**, **5** and **6** were investigated in pyrotechnic mixtures and showed a mainly smokeless burn down with different color performances.

4 Experimental section

The synthesis of 4,5-dinitroimidazolate was performed according to literature [3]. All salts were synthesized by the same procedure. To a solution of 4,5-dinitroimidazole in acetone the corresponding metal carbonate (1.5 mol excess) was added. The reaction mixture was stirred at room temperature for two hours and then filtered off. After removing the solvent and recrystallization from ethylacetate yellow solids as products were obtained.

Lithium 4,5-dinitroimidazolate trihydrate (1)

yield: 55%

^{1}H-NMR (DMSO-d_6): 3.41 (s, 12H, H_2O), 6.90 (s, 1H, CH) ppm.

^{13}C-NMR (DMSO-d_6): 139.80 (2C, C-NO_2), 140.52 (1C, N-CH-N) ppm.

EA: $C_3HN_4O_4Li \cdot 3\ H_2O$ (218.07): calculated: C, 16.52; H, 3.24; N, 25.69; found: C, 15.87; H, 3.87; N, 24.99.

M/z (FAB$^+$): 7.9 (cation), (FAB$^-$): 156.9 (anion).

Sodium 4,5-dinitroimidazolate monohydrate (2)

yield: 50%

^{1}H-NMR (DMSO-*d*$_6$): 3.36 (s, 2H, H_2O), 6.93 (s, 1H, CH) ppm.

^{13}C-NMR (DMSO-*d*$_6$): 139.38 (2C, C-NO_2), 140.30 (1C, N-CH-N) ppm.

EA: $C_3HN_4O_4Na \cdot H_2O$ (198.07): calculated: C, 18.19; H, 1.53; N, 28.29; found: C, 18.40; H, 1.49; N, 27.91.

M/z (FAB$^+$): 23.1 (cation), (FAB$^-$): 156.9 (anion).

Potassium 4,5-dinitroimidazolate monohydrate (3)

yield: 65%

^{1}H-NMR (DMSO-*d*$_6$): 3.40 (s, 2H, H_2O), 6.88 (s, 1H, CH) ppm.

^{13}C-NMR (DMSO-*d*$_6$): 139.36 (2C, C-NO_2), 140.02 (1C, N-CH-N) ppm.

EA: $C_3HN_4O_4K \cdot 1\ H_2O$ (214.18): calculated: C, 16.82; H, 1.41; N, 26.16; found: C, 17.36; H, 1.43; N, 25.28.

M/z (FAB$^+$): 38.9 (cation), (FAB$^-$): 156.9 (anion).

Calcium 4,5-dinitroimidazolate trihydrate (4)

yield: 49%

^{1}H-NMR (DMSO-*d*$_6$): 3.31 (s, 2H, H_2O), 6.83 (s, 1H, CH) ppm.

^{13}C-NMR (DMSO-*d*$_6$): 139.91 (2C, C-NO_2), 140.56 (1C, N-CH-N) ppm.

EA: $C_6H_2N_8O_8Ca \cdot 3\ H_2O$ (408.25): calculated: C, 17.65; H, 1.98; N, 27.45; found: C, 18.24; H, 1.87; N, 26.76.

M/z (FAB$^-$): 156.9 (anion).

Strontium 4,5-dinitroimidazolate pentahydrate (5)

yield: 68%

^{1}H-NMR (DMSO-*d*$_6$): 3.40 (s, 2H, H_2O), 6.95 (s, 1H, CH) ppm.

^{13}C-NMR (DMSO-*d*$_6$): 139.95 (2C, C-NO_2), 140.60 (1C, N-CH-N) ppm.

EA: $C_6H_2N_8O_8Sr \cdot 5\ H_2O$ (491.83): calculated: C, 14.65; H, 2.46; N, 22.78; found: C, 14.40; H, 2.39; N, 22.19.

M/z (FAB$^-$): 156.9 (anion).

Barium 4,5-dinitroimidazolate tetrahydrate (6)

yield: 70%

^{1}H-NMR (DMSO-*d*$_6$): 3.38 (s, 2H, H_2O), 6.92 (s, 1H, CH) ppm.

^{13}C-NMR (DMSO-*d*$_6$): 139.48 (2C, C-NO_2), 140.33 (1C, N-CH-N) ppm.

EA: $C_6H_2N_8O_8Ba \cdot 4\ H_2O$ (523.52): calculated: C, 13.77; H, 1.92; N, 21.40; found: C, 14.01; H, 1.88; N, 21.03.

M/z (FAB$^-$): 156.9 (anion).

Acknowledgments

Financial support of this work by the Ludwig-Maximilian University of Munich (LMU), the U.S. Army Research Laboratory (ARL), the Armament Research, Development and Engineering Center (ARDEC), the Strategic Environmental Research and Development Program (SERDP) and the Office of Naval Research (ONR Global, title: “Synthesis and Characterization of New High Energy Dense Oxidizers (HEDO) - NICOP Effort ”) under contract nos. W911NF-09-2-0018 (ARL), W911NF-09-1-0120 (ARDEC), W011NF-09-1-0056 (ARDEC) and 10 WPSEED01-002 / WP-1765 (SERDP) is gratefully acknowledged. The authors acknowledge collaborations with Dr. Mila Krupka (OZM Research, Czech Republic) in the development of new testing and evaluation methods for energetic materials and with Dr. Muhamed Sucesca (Brodarski Institute, Croatia) in the development of new computational codes to predict the detonation and propulsion parameters of novel explosives. We are indebted to and thank Drs. Betsy M. Rice and Brad Forch (ARL, Aberdeen, Proving Ground, MD) and Mr. Gary Chen (ARDEC, Picatinny Arsenal, NJ) for many helpful and inspired discussions and support of our work.

References

[1] A. J. Bracuti, Crystal structure of 4,5-dinitroimidazole, *J. Chem. Crystallogr.*, 28(5), 367-371, **1998**.

[2] G.-F. Zhang, M.-Y. Cai, P. Jing, C. He, P. Li, F.-Q. Zhao, J.-Z. Li, X.-Z. Fan, S. W. Ng, Crystal Structure and Thermal Properties of Two Transition Metal Compounds $\{[Ni(DNI)_2(H_2O)_3][Ni(DNI)_2(H_2O)_4]\}\cdot 6H_2O$ and $Pb(DNI)_2(H_2O)_4$ (DNI = 2,4-Dinitroimidazolate), *J. Chem. Crystallogr.*, 40(3), 278-282, **2010**.

[3] A. R. Katritzky, S. Singh, K. Kirichenko, M. Smiglak, J. D. Holbrey, W. M. Reichert, S. K. Spear, R. D. Rogers, In Search of Ionic Liquids Incorporating Azolate Anions, *Chem. Eur. J.*, 12(17), 4630-4641, **2006**.

[4] A. Altomare, M. C. Burla, M. Camalli, G. L. Cascarano, C. Giacovazzo, A. Gagliardi, A. G. G. Moliterni, G. Polidori, R. Spagna, *J. Appl. Crystallogr.*, 32, 115-119, **1999**.

[5] G. M. Sheldrick, SHELXL-97, Programm for Crystal Structure Refinement, Universität Göttingen, **1997**.

[6] http://www.bam.de

DOI: 10.1002/zaac.201400233

Metal Salts of Dinitro-, Trinitropyrazole, and Trinitroimidazole

Ines E. Drukenmüller,[a] Thomas M. Klapötke,*[a] Yvonne Morgenstern,[a] Magdalena Rusan,[a] and Jörg Stierstorfer[a]

Keywords: Nitropyrazolate salts; Trinitroimidazole; Synthesis; Nitrogen-rich compounds; Green-burning pyrotechnic formulations; Red-burning pyrotechnic formulations

Abstract. The syntheses of alkali and earth alkaline dinitropyrazolate (DNP), trinitropyrazolate (TNP), and trinitroimidazolate (TNI) salts are reported. Additionally, copper trinitroimidazolate was synthesized. Their characterization by NMR spectroscopy, mass spectrometry, elemental analysis, and vibrational spectroscopy is reported as well. Crystal structures of compound $Ba(DNP)_2$ (**9**), which crystallizes with one molecule of methanol and ethyl ether as well as of compounds $Sr(TNP)_2 \cdot 3H_2O$ (**12**), $Ba(TNP)_2 \cdot 3H_2O$ (**13**), and $LiTNI \cdot 3H_2O$ (**14**) were determined. The energetic and thermal properties were measured as well. Green- and red-burning pyrotechnic formulations containing barium salts **9** and **13** as well as strontium salts **8** and **12** serving as colorants are tested. Additionally, formulations using $Sr(TNP)_2 \cdot 3H_2O$ (**12**) and $Ba(TNP)_2 \cdot 3H_2O$ (**13**) as the oxidizer and colorant at the same time were examined. The formulations were investigated with regard to their combustion behavior and performances such as burn time, dominant wavelength, spectral purity, luminous intensity, and luminous efficiency. The sensitivities towards ignition stimuli and the decomposition temperatures were determined as well.

Introduction

Energetic materials based on five-membered nitrogen-containing heterocycles such as tetrazole and triazole have been widely investigated.[1] The introduction of nitro groups enhances the oxygen balance and density of energetic compounds and therefore improves the detonation properties.[2] Various nitrogen-rich 3,4,5-trinitropyrazolate and 2,4,5-trinitroimidazolate salts are reported in literature.[2,3] 3,5-Dinitropyrazole as well as salts of 3,4,5-trinitropyrazole and 2,4,5-trinitroimidazole with nitrogen-rich cations are reported to be insensitive and reveal good oxygen balance, high thermal stability, and high positive molar enthalpies of formation.[2,3] Although metal 3,4,5-trinitropyrazolate salts are mentioned in patents,[4] their full characterization and energetic properties are not described. The synthesis of potassium 2,4,5-trinitroimidazolate is reported by *Duddu* et al.[5] Nitrogen-rich compounds based on 3,5-dinitropyrazole, 3,4,5-trinitropyrazole, and 2,4,5-trinitroimidazole are investigated as potential energetic materials and propellants, respectively,[2,3] but the corresponding metal salts could also be of interest for the use as colorants in pyrotechnical applications. The development of environmentally friendly pyrotechnics, which is of high relevance, requires a smokeless or smoke-reduced combustion as well as the formation of less toxic decomposition products. Nitrogen-rich compounds are considered to be suitable candidates since their main decomposition product is molecular nitrogen, which also means improved color brilliance. But also high performance and stability are important properties. For these reasons alkali and earth alkali salts of 3,5-dinitropyrazolate (3,5-DNP), 3,4,5-trinitropyrazole (TNP), and 2,4,5-trinitroimidazole (TNI) are interesting compounds as potential coloring agents since they may fit these requirements.

In this contribution the syntheses of alkali and earth alkaline dinitropyrazolate, trinitropyrazolate, and trinitroimidazolate salts are described. The characterization was performed using NMR and IR spectroscopy as well as elemental analysis and mass spectrometry. Crystal structures of barium bis(2,5-dinitropyrazolate) crystallizing with one molecule of methanol and ethyl ether, strontium bis(trinitropyrazolate) trihydrate, barium bis(trinitropyrazolate) trihydrate, and lithium trinitroimidazolate trihydrate were determined. Also copper bis(trinitroimidazolate) tetrahydrate was synthesized and characterized. Green- and red-burning formulations containing selected metal salts were prepared and investigated with respect to their color performance and thermal and energetic properties. Compounds $Sr(TNP)_2 \cdot 3H_2O$ (**12**) and $Ba(TNP)_2 \cdot 3H_2O$ (**13**) were tested in pyrotechnic formulations serving as the oxidizer and colorant at the same time.

Results and Discussion

Syntheses

The first starting material 3,5-dinitropyrazole (**1**) was synthesized according to literature procedures by stepwise nitration of commercially available pyrazole.[6,7] The second starting material 3,4,5-trinitropyrazole (**2**) was synthesized by

---

* Prof. Dr. T. M. Klapötke
Fax: +49-89-2180-77492
E-Mail: tmk@cup.uni-muenchen.de
[a] Department of Chemistry
Energetic Materials Research
Ludwig-Maximilian University
Butenandtstr. 5–13 (D)
81377 München, Germany

nitration of compound **1** with concentrated HNO_3/H_2SO_4 (Figure 1). The third starting compound 2,4,5-trinitroimidazole (**3**) was obtained by nitration of 4-nitroimidazole with concentrated HNO_3 and glacial acetic acid obtaining 2,4-dinitroimidazole as intermediate compound followed by a second nitration reaction with concentrated HNO_3/H_2SO_4 yielding compound **3** (Figure 2).

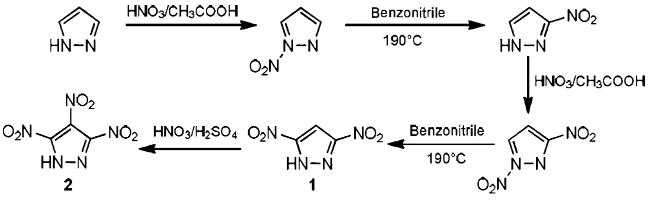

Figure 1. Synthesis of compounds **1** and **2**.

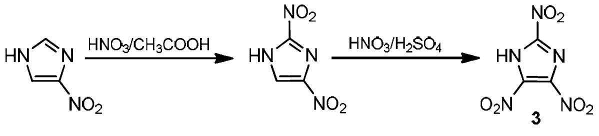

Figure 2. Synthesis of compound **3**.

The alkali and earth alkaline salts of 3,5-dinitropyrazole were obtained by the reaction of compound **1** with the corresponding metal hydroxides in water at room temperature (Figure 3). After removing the solvent products **4–9** were obtained as yellow solids. Estimation of the amount of crystal water is based on elemental analysis.

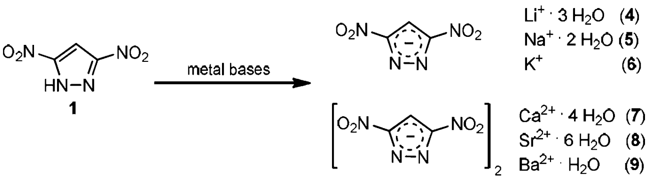

Figure 3. Synthesis of metal 3,5-dinitropyrazolate salts.

The synthesis of 3,4,5-trinitropyrazolate salts was reported in a patent but no analytical data was provided.[4] The alkali and earth alkaline salts of 3,4,5-trinitropyrazolate were synthesized by deprotonating compound **2** with the corresponding metal carbonates in ethanol at room temperature (Figure 4). Removing the solvent resulted in the formation of products **10–13** as slightly yellow solids.

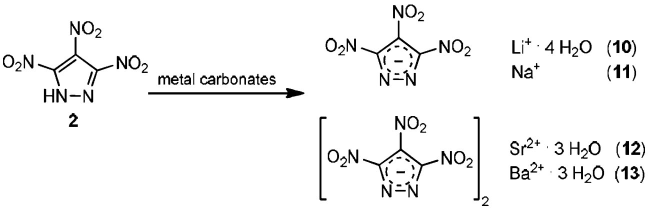

Figure 4. Synthesis of metal 3,4,5-trinitropyrazolate salts.

The synthesis of potassium 2,4,5-trinitroimidazolate was reported by *Duddu* et al.[5] The herein reported compounds **14–20** were obtained by the reacting of a solution of compound **3** in ethyl ether with the corresponding metal carbonates (Figure 5). After removing the solvent and recrystallization from ethyl acetate the products were gained.

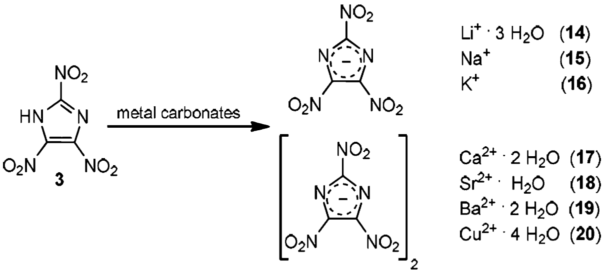

Figure 5. Synthesis of metal 2,4,5-trinitroimidazolate salts.

IR Spectroscopy

All product compounds were characterized by infrared spectroscopy. The assignment of absorptions is based on the values given in the literature.[8] The 3,5-dinitropyrazole salts exhibit symmetrical and asymmetrical nitro groups stretching vibrations between 1282–1284 cm^{-1} and 1608–1636 cm^{-1}. The C–NO_2 stretching vibrations are observable in the regions of 1333–1351 cm^{-1} and 1528–1555 cm^{-1}. The 3,4,5-trinitropyrazole salts show C–C valence vibration in the region between 1454 cm^{-1} and 1668 cm^{-1}. The ring vibrations appear in the range between 841 cm^{-1} and 850 cm^{-1}. The symmetrical and asymmetrical valence vibrations of the nitro groups are visible between 1318–1328 cm^{-1} and 1512–1540 cm^{-1}. The vibrations of the crystal water were detected at 3582 cm^{-1} and 3512 cm^{-1}. The ring vibrations of the 2,4,5-trinitroimidazolate salts are visible in the range between 650 cm^{-1} and 690 cm^{-1}. The symmetrical and asymmetrical vibrations of the nitro groups as well as the crystal water vibrations appear in at the same range like that of the 3,4,5-trinitropyrazole salts.

Crystal Structures

In order to round out characterization low temperature single-crystal X-ray diffraction was carried out and the results are described in the following. Selected data and parameter of the measurements and solutions are gathered in Table 1. Salts of 3,5-dinitropyrazole do not tend to form single crystals. Up to now only the gold complex DNP-Au-PPh_3[9] has been submitted to the CCDC database. Also barium dinitropyrazolate (**9**) could only be obtained single crystalline with inclusion of the two solvent molecules methanol and diethyl ether, which is shown in Figure 6. The compound crystallizes in the monoclinic space group $P2_1/c$ with (due to the solvent inclusion) a relatively low density of 1.86 $g \cdot cm^{-3}$ at 173 K in comparison to other barium salts. Both pyrazolate anions are arranged almost planar. The nitro groups are twisted only very little out

Table 1. Crystallographic data of **9**, **12**, **13**, and **14**.[12–18]

	9	**12**	**13**	**14**
Formula	$C_{11}H_{16}BaN_8O_{10}$	$C_6H_6N_{10}O_{15}Sr$	$C_6H_6BaN_{10}O_{15}$	$C_3H_6LiN_5O_9$
FW /g·mol^{-1}	557.65	545.83	595.54	263.07
Crystal system	monoclinic	orthorhombic	orthorhombic	triclinic
Space group	$P2_1/c$ (No. 14)	Fdd_2 (No. 43)	Fdd_2 (No. 43)	$P\bar{1}$ (No. 2)
Color / habit	colorless plate	colorless block	colorless block	colorless plate
Size /mm	0.09 × 0.18 × 0.34	0.14 × 0.15 × 0.20	0.08 × 0.13 × 0.22	0.08 × 0.15 × 0.32
a /Å	10.1288(3)	28.5318(8)	28.6910(8)	7.3642(9)
b /Å	9.4139(2)	28.4016(8)	28.8940(9)	8.2851(10)
c /Å	21.4156(8)	8.5108(2)	8.8301(2)	9.1092(12)
α /°	90	90	90	94.148(11)
β /°	103.197(3)	90	90	104.721(11)
γ /°	90	90	90	108.607(11)
V /Å^3	1988.08(11)	6896.7(3)	7320.1(3)	502.25(12)
Z	4	16	16	2
$\rho_{calcd.}$ /g·cm^{-3}	1.863	2.103	2.162	1.740
μ /mm^{-1}	2.066	3.238	2.275	0.172
F(000)	1096	4320	4608	268
λ Mo-K_α /Å	0.71073	0.71073	0.71073	0.71073
T /K	173	173	100	173
θ min-max /°	4.2, 26.0	4.4, 26.0	4.3, 27.0	4.3, 26.0
Dataset h; k; l	–12:12; –11:11; –26:26	–35:26; –34:32; –7:10	–36: 36; –36:36; –11:11	–8: 9; –10:10; –11:11
Reflect. coll.	19502	8806	19700	3859
Independ. refl.	3892	3059	3977	1963
R_{int}	0.048	0.028	0.029	0.025
Reflection obs.	3283	2898	3827	1640
No. parameters	283	313	313	187
R_1 (obs)	0.0254	0.0225	0.0165	0.0335
wR_2 (all data)	0.0580	0.0504	0.0384	0.0881
S	1.03	1.04	1.04	1.04
Resd. dens. /e·Å^{-3}	–0.41, 0.61	–0.35, 0.50	–0.25, 0.57	–0.24, 0.24
Device type	Oxford Xcalibur3 CCD	Oxford Xcalibur3 CCD	Oxford Xcalibur3 CCD	Oxford Xcalibur3 CCD
Solution	SIR-92	SIR-92	SHELXS-97	SIR-92
Refinement	SHELXL-97	SHELXL-97	SHELXL-97	SHELXL-97
Absorpt. corr.	multi-scan	multi-scan	multi-scan	multi-scan
CCDC	1002135	1002137	1002138	1002136

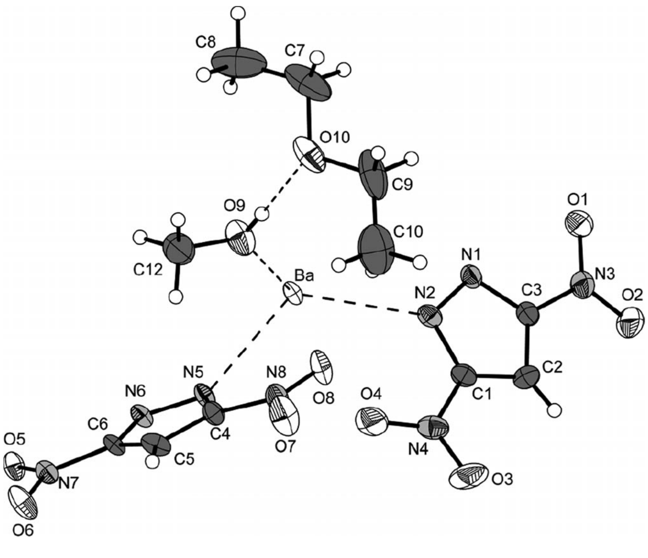

Figure 6. Representation of the molecular unit of **9**, showing the atom-labeling scheme. Thermal ellipsoids represent the 50 % probability level and hydrogen atoms are shown as small spheres of arbitrary radius. Selected anion bond lengths /Å: O1–N3 1.238(3), O2–N3 1.227(3), O3–N4 1.224(4), O4–N4 1.242(4), N1–C3 1.347(4), N1–N2 1.355(3), N2–C1 1.352(4), N3–C3 1.439(4), N4–C1 1.431(4), C1–C2 1.373(5), C2–C3 1.372(4); selected anion bond angles /°: O2–N3–O1 124.0(3), O2–N3–C3 117.3(3) O1–N3–C3 118.7(3); selected anion torsion angles /°: N1–C3–N3–O1 6.8(5), C2–C1–N4–O3 11.4(5).

of the ring plane. Including coordination up to a distance of 3 Å, the barium cations are surrounded by the atoms N5, N2, O4, O8, N1^{i}, O1^{i}, O6^{ii}, and O9 (symmetry codes: (i) –x, 0.5+y, 0.5–z, (ii) x, –1+y, z).

In contrast to dinitropyrazole, structures of 3,4,5-trinitropyrazole and derivatives have been described in the literature more often. Prominent examples are neutral 3,4,5-trinitropyrazole[10] and its ammonium salt.[11] It was possible to obtain single crystals of strontium as well as barium trinitropyrazolate both as their trihydrates. Interestingly, both salts crystallize isotypically (see Table 1) in the non-centrosymmetric orthorhombic space group Fdd_2 with 16 anion/cation pairs in the unit cell. The density of the barium salt is only slightly higher (2.162 g·cm^{-3} at 100 K) than that of the strontium salt (2.103 g·cm^{-3} at 173 K). The molecular moieties are depicted in Figure 7 and Figure 8. Also the coordination distances are in the same range. The structure of the trinitropyrazolate anion is comparable to that observed for the ammonium salt,[11] in which the inner nitro group significantly is twisted out of the planar ring plane due to steric reasons.

Lithium 2,4,5-trinitroimidazolate trihydrate (**14**) crystallizes in the triclinic space group $P\bar{1}$ with a density of 1.740 g·cm^{-3}. The structure of the anions is comparable to the structure published for dimethylammonium 2,4,5-trinitro-imidazolate.[3] The nitro group bonded to carbon atom C3 follows the planar ring structure. The adjacent nitro groups are slightly rotated

Table 2. Thermal properties of compounds **4**–**9**.

	4	**5**	**6**	**7**	**8**	**9**
FS /N	>360	>360	216	360	>360	72
IS /J	>40	>40	20	8	>40	30
ESD /J	0.7	0.5	0.1	0.5	0.2	0.1
Grain size /µm	<100	<100	100–500	100–500	100–500	500–1000
T_{dehydro} /°C	78	98	–	120	89	150
T_{m} /°C	145	295	–	–	–	–
T_{dec} /°C	325	324	306	>400	398	361

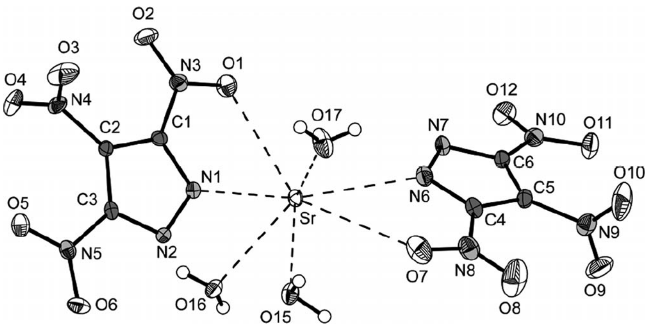

Figure 7. Molecular unit of **12**, showing the atom-labeling scheme. Thermal ellipsoids represent the 50 % probability level and hydrogen atoms are shown as small spheres of arbitrary radius. Selected strontium coordination distances /Å: O1–Sr 2.863(2), N–Sr 2.704(2), Sr–O17 2.531(2), Sr–O16 2.691(2), Sr–O15 2.816(2), Sr1–N6 2.840(2).

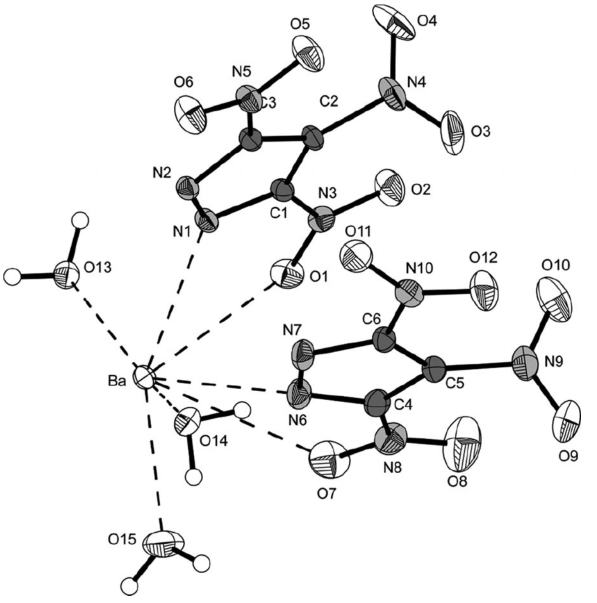

Figure 8. Representation of the molecular unit of **13**, showing the atom-labeling scheme. Thermal ellipsoids represent the 30 % probability level and hydrogen atoms are shown as small spheres of arbitrary radius. Selected barium coordination distances /Å: Ba–O15 2.700(2), Ba–O13 2.874(2), Ba–N1 2.898(2), Ba–N6 2.913(2), Ba–O14 2.943(2), Ba–O1 3.052(2).

out of the ring system [torsion angles: N1–C1–N3–O1 28.2(2)° and C1–C2–N4–O3 14.1(3)°]. A O2–N3–N4–O3 bent angle of 43.9(1)° is observed due to steric repulsion. The anions do not coordinate to the lithium cations, which are coordinated tetrahedrally by four water molecules. A dimeric dicationic motive is formed by two bridging water molecules, which is shown in Figure 9.

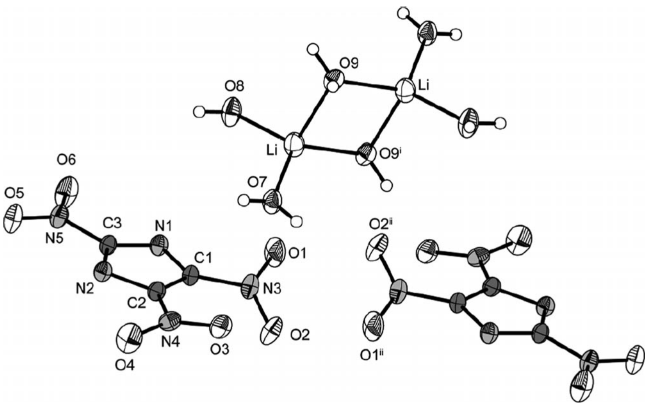

Figure 9. Illustration of the dimeric lithium coordination and two trinitroimidazolate anions in the crystal structure of LiTNI (**14**). Thermal ellipsoids represent the 50 % probability level and hydrogen atoms are shown as small spheres of arbitrary radius. Lithium-oxygen distances /Å: : Li–O7 1.916(3), Li–O8 1.910(3), Li–O9 2.064(3), Li–O9^{i} 1.999(3); symmetry codes (i) 1–*x*, 1–*y*, 1–*z*; (ii) 1–*x*, –*y*, 1–*z*.

Thermal and Energetic Properties

Table 2, Table 3, and Table 4 show the dehydration (T_{dehydro}), melting (T_{m}) and decomposition (T_{dec}) temperatures of compounds **4**–**9** (dinitropyrazolate salts), compounds **10**–**13** (trinitropyrazolate salts), and compounds **14**–**20** (trinitroimidazolate salts) measured by differential scanning calorimetry (DSC). The friction (FS) and impact (IS) sensitivities as well as the sensitivity towards electrostatic discharge (ESD) were determined and are summarized in Table 2, Table 3, and Table 4.

Table 3. Thermal properties of compounds **10**–**13**.

	10	**11**	**12**	**13**
FS /N	96	80	80	144
IS /J	40	25	40	5
ESD /J	0.2	0.2	0.2	0.1
Grain size /µm	100–500	100–500	100–500	100–500
T_{dehydro} /°C	104	–	121	115
T_{m} /°C	–	–	–	158
T_{dec} /°C	274	254	193	302

Table 4. Thermal properties of compounds **14**–**20**.

	14	**15**	**16**	**17**	**18**	**19**	**20**
FS /N	>360	>360	120	>360	>360	>360	80
IS /J	>40	>40	25	>40	>40	>40	3
ESD /J	0.5	0.6	0.2	0.7	0.7	0.6	0.1
Grain size /µm	<100	<100	100–500	100–500	<100	100–500	100–500
$T_{dehydro}$ /°C	79	–	–	110	104	98	107
T_m /°C	152	–	–	–	–	123	–
T_{dec} /°C	252	249	231	188	239	166	170

The 3,5-dinitropyrazolate salts (**4**–**9**) are predominantly friction insensitive. Only the potassium (**6**) and barium (**9**) salts are friction sensitive. The impact sensitivities vary from insensitive to very sensitive (compound **7**). All salts **4**–**9** show high decomposition temperatures and the DSC curves reveal endothermic peaks between 78 °C and 150 °C, which can be assigned to the loss of crystal water (Table 2).

3,4,5-Trinitropyrazolate salts are friction and impact sensitive. The DSC curves reveal peaks between 104 °C and 121 °C corresponding to the crystal water loss (Table 3). As can been seen in Table 4 the 2,4,5-trinitroimidazolate salts are impact and friction insensitive. Only the potassium (**16**) and copper (**20**) salts are impact and friction sensitive.

The DSC curves of compounds **14** and **17**–**20** show endothermic peaks between 79 °C and 110 °C, which can be assigned to the loss of crystal water. All salts show high decomposition temperatures ranging from 166 °C to 252 °C (Table 4).

Pyrotechnical Formulations

The investigation of perchlorate-free formulations is performed. The barium compounds **9** and **13** and the strontium compounds **8** and **12** were tested as nitrogen-rich colorants in pyrotechnic formulations. Several formulations containing besides the metal salts ammonium nitrate and ammonium dinitramide (ADN) as oxidizer were prepared and compared to the US Army′s in-service green (M125A1) and red (M126A1) formulations. Formulations without additional NH_4NO_3 or ADN but containing compounds **12** and **13**, which served as the oxidizer and colorant, were prepared and investigated. Magnesium was used as fuel. The pyrotechnical compositions were prepared by mixing all substances, except the binder, in a mortar. Then the binder, a solution of 25 % vinyl alcohol acetate resin (VAAR), was added. After drying in high vacuum for 3 h the mixtures were grinded again. Pellets of 0.6 g each were pressed using a consolidation dead load of 2000 kg. The pellets were dried overnight at ambient temperature. The performance of each composition has been evaluated with respect to color emission, smoke generation, and the amount of solid residues. The dominant wavelength and spectral purity was measured based on the 1931 CIE method using illuminant C as the white reference point. Five samples were measured for each formulation and all given values are averaged based on the full burn of the mixture.

Red-Burning Formulations

The strontium control M126A1 was mixed in a small-scale (0.6 g) and the color properties as well as thermal and energetic properties were measured and are summarized in Table 5, Table 6, and Table 7.

Table 5. US Army′s composition M126A1 /wt-%.

	$Sr(NO_3)_2$	$KClO_4$	Mg	PVC	VAAR
Sr-control	39.9	9.8	29.4	14.7	6.8

Table 6. US Army′s composition M126A1.

	Burn time /s	Dw /nm	Sp /%	LI /cd	LE /cdsg^{-1}
Sr-control	4	617	91	992	6613

Table 7. US Army′s composition M126A1.

	Impact /J	Friction /N	Grain size /µm	T_{dec} /°C
Sr-control	10	360	<100	266

In Table 8 the content of formulation SrDNP_1 containing compound **8**, ammonium nitrate, magnesium, and poly(vinyl chloride) serving as colorant, the oxidizer, fuel and chlorine donor is summarized. The content of formulations SrDNP_2 and SrDNP_3 consisting of compound **8**, ammonium dinitramide, and magnesium is shown in Table 9. Formulation SrDNP_3 contains additionally PVC.

Table 8. Formulation /wt-% SrDNP_1.

	8	NH_4NO_3	Mg	PVC	VAAR
SrDNP_1	13	67	13	3	4

Table 9. Formulations /wt-% SrDNP_2 and SrDNP_3.

	8	ADN	Mg	PVC	VAAR
SrDNP_2	15	72	8	–	5
SrDNP_3	10	62	13	10	5

All three formulations burned smokeless with a red flame color. In Table 11 the burn time and the color performance values are summarized. While formulations SrDNP_2 and SrDNP_3 show comparable spectral purities to the strontium control, formulation SrDNP_1 exhibits a lower spectral purity (Table 6 and Table 11). The luminous intensities of all three formulations are lower than that of the strontium control formulation (Table 6 and Table 11). In Table 12 the impact and friction sensitivities as well as the decomposition temperatures are shown. Formulation SrDNP_1 containing NH_4NO_3 instead ADN is neither friction nor impact sensitive and reveals a higher decomposition temperature than formulations SrDNP_2 and SrDNP_3, which are also friction and impact sensitive.

Two formulations containing compound **12** as the oxidizer and colorant were tested. Both formulations do not contain any additional oxidizer. Magnesium was used as fuel and only composition SrTNP_1 contains PVC. The content of these formulations is summarized in Table 10.

Table 10. Formulations /wt-% SrTNP_1 and SrTNP_2.

	12	Mg	PVC	VAAR
SrTNP_1	68	20	5	7
SrTNP_2	68	25	–	7

Both formulations revealed a smokeless burn down. An intensive-red flame color and no remaining residues could be observed. Compared to the Sr-control formulation both compositions showed long burn times of 8.5 s and 9 s. The spectral purity of SrTNP_1 is 89 % and hence lower than that of the Sr-control, whereas SrTNP_2 shows a spectral purity of 94 % exceeding that of the control. The luminous intensities are 370 cd (SrTNP_1) and 390 cd (SrTNP_2), respectively. Additionally, it is worth to mention that formulation SrTNP_2 does not contain PVC, but shows better color properties than SrTNP_1 containing PVC (Table 11). Both formulations show high decomposition temperatures and are relatively less impact and friction sensitive (Table 12).

Table 11. Color properties of Sr-formulations.

	Burn time /s	Dw /nm	Sp /wt-%	LI /cd	LE /cdsg^{-1}
SrDNP_1	4	605	68	90	600
SrDNP_2	5	610	90	192	1600
SrDNP_3	5	610	90	150	1250
SrTNP_1	8	608	89	390	5200
SrTNP_2	5	603	94	390	3250

Table 12. Energetic and thermal properties of Sr-formulations.

	Impact /J	Friction /N	Grain size /µm	T_{dec} /°C
SrDNP_1	>40	>360	< 100	214
SrDNP_2	30	168	< 100	159
SrDNP_3	30	144	< 100	161
SrTNP_1	40	120	< 100	201
SrTNP_2	40	180	< 100	196

Green-Burning Formulations

The barium control M125A1 was mixed in a small-scale (0.6 g) and the color properties as well as thermal and energetic properties were measured and are summarized in Table 13, Table 14, and Table 15.

Table 13. US Army′s composition M125A1 /wt-%.

	$Ba(NO_3)_2$	Mg	PVC	VAAR
Ba-control	46	33	16	5

Table 14. US Army′s composition M125A1.

	Burn time /s	Dw /nm	Sp /%	LI /cd	LE /cdsg^{-1}
Ba-control	3	558	75	390	1950

Table 15. US Army′s composition M125A1.

	Impact /J	Friction /N	Grain size /µm	T_{dec} /°C
Ba-control	15	360	<100	258

Two formulations containing compound **9** as colorant and ammonium nitrate (Table 16) and ammonium dinitramide (Table 17) as the oxidizer are shown. Both formulations contain additionally magnesium as fuel and PVC as the chlorine-source. Both formulations burned smokeless with a green flame color. The color properties are summarized in Table 19. The spectral purities are in the same range like the barium control formulation; however, lower luminous intensities were observed (Table 14 and Table 19). Whereas formulation BaDNP_1 is rather less impact and friction sensitive, formulation BaDNP_2 shows a high impact sensitivity of 5 J (Table 20).

Table 16. Formulation /wt-% BaDNP_1.

	9	NH_4NO_3	Mg	PVC	VAAR
BaDNP_1	13	70	8	5	4

Table 17. Formulation /wt-% BaDNP_2.

	9	ADN	Mg	PVC	VAAR
BaDNP_2	15	62	8	10	5

Three formulations using compound **13** as colorant were investigated. Two formulations (BaTNP_1 and BaTNP_2) contain compound **13**, ammonium nitrate, magnesium, and PVC. Formulations BaTNP_3 and BaTNP_4 do not contain any additional oxidizer (Table 18). Formulations BaTNP_1, BaTNP_3, and BaTNP_4 burned smokeless with an intensive green flame color. Formulation BaTNP_2 burned with a pale-green flame color. As can be seen in Table 19 formulations BaTNP_1 and BaTNP_2 show lower spectral purities compared to the barium control formulation, whereas the spectral purities of formulations BaTNP_3 and BaTNP_4 exceed that of the control formulation. Formulation BaTNP_3 exhibits the

Table 18. Formulations /wt-% containing compound **13**.

	13	NH_4NO_3	Mg	PVC	VAAR
BaTNP_1	35	40	13	5	7
BaTNP_2	38	40	15	–	7
BaTNP_3	53	–	30	10	7
BaTNP_4	58	–	20	15	7

highest luminous intensity among the investigated formulations, which is also in the range of the barium control formulation (Table 14 and Table 19). The BaTNP formulations reveal rather less impact and friction sensitivities and show high decomposition temperatures (Table 20).

Table 19. Color properties of Ba-formulations.

	Burn time /s	Dw /nm	Sp /wt%	LI /cd	LE /cdsg^{-1}
BaDNP_1	4	560	75	159	1060
BaDNP_2	3	559	79	189	945
BaTNP_1	3	552	66	169	845
BaTNP_2	3	497	46	109	545
BaTNP_3	6	558	80	359	3590
BaTNP_4	5	559	79	278	2317

Table 20. Energetic and thermal properties of Ba-formulations.

	Impact /J	Friction /N	Grain size /µm	T_{dec} /°C
BaDNP_1	30	360	< 100	194
BaDNP_2	5	168	< 100	170
BaTNP_1	40	192	< 100	165
BaTNP_2	30	324	< 100	186
BaTNP_3	40	>360	< 100	210
BaTNP_4	35	360	< 100	234

The investigation of SrTNP- and BaTNP-containing formulations revealed that brilliant flame colors and good color properties can be achieved without the use of additional oxidizer. In addition, formulation SrTNP_2 showed that PVC, which is used as chlorine-source to generate the red-light-emitting species SrCl, is not necessary to produce intensive red-burning flame colors.

Conclusions

Alkali and earth alkaline salts of 3,5-dinitropyrazole (DNP), 3,4,5-trinitropyrazole (TNP), and 2,4,5-trinitroimidazole (TNI) as well as copper 2,4,5-trinitroimidazolate were synthesized and fully characterized. Crystal structures of $Ba(DNP)_2$ (**9**) crystallizing with one molecule of methanol and ethyl ether as well as of $Sr(TNP)_2{\cdot}3H_2O$ (**12**), $Ba(TNP)_2{\cdot}3H_2O$ (**13**), and $LiTNI{\cdot}3H_2O$ (**14**) were determined. Energetic and thermal analysis of all compounds were performed and revealed predominantly low friction and impact sensitivities and high decomposition temperatures. Pyrotechnic formulations using $Sr(DNP)_2{\cdot}6H_2O$ (**8**), $Ba(DNP)_2{\cdot}H_2O$ (**9**), $Sr(TNP)_2{\cdot}3H_2O$ (**12**), and $Ba(TNP)_2{\cdot}3H_2O$ (**13**) as red and green colorants were investigated. Especially formulations based on $Sr(TNP)_2{\cdot}3H_2O$ (**12**) and $Ba(TNP)_2{\cdot}3H_2O$ (**13**) showed good color properties as well as low friction and impact sensitivities and high decomposition temperatures. The best performance values were observed for the red-burning formulation SrTNP_2 and the green-burning formulation BaTNP_3 revealing the highest spectral purities and the highest luminous intensities.

Experimental Section

CAUTION! The compounds described in this work are potential explosives, which are sensitive to environmental stimuli such as impact, friction, heat or electrostatic discharge. While no issues in the handling of these materials were encountered, appropriate precautions and proper protective measures (safety glasses, face shields, leather coat, Kevlar gloves and ear protectors) should be taken when preparing and manipulating these materials.

General: All reagents and solvents were purchased from Sigma-Aldrich, Fluka and Acros Organics. Melting and decomposition points were measured with a Linseis PT10 DSC using heating rates of 5 °C min^{-1}, which were checked with a Büchi Melting Point B-450 apparatus. ^{1}H, ^{13}C and ^{14}N NMR spectra were measured with a JEOL Eclipse 400, JEOL Eclipse 270 or JEOL EX400 instrument at an ambient temperature of 25 °C if not stated otherwise. All chemical shifts are quoted in ppm relative to TMS (^{1}H, ^{13}C), nitromethane (^{14}N) or boron trifluoro etherate (^{11}B) as external standards. Infrared spectra were measured using a Perkin-Elmer Spectrum BX-FTIR spectrometer with a Smiths DuraSampl IR-ATR unit. Elemental analyses were performed with an Elementar Vario EL or an Elementar Vario EL micro cube. Mass spectra were measured with a JEOL MS station JMS 700 instrument. The impact and friction sensitivity was determined with a BAM drophammer and a BAM friction tester.[19] The sensitivities of the compounds are indicated according to the UN Recommendations on the Transport of Dangerous Goods (+):[19] impact: insensitive > 40 J, less sensitive > 35 J, sensitive > 4 J, very sensitive < 4 J; friction: insensitive > 360 N, less sensitive = 360 N, sensitive < 360 N > 80 N, very sensitive < 80 N, extreme sensitive < 10 N. The controlled burn down of the pyrotechnic formulations was filmed with a digital video camera recorder (SONY, DCR-HC37E). Spectrometric measurements of the formulations were performed with a HR2000+ES spectrometer with an ILX511B linear silicon CCD-array detector and included software from Ocean Optics with a detector-sample distance of 1 meter.

Metal 3,5-Dinitropyrazolate Salts: 3,5-Dinitropyrazolate salts were synthesized by the reaction of 3,5-dinitropyrazole[6,7] (**1**) and the corresponding metal bases in stoichiometric amounts in water at room temperature. After stirring overnight the solvent was evaporated and the obtained solids were recrystallized from hot ethanol.

Lithium 3,5-Dinitropyrazolate Trihydrate (4): Slightly brown crystals (97 %) were obtained as product. **IR** (ATR): $\tilde{\nu}$ = 3156 (w), 1738 (m), 1641 (m), 1531 (m), 1470 (m), 1443 (s), 1353 (s), 1318 (m), 1273 (m), 1171 (m), 1016 (m), 997 (m), 821 (m), 749 (m), 681 (w) cm^{-1}. **^{1}H NMR** ([D$_6$]acetone): δ = 4.07 (s, H_2O), 7.26 (s, 1 H, CH) ppm. **^{13}C NMR** ([D$_6$]acetone): δ = 97.6 (C–H), 156.4 (C–NO_2) ppm. **^{14}N NMR** ([D$_6$]acetone): δ = –18 (C–NO_2) ppm. **EA** $C_3HN_4O_4Li{\cdot}3\ H_2O$ (218.05): calcd. C 16.53, H 3.24, N 25.69 %; found C 16.97, H 3.12, N 25.84 %. **MS** (FAB$^+$): *m/z* for Li$^+$: calculated 7.02, found 7.0. **MS** (FAB$^-$): *m/z* for $C_3HN_4O_4^-$: calculated 157.00; found 156.9. **IS:** >40 J (grain size < 100 µm). **FS:** 360 N (grain size < 100 µm). **ESD:** 0.7 J (grain size < 100 µm). **DSC:** 325 °C (dec.).

Sodium 3,5-Dinitropyrazolate Dihydrate (5): As product a brownish solid was gained (99 %). **IR** (ATR): $\tilde{\nu}$ = 3570 (m), 3156 (m), 2362 (m), 2337 (m), 1683 (m), 1645 (m), 1560 (w), 1532 (m), 1507 (m), 1472 (s), 1443 (s), 1355 (s), 1316 (s), 1272 (m), 1166 (m), 1072 (w), 1012 (m), 994 (m), 837 (s), 820 (s), 750 (s), 686 (w) cm^{-1}. **^{1}H NMR** ([D$_6$]acetone): δ = 3.42 (s, H_2O), 7.30 (s, 1 H, CH) ppm. **^{13}C NMR** ([D$_6$]acetone): δ = 97.8 (C–H), 156.4 (C–NO_2) ppm. **^{14}N NMR** ([D$_6$]acetone): δ = –18 (C–NO_2) ppm. **EA** $C_3HN_4O_4Na{\cdot}2\ H_2O$ (216.09): calcd. C 16.67, H 2.33, N 25.92 %; found C 16.61, H 2.43, N 25.23 %. **MS** (FAB$^+$): *m/z* for Na$^+$: calculated 22.99; found 23.0. **MS** (FAB$^-$): *m/z* for $C_3HN_4O_4^-$: calculated 157.00; found 157.0. **IS:**

>40 J (grain size < 100 μm). **FS:** 360 N (grain size < 100 μm). **ESD:** 0.5 J (grain size < 100 μm). **DSC:** 324 °C (dec.).

Potassium 3,5-Dinitropyrazolate (6): Yellow crystals were obtained as product (99 %). **IR** (ATR): ṽ = 3156 (w), 2596 (w), 2294 (w), 1738 (w), 1539 (m), 1476 (s), 1443 (s), 1378 (m), 1353 (s), 1338 (s), 1310 (s), 1270 (m), 1151 (m), 1064 (w), 1003 (s), 993 (m), 830 (s), 754 (s) cm^{-1}. **^{1}H NMR** ([D_6]acetone): δ = 7.21 (s, 1 H, CH) ppm. **^{13}C NMR** ([D_6]acetone): δ = 97.8 (C–H), 156.9 (C–NO_2) ppm. **^{14}N NMR** ([D_6]acetone): δ = –17 (C–NO_2) ppm. **EA** $C_3HN_4O_4K$ (196.16): calcd. C 18.37, H 0.51, N 28.56 %; found C 18.42, H 0.62, N 27.96 %. **MS** (FAB^+): *m/z* for K^+: calculated 38.96; found 39.0. **MS** (FAB^-): *m/z* for $C_3HN_4O_4^-$: calculated 157.00; found 156.9. **IS:** 20 J (grain size 100–500 μm). **FS:** 216 N (grain size 100–500 μm). **ESD:** 0.1 J (grain size 100–500 μm). **DSC:** 306 °C (dec.).

Calcium Bis(3,5-dinitropyrazolate) Tetrahydrate (7): As the product yellow-brownish crystals were obtained (77 %). **IR** (ATR): ṽ = 3638 (m), 3549 (m), 3166 (m), 1636 (m), 1540 (m), 1511 (m), 1483 (s), 1450 (m), 1344 (s), 1318 (s), 1280 (m), 1204 (w), 1175 (m), 1017 (s), 998 (m), 842 (s), 818 (w), 748 (s) cm^{-1}. **^{1}H NMR** ([D_6]acetone): δ = 3.91 (s, H_2O), 7.29 (s, 1 H, CH) ppm. **^{13}C NMR** ([D_6]acetone): δ = 97.6 (C–H), 156.3 (C–NO_2) ppm. **^{14}N NMR** ([D_6]acetone): δ = –18 (C–NO_2) ppm. **EA** $C_6H_2N_8O_8Ca\cdot4\ H_2O$ (426.27): calcd. C 16.91, H 2.36, N 26.29 %; found C 17.05, H 2.34, N 25.72 %. **MS** (FAB^+): *m/z* for $C_3HN_4O_4Ca^+$: calculated 196.96; found 197.0. **MS** (FAB^-): *m/z* for $C_3HN_4O_4^-$: calculated 157.00; found 156.9. **IS:** 8 J (grain size 100–500 μm). **FS:** 360 N (grain size 100–500 μm). **ESD:** 0.5 J (grain size 100–500 μm). **DSC:** >400 °C (dec.).

Strontium Bis(3,5-dinitropyrazolate) Hexahydrate (8): Yellow-brownish crystals were gained as product (98 %). **IR** (ATR): ṽ = 2971 (w), 2170 (w), 1739 (s), 1618 (m), 1540 (m), 1475 (m), 1443 (m), 1354 (s), 1322 (m), 1279 (w), 1229 (m), 1217 (m), 1073 (w), 1017 (m), 999 (w), 835 (m), 826 (m), 749 (m) cm^{-1}. **^{1}H NMR** ([D_6]acetone): δ = 3.68 (s, H_2O), 7.27 (s, 1 H, CH) ppm. **^{13}C NMR** ([D_6]acetone): δ = 98.3 (C–H), 157.0 (C–NO_2) ppm. **^{14}N NMR** ([D_6]acetone): δ = –18 (C–NO_2) ppm. **EA** $C_6H_2N_8O_8Sr\cdot6H_2O$ (509.84): calcd. C 14.14, H 2.77, N 21.98 %; found C 14.43, H 2.68, N 21.71 %. **MS** (FAB^+): *m/z* for $C_3HN_4O_4Sr^+$: calculated 244.91; found 245.0. **MS** (FAB^-): *m/z* for $C_3HN_4O_4^-$: calculated 157.00; found 157.0. **IS:** >40 J (grain size 100–500 μm). **FS:** 360 N (grain size 100–500 μm). **ESD:** 0.2 J (grain size 100–500 μm). **DSC:** >400 °C (dec.).

Barium Bis(3,5-dinitropyrazolate) Hydrate (9): Brownish crystals were obtained as product (86 %). **IR** (ATR): ṽ = 3610 (w), 3156 (w), 2361 (w), 1739 (m), 1611 (m), 1548 (s), 1494 (s), 1444 (m), 1369 (m), 1342 (s), 1321 (s), 1230 (w), 1172 (m), 1070 (w), 1010 (m), 1000 (w), 840 (s), 821 (w), 744 (s), 669 (w) cm^{-1}. **^{1}H NMR** ([D_6]acetone): δ = 2.88 (s, H_2O), 7.28 (s, 1 H, CH) ppm. **^{13}C NMR** ([D_6]acetone): δ = 98.6 (C–H), 157.3 (C–NO_2) ppm. **^{14}N NMR** ([D_6]acetone): δ = –19 (C–NO_2) ppm. **EA** $C_6H_2N_8O_8Ba\ H_2O$ (469.47): calcd. C 15.32, H 0.86, N 23.84 %; found C 15.36, H 0.92, N 23.18 %. **MS** (FAB^+): *m/z* for $C_6H_2N_8O_8Ba^+$: calculated 451.90; found 448.0. **MS** (FAB^-): *m/z* for $C_3HN_4O_4^-$: calculated 157.00; found 157.0. **IS:** 30 J (grain size 500–1000 μm). **FS:** 72 N (grain size 500–1000 μm). **ESD:** 0.1 J (grain size 500–1000 μm). **DSC:** 361 °C (dec.).

Metal 3,4,5-Trinitropyrazolate Salts: All metal 3,4,5-trinitropyrazolate salts were obtained by the same synthesis procedure. To a solution of 3,4,5-trinitropyrazole[20] (**2**) in ethanol the corresponding metal carbonates were added in stoichiometric amounts. The solutions were stirred overnight at room temperature. After removing the solvent the products were obtained as solids.

Lithium 3,4,5-Trinitropyrazolate Tetrahydrate (10): A yellow solid (86 %) was obtained as product. **IR** (ATR): ṽ = 3620 (m), 3582 (w), 3512 (m), 3343 (w), 3209 (w), 2628 (w), 1668 (m), 1630 (w), 1540 (m), 1522 (s) 1456 (s), 1351 (s), 1325 (s), 1299 (s), 1172 (w), 1133 (m), 1024 (m), 850 (s), 806 (m), 763 (m), 731 (m), 680 (m) cm^{-1}. **^{1}H NMR** ([D_6]acetone): δ = 3.37 (s, H_2O) ppm. **^{13}C NMR** ([D_6]acetone): δ = 145.9 ppm. **^{14}N NMR** ([D_6]acetone): δ = –22 (C–NO_2) ppm. **EA** $C_3N_5O_6Li\cdot4\ H_2O$ (281.06): calcd. C 12.82, H 2.87, N 24.92 %; found C 12.98, H 2.80, N 24.45 %. **MS** (FAB^+): *m/z* for Li^+: calculated 7.02, found 7.0. **MS** (FAB^-): *m/z* for $C_3N_5O_6^-$: calculated 201.98; found 202.0. **IS:** 40 J (grain size 100–500 μm). **FS:** 96 N (grain size 100–500 μm). **ESD:** 0.2 J (grain size 100–500 μm). **DSC:** 274 °C (dec.).

Sodium 3,4,5-Trinitropyrazolate (11): As product (96 %) yellow crystals were gained. **IR** (ATR): ṽ = 3638 (w), 1605 (w), 1560 (w), 1546 (m), 1512 (s), 1456 (m), 1357 (m), 1319 (s), 1296 (w), 1170 (w), 1132 (w), 1024 (w), 850 (s), 808 (m), 762 (w), 682 (w) cm^{-1}. **EA** $C_3N_5O_6Na$ (225.05): calcd. C 16.01, N 31.12 %; found C 16.15, N 30.85 %. **^{13}C NMR** ([D_6]acetone): δ = 146.8 ppm. **^{14}N NMR** ([D_6]acetone): δ = –22 (C–NO_2) ppm. **MS** (FAB^+): *m/z* for Na^+: calculated 22.99; found 23.0. **MS** (FAB^-): *m/z* for $C_3N_5O_6^-$: calculated 201.98; found 202.0. **IS:** 25 J (grain size 100–500 μm). **FS:** 80 N (grain size 100–500 μm). **ESD:** 0.2 J (grain size 100–500 μm). **DSC:** 254 °C (dec.).

Strontium Bis(3,4,5-trinitropyrazolate) Trihydrate (12): As product yellow crystals were obtained (74 %). **IR** (ATR): ṽ = 3616 (w), 3139 (m), 2924 (m), 1596 (w), 1518 (s), 1493 (m), 1454 (m), 1358 (m) 1328 (s), 1131 (m), 1025 (s), 841 (m), 787 (w), 760 (m), 672 (w) cm^{-1}. **^{1}H NMR** ([D_6]acetone): δ = 3.06 (s, H_2O) ppm. **^{13}C NMR** ([D_6]acetone): δ = 146.1 ppm. **^{14}N NMR** ([D_6]acetone): δ = –22 (C–NO_2) ppm. **EA** $C_6N_{10}O_{12}Sr\cdot3H_2O$ (545.79): calcd. C 13.20, H 1.11, N 25.66 %; found C 12.99, H 1.14, N 25.10 %. **MS** (FAB^-): *m/z* for $C_3N_5O_6^-$: calculated 201.98; found 202.0. **IS:** 40 J (grain size 100–500 μm). **FS:** 80 N (grain size 100–500 μm). **ESD:** 0.2 J (grain size 100–500 μm). **DSC:** 193 °C (dec.).

Barium Bis(3,4,5-trinitropyrazolate) Trihydrate (13): As product yellow crystals were obtained (55 %). **IR** (ATR): ṽ = 3582 (m), 1619 (m), 1540 (s), 1514 (s), 1457 (m), 1354 (m), 1322 (s), 1303 (m), 1132 (m), 1028 (w), 850 (s), 806 (m), 766 (w) cm^{-1}. **^{1}H NMR** ([D_6]acetone): δ = 2.99 (s, H_2O) ppm. **^{14}N NMR** ([D_6]acetone): δ = –23 (C–NO_2) ppm. **EA** $C_6N_{10}O_{12}Ba\ \cdot3\ H_2O$ (595.56): calcd. C 12.10, H 1.02, N 23.52 %; found C 12.13, H 1.04, N 23.10 %. **MS** (FAB^-): *m/z* for $C_3N_5O_6^-$: calculated 201.98; found 202.0. **IS:** 5 J (grain size 100–500 μm). **FS:** 144 N (grain size 100–500 μm). **ESD:** 0.1 J (grain size 100–500 μm). **DSC:** 302 °C (dec.).

Metal 2,4,5-Trinitroimidazolate Salts: To a solution of trinitroimidazole[21] (**3**) in ethyl ether the corresponding metal carbonates were added in stoichiometric amounts and the solutions were stirred overnight at room temperature. Evaporation of the solvent and recrystallization from ethyl acetate resulted in the formation of the products.

Lithium 2,4,5-Trinitroimidazolate Trihydrate (14): A yellow-orange solid (79 %) was obtained as product. **IR** (ATR): ṽ = 3563 (m), 3321 (w), 1648 (m), 1538 (s), 1467 (s), 1426 (m), 1328 (s), 1301 (s), 1111 (m), 868 (s), 832 (m), 812 (s), 755 (w), 650 (m) cm^{-1}. **^{1}H NMR** ([D_6]DMSO): δ = 3.37 (s, H_2O) ppm. **^{14}N NMR** ([D_6]DMSO): δ = –21 (C–NO_2) ppm. **EA** $C_3N_5O_6Li\cdot3H_2O$ (263.05): calcd. C 13.70, H 2.30, N 26.62 %; found C 14.01, H 2.25, N 26.67 %. **MS** (FAB^+): *m/z* for Li^+: calculated 7.02, found 7.0. **MS** (FAB^-): *m/z* for $C_3N_5O_6^-$: calculated 201.98; found 201.9. **IS:** >40 J (grain size

< 100 μm). **FS:** >360 N (grain size < 100 μm). **ESD:** 0.5 J (grain size < 100 μm). **DSC:** 252 °C (dec.).

Sodium 2,4,5-Trinitroimidazolate (15): As product a yellow-orange solid (80 %) was obtained. **IR** (ATR): $\tilde{\nu}$ = 3600 (w), 2978 (w), 1693 (s), 1545 (s), 1470 (s), 1425 (m), 1378 (m), 1325 (s), 1297 (s), 1170 (w), 1111 (s), 1035 (s), 867 (s), 835 (m), 810 (s), 753 (m), 645 (m) cm^{-1}. **^{14}N NMR** ([D$_6$]DMSO): δ = –21 (C–NO$_2$) ppm. **EA** $C_3N_5O_6Na$ (225.05): calcd. C 16.01, N 31.12 %; found C 16.45, N 30.67 %. **MS** (FAB$^+$): *m/z* for Na$^+$: calculated 22.99; found 23.0. **MS** (FAB$^-$): *m/z* for $C_3N_5O_6^-$: calculated 201.98; found 201.9. **IS:** >40 J (grain size < 100 μm). **FS:** N (grain size < 100 μm). **ESD:** 0.6 J (grain size < 100 μm). **DSC:** 249 °C (dec.).

Potassium 2,4,5-Trinitroimidazolate (16): As product a yellow crystals (83 %) were obtained. **IR** (ATR): $\tilde{\nu}$ = 2629 (w), 1530 (s), 1465 (s), 1426 (m), 1315 (s), 1302 (s), 1280 (m), 1110 (m), 869 (s), 832 (m), 812 (s), 764 (m), 758 (m), 690 (w) cm^{-1}. **^{14}N NMR** ([D$_6$]DMSO): δ = –21 (C–NO$_2$) ppm. **EA** $C_3N_5O_6K$ (241.16): calcd. C 14.94, N 29.04 %; found C 14.93, N 28.67 %. **MS** (FAB$^+$): *m/z* for K$^+$: calculated 38.96; found 39.0. **MS** (FAB$^-$): *m/z* for $C_3N_5O_6^-$: calculated 201.98; found 201.9. **IS:** 25 J (grain size 100–500 μm). **FS:** 120 N (grain size 100–500 μm). **ESD:** 0.2 J (grain size 100–500 μm). **DSC:** 231 °C (dec.).

Calcium Bis(2,4,5-trinitroimidazolate) Dihydrate (17): Orange crystals (78 %) were obtained as product. **IR** (ATR): $\tilde{\nu}$ = 3582 (m), 3347 (w), 1643 (w), 1619 (m), 1535 (s), 1468 (s), 1422 (w), 1327 (s), 1304 (s), 1109 (m) 865 (s), 830 (w), 808 (s), 752 (m), 672 (m) cm^{-1}. **^{1}H NMR** ([D$_6$]DMSO): δ = 3.18 (s, H$_2$O) ppm. **^{14}N NMR** ([D$_6$]DMSO): δ = –20 (C–NO$_2$) ppm. **EA** $C_6N_{10}O_{12}Ca{\cdot}2H_2O$ (480.24): calcd. C 15.01, H 0.84, N 29.17 %; found C 15.12, H 1.01, N 28.18 %. **MS** (FAB$^-$): *m/z* for $C_3N_5O_6^-$: calculated 201.98; found 201.9. **IS:** >40 J (grain size 100–500 μm). **FS:** >360 N (grain size 100–500 μm). **ESD:** 0.7 J (grain size 100–500 μm). **DSC:** 188 °C (dec.).

Strontium Bis(2,4,5-trinitroimidazolate) Hydrate (18): A yellow-orange solid (78 %) was gained as product. **IR** (ATR): $\tilde{\nu}$ = 3616 (w), 2988 (w), 1693 (s), 1545 (s), 1470 (s), 1425 (m), 1378 (m), 1321 (s), 1297 (s), 1189 (w), 1111 (s), 1041 (s), 867 (s), 833 (m), 810 (s), 753 (m), 650 (m) cm^{-1}. **^{1}H NMR** ([D$_6$]DMSO): δ = 3.47 (s, H$_2$O) ppm. **^{14}N NMR** ([D$_6$]DMSO): δ = –20 (C–NO$_2$) ppm. **EA** $C_6N_{10}O_{12}Sr{\cdot}H_2O$ (509.76): calcd. C 14.14, H 0.39, N 27.48 %; found C 14.11, H 0.50, N 26.75 %. **MS** (FAB$^-$): *m/z* for $C_3N_5O_6^-$: calculated 201.98; found 201.9. **IS:** >40 J (grain size < 100 μm). **FS:** >360 N (grain size < 100 μm). **ESD:** 0.7 J (grain size < 100 μm). **DSC:** 239 °C (dec.).

Barium Bis(2,4,5-trinitroimidazolate) Dihydrate (19): Orange crystals (73 %) were obtained as product. **IR** (ATR): $\tilde{\nu}$ = 3229 (w), 1589 (s), 1413 (m), 1306 (s), 1222 (w), 1184 (w), 1130 (w), 855 (m), 769 (m), 692 (m) cm^{-1}. **^{1}H NMR** ([D$_6$]DMSO): δ = 3.52 (s, H$_2$O) ppm. **^{14}N NMR** ([D$_6$]DMSO): δ = –20 (C–NO$_2$) ppm. **EA** $C_6N_{10}O_{12}Ba{\cdot}2H_2O$ (577.48): calcd. C 12.48, H 0.70, N 24.25 %; found C 12.23, H 0.82, N 23.98 %. **MS** (FAB$^-$): *m/z* for $C_3N_5O_6^-$: calculated 201.98; found 201.9. **IS:** >40 J (grain size 100–500 μm). **FS:** >360 N (grain size 100–500 μm). **ESD:** 0.6 J (grain size 100–500 μm). **DSC:** 166 °C (dec.).

Copper Bis(2,4,5-trinitroimidazolate) Tetrahydrate (20): A turquoise solid (65 %) was obtained as product. **IR** (ATR): $\tilde{\nu}$ = 2745 (w), 1610 (s), 1469 (s), 1400 (m), 1315 (s), 1302 (s), 1280 (m), 1143 (m), 869 (s), 832 (m), 824 (s), 764 (m), 758 (m), 680 (w) cm^{-1}. **^{1}H NMR** ([D$_6$]DMSO): δ = 3.17 (s, H$_2$O) ppm. **^{14}N NMR** ([D$_6$]DMSO): δ = –20 (C–NO$_2$) ppm. **EA** $C_6N_{10}O_{12}Cu \cdot 4\,H_2O$ (539.73): calcd. C 13.35, H 1.49, N 25.95 %; found C 13.49, H 1.49, N 25.92 %. **MS** (FAB$^-$): *m/z* for $C_3N_5O_6^-$: calculated 201.98; found 201.9. **IS:** 3 J (grain size 100–500 μm). **FS:** 80 N (grain size 100–500 μm). **ESD:** 0.1 J (grain size 100–500 μm). **DSC:** 170 °C (dec.).

Crystallographic data (excluding structure factors) for the structures in this paper have been deposited with the Cambridge Crystallographic Data Centre, CCDC, 12 Union Road, Cambridge CB21EZ, UK. Copies of the data can be obtained free of charge on quoting the depository numbers CCDC-1002135, CCDC-1002137, CCDC-1002138, and CCDC-1002136 for **9**, **12**, **13**, and **14** (Fax: +44-1223-336-033; E-Mail: deposit@ccdc.cam.ac.uk, http://www.ccdc.cam.ac.uk).

Acknowledgements

Financial support of this work by the Ludwig-Maximilian University of Munich (LMU), the U.S. Army Research Laboratory (ARL) under grant no. W911NF-09–2-0018, the Armament Research, Development and Engineering Center (ARDEC) under grant no. W911NF-12–1-0467, and the Office of Naval Research (ONR) under grant nos. ONR.N00014–10–1-0535 and ONR.N00014–12–1-0538 is gratefully acknowledged. The authors acknowledge collaborations with *Dr. Mila Krupka* (OZM Research, Czech Republic) in the development of new testing and evaluation methods for energetic materials and with *Dr. Muhamed Suceska* (Brodarski Institute, Croatia) in the development of new computational codes to predict the detonation and propulsion parameters of novel explosives. The authors are indebted to and thank *Drs. Betsy M. Rice* and *Brad Forch* (ARL, Aberdeen, Proving Ground, MD) for many inspired discussions. The Cusanuswerk is gratefully acknowledged for the award of a Ph.D. scholarship (*M. Rusan*).

References

[1] a) T. M. Klapötke, G. Steinhauser, *Angew. Chem. Int. Ed.* **2008**, *47*, 3330; b) G. Steinhauser, K. Tarantik, T. M. Klapötke, *J. Pyrotech.* **2008**, *27*, 3; c) T. J. Groshens, *J. Coord. Chem.* **2010**, *63*, 1882; d) D. Lu, C. H. Winter, *Inorg. Chem.* **2010**, *49*, 5795; e) Z. Zeng, B. Twamley, J. M. Shreeve, *Organometallics* **2007**, *26*, 1782.
[2] Y. Zhang, Y. Guo, Y.-H. Joo, D. A. Parrish, J. M. Shreeve, *Chem. Eur. J.* **2010**, *16*, 10778.
[3] H. Gao, C. Ye, O. D. Gupta, J.-C. Xiao, M. A. Hiskey, B. Twamley, J. M. Shreeve, *Chem. Eur. J.* **2007**, *13*, 3853.
[4] G. Hervé, US Pat. US 0186931, **2009**.
[5] R. Duddu, P. Dave, R. Davamarapu, R. Surapaneni, US Pat. US 8153786, **2012**.
[6] R. Hüttel, F. Büchele, *Chem. Ber.* **1955**, *88*, 1586.
[7] J. W. A. M. Janssen, H. J. Koeners, C. G. Kruse, C. L. Habrakern, *J. Org. Chem.* **1973**, *38*, 1777.
[8] a) G. Socrates, *Infrared and Raman Characteristic Group Frequencies – Tables and Charts*, 3rd ed., John Wiley & Sons: Chichester, **2004**; b) M. Hesse, H. Meier, B. Zeeh, *Spektroskopische Methoden in der Organischen Chemie*, 6. Auflage, Thieme, Stuttgart, **2002**.
[9] R. Galassi, A. Burini, S. Ricci, M. Pellei, M. P. Rigobello, A. Citta, A. Domella, V. Gandin, C. Marzano, *Dalton Trans.* **2012**, *41*, 5307.
[10] G. Herve, C. Roussel, H. Graindorge, *Angew. Chem.* **2010**, *122*, 3177.
[11] Y. Zhang, D. A. Parrish, J. M. Shreeve, *J. Mater. Chem.* **2012**, *22*, 12659.
[12] *CrysAlisPro*, Oxford Diffraction Ltd., version 171.33.41, **2009**.
[13] *SIR-92*, A Program for Crystal Structure Solution: A. Altomare, G. Cascarano, C. Giacovazzo, A. Guagliardi, *J. Appl. Crystallogr.* **1993**, *26*, 343.

[14] a) A. Altomare, G. Cascarano, C. Giacovazzo, A. Guagliardi, A. G. G. Moliterni, M. C. Burla, G. Polidori, M. Camalli, R. Spagna, *SIR97*, **1997**; b) A. Altomare, M. C. Burla, M. Camalli, G. L. Cascarano, C. Giacovazzo, A. Guagliardi, A. G. G. Moliterni, G. Polidori, R. Spagna, *J. Appl. Crystallogr.* **1999**, *32*, 115–119.

[15] a) G. M. Sheldrick, *SHELX-97*, University of Göttingen, Göttingen, Germany, **1997**; b) G. M. Sheldrick, *Acta Crystallogr., Sect. A* **2008**, *64*, 112–122.

[16] A. L. Spek, *PLATON*, A Multipurpose Crystallographic Tool, Utrecht University, The Netherlands, **1999**.

[17] L. J. Farrugia, *J. Appl. Crystallogr.* **1999**, *32*, 837–838.

[18] *SCALE3 ABSPACK*, An Oxford Diffraction Program (1.0.4, gui: 1.0.3), Oxford Diffraction Ltd., **2005**.

[19] *UN Recommendations on the Transport of Dangerous Goods*, Model Regulations 15th ed., United Nations, New York, Geneva, **2007**.

[20] G. Herve, C. Roussel, H. Graindorge, *Angew. Chem. Int. Ed.* **2010**, *49*, 3177.

[21] A. R. Katriszky, D. J. Cundy, J. Chen, *J. Energ. Mater.* **1993**, *11*, 345.

Received: May 13, 2014

DOI: 10.1002/zaac.201100263

Alkaline Earth Metal Salts of 5,5′-Bistetrazole – from Academical Interest to Practical Application

Niko Fischer,[a] Thomas M. Klapötke,*[a] Kristina Peters,[a] Magdalena Rusan,[a] and Jörg Stierstorfer[a]

In Memory of Professor Kurt Dehnicke

Keywords: Alkaline earth metals; Tetrazoles; Crystal structures; IR spectroscopy; Pyrotechnics

Abstract. The alkaline earth metal salts of 5,5′-BT, $[Be(H_2O)_4](5,5'\text{-}BT)\cdot H_2O$ (**1**), $[Mg(H_2O)_6(5,5'\text{-}BT)\cdot 3H_2O$ (**2**), $[Ca(H_2O)_4(5,5'\text{-}BT)]\cdot H_2O$ (**3**), $[Sr(H_2O)_4(5,5'\text{-}BT)]\cdot 2DMF$ (**4**), and $[Ba(H_2O)_4(5,5'\text{-}BT)]$ (**5**) were fully characterized by low temperature X-ray diffraction, vibrational (IR, Raman) and NMR spectroscopy, elemental analysis and differential scanning calorimetry (DSC). A detailed description of the crystal structures is given. In addition, the potential use of **4** and **5** in coloring pyrotechnical compositions was investigated.

Introduction

5,5′-Bistetrazole (**5,5-H$_2$BT**) can be obtained in good yield and high purity from the reaction of sodium azide, sodium cyanide and manganese dioxide in water.[1] Surprisingly since the determination of the crystal structure of 5,5′-bistetrazole in 1996[2] only very few examples of ionic compounds containing this heterocycle have been reported. In 2008 a row of rare earth metal salts have been structurally investigated by *Klein* et al..[3] Having a nitrogen content of more than 82 %, the 5,5′-bistetrazolate anion is one of the anions with the highest nitrogen contents known, thus it can be considered as a building block for energetic compounds. *Hiskey* et al. reported on several nitrogen-rich ionic compounds based on 5,5′-bistetrazole and their possible application as high nitrogen fuels in low smoke pyrotechnics in 1999,[1] however they did not give a complete characterization including the crystal structure of these compounds. The use of alkaline earth metal salts of nitrogen-rich anions in pyrotechnics combines the advantage of a fuel on the one hand and a colorant on the other hand in one compound. Usually calcium, strontium or barium salts are used for red and green flame colors, respectively.

Here we report on the full characterization including the crystal structures of the alkaline earth metal salts beryllium, magnesium, calcium, strontium, and barium 5,5′-bistetrazolate. Of course, the potential use of these compounds decreases within this row. The heavier alkaline earth metal salts can be used in pyrotechnical compositions and have also been tested towards their behavior in pyrotechnical mixtures together with a vinyl alcohol based binder, magnesium or boron as fuel and ammonium nitrate as oxidizer.

A different approach of this work is the structural determination of the alkaline earth metal salts and a comparison of the different coordination modes found in the structures. Some of the metal centers are coordinated by their hydration shell only, but there are also examples of metal centers in which 5,5′-bistetrazole serves as a bidentate ligand.

Results and Discussion

Synthesis

Since 5,5′-bistetrazole, which can be synthesized according to literature,[1] bears two protons which are readily available in aqueous solution, it can be deprotonated by reaction with the respective metal hydroxide or carbonate. This procedure was used for the preparation of the magnesium (**2**), calcium (**3**), strontium (**4**), and barium (**5**) 5,5′-bistetrazolate. The solubility of 5,5′-bistetrazole is fairly good in hot water, but poor in cold water. The reactions therefore were carried out under reflux conditions in water, ensuring that the starting material is fully dissolved. Also the choice of the metal source has to depend on the solubility of the respective material. The calcium (**3**), strontium (**4**), and barium (**5**) salt was prepared using the hydroxides since their solubility in water than the respective carbonates is higher by about a factor of 1000. For the preparation of the magnesium salt **2**, basic magnesium carbonate was used. For availability reasons, beryllium sulfate was used for the preparation of the beryllium salt **1** via a metathesis reaction using the barium salt of 5,5′-bistetrazole, whereas barium sulfate was filtered off and the beryllium 5,5′-bistetrazolate could be crystallized from the hot aqueous solution. The

---

* Prof. Dr. T. M. Klapötke
Fax: +49-89-2180-77492
E-Mail: tmk@cup.uni-muenchen.de
[a] Ludwig Maximilian University Munich (LMU)
Department of Chemistry
Energetic Materials Research
Butenandtstr. 5–13 (D)
81377 Munich, Germany

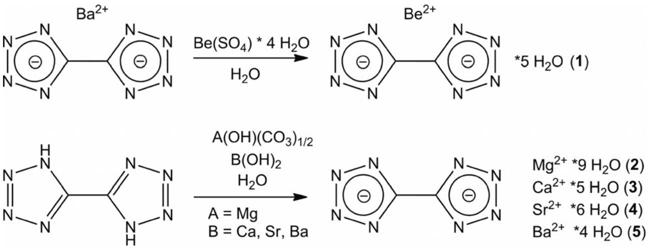

Scheme 1. Synthesis of the alkaline earth metal salts of 5,5′-bistetrazole.

synthetic procedures to compounds **1–5** are summarized in Scheme 1.

Molecular Structures

To determine the molecular structures of **1–5** in the crystalline state an Oxford Xcalibur3 diffractometer with a Spellman generator (voltage 50 kV, current 40 mA) and a KappaCCD detector was used. The data collections at 173 K were performed using the CrysAlis CCD software,[4] the data reductions with the CrysAlis RED software.[5] The solution and refinement of all structures were performed using the programs SIR-92,[6] SHELXS-97,[7] and SHELXL-97[8] implemented in the WinGX software package[9] and finally checked with the PLATON software.[10] In all crystal structures the hydrogen atoms were located and refined. The absorptions were corrected with the SCALE3 ABSPACK multi-scan method.[11] Selected data and parameters of the X-ray determinations are given in Table 1.

Beryllium 5,5′-bistetrazolate pentahydrate (**1**) (Figure 1) crystallizes in the monoclinic space group $P2_1/c$ with four molecules in the unit cell. The N–N bond lengths in the two C–C linked tetrazolate rings are between N–N single bonds (1.454 Å) and N=N double bonds (1.245 Å). The shortest distance is between the atoms N2–N3 (1.3094(17)Å), the longest between the atoms N1–N2 1.3445(17) Å. The C–C bond length (1.4629(19) Å) is closer to a single bond (1.52 Å) than to a double bond (1.32 Å). In comparison to neutral 5,5′-bistetrazole there are no significant changes regarding the bond lengths (N2–N3 = 1.2976(14) Å, N1–N2 = 1.3439(14) Å, C1–C2 = 1.4535(15) Å). The bond angle in **1** N2–N1–C1 is smaller (104.40(11)°) than in 5,5′-bistetrazole (108.37(9)°),[12] whereas the angle N1–N2–N3 is larger (109.70(11)°) than in the free acid (106.46(10)°). The five membered 6π electron aromatic tetrazole rings are almost planar for 5,5′-BT (torsion

Table 1. X-ray data and parameters.

	1	**2**	**3**	**4**	**5**
formula	$BeC_2H_{10}N_8O_5$	$MgC_2H_{18}N_8O_9$	$CaC_2H_{10}N_8O_5$	$SrC_8H_{22}N_{10}O_6$	$BaC_2H_8N_8O_4$
form. mass /g•mol^{-1}	235.19	322.55	266.26	441.98	345.49
crystal system	monoclinic	monoclinic	monoclinic	orthorhombic	triclinic
space group	$P2_1/c$ (No. 14)	$P2_1/n$ (No. 14)	$P2_1/c$ (No. 14)	*Pcca* (No. 54)	$P\bar{1}$ (No. 2)
color / habit	colorless plate	colorless rod	colorless block	colorless plate	colorless rod
size /mm	0.23 × 0.22 × 0.08	0.30 × 0.20 × 0.20	0.25 × 0.20 × 0.10	0.23 × 0.22 × 0.10	0.17 × 0.10 × 0.10
a /Å	11.5764(8)	12.117(4)	6.7848(2)	22.378(5)	7.4679(5)
b /Å	11.8368(7)	6.955(5)	13.6768(3)	5.8533(9)	7.5004(5)
c /Å	7.1908(6)	16.081(6)	10.8009(2)	13.940(3)	9.4148(7)
α /°	90	90	90	90	73.119(6)
β/°	99.035(7)	93.413(5)	91.147(2)	90	70.842(7)
γ /°	90	90	90	90	81.251(5)
V /Å^3	973.11(12)	1352.8(12)	1002.06(4)	1825.9(6)	475.73(6)
Z	4	4	4	4	2
$\rho_{calcd.}$ /g•cm^{-3}	1.605	1.584	1.765	1.608	2.412
μ /mm^{-1}	0.145	0.192	0.654	3.000	4.189
F(000)	488	680	552	904	328
λ(Mo-K_α) /Å	0.71073	0.71073	0.71073	0.71073	0.71073
T /K	173	173	173	173	173
θ min-max /°	4.5, 26.0	4.2, 26.0	4.2, 25.7	4.2, 25.0	4.2, 26.0
dataset *h; k; l*	–12:14;-14:14;-8: 7	–14:14;-5:8;-18:19	–8:8; –16:16; –13:13	–17: 26;-6: 6;-16:16	–9: 9;-9: 9;-11:11
reflect. coll.	4876	6818	14722	7853	4862
independ. refl.	1888	2647	1908	1598	1866
R_{int}	0.032	0.027	0.024	0.023	0.041
reflection obs.	295	1996	1678	1245	1648
No. Parameters	185	253	185	134	168
R_1 (obs)	0.0289	0.0294	0.0202	0.0230	0.0219
wR_2 (all data)	0.0503	0.0677	0.0566	0.0662	0.0488
S	0.77	0.91	1.03	1.06	0.98
resd. dens. /e·Å^{-3}	–0.14, 0.19	–0.18, 0.28	–0.23, 0.30	–0.46, 0.35	–0.89, 0.48
device type	Oxford Xcalibur3 CCD	Oxford Xcalibur3 CCD	Oxford Xcalibur3 CCD	Oxford Xcalibur3 CCD	Oxford Xcalibur3 CCD
solution	SHELXS-97	SIR-92	SIR-92	SIR-92	SIR-92
refinement	SHELXL-97	SHELXL-97	SHELXL-97	SHELXL-97	SHELXL-97
absorpt. corr.	multi-scan	multi-scan	multi-scan	multi-scan	multi-scan
CCDC	827503	827502	827501	827504	827500

angle N1–N2–N3–N4 = 0.05(12)) as well as for its alkaline earth metal salts (torsion angle N1–N2–N3–N4 = 0.03(16)°). Exact bond lengths and angles are listed in Table 2. In this structure beryllium is coordinated tetrahedral by four water molecules with bond lengths between 1.60 Å and 1.61 Å and bond angles between 105.1° and 115.1°. The packing is affected by layers of 5,5′-BT anions connected by strong hydrogen bonds involving all water hydrogen atoms (Figure 2).

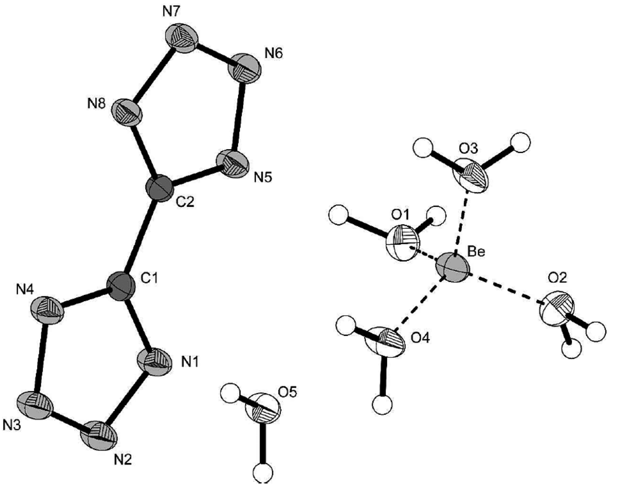

Figure 1. Molecular unit of **1**. Thermal ellipsoids of non-hydrogen atoms represent the 50 % probability level.

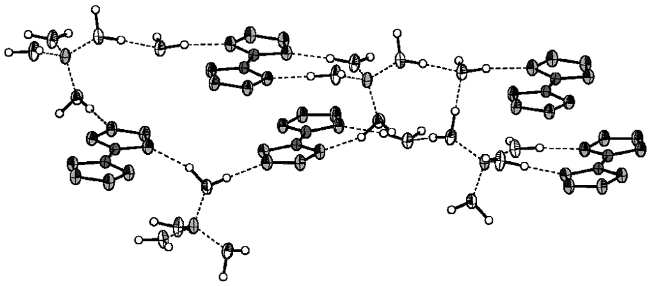

Figure 2. Hydrogen bonding in the structure of **1** forming layers of 5,5′-BT dianions connected by the tetrahedrally solvated beryllium cations.

Basically all of the metal atoms are coordinated by crystal water molecules and partly by the bistetrazolate dianions. The coordination numbers follow an increasing trend by raising the period (CN: Be^{2+} = 4, Mg^{2+} = 6, Ca^{2+} = 6, Sr^{2+} = 8, Ba^{2+} = 9). The densities do not follow a corresponding trend (ρ (**5**) $>$ ρ(**3**) $>$ ρ(**4**) $>$ ρ(**1**) $>$ ρ(**2**)), due to the varying water content.

Magnesium 5,5′-bistetrazolate nonahydrate (**2**) crystallizes in the monoclinic space group $P2_1/n$ with four molecular moie-

Table 2. Selected bond lengths /Å, angles /° and torsion angles /° of the anions of compounds **1**–**5**.

	5,5BT	Be-BT (1)	Mg-BT (2)	Ca-BT (3)	Sr-BT (4)	Ba-BT (5)
Atom 1–2 /Å	*d*(1–2)	*d*(1–2)	*d*(1–2)	*d*(1–2)	*d*(1–2)	*d*(1–2)
N1–N2	1.3439(14)	1.3445(17)	1.343(2)	1.3483(15)	1.349(3)	1.349(5)
N2–N3	1.2976(14)	1.3094(17)	1.315(2)	1.3107(15)	1.313(3)	1.316(4)
N3–N4	1.3583(14)	1.3430(17)	1.343(2)	1.3512(15)	1.352(3)	1.345(4)
N4–C1	1.3178(14)	1.3307(18)	1.332(2)	1.3353(15)	1.329(3)	1.346(5)
N1–C1	1.3289(14)	1.3333(18)	1.336(2)	1.3332(15)	1.331(3)	1.338(5)
C1–C2	1.4535(15)	1.4629(19)	1.461(2)	1.4549(16)	1.465(4)	1.466(5)
N5–C2	1.3178(14)	1.3333(18)	1.332(2)	1.3334(16)		1.331(5)
N5–N6	1.3583(14)	1.3466(17)	1.347(2)	1.3495(15)		1.342(5)
N6–N7	1.2976(14)	1.3032(17)	1.314(2)	1.3126(14)		1.316(4)
N7–N8	1.3439(14)	1.3446(17)	1.346(2)	1.3460(14)		1.342(5)
N8–C2	1.3289(14)	1.3299(18)	1.333(2)	1.3362(15)		1.328(5)
Atoms 1–2–3 /°	<(1–2–3)	<(1–2–3)	<(1–2–3)	<(1–2–3)	<(1–2–3)	<(1–2–3)
N2–N1–C1	108.37(9)	104.40(11)	104.23(12)	104.81(10)	104.02(19)	103.9(3)
N1–N2–N3	106.46(10)	109.70(11)	109.90(12)	109.11(9)	109.7(2)	110.1(3)
N2–N3–N4	110.57(10)	109.28(11)	109.08(12)	109.92(10)	109.3(2)	109.5(3)
N3–N4–C1	105.52(9)	104.80(11)	104.85(12)	104.13(9)	104.16(19)	104.2(3)
N6–N5–C2	105.52(9)	104.50(11)	104.66(12)	103.88(9)		104.9(3)
N5–N6–N7	110.57(10)	109.68(11)	109.24(12)	110.05(9)		108.7(3)
N6–N7–N8	106.46(10)	109.36(11)	109.62(12)	109.22(9)		110.1(3)
N7–N8–C2	108.37(9)	104.89(11)	104.49(12)	104.46(9)		104.2(3)
N1–C1–N4	109.07(10)	111.82(12)	111.94(13)	112.03(10)	112.8(2)	112.3(3)
N4–C1–C2	126.23(10)	124.20(13)	123.94(13)	126.94(11)	124.1(2)	122.1(3)
N1–C1–C2	124.67(9)	123.98(13)	124.10(13)	121.02(10)	123.1(2)	125.4(3)
N5–C2–C1	126.23(10)	124.20(13)	123.63(13)	121.89(10)		124.2(3)
N8–C2–C1	124.67(9)	124.22(13)	124.34(13)	125.69(11)		123.6(3)
N5–C2–N8	109.07(10)	111.58(12)	112.00(13)	112.40(10)		112.2(3)
Atoms 1–2–3–4 /°	<(1–2–3–4)	<(1–2–3–4)	<(1–2–3–4)	<(1–2–3–4)	<(1–2–3–4)	<(1–2–3–4)
N1–C1–C2–N5	–1.94(18)	0.9(2)	–18.9(2)	0.80(18)	0.1(4)	–9.9(6)
N1–C1–C2–N8	–180.00(11)	–179.60(13)	163.35(14)	178.57(11)	178.6(2)	173.6(4)

ties in the unit cell. The magnesium dications are coordinated octahedrally by water molecules, with bond lengths in the range of 2.1 Å (Figure 3). Additionally, there are three free water molecules in each molecular unit. The packing of **2** can be described as a vertical layer structure along the *a* axis, with alternating alignments of octahedrally coordinated Mg^{2+}-cations as well as the 5,5′-BT anions and free water molecules (Figure 4).

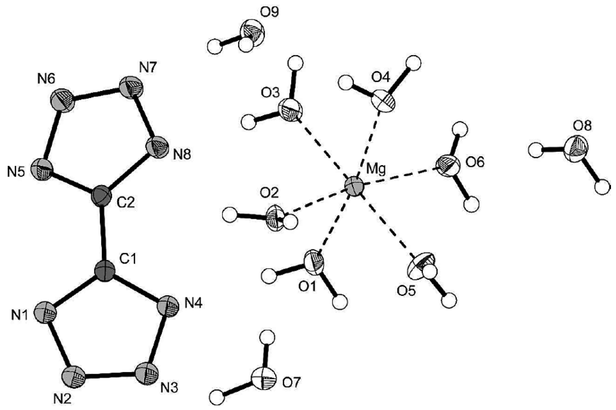

Figure 3. Molecular unit of **2**. Thermal ellipsoids of non-hydrogen atoms represent the 50 % probability level. Coordination distances /Å: Mg–O1 2.067(2), Mg–O2 2.069(2), Mg–O3 2.037(2), Mg–O4 2.089(2), Mg–O5 2.086(2), Mg–O6 2.0745(19).

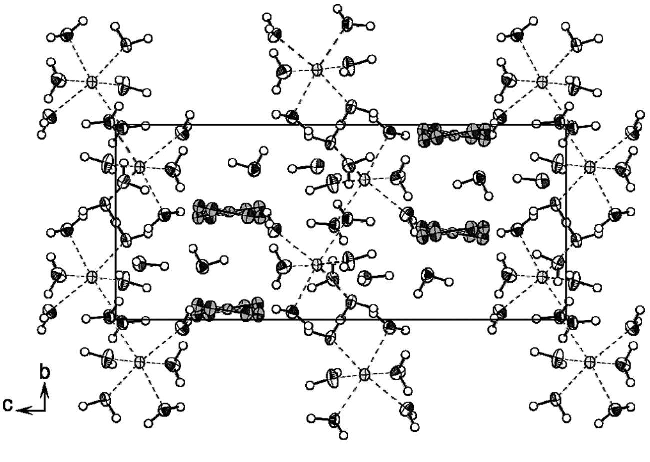

Figure 4. Packing of the magnesium salt **2**, showing the alternating layers within the *a,b* plane.

Calcium 5,5′-bistetrazolate pentahydrate (**3**) crystallizes in the monoclinic space group $P2_1/c$ with four molecular moieties in the unit cell. Calcium is coordinated sixfold by four water molecules, with shorter bond lengths (Ca–O1 = 2.3576(11) Å, Ca–O2 = 2.3955(10) Å, Ca–O3 = 2.3770(10) Å, Ca–O4 = 2.3263(11) Å], and two nitrogen atoms of two different 5,5-BT anions, with longer bond lengths (Ca–N1 = 2.5049(11) Å, Ca–$N6^i$ = 2.5293(10) Å) (Figure 5). A further contact, indicated in Figure 6, is formed by Ca–N5 with a distance of 2.8739(10) Å, which is slightly above the sum of the *van der Waals* radii. The packing along the *c* axis can be described as a horizontal alternating layer structure between the coordinated cations and the anions with the free water molecules. Within the *b*,*c* planes the structure shows alternating vertical layers. The one layer is made up of the 5,5′-BT anions, the calcium cations as well as the free water molecule, while the other one contains just the water coordination sphere of the calcium cation. The packing is affected by several strong hydrogen bonds.

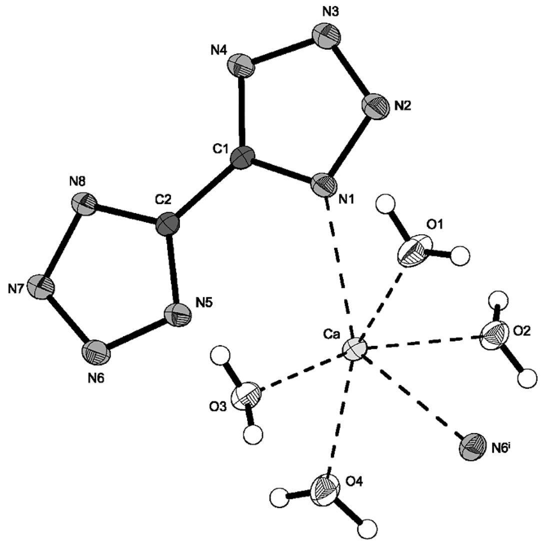

Figure 5. View on the molecular unit of **3** indicating the distorted octahedral coordination sphere of the calcium cations. Thermal ellipsoids represent the 50 % probability level. Symmetry code: (i) *x*, 0.5–*y*, 0.5+*z*.

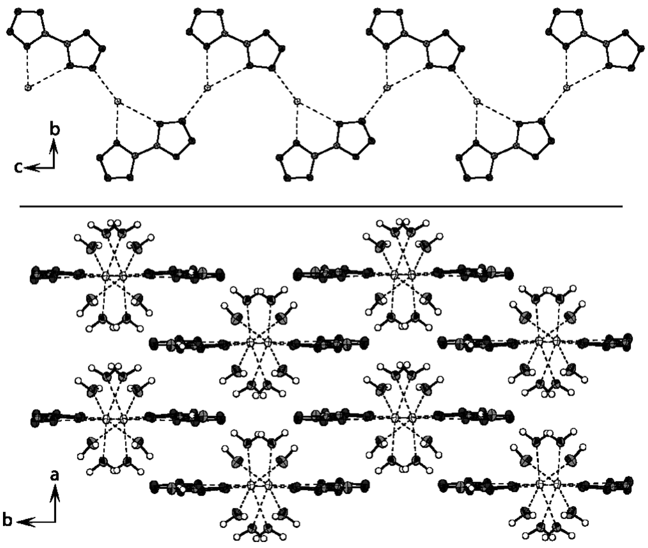

Figure 6. Structural motive within **3**. Top: Strings of Ca^{2+} and 5,5′-BT anions along *c*; bottom: View along *c* axis showing the alternating layers formed by the strings.

Strontium 5,5′-bistetrazolate (**4**) could only be obtained crystalline as its tetrahydrate with two additional DMF molecules per molecular unit. It crystallizes in the orthorhombic space group *Pcca*, with four molecular moieties in its unit cell. The bond lengths and angles in the 5,5′-BT anion are similar to the other alkaline earth metal salts. The strontium cations are coordinated eightfold by two water molecules and two nitrogen atoms of two different 5,5′-bistetrazolate anions. Both oxygen and nitrogen atoms are doubled by symmetry. The Sr–O bond lengths are shorter (Sr–O1 = 2.579(19) Å, Sr–O2 = 2.594(2) Å) than the Sr–N bond lengths (Sr–N1 = 2.802(2) Å, Sr–N4^{i} = 2.787(19) Å) (Figure 7). The packing along the *a* axis could be described as a stacking of alternating layers of the strontium 5,5′-bistetrazolate tetrahydrate and the DMF molecules, which are connected by strong hydrogen bonds e.g. O2–H2A•••O3: D–A = 2.688(3), 175(2)°. A view along the *c* axis shows the angulated packing of two 5,5′-bistetrazolate moieties above each other (Figure 8).

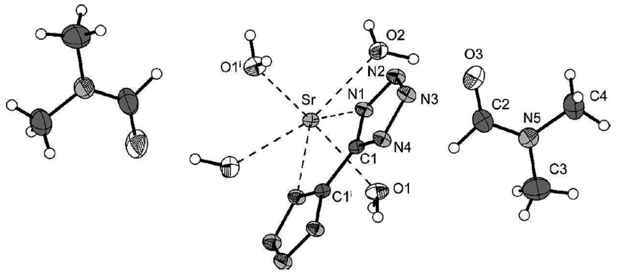

Figure 7. View on the molecular unit of **4**. Thermal ellipsoids represent the 50 % probability level. Symmetry code: (i) = 0.5–*x*, 1 –*y*, *z*.

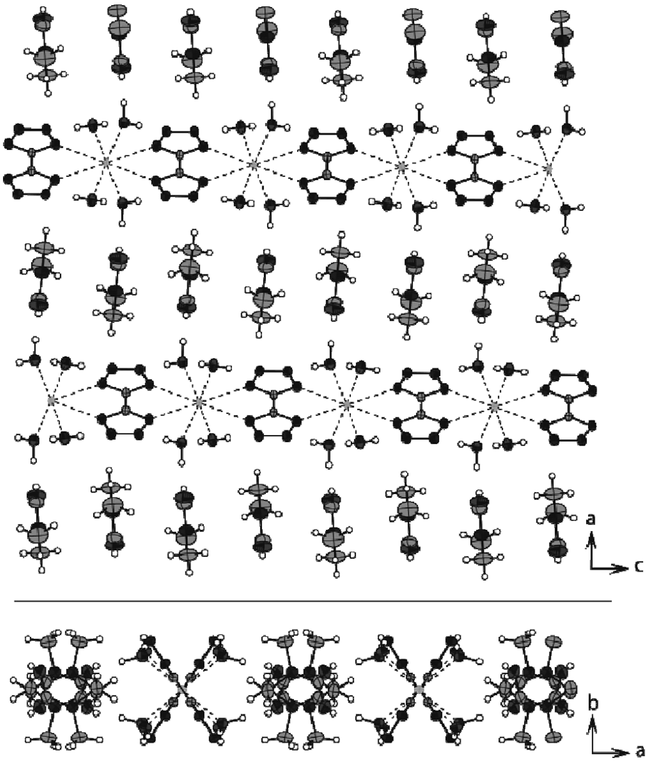

Figure 8. View along the *b*- and *c* axis in the crystal structure of **4** showing the alternating layers.

Barium 5,5′-bistetrazolate tetrahydrate (**5**) crystallizes in the triclinic space group $P\bar{1}$ with two molecular moieties in the unit cell. A view on the molecular unit is shown in Figure 9. The bond lengths are in agreement to the previously discussed structures and given in Table 2. The barium atoms are coordinated ninefold, by six oxygen and three nitrogen atoms, as shown in Figure 9 (Ba–O1 = 2.830(3) Å, Ba–O2 = 2.712(4) Å, Ba–O3 = 2.829(3) Å, Ba–O4 = 2.702(4) Å, Ba–N1 = 2.984(3) Å, Ba–N3^{i} = 2.975(3) Å, Ba–O3^{ii} = 2.919(3) Å, Ba–O^{iii} = 2.892(3) Å, Ba–N2^{iii} = 2.912(3) Å). The packing along the *c* axis shows an alternating horizontal layer structure between tilted 5,5′-BT anions and barium cations with its water coordination sphere. A view along the *a* axis (Figure 10) presents vertical rows of 5,5′-BT, which are separated from each other through a zig-zag pattern of coordinated barium atoms. Again the structure of **5** is stabilized by various strong hydrogen bonds.

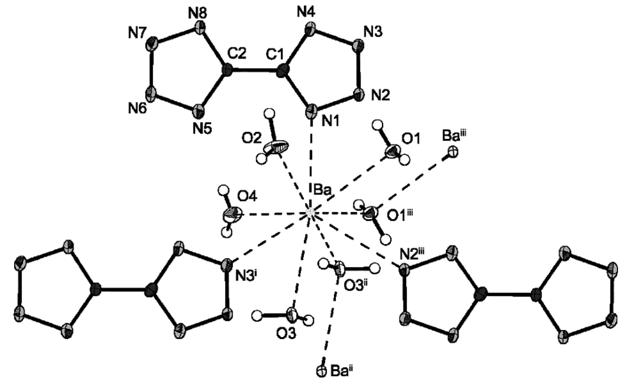

Figure 9. Molecular unit of **5**. Thermal ellipsoids of non-hydrogen atoms represent the 50 % probability level. Symmetry codes: (i) *x*, –1+*y*, *z*, (ii) 1 –*x*, –*y*, –*z*, (iii) 1 –*x*, 1 –*y*, -*z*.

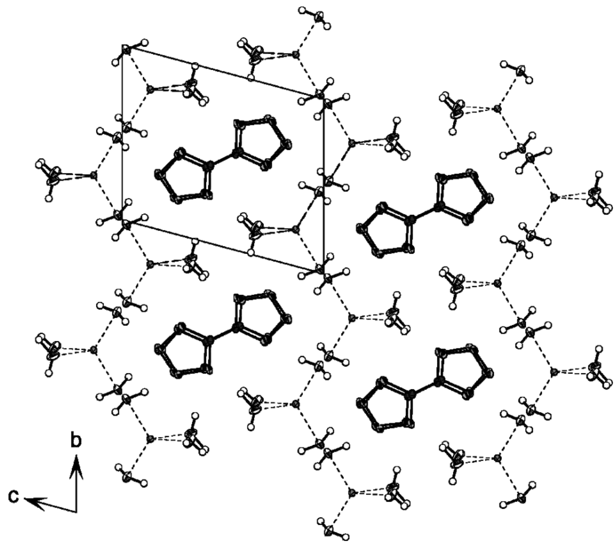

Figure 10. View along the *a* axis showing columns of staggered 5,5′-BT dianions.

Vibrational Spectroscopy

IR- as well as Raman spectroscopy are suitable methods for the detection of the 5,5′-bistetrazolates **1**–**5**. After deprotonation of the free acid, the N–H stretching vibration disappears. The values for the stretching and deformation vibrations in the IR and Raman spectra of the examined substances were compared to values found in literature.[13–15] The most intensive absorption bands in the raman spectra are the symmetrical stretching mode between the C–C linked tetrazole rings at around 1576 cm^{-1} and a typical tetrazole ring deformation vibration at around 1143 cm^{-1}. The most intensive absorption bands in the IR spectra can be assigned to asymmetrical >C=N– stretching modes of the tetrazole ring system in the range of 1690 and 1640 cm^{-1}. Further, O-H stretching vibrations of the crystal water, which is contained in all compounds, are found in the range of 3600–3100 cm^{-1}. Apart from >C=N– stretching modes at 1690 and 1640 cm^{-1} further sets of tetrazole ring stretching and deformation vibrations in a range of 1390–700 cm^{-1} [ν(NCN), ν(NN), δ(ring), δ(NCN),] can be identified.

Physico-Chemical Properties

Thermal Behavior

Differential scanning calorimetry (DSC) measurements to determine the melt- and decomposition temperatures of **1–5** (about 1.5 mg of each energetic material) were performed in covered aluminum containers with a hole (0.1 mm) in the lid for gas release and a nitrogen flow of 20 mL per minute with a Linseis PT 10 DSC[16] calibrated by standard pure indium and zinc at a heating rate of 5 °C·min^{-1}.

In the DSC curves of the salts **1–5** several endothermic peaks between 92 °C and 190 °C can be detected, which can be assigned to the stepwise dehydration of the salts. Except from the strontium salt all compounds show two endothermic peaks, the first one of which is due to the loss of water molecules, which are not coordinated by the metal atoms (**1**: 123 °C, **2**: 138 °C, **3**: 98 °C, **4**: 130 °C, **5**: 92 °C). The second endothermic peaks, which are observed for **1**, **2**, **3** and **5** can be assigned to the loss of the hydration shells of the metal centers (**1**: 186 °C, **2**: 148 °C, **3**: 190 °C, **5**: 166 °C). For the determination of the exact amount of released water thermogravimetrical measurements had to be accomplished. Despite the high nitrogen content of the investigated 5,5′-bistetrazolate salts, no exothermic decomposition of any of the compounds could be observed in a temperature range up to 400 °C.

Water Solubility

From recrystallization attempts in water and NMR measurements, which were carried out in deuterium oxide, a trend of the water solubility of the salts **1–5** could be observed. For the salts **2** to **5** the water solubility decreases rapidly with increasing molecular weight of the cation just as it also is observed for the alkaline earth metal sulfates. In this context, the beryllium salt plays a special role, since, against expectations from the above mentioned trend, its solubility in water is similar to that of the barium salt. A possible explanation for this behavior could be the same argumentation as it is applied for diagonal relationships in the periodic table saying that lithium salts behave like magnesium salts rather than the other alkali salts or beryllium salts behave like aluminum salts rather than other alkaline earth metal salts because of the similar charge to diameter ratio of the diagonally related ions.

Sensitivities

The impact sensitivity tests were carried out according to STANAG 4489[17] modified instruction[18] using a BAM (Bundesanstalt für Materialforschung) drophammer.[19] The friction sensitivity tests were carried out according to STANAG 4487[20] modified instruction[21] using the BAM friction tester. The classification of the tested compounds results from the "UN Recommendations on the Transport of Dangerous Goods".[22] All compounds were tested upon the sensitivity towards electrical discharge using the Electric Spark Tester ESD 2010 EN.[23] Apart from the beryllium salt, the sensitivities of all alkaline earth metal salts were determined. To dehydrate the compounds, all substances were dried at 200 °C previously to sensitivity testing. Also for the sensitivities, a trend from lower to higher molecular weight of the cation can be observed. The impact sensitivities are in a range from 40 J to 30 J with the higher values for the lighter elements (**2**: 40 J, **3**: 40 J, **4**: 35 J, **5**: 30 J). Therefore, the dry magnesium and calcium salts can be considered as insensitive, the strontium salt as less sensitive and the barium salt as sensitive. Also the sensitivity towards electrical discharge shows the same trend. The values reach from 0.30 J for the magnesium salt to 0.15 J for both, the strontium and the barium salt (**2**: 0.30 J, **3**: 0.20 J, **4**: 0.15 J, **5**: 0.15 J). Only the friction sensitivities do not change within the row of the alkaline earth metal salts and were determined to 360 N for all compounds. They can therefore be considered as less sensitive towards friction.

Pyrotechnical Compositions

Nitrogen-rich compounds are promising substances in the development of ecologically friendly coloring agents in pyrotechnical formulations. The formation of mainly gaseous products like nitrogen is an important requirement for smokeless combustion, therefore the investigation of nitrogen-rich compounds as coloring substances is focused. For this reason several pyrotechnical formulations with the barium and strontium salts of 5,5′-bistetrazole were tested.

The pyrotechnic mixtures were prepared by mixing all substances, except the binder, in a mortar. Then the binder, a solution of 25 % vinyl alcohol acetate resin (VAAR), was added. The mixture was formed by hand and dried under high vacuum for three hours. The controlled burn down was filmed with a digital video camera recorder (SONY, DCR-HC37E). The performance of each composition has been evaluated with respect to color emission (subjective impression), smoke generation and the amount of solid residues. As red and green coloring agents the strontium and barium salts (MBT) were used. In all pyrotechnic formulations ammonium nitrate served as oxidizer. Magnesium and amorphous boron in the case of the formulations with the barium salt were used as fuels. Polyvinyl chloride (PVC) was added to a barium formulation and served as chlorine source for the generation of the green-emitting species $BaCl_2$. In Table 3 the content of the compositions (mass percent) is summarized.

Table 3. Composition of pyrotechnical mixtures containing **4** and **5**.

Formulations	Sr-BT_1	Sr-BT_2	Ba-BT_1	Ba-BT_2	Ba-BT_3
MBT /wt.-%	35	39	35	30	40
NH_4NO_3 /wt.-%	40	44	40	35	44
Mg /wt.-%	18	10	–	11	–
B /wt.-%	–	–	18	–	9
PVC /wt.-%	–	–	–	17	–
VAAR /wt.-%	7	7	7	7	7

The pyrotechnic composition Sr-BT_1 consists of 35 % Sr-BT, 40 % NH_4NO_3, 18 % magnesium and 7 % VAAR. The observed flame color is intense red and the combustion occurs fast and smokeless and no residues were observed. Formulation Sr-BT_2 with an increased oxidizer and Sr-BT content of 44 % NH_4NO_3 and 39 % Sr-BT and a decreased amount of 10 % magnesium burned smokeless with an orange-red flame color (Figure 11). The combustion velocity was slower than that of composition Sr-BT_1 and some magnesium sparks and solid residues could be observed.

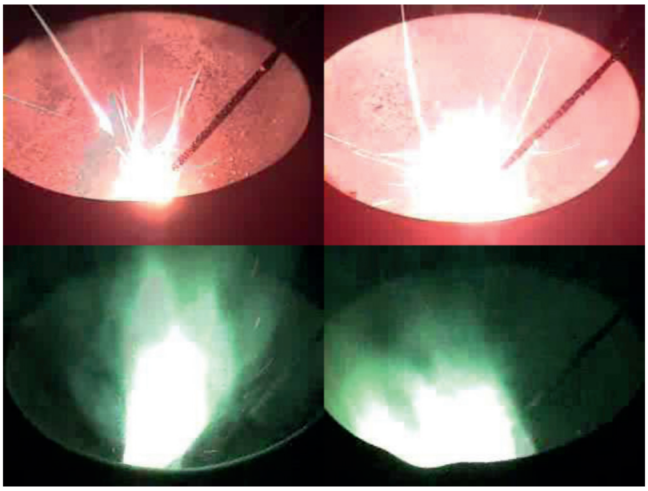

Figure 11. Flame colors of Sr-BT_1 (top left), Sr-BT_2 (top right), Ba-BT_1 (bottom left) and Ba-BT_3 (bottom right).

Both formulations Ba-BT_1 and Ba-BT_3 with 35 % Ba-BT, 40 % NH_4NO_3, 18 % boron, 7 % VAAR and 40 % Ba-BT, 44 % NH_4NO_3, 9 % boron, 7 % VAAR respectively burned fast with an intense green flame color and no residues remained, however a slight generation of smoke was observed for both compositions. The composition Ba-BT_2 containing 30 % Ba-BT, 35 % NH_4NO_3, 11 % magnesium, 17 % PVC and 7 % VAAR combusted fast with an intense white flame color without smoke and no solid residues remained.

Conclusions

5,5′-Bistetrazole was deprotonated in aqueous solution using the alkaline earth metal hydroxides or, in case of the magnesium salt, the basic carbonate to synthesize the corresponding alkaline earth metal salts **2**, **3**, **4**, and **5**. Due to the low solubility of the alkaline earth metal hydroxides in water, the yields of the described reactions are not quantitative. The beryllium salt **1** of 5,5′-bistetrazole was synthesized in a metathesis reaction using the barium salt of 5,5′-bistetrazole and beryllium sulfate.

The water solubility of the alkaline earth metal salts of 5,5′-bistetrazole in water drops with increasing molecular weight of the cation. As an exception, the solubility of the beryllium salt **1** is almost as low as the solubility of the barium salt **5**.

The salts crystallize in the common mono- and triclinic space groups $P2_1/c$ (**1**, **3**), $P2_1/n$ (**2**), *Pcca* (**4**) and $P\bar{1}$ (**5**) as tetrahydrate (**4**, **5**), pentahydrate (**1**, **3**) or nonahydrate (**2**). Single crystals of **4** could only be obtained from DMF, where it crystallizes with two molecules of DMF per molecular unit.

All salts can be dehydrated at temperatures between 92 °C and 190 °C. They do not decompose at temperatures lower than 400 °C.

The impact and friction sensitivities were determined of previously dried substances. They reach from 30 J (**5**) to 40 J (**2**, **3**) impact sensitivity. The friction sensitivity of all compounds is 360 N. The salts therefore are comparatively insensitive towards impact and friction.

The strontium (**4**) and the barium salt (**5**) were tested in pyrotechnical compositions as red respectively green colorants. Their color performance for the strontium salt was best in a formulation containing 35 % Sr-BT, 40 % NH_4NO_3, 18 % magnesium and 7 % VAAR. Regarding smokeless combustion, the best performing mixture for the barium salt consists of 40 % Ba-BT, 44 % NH_4NO_3, 9 % boron and 7 % VAAR.

Experimental Section

All chemicals and solvents were employed as received (Sigma–Aldrich, Fluka, Acros). ^1H and ^{13}C spectra were recorded using a JEOL Eclipse 270, JEOL EX 400 or a JEOL Eclipse 400 instrument. The chemical shifts quoted in ppm in the text refer to typical standards such as tetramethylsilane (^1H, ^{13}C). To determine the melting and decomposition temperatures of the described compounds a Linseis PT 10 DSC (heating rate 5 °C min^{-1}) was used. Infrared spectra were measured using a Perkin–Elmer Spectrum One FT-IR spectrometer as KBr pellets. Raman spectra were recorded with a Bruker MultiRAM Raman Sample Compartment D418 equipped with a Nd-YAG-Laser (1064 nm) and a LN-Ge diode as detector. Mass spectra of the described compounds were measured at a JEOL MStation JMS 700 using FAB technique. To measure elemental analyses a Netsch STA 429 simultaneous thermal analyzer was employed.

Beryllium 5,5′-bistetrazolate pentahydrate (1): Barium bistetrazolate tetrahydrate (2.73 g, 10.0 mmol, 1 equiv.) was dissolved in boiling water (75 mL) and combined with beryllium sulfate tetrahydrate (1.77 g, 10.0 mmol, 1.0 equiv.), which previously was dissolved in hot water (25 mL). Barium sulfate precipitated instantly. Then the mixture was boiled for 20 min and filtered. To remove the remaining barium sulfate, the solution was centrifuged. Lastly, the water was evaporated and the colorless product was recrystallized from ethanol/water in 86 % yield (2.02 g).

DSC (5 °C·min^{-1}): 123 °C (dehydr.), 186 °C (endoth.), >400 °C (no dec.). **IR** (KBr): $\tilde{\nu}$ = 2931 (s), 2235 (s), 1679 (m), 1593 (m), 1384 (m), 1339 (s), 1319 (m), 1229 (m), 1204 (s), 1167 (m), 1066 (s), 1054 (s), 1038 (vs), 983 (s), 880 (s), 788 (s), 719 (s), 675 (s), 533 (m), 488 (w) cm^{-1}; **Raman** (1064 nm, 200 mW, 25 °C): $\tilde{\nu}$ = 1595 (100), 1231

(15), 1159 (14), 1138 (31), 1101 (16), 782 (3), 540 (1), 489 (3), 426 (5), 392 (11) cm^{-1}. **^{1}H NMR** (D_2O, 95 °C): $\delta = 4.78$ (H_2O). **^{13}C NMR** (D_2O, 95 °C): $\delta = 154.8$ (CN_4); ***m/z* (FAB$^-$)** 137.0 [$C_2HN_8^-$]; **EA** ($C_2H_{10}BeN_8O_5$, 235.16): calcd.: C 10.21; H 4.29; N 47.65 %; found: C 10.69; H 4.11; N 47.72 %.

Magnesium 5,5′-bistetrazolate nonahydrate (2): 5,5′-Bistetrazole (1.38 g, 9.99 mmol, 1.0 equiv.) was dissolved in hot water (20 mL) and combined with basic magnesium carbonate ($Mg(OH)_2{\cdot}MgCO_3$) (0.86 g, 12.06 mmol, 1.21 equiv.). The mixture was boiled for 40 min and filtered hot, to remove remaining basic magnesium carbonate. The product crystallized from the solution at room temperature in 45 % yield (1.45 g).

DSC (5 °C·min^{-1}): 138 °C (dehydr.), 148 °C (dehydr.), <400 °C (no dec.). **IR** (KBr): ṽ = 3553 (s), 3316 (s), 3213 (vs), 2399 (m), 2224 (w), 1876 (w), 1696 (m), 1666 (m), 1384 (w), 1334 (s), 1314 (m), 1300 (m), 1204 (m), 1197 (m), 1161 (m), 1104 (w), 1070 (w), 1053 (w), 1026 (m), 940 (w), 730 (m), 688 (m), 452 (w) cm^{-1}; **Raman** (1064 nm, 200 mW, 25 C): ṽ = 2859 (1), 1591 (100), 1565 (8), 1221 (6), 1155 (6), 1129 (15), 1091 (9), 783 (3), 486 (2), 428 (2), 391 (4) cm^{-1}. **^{1}H NMR** (D_2O, 95 °C): $\delta = 4.83$ (H_2O). **^{13}C NMR** (D_2O, 25 °C): $\delta = 154.7$ (CN_4); ***m/z* (FAB$^-$)** 137.0 [$C_2HN_8^-$]; **EA** ($C_2H_{18}MgN_8O_9$, 322.52): calcd.: C 7.45; H 5.63; N 34.74 %; found: C 9.57, H 4.13, N 41.49 %. **BAM drophammer**: 40 J; **friction tester**: 360 N; **ESD**: 0.30 J (at grain size <100 µm).

Calcium 5,5′-bistetrazolate pentahydrate (3): 5,5′-Bistetrazole (1.38 g, 9.99 mmol, 1 equiv.) was dissolved in hot water (20 mL) and combined with calcium hydroxide (0.89 g, 12.01 mmol, 1.20 equiv.). The mixture was boiled for 40 min and filtered hot. During the following days the product crystallized from the solution at room temperature in light yellowish blocks in 72 % yield (1.92 g).

DSC (5 °C·min^{-1}): 98 °C (dehydr.), 190 C (endoth.), >400 °C (no dec.). **IR** (KBr): ṽ = 3468 (s), 3416 (s), 3234 (vs), 2224 (m), 2195 (m), 1685 (m), 1649 (m), 1444 (m), 1384 (m), 1350 (s), 1319 (m), 1220 (m), 1202 (m), 1166 (m), 1154 (m), 1103 (m), 1082 (m), 1062 (m), 1049 (m), 1025 (m), 818 (m), 728 (m), 687 (s), 486 (m) cm^{-1}; **Raman** (1064 nm, 200 mW, 25 °C): ṽ = 3203 (2), 2859 (3), 1604 (100), 1566 (3), 1223 (14), 1148 (5), 1123 (19), 1084 (9), 783 (4), 493 (6), 433 (6) cm^{-1}. **^{1}H NMR** (D_2O, 25 °C): $\delta = 4.78$ (H_2O). **^{13}C NMR** (D_2O, 25 °C): $\delta = 154.8$ (CN_4), ***m/z* (FAB$^-$)** 137.0 [$C_2HN_8^-$]; **EA** ($C_2H_{10}N_8CaO_5$, 266.23): calcd.: C 9.02; H 3.79; N 42.09 %; found: C 9.35; H 3.43; N 41.66 %. **BAM drophammer**: 40 J; **friction tester**: 360 N; **ESD**: 0.20 J (at grain size <100 µm).

Strontium 5,5′-bistetrazolate tetrahydrate (4): 5,5′-Bistetrazole (1.38 g, 9.99 mmol, 1 equiv.) was dissolved in hot water (20 mL) and combined with strontium hydroxide octahydrate (3.19 g, 12.00 mmol, 1.20 equiv.). The mixture was boiled for 40 min and filtered hot. After a short period, precipitation of the yellowish product could be observed. Crystals suitable for single-crystal X-ray diffraction could only be obtained by recrystallization from DMF. Yield: 68 % after recrystallization of the DMF adduct (3.00 g).

DSC (5 °C·min^{-1}): 130 °C (dehydr.), >400 °C (no dec.). **IR** (KBr): ṽ = 3614 (s), 3358 (vs), 3178 (s), 2689 (w), 2450 (w), 2430 (w), 2213 (w), 2172 (w), 2125 (w), 1656 (m), 1629 (w), 1590 (w), 1457 (w), 1426 (w), 1384 (w), 1329 (m), 1309 (m), 1208 (w), 1181 (m), 1156 (w),, 1128 (w), 1101 (w), 1051 (w), 1022 (w), 1031 (w), 782 (w), 733 (w), 591 (w) cm^{-1}; **Raman** (1064 nm, 200 mW, 25 °C): ṽ = 1590 (100), 1565 (8), 1210 (10), 1181 (1), 1156 (3), 1127 (25), 1083 (19), 1033 (1), 783 (4), 481 (2), 427 (4), 401 (7) cm^{-1}. **^{1}H NMR** (D_2O, 25 °C): $\delta = 4.78$ (H_2O), **^{13}C NMR** (D_2O, 25 °C): $\delta = 154.8$ (CN_4); ***m/z* (FAB$^-$)** 137.0 [$C_2HN_8^-$]; **EA** ($C_2H_8N_8O_4Sr$, 295.76): calcd.: C 8.12; H 2.73; N 37.89 %; found: C 8.54; H 2.55; N 37.86 %. **BAM drophammer**: 35 J; **friction tester**: 360 N; **ESD**: 0.15 J (at grain size <100 µm).

Barium 5,5′-bistetrazolate tetrahydrate (5): 5,5′-Bistetrazole (1.38 g, 9.99 mmol, 1 equiv.) was dissolved in hot water (20 mL) and combined with barium hydroxide octahydrate (3.78 g, 12.00 mmol, 1.20 equiv.). The mixture was boiled for 40 min and filtered hot. After standing for a few minutes, **5** crystallizes in small colorless blocks in 66 % yield (2.28 g).

DSC (5 °C·min^{-1}): 92 °C (dehydr.), 166 °C (endoth.), >400 °C (no dec.). **IR** (KBr): ṽ = 3526 (vs), 3386 (s), 3090 (s), 2677 (w), 2195 (w), 1631 (m), 1435 (w), 1384 (w), 1340 (s), 1326 (m), 1310 (s), 1218 (w), 1186 (m), 1151 (w), 1143 (w), 1081 (w), 1047 (w), 1030 (w), 1020 (m), 824 (w), 782 (w), 731 (w), 726 (w), 681 (w), 581 (m), 551 (m), 485 (w) cm^{-1}; **Raman** (1064 nm, 200 mW, 25 °C): ṽ = 1588 (100), 1565 (11), 1219 (5), 1206 (9), 1146 (4), 1125 (24), 1081 (17), 784 (5), 480 (2), 427 (4), 399 (8) cm^{-1}. **^{1}H NMR** (D_2O, 25 °C): $\delta = 4.78$ (H_2O), **^{13}C NMR** (D_2O, 25 °C): $\delta = 154.8$ (CN_4); ***m/z* (FAB$^-$)** 137.0 [$C_2HN_8^-$]; **EA** ($BaC_2H_8N_8O_4$, 345.46): calcd.: C 6.95; H 2.33; N 32.44 %; found: C 7.34; H 2.07; N 32.89 %. **BAM drophammer**: 30 J; **friction tester**: 360 N; **ESD**: 0.15 J (at grain size 100–500 µm).

Acknowledgement

Financial support of this work by the *Ludwig Maximilian University of Munich* (LMU), the *U.S. Army Research Laboratory* (ARL), the *Armament Research, Development and Engineering Center* (ARDEC), the *Strategic Environmental Research and Development Program* (SERDP) and the *Office of Naval Research* (ONR Global, title: "*Synthesis and Characterization of New High Energy Dense Oxidizers* (HEDO) - NICOP Effort") under contract nos. W911NF-09–2-0018 (ARL), W911NF-09–1-0120 (ARDEC), W011NF-09–1-0056 (ARDEC) and 10 WPSEED01–002 / WP-1765 (SERDP) is gratefully acknowledged. The authors acknowledge collaborations with *Dr. Mila Krupka* (OZM Research, Czech Republic) in the development of new testing and evaluation methods for energetic materials and with *Dr. Muhamed Sucesca* (Brodarski Institute, Croatia) in the development of new computational codes to predict the detonation and propulsion parameters of novel explosives. We are indebted to and thank *Drs. Betsy M. Rice* and *Brad Forch* (ARL, Aberdeen, Proving Ground, MD) and Mr. *Gary Chen* (ARDEC, Picatinny Arsenal, NJ) for many helpful and inspired discussions and support of our work. Mr. *Stefan Huber* is thanked for performing the sensitivity tests. The *Cusanuswerk* is gratefully acknowledged for a PhD scholarship (M.R.).

References

[1] D. E. Chavez, M. A. Hiskey, D. L. Naud, *J. Pyrotech.* **1999**, *10*, 17–36.
[2] P. J. Steel, *J. Chem. Crystallogr.* **1996**, *26*, 399.
[3] P. J. Eulgem, A. Klein, N. Maggiarosa, D. Naumann, P. W. H. Pohl, *Chem. Eur. J.* **2008**, *14*, 3727.
[4] *CrysAlis CCD*, Version 1.171.27p5 beta; Oxford Diffraction Ltd.
[5] *CrysAlis RED*, Version 1.171.27p5 beta; Oxford Diffraction Ltd.
[6] A. Altomare, G. Cascarano, C. Giacovazzo, A. Guagliardi, *J. Appl. Crystallogr.* **1993**, *26*, 343.
[7] G. M. Sheldrick, *SHELXS-97, Program for Crystal Structure Solution*; University of Göttingen: Göttingen, Germany, **1997**.
[8] G. M. Sheldrick, *SHELXL-97, Program for the Refinement of*

Crystal Structures; University of Göttingen: Göttingen, Germany, **1994**.
[9] L. J. Farrugia, *WinGX* suite for small-molecule single-crystal crystallography, *J. Appl. Crystallogr.* **1999**, *32*, 837–838.
[10] A. Spek, A. L. *PLATON, A Multipurpose Crystallographic Tool*; Utrecht, The Netherlands, **1999**.
[11] *SCALE3 ABSPACK*-An Oxford Diffraction program; Oxford Diffraction Ltd., **2005**.
[12] Personal X-ray redetermination of neutral 5,5′-BT at 173 K.
[13] T. M. Klapötke, M. Stein, J. Stierstorfer, *Z. Anorg. Allg. Chem.* **2008**, *634*, 1711–1723.
[14] A. Hammerl, G. Holl, T. M. Klapötke, P. Meyer, H. Nöth, H. Piotrowski, M. Warchhold, *Eur. J. Inorg. Chem.* **2002**, 834–845.
[15] M. Hesse, H. Meier, B. Zeeh, *Spektroskopische Methoden in der organischen Chemie*, Thieme, **2002**, vol. 6, pp. 41–46.
[16] http://www.linseis.com.
[17] NATO standardization agreement (STANAG) on explosives, *impact sensitivity tests*, no. 4489, 1st ed., Sept. 17, **1999**.
[18] WIWEB-Standardarbeitsanweisung 4–5.1.02, Ermittlung der Explosionsgefährlichkeit, hier der Schlagempfindlichkeit mit dem Fallhammer, Nov. 8, **2002**.
[19] http://www.bam.de.
[20] NATO standardization agreement (STANAG) on explosive, *friction sensitivity tests*, no. 4487, 1st ed., Aug. 22, **2002**.
[21] WIWEB-Standardarbeitsanweisung 4–5.1.03, Ermittlung der Explosionsgefährlichkeit or der Reibeempfindlichkeit mit dem Reibeapparat, Nov. 8, **2002**.
[22] Impact: Insensitive $>$ 40 J, less sensitive $\geq$ 35 J, sensitive $\geq$ 4 J, very sensitive $\leq$ 3 J; friction: Insensitive $>$ 360 N, less sensitive = 360 N, sensitive $<$ 360 N a. $>$ 80 N, very sensitive $\leq$ 80 N, extreme sensitive $\leq$ 10 N; According to the UN Recommendations on the Transport of Dangerous Goods (+) indicates: not safe for transport.
[23] http://www.ozm.cz.

Received: June 14, 2011
Published Online: August 11, 2011

Full Paper

Propellants, Explosives, Pyrotechnics

DOI: 10.1002/prep.201200177

A Selection of Alkali and Alkaline Earth Metal Salts of 5,5′-Bis(1-hydroxytetrazole) in Pyrotechnic Compositions

Niko Fischer,[a] Thomas M. Klapötke,*[a] Stefan Marchner,[a] Magdalena Rusan,[a] Susanne Scheutzow,[a] and Jörg Stierstorfer[a]

Abstract: The dilithium (**1**), disodium (**2**), dipotassium (**3**) and dicesium (**4**) salt as well as the calcium (**5**), strontium (**6**) and barium (**7**) salt of 5,5′-bis(1-hydroxytetrazole) were prepared and characterized including NMR-, IR- and Raman spectroscopy, mass spectrometry, elemental analysis and differential scanning calorimetry. The crystal structures of **1**, **2** and **4**–**6** were additionally determined by single-crystal X-ray diffraction. The sensitivities of the salts towards impact, friction and electrostatic discharge were determined by means of BAM (Bundesanstalt für Materialforschung- und prüfung) methods. The potential use of **1**, **6** and **7** as coloring agents in pyrotechnical mixtures as well as the utilization of **3** and **4** as additives in near infrared (NIR) emitting pyrotechnical formulations was examined.

Keywords: Tetrazoles · Crystal structures · NIR flares · Pyrotechnics · Sensitivities

1 Introduction

The research in the various classes of energetic materials is an ongoing project of interest. Recently several strong achievements were described in the field of high explosives [1,2] as well as pyrotechnics [3,4]. Due to an increase in environmental awareness, today's research in the field of high explosives however is more and more based on the interest of synthesizing so called green energetic materials [5,6]. This trend progressively is also observed for the examination of new materials for pyrotechnic applications [7]. The concept of these compounds rests upon a high nitrogen content in order to promote the release of environmentally benign N_2 after decomposition or degradation. Nitrogen-rich azoles [8] such as triazole- and tetrazole derivatives especially in their ionic forms [9] benefit from a high-nitrogen content to release the desirable N_2. In contrast cyclic and caged nitramines mainly decompose into toxic reaction products like nitro- and nitrosoamines [10]. Next to only releasing N_2, the heat of formation of these compounds is fairly high due to a large number of inherently energetic C–N and N–N bonds. Beside a high heat of formation, a high density, high thermal stability and low sensitivities towards impact, friction and electrical discharge are further goals of interest. An energetic building block which fulfills a multitude of the desired features is 5,5′-bis(1-hydroxytetrazole) [11,12]. After abstracting both highly acidic protons of the dihydroxylated bistetrazole an anion for different energetic salts for applications in the high explosives sector as well as for pyrotechnic compositions is created. The tetrazole N-oxide [13,14] not only reveals a high thermal stability, it also leads to a higher density compared to non-oxidized tetrazoles because of further possibilities to form hydrogen bonds. In this context alkali metal and alkaline earth metal salts of the aforementioned anion are further investigated for applications in the fields of "green pyrotechnics" or primary explosives. Whereas the disodium salt has also been described as an intermediate in the synthesis of dihydroxylammonium 5,5′-bis(tetrazole-1-oxide) (TKX50) [11], the use of dilithium as well as of the alkaline earth metal salts strontium and barium 5,5′-bis(tetrazole-1-oxide) as coloring agents in pyrotechnical mixtures [15] is investigated. Furthermore the dipotassium and dicesium salt are possible additives [16] in pyrotechnical compositions emitting in the near infrared region (NIR) of the electromagnetic spectrum and thus their utilization as ingrediant in NIR flares is examined.

Here we report on the full characterization including the crystal structures of most of the alkali metal salts dilithium (**1**), disodium (**2**), dipotassium (**3**) and dicesium (**4**) as well as the alkaline earth metal salts calcium (**5**), strontium (**6**) and barium (**7**) 5,5′-bis(tetrazol-1-oxide).

---

[a] N. Fischer, T. M. Klapötke, S. Marchner, M. Rusan, S. Scheutzow, J. Stierstorfer
Department Chemie, LMU München, Butenandtstr. 5–13, 81377 München, Germany
*e-mail: tmk@cup.uni-muenchen.de

Supporting information for this article is available on the WWW under http://dx.doi.org/10.1002/prep.201200177 or from the author.

2 Results and Discussion

2.1 Synthesis

The starting material 5,5′-bis(1-hydroxytetrazole) was synthesized according to Ref. [11] and further converted into the various metal salts by adding the respective metal hydroxides to the aqueous solution of 5,5′-bis(1-hydroxytetrazole), which is a divalent acid bearing two highly acidic protons.

The solubility of 5,5′-bis(1-hydroxytetrazole) is fairly good in hot water but poor in cold water. Regarding this, all reactions were carried out under reflux conditions to make sure that all starting material is entirely dissolved. Due to the lower solubility of the alkaline earth metal hydroxides compared to the alkali metal hydroxides in water, an excess of 1.2 equivalents relative to 5,5′-bis(1-hydroxytetrazole) of the respective alkaline earth metal hydroxide were used in order to achieve better yields. After addition of the base, all batches were filtered hot and slowly cooled down to room temperature. Faster crystallization in the cases of the better soluble alkali metal salts could be achieved by reducing the mother liquors under reduced pressure. The synthetic procedure to compounds **1**–**7** is summarized in Scheme 1.

The dilithium (**1**), the disodium (**2**) as well as the calcium (**5**) and the strontium salts (**6**) crystallize as tetrahydrates as evidenced by single-crystal X-ray diffraction. Unfortunately, no single crystals of the potassium (**3**) and the barium salts (**7**) suitable for X-ray diffraction could be obtained, so that the assumption of a crystal water free compound is only based on elemental analysis. The dicesium salt (**4**) crystallizes water free.

2.2 Single Crystal X-ray Structure Analysis

Selected data and parameter of the X-ray determinations are given in Table 1. In the crystal structures od **1**, **2** and **4**–**6** the 5,5′-bis(tetrazole-1-oxide) anion reveals similar structural properties. Due to the torsion angles N4^{i}–C1^{i}–C1–N1 closely varying from 0.3–1.2° the dianion can be considered planar and also the tetrazole rings show no distortion. The N–N and C–N bond lengths of the tetrazole rings vary between the lengths typically observed for N–N single and N=N double bonds as well as C–N single and C=N double bonds. Also the C–C bond connecting the two tetrazole moieties as well as the N–O bonds are between a C–C single and a C=C double bond and a N–O single and N=O double bond, respectively.

Dilithium 5,5′-bis(tetrazole-1-oxide) tetrahydrate (**1**) crystallizes in the triclinic space group $P\bar{1}$ with only one molecular unit (shown in Figure 1) in the unit cell. With an ionic radius of 76 pm, the lithium cations have coordinative bonds to the oxygen atom O1 of the anion (Li1–O1 214.3(2) pm) and also to the nitrogen atoms of the anion (Li1–N4^{i} 218.7(2) pm). The lithium cations in the structure of **1** are similarly coordinated by four hydrate water molecules revealing different bond lengths each. The anion is coordinated by eight hydrate water molecules which are stabilized by hydrogen bond formation.

Disodium 5,5′-bis(tetrazole-1-oxide) tetrahydrate (**2**) (Figure 2) crystallizes in the triclinic space group $P\bar{1}$ with two molecular units per unit cell and a density of 1.767 g cm^{-3}. Each sodium ion is coordinated sixfold by four oxygen atoms of hydrate water molecules and one oxygen as well as one nitrogen atom of the anion. The coordination sphere can be described as a distorted octahedron. A view onto the *a*/*c* plane reveals alternating layers of the dianions and the sodium cations including their coordination sphere. Chains of 5,5′-bis(tetrazole-1-oxide)

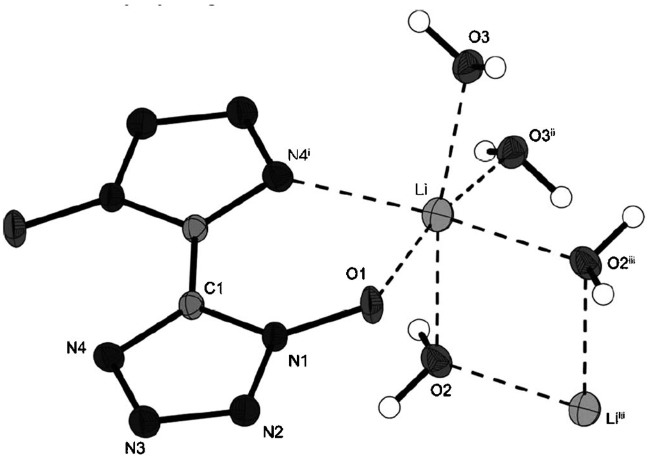

Figure 1. Molecular structure of dilithium 5,5′-bis(tetrazole-1-oxide) tetrahydrate (**1**). Ellipsoids are drawn at the 50% probability level. Coordination distances/pm: Li–O1 214.3(2), Li–N4^{i} 218.7(2), Li–O2 224.1(2), Li–O3 204.7(2), Li–O3^{ii} 232.6(3), Li–O2^{iii} 211.6(3). Symmetry codes: (i) −*x*, −*y*, −*z*; (ii) −*x*, 1−*y*, 1−*z*; (iii) 1−*x*, 1−*y*, 1−*z*. A colored version of the Figure can be found in the Supporting Information.

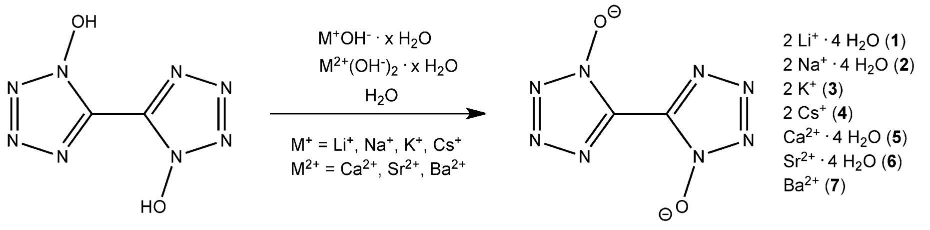

Scheme 1. Synthesis of the alkali metal and alkaline earth metal salts of 5,5′-bis(tetrazole-1-oxide).

Table 1. X-ray data and parameters of **1**, **2** and **4**–**6**.

	1	**2**	**4**	**5**	**6**
Formula	$C_2H_8Li_2N_8O_6$	$C_2H_8N_8Na_2O_6$	$C_2Cs_2N_8O_2$	$C_2CaH_8N_8O_6$	$C_2H_8N_8O_6Sr$
FW/g mol^{-1}	254.04	286.14	433.92	280.24	327.78
Crystal system	triclinic	triclinic	orthorhombic	monoclinic	monoclinic
Space Group	$P\bar{1}$	$P\bar{1}$	*Pbca*	*C*2/*c*	*C*2/*c*
Color/Habit	colorless block	colorless block	colorless rod	colorless block	colorless block
Size/mm	0.30×0.30×0.10	0.17×0.22×0.34	0.09×0.10×0.18	0.18×0.21×0.23	0.17×0.18×0.19
a/pm	528.96(5)	564.23(6)	1148.69(3)	1164.97(15)	1193.80(8)
b/pm	637.41(7)	644.12(8)	1157.51(4)	567.03(4)	574.26(3)
c/pm	825.52(9)	829.25(10)	1319.72(4)	1619.2(2)	1545.6(1)
α/°	105.928(9)	100.108(10)	90	90	90
β/°	98.073(9)	96.877(10)	90	116.988(17)	107.484(7)
γ/°	111.86(1)	112.214(11)	90	90	90
V/pm^3	2390500(500)	2688900(600)	17547300(900)	953100(200)	10106400(1100)
Z	1	1	8	4	4
$\rho_{calcd.}$/g cm^{-3}	1.765	1.767	3.285	1.953	2.154
μ/mm^{-1}	0.161	0.228	8.300	0.701	5.375
F(000)	130	146	1552	576	648
$\lambda_{MoK\alpha}$/pm	71.073	71.073	71.073	71.073	71.073
T/K	173	173	298	173	173
θmin–max/°	4.3, 26.5	4.3, 26.0	4.2, 25.0	4.4, 26.2	4.4, 25.5
Dataset	−6:6; −7:7; −10:10	−6:6; −7:7; −10:10	−13:8; −12:13; −15:14	−12:14; −7:7; −20:20	−14:10; −6:6; −18:18
Reflections collected	2516	2694	7700	2364	2352
Independent refl.	987	1046	1536	950	926
R_{int}	0.024	0.029	0.037	0.022	0.040
Observed reflections	791	803	1242	809	825
Parameters	98	98	128	94	89
R_1 (obs)^a	0.0272	0.0284	0.0225	0.0246	0.0248
wR_2 (all data)^b	0.0703	0.0715	0.0526	0.0661	0.0488
GooF^c	1.01	0.94	1.08	1.03	0.94
Resd. Dens./e pm^{-3}	-0.24×10^{-6}, 0.19×10^{-6}	-0.27×10^{-6}, 0.23×10^{-6}	-0.66×10^{-6}, 1.24×10^{-6}	-0.22×10^{-6}, 0.29×10^{-6}	-0.39×10^{-6}, 0.66×10^{-6}
Device type	Oxford Xcalibur3 CCD	Oxford Xcalibur3 CCD	Oxford Xcalibur3 CCD	Oxford Xcalibur3 CCD	Oxford Xcalibur3 CCD
Solution	SIR-92	SIR-92	SIR-92	SIR-92	SIR-92
Refinement	SHELXL-97	SHELXL-97	SHELXL-97	SHELXL-97	SHELXL-97
Absorption correction	multi-scan	multi-scan	multi-scan	multi-scan	multi-scan
CCDC	906341	906342	906343	906339	906340

a) $R_1=\Sigma||F_o|-|F_c||/\Sigma|F_o|$; b) $wR_2=[\Sigma[w(F_o^2-F_c^2)^2]/\Sigma[w(F_0)^2]]^{1/2}$; $w=[\sigma_c^2(F_o^2)+(xP)^2+yP]^{-1}$ and $P=(F_o^2+2F_c^2)/3$; c) $\mathrm{GooF}=\{\Sigma[w(F_o^2-F_c^2)^2]/(n-p)\}^{1/2}$ (*n* = number of reflections; *p* = total number of parameters).

anions, sodium cations and hydrate water are detected in a view onto the *b*/*c* plane.

Dicesium-5,5′-bis(tetrazole-1-oxide) (**4**) (Figure 3) crystallizes in the orthorhombic space group *Pbca* with a density of 3.285 g cm^{-3}. The unit cell contains eight molecular units. Each cesium atom is coordinated eightfold by four oxygen atoms and four nitrogen atoms. The coordination sphere can be described as a distorted cube. A view along the *c* axis presents alternating layers of the dianions and cesium cations, which are arranged in a zig-zag pattern.

Calcium 5,5′-bis(tetrazole-1-oxide) tetrahydrate (**5**) (Figure 4) crystallizes in the monoclinic space group *C*2/*c* with four molecular units per unit cell and a density of 1.953 g cm^{-3}. Calcium is coordinated eightfold by four water molecules as well as two oxygen atoms and two nitrogen atoms of two different 5,5′-bis(tetrazole-1-oxide) anions each which all together form a distorted dodecahedron. The packing parallel to the *a*/*b* planes can be described as alternating layers of calcium, water and the dianions. Along the *c* axis chains of calcium and water molecules are formed.

Strontium 5,5′-bis(tetrazole-1-oxide) tetrahydrate (**6**) (Figure 5) crystallizes very similar to **5** also in the monoclinic space group *C*2/*c* with four formula units in the unit cell. Compared to the ionic interaction in the structure of **5**, the different sizes of the ions and also the minor difference of the electronegativity (EN) of the strontium ion lead to collectively larger ionic interactions between Sr and N as well as Sr and O.

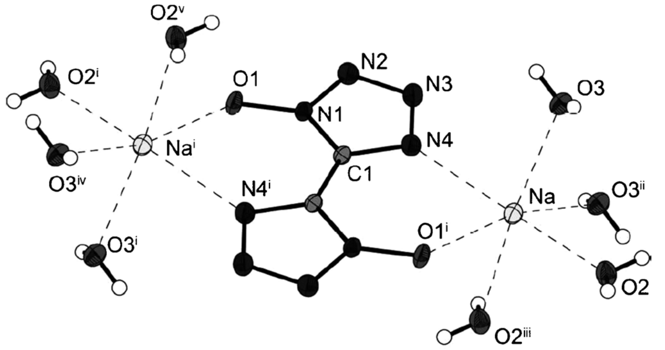

Figure 2. Extended molecular structure of disodium 5,5′-bis(tetrazole-1-oxide) tetrahydrate (**2**). Ellipsoids are drawn at the 50% probability level. Coordination distances/pm: Na–O2 235.88(15), Na–O3 234.82(15), Na–N4 241.44(15), Na–O1^{i} 235.96(14), Na–O3^{ii} 241.40(14), Na–O2^{iii} 249.41(17). (Symmetry codes: (i) $-x$, $-y$, $-z$; (ii); $-x$, $1-y$, $1-z$; (iii) $1-x$, $1-y$, $1-z$, (iv); x, $-1+y$,$-1+z$, (v); $-1+x$, $-1+y$, $-1+z$.). A colored version of the Figure can be found in the Supporting Information.

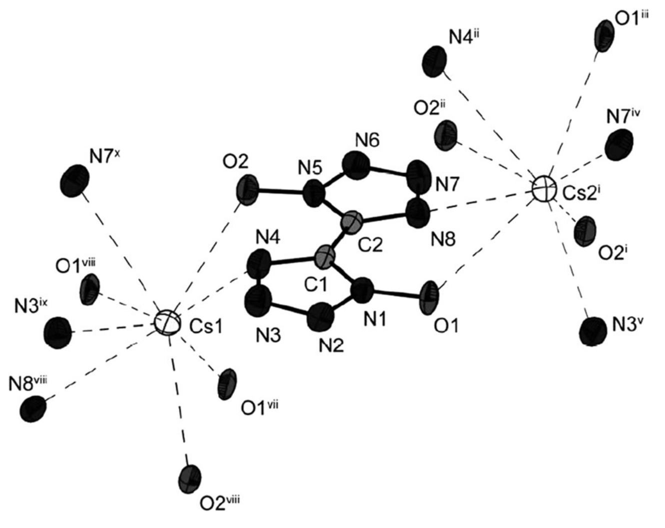

Figure 3. Extended molecular structure of dicesium-5,5′-bis(tetrazole-1-oxide) (**4**). Ellipsoids are drawn at the 50% probability level. Coordination distances/pm: Cs1–O1^{viii} 308.3(3), Cs1–O1^{vii} 314.6(3), Cs1–O2 305.1(3), Cs1–O2^{viii} 315.5(3), Cs1–N3^{ix} 327.4(4), Cs1–N4 328.4(4), Cs1–N7^{x} 339.5(4), Cs1–N8^{viii} 332.4(4), Cs2^{i}–O1 313.1(4), Cs2^{i}–O1^{iii} 326.0(4), Cs2^{i}–O2^{ii} 312.5(3), Cs2^{i}–N8 331.2(4), Cs2^{i}–N3^{v} 331.1(4), Cs2^{i}–N4^{ii} 331.7(4), Cs2^{i}–N7^{iv} 327.5(4), Cs2^{i}– O2^{i} 323.3(3). Symmetry codes: (i) $0.5-x$, $1-y$, $-0.5+z$; (ii) $1-x$, $1-y$, $-z$; (iii) $1-x$, $0.5+y$, $-0.5-z$; (iv) $0.5+x$, y, $-0.5-z$; (v) x, $0.5-y$, $-0.5+z$; (vi) $-0.5+x$, $0.5-y$, $-z$; (vii) $0.5-x$, $-0.5+y$, z; (viii) x, $0.5-y$, $0.5+z$; (ix) $-0.5+x$, y, $0.5-z$; (x) $0.5-x$, $1-y$, $0.5+z$. A colored version of the Figure can be found in the Supporting Information.

Comparing the coordination geometry of **5** with that of **6** one can see that both cations exhibit a highly distorted octahedral coordination sphere consisting of four hydrate water molecules and two further oxygen atoms of the anions.

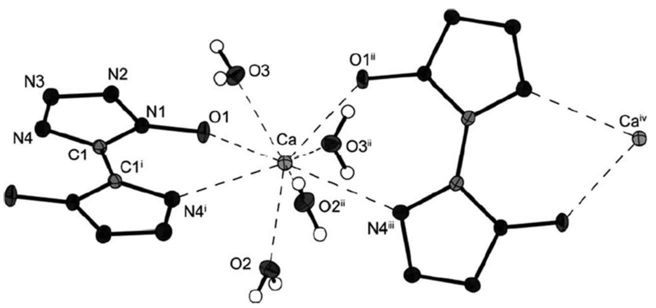

Figure 4. Extended molecular structure of calcium 5,5′-bis(tetrazole-1-oxide) tetrahydrate (**5**). Ellipsoids are drawn at the 50% probability level. Coordination distances/pm: Ca–O1 247.91(12), Ca–O2 236.97(14), Ca–O3 239.96(13), Ca–N4i 266.45(14). Symmetry codes: (i) $1.5-x$, $0.5-y$, $-z$; (ii) 2 $-x$, y, $0.5-z$; (iii) $0.5+x$, $0.5-y$, $0.5+z$; (iv) $2.5-x$, $0.5-y$, $1-z$. A colored version of the Figure can be found in the Supporting Information.

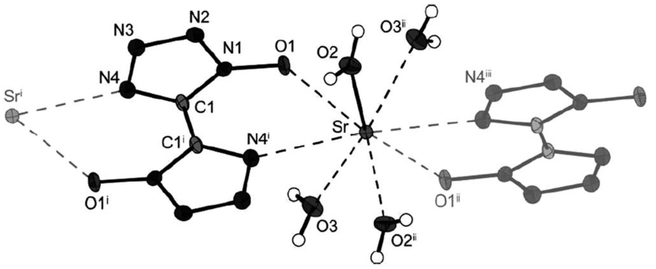

Figure 5. Extended molecular structure of strontium 5,5′-bis(tetrazole-1-oxide) tetrahydrate (**6**). Ellipsoids are drawn at the 50% probability level. Coordination distances/pm: Sr1–N4^{i} 275.1(4), Sr1–O1 257.6(2), Sr1–O2/Sr1–O2^{ii} 252.2(2), Sr1–O3/Sr1–O3^{ii} 254.3(2). Symmetry codes: (i) $-x$, $2-y$, $-z$; (ii) $-x$, y, $0.5-z$; (iii) x, $2-y$, $0.5+z$. A colored version of the Figure can be found in the Supporting Information.

2.3 IR Spectroscopy

Both IR- and Raman spectroscopy can be consulted for the identification of the 5,5′-bis(tetrazole-1-oxide) salts **1**–**7**. The assignment of absorptions to the different functional groups is based on the values given in literature [17]. The most intensive absorption band in the Raman spectra is the symmetrical stretching mode between the C–C linked tetrazole rings at around 1627–1586 cm^{-1}. The typical ring vibrations of the 5,5′-bis(tetrazole-1-oxide) anion are observed at around 1690–1640 cm^{-1} (γ(CN)) and 1440–700 cm^{-1} (ν(NN), ν(NCN), δ (aromatic tetrazole-oxide ring), δ (NCN)), which partially are in the fingerprint region. Further absorptions based on the N–O valence vibration are visible in the range of 1250–1230 cm^{-1}. All IR spectra additionally show O–H stretching vibrations in the range of 3600–3100 cm^{-1} indicating the presence of the crystal water or moisture.

2.4 Sensitivities and Thermal Stability

With impact sensitivities of 27–40 J, compounds **1**, **5** and **6** can be classified as less sensitive. The sodium salt **2** can be even considered as insensitive towards impact with a value higher than 40 J. These low sensitivities can be attributed probably to the presence of crystal water. The determined values of 2 J (**3**, **4**) and 12 J (**7**) indicate, that these salts are regarded as very sensitive (**3**, **4**) or sensitive towards impact (**7**) respectively, which presumably is due to the fact, that these salts crystallize solvent free.

For the friction sensitivity nearly the same trends as for the impact sensitivity can be observed.

Therefore, the sodium (**2**) and strontium (**6**) salts can be considered as less sensitive with regard to their friction sensitivities of 360 N. Compound **1** is regarded as sensitive (324 N) towards friction. Surprisingly, the calcium salt **5** is fairly friction sensitive (56 N) although it is less sensitive towards impact comparable to **1** and **6**. The potassium (**3**), cesium (**4**) and barium salts (**7**) however follow the observed trend, like the friction sensitivities (2, 2 and 12 N) show. Therefore, compounds **3** and **4** have to be classified as very sensitive and compound **7** as sensitive towards friction.

Except compounds **5** (0.2 J) and **7** (0.1 J) all values for the sensitivity towards electrical discharge (ESD) reach from 0.5 J for the strontium salt **6** to 1 J for the lithium salt **1** (**1**: 1.0, **2**: 0.7, **3**: 0.7, **4**: 0.7, **6**: 0.5) implying only low ESD sensitivities.

In order to determine the melt- and decomposition temperatures as well as the dehydration temperatures of the partially crystal water containing salts of **1**–**7** differential scanning calorimetry measurements (DSC) were carried out. All experiments were performed in covered aluminum containers (about 1.5 mg of each energetic material) with a hole (0.1 mm) in the lid for gas release and a nitrogen flow of 20 mL per minute with a Linseis PT 10 DSC [18] calibrated by standard pure indium and zinc at a heating rate of 5 K min^{-1}. The decomposition temperatures are given as absolute onset temperatures.

The decomposition temperatures of the investigated alkali salts **1**–**4** (**1**: 225 °C, **2**: 330 °C, **3**: 335 °C, **4**: 314 °C) as well as the alkaline earth metal salts **5**–**7** (**5**: 300 °C, **6**: 300 °C, **7**: 290 °C) lie in the vicinity of 300 °C except for the dilithium salt **1**, which already decomposes at 225 °C.

The hydrated compounds **1**, **2**, **5** and **6** also show endothermic steps based on the loss of crystal water. Dependent on the geometrical parameters of the crystal structure and its coordination of water the loss is either single or multi stage. In the cases of **5** (144 °C) and **6** (132 °C) the dehydration can be observed as single step, whereas compounds **1** (104, 178 °C) and **2** (124, 154, 180 °C) show two and three endothermic signals indicating a stepwise dehydration of the salt. The barium salt **7** shows no endothermic signal in its DSC curve although the low sensitivity towards impact and friction indicates inclusion of crystal water. This finding however was proved by elemental analysis, which rather indicates a crystal water free structure. Unfortunately also no X-ray structure of the compound could be obtained to ascertain the inclusion or the lack of crystal water molecules in this compound.

In order to determine the exact amount of released crystal water in any of the salts, thermogravimetrical measurements had to be accomplished.

2.5 Dipotassium (3) and Dicesium 5,5′-Bis(tetrazole-1-oxide) (4) as Additives in Near Infrared (NIR) Pyrotechnic Compositions

For the development of night vision devices new pyrotechnic formulations emitting in the NIR region of the electromagnetic spectrum are of major interest. The mainly used spectral region for night vision detection is in the range of 700 to 1000 nm [19]. NIR pyrotechnics find therefore their applications in clandestine night operations and are used for instance as hand-held signal flares or parachute flares to illuminate large areas or aiding in emergency landings of aircrafts. IR illuminants are specified by *radiometric* measurements. Important radiometric parameters are the ‘radiant intensity’ and the introduced ‘concealment index’.

The concealment index χ gives the ratio of the emitted NIR radiation to the emitted visible light (Equation (1)).

$$\chi = \frac{I_{\mathrm{NIR}}}{I_{\mathrm{VIS}}} \tag{1}$$

with $\lambda_{\mathrm{NIR}} = 700–1000$ nm and $\lambda_{\mathrm{VIS}} = 400–700$ nm. It is favored to obtain a high concealment index χ, which means a high NIR emission, and low emission in the visible area. A commonly known disadvantage of many conventional compositions is the high emission of visible light which leads by mischance to a low concealment index. Therefore, compounds which burn with an invisible diffuse flame and furthermore produce large amounts of nitrogen to disseminate condensed reaction products are favored additives in NIR formulations.

For pyrotechnic formulations the following compounds were used: Epon 828 (70%), Epicure 3140 (30%) (binder system) and silicon (mesh 250). Hexamine, potassium nitrate and cesium nitrate were received from Sigma–Aldrich, pulverized separately in a ball mill from Harbor Freight Tools for several hours, sieved and dried at 60 °C for at least 12 h prior to use. All compounds were mixed in a mortar and prepared as 50 g (5 × 10 g) batches according to the respective weight percentages of the formulations given in Table 2. 10 g of the composition was pressed with 2–3 t in a 54PM250 hydraulic press using a corresponding 20 mm die set from Maassen GmbH.

Radiometric emissive properties of the formulations were characterized using a *HR2000 + ES* spectrometer with an ILX511B linear silicon CCD-array detector and included soft-

Table 2. Sensitivities and thermal behavior of **1**–**7**.

IS/J	FS/N	ESD/J	T_{dehydr}/°C	T_{dec}/°C
40	324	1.00	104, 178	225
>40	360	0.70	124, 154, 180	330
2	20	0.70	–	335
2	60	0.70	–*	314
27	56	0.20	144	300
30	360	0.50	132	300
12	216	0.50	–	290

* no crystal water contained

Table 3. Composition of pyrotechnic formulations containing dipotassium and dicesium 5,5′-bis(tetrazole-1-oxide) **3** and **4** as well as the reference compositions 1 and 2.

/wt-% in form.	Ref. 1	Ref. 2	BTO1	BTO2
KNO_3	70	30	70	30
$CsNO_3$	–	40	–	40
Hexamine	16	16	11	15
3	–	–	5	–
4	–	–	–	1
Silicon	10	10	10	10
Binder	4	4	4	4

ware from Ocean Optics. The spectrometer comprises a wavelength region from 200–1100 nm, in which the measurements for NIR calculations were in the range of 400–1100 nm. The standard integration time was 100 ms and the average scan time 35 s. Radiometric data obtained from the spectrometer were normally given in counts and converted to Watts per steradian (W/sr) and Candela (Cd) with an in-house Matlab program. The distance between detector and NIR pellet was 1 m. To assess the utility of **3** and **4** as ingredients in NIR pyrotechnic compositions, two formulations BTO1 and BTO2 were prepared and the radiometric emissive properties measured and compared to reference compositions 1 and 2, which are currently used compositions [19] containing cesium and/or potassium nitrate as oxidizer (Table 3).

The average weight of the BTO1 pellets was 9.9 g at a density of 1.68 g cm^{-1} and for BTO2 pellets 9.8 g at a density of 1.71 g cm^{-1}, respectively. Both compositions are insensitive against friction, impact, and electric discharge (360 N, 40 J, 1.5 J). Due to the surprisingly poor burning behavior, only two compositions were tested whereas the amount of **4** in composition 2 was reduced to 1 %. The size of the observed flame for BTO1 and 2 was diminutive compared to the flame surface of both references. The maximum intensity of 20 g of reference 1 was about 13 W/sr with a concealment index of 34 and a burning time of 25 s to 30 s. The maximum intensity of reference 2 was about 12 W/sr for 20 g of the composition, a concealment index of around 60 and a burning time of 30 s. The maximum intensities of BTO1 (20 g flare) was around 5 W/sr with a concealment index of 25 and a burning time of larger than 30 s, and for BTO2 around 15 W/sr (20 g), a concealment index of 33 and a burning time of 33 s, respectively (Figure 6, Figure 7).

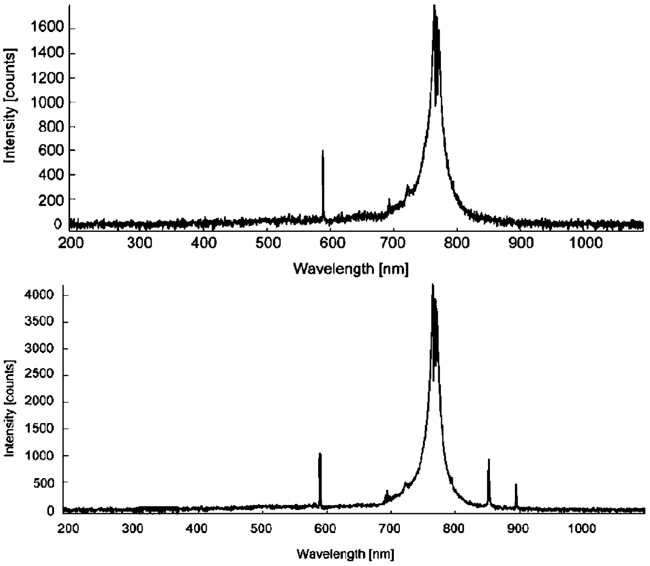

Figure 6. Intensity plots of formulations BTO1 (20 g) and BTO2 (10 g).

Although the burning times of both formulations are high, the maximum intensity values in BTO1 containing 5 % of **3** are very low. The value for the formulation BTO2 containing only 1 % of **4** are slightly better than the values obtained for reference 2.

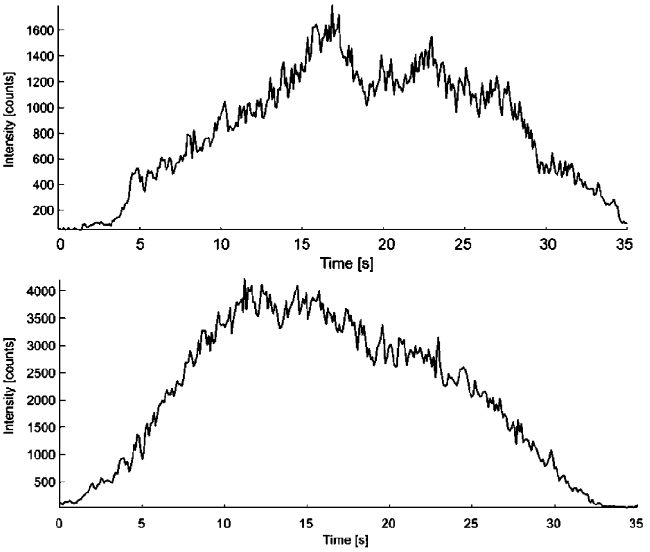

Figure 7. Burning time plots of formulations BTO1 (20 g) and BTO2 (10 g).

2.6 Pyrotechnic Compositions using Strontium (6) and Barium 5,5′-Bis(tetrazole-1-oxide) (7) as Coloring Agents

In order to obtain pyrotechnics with high color brilliance it is necessary to avoid the generation of smoke during the combustion. Therefore, compounds with high nitrogen content are suitable as coloring agents [20,21]. Due to the formation of nitrogen as main decomposition product these compounds are additionally promising substances in the development of ecologically friendly pyrotechnic. Therefore investigations of several pyrotechnical mixtures with strontium and barium 5,5′-bis(tetrazole-1-oxide) were performed.

Table 4. Composition of pyrotechnical formulations containing **6** as red coloring agent.

/wt-%	Sr-control	Sr-BTO_1	Sr-BTO_2	Sr-BTO_3	Sr-BTO_4
MBTO	–	40	43	39	39
$Sr(NO_3)_2$	39.3	–	–	–	–
NH_4NO_3	–	45	–	–	41
ADN	–	–	42	41	–
$KClO_4$	9.8	–	–	–	–
Mg	29.4	8	8	8	8
PVC	14.7	–	–	5	5
VAAR	6.8	7	7	7	7

Several pyrotechnic formulations of **6** and **7** were investigated and compared to the US Army's in-service green (M125A1 Ba-control) and red (M126A1 Sr-control) burning compositions (Table 4 and Table 5). The pyrotechnical compositions were prepared by mixing all substances, except the binder, in a mortar. Then the binder, a solution of 25% vinyl alcohol acetate resin (VAAR), was added. The mixtures of 0.6 g each were formed by hand and dried under high vacuum for three hours. The controlled burn down was filmed with a digital video camera recorder (SONY, DCR-HC37E). The performance of each composition has been evaluated with respect to color emission, smoke generation and the amount of solid residues. Spectrometric measurements were performed using a *HR2000+ES* spectrometer with an ILX511B linear silicon CCD-array detector and included software from Ocean Optics with a detector-sample distance of 1 meter. The dominant wavelength and spectral purity was measured based on the 1931 CIE method using illuminant C as the white reference point. 5 samples were measured for each formulation and all given values are averaged based on the full burn of the mixture. **6** and **7** were used as red and green coloring agents. Ammonium nitrate or ammonium dinitramide (ADN) and magnesium or boron were used as oxidizer and fuel, respectively. In Table 4 and Table 5 the content of the compositions (mass percent) is summarized.

The formulation Sr-BTO_1 consists of 40% of the metal salt, 45% of NH_4NO_3, 8% of magnesium and 7% of binder and burned fast with a red flame color (Color figures are shown in the Supporting Information). Some smoke was produced and some residues could be observed. The compositions Sr-BTO_2 and Sr-BTO_3 contain 43% and 39% of the Sr-salt, 42% and 41% of ammonium dinitramide (ADN) as oxidizer, 8% of magnesium as fuel for both and 5% of poly(vinyl chloride) (PVC) as chlorine source in the case of Sr-BTO_3 and 7% of binder. Both compositions burned smokeless with an intense red flame color and almost no residues remained. The composition Sr-BTO_4 with 39% of the metal salt, 41% of ammonium nitrate, 8% of magnesium, 5% of PVC and 7% of binder burned with a red flame

Table 5. Composition of pyrotechnical formulations containing **7** as green coloring agent.

/wt-%	Ba-control	Ba-BTO_1	Ba-BTO_2	Ba-BTO_3	Ba-BTO_4
MBTO	–	43	43	43	40
$Ba(NO_3)_2$	46	–	–	–	–
NH_4NO_3	–	42	42	–	42
ADN	–	–	–	42	–
Mg	33	–	8	8	7
B	–	8	–	–	–
PVC	16	–	–	–	4
VAAR	5	7	7	7	7

color and no smoke and almost no residues could be observed.

In the case of the green-burning compositions, formulations Ba-BTO_1 and Ba-BTO_2 consist of 43 % of the barium salt, 42 % of ammonium nitrate and 7 % of binder. Composition Ba-BTO_1 contains 8 % of amorphous boron and Ba-BTO_2 8 % of magnesium as fuel. The formulation Ba-BTO_3 has the same composition like Ba-BTO_2 except the oxidizer. In Ba-BTO_3 ADN is used instead of NH_3NO_3. Formulation Ba-BTO_4 consists of 40 % of the metal salt, 42 % of NH_3NO_3, 7 % of magnesium, 4 % of PVC and 7 % of binder. All compositions burned smokeless. While compositions Ba-BTO_3 and Ba-BTO_4 showed no residues, after the burn down of formulations Ba-BTO_1 and Ba-BTO_2 some solid residues remained. The first formulation Ba-BTO_1 showed a pale-green flame color. Ba-BTO_2 and Ba-BTO-4 showed green flame colors and sparkles. Ba-BTO-3 revealed an intense green flame color.

In the Table 6 and Table 7 the measured burning times and the dominant wavelength and spectral purity values of the tested and control formulations are summarized.

The Sr-containing formulations of 0.6 g each show burning times from 3 to 5 s and are in the range of the Sr-control formulation, which revealed a burning time of 4 s. The compositions Sr-BTO_2 and Sr-BTO_3 with ADN as oxidizer show high spectral purities of 96 % and of 98 %, which exceed the spectral purity of the Sr-control of 91 %. In contrast the formulations with NH_4NO_3 as oxidizer show lower spectral purities of 62 % and of 66 %. The color values (x, y) of the investigated formulations as well as those of the Sr-control are plotted in the 1931 CIE chromaticity diagram (Figure 8). As can be seen in the diagram, the position of the color values is shifted furthest to the red boundary of the diagram and therefore Sr-BTO_3 is the best performing formulation.

In the case of the Ba-containing formulations the burning times are in the range of 4 to 7 s and hence are higher than the burning time of the Ba-control of 3 s. Compositions Ba-BTO_1 and Ba-BTO_3 show the highest spectral purities of 79 % and of 85 %, however the color values of Ba-BTO_1 are rather in the white region of the CIE 1931 di-

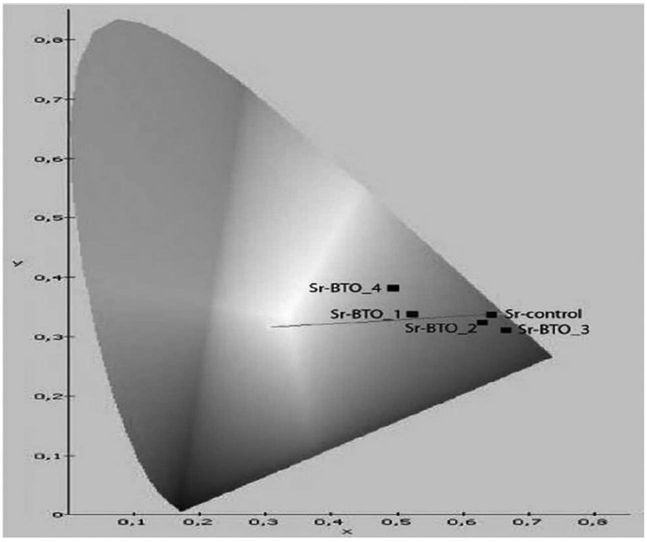

Figure 8. Color values of Sr-containing formulations in the CIE 1931 diagram. A colored version of the Figure can be found in the Supporting Information.

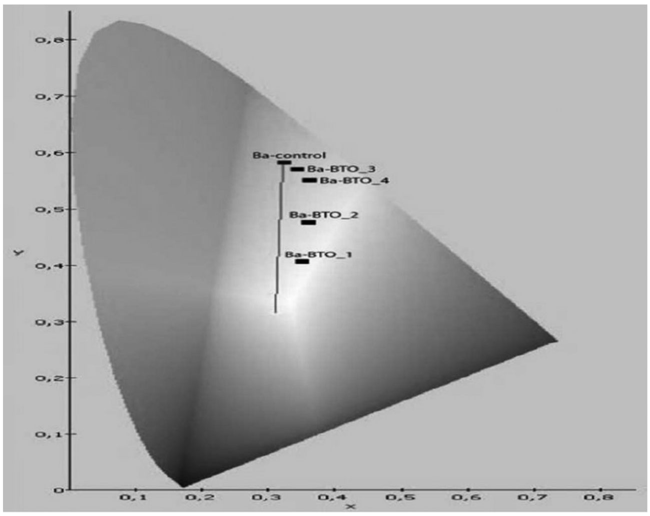

Figure 9. Color values of Ba-containing formulations in the CIE 1931 diagram. A colored version of the Figure can be found in the Supporting Information.

Table 6. Performance of Sr-containing formulations.

	Sr-control	Sr-BTO_1	Sr-BTO_2	Sr-BTO_3	Sr-BTO_4
Burning time/s	4	5	5	4	3
Dominant wavelength/nm	617	604	600	614	592
Spectral purity/%	91	62	96	98	66

Table 7. Performance of Ba-containing formulations.

	Ba-control	Ba-BTO_1	Ba-BTO_2	Ba-BTO_3	Ba-BTO_4
Burning time/s	3	4.5	7	4	5
Dominant wavelength/nm	558	570	565	559	560
Spectral purity/%	75	79	61	85	42

agram which is in good accordance to the visual observation of the burning of Ba-BTO_1 (Figure 9). The position of the color values of Ba-BTO_3 is close to that of the Ba-control, but the spectral purity with a value of 85 % is higher. The formulations Ba-BTO_2 and Ba-BTO_4 reveal with 61 % and 42 % lower spectral purities, therefore among the investigated BaBTO-containing compositions the formulation Ba-BTO_3 is the best performing one.

3 Experimental Section

Caution! The herein described alkali and alkaline earth metal salts are energetic materials and show increased sensitivities towards shock and friction, especially if crystal water free or dehydrated. Therefore, proper safety precautions (safety glass, face shield, earthed equipment and shoes, Kevlar® gloves and ear plugs) have to be applied while synthesizing and handling the described compounds.

All chemicals and solvents were employed as received (Sigma–Aldrich, Fluka, Acros). ^{1}H and ^{13}C NMR spectra were recorded using a JEOL Eclipse 270, JEOL EX 400 or a JEOL Eclipse 400 instrument. The chemical shifts quoted in ppm in the text refer to typical standards such as tetramethylsilane (^{1}H, ^{13}C). To determine the melting and decomposition temperatures of the described compounds a Linseis PT 10 DSC (heating rate 5 K min^{-1}) was used. Infrared spectra were measured using a Perkin–Elmer Spectrum One FT-IR spectrometer as KBr pellets. Raman spectra were recorded on a Bruker MultiRAM Raman Sample Compartment D418 equipped with a Nd-YAG-Laser (1064 nm) and a LN-Ge diode as detector. Mass spectra of the described compounds were measured at a JEOL MStation JMS 700 using FAB technique. To measure elemental analyses a Netsch STA 429 simultaneous thermal analyzer was employed.

The low temperature determination of the crystal structures of **1**, **2** and **4–6** were performed with a Oxford Xcalibur3 diffractometer with a Spellman generator (voltage 50 kV, current 40 mA) and a KappaCCD detector. The data collection and reduction were carried out using the CrysAlisPro software [22]. The structures were solved either with SIR-92 [23] or SHELXS-97 [24], refined with SHELXL-97 [25] and finally checked using the Platon [26] software integrated in the WinGX [27] software suite. The non-hydrogen atoms were refined anisotropically and the hydrogen atoms were located and freely refined. The absorptions were corrected by a Scale3 Abspack multi-scan method [28].

The impact sensitivity tests were carried out according to STANAG 4489 [29] modified instruction [30] using a BAM (Bundesanstalt für Materialforschung) drophammer [31] The friction sensitivity tests were carried out according to STANAG 4487 [32] modified instruction [33] using the BAM friction tester. The classification of the tested compounds results from the "UN Recommendations on the Transport of Dangerous Goods" [34]. Additionally all compounds were tested upon the sensitivity towards electrical discharge using the Electric Spark Tester ESD 2010 EN [35].

3.1 General Procedure for Alkali Metal Salts

5,5′-Bis(1-hydroxytetrazole) dihydrate (2.06 g, 10 mmol) was suspended in water (80 mL). The mixture was heated to reflux to obtain a clear solution. The alkali metal hydroxide (20 mmol) was added and the solution was cooled down to room temperature causing the precipitation of the salts, all of which only show moderate water solubility. In some cases the mother liquors had to be concentrated on a rotary evaporator to app. 60 % of their original volume to initiate precipitation of the products.

Dilithium 5,5′-Bis(tetrazole-1-oxide) Tetrahydrate (1): The colorless crystalline precipitate was filtered and 2.11 g of **1** (8.31 mmol, 83 %) were obtained.

DSC (5 K min^{-1}): 104, 178 °C (dehydr.), 225 °C (dec.). IR (KBr, cm^{-1}): $\tilde{\nu}=3538$ (s), 3311 (vs), 2725 (w), 2187 (w), 2021 (w), 1669 (s), 1434 (s), 1368 (m), 1243 (s), 1181 (m), 1064 (m), 1009 (m), 757 (m), 704 (m), 618 (m), 509 (w); Raman (1064 nm, 300 mW, 25 °C, cm^{-1}): $\tilde{\nu}=1627$ (100), 1603 (4), 1481 (2), 1248 (15), 1150 (11), 1130 (7), 1019 (5), 791 (2), 745 (1), 620 (1), 423 (2), 411 (2). ^{1}H NMR (DMSO-d_6, 25 °C, ppm): $\delta=4.56$. ^{13}C NMR (DMSO-d_6, 25 °C, ppm): $\delta=135.5$. MS (FAB$^-$) $m/z=169.1$ ($C_2HN_8O_2^-$); EA ($C_2H_8N_8O_6Li_2$, MW 254.02): calcd.: C 9.46, H 3.17, N 44.11 %; found: C 9.97, H 2,99, N 44.42 %; BAM drophammer: 40 J; friction tester: 324 N; ESD: 1.0 J.

Disodium 5,5′-Bis(tetrazole-1-oxide) Tetrahydrate (2): Filtration of the colorless crystalline precipitate yielded 2.30 g (8.04 mmol, 80 %) of **2**.

DSC (5 K min^{-1}): 124, 154, 180 °C (dehydr.), 330 °C (dec.). IR (KBr, cm^{-1}): $\tilde{\nu}=3496$ (vs), 3404 (vs), 3308 (s), 3269 (s), 2192 (w), 1672 (m), 1423 (s), 1382 (w), 1359 (w), 1239 (s), 1178 (m), 1149 (w), 1067 (m), 1007 (m), 755 (m), 718 (w), 656 (m), 620 (m), 501 (m); Raman (1064 nm, 300 mW, 25 °C, cm^{-1}): $\tilde{\nu}=1605$ (100), 1581 (3), 1468 (2), 1248 (13), 1154 (11), 1131 (4), 1016 (4), 791 (3), 614 (1), 410 (2). ^{1}H NMR (DMSO-d_6, 25 °C, ppm): $\delta=3.43$. ^{13}C NMR (DMSO-d_6, 25 °C, ppm): $\delta=134.7$; EA ($C_2H_8N_8O_6Na_2$, MW 286.11): calcd.: C 8.40, H 2.82, N 39.16 %; found: C 8.99, H 2.76, N 38.79 %; BAM drophammer: >40 J; friction tester: 360 N; ESD: 0.7 J.

Dipotassium 5,5′-Bis(tetrazole-1-oxide) (3): The precipitate was filtered to yield 2.15 g (8.73 mmol, 87 %) of **3** as slightly yellow octahedral crystals.

DSC (5 K min^{-1}): 335 °C (dec.). IR (KBr, cm^{-1}): $\tilde{\nu}=3496$ (s), 3407 (s), 3252 (m), 2165 (w), 1663 (w), 1637 (w), 1510 (w), 1409 (s), 1356 (m), 1234 (vs), 1164 (s), 1058 (m), 997 (m), 732 (m), 713 (w), 614 (w), 502 (m); Raman (1064 nm, 300 mW, 25 °C, cm^{-1}): $\tilde{\nu}=2012$ (1),1605 (100), 1458 (5), 1240 (27), 1142 (6), 1131 (9), 1118 (17), 1000 (11), 781 (27), 741 (2), 620 (8); 434 (4), 411 (6), 285 (7). ^{1}H NMR (DMSO-d_6, 25 °C, ppm): $\delta=4.67$. ^{13}C NMR (DMSO-d_6, 25 °C, ppm): $\delta=140.0$. MS (FAB$^-$): $m/z=169.0$ ($C_2HN_8O_2^-$); EA ($C_2N_8O_2K_2$, MW

246.27): calcd.: C 9.75, N 45.50 %; found: C 10.19,N 45.21 %; BAM drophammer: 2 J; friction tester: 20 N; ESD: 0.7 J.

Dicesium 5,5′-Bis(tetrazole-1-oxide) (4): After filtration of the precipitate 3.92 g (9.03 mmol, 90 %) of **4** as colorless crystals could be isolated.

DSC (5 K min^{-1}): 314 °C (dec.). IR (KBr, cm^{-1}): $\tilde{\nu} = 3495$ (vs), 3407 (vs), 2163 (w), 1663 (w), 1409 (s), 1382 (m), 1355 (m), 1234 (m), 1163 (w), 1057 (w), 997 (w), 732 (w), 501 (w), 488 (w); Raman (1064 nm, 300 mW, 25 °C, cm^{-1}): $\tilde{\nu} = 3162$ (1), 1981 (1), 1586 (100), 1447 (3), 1285 (1), 1229 (22), 1187 (1), 1138 (8), 1100 (11), 997 (6), 755 (9), 739 (2), 702 (1), 609 (4), 416 (5). ^{1}H NMR (DMSO-d_6, 25 °C, ppm): $\delta = 4{:}67$. ^{13}C NMR (DMSO-d_6, 25 °C, ppm): $\delta = 134.0$. MS (FAB$^-$): $m/z = 169.0$ ($C_2HN_8O_2^-$); EA ($C_2N_8O_2Cs_2$, MW 206.12): calcd.: C 5.54, N 25.83 %; found: C 5.48, H 0.34, N 23.33 %; BAM drophammer: 2 J; friction tester: 60 N; ESD: 0.7 J.

3.2 General Procedure of Alkaline Earth Metal Salts

5,5′-Bis(1-hydroxytetrazole) dihydrate (2.06 g, 10 mmol) was suspended in water (80 mL). The mixture was heated to reflux in order to dissolve the acid. After obtaining a clear solution the alkaline earth metal hydroxide (24 mmol) was added. The solution was kept boiling for 5 min. followed by filtration of the hot solution. The filtrate was then cooled down to room temperature and the alkali earth metal salts precipitated within a few minutes.

Calcium 5,5′-Bis(tetrazole-1-oxide) Tetrahydrate (5): After filtration of the colorless crystalline precipitate 2.11 g (7.53 mmol, 75 %) of **5** were obtained.

DSC (5 K min^{-1}): 144 °C (dehydr.), 300 °C (dec.). IR (KBr, cm^{-1}): $\tilde{\nu} = 3477$ (vs), 3360 (s), 3241 (s), 2207 (w), 2032 (w), 1678 (w), 1640 (m), 1424 (s),1414 (s), 1358 (w), 1242 (s), 1189 (m), 1152 (w), 1073 (m), 1010 (m), 746 (m), 591 (w), 506 (w); Raman (1064 nm, 300 mW, 25 °C, cm^{-1}): $\tilde{\nu} = 2032$ (1), 1614 (100), 1590 (3), 1469 (2), 1296 (1), 1257 (13), 1158 (9), 1141 (6), 1019 (4), 790 (4), 742 (1), 704 (1), 422 2, 294 (1), 183 (2), 119 (10); EA ($C_2H_8N_8O_6Ca$, MW 280.21): calcd.: C 8.57, H 2.88, N 39.99 %; found: C 8.98, H 2.75, N 39.92 %; BAM drophammer: 27 J; friction tester: 56 N; ESD: 0.2 J.

Strontium 5,5′-Bis(tetrazole-1-oxide) Tetrahydrate (6): The colorless crystalline precipitate was filtered yielding 2.33 g (7.11 mmol, 71 %) of **6**.

DSC (5 K min^{-1}): 132 °C (dehydr.), 300 °C (dec.). IR (KBr, cm^{-1}): $\tilde{\nu} = 3495$ (vs), 3387 (s), 2703 (w), 2198 (w), 2027 (w), 1672 (w), 1627 (m), 1535 (w), 1421 (m), 1412 (s), 1242 (s), 1184 (m), 1069 (m), 1008 (m), 747 (m), 573 (w), 499 (w); Raman (1064 nm, 300 mW, 25 °C, cm^{-1}): $\tilde{\nu} = 1603$ (100), 1466 (3), 1295 (1), 1256 (15), 1154 (10), 1135 (6), 1017 (4), 791 (4), 741 (1), 703 (1); 418 (2). MS (FAB$^-$): $m/z = 169.0$ ($C_2HN_8O_2^-$); EA ($C_2H_8N_8O_6Sr$, MW 327.75): calcd.: C 7.33, H 2.46, N 34.19 %; found: C 7.66, H 2.27, N 34.18 %; BAM drophammer: 30 J; friction tester: 360 N; ESD: 0.5 J.

Barium 5,5′-Bis(tetrazole-1-oxide) Hydrate (7): The precipitate was filtered to yield 2.39 g (7.83 mmol, 78 %) of **7** as a slightly yellow solid.

DSC (5 K min^{-1}): 290 °C (dec.). IR (KBr, cm^{-1}): $\tilde{\nu} = 3435$ (s), 3280 (m), 2010 (w), 1652 (m), 1515 (w), 1425 (s), 1414 (s), 1358 (m), 1236 (vs), 1173 (s), 1050 (m), 1004 (m), 734 (m), 716 (w), 597 (w), 506 (m); Raman (1064 nm, 300 mW, 25 °C, cm^{-1}): $\tilde{\nu} = 3219$ (1), 1613 (100), 1590 (3), 1476 (2), 1464 (1), 1291 (1), 1243 (18), 1143 (6), 1125 (6), 1011 (6), 783 (8), 742 (1), 623 (3), 427 (1), 410 (3); EA ($C_2H_8N_8O_6Ba$, MW 206.12): calcd.: C 7.87, N 36.69 %; found: C 7.32, N 32.83 %; BAM drophammer: > 40 J; friction tester: 216 N; ESD: 0.5 J.

Supporting Information (see footnote on the first page of this article): Colored versions of the Figures.

4 Conclusions

From the experimental study of alkali and alkaline earth metal salts of 5,5′-bis(1-hydroxytetrazole) the following conclusions can be drawn:

By reacting aqueous solutions of 5,5′-bis(1-hydroxytetrazole) with alkali and alkaline earth metal hydroxides, the dilithium (**1**), disodium (**2**), dipotassium (**3**), dicesium (**4**), calcium (**5**) strontium (**6**) and barium (**7**) 5,5′-bis(tetrazole-1-oxide) can be isolated. Due to their only moderate (**1**–**4**) or poor (**5**–**7**) water solubility they either crystallize from their original aqueous mother liquors or after reducing the volume of the mother liquor to approximately 60 %.

The salts studied crystallize in the space groups *P*$\bar{1}$ (**1**, **2**), *Pbca* (**4**) and *C*2/*c* (**5**, **6**) with densities between 1.765 g cm^{-3} for the dilithium salt **1** and 3.285 g cm^{-3} for the dicesium salt **4** either as tetrahydrates (**1**, **2**, **5**, **6**) or water free (**4**). No crystal structures of **3** and **7** were measured; however, their elemental analyses indicate a solvent free crystallization of these salts.

All salts decompose at temperatures higher than 200 °C (**1**: 225 °C, **5**, **6**: 300 °C, **7**: 290 °C) or higher than 300 °C (**2**: 330 °C, **3**: 335 °C, **4**: 314 °C). The (stepwise) loss of crystal water is observed in their DSC curves at 104 and 178 °C (**1**), 124, 154 and 180 °C (**2**), 144 °C (**5**) and 132 °C (**6**) as endothermic events.

If the salts are crystal water free (**3**, **4**), they are highly sensitive towards impact and friction (IS: 2 J; FS 20 N (**3**), 60 N (**4**)). If hydrated the sensitivities are moderate to low (IS: 40 J (**1**, **2**), 12 J (**7**), 30 J (**6**), 27 J (**5**); FS: 360 N (**2**, **6**), 324 N (**1**), 216 (**7**), 56 N (**5**)).

If used as additives in pyrotechnic formulations for NIR flares, compositions containing **3** (BTO1: 5 W/sr, $\chi = 25$) and **4** (BTO2: 15 W/sr, $\chi = 33$) do not reach the radiant intensities and concealment indices observed for the commonly used reference formulations 1 (Ref1: 13 W/sr, $\chi = 34$) and 2 (Ref2: 12 W/sr, $\chi = 60$).

The strontium (**6**) and the barium salt (**7**) were tested in pyrotechnical compositions as red respectively green colorants. The color performance of both formulations containing **6** shows no noteworthy difference. Both mixtures burned with less smoke and some residues remained. Among the formulations containing the barium salt **7**, the composition Ba-BTO_2 with the highest content of the metal salt showed the most intense green flame color and no sparks. Only the Ba-BTO_1 mixture revealed no smoke during the combustion, but residues were observable.

Symbols and Abbreviations

BAM	Bundesanstalt für Materialforschung und -prüfung
BTO	5,5′-bis(tetrazole-1-oxide)
CCDC	Cambridge crystallographic data centre
DSC	differential scanning calorimetry
FW	formula weight/g mol^{-1}
IS	impact sensitivity/J
FS	friction sensitivity/N
ESD	electrostatic discharge/J
EN	electronegativity
GooF	goodness of fit
IR	infrared
$\lambda_{\mathrm{MoK}\alpha}$	X-ray laser wavelength
MS	mass spectrometry
N	nitrogen content/%
NIR	near infrared
NMR	nuclear magnetic resonance
ρ	density/g cm^{-3}
STANAG	standardization agreement
$T_{\mathrm{dec.}}$	decomposition temperature/°C
$T_{\mathrm{dehydr.}}$	dehydration temperature/°C
χ	concealment index
VAAR	vinyl alcohol acetate resin
Z	number of molecular units per unit cell

Acknowledgments

Financial support of this work by the Ludwig-Maximilian University of Munich (LMU), the European Research Office (ERO) of the U.S. Army Research Laboratory (ARL), the Armament Research, Development and Engineering Center (ARDEC) and the Strategic Environmental Research and Development Program (SERDP) under contract nos. W911NF-09-2-0018 (ARL), W911NF-09-1-0120 (ARDEC), W011NF-09-1-0056 (ARDEC) and 10 WPSEED01-002/WP-1765 (SERDP) is gratefully acknowledged. The authors acknowledge collaborations with *Dr. Mila Krupka* (OZM Research, Czech Republic) in the development of new testing and evaluation methods for energetic materials and with *Dr. Muhamed Sucesca* (Brodarski Institute, Croatia) in the development of new computational codes to predict the detonation and propulsion parameters of novel explosives. We are indebted to and thank *Drs. Betsy M. Rice* and *Brad Forch* (ARL, Aberdeen, Proving Ground, MD) and Mr. *Gary Chen* (ARDEC, Picatinny Arsenal, NJ) for many helpful and inspired discussions and support of our work. The authors thank Mr. *Stefan Huber* for the sensitivity measurements. The Cusanuswerk is greatfully acknowledged for the award of a PhD scholarship (M. R.).

References

[1] V. Thottempudi, F. Forohor, D. A. Parrish, J. M. Shreeve, Tris-(triazolo)benzene and Its Derivatives: High-Density Energetic Materials, *Angew. Chem. Int. Ed.* **2012**, *51*, 9881–9885.

[2] L. Liang, H. Huang, K. Wang, C. Bian, S. Chengming; L. Jinhong; L. Ling, Z. Liming; F. Zhao, Z. Zhou, Oxy-bridged bis(1H-tetrazol-5-yl)furazan and its Energetic Salts Paired with Nitrogen-rich Cations: Highly Thermally Stable Energetic Materials with Low Sensitivity, *J. Mater. Chem.* **2012**, *22*, 21954–21964.

[3] E.-C. Koch, V. Weiser, E. Roth, 2,4,6-Trinitrotoluene: A Surprisingly Insensitive Energetic Fuel and Binder in Melt-Cast Decoy Flare Compositions, *Angew. Chem. Int. Ed.* **2012**, *51*, 10038–10040.

[4] E.-C. Koch, A. Hahma, Metal-Fluorocarbon Pyrolants. XIV: High Density-High Performance Decoy Flare Compositions Based on Ytterbium/Polytetrafluoroethylene/Viton®, *Z. Anorg. Allg. Chem.* **2012**, *638,* 721–724.

[5] P. Pagoria, M. Z. A. DeHope, G. Lee, A. Mitchell, P. Leonard, "Green" Energetic Materials Synthesis at LLNL, *15th Seminar New Trends in Research of Energetic Materials*, Pardubice, Czech Republic, April 18–20, **2012**, 55–65.

[6] M. B. Talawar, R. Sivabalan, T. Mukundan, H. Muthurajan, A. K. Sikder, B. R. Gandhe, A. Subhananda Rao, Environmentally Compatible Next Generation Green Energetic Materials (GEMs), *J. Hazard. Mater.* **2009**, *161*, 589–607.

[7] G. Steinhauser, T. M. Klapötke, "Green" Pyrotechnics: A Chemists' Challenge, *Angew. Chem. Int. Ed.* **2008**, *47*, 3330–3347.

[8] H. Gao, J. M. Shreeve, Azole-Based Energetic Salts, *Chem. Rev.* **2011** *111*, 7377–7436.

[9] R. P. Singh, R. D. Verma, D. T. Meshri, J. M. Shreeve, Energetic Nitrogen-Rich Salts and Ionic Liquids, *Angew. Chem. Int. Ed.* **2006**, *45*, 3584–3601.

[10] S. A. Meyer, A. J. Marchand, J. L. Hight, G. H. Roberts, L. B. Escalon, L. S. Inouye, D. K. MacMillan, Up- and Down-Procedure (UDP) Determinations of Acute Oral Toxicity of Nitroso Degradation Products of Hexahydro-1,3,5-trinitro-1,3,5-triazine (RDX), *J. Appl. Toxicol.* **2005**, *25*, 427–434.

[11] N. Fischer, D. Fischer, T. M. Klapötke, D. Piercey, J. Stierstorfer, Pushing the Limits of Energetic Materials – The Synthesis and Characterization of Dihydroxylammonium 5,5′-bistetrazole-1,1′-diolate, *J. Mater. Chem.* **2012**, *22*, 20418–20422.

[12] I. V. Tselinskii, S. F. Mel'nikova, T. V. Romanova, Synthesis and Reactivity of Carbohydroximoyl Azides: I. Aliphatic and Aromatic Carbohydroximoyl Azides and 5-Substituted 1-Hydroxytetrazoles based Thereon, *Russ. J. Org. Chem.* **2001**, *37*, 430–436.

[13] M. Göbel, K. Karaghiosoff, T. M. Klapötke, D. G. Piercey, J. Stierstorfer, Nitrotetrazolate-2N-oxides and the Strategy of N-Oxide Introduction, *J. Am. Chem. Soc.* **2010**, *132,* 17216–17226.

[14] A. M. Churakov, V. A. Tartakovsky, Progress in 1,2,3,4-Tetrazine Chemistry, *Chem. Rev.* **2004**, *104,* 2601–2616.

[15] E.-C. Koch, Special Materials in Pyrotechnics: III. Application of Lithium and its Compounds in Energetic Systems, *Propellants Explos. Pyrotech.* **2004**, *29*, 67–80.

[16] P. A. Jemmett, K. Patel, Enhanced Near Infrared Illuminating Compositions, *36th International Pyrotechnics Seminar*, August 23–29, **2009**, Rotterdam, The Netherlands, pp. 73–86.

[17] M. Hesse, H. Meier, B. Zeeh, S. Bienz, L. Bigler, T. Fox, in *Spektroskopische Methoden in der organischen Chemie*, Vol. 8, Thieme, Stuttgart, New York, **2012**.

[18] http://www.linseis.com.

[19] E.-C. Koch, *Survey on State-of-the-art Near-Infrared Emitting Compositions for Flares and Tracers*, NATO-MSIAC, Belgium, **2009**, and literature therein.

[20] D. E. Chavez, M. A. Hiskey, D. L. Naud, High-Nitrogen Fuels for Low-Smoke Pyrotechnics, *J. Pyrotech.* **1999**, *10*, 17–36.

[21] D. E. Chavez, M. A. Hiskey, High-Nitrogen Pyrotechnic Compositions, *J. Pyrotech.* **1998**, *7*, 11–14.

[22] *CrysAlisPro*, Oxford Diffraction Ltd., Version 171.33.41, **2009**.

[23] A. Altomare, G. Cascarano, C. Giacovazzo, A. Guagliardi, Completion and Refinement of Crystal Structures with SIR92, *J. Appl. Crystallogr.* **1993**, *26*, 343.

[24] G. M. Sheldrick, *SHELXS-97, Program for Crystal Structure Solution*, University of Göttingen, Germany, **1997**.

[25] G. M. Sheldrick, *SHELXL-97*, *Program for the Refinement of Crystal Structures*, University of Göttingen, Germany, **1997**.

[26] A. L. Spek, *PLATON, A Multipurpose Crystallographic Tool*, Utrecht University, Utrecht, The Netherlands, **1998**.

[27] L. J. Farrugia, WinGX Suite for Small-Molecule Single-Crystal Crystallography, *J. Appl. Crystallogr.* **1999**, *32*, 837–838.

[28] Empirical Absorption Correction Using Spherical Harmonics, Implemented in *SCALE3 ABSPACK Scaling Algorithm* (CrysAlisPro Oxford Diffraction Ltd., Version 171.33.41, **2009**).

[29] *NATO Standardization Agreement (STANAG) on Explosives, Impact Sensitivity Tests*, no. 4489, 1st ed., Sept. 17, **1999**.

[30] *WIWEB-Standardarbeitsanweisung 4–5.1.02, Ermittlung der Explosionsgefährlichkeit*, hier der Schlagempfindlichkeit mit dem Fallhammer, Nov. 8, **2002**.

[31] http://www.bam.de.

[32] *NATO Standardization Agreement (STANAG) on Explosive, Friction Sensitivity Tests*, no. 4487, 1st ed., Aug. 22, **2002**.

[33] *WIWEB-Standardarbeitsanweisung 4–5.1.03, Ermittlung der Explosionsgefährlichkeit oder der Reibeempfindlichkeit mit dem Reibeapparat*, Nov. 8, **2002**.

[34] Impact: insensitive $>$40 J, less sensitive 35 J, sensitive 4 J, very sensitive 3 J. Friction: insensitive $>$360 N, less sensitive $=$ 360 N, sensitive $<$360 N, $>$80 N, very sensitive $<$80 N, extremely sensitive $<$10 N. According to the UN Recommendations on the Transport of Dangerous Goods, (+) indicates not safe for transport.

[35] http://www.ozm.cz..

Received: October 23, 2012
Revised: December 21, 2012

Angewandte Chemie International Edition

Energetic Materials Hot Paper

DOI: 10.1002/anie.201405195

Chlorine-Free Pyrotechnics: Copper(I) Iodide as a “Green” Blue-Light Emitter**

Thomas M. Klapötke, Magdalena Rusan, and Jesse J. Sabatini**

Abstract: *The generation of blue-light-emitting pyrotechnic formulations without the use of chlorine-containing compounds is reported. Suitable blue-light emission has been achieved through the generation of molecular emitting copper(I) iodide. The most optimal copper(I) iodide based blue-light-emitting formulation was found to have performances exceeding those of chlorine-containing compositions, and was found to be insensitive to various ignition stimuli.*

The generation of a blue flame in pyrotechnics is very challenging and requires the exact tuning of different parameters such as the specific ratio of the ingredients, reactivity, and combustion temperature.[1] Blue flame colors are obtained by using copper or copper-containing compounds, which in the presence of a chlorine source, produce the blue-emitting species copper(I) chloride (CuCl). This light-emitting species is currently believed to be the best emitter in the blue region of the visible spectrum, ranging from 435 to 480 nm. A series of bands in the region from 428 to 452 nm with additional peaks between 476–488 nm are obtained from this molecular species.[1,2] It has been hypothesized that CuCl is an especially unstable species, and that decomposition occurs at temperatures above 1200 °C. The decomposition is believed to occur in an oxygen-rich flame, producing copper(II) oxide (CuO) and copper(I) hydroxide (CuOH). While CuOH emits in the green region from 525 to 555 nm, CuO emits bands in the red region, which is often observable at the top of blue flames.[3] The theory as to whether CuCl decomposes at 1200 °C has been disputed in a theoretical sense by Sturman. He carried out thermodynamic modeling investigations using the NASA-CEA code revealing that excellent blue flame colors can be obtained at much higher temperatures.[4]

Potassium perchlorate and ammonium perchlorate oxidizers are often employed as the chlorine source in blue-light-emitting flames. Unfortunately, the use of perchlorates in today’s pyrotechnic formulations is discouraged due to environmental concerns.[5] To encourage the production of CuCl, polychlorinated organic compounds such as polyvinyl chloride are commonly employed in blue-light-emitting formulations to provide a large excess of chlorine.[1] In the literature, there are contradictory opinions concerning the amount of toxic polychlorinated organic compounds generated during the combustion of chlorine-containing pyrotechnic formulations. Such toxic compounds include the highly carcinogenic polychlorinated biphenyls (PCBs), polychlorinated dibenzo-*p*-dioxins (PCDDs), and polychlorinated dibenzofurans (PCDFs). Although Fleischer et al.[6] state that low concentrations of PCBs, PCDDs, and PCDFs are generated following fireworks displays, Dyke and Coleman[7] found significantly higher concentrations of these carcinogenic materials following such displays. Given the presence of perchlorates and chlorinated organic compounds in blue-light-emitting compositions, it was of interest to develop formulations of this color that are entirely devoid of these materials.

It was hypothesized that copper(I) iodide (CuI) could serve as an environmentally benign alternative in blue-light emission. Spectroscopically, CuI is known to emit in the blue region at 460 nm,[8] though this emitter has not been known to form a blue light of high quality in pyrotechnic formulations. Presumably, with a CuI-based blue flame, the formation of polyiodated bisphenyls (PIBs) is likely. Fortunately, PIBs are not believed to be associated with health hazards; these materials are also used as contrast agents for radiological purposes in medicine.[9]

In the design of a chlorine-free blue flame, copper iodate ($Cu(IO_3)_2$) was believed to be a suitable oxidizer in CuI-based formulations, as it also can form this light emitter during the combustion process. $Cu(IO_3)_2$ is easy to prepare from potassium iodate and copper nitrate,[10] and is insensitive towards various ignition stimuli. Formulations based on CuCl as a blue-light emitter have been reported to yield a blue flame of the highest quality.[11]

To investigate blue-light-emitting formulations based on copper iodate as the oxidizer and colorant without any additional chlorine-containing compound, we chose Shimizu’s blue-light-emitting formulation[11a] consisting of 68 % potassium perchlorate, 15 % copper, 17 % polyvinyl chloride, and 5 % starch as the control (Table 1), and reinvestigated it using our equipment.

Table 1: Shimizu’s chlorine-containing blue-light-emitting formulation.

	$KClO_4$ [wt %]	Cu [wt %]	PVC [wt %]	Starch [wt %]
Control	68	15	17	5

---

[*] Prof. Dr. T. M. Klapötke, Dr. M. Rusan
Ludwig Maximilian University Munich
Department of Chemistry
Butenandtstrasse 5-13, Haus D, 81377 München (Germany)
E-mail: tmk@cup.uni-muenchen.de
Dr. J. J. Sabatini
Pyrotechnics Technology and Prototyping Division
U.S. Army RDECOM-ARDEC
Picatinny Arsenal, NJ 08706-5000 (USA)
E-mail: jesse.j.sabatini.civ@mail.mil

[**] Financial support of this work by LMU, ARL, ONR, and ARDEC is gratefully acknowledged.

Table 2: Performance and sensitivity of the chlorine-containing control.

	BT [s]	DW [nm]	SP [%]	LI [cd]	LE [cdsg^{-1}]	IS [J]	FS [N]	T_{dec} [°C]
Control	4	475 (552)	61	54	360	8	324	307

The performance of the chlorine-containing control **A** is summarized in Table 2. The burn time (BT), dominant wavelength (DW), spectral purity (SP), luminous intensity (LI), and luminous efficiency (LE) have been determined. The impact sensitivity (IS) and friction sensitivity (FS), as well as the decomposition temperature (T_{dec}) were measured. Although the control yielded an intense blue flame during the combustion process, two dominant wavelength values were detected appearing at 475 nm in the blue region and at 552 nm in the green region. The latter band can be attributed to the formation of CuOH during the combustion process. A spectral purity of 61 % and a luminous intensity of 54 cd were obtained. The control was relatively insensitive toward various ignition stimuli, revealing an impact sensitivity of 8 J, a friction sensitivity of 324 N, and a decomposition temperature of 307 °C.

Formulations using copper iodate and several different fuels such as 5-aminotetrazole, guanidinium nitrate, copper, and starch have been investigated; however, they did not burn efficiently. Either the formulations glowed or they did not yield blue light.

Although 5-aminotetrazole as the sole fuel source did not produce the energy necessary for a combustion reaction, magnesium was added in an effort to raise the formulation's combustion temperature and to facilitate efficient propagation. The compositions of these formulations are summarized in Table 3. Formulation **1**, containing only 53 % copper iodate, exhibited a poor burning behavior, and blue light was not observed. Formulations **2**–**4** burned with a blue flame, with smoke and residues being observed. While formulations **2**–**4** exhibited a reasonable sensitivity to ignition stimuli, the quality of these flames was poor, as all spectral purities were lower than those of the control (Table 4).

Table 3: Formulations **1**–**4**.

	$Cu(IO_3)_2$ [wt %]	5-At [wt %]	Mg [wt %]	Epon 828/Epikure 3140 [wt %]
1	53	35	5	7
2	65	15	15	5
3	75	5	15	5
4	75	12	8	5

Table 4: Performance and sensitivity of formulations **2**–**4**.

	BT [s]	DW [nm]	SP [%]	LI [cd]	LE [cdsg^{-1}]	IS [J]	FS [N]	Grain size [μm]	T_{dec} [°C]
2	5	468 (546)	58	45	375	10	>360	<100	164
3	5	480 (555)	51	76	633	10	>360	<100	167
4	6	465 (532)	56	80	800	8	>360	<100	170

Table 5: Formulations **5**–**8**.

	$Cu(IO_3)_2$ [wt %]	5-At [wt %]	Mg [wt %]	CuI [wt %]	Urea [wt %]	Cu [wt %]	Epon 828/ Epikure 3140 [wt %]
5	65	7	15	8	–	–	5
6	65	7	5	18	–	–	5
7	65	7	5	10	4	–	5
8	65	–	13	10	–	7	5

Compared to these formulations, formulations **5**–**8** contain copper iodide as an additional colorant, with formulation **7** containing urea, and formulation **8** containing copper powder in lieu of 5-aminotetrazole (Table 5). Although the luminous intensities of these formulations were below those of the chlorine-containing control, formulations **6** and **8** were observed to have better spectral purities than the control, with a dominant wavelength in the blue-light-emitting region (Table 6). The large excess of CuI employed in formulation **6** contributed to its enhanced spectral purity. Unfortunately, the composition suffers from a moderate sensitivity to impact.

Table 6: Performance and sensitivity of formulations **5**–**8**.

	BT [s]	DW [nm]	SP [%]	LI [cd]	LE [cdsg^{-1}]	IS [J]	FS [N]	Grain size [μm]	T_{dec} [°C]
A	4	475 (552)	61	54	360	8	324	307	307
5	4	470 (555)	59	67	447	10	>360	<100	173
6	4	473 (555)	65	42	280	5	>360	<100	161
7	3	480 (527)	56	32	160	5	>360	<100	167
8	4	470 (551)	60	41	273	5	>360	<100	170

Jennings-White reported a blue-light-emitting formulation, consisting of 50 % guanidinium nitrate, 20 % parlon, 15 % copper, and 15 % magnesium.[12] Using this formulation as a guide, we prepared and investigated compositions containing copper iodate and guanidinium nitrate (Table 7). The combination of magnesium with two further fuels—urea and copper—was tested. While formulation **9** could not be ignited, formulations **10** and **11** burned efficiently, yielding an intense blue flame. Unlike the previous formalations that provided a CuI-based blue flame, formulations **10** and **11** exhibited no smoke and no residues.

Table 7: Formulations **9**–**11**.

	$Cu(IO_3)_2$ [wt %]	Guanidinium nitrate [wt %]	Mg [wt %]	Urea [wt %]	Cu [wt %]	Epon 828/ Epikure 3140 [wt %]
9	15	50	9	21	–	5
10	20	50	10	–	15	5
11	30	35	9	21	–	5

Formulations **10** and **11** both exhibited longer burn times, higher spectral purities, and higher luminosities than the control. Formulation **10** is particularly noteworthy, as this formulation has a luminous intensity 33 % brighter and a luminous efficiency value three times better than the control formulation. Moreover, formulations **10** and **11** were found to have very low impact and friction sensitivities, with reasonably high decomposition temperatures (Table 8).

Table 8: Performance and sensitivity of formulations **10** and **11**.

	BT [s]	DW [nm]	SP [%]	LI [cd]	LE [cdsg^{-1}]	IS [J]	FS [N]	Grain size [μm]	T_{dec} [°C]
A	4	475 (552)	61	54	360	8	324	307	307
10	6	477 (555)	64	80	1067	>40	>360	<100	198
11	6	476 (525)	63	78	780	>40	>360	<100	180

In addition to the experimental evidence, the CIE chromaticity diagram of formulations **10** and **11** show them to be suitable blue-light emitters (Figure 1).

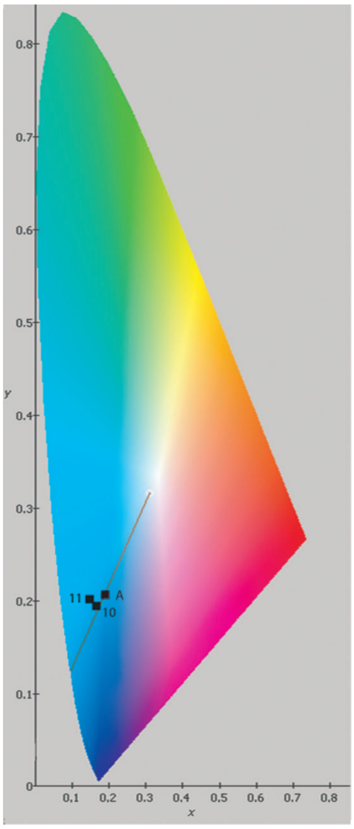

Figure 1. CIE 1931 chromaticity diagram of formulations **A**, **10**, and **11**.

Several blue-light-emitting formulations based on copper(I) iodide as the molecular emitter have been investigated. $Cu(IO_3)_2$ was determined to serve as a suitable oxidizer for achieving blue-light emission based on molecular copper(I) iodide. Only formulations containing magnesium in addition to various high-nitrogen-containing fuels displayed a useful and practical burning behavior. The best results were achieved for mixtures containing copper iodate/magnesium/guanidinium nitrate, with urea or copper serving as an additional fuel source (formulations **10** and **11**). Formulation **10** exhibited the best performance, with a burn time, spectral purity, and luminous output greatly exceeding those of the chlorine-containing control. It can be concluded that for the generation of blue-flame colors, CuCl is not the only suitable blue-light emitter. CuI can also serve this purpose in a properly tuned formulation. This is advantageous from the "greener" pyrotechnics perspective, as the potential formation of highly toxic PCBs, PCDFs, and PCDDs is avoided.

Experimental Section

CAUTION! The mixtures described here are potential explosives, which are sensitive to environmental stimuli such as impact, friction, heat, and electrostatic discharge. While we encountered no problems in handling of these materials, appropriate precautions and proper protective measures (safety glasses, face shields, leather coats, Kevlar gloves, and ear protectors) should be taken when preparing and manipulating these materials.

Copper iodate was purchased from abcr. Copper, potassium perchlorate, urea, 5-aminotetrazole, nitroguanidine, guanidinium nitrate, polyvinyl chloride, magnesium, and copper iodide were purchased from Aldrich, Fluka and Acros, and were used as received. The pyrotechnical compositions were prepared by rigorously grinding all substances in a mortar with a pestle. The mixtures were introduced to Epon 828/Epikure 3140 binder system, mixed by hand with a plastic spatula for 15 min, and ground in a mortar again. Pellets, each 0.6 g, were pressed in one increment using a consolidation dead load of 2000 kg. The pellets were dried overnight in an oven at 60 °C. The controlled burn was filmed with a digital video camera recorder (SONY, DCR-HC37E). The performance of each composition was evaluated with respect to color emission, smoke generation, and the amount of solid residues. Spectrometric measurements were performed using a HR2000 + ES spectrometer with an ILX511B linear silicon CCD-array detector and included software from Ocean Optics with a detector–sample distance of 1 m. The dominant wavelength (DW) and spectral purity (SP) were measured based on the 1931 CIE method using illuminant C as the white reference point. Luminous intensities (LI) and luminous efficiencies (LE) were determined using pellets each weighing 0.6 g. Five samples were measured for each formulation and all given values are averaged based on the full burn of the mixture. Decomposition points were measured with a Linseis PT10 DSC apparatus using heating rates of 5 °C min^{-1}.[13] The impact and friction sensitivities were determined using a BAM drophammer and a BAM friction tester.[14–18] The sensitivities of the compounds are indicated according to the U.N. Recommendations on the Transport of Dangerous Goods (+):[19] impact: insensitive >40 J, less sensitive >35 J, sensitive >4 J, very sensitive 4 J; friction: insensitive >360 N, less sensitive $=360$ N, sensitive <360 N >80 N, very sensitive <80 N, extreme sensitive <10 N.

Received: May 12, 2014

Keywords: blue flame colors · color performance · copper · pyrotechnics · sensitivities

---

[1] J. A. Conkling, C. J. Mocella, *Chemistry of Pyrotechnics: Basic Principles and Theory, 2nd ed.*, Taylor and Francis, Boca Raton, **2011**.

[2] a) B. E. Douda, RDTN 71, Crane, IN: U.S. Naval Ammunition Depot, **1964**; b) K. L. Kosanke, B. J. Kosanke, *Pyrotechnic Chemistry, Journal of Pyrotechnics*, Pyrotechnica, Whitewater, **2004**, Chap. 9.

[3] T. Shimizu, *Fireworks: The art, science and technique*, Tokyo: T. Shimizu, **1981**.
[4] B. T. Sturman, *Propellants Explos. Pyrotech.* **2006**, *31*, 70.
[5] a) United States Environmental Protection Agency, *Interim Health Advisory for Perchlorate*, **2008**, pp. 1–35, http://www.epa.gov/safewater/contaminants/unregulated/pdfs/healthadvisoryperchlorate_interim.pdf; b) C. Hogue, *Chem. Eng. News* **2011**, *89*, 6.
[6] O. Fleischer, H. Wichmann, W. Lorenz, *Chemosphere* **1999**, *39*, 925.
[7] D. Dyke, P. Coleman, *Organohalogen Compd.* **1995**, *24*, 213.
[8] A. P. Hardt, *Pyrotechnics* **2001**, Post Falls, ID: Pyrotechnica Publications.
[9] M. Dugast-Zrihen, D. Meyer, US Patent US005618977A, **1997**.
[10] K. Nassau, A. S. Cooper, J. W. Shiever, B. E. Prescott, *J. Solid State Chem.* **1973**, *8*, 260.
[11] a) T. Shimizu, *Pyrotechnica* **1980**, *6*, 5; b) C. Jennings-White, *Pyro. Guild Int. Bull.* **1988**, *59*, 31; c) T. Shimizu, *Fireworks. The Art, Science and Technique Vol. II* (Ed.: A. Schuman), Pyrotechnica, Austin, **1983**, p. 81.
[12] C. Jennings-White, *Pyrotechnica XV*, Pyrotechnica, Austin, **1993**.
[13] http://www.linseis.com.
[14] NATO standardization agreement (STANAG) on explosives, *impact sensitivity tests*, no. 4489, *1st ed.*, Sept. 17, **1999**.
[15] WIWEB-Standardarbeitsanweisung 4–5.1.02, Ermittlung der Explosionsgefährlichkeit, hier der Schlagempfindlichkeit mit dem Fallhammer, Nov. 8, **2002**.
[16] http://www.bam.de.
[17] NATO standardization agreement (STANAG) on explosive, friction sensitivity tests, no. 4487, 1st ed., Aug. 22, **2002**.
[18] WIWEB-Standardarbeitsanweisung 4–5.1.03, Ermittlung der Explosionsgefährlichkeit hier der Reibeempfindlichkeit mit dem Reibeapparat, Nov. 8, **2002**.
[19] U.N. Recommendations on the Transport of Dangerous Goods, Model Regulations, *15th ed.*, United Nations, New York and Geneva, **2007**.

The investigation of copper iodate and tris(2,2,2-trinitroethyl)borate in pyrotechnical formulations

Thomas M. Klapötke[a], Burkhard Krumm[a], Magdalena Rusan[a] and Jesse J. Sabatini[b]

[a]Energetic Materials Research, University of Munich (LMU), Butenandtstr. 5-13, 81377 Munich, Germany, Fax: +49 89 2180 77492, tmk@cup.uni-muenchen.de
[b]US Army RDECOM-ARDEC, Pyrotechnics Technology and Prototyping Division, Building 3124, Picatinny Arsenal, NJ 07806, USA, Fax: 973-724-8449, E-Mail: jesse.j.sabatini.civ@mail.mil

ABSTRACT

The replacement of noxious perchlorate-containing oxidizers in pyrotechnical formulations by non-hazardous materials is desired and the object of current research. The investigation of two compounds – copper(II) iodate and tris(2,2,2-trinitroethyl)borate (TNEB) – as oxidizers in pyrotechnical compositions is reported here. Several formulations using $Cu(IO_3)_2$ and TNEB, respectively, have been tested with respect to the flame color, color properties and energetic and thermal properties.

Introduction

Green-burning pyrotechnic formulations, whether in civilian or military applications traditionally use barium compounds as green-light-emitting species.[1] Often these formulations additionally contain perchlorates and chlorine-sources such as PVC to generate metastable BaCl, which is responsible for the green color.[1] But due to health and environmental issues the replacement of barium compounds by less hazardous materials is desired and currently investigated.[2] The use of green-burning boron-containing compounds as substituents for barium nitrate is described in literature.[3] Sabatini et al reported the investigation of formulations based on amorphous boron and boron carbide. While formulations containing amorphous boron, potassium nitrate and binder are reported to burn too rapidly for practical use, the formulations using boron carbide, potassium nitrate and binder show an intensive green flame color, suitable combustion properties and an acceptable performance.[3] Replacing potassium nitrate by metal-free oxidizer could improve the color properties. Therefore the use of a metal-free and boron-containing oxidizer is of interest. Tris(2,2,2-trinitroethyl)borate (TNEB) is considered to be one potential compound[4], which combines a boron centre and energetic ligands in one molecule. Tris(2,2,2-trinitroethyl)borate (TNEB) has been synthesized and characterized by Klapötke et al.[4] The facile reaction of boron oxide and trinitroethanol in acetonitrile led to the formation of TNEB in high yield and purity. A good oxygen performance is reported, which makes it a suitable oxidizing compound.

The generation of blue flame colors in pyrotechnics is very challenging and requires an eligible tuning of different parameters such as a specific ratio of the ingredients, molecular behavior and combustion temperature for instance.[5] Blue flame colors are obtained by using copper or copper-containing compounds, which produce during the combustion in the presence of a chlorine-source the blue-emitting species CuCl, which is the best emitter in the blue region of the visible spectrum ranking from 435 nm to 480 nm. A series of bands in the region from 428 nm to 452 nm with additional peaks between 476 nm and 488 nm are obtained from this molecular species.[5, 6] But when the temperature rises above 1200 °C, which occurs in an oxygen-rich flame, CuCl decomposes resulting in the formation of CuO and CuOH. While CuOH emits in the green region from 525 nm to 555 nm, CuO emits bands in the red region, which is often observable at the top of blue flames.[7] As the chlorine-source potassium perchlorate is often used serving as the oxidizer at the same time. But also chlorinated organic compounds such as polyvinyl chloride, parlon or dechlorane for example are employed as chlorine donors.[5] In literature there are contradictory opinions concerning the extent of toxicity of the during the combustion emerging polychlorinated dibenzo-*p*-dioxins (PCDD) and dibenzofurans (PCDF). While Fleischer et al[8] stated a too low concentration of PCDD and PCDF to be harmful, Dyke and Coleman[9] found a significantly higher concentration. However, toxicity and environmental aspects should be considered and potential hazards should be avoided when possible. Therefore blue colorants, which do not base on CuCl as the blue-light-emitting species but on CuI, which emits in the blue region at 460 nm[10] as well and hence do not need any chlorine donors, would be alternatives. Such a compound is copper iodate, which is easy to prepare from potassium iodate and copper nitrate[11] and insensitive towards ignition stimuli. It possesses a high decomposition temperature and oxidizing character and therefore suitable as blue colorant and oxidizer at the same time. In literature only blue-burning formulations based on CuCl as blue-light-emitter are reported so far.[12] In this work blue-burning formulations based on copper iodate serving as the oxidizer and colorant at the same time are investigated. Formulations mixing copper iodate with a series of fuels have been prepared and investigated regarding their color performance and combustion behavior as well as their energetic and thermal properties.

Results and Discussion

1. Formulations based on tris(2,2,2-trinitroethyl)borate

The green-burning formulation containing potassium nitrate and boron carbide was reported by Sabatini et al and is reinvestigated with the herein used equipment. Although formulation **1** (Table 1.1) using potassium nitrate and boron carbide burns with a green flame color the spectral purity is reported to be lower than 70 %. In Table 1.2 the color properties like dominant wavelength (Dw), spectral purity (Sp), luminous intensity (LI) and luminous efficiency (LE) of formulation **1** are summarized. Formulation **1** is impact and friction insensitive and decomposes above 400°C.[3]

Table 1.1. Formulation **1.**

	KNO_3 [wt%]	**B_4C [wt%]**	**Epon 828/Epikure 3140 [wt%]**
1	83	10	7

Table 1.2. Color properties of formulation **1.**

	burn time [s]	**Dw [nm]**	**Sp [%]**	**LI [cd]**	**LE [$cdsg^{-1}$]**
1	6	560	69	25	250

Increased spectral purities can be obtained by replacing potassium nitrate by metal-free oxidizers. Therefore several formulations using ammonium nitrate, ammonium dinitramide (ADN) and tris(2,2,2-trinitroethyl)borate (TNEB) have been investigated.

Two formulations using NH_4NO_3 were prepared (Table 1.3). Formulation **2** consisting of 83 % ammonium nitrate, 10 % boron carbide and 7 % binder was not ignitable and formulation **3** employing 75 % ammonium nitrate, 10 % boron carbide, 8 % magnesium and 7 % binder also was not ignitable, although magnesium was added to enhance the burning temperature.

Table 1.3. Formulations **2** and **3.**

	NH_4NO_3 [wt%]	B_4C [wt%]	Mg [wt%]	Epon 828/Epikure 3140 [wt%]
2	83	10	-	7
3	75	10	8	7

In the next two formulations (Table 1.4) ammonium nitrate was replaced by ammonium dinitramide, which produces higher burning temperatures. The other components were employed in the same ratio like formulations **2** and **3**. Both formulations **4** and **5** did not burn with a green flame color.

Table 1.4. Formulations **4** and **5.**

	ADN [wt%]	B_4C [wt%]	Mg [wt%]	Epon 828/Epikure 3140 [wt%]
4	80	10	-	7
5	75	10	8	7

Tris(2,2,2-trinitroethyl)borate (TNEB) possesses oxidizing character and contains a boron centre. Due to this combination TNEB is considered to be a suitable green-burning oxidizer and was investigated in pyrotechnic formulations.

As summarized in Table 1.5 three formulations were prepared replacing stepwise potassium nitrate by TNEB. Formulation **6** contains 63 % KNO_3 and 20 % TNEB, while in formulation **7** KNO_3 and TNEB are used in a 1:1 ratio. Formulation **8** contains only TNEB as oxidizer. While formulations **6** and **7** did not burn with a green flame color, formulation **8** did not burn at all and only soaked through.

Table 1.5. Formulations **6**, **7** and **8.**

	TNEB [wt%]	KNO_3 [wt%]	B_4C [wt%]	Binder [wt%]
6	20	63	10	7
7	41.5	41.5	10	7
8	83	-	10	7

As binders VAAR and Epon 828/Epikure 3140 were investigated and revealed no difference concerning the combustion behaviour.

All other following formulations were also prepared once using VAAR binder and once again using Epon 828/Epikure 3140 and showed the same burning behaviour as well as no difference concerning the color performance, the sensitivity and the thermal properties. But all formulations whether using VAAR or Epon 828/Epikure 3140 have in common that after several days the decomposition of TNEB could be observed. It is believed that the boron ester is attacked by the ethylacetate containing in the VAAR binder and the epoxy moieties containing in the Epon 828/Epikure 3140 binder system. Additionally, all formulations were prepared without a binder and were investigated with regard to their stability exposed to air moisture. Like the formulations using a binder they also started to decompose after several days. To avoid the decomposition of TNEB and hence to ensure the stability of TNEB-containing formulations paraffin was added to the formulations instead of binder. By mixing all solid formulation components with warm liquid paraffin the particle surface is assumed to be sealed and therefore TNEB is protected from air-moisture.

In Table 1.6 the content of two formulations using only TNEB as oxidizer, boron carbide, magnesium and paraffin are summarized. To increase the combustion temperature formulations **9** and **10** were prepared using magnesium besides TNEB, B_4C and paraffin. The content of both formulations **9** and **10** is shown in Table 1.6. Both mixtures burned smokeless with an intensive green flame color.

Table 1.6. Formulations **9** and **10.**

	TNEB [wt%]	**B_4C [wt%]**	**Mg [wt%]**	**Paraffin [wt%]**
9	75	10	8	7
10	79	10	4	7

The performances of both mixtures as well as the energetic and thermal properties are summarized in Table 7. Formulations **9** and **10** reveal spectral purities of 85% and 86%, which exceed the spectral purity of formulation **1** due to the absence of potassium nitrate. The luminous intensity of composition **9**, which shows a burn time of 4 seconds is 89 cd and higher than the luminous intensity of composition **10** with 50 cd and a burn time of 7 seconds. The comparison with formulation **1** showing a luminous intensity of 25 cd reveals that both formulations **9** and **10** possess higher luminous intensities, most likely due to the presence of magnesium.

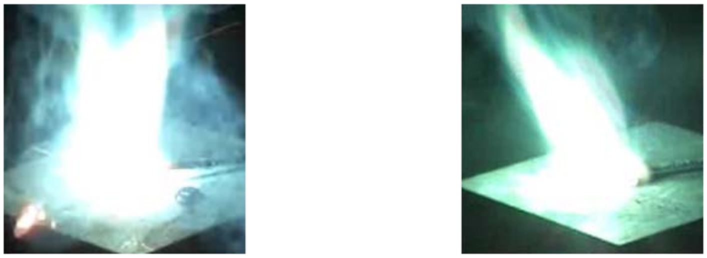

Figure 1.1: Burn down of formulations **9** (left) and **10** (right).

Table 1.7. Color performances and energetic and thermal properties of formulations **9** and **10.**

	burn time [s]	**Dw [nm]**	**Sp [%]**	**LI [cd]**	**LE [cdsg^{-1}]**	**Impact [J]**	**Friction [N]**	**grain size [µm]**	**T_{dec} [°C]**
9	4	562	85	89	593	> 40	> 360	< 100	168
10	7	561	86	50	583	> 40	> 360	< 100	170

The impact and friction sensitivities of both formulations were determined. Both compositions revealing an impact sensitivity higher than 40 J and a friction sensitivity higher than 360 N, therefore can be classified as not sensitive. The decomposition temperatures are found to be at 168°C and 170°C.

In the following two formulations **11** and **12** amorphous boron was employed as fuel. In composition **11** (Table 1.8) only boron is used, whereas formulation **12** (Table 1.9) contains boron and boron carbide. The ratios of oxidizer to fuel and binder are according to formulation **1**.

Table 1.8. Formulation **11.**

	TNEB [wt%]	**B [wt%]**	**Paraffin [wt%]**
11	83	10	7

Table 1.9. Formulation **12.**

	TNEB [wt%]	**B_4C [wt%]**	**B [wt%]**	**Paraffin [wt%]**
12	83	5	5	7

Formulation **11** shows a spectral purtiy of 80% and a luminous intensity of 13 cd (Table 1.10). Compared to formulation **1** a higher spectra purity but a lower luminous intensity could be obtained. But both performance values are below that of formulations **9** and **10** using boron carbide and magnesium as fuels. Additionally an impact sensitivity of 10 J was determined.

Table 1.10. Color performance and energetic and thermal properties of formulation **11.**

	burn time [s]	**Dw [nm]**	**Sp [%]**	**LI [cd]**	**LE [$cdsg^{-1}$]**	**Impact [J]**	**Friction [N]**	**grain size [µm]**	**T_{dec} [°C]**
11	4	565	80	13	87	10	> 360	< 100	171

When using boron and boron carbide as fuels in combination with TNEB a long burn time of 8 seconds, a low spectral purity of 45% and a lower luminous intensity of 10 cd were achieved (Table 1.11). Compared to formulation **1** and formulations **9** and **10**, mixture **12** shows a lower performance.

Table 1.11. Color performance and energetic and thermal properties of formulation **12.**

	burn time [s]	**Dw [nm]**	**Sp [%]**	**LI [cd]**	**LE [$cdsg^{-1}$]**	**Impact [J]**	**Friction [N]**	**grain size [µm]**	**T_{dec} [°C]**
12	8	563	45	10	133	40	> 360	< 100	178

2. Formulations based on copper iodate

In order to investigate blue-burning formulations using copper iodate as the oxidizer and colorant without any additional chlorine-containing compound, an established blue-burning formulation was prepared and compared with the new formulations.

Shimizu´s blue formulation[12a] consisting of 68% potassium perchlorate, 15% copper, 17% polyvinyl chloride and 5% starch (Table 2.1) was chosen and reinvestigated with the herein used equipment.

Table 2.1. Formulation **A** - Shimizu´s blue formulation.

	$KClO_4$ [wt%]	Cu [wt%]	PVC [wt%]	Starch [wt%]
A	68	15	17	5

The performance of formulation **A** is summarized in Table 2.2. The burn time, the dominant wavelength (Dw), the spectral purity (Sp), the luminous intensity (LI) and the luminous efficiency (LE) have been determined. The sensitivity towards impact and friction as well as the decomposition temperature (T_{dec}) were measured. Although formulation **A** burned with an intensive blue flame color two dominant wavelength values were measured appearing at 475 nm in the blue region and at 552 nm in the green region, which can be attributed to the formation of CuOH during the combustion. A spectral purity of 61% and a luminous intensity of 54 cd were measured. Formulation **A** revealed an impact sensitivity of 8 J, a friction sensitivity of 324 N and a decomposition temperature of 307°C (Table 2.2).

Table 2.2. Performance and sensitivity of formulation **A**.

	burn time [s]	Dw [nm]	Sp [%]	LI [cd]	LE [$cdsg^{-1}$]	Impact [J]	Friction [N]	T_{dec} [°C]
A	4	475 (552)	61	54		8	324	307

In Table 2.3 the content of formulations using copper iodate and several different fuels is shown. In all formulations the binder system Epon 828/Epikure 3140 is employed. Formulations **1** and **2** contain beside the binder copper iodate and 5-aminotetrazole in different ratios. Both formulations did not burn but only glowed down. Formulation **4** containing copper iodate and nitroguanidine as fuel and formulation **5** containing copper iodate, copper and starch did not burn as well and both only glowed down. In contrast formulation **3** using copper iodate and the very reactive fuel amorphous boron self-ignited by grinding the mixture in the mortar.

Table 2.3. Formulations **1**, **2**, **3**, **4** and **5**.

	$Cu(IO_3)_2$ [wt%]	5-At [wt%]	B [wt%]	Nitroguanidine [wt%]	Cu [wt%]	starch [wt%]	Epon 828/Epikure 3140 [wt%]
1	60	33	-	-	-	-	7
2	80	15	-	-	-	-	5
3	75	-	20	-	-	-	5
4	75	-	-	20	-	-	5
5	70	-	-	-	20	5	5

While the use of boron makes a formulation to reactive, 5-aminotetrazole as the only fuel does not produce the energy, which is required for the combustion reaction. To enhance the reaction temperature formulations were prepared using copper iodate, 5-aminotetrazole and magnesium. The content of these formulations is summarized in Table 2.4. Formulation **6**, containing only 53% of copper iodate did not burn but only glowed down. Formulations **7** and **8** burned with a blue flame color and some smoke and residues could be observed. Formulation **9** burned also with a blue flame color, but some slightly red smoke was observable and residues remained.

Table 2.4. Formulations **6**, **7**, **8** and **9**.

	$Cu(IO_3)_2$ [wt%]	5-At [wt%]	Mg [wt%]	Epon 828/Epikure 3140 [wt%]
6	53	35	5	7
7	65	15	15	5
8	75	5	15	5
9	75	12	8	5

Figure 2.1: Burn down of formulations **7**, **8** and **9**.

In Table 2.5 the performance data, the impact and friction sensitivities as well as the decomposition temperatures of formulations **7**, **8** and **9** are summarized. While formulations **7** and **8** revealed burn times of 5 seconds, formulation **9** showed a burn time of 6 seconds. The spectral purities of all three formulations are below 60% and therefore lower than that of formulation **A**. The dominant wavelength values indicate, that beside the main blue emitter also green-light-emitting species occur, which are responsible for the dominant wavelength values in the green region of the visible spectrum. Among these three formulations mixture **7** shows the highest spectral purity of 58% and mixture **9** achieved the highest luminous intensity of 80 cd. All three formulations are friction insensitive but very sensitive towards impact and the decomposition temperatures are in the range from 164°C to 170°C (Table 2.5).

Table 2.5. Performance and sensitivity of formulations **7**, **8** and **9**.

	burn time [s]	Dw [nm]	Sp [%]	LI [cd]	LE [$cdsg^{-1}$]	Impact [J]	Friction [N]	grain size [µm]	T_{dec} [°C]
7	5	468 (546)	58	45	375	10	> 360	< 100	164
8	5	480	51	76	633	10	> 360	< 100	167

		(555)							
9	6	465 (532)	56	80	800	8	> 360	< 100	170

The next four investigated formulations **10**, **11**, **12** and **13** contain besides copper iodate, 5-aminotetrazole and magnesium also copper iodide, which was used as an additional colorant. Formulation **12** contains urea in addition. Formulation **13** consists of copper iodate, magnesium, copper iodide and copper instead of 5-aminotetrazole. The content of these formulations is summarized in Table 2.6.

Table 2.6. Formulations **10**, **11**, **12** and **13**.

	$Cu(IO_3)_2$ [wt%]	**5-At [wt%]**	**Mg [wt%]**	**CuI [wt%]**	**Urea [wt%]**	**Cu [wt%]**	**Epon 828/Epikure 3140 [wt%]**
10	65	7	15	8	-	-	5
11	65	7	5	18	-	-	5
12	65	7	5	10	4	-	5
13	65	-	13	10	-	7	5

Formulations **10** and **11** burned with a blue flame color and produced some smoke and residues. Formulations **12** and **13** also showed blue flame colors and a slightly reddish smoke and residues remained.

Figure 2.2: Burn down of formulations **10**, **11**, **12** and **13**.

The burn times and the performance as well as the impact and friction sensitivities and the decomposition temperatures of formulations **10**, **11**, **12** and **13** are summarized in Table 2.7.

Table 2.7. Performance and sensitivity of formulations **10**, **11**, **12** and **13**.

	burn time [s]	**Dw [nm]**	**Sp [%]**	**LI [cd]**	**LE [$cdsg^{-1}$]**	**Impact [J]**	**Friction [N]**	**grain size [µm]**	**T_{dec} [°C]**
10	4	470 (555)	59	67	447	10	> 360	< 100	173
11	4	473	65	42	280	5	> 360	< 100	161

		(555)							
12	3	480 (527)	56	32	160	5	> 360	< 100	167
13	4	470 (551)	60	41	273	5	> 360	< 100	170

Formulations **10**, **11** and **13** show burn times of 4 seconds and formulation **12** shows a burn time of 3 seconds. The spectral purities are found to be between 56% and 65%. While formulation **13** shows the same spectral purity of 60% like formulation **A**, composition **11** possesses a spectral purity of 65%, which exceeds that of formulation **A**. Among these four formulations, composition **10** reveals the highest luminous intensity of 67 cd, which is higher than that of formulation **A**. Comparing these formulations with formulations **7**, **8** and **9**, it can be assumed, that the addition of CuI improves the spectral purity. All formulations show very high impact sensitivities but are not friction sensitive (Table 2.7). The decomposition temperatures are from 161°C to 173°C.

J. Jennings-White reported a blue-burning formulation, which consists of 50% guanidine nitrate, 20% parlon, 15% copper and 15% magnesium.[13] According to this formulation compositions containing copper iodate and guanidine nitrate were prepared and investigated (Table 2.8). Formulations **14**, **15** and **16** contain copper iodate, guanidine nitrate and magnesium. Formulation **17** contains no guanidine nitrate. Except formulation **15**, the other formulations contain 21% urea. Formulation **15** contains copper instead of urea. The highest amount of copper iodate was used in formulation **17**, the lowest in formulation **14**. While formulation **14** could not be ignited, formulations **15**, **16** and **17** burned with an intensive blue flame color. No smoke and no residues were observable for all three formulations.

Table 2.8. Formulations **14**, **15**, **16** and **17**.

	$Cu(IO_3)_2$ [wt%]	Guanidine nitrate [wt%]	Mg [wt%]	Urea [wt%]	Cu [wt%]	Epon 828/Epikure 3140 [wt%]
14	15	50	9	21	-	5
15	20	50	10	-	15	5
16	30	35	9	21	-	5
17	65	-	9	21	-	5

Figure 2.3: Burn down of formulations **15**, **16** and **17**.

In Table 2.9 the performance data of formulations **15**, **16** and **17** is shown. Also the impact and friction sensitivities as well as the decomposition temperatures are summarized. Formulation **15** reveals a rather long burn time of 8 seconds. Formulations **16** and **17** show both a burn time of 6 seconds. The spectral purity of composition **16** is measured to be 63%. Like in the case of all previous discussed formulations, compositions **15**, **16** and **17** exhibit dominant wavelengths in the blue and green region of the visible spectrum (Table 2.9). Formulations **15** and **17** show a slightly higher spectral purity of 64% (Table 2.9). But compared to formulation **A** all three formulations possess an increased spectral purity. Although formulation **15** exhibits the highest burn time, the highest luminous intensity of 80 cd was obtained as well. Compositions **16** and **17** reveal luminous intensities of 78 cd and 74 cd, respectively. Formulations **15** and **16** containing a low quantity of copper iodate are impact insensitive, while formulation **17** with 65% of copper iodate is very impact sensitive. But all three formulations are friction insensitive. Among these three formulations the decomposition temperatures decrease with increasing amount of copper iodate. Formulation **15** shows the highest decomposition temperature of 198°C (Table 2.9).

Table 2.9. Performance and sensitivity of formulations **15**, **16** and **17**.

	burn time [s]	**Dw [nm]**	**Sp [%]**	**LI [cd]**	**LE [cdsg^{-1}]**	**Impact [J]**	**Friction [N]**	**grain size [µm]**	**T_{dec} [°C]**
15	8	477 (555)	64	80	1067	> 40	> 360	< 100	198
16	6	476 (525)	63	78	780	> 40	> 360	< 100	180
17	6	475 (553)	64	74	740	5	> 360	< 100	151

Summary and Conclusions

The replacement of potassium nitrate by TNEB in pyrotechnic formulation leads to a significant increase of the spectral purity and luminous intensity, when combining TNEB with boron carbide and magnesium. These formulations are determined not to be impact and friction sensitive. Formulations using TNEB combined with or without potassium nitrate and only boron carbide did not yield green flame colors. The combination of TNEB and amorphous boron only shows a higher spectral purity than formulations using potassium nitrate but also an increased impact sensitivity. The addition of paraffin instead of an epoxy or VAAR binder protects from hydrolysis by air moisture.

Several blue-burning formulations using copper iodate as the oxidizer and colorant have been investigated. Formulations combining copper iodate with a series of fuels such as 5-aminotetrazole, magnesium, boron, nitroguanidine and copper and other additives such as copper iodide, urea and guanidine nitrate were prepared and examined. Only formulations containing magnesium in addition did burn. Different component ratios have been tested and investigated with respect to the combustion behaviour. While low amounts of copper iodate impede the combustion, the use of higher quantities of copper iodate seems to cause smoke during the combustion and high impact sensitivities. Best results have been achieved when using copper iodate between 20% and 30% together with magnesium, guanidine nitrate and urea or copper (Formulations **15** and **16**). These two formulations show the highest spectral purities of 64% and 63% as well as the highest luminous intensities of 80 cd and 78 cd revealing also the longest burn times of 8 and 6 seconds at the same time. Furthermore, both formulations are neither impact nor friction sensitive and possess the highest decomposition temperatures of 198°C and

180°C as well. From the comparison with the performance of formulation **A** (Shimizu´s blue) it can be concluded that for the generation of blue-flame colors not only the combination of copper or copper compounds with a chlorine donor resulting in the formation of blue-emitting CuCl is necessary. Copper iodate forming very likely CuI during the combustion also produces brilliant blue flame colors when combining with magnesium and guanidine nitrate in a proper tuned formulation.

Experimental

TNEB was synthesized according to literature procedure.[4] Boron carbide, copper iodate, amorphous boron, potassium nitrate, ammonium nitrate, potassium perchlorate copper, 5-aminotetrazole, magnesium, urea and paraffin were purchased from Aldrich, Fluka and Acros and were used as received. ADN was supplied by EURENCO, Karlskoga, Sweden. The pyrotechnical compositions were prepared by grinding all substances in a mortar. Then the mixture was introduced to the Epon 828/Epikure 3140 binder system, mixed by hand with a plastic spatula for 15 minutes and grinded in a mortar again. In the case of the TNEB-formulations the mixtures were introduced slowly to warm liquid paraffin after grinding. After cooling to room temperature the mixtures were grinded again. Pellets of 0.6 g each were pressed using a consolidation dead load of 2000kg. The pellets were dried over night at ambient temperature. The controlled burn down was filmed with a digital video camera recorder (SONY, DCR-HC37E). The performance of each composition has been evaluated with respect to color emission, smoke generation and the amount of solid residues. Spectrometric measurements were performed using a HR2000+ES spectrometer with an ILX511B linear silicon CCD-array detector and included software from Ocean Optics with a detector-sample distance of 1 meter. The dominant wavelength (Dw) and spectral purity (Sp) were measured based on the 1931 CIE method using illuminant C as the white reference point. Luminous intensities (LI) and luminous efficiencies (LE) were determined using pellets of 0.6g each. Five samples were measured for each formulation and all given values are averaged based on the full burn of the mixture. Decomposition points were measured with a Linseis PT10 DSC using heating rates of 5 °C min^{-1}.[14] The impact and friction sensitivity was determined using a BAM drophammer and a BAM friction tester.[15-19] The sensitivities of the compounds are indicated according to the UN Recommendations on the Transport of Dangerous Goods (+):[20] impact: insensitive >40 J, less sensitive >35 J, sensitive >4 J, very sensitive 4< J; friction: insensitive >360 N, less sensitive = 360 N, sensitive <360 N>80 N, very sensitive <80 N, extreme sensitive <10 N.

Acknowledgement

Financial support of this work by the Ludwig-Maximilian University of Munich (LMU), the U.S. Army Research Laboratory (ARL) under grant no. W911NF-09-2-0018, the Armament Research, Development and Engineering Center (ARDEC) under grant no. W911NF-12-1-0467, and the Office of Naval Research (ONR) under grant nos. ONR.N00014-10-1-0535 and ONR.N00014-12-1-0538 is gratefully acknowledged. The authors acknowledge collaborations with Dr. Mila Krupka (OZM Research, Czech Republic) in the development of new testing and evaluation methods for energetic materials and with Dr. Muhamed Suceska (Brodarski Institute, Croatia) in the development of new computational codes to predict the detonation and propulsion parameters of novel explosives. We are indebted to and thank Drs. Betsy M. Rice and Brad Forch (ARL, Aberdeen, Proving Ground, MD) for many inspired discussions. The Cusanuswerk is gratefully acknowledged for the award of a PhD scholarship (M. Rusan).

References

[1] a) G. Steinhauser, T. M. Klapötke, *Angew. Chem. Int. Ed.* **2008**, *47*, 3330; b) J. A. Conkling, *Chemistry of Pyrotechnics: Basic Principles and Theory*, Taylor & Francis Group, New York, **1985**, 156; c) G. Steinhauser, T. M. Klapötke, *J. Chem. Educ.* **2010**, *87*, 150.

[2] a) J. J. Sabatini, A. V. Nagori, E. A. Latalladi, J. C. Poret, G. Chen, R. Damavarapu, T. M. Klapötke, *Propellants Explos. Pyrotech.* **2011**, *36*, 373; b) J. J. Sabatini, A. V. Nagori, G. Chen, P. Chu, R. Damavarapu, T. M. Klapötke, *Chem. Eur. J.* **2012**, *18*, 628; c) J. J. Sabatini, J. M. Raab, R. K. Hann Jr., C. T. Freeman, *Z. Anorg. Allg. Chem.* **2013**, *639*, 25.

[3] J. J. Sabatini, J. C. Poret, R. N. Broad, *Angew. Chem. Int. Ed.* **2011**, *50*, 4624.

[4] T. M. Klapötke, B. Krumm, R. Moll, *Chem. Eur. J.* **2013**, *19*, 12113.

[5] J. A. Conkling, C. J. Mocella, *Chemistry of Pyrotechnics: Basic Principles and Theory*, *2nd Ed*, **2011**, Boca Raton, FL: Taylor and Francis Group.

[6] a) B. E. Douda, RDTN 71, Crane, IN: U.S. Naval Ammunition Depot, **1964**; b) K. L. Kosanke, B. J. Kosanke, *Pyrotechnic Chemistry*, *Journal of Pyrotechnics*, Whitewater, CO, **2004**, chap. 9.

[7] T. Shimizu, *Fireworks: The art, science and technique*, Tokyo: T. Shimizu, **1981**.

[8] O. Fleischer, H. Wichmann, W. Lorenz, *Chemosphere* **1999**, *39*, 925.

[9] D. Dyke, P. Coleman, *Organohalogen Compounds* **1995**, *24*, 213.

[10] A. P. Hardt, *Pyrotechnics*, **2001**, Post Falls, ID: Pyrotechnica Publications.

[11] K. Nassau, A. S. Cooper, J. W. Shiever, B. E. Prescott, *J. Solid State Chem.* **1973**, *8*, 260.

[12] a) T. Shimizu, *Pyrotechnica* **1980**, *6*, 5; b), C. Jennings-White, *Pyro. Guild Int. Bull.* **1988**, *59*, 31; c) T. Shimizu, Pyrotechnica Publications, Austin , Texas **1983**, Vol. II, trans. A. Schuman, p.81.

[13] C. Jennings-White, *Pyrotechnica XV*, Austin, TX: Pyrotechnica Publications, **1993**.

[14] http://www.linseis.com.

[15] NATO standardization agreement (STANAG) on explosives, *impact sensitivity tests*, no. 4489, 1st ed., Sept. 17, 1999.

[16] WIWEB-Standardarbeitsanweisung 4–5.1.02, Ermittlung der Explosionsgefährlichkeit, hier der Schlagempfindlichkeit mit dem Fallhammer, Nov. 8, **2002**.

[17] http://www.bam.de.

[18] NATO standardization agreement (STANAG) on explosive, *friction sensitivity tests*, no. 4487, 1st ed., Aug. 22, **2002**.

[19] WIWEB-Standardarbeitsanweisung 4–5.1.03, Ermittlung der Explosionsgefährlichkeit or der Reibeempfindlichkeit mit dem Reibeapparat, Nov. 8, **2002**.

[20] *UN Recommendations on the Transport of Dangerous Goods, Model Regulations*, 15th ed., United Nations, New York a. Geneva, **2007**.

List of Publications (author names are given in alphabetical order)

Papers

[1] Thomas M. Klapötke, Carles Miró Sabaté, Magdalena Rusan, *Z. Anorg. Allg. Chem.* **2008**, *634*, 688-695.

[2] Thomas M. Klapötke, Carles Miró Sabaté, Alexander Penger, Magdalena Rusan, Jan M. Welch, *Eur. J. Inorg. Chem.* **2009**, 880-896.

[3] Margaret-Jane Crawford, Thomas M. Klapötke, Franz A. Martin, Carles Miró Sabaté, Magdalena Rusan, *Chem. Eur. J.* **2011**, *17*, 1683-1695.

[4] Niko Fischer, Thomas M. Klapötke, Kristina Peters, Magdalena Rusan, Jörg Stierstorfer, *Z. Anorg. Allg. Chem.* **2011**, *637*, 1693–1701.

[5] Thomas M. Klapötke, Thomas G. Müller, Magdalena Rusan, *New Trends in Research of Energetic Materials*, 14th, Pardubice, Czech Republic, Apr. 13– 15, **2011**, 729-741.

[6] Thomas M. Klapötke, Magdalena Rusan, Jörg Stierstorfer, *38th International Pyrotechnics Seminar*, Proceedings, Denver, Colorado, USA, June 10-15, **2012**, 527-550.

[7] Niko Fischer, Thomas M. Klapötke, Stefan Marcher, Magdalena Rusan, Susanne Scheutzow, Jörg Stierstorfer, *Propellants Explos. Pyrotech.* **2013**, *35*, 1-12.

[8] Thomas M. Klapötke, Magdalena Rusan, Véronique Sproll, Jörg Stierstorfer, *39th International Pyrotechnics Seminar*, Proceedings, Valencia, Spain, May 27-31. **2013**, 1-7.

[9] Thomas M. Klapötke, Magdalena Rusan, Véronique Sproll, *Z. Anorg. Allg. Chem.* **2013**, *639*, (14), 2433-2443.

[10] Thomas M. Klapötke, Magdalena Rusan, Véronique Sproll, *Z. Anorg. Allg. Chem.* **2014**, *640*, (*10*), 1892-1899.

[11] Thomas M. Klapötke, Thomas G. Müller, Magdalena Rusan, Jörg Stierstofer, *Z. Anorg. Allg. Chem.* **2014**, *640*, (*7*), 1347-1354.

[12] Ines E. Drukenmüller, Thomas M. Klapötke, Yvonne Morgenstern, Magdalena Rusan, Jörg Stierstorfer, *Z. Anorg. Allg. Chem.* **2014**, *640*, (*11*), 2139-2148.

[13] Thomas M. Klapötke, Magdalena Rusan, Jesse J. Sabatini, *Angew. Chem. Int. Ed.* **2014**, *53*, 9665-9668.

[14] Thomas M. Klapötke, Burkhard Krumm, Magdalena Rusan, Jesse J. Sabatini, *40th International Pyrotechnics Seminar,* Proceedings, Colorado Springs, Colorado, USA, July 13-18, **2014**, 15-27.

[15] Johann Glück, Thomas M. Klapötke, Magdalena Rusan, Jörg Stierstofer, *Chem Eur. J.* **2014**, *20*, 15947-15960.

[16] Thomas M. Klapötke, Burkhard Krumm, Magdalena Rusan, Jesse J. Sabatini, *Chem. Commun.* **2014**, 50, 9581-9583.

[17] Thomas M. Klapötke, Magdalena Rusan, *Z. Naturforsch.* **2014**, *69b*, 1241-1247.

[18] Thomas M. Klapötke, Magdalena Rusan, Jörg Stierstofer, *J. Pyrotech.* **2014**, in press.

Poster

Thomas M. Klapötke, Thomas G. Müller, Magdalena Rusan, *New Trends in Research of Energetic Materials*, 14th, Pardubice, Czech Republic, Apr. 13– 15, **2011**.

Oral Presentations

[1] Thomas M. Klapötke, Magdalena Rusan: Some Recent Aspects of Silicon and Boron in Energetic Materials, *8th Workshop on Pyrotechnic Combustion Mechanisms*, Reims, France, May 14, **2011**.

[2] Thomas M. Klapötke, Magdalena Rusan, Jörg Stierstorfer: The Synthesis and Investigation of Nitrogen-rich and Boron-based Compounds as Coloring Agents in Pyrotechnics, *38th International Pyrotechnics Seminar*, Denver, Colorado, USA, June 10-15, **2012.**

[3] Thomas M. Klapötke, Magdalena Rusan, Véronique Sproll, Jörg Stierstorfer: Energetic Materials Based on Azole Borates, *10th Workshop on Pyrotechnic Combustion Mechanisms*, Valencia, Spain, May 25, **2013**.

[4] Thomas M. Klapötke, Magdalena Rusan, Véronique Sproll, Jörg Stierstorfer: Energetic Materials Based on Azole Borates, *39th International Pyrotechnics Seminar*, Valencia, Spain, May 27-31. **2013.**

[5] Thomas M. Klapötke, Magdalena Rusan, Jesse J. Sabatini: Development of environmentally benign pyrotechnic formulations based on energetic boron compounds, nitrogen-rich metal salts and copper iodate, *11th Workshop on Pyrotechnic Combustion Mechanisms*, Colorado Springs, Colorado, USA, July 12, **2014**.

[6] Thomas. M. Klapötke, Magdalena Rusan, Jesse J. Sabatini: Copper iodate as an oxidizer in blue-light-emitting pyrotechnic compositions, *40th International Pyrotechnics Seminar*, Colorado Springs, Colorado, USA, July 13-18, **2014.**

[7] Thomas M. Klapötke, Magdalena Rusan, Jesse J. Sabatini: Investigation of tris(2,2,2-trinitroethyl)borate in green-light-emitting pyrotechnical formulations, *40th International Pyrotechnics Seminar*, Colorado Springs, Colorado, USA, July 13-18, **2014.**

Press Release

Deutschlandradio: Strontiumtetrazolat – bitte abbrennen und in Luft auflösen! http://www.deutschlandfunk.de/strontiumtetrazolat-bitte-abbrennen-und-in-luft-aufloesen.676.de.html?dram:article_id=29031

Feuer frei!: Newton - ORF eins - tv.ORF.at

Contact

Magdalena Rusan
Graf-Konradstr. 10 80809 Munich, Germany
magda.rusan@gmx.net

Born: November 09, 1983, Munich, Germany
Nationality: German, Croatian

Education

July 2009 – July 2014	PhD thesis, Inorganic Chemistry, Ludwig Maximilian University Munich, Germany, Research Group of Prof. Dr. T. M. Klapötke, Main research subject: ‘Synthesis of nitrogen-rich boron compounds and their investigation as colorants in pyrotechnics’
October 2005 - April 2009	Diplom (equiv. to M.Sc.), Chemistry, Ludwig Maximilian University Munich, Germany, Research subject: ‘Synthesis and investigation of energetic borazine and aminborane compounds’
October 2003 - October 2005	Vordiplom (equiv. to B.Sc.), Chemistry, Ludwig Maximilian University Munich, Germany
September 1994 - May 2003	Allgemeine Hochschulreife (equiv. to A-levels), Lion Feuchtwanger Gymnasium, Munich, Germany

Work Experience

August 2009 - September 2009	Research Project with Philip Morris Products S.A. ‘Impregnation of carbon heat sources with energetic materials’

June 2007 - July 2007	Working student at Aromalab AG ‘Synthesis of Grignard reagents’
October 2009 - November 2013	Supervisor for undergraduate and graduate students

Languages

German (native), Croatian (native), Polish (native), English (fluent), French (advanced)

Scholarship

February 2010 - February 2013	PhD scholar of the Cusanuswerk